RECORDS OF THE AUSTRALIAN MUSEUM

Volume 63 Numbers 2 & 3 30 November 2011

nature culture **discover**

Australian museum

Volume 63 Numbers 2 and 3

Published 30 November 2011

Price: AU$60.00

Printed by RodenPrint Pty Ltd, Sydney

ISSN 0067-1975

The Australian Museum is a statutory authority of, and principally funded by, the NSW State Government.

NSW GOVERNMENT

Cover images—Comparison is an essential aspect of discovery in the natural sciences. In 1913 Fry published images—in *Rec. Aust. Mus.*—of three kinds of *Limnodynastes* frog: a variety from the Riverina (cover image, left, *L. dorsalis* Gray, var. *interioris*), a variety from Western Australia (middle, *L. dorsalis*, var. *typica*), and one from Somerset, Cape York (right, *L. dorsalis*, var. *dumerilii*). Later, Australian Museum herpetologists Kinghorn (1924), Cogger (1979), and Shea and Sadlier (1999), greatly expanded our knowledge of this genus and its species and further developed the taxonomy. All of these works have been published by the Australian Museum and may be read online at the Australian Museum website (to resolve any DOI, insert *http://dx.doi.org/* before the *10* and use as a hyperlink)

Fry (1913)	doi:10.3853/j.0067-1975.10.1913.894
Kinghorn (1924)	doi:10.3853/j.0067-1975.14.1924.840
Cogger (1979)	doi:10.3853/j.0067-1975.32.1979.455
Shea & Sadlier (1999)	doi:10.3853/j.1031-8062.15.1999.1290

Since 2009 the entire legacy of the primary scientific literature published in print by the Australian Museum has been freely accessible online. *Records of the Australian Museum* and *Supplements (*from 1890), *Australian Museum Memoirs* (from 1851) and *Technical Reports of the Australian Museum*, have been digitized and OCR-enhanced, making this huge resource fully searchable at:
www.australianmuseum.net.au/Scientific-Publications

Records of the Australian Museum is covered in the Thomson Scientific services: Current Contents ® / Agriculture, Biology, and Environmental Sciences, and Science Citation Index Expanded (also known as SciSearch ®)

We encourage cross-linking in the scientific literature by applying *doi* registration to Australian Museum publications via CrossRef ®

The Australian Museum houses some of the world's most important collections of Australian animal, fossil and geological specimens and cultural objects. Research on these millions of specimens and artefacts yields insights into how our world changes through time and how its diversity can be classified and interpreted. This knowledge, when shared among the scientific and broader community—initially through publication—helps us understand human impact on our environment and what reasonable steps society can take now for the well-being of future generations. Our responsibility is to inspire the exploration of nature and cultures; our vision is a beautiful and sustainable natural world with vibrant and diverse cultures.

Since 1889 the *Records of the Australian Museum* (ISSN 0067-1975) has published the results of studies that derive in large part from Australian Museum collections or studies that more generally lead to a better understanding of nature and cultures in the Australian Region. Three issues of the *Records* are published annually and circulated to numerous countries. All that is published in print is, within several days, also freely available online. *Records of the Australian Museum*, volume 61, was published in 2009, volume 62 in 2010. Monographic works of particular significance are published irregularly as *Records of the Australian Museum, Supplements*, the last in 2006. Catalogues and checklists have, in the past, been published in print as numbered *Technical Reports of the Australian Museum* (ISSN 1031-8062 print). From number 20 (December 2007) onwards, *Technical Reports of the Australian Museum, Online* (ISSN 1835-4211 online) has been published online only. *Australian Museum Memoirs* (ISSN 0067-1967) ceased in 1983.

Librarians or publishers of similar scientific and academic journals may propose exchange agreements with the *Australian Museum Research Library*.

Authors are invited to submit manuscripts to The Editor. Manuscripts meeting subject and stylistic requirements outlined in the *Instructions to Authors* (see inside back cover) are assessed by external referees.

The Editor, *Records of the Australian Museum*
Australian Museum
6 College Street
Sydney NSW 2010, Australia
editor@austmus.gov.au

www.australianmuseum.net.au/Scientific-Publications

Australian museum

nature culture **discover**

Our logo is based on a distinctive and local Aboriginal rock engraving of the echidna. This image has special meaning for the Australian Museum as it represents both nature and culture—a fitting symbol for all that we do.

Records of the Australian Museum (2011) Vol. 63: 113–166. ISSN 0067-1975
doi:10.3853/j.0067-1975.63.2011.1585

Observations on Antennal Morphology in Diptera, with Particular Reference to the Articular Surfaces between Segments 2 and 3 in the Cyclorrhapha

DAVID K. MCALPINE

Australian Museum, 6 College Street, Sydney NSW 2010, Australia

ABSTRACT. The main features of antennal segments 2 and 3 seen in the higher Diptera are described, including many that are not or inadequately covered in available publications. The following terms are introduced or clarified: for segment 2 or the pedicel—annular ridge, caestus, chin, collar, conus, distal articular surface, encircling furrow, foramen of articulation, foraminal cusp, foraminal ring, pedicellar button, pedicellar cup, rim; for segment 3 or the postpedicel—basal foramen, basal hollow, basal stem, postpedicellar pouch, sacculus, scabrous tongue, sub-basal caecum; for the stylus or arista—stylar goblet. Particular attention is given to the occurrence and position of the pedicellar button. The button is the cuticular component of a chordotonal organ, which perhaps has the role of a baroreceptor. It is present in the majority of families of Diptera, and possibly was present in the ancestral dipteran. Some generalizations about antennal structure are made, and a diagram showing the main trends in antennal evolution in the Eremoneura is provided. The general form of the antenna shows a transition from approximate radial symmetry (e.g., in *Empis*, *Microphor*, and *Opetia*) through to superficial bilateral symmetry (in many taxa of Eumuscomorpha), though there is usually much asymmetry in detail. More detailed descriptions and illustrations are given for selected taxa of Cyclorrhapha. The phenomenon of an additional concealed segment-like structure between segments 2 and 3, found among the Chloropidae, Pyrgotidae, etc., and formed from the basally flexible conus, is described. Some antennal features of the Calyptratae suggest a relationship to the Tephritoidea. Critical comments are made with regard to the recently published phylogenetic association of the Ironomyiidae with the Phoridae and the Pallopteridae with the Neurochaetidae. In discussing relationships of some taxa, a few non-antennal features, some needing further study, are mentioned, e.g., variation in separation of abdominal tergites 1 and 2 in the Opetiidae and other lower cyclorrhaphous families; the presence of supplementary claw-like terminal tarsal processes in the Lonchopteridae; the apparent restriction of the presence of barbed macrotrichia to the Phoridae, among lower cyclorrhaphans; variation in structure of the prelabrum in the Pyrgotidae; the microstructure of the facial cuticle in the Syringogastridae as compared with that of other families; the calyptrate-like development of the squama in some tephritoid taxa; variation in the subscutellum in the Conopidae; a feature of the larval posterior spiracles diagnostic for Coelopidae.

MCALPINE, DAVID K. 2011. Observations on antennal morphology in Diptera, with particular reference to the articular surfaces between segments 2 and 3 in the Cyclorrhapha. *Records of the Australian Museum* 63(2): 113–166.

Table of Contents

Introduction

From morphological studies relating to my taxonomic research on cyclorrhaphous Diptera, it has become apparent that much of the structural diversity in the antenna of these insects remains unrecorded, and that established terminology does not adequately cover this diversity. Difficulties in observation have occurred because some structures are concealed until careful separation of certain segments is carried out, and in the past access to electron microscopy was more limited.

It is probable that much of the diversity now described has phylogenetic significance, but I do not here propose alterations to current classification. Antennal characters will need to be further checked for consistency and correlated with other data, if such changes are to be made, as I find much evidence of homoplasy. However, the broader trends in at least some aspects of antennal morphology in the higher Diptera seem to follow the course outlined (and simplified) in Fig. 23.

In order to present my more significant findings within a reasonable time, I have limited the range of taxa for detailed study to those of more immediate interest and availability, and some other significant groups have been omitted or given slight attention. Therefore, there remains a large field for investigation by other students, e.g., in the Muscoidea or Calyptratae. Theodor (1967) has described the extraordinary antennal features of the Nycteribiidae. I have omitted my observations on the superfamily Nerioidea and the families Somatiidae and Heteromyzidae s.l. (including Heleomyzidae, Rhinotoridae, Sphaeroceridae, Trixoscelididae, etc.), as these show such diversity as to require separate studies.

Morphological study for this paper has been performed using a stereo light microscope (SLM), a compound light microscope (CLM), and a scanning electron microscope (SEM).

Collections mentioned in the text are: Australian Museum, Sydney (AM); Natural History Museum, London (BMNH); Zoological Museum, Copenhagen (ZMUC).

Terminology—orientation

For descriptive purposes the antenna is assumed to lie, in its primitive position, directed anteriorly from the frontal surface. The terms **dorsal** and **ventral** are applied according to this orientation. The surfaces of the two antennae which are nearest to one another and to the median or sagittal plane of the insect are described as **medial**. The surface of each antenna most remote from the median line is described as **lateral**. The segments are numbered from the basal one (joining the head capsule) to the free distal end, and the adjectives **basal** and **distal** are accordingly applied to the parts of each segment.

Terminology—segmental structure

In the Cyclorrhapha the antenna is most frequently six-segmented and it seems probable (but not certain) that this is the groundplan condition for the Cyclorrhapha (D. McAlpine, 2002). The simplest system of indicating the individual segments is therefore by numbering them 1 to 6 from the base, but names for the differentiated segments or groups of segments are in fairly general use and have application to descriptive morphology, physiology, and taxonomy. I do not use the system of numbering for flagellar segments deduced by Stuckenberg (1999) from study of the reduction series found in extant taxa of Vermileonidae, as the basal eremoneuran was not evolved from that somewhat derived homoeodactylous family. In fact there is no surviving evidence of a multisegmental origin for the postpedicel in the Eremoneura, and, although a very early multisegmental origin is conceivable, it is unlikely that we could ascertain the details of such an origin using present methodology.

Segment 1 is widely termed the **scape** in insects. It is often relatively short, subcylindrical, and assumed to be of simple structure. Its comparative morphology has therefore received little attention. It probably generally contains muscles arising in its basal part, which connect with the base of segment 2 and effect movement between the segments (Snodgrass 1935: 132; Soenen 1940: fig. 2).

Segment 2 is generally termed the **pedicel**. Its external structure is often complex and taxonomically variable (e.g., Figs 1, 2). Internally it probably usually contains two sensory organs, which have been examined in very few cyclorrhaphans. These are the relatively large Johnston's organ and the outer chordotonal organ or inappropriately "organe de Hicks" (Soenen 1940). The distal surface of segment 2 in the Cyclorrhapha is usually at least partly flattened to concave and encircled by an angular or flange-like **rim** delimiting the **distal articular surface**. This condition contrasts with that of most non-cyclorrhaphous brachycerans, in which segment 2 is generally more or less rounded in distal profile. In some schizophorans the dorsal part of the rim is extended into a pair of **dorsal lobes**, which may be hood-like or cucullate, concealing part of the distal articular surface. This surface is penetrated by the **foramen of articulation** for attachment to the base of segment 3. The foramen is primitively placed in the centre of the distal articular surface and faces distally, but it may be very asymmetrically placed and inclined in advanced taxa. Immediately surrounding the foramen there is often a slender ridge, the **foraminal ring** (*anneau de renforcement* of Soenen 1940: fig. 2) which is devoid of microtrichia. In some schizophorans the foraminal ring is vertically elongate and may form a dorsal and a ventral projection, each termed a **foraminal cusp** (Figs 95, 101). Outside of this ring there is an often more prominent **annular ridge** (Figs 1, 24, 29, 95). The latter is often armed with spinules, complex denticles, or simple microtrichia. In *Periscelis*, *Neurochaeta* and some diverse other genera there is on each side of the foraminal ring a stout, rounded, and usually nodulose vertical ridge, which I term a **caestus** (Figs 95, 101, 113). The paired caesti are surrounded by the innermost whorl of spinescent microtrichia on the annular ridge. In many taxa of Cyclorrhapha part of the distal articular surface rises into a bulky or elongate projection termed the **conus** (articulatory peg of Colless, 1994). The conus, which can only be examined adequately after separation of segment 3, bears the foramen of articulation on its distal, lateral, or dorsal surface. The surface of the conus is usually roughened by the presence of numerous hair-like or spinescent microtrichia, denticles, simple or denticulate ridges, or overlapping plates. In some taxa of Schizophora the partly reduced conus is prominent only on the medial side or only on the ventral side of the foramen of articulation, but in these taxa there is no prominence on its outer or lateral side (except sometimes for a slight development of the annular ridge). In some schizophorans the conus is produced into a broad, rounded prominence below the annular ridge, termed the **chin** (Fig. 63). In several acalyptrate families the general region of the conus has become secondarily flattened and almost symmetrical and the region of the annular ridge is sunk into a rounded cavity, termed the **pedicellar cup** when sharply differentiated from the rest of the distal articular surface (Figs 99, 112, 151). A further development of the conus is that described below for the Chloropidae and repeated in at least some taxa of Pyrgotidae. In these forms and some others the conus appears to be moveable in relation to the rest of segment 2, and in extreme forms may resemble an additional segment interposed between segments 2 and 3 (see Figs 63, 66, 67, 134–136).

The **pedicellar button** is a term recently introduced (D. McAlpine, 2008) for a somewhat button-like modification of the cuticle on the distal articular surface of the second antennal segment or pedicel in a majority of families of Diptera. This structure, hereafter referred to simply as the "button", has been generally overlooked by dipterists. There are several apparent reasons for this oversight: it is too small and too slightly prominent to be noticeable in most studies using SLM, and, when slide mounts are examined with higher magnification under CLM the line of view is often almost parallel to the button-bearing surface; the button-bearing surface is normally concealed between segments 2 and 3 until these are artificially separated, and even then the complex articular surface makes detection difficult in some taxa (e.g., in *Musca* spp., *Neurochaeta* spp., *Drosophila* [or *Sophophora*] spp.). For these reasons I have used the SEM on disarticulated antennae in order to locate the button in various dipterous taxa.

The button consists of an almost smooth, bare area, usually in a microtrichose field, and has a central dome or convexity, which is almost circular or tear-drop shaped, and a peripheral ring which is usually also slightly convex (typical examples of button shown in Figs 1, 9, 10, 14, etc.). Although

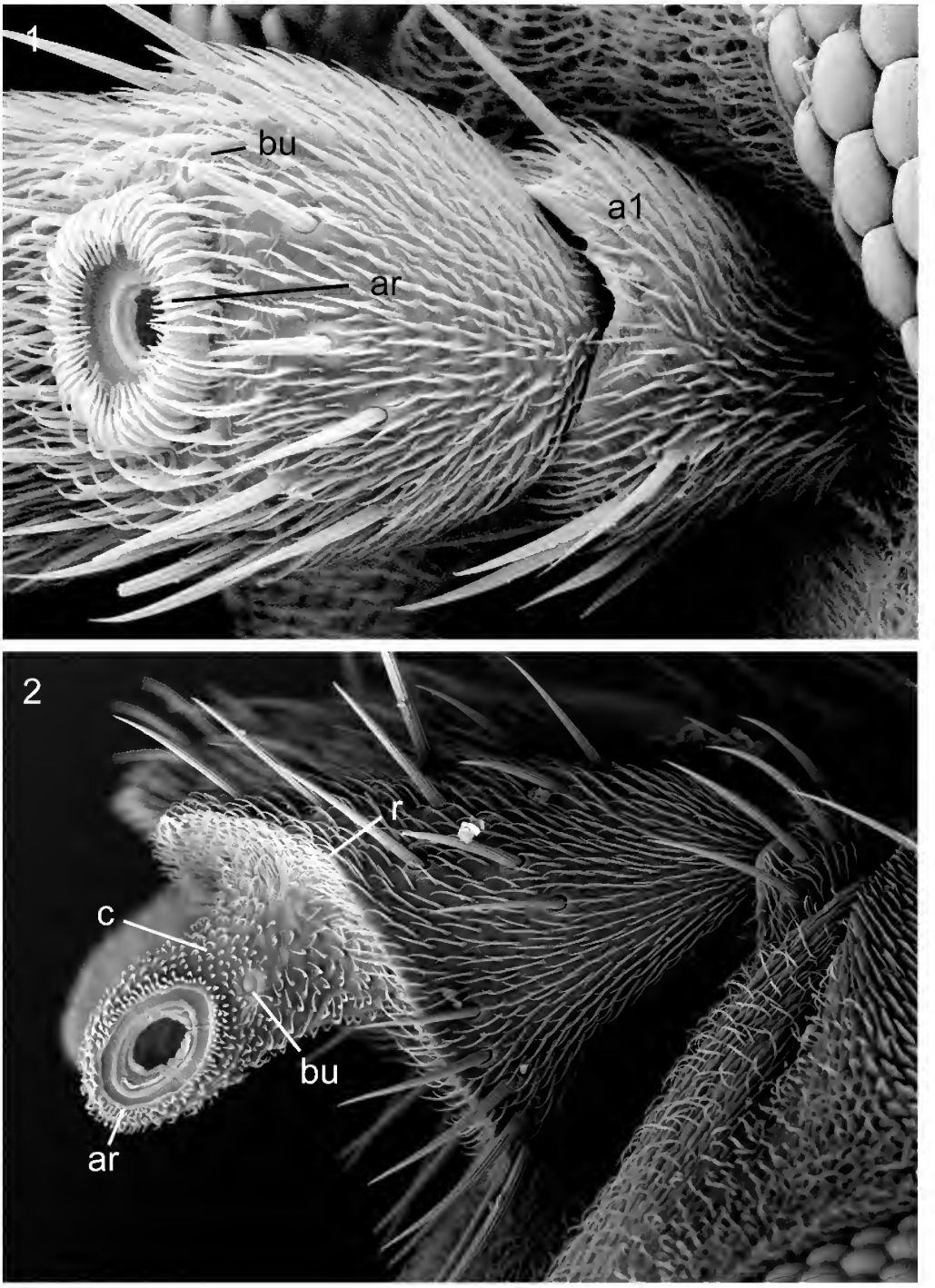

Figures 1, 2. Segments 1 and 2 (scape and pedicel) of left antenna, after removal of seg. 3, lateral view, of two cyclorrhaphans of different grade. *(1) Opetia nigra* Meigen (fam. Opetiidae). *(2) Huttonina abrupta* Tonnoir & Malloch (fam. Huttoninidae). *a1*, antennal seg. 1; *ar,* annular ridge (surrounding distal articular foramen); *bu*, pedicellar button; *c*, conus (absent in *Opetia*); *r*, rim (absent in *Opetia*).

the central dome is separated from the peripheral ring by an encircling groove, in no case have I been able to detect any slit or aperture associated with the groove, which could lead to a subcuticular cavity. Measurements for greatest diameter of the central dome made over a wide range of dipterous families give a range of c. 2.1 μm (Neurochaetidae) to 8.8 μm (Asilidae). Because the limits of the peripheral ring are often less defined, meaningful measurements of it were not obtained.

In these external features the button conforms to at least some cases of a campaniform sensillum, a sensory structure occurring widely on insect cuticle (Imms *et al.*, 1957; Chapman, 1971; McIver, 1975) and apparently of variable internal structure and function. The button differs from the sensillum placodeum (placoid sensillum) found in the antenna of certain Trichoptera and Lepidoptera (Faucheux, 2004a; 2004b) in the smooth, non-porous surface of the central dome.

The button is, so far as known, the external, supporting component of a special chordotonal sense organ (see Heymons, 1943: 107) which is distinct from the larger Johnston's organ, also contained in segment 2 of the dipterous antenna, and which encircles the central antennal nerve. According to Imms *et al.* (1957: 88), chordotonal sensilla "are stimulated by tension and are used for various purposes, including proprioception, the perception of internal pressure changes, mechanical vibrations, and sound. They have been reported for most orders of insects and occur on various parts of the body… "

The button surface is generally concealed by overlapping structures and often also deeply recessed in a cavity, though not sealed off from the atmosphere. This degree of protection from the exterior seems not to be appropriate for an auditory organ, a role probably fulfilled in most dipterans by vibration of the flagellum in connection with Johnston's organ, nor with detection of substrate vibrations. But such conditions are in accord with the possibility that the organ can detect either internal pressure changes or changes in atmospheric pressure.

Wellington (1946) recorded reactions of muscoid (or calyptrate) flies to sudden changes in atmospheric pressure produced by a controlled wave of the hand (visual stimuli being excluded), and demonstrated that reception was dependent on the arista. However, he also noted behaviour under differing static levels of air pressure, and stated: "While it is evident that the aristae function as external baroreceptors, it is equally evident that the transmission of the stimulus to the brain is intimately linked with some apparatus present in the pedicels of the antennae. Exposure of the conjunctival plates of these second segments [i.e. of the button-bearing distal articular surfaces] results in partial retention of pressure sensitivity, while the removal of the pedicels or their coverage with collodion results in the loss of wave sensitivity;" —also in general pressure sensitivity in his second (II) set of experiments.

Wellington (1946: 113) inclined to attribute this latter sensory stimulus to Johnston's organ in segment 2, but the various investigations of that organ seem to show that it forms a larger separate body whose chordotonal elements are directly connected to the base of the flagellum via the intersegmental foramen, not to the button-bearing surface (see Heymons, 1943, in particular).

Pending further experimental tests, I propose the hypothesis that the button-connected chordotonal organ is likely to be the pedicellar baroreceptor inferred but not seen by Wellington. Wellington's further discussion (1946: 114–117) gives some indications of the importance of baroreception in dipterous biology.

The tendency for the button to be recessed or protected may be due to the fact that, when its cuticle is perforated by abrasion, no difference is maintained between external and internal pressure, and the baroreceptor becomes inoperative. It is possible that the dorsal cleft or seam of segment 2 in the Ephydroidea, Muscoidea, etc. ensures that, in at least some taxa, complete separation of the button from the atmosphere does not take place, while extensive abrasion of the segment (as in Fig. 87) is unlikely to reach the button.

I am uncertain if a typical pedicellar button occurs on the antenna of any non-dipterous insect. In *Nannochorista dipteroides* Tillyard (order Mecoptera or Nannomecoptera) the pedicel bears some button-like structures (Figs 3–5) but these appear to have a lateral or annular opening leading to an internal cavity, and this apparent difference suggests a difference in function in the nannochoristid structure. Somewhat button-like surface features on the pedicel of *Panorpa* sp. and *Chorista* sp. (order Mecoptera) need detailed investigation.

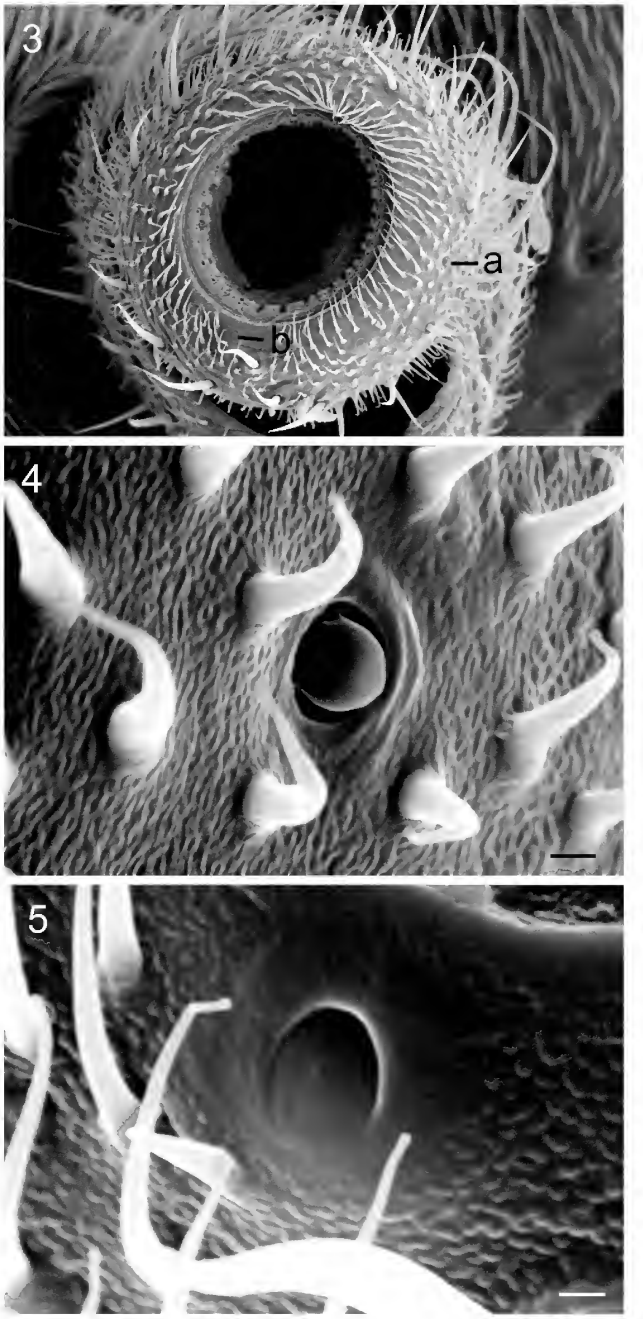

Figures 3–5. *Nannochorista dipteroides* Tillyard (fam. Nannochoristidae), antenna. *(3)* Distal view of seg. 2, after removal of seg. 3, showing positions of sensory structures. *(4, 5)* Detail of sensory structures at positions a, b in Fig. 3; scale = 1 μm.

According to Grimaldi & Engel (2005) four extant infraorders of Diptera (or suborders in the modern sense) were present in the late Triassic (at least 210 MYA), and it is clear that the dipterous button must have existed at this time level. Further data are discussed below under Grade Nematocera.

There is some disagreement in available literature on terminology of antennal sense organs. Soenen (1940: 20) stated that he could confirm the absence of the pedicellar chordotonal organ in the rhagionid and chloropid flies which he studied, thus excluding both Johnston's organ and the outer button-connected organ from this category. Wigglesworth (1950: 164–166) appeared to regard Johnston's organ as a special type of chordotonal organ, as did Chapman (1991: 44–45). Soenen (1940: fig. 2) apparently identified the button-connected sensillum in his rhagionid fly as "organe de Hicks", but this is not the antennal structure (on segment 3) described by Hicks (1857). Wigglesworth (1950: 162, 170) and others have referred to "Hicks' papillae" on the halteres of Diptera, a term arising from other studies by Hicks.

It should be noted that the "antennal pulsating organ" of nematocerous dipterans (Clements, 1956) is in the head capsule, not in the antenna, and is termed the "tambour organ" by Day (1955).

Those segments of the insect antenna distal to segment 2 are collectively termed the **flagellum**, and in their more primitive state (as in the dipterous grade Nematocera) they are little differentiated from one another. However the usual four flagellar segments of cyclorrhaphous flies are strongly differentiated structurally, so that the collective term is less appropriate. While segment 3 is often called the first flagellomere, the term flagellomere or flagellar segment is not generally applied to the succeeding segments, which are taken as constituting the **arista** or **stylus**. The view that the flagellum consists of a single segment, the dipterous antenna thus consisting of only three segments, is expressed by J. McAlpine (1981) and a few other entomologists. However, comparative study reveals no likely three-segmented stage in the ancestral line of the Hexapoda and that of the Insecta (though the intersegmental or intrinsic musculature has been lost in the insect flagellum, it is retained in such basal hexapod groups as the Diplura and Collembola). Treatment of the flagellomeres as segments remains the standard practice in the majority of insect orders, and it does not seem reasonable to designate those concerned as misled. For these reasons, I do not follow J. McAlpine's system.

Segment 3 (postpedicel, funiculus, first flagellomere) is often the bulkiest antennal segment in the Eremoneura (including the Cyclorrhapha). In those cyclorrhaphans which have a substantial conus, this is inserted into the corresponding **basal hollow** of segment 3. Such basal hollow typically contains the articular foramen connecting segment 3 with the conus of segment 2 (Figs 36, 47). Alternatively, in those schizophoran taxa with reduced conus and the distal articular foramen of segment 2 sunk into a concavity of that segment (e.g., *Neurochaeta*, *Psila*, *Cyamops*, *Hydrellia*, *Drosophila*), segment 3 is narrowed into a **basal stem** contained within that cavity. This basal stem (proximale Lappenfortsatz of Hennig, 1971, but unfortunately termed the conus by Grimaldi, 1990, misinterpreting Disney, 1988) is formed by extension of the ventrobasal convexity of segment 3 into a narrow process and migration of the basal foramen on to the process not far from its basal end. This development results in modification of the shape of segment 3 (compare Figs 93, 91). In such forms segment 3 may be considered as divided into the narrow basal stem and the broad **disc**, which constitutes the greater part of the segment, but numerous intermediate states occur. Often, in these taxa lacking a well-developed conus, segment 3 has the basal hollow much reduced or represented by the **sub-basal caecum** opening on the medial side of the basal stem (Fig. 91). A narrow band of thickened, rough-surfaced cuticle often runs from the medial surface of the basal stem into the extremity of the sub-basal caecum (e.g., Fig. 96). This roughened tract is termed the **scabrous tongue**.

I have seen evidence that the basal stem may be flexible in relation to the disc of segment 3. The cuticle near the junction of the basal stem with the disc is often modified by the presence of transverse ridging with softer interstices (e.g., Fig. 83), and this structure probably confers a limited flexibility.

A feature of segment 3 in most eumuscomorphans is the presence of one or few **sacculi** (Lowne, 1895; Shanbhag *et al.*, 1995; D. McAlpine, 2008). A sacculus is a deep, sac-like invagination of the cuticle of segment 3 containing several trichoid sensilla and opening to the exterior by a relatively small pore, most often on the exposed lateral surface. This structure is distinct from the often numerous simple pits in the cuticle, each of which may be associated with a single sensillum, or various saucer-like pits which sometimes contain one or more trichoid sensilla. Smith (1919) has given information on the various sensory pits on antennal segment 3 in various families of Diptera. Where both simple sensory pits and a true sacculus occur together, as in *Musca* (see Smith, 1919: text-fig. 38) and *Cryptochetum* (see below) the two structures are usually very distinct. Stocker (2001) has investigated the distribution of olfactory sensilla on segment 3 of *Drosophila*. Hu *et al.* (2010) characterizedthe sensilla of segment 3 in certain species of Tephritidae and provided references to much earlier work.

My recent studies (following D. McAlpine, 2008) indicate the possibility that, among the Eremoneura, segment 3 has true sacculi only in the Ironomyiidae (see below) and the Eumuscomorpha (i.e. Syrphidae, Pipunculidae, and Schizophora). In *Hormopeza* (Orthogenya or Empidoidea) and *Microsania* (Cyclorrhapha, Platypezidae), segment 3 has two well-developed sac-like cavities, which I term **postpedicellar pouches**. Though these are suggestive of eumuscomorphan sacculi, they differ in their simple lining and complete lack of trichoid sensilla (author's studies with CLM). Each of these genera seems to be phylogenetically remote from any other known taxon with similar pouches on segment 3, and I am convinced that these structures have evolved independently in each genus. I also use the term postpedicellar pouch below for somewhat similar structures in certain taxa of Conopidae and Muscidae.

Further information on sacculi is given below under the taxonomic headings (particularly for Ironomyiidae).

Segments 4 to 6 of the cyclorrhaphous antenna constitute the arista or stylus. I have given an account of variation in segmentation of the arista and noted among cyclorrhaphous taxa 29 separate derivations of reduction from the plesiomorphic three-segmented condition (D. McAlpine, 2002). I have now observed some additional cases of segment reduction in the Curtonotidae, Natalimyzidae, Platystomatidae, and Pyrgotidae as noted below, and Buck (2006) has recorded a case for the Inbiomyiidae.

In the Apystomyiidae the basal segment of the stylus has on its terminal surface a capsule-like structure, here termed the **stylar goblet**. See under that family and Fig. 177.

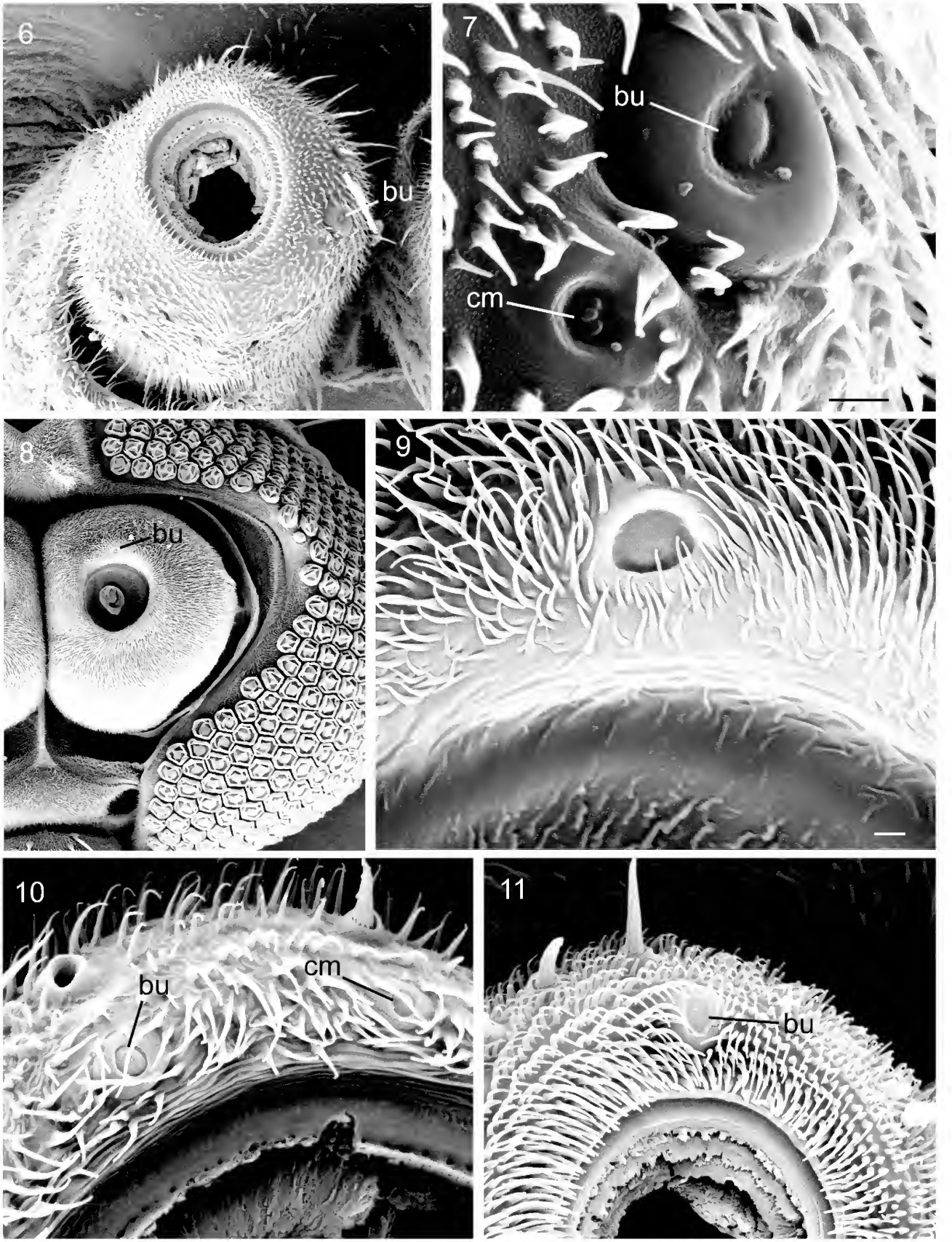

Figures 6–11. Details of antennal seg. 2 in nematocerous dipterans. *(6) Ptychoptera capensis* Alexander (fam. Ptychopteridae), right segs. 1 and 2, distal view. *(7)* The same, sensory structures; scale = 3 µm. *(8) Chironomus* (s.l.) sp. (fam. Chironomidae), left side of head after removal of flagellum. *(9)* The same, part of distal articular surface showing pedicellar button; scale = 2 µm. *(10) Macrocera* sp. (fam. Keroplatidae), part of distal articular surface (left antenna) showing button and possible campaniform sensillum. *(11) Sciara* sp. (fam. Sciaridae), part of distal articular surface (left antenna) showing button. *bu*, pedicellar button; *cm*, campaniform sensillum (?).

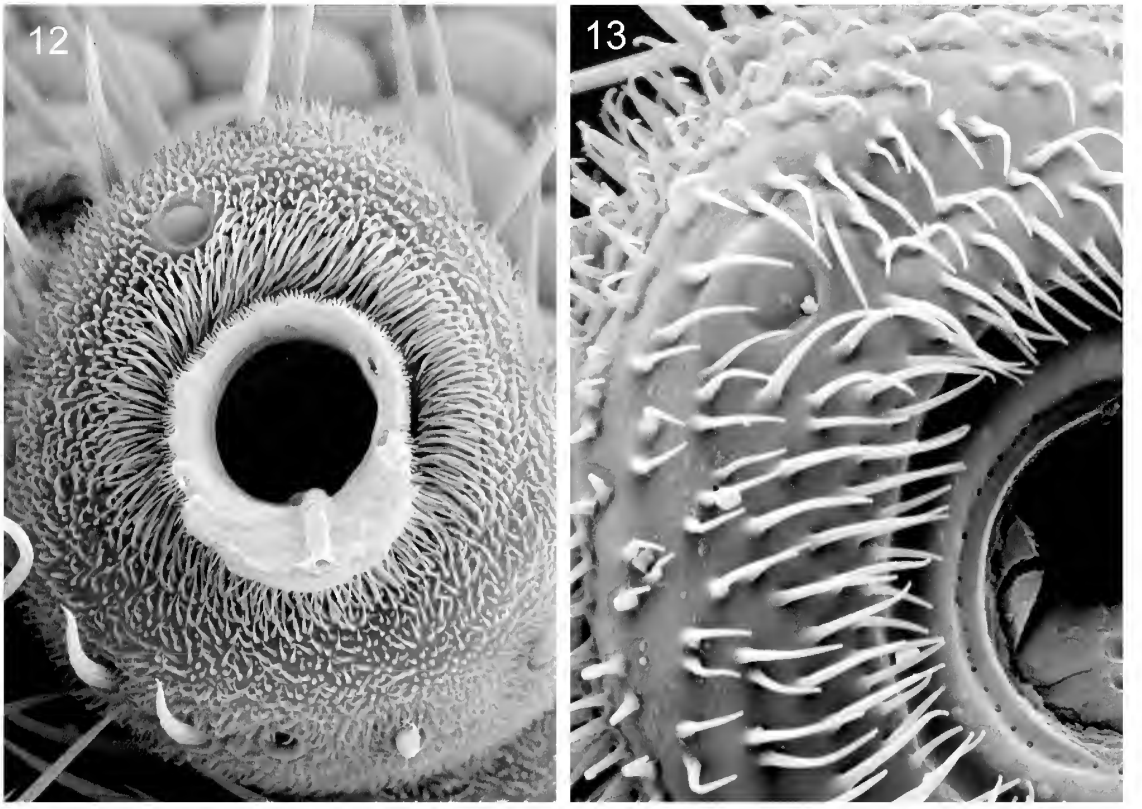

Figures 12–13. Details of antennal seg. 2 in nematocerous dipterans. *(12) Sylvicola* sp. (fam. Anisopodidae), distal view (left antenna), showing button. *(13) Limonia marina* (Skuse) (fam. Tipulidae s.l.), part of distal articular surface (left antenna), showing button.

The grade Nematocera

The non-brachyceran families of Diptera have not been a main focus in this study. General information on the antenna has been given in numerous publications (e.g., Crampton, 1942; Hennig, 1973), and information on Johnston's organ within the pedicel by Eggers (1923), Soenen (1940), and others, who acknowledged that this organ was evidently present in a very early ancestral insect.

The occurrence and position of the pedicellar button within this grade has not been recorded, and I have made a preliminary survey only of this subject. My observations using SEM on the distal surface of segment 2 shows the button to be present in at least some taxa of the following families: Anisopodidae, Bibionidae, Chironomidae, Dixidae, Keroplatidae, Mycetophilidae (s.str.), Psychodidae, Ptychopteridae, Sciaridae, Tipulidae (s.l.), Trichoceridae (see Figs 6–18). In *Ptychoptera capensis* Alexander (Fig. 7) there are two somewhat button-like structures on segment 2, but probably only one is homologous and functionally equivalent to the typical button. The position of the button in these families varies from medial to dorsal in relation to the distal foramen of the segment.

In examples of several nematocerous families (e.g., the Culicidae) I have failed to demonstrate the presence of a pedicellar button. It is probable that in some of these taxa the button is really absent, but it is also possible that the position or nature of the button has sometimes made it difficult to detect using standard SEM methodology. Rather than listing such taxa at present, I leave detailed interpretations open for future research.

The taxonomic diversity of the above-listed families, for which the presence of the pedicellar button is confirmed, demonstrates its presence within a wide range of nematocerous groupings, whether one uses the cladogram of Oosterbroek & Courtney (1995: fig. 9) or the rather different version of Grimaldi & Engel (2005: fig. 12.25). On the reasonable assumption that the button has not originated more than once in the Diptera, the question arises whether it was present in the groundplan of the order. Of the seven "nematocerous" suborders in the revised classification by Amorim & Yeates (2006), I have found the pedicellar button to occur in five, viz. Tipulomorpha, Psychomorpha (or Psychodomorpha), Ptychopteromorpha, Culicomorpha, and Bibionomorpha. This leaves only the suborders Blephariceromorpha and Axymyiomorpha in which the button has not yet been observed, but the latter is included in the Bibionomorpha by Oosterbroek & Courtney (1995) and Grimaldi & Engel (2005). If the hypothesis of Oosterbroek & Courtney, that the Ptychopteromorpha + Culicomorpha form a monophyletic sister-group to all other Diptera, be confirmed, then presence of the button in the dipterous groundplan would be inferred. Alternatively, under the new system of Wiegmann *et al.* (2011: fig. 1), presence of the button is inferred for the deduced clade that includes all extant dipterous families except the Deuterophlebiidae and Nymphomyiidae (for which antennal microstructure is unrecorded).

The lower brachycerans

I use this designation to include those taxa of the suborder Brachycera other than the Eremoneura (= Orthogenya,

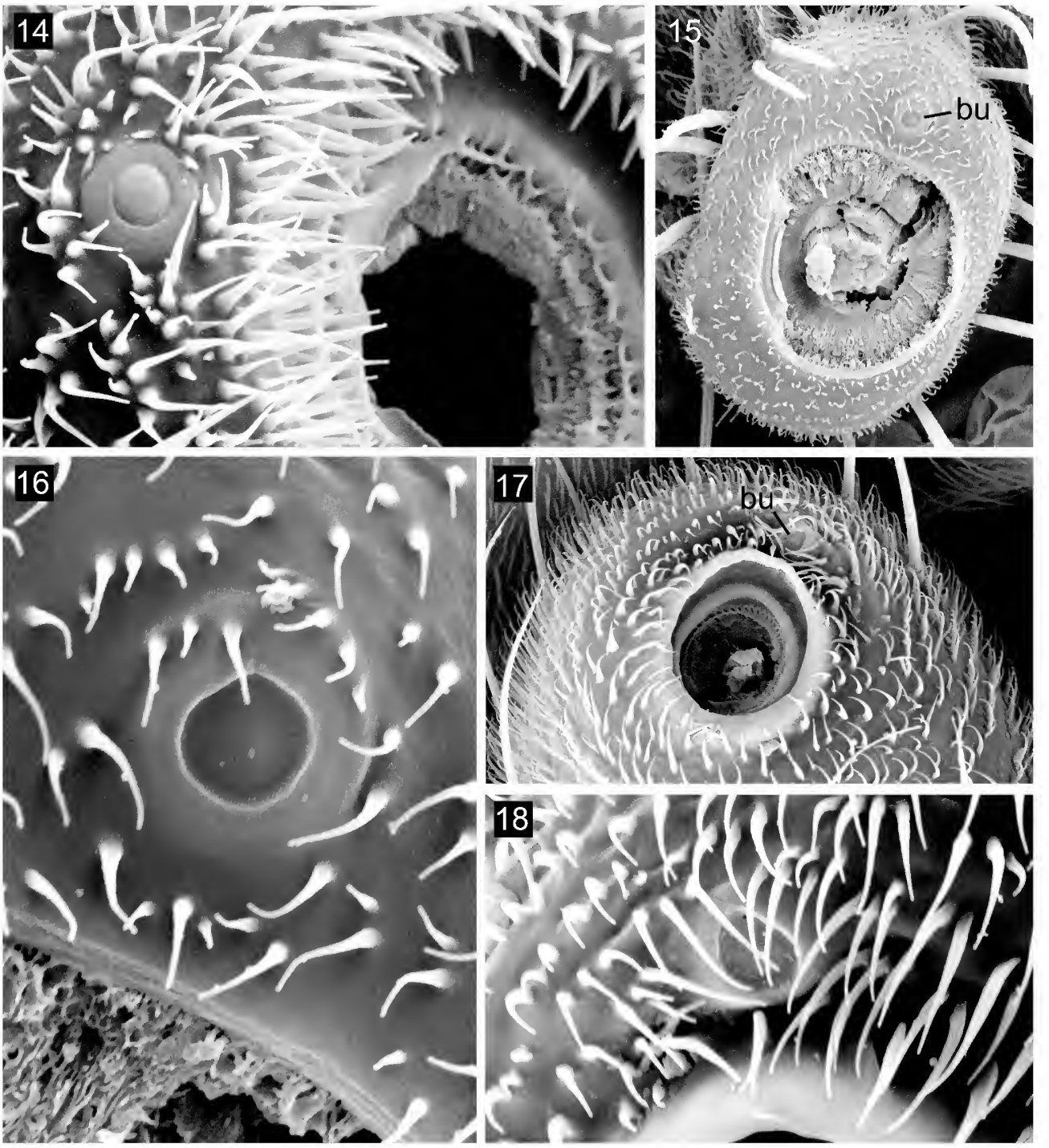

Figures 14–18. Details of antennal seg. 2 in nematocerous dipterans. *(14) Plecia dimidiata* Macquart (fam. Bibionidae), part of distal articular surface (left antenna), showing button. *(15) Nemapalpus capensis* Edwards (fam. Psychodidae), seg. 2, distal view (left antenna). *(16)* The same, detail of part of distal articular surface, showing button. *(17) Dixella* sp. (fam. Dixidae), seg. 2, distal view (left antenna). *(18)* The same, detail of button (right antenna). *bu*, pedicellar button.

Cyclorrhapha, and their possible immediate outgroups Chimeromyiidae and Apystomyiidae). These taxa are not usually considered to constitute a clade and are therefore without a formal group name.

Variation in antennal segmentation and external form has been covered in much taxonomic literature. Excellent descriptions and illustrations of antennae of many families can be found in such works as J. McAlpine *et al.* (editors 1981: chapters 30–46), but, as usual, details of the articular surfaces are omitted. I am concerned with only a few points here.

Segment 2 of lower brachycerans is most frequently almost radially symmetrical, with terminal surface somewhat convex and commonly lacking an angular or flange-like rim encircling the distal articular surface (Figs 19, 21). Sometimes a distinct distal rim is present, in which case the distal articular surface is flat or concave. The distal articular surface bears a usually well-developed pedicellar button located almost mid dorsally to laterally in relation to the distal foramen. This is a derived condition relative to the more medially located button generally seen in taxa of nematoceran grade. The distal

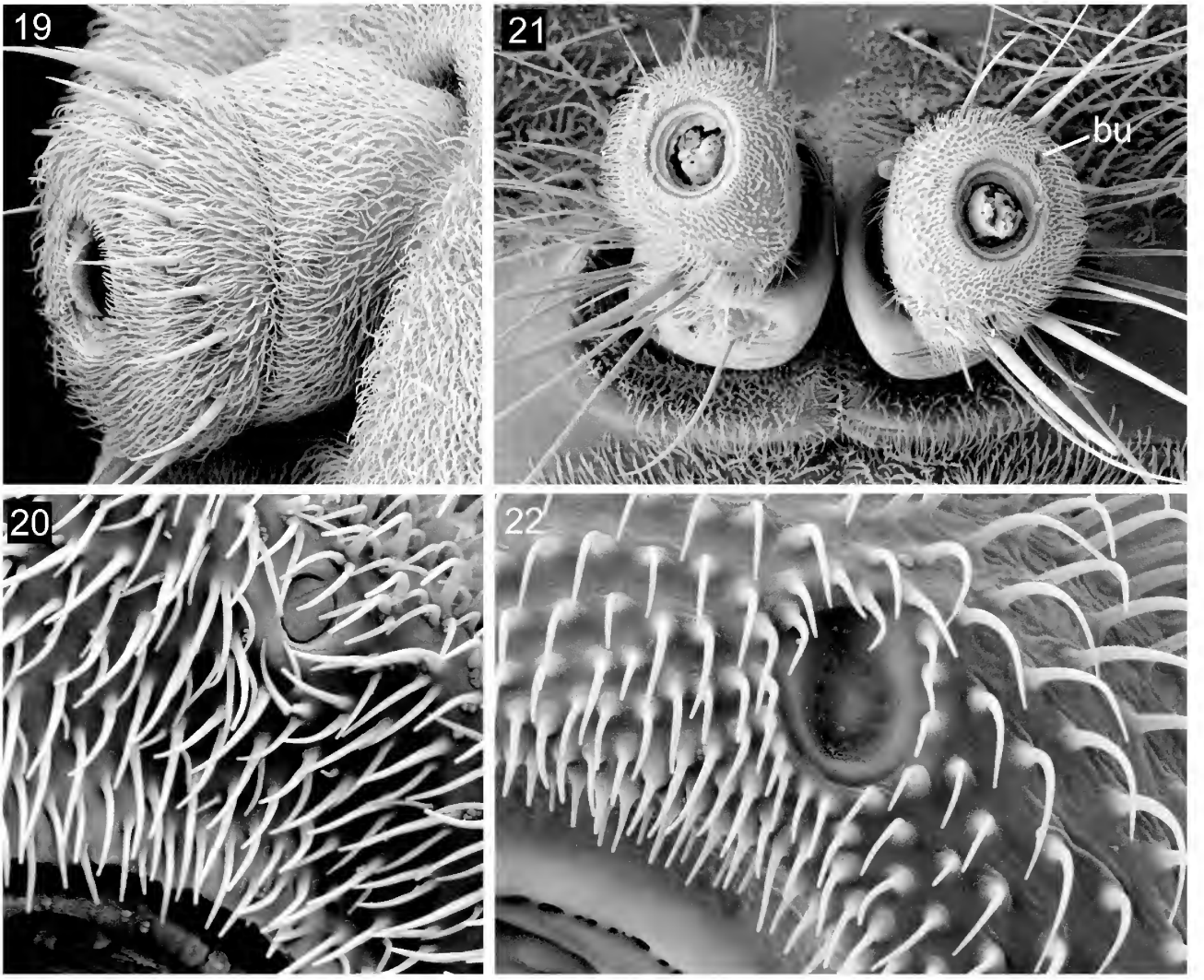

Figures 19–22. Details of antennal structure in lower brachycerans. *(19) Spaniopsis clelandi* Ferguson (fam. Rhagionidae), left antennal segs. 1 and 2, after removal of seg. 3, lateral view. *(20)* The same, detail of distal articular surface, showing button. *(21) Daptolestes* sp. (fam. Asilidae), distal view of antennae after removal of segs. 3, showing button. *(22)* The same, part of distal articular surface (left antenna) including button. *bu*, pedicellar button.

articular surface generally lacks any prominence comparable with the conus of more advanced cyclorrhaphans. The distal foraminal ring is often slightly recessed to receive the narrowed basal prominence of segment 3. Figs 1, 19, 21, 25 show slight variation in this probably plesiomorphic condition for segment 2 of the Brachycera, including some more basal taxa of the Eremoneura.

In the Stratiomyidae the more basal segments of the flagellum often form a compact unit or may even be fused into an apparent single stoutly rounded segment. These often bear numerous sense organs, sometimes but not always compactly grouped in shallow pits. This subject is touched on by Smith (1919). Schlinger (1981) recorded such a sensory pit, somewhat resembling a shallow sacculus, on segment 3 of some taxa of the family Acroceridae.

The Eremoneura

Since the work of Griffiths (1972) and Hennig (1976) the monophyly of the group Cyclorrhapha + Orthogenya (or Empidoidea) has gradually achieved general acceptance as the clade Eremoneura. More recently, Grimaldi *et al.* (2009) have added the Cretaceous family Chimeromyiidae to the Eremoneura, but its more precise relationships within this division are undecided. Hennig (1976: 54–56, figs 58–62) described the structural relations between antennal segments 2 and 3 in some lower eremoneurans. The plesiomorphic conditions for Eremoneura, present in what appear to be the most basal examples of Orthogenya and Cyclorrhapha, are described below. My understanding of the main evolutionary stages leading from such basal eremoneuran antennal structure to that of the Eumuscomorpha is shown in Fig. 23.

My studies suggest that the pedicellar conus and prominent rim are absent in the groundplan of both the Orthogenya (see Sinclair & Cumming, 2006) and the Cyclorrhapha, and that they have evolved independently in each of these groups. Thus the general nature of the articulation between segments 2 and 3 found in the Opetiidae and Platypezidae probably resembles the groundplan condition for the Eremoneura (compare my Figs 1, 26 with 24, 25).

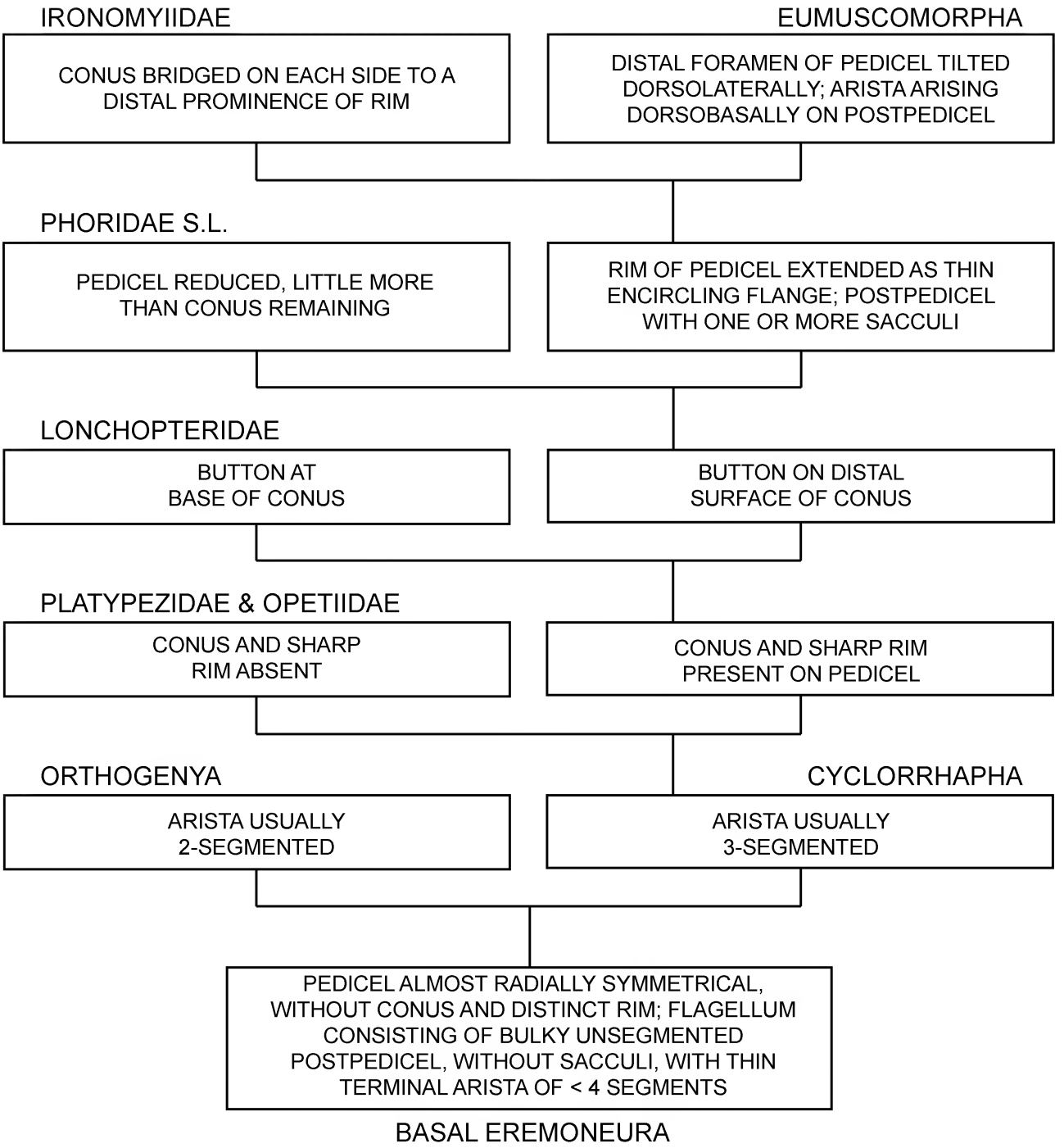

Figure 23. Gradogram, showing possible history of some antennal structures in the Eremoneura. The diagram is intended to show grades as much as clades, and shows the probable basal condition for each broad grouping or taxon, particularly if this condition is a probable apomorphy (polarity of some characters doubtful). As character reversals and convergences occur in numerous taxa, it is not an identification aid.

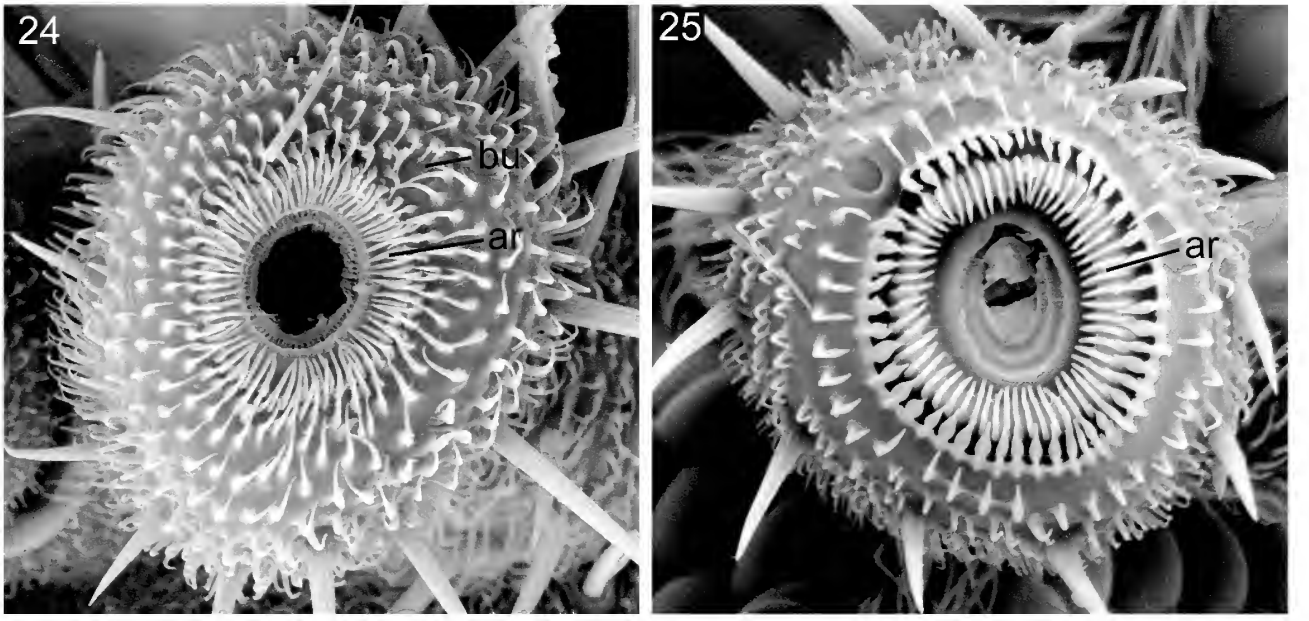

Figures 24, 25. Antennal seg. 2 of Orthogenya, seg. 3 removed. *(24) Empis* sp. (Empididae, Empidinae), distal view of left antenna. *(25) Leptopeza* sp. (Hybotidae, Ocydromiinae), distal view of right antenna. *ar*, annular ridge; *bu*, pedicellar button.

The Chimeromyiidae

The family Chimeromyiidae was established by Grimaldi *et al.* (2009) for the Early Cretaceous genera *Chimeromyia* and *Chimeromyina*. My information on the family is only that provided by these authors.

At least some taxa of Chimeromyiidae have a bulky conus inserted into antennal segment 3 (see figs 7A and 13B in Grimaldi *et al.*, 2009). The pedicel of *Chimeromyia burmitica* Grimaldi & Cumming is described as "cup-shaped" and the basal flagellomere (postpedicel) is described as "possibly with inserted condyle on mesal surface," presumably referring to a conus arising from the concave distal articular surface of the pedicel. The three-segmented arista may be clearly terminal to dorsal and sub-basal on segment 3 in the various chimeromyiid taxa.

To what degree the presence of a conus in the Chimeromyiidae affects the above hypothesis as to the groundplan state of the eremoneuran pedicel is at present hard to determine, and has not been considered in the design of Fig. 23. The three-segmented condition of the chimeromyiid arista suggested to Grimaldi *et al.* that this is possibly the plesiomorphic state for the Eremoneura.

The Orthogenya (Empidoidea)

If two taxa are sister groups, they should have the same rank, as recognized by Hennig (1973, and elsewhere). As this taxon is widely accepted as the monophyletic sister-group to the Cyclorrhapha (which includes numerous superfamilies), I use the name Orthogenya (following Griffiths, 1972; Zatwarnicki, 1996), instead of the superfamily name Empidoidea; it takes priority over the names Empidiformia and Empidiformae sometimes used by dipterists; see Sabrosky (1999) for publication details.

The antennal structure in the apparently primitive forms is essentially similar to that of such basal cyclorrhaphans as Platypezidae, but there are also examples of more complex antennal types within the group (see Chvala, 1983, and Sinclair & Cumming, 2006, for numerous examples). I am here mainly concerned with the plesiomorphic conditions for the group, which are likely to approach those for the Eremoneura as a whole.

In its simplest form (e.g., Figs 24, 25) segment 2 is moderately compact and maintains an approach to radial symmetry as in many lower brachycerans. The distal profile is rounded, there being neither an encircling rim nor a conus. The pedicellar button is generally present on the distal articular surface, dorsolaterally or laterally to the distal articular foramen. Segment 3 may bear the terminal section of the antenna (arista or stylus) terminally or dorsolaterally, but is not known to have a typical sacculus in any species (see below for comment on *Hormopeza*). The arista is usually two-segmented.

The Apystomyiidae

The Nearctic genus *Apystomyia*, originally placed in the Bombyliidae, was elevated to a separate monotypic family, Apystomyiidae, in the Asiloidea by Nagatomi & Liu (1994). The placement of Apystomyiidae alone as the sister-group to the Cyclorrhapha by Trautwein *et al.* (2010) and Wiegmann *et al.* (2011) has brought this taxon into prominence. Shaun Winterton has generously supplied me with specimens of *A. elinguis* Melander for antennal study from the type locality, Sheep Creek Canyon, Bernadino Co., California.

Nagatomi & Liu (1994) gave a general account of the morphology of *Apystomyia*, including the gross features of the antenna. As in many of the less advanced brachycerans, the general form of the antenna approximates to radial symmetry, except for the bilateral compression of segment 3.

Segment 1 is small, collar-like, with many microtrichia, not evenly distributed, and few dorsal setulae.

Segment 2 (Fig. 174) is considerably larger than segment 1, rotund, slightly bilaterally compressed, slightly higher

than long, without trace of a rim or conus, with the usual covering of microtrichia and a small but variable number of large dorsal and ventral bristles, not forming an encircling series. The annular ridge is scarcely raised above the distal surface of the segment, but bears numerous moderately short, inwardly directed microtrichia. The foraminal ring is slightly raised and finely crenulated. There are two dorsal to dorsolateral buttons (in both sexes) with their peripheral convex rings in contact or partly fused (Fig. 175).

Segment 3 (Fig. 176) is ovoid, slightly bilaterally compressed, with small basal stem fitting into the annular ridge of segment 2. The surface is rugose, more coarsely and irregularly so distally, with many small microtrichia and larger projections, probably trichoid sensilla, but typical macrotrichia are absent. There are no sensory pits, nor anything resembling the sacculi or pedicellar pouches which are present in various cyclorrhaphans.

The slender distal part of the antenna, here termed stylus (though with some doubt regarding its homology with the eremoneuran stylus or arista), arises terminally and symmetrically on segment 3. It consists of two sections (? segments). The more basal section is subcylindrical with its surface broken by many deep grooves into a series of transverse microtrichose plates or sclerites. The terminal surface of the basal section has, ventrally to the base of the terminal section, the structure here termed the stylar goblet (Fig. 177, *go*). The goblet consists in both sexes of a smooth hemispherical cuticular prominence of c. 4.1 μm diameter, with, at its summit, a subcircular aperture of c. 2.1 μm diameter. The aperture clearly leads into a capacious cavity, but further details are not visible because of the condition of the specimens and the minute size of the goblet. On further examination it may be possible to identify the goblet with a particular category of arthropod sense organ. The smaller terminal section of the stylus is articulated with the basal section and has a smooth outer surface (surface contaminated as seen in Fig. 177). Examination with CLM shows it to be hollow, with the inner surface of its cuticle densely micropustulose.

The Apystomyiidae are not morphologically typical of the Cyclorrhapha, because the male postabdomen has a full complement of symmetrical tergites and sternites (which suggests that there is no circumversion of the genital segment), and abdominal plaques can be detected under SEM (which suggests that there is no puparium). I am aware of no other brachyceran with two buttons on each pedicel, but the pedicellar distal articular surface has been examined for very few asiloid flies. I am not aware of any structure resembling the stylar goblet in any other family of Diptera, but this is perhaps due to its minute size and the lack of SEM study of most lower brachycerans. At present I regard the antennal morphology of *Apystomyia* as an ambiguous indicator of relationships, as it resembles that of some more reduced asiloid taxa as well as that of certain more or less basal eremoneurans. The articulation between antennal segments 2 and 3 is unlike that of the Chimeromyiidae and probably more plesiomorphic. If the Apystomyiidae constitute a plesiomorphic sister-group to the Cyclorrhapha, then this would seem to confirm the basal conditions for the eremoneuran antenna indicated in Fig. 23.

The Platypezidae and Opetiidae

I treat these two families together primarily because of similarity in antennal structure. The molecular study by Moulton & Wiegmann (2004) indicates that they probably together form a clade. See also Chandler (1998) and Collins & Wiegmann (2002a).

Segment 2 in platypezids is generally of primitive form for the Cyclorrhapha, but is variable in some significant characters. I believe that true platypezids, in common with Opetiidae, lack a conus, and that the attribution of a conus to *Plesioclythia* (now included in *Lindneromyia*) by Disney (1988: fig. 5) is due to a slightly prominent annular ridge only. Sometimes the distal articular surface is flattened (as in *Melanderomyia* and *Lindneromyia* sensu Chandler, 1994; see D. McAlpine, 2008: figs 5, 8) but the rim is either indistinct or only slightly angular. The annular ridge in these genera (also in *Agathomyia* and *Microsania*) defines an area of variable size near the centre of the articular surface, and is well marked by its prominent, coarse, incurved microtrichia. In *Opetia* the annular ridge is particularly incrassate, but the rim is quite absent (Fig. 1). In *Lindneromyia* the rest of the articular surface is covered with many short, inwardly inclined, tile-like ridges, each bearing a row of microtrichia. The button in the Platypezidae and Opetiidae is located on the dorsolateral part of the distal articular surface, as in most flies of orthorrhaphous grade.

Segment 3 of the Platypezidae and Opetiidae much resembles that of more plesiomorphic taxa of Orthogenya in that it usually tapers distally to the terminal arista and is probably always without true sacculi such as those present in most taxa of Eumuscomorpha. The smoke flies, *Microsania*, are perhaps unique among the platypezids in possessing two deep pit-like hollows, one dorsomedial and one ventral, on segment 3, the postpedicellar pouches (see Fig. 28). However, this condition is almost identical to that of the orthogenyan genus *Hormopeza*, which is also attracted to smoke by odour (Kessel, 1960; Sinclair & Cumming, 2006). The latter authors refer to these hollows as "sensory pits" in their text (2006: 73) and as "pit glands" on their figs 8 and 47. The taxonomic distribution of the pedicellar pouches renders it improbable that they are homologous structures in *Hormopeza* and *Microsania*, or that they can be homologous with the sensory sacculi in typical taxa of Eumuscomorpha. Also, the pouches in *Microsania* and *Hormopeza* do not contain trichoid sensilla, which characterize the sacculi of those eumuscomorphans in which they have been investigated. More detailed examination of ultramicroscopic structure is beyond the scope of the present work. In *Opetia* and some platypezids (e.g., *Microsania*, Fig. 28) segment 3 bears one or more relatively large socket-based bristles or macrotrichia. This is an unusual condition in the Eremoneura.

The arista of typical platypezids is three-segmented, but that of *Opetia* has fewer segments (Fig. 27), as recorded by Hennig (1976), Chandler (1998), and Sinclair & Cumming (2006). In view of the many independent examples of secondary reduction in aristal segmentation in Cyclorrhapha (D. McAlpine, 2002), I have suggested that the condition in *Opetia* may not be plesiomorphic or indicative of wide phylogenetic isolation of the taxon. The Cretaceous *Electrosania cretica* Grimaldi & Cumming, 1999, is also a platypezid-like fly with a two-segmented arista.

While the partial to complete fusion of abdominal tergites

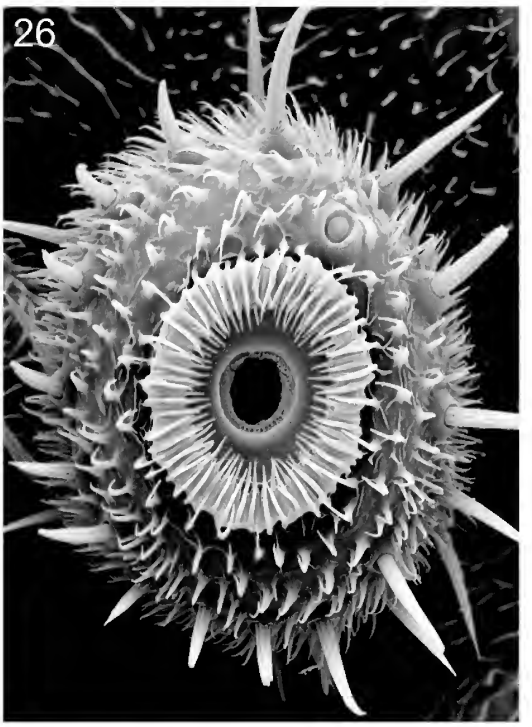

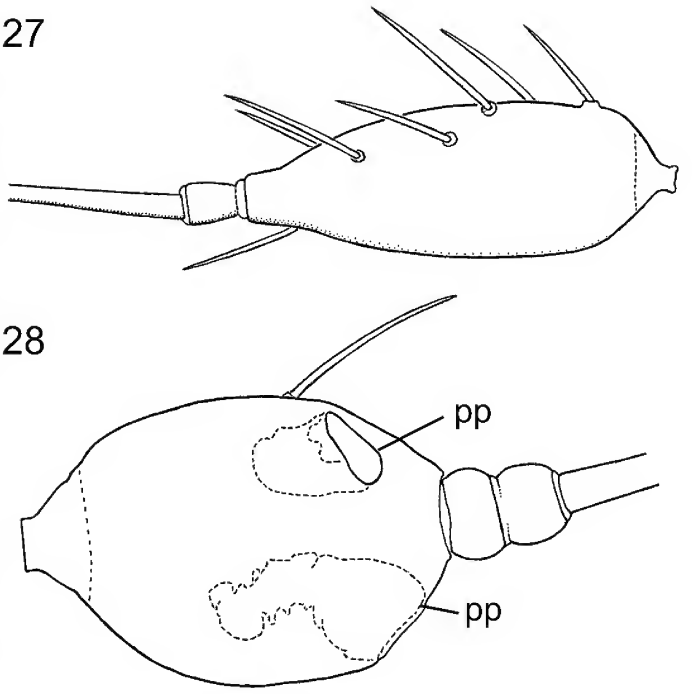

Figures 26–28. Antennal structure in some basal cyclorrhaphans. *(26) Opetia nigra* Meigen, male (fam. Opetiidae), left antennal seg. 2 after removal of seg. 3, distal view. *(27)* The same, left seg. 3 and arista, lateral view. *(28) Microsania arthuri* Chandler (fam. Platypezidae), left seg. 3 and arista, medial view. *pp*, postpedicellar pouches.

1 and 2 is usual among the Cyclorrhapha (generally quite free in Orthogenya, but also in Phoridae s.l.), *Opetia nigra* Meigen shows sexual dimorphism in this character. The male has tergites 1 and 2 fused so as to leave no intervening intersegmental membrane, but a line of demarcation is generally visible, taking the form of a slight groove in available specimens. This condition is essentially similar to that of both sexes of typical platypezids (e.g., *Lindneromyia* spp.). The female of *O. nigra* has tergites 1 and 2 completely separated by intersegmental membrane so that the posterior margin of tergite 1 is free to overlap broadly the anterior margin of tergite 2, and tergite 1 is shorter than in the male of the species. I have examined dried specimens and others cleared in lactic acid of both sexes of *O. nigra* for this character. The condition for the female can also be inferred from the illustration by Chandler (1998: fig. 2.12).

Cyclorrhaphans with a conus

The remaining families of Brachycera-Cyclorrhapha either have a distinct conus on segment 2 (see Hennig, 1976: 54–56) or are derived from forms possessing a conus with subsequent reduction (e.g., *Periscelis*, Fig. 100). Almost all these taxa also have an angular or flange-like, more or less encircling pedicellar rim.

The lower cyclorrhaphous families Lonchopteridae,

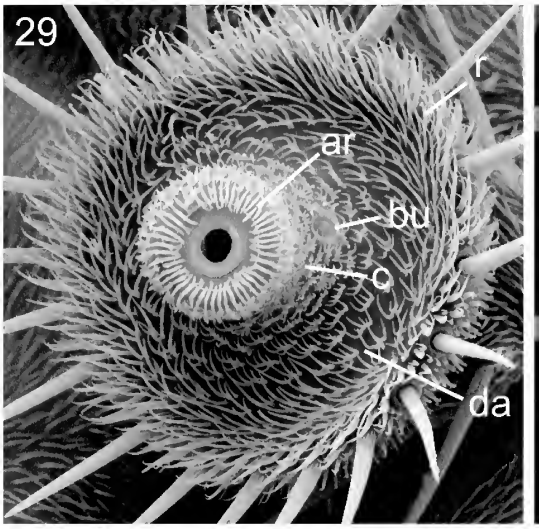

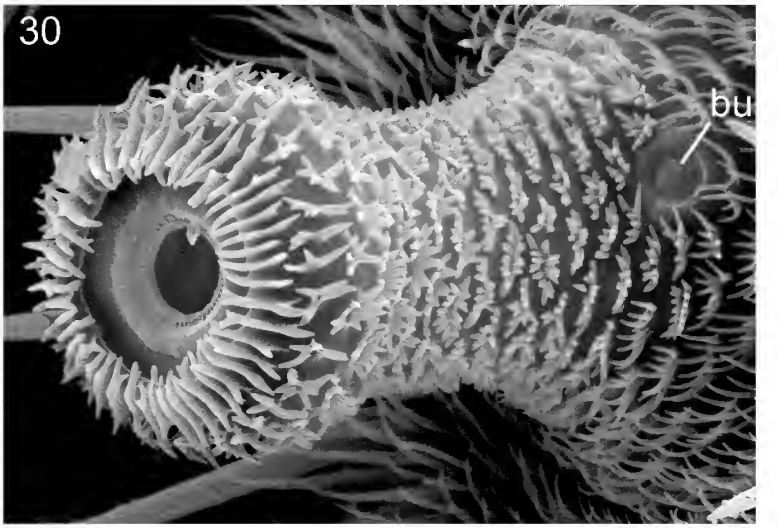

Figures 29, 30. *Lonchoptera bifurcata* Fallén (fam. Lonchopteridae). *(29)* Left seg. 2, distal view. *(30)* Conus, lateral view. *ar*, annular ridge; *bu*, pedicellar button; *c*, conus; *da*, distal articular surface; *r*, rim.

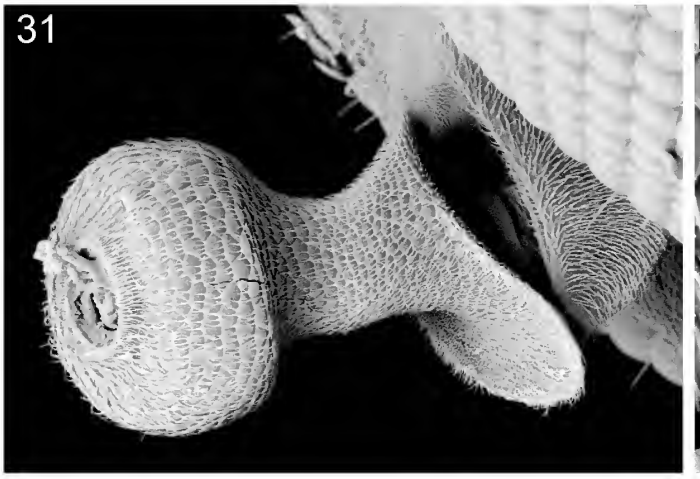

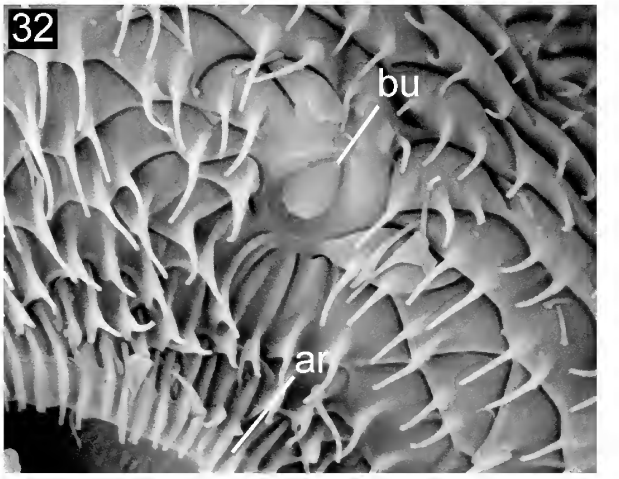

Figures 31, 32. *Sciadocera rufomaculata* White (fam. Phoridae). *(31)* Left antenna, seg. 2 after removal of seg. 3, lateral view. *(32)* Part of distal surface of conus, showing button. *ar*, annular ridge; *bu*, pedicellar button.

Opetiidae, and Platypezidae are misplaced in the otherwise informative cladogram for the Eremoneura by Grimaldi & Engel (2005: fig. 12.78), through errors regarding the development of the conus (op. cit.: table 12.7, character 19).

The Lonchopteridae

In *Lonchoptera bifurcata* (Fallén) (*L. furcata* auct.), which may be taken as morphologically typical of extant taxa of Lonchopteridae, segment 2 shows an apparent combination of plesiomorphic and derived conditions (Figs 29, 30). The approximate radial symmetry of the segment resembles the plesiomorphic one for the Cyclorrhapha. However, the strongly developed angular rim surrounding the partly concave distal articular surface, and the presence of a well developed, elongate conus arising from the centre of this surface suggest the possibility of apomorphies shared with more advanced cyclorrhaphans, but some features of the conus indicate that this may not be so. The conus in the Phoridae and Ironomyiidae bears the button on its distal surface, and this is the usual and perhaps the primitive position for the button in the Eumuscomorpha. However, in *Lonchoptera* the button is situated at the extreme base of the conus where it adjoins the distal articular surface. I therefore point out the possibility that the lonchopterid conus is an independently derived structure resulting from the simple protrusion of the annular ridge and its associated foramen, in a primitively platypezid-like taxon, into the base of segment 3, without affecting the position of the button. This hypothesis allows for the independent evolution of the conus at least twice in the Cyclorrhapha, but this may not be surprising in view of the fact that a centrally inserted conus has also developed in the orthogenyan genus *Dolichopus* (Sinclair & Cumming 2006), and such concealed structure may well have been overlooked in other non-cyclorrhaphous taxa.

Lonchoptera also differs from the Phoridae in retaining a relatively massive main body of segment 2 with a well developed encircling series of setulae, whereas extant phorid taxa have the segment reduced as explained below. A generally overlooked feature of at least some *Lonchoptera* spp. is the presence of a pair of secondary claw-like structures on the terminal surface of tarsal segment 5. These are concealed by the true claws so that detailed study is difficult (author's observations with SEM).

The Cretaceous genus *Lonchopteromorpha* (see Grimaldi & Cumming, 1999), though described under "family Lonchopteridae (?)", clearly has a bilaterally subsymmetrical (rather than radially subsymmetrical) antennal type, and possibly separate abdominal tergites 1 and 2 (op. cit. fig. 54); it therefore is probably not closely related to the Lonchopteridae. *Lonchopteromorpha* also differs from *Lonchoptera* in its short, strongly incrassate hind basitarsus.

The Phoridae (including Sciadoceridae)

It has been clear for some time that the Phoridae and Sciadoceridae are very closely related to each other. Disney (2001) combined the two families, and Brown (2007) demonstrated the difficulty of supporting a monophyletic group Sciadoceridae (or Sciadocerinae) when the numerous fossil taxa are considered. Study of phorid antennal structure has been limited because of the difficulty in separating segments 2 and 3 to expose the conus without fragmentation.

Segment 2 of *Sciadocera rufomaculata* White (Figs 31, 32) is very largely concealed in the intact antenna. This is because the main body of the segment is reduced to a narrowly or scarcely visible flange representing the rim, and the large conus is deeply embedded within the basal hollow of segment 3. After removal of segment 3, the conus is seen to be relatively slender basally, with a large, rounded distal club bearing the foramen of articulation on the centre of its apical surface (Fig. 31). The foramen is surrounded by an annular ridge bearing ridge-like denticles. The button is situated dorsolaterally on the distal surface of the conus (Fig. 32). Much of the surface of the conus is covered with tile-like microtrichose ridges as described for *Lindneromyia* sp. above (family Platypezidae). In contrast to that of most cyclorrhaphans, the region of the rim lacks obvious setulae.

In the Phoridae s.str. (or Euphorida of Brown, 2007) segment 2 shows the essential features described above for *Sciadocera* (see also Disney, 1988; 1994). This is the reason why many phorids appear to have only two prearistal segments in the antenna. In specimens of several genera I find the conus to have similar surface sculpture and annular ridge and a similarly situated button to that of *Sciadocera*. The

rim may bear a few moderately small, socket-based setulae.

Segment 3 of *Sciadocera* has a deep basal hollow enclosing the conus and bears a subterminal three-segmented arista (Hennig, 1976: fig. 62; Disney, 2001: fig. 7). It lacks macrotrichia and typical sacculi, but the general surface has diverse microtrichia and sensilla, and the dorsobasal external surface bears numerous (more than 25) saucer-shaped pits packed with trichoid sensilla (author's observations). These pits bear some resemblance to the sensory pits of *Cryptochetum* (family Cryptochetidae, see Figs 69, 70), but in that genus they coexist with a typical schizophoran sacculus. Both *Sciadocera* and *Diplonevra* sp. (examined by me) have neither sacculi (as described above and under Ironomyiidae) nor the subcuticular pit sensilla (SPS) described by Disney (2003) and Pfeil *et al.* (1994) for certain phorids. Sukontason *et al.* (2005) and Chen & Fadamiro (2008) described the surface sensilla on segment 3 of certain phorids, demonstrating some diversity in these.

The arista of various phorids is not consistently terminal and consists of one to three segments, or it may be absent (Peterson, 1987; Disney, 1994).

A general condition for the Phoridae, sometimes noted by specialists, is the presence of barbed ("feathered", or "fringed") larger macrotrichia on many parts of the insect (see Peterson, 1987: fig. 99). The barbed condition is confirmed by our SEM work on such phylogenetically diverse phorids as *Diplonevra nigrita* (Malloch) and *Sciadocera rufomaculata*, and is therefore probably in the groundplan of the family. Detailed SEM examination of representatives of each of the other families of lower (non-eumuscomorphan) Cyclorrhapha (Opetiidae, Platypezidae, Lonchopteridae, Ironomyiidae, also Apystomyiidae) suggests the absence of barbs on all macrotrichia for these families. Extensive experience also suggests that barbed macrotrichia may be absent from the numerous other cyclorrhaphous families, but a thorough search has not been made. The barbed condition is therefore likely to be, to a large extent, diagnostic for the Phoridae, though reduced or perhaps lost in some highly derived phorid taxa.

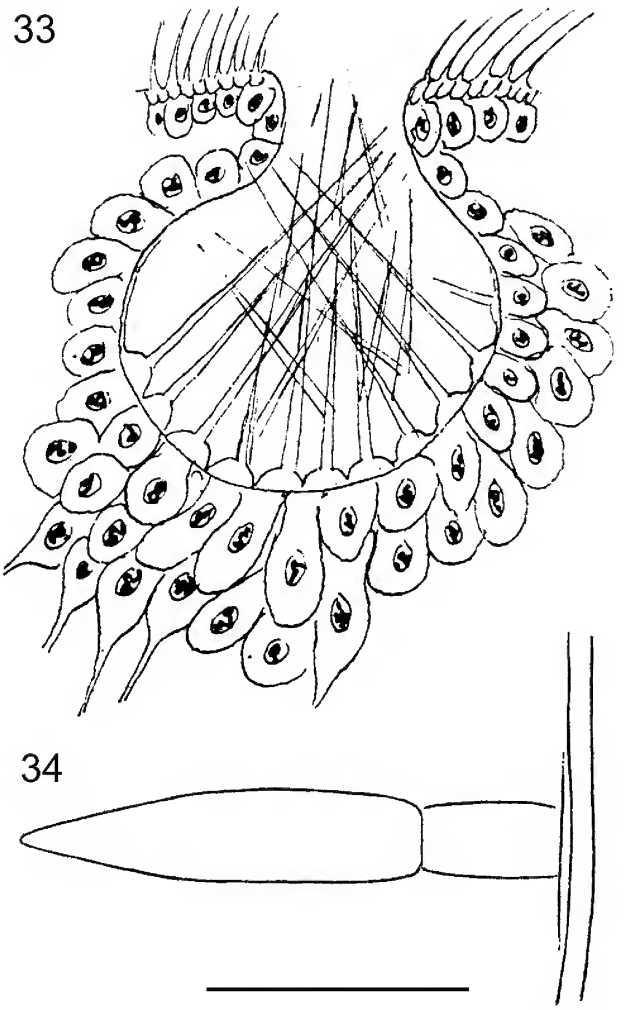

Figures 33, 34. Details of sacculus. *(33) Calliphora vicina* Robineau-Desvoidy (fam. Calliphoridae), longitudinal section of sacculus (after Lowne, 1895). *(34) Ironomyia nigromaculata* White (fam. Ironomyiidae), sensillum from lining of sacculus, approximate outline as seen with CLM; scale = 5 μm.

The Ironomyiidae

I have already given some details of the antenna of *Ironomyia nigromaculata* White (D. McAlpine, 2008: figs 1, 2, 6, 7).

Segment 2 of *I. nigromaculata* has the basal body well developed, encircled by setulae and with prominent, flange-like rim surrounding its largely concave distal articular surface. The rim has a pair of opposed angular projections (dorsomedial and ventrolateral). The centre of the distal articular surface bears a large, distally swollen conus with dorsolateral button on its terminal surface. The conus is connected to each of the two angular projections of the rim by a separate bridge.

Segment 3 has a characteristic shape, as previously described. Study of more material shows that the number of sacculi in segment 3 can sometimes be more than two, as one male specimen shows two sacculi in the ventral gibbosity of the left antenna as well as one in the dorsal gibbosity, but, as the right antenna has an irregularly divided ventral sacculus, this may be regarded as an abnormal specimen. As this is the first occurrence of sacculi in the standard taxonomic sequence of higher Diptera (or Eremoneura), I have given it some attention.

The sacculus contains a large number of slender sensilla. These appear to be of several kinds but detail is at about the limit of resolution of available CLM. Sensilla on the floor and lower sides of the sacculus have the approximate form shown in Fig. 34. These are almost circular in cross-section, without a finely filiform apex, and at least some show a division into two segments. Those on the wall nearer the orifice are closely packed and either more slender than the above or at least very slender and filiform apically. This rather limited information may be adequate to suggest a homology of the ironomyiid sacculus with that of *Drosophila* (Drosophilidae; Stocker, 2001), *Delia* (Anthomyiidae; Ross & Anderson, 1987 and 1991), *Hippelates* (Chloropidae; DuBose & Axtell, 1968), *Calliphora* (Calliphoridae; Fig. 33 reproduced here from Lowne, 1895), and other schizophorans. However, my data are insufficient to draw precise comparisons with the types of sensilla described in the sacculi of these flies.

I have previously summarizedevidence for a possible but uncertain close relationship between the Ironomyiidae and the Eumuscomorpha (D. McAlpine, 2008). Alternatively,

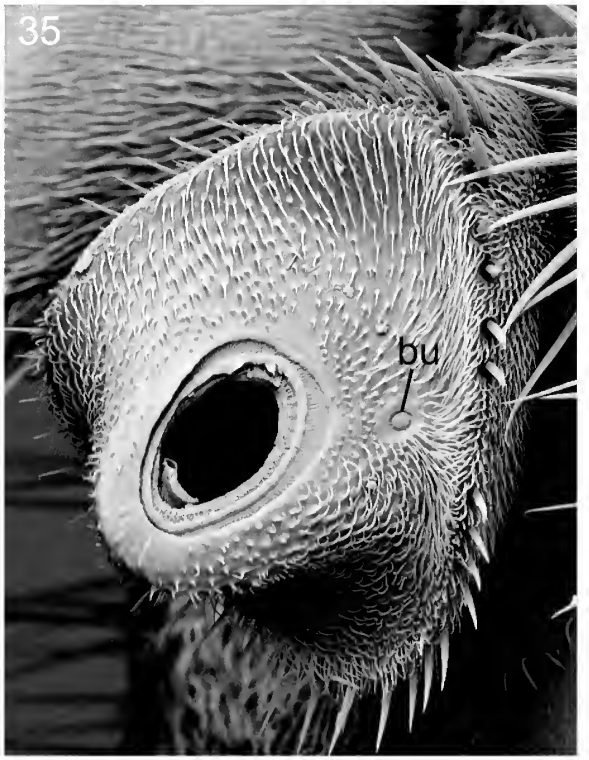

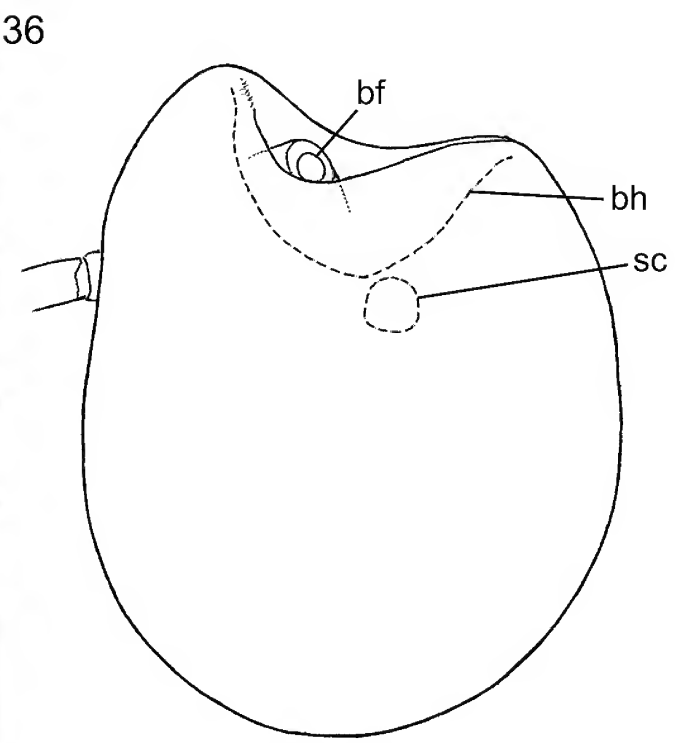

Figures 35, 36. *Melangyna* sp. (fam. Syrphidae). *(35)* Left antennal seg. 2, distolateral view after removal of seg. 3. *(36)* Right seg. 3. *bf*, basal foramen; *bh*, basal hollow; *bu*, pedicellar button; *sc*, sacculus.

Wiegmann *et al.* (2011) treated Ironomyiidae and Phoridae s.l. as sister groups, which separated c. 90 MYA. However, *Euliphora grimaldii* Arillo & Mostovski, 1999, dating from c. 110 MYA (Early Cretaceous), showed to a significant extent the venational apomorphies of early but not basal phorids (see Brown, 2007), and apparently also (my interpretation of the illustrations by Arillo & Mostovski) the characteristic phorid reduction of antennal segment 2. The Ironomyiidae resemble the Phoridae in the partial fusion of the subcosta and vein 1, but otherwise possess none of these phorid apomorphies. Therefore, if the two families are sister groups, their initial divergence must have occurred at a much earlier time level, especially so if the sinolestine fossils (discussed by D. McAlpine, 2008) are close to true ironomyiids. The date of separation indicated by Grimaldi & Engel (2005: fig. 12.78)—between 130 and 140 MYA—is more credible. Arillo & Mostovski placed *Euliphora*, together with *Prioriphora* (Late Cretaceous), in the phorid subfamily Prioriphorinae. It remains to be recorded whether these fossils have abdominal tergites 1 and 2 quite separate, as in Recent phorids (and apparently the Late Cretaceous *Sciadophora*), or partly fused as in *Ironomyia* and most other cyclorrhaphans.

Contrary to the statement of J. McAlpine (1989: 1422), *Ironomyia* differs from almost all Phoridae in the holoptic condition of the males, the derived phorid genus *Postoptica* being an exception. It also differs from the Phoridae in the sexual dimorphism of the prelabrum (a condition met with in many taxa of Eumuscomorpha, see D. McAlpine, 2008: 22–23), and in the absence of barbed macrotrichia on the head, thorax, wing, and abdomen.

The Eumuscomorpha

Following Wada (1991) this apparently monophyletic group includes the Syrphidae, Pipunculidae, and the numerous families of Schizophora. Despite the great present diversity of the Eumuscomorpha, there appear to be very few undoubted fossils of the group from before the Tertiary (Cenozoic era). There is much diversity in structure of segment 2 in the Eumuscomorpha, but the groundplan conditions are probably those shared with certain syrphids and the less modified taxa in several superfamilies of Schizophora, e.g., the Sciomyzoidea. The accumulated antennal apomorphies of the basal Eumuscomorpha, probably absent in the groundplan of the Eremoneura, are as follows: segment 2 with rim extended as encircling flange; conus present, with button on its distal surface; annular ridge and distal foramen of segment 2 tilted dorsolaterally; segment 3 with one or more sacculi; arista arising dorsobasally from segment 3; arista three-segmented (doubtful apomorphy).

The Syrphidae

The Syrphidae, whether they form a sister-group to the Pipunculidae alone or to the whole remainder of the Eumuscomorpha (i.e. Pipunculidae + Schizophora, see Collins & Wiegmann, 2002) must be considered a key group to understanding much of the basal morphology of the Schizophora. I have taken for initial study representatives of the syrphid genera *Melangyna*, *Microdon*, *Psilota*, *Eristalis*, *Chalcosyrphus*, *Ceriana*. These show slight variation, mainly in proportions of certain parts and degree of symmetry.

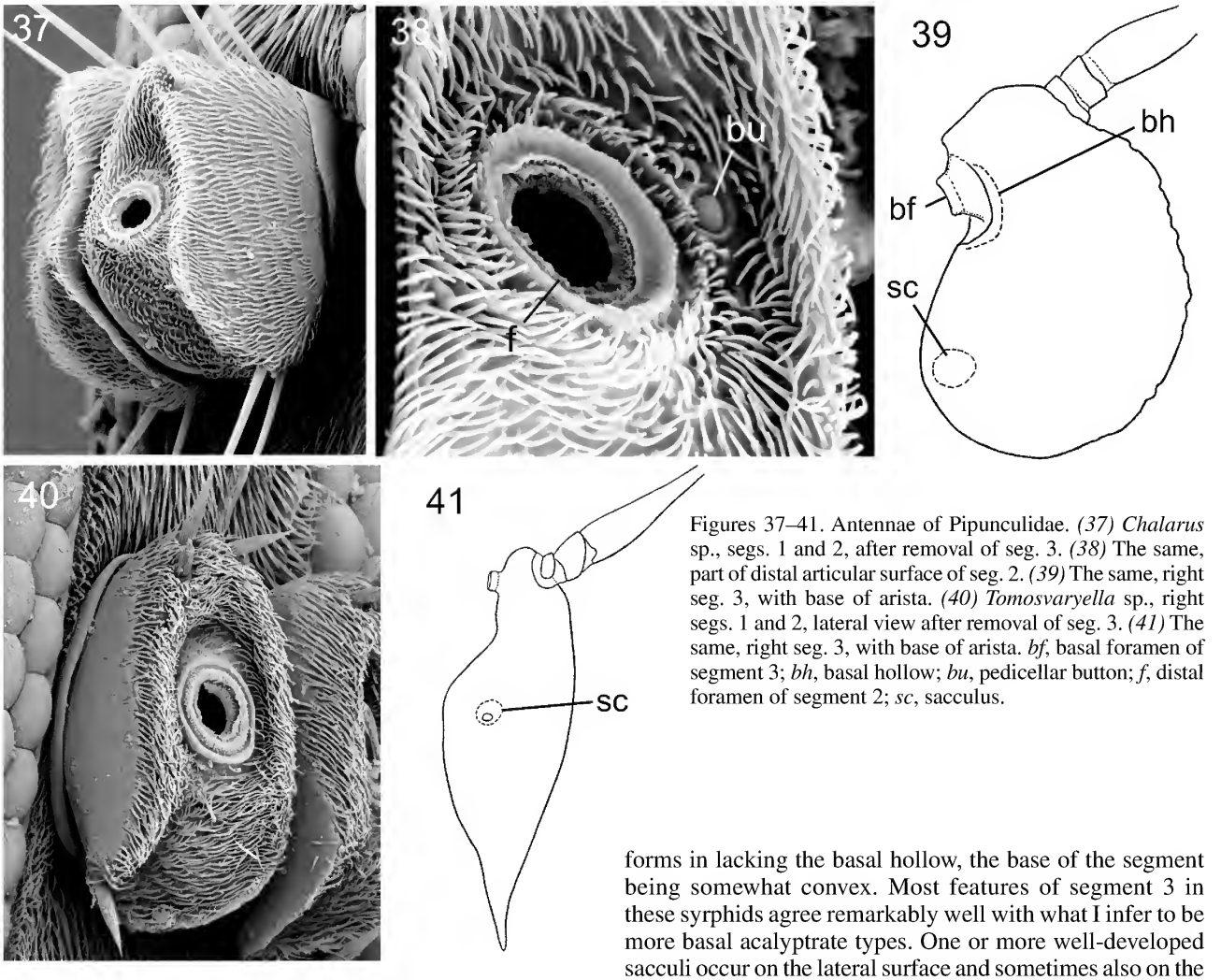

Figures 37–41. Antennae of Pipunculidae. *(37) Chalarus* sp., segs. 1 and 2, after removal of seg. 3. *(38)* The same, part of distal articular surface of seg. 2. *(39)* The same, right seg. 3, with base of arista. *(40) Tomosvaryella* sp., right segs. 1 and 2, lateral view after removal of seg. 3. *(41)* The same, right seg. 3, with base of arista. *bf*, basal foramen of segment 3; *bh*, basal hollow; *bu*, pedicellar button; *f*, distal foramen of segment 2; *sc*, sacculus.

Segment 2 (Fig. 35) is generally of moderate size, with largely concave distal articular surface and completely encircling rim. The rim is usually notched or sinuate on its dorsal margin, but is scarcely so in *Microdon* and *Ceriana*. Typically, the conus is moderately large, broad, and rather short, with a short ventral chin, and the foramen of articulation is inclined laterally with a tendency to become vertically elongate in some forms. The button is located at the lateral base of the conus where the latter merges with the surrounding articular surface, or is located more dorsally, especially so in *Microdon*.

In *Ceriana ornata* (Saunders) segment 2 is very different from that of other examined taxa. Both the segment as a whole and the conus are elongate and almost radially symmetrical, the latter distally rounded and clavate. As in the Phoridae, the clavate condition of the conus renders the separation of segments 2 and 3 for study difficult, even after the connective membrane is snapped by rotation.

Segment 3 in *Melangyna* (Fig. 36) is typical of a number of syrphid genera. The segment is broadly bilaterally compressed, has a broad, relatively shallow basal hollow, and the basal articular foramen is situated on a slight prominence arising within this cavity, but there is no indication of a sub-basal caecum. The arista arises before mid length of the segment on the lateral surface very close to the dorsal margin. Segment 3 of *Eristalis copiosa* Walker (and possibly that of related species) differs from the above forms in lacking the basal hollow, the base of the segment being somewhat convex. Most features of segment 3 in these syrphids agree remarkably well with what I infer to be more basal acalyptrate types. One or more well-developed sacculi occur on the lateral surface and sometimes also on the medial surface. The number can sometimes differ between the right and the left antenna, but often there is just one sacculus, which is located on the lateral surface as in most acalyptrate taxa.

In *Ceriana* (already noted for its unusual segment 2) and some related genera (see Vockeroth & Thompson, 1987) the arista is much shortened and located apically on segment 3. Comparison with probable outgroups leads me to believe that the peculiarities of *Ceriana* and its allies (tribe Cerioidini) are autapomorphies for this group. Thus, the presence of a terminal arista (or style) on a distally tapered segment 3 is an evolutionary reversal, simulating the conditions present in basal eremoneurans.

The Pipunculidae

I have taken for study antennae of the genera *Chalarus* and *Tomosvaryella*.

In *Chalarus* segment 2 (Figs 37, 38) is bilaterally compressed and otherwise resembles that of the less modified taxa of Syrphidae. The distal articular surface is moderately concave with moderately developed rim, receding ventrally. The conus is broad, little raised, and approximated to the medial side of the segment. The annular ridge and distal foramen are tilted dorsolaterally and the button lies in the relatively slight concavity between the conus and the mid-lateral part of the rim.

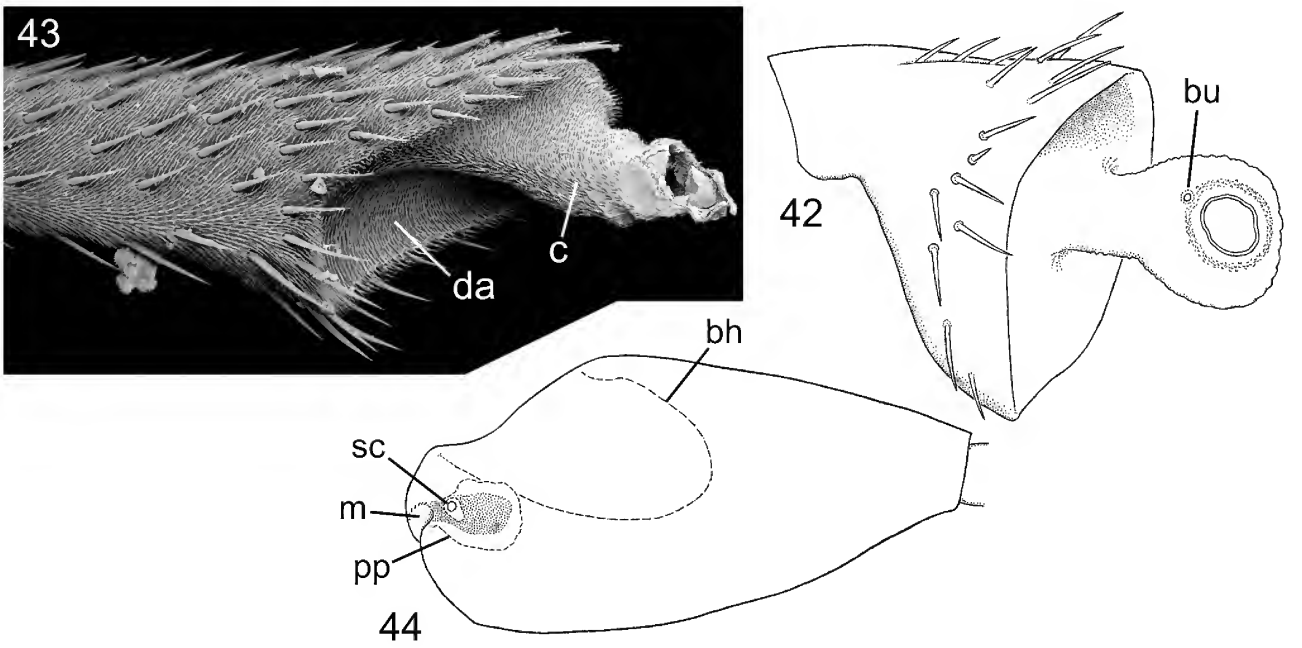

Figures 42–44. Antennae of Conopidae. *(42) Myopa* sp., right antennal seg. 2. *(43) Australoconops unicinctus* (Kröber), part of right antennal seg. 2. *(44)* The same, right antennal seg. 3. *bh*, basal hollow; *bu*, pedicellar button; *c*, conus; *da*, distal articular surface; *m*, mouth of postpedicellar pouch; *pp*, postpedicellar pouch; *sc*, sacculus (seen superimposed on postpedicellar pouch).

Segment 3 in *Chalarus* (Fig. 39) is broadly rounded and bilaterally compressed. The basal hollow is present, but too small to contain the prominence bearing the basal articular foramen and there is no sub-basal caecum. The single sacculus is located on the ventral side of the segment and opens on the lateral surface. Much of the surface is covered with relatively large, saucer-like pits. The arista is inserted dorsally not far from the base of the segment; it is three-segmented with segment 4 forming a complete annulus.

The notable differences in antennal structure of *Tomosvaryella* from the above are probable apomorphies (see Figs 40, 41). The conus is absent and the smooth annular ridge, together with the distal foramen, is sunk into a deep, narrow cavity on the distal articular surface of segment 3. The annular ridge and foramen are located centrally on this surface and are almost symmetrical, not tilted. The button (not visible in the preparation) is apparently concealed in the narrow cavity between the annular ridge and the lateral part of the rim.

Segment 3 is much prolonged ventrally and has no basal hollow. The basal segment of the arista (segment 4) is sclerotized only on the dorsal side.

The antenna of the Pipunculidae shows the basic structure of the Eumuscomorpha, but does not appear to provide evidence as to whether this family is the sister group of the Syrphidae or the Schizophora. Neither J. McAlpine (1989) nor Zatwarnicki (1996) gave very convincing synapomorphies for the Syrphoidea (Syrphidae + Pipunculidae) as a monophyletic group. The work of Collins & Wiegmann (2002b) suggested that the Pipunculidae alone represent the sister group to Schizophora, and that the Syrphoidea (*sensu* J. McAlpine, 1989) are paraphyletic. These conclusions are supported by Wiegmann *et al.* (2011).

The Conopidae

Examples used in this study include *Myopa* sp. (subfamily Myopinae), *Australoconops unicinctus* (Kröber), and *Heteroconops* sp. (subfamily Conopinae). Though these species show a range of variation, a wider range of observations will be necessary to make generalizations for the family.

In *Myopa* sp. segment 2 is moderately short and stout, narrowed basally and broadly funnel-like distally (Fig. 42). The flange-like rim is continuous without division into dorsal lobes. The external surface is densely microtrichose and bears a number of stout setulae. In several observed examples the setulae on the medial surface are partly or extensively broken or abraded. The distal articular surface is broadly concave and bears numerous fine, simple microtrichia which are not grouped into combs nor located on ridges. The conus rises from the dorsomedial part of the articular surface. It is narrow basally and dilated and bilaterally compressed distally, apparently well sclerotized and rigid; the distal foramen is located subterminally on the outer lateral surface; it has a narrow foraminal ring; the annular ridge is only slightly prominent and bears a moderate number of small compact tubercles, some rounded, some bearing a minute microtrichium. The general surface of the conus is almost devoid of microtrichia, but bears many short, smooth transverse ridges.

Segment 3 is rather short, inflated, and without basal stem. The apparent sacculus is situated on the outer lateral surface, slightly ventrobasally of its centre, and is only slightly larger than numerous sensory pits on this surface, but it is differentiated by the possession of fine trichoid sensilla in the mouth region, as well as one larger ovoid-cylindrical sensillum arising from the floor of the cavity. The arista is shorter than segment 3, inserted slightly laterad of mid-dorsal position on segment 3, and is three-segmented.

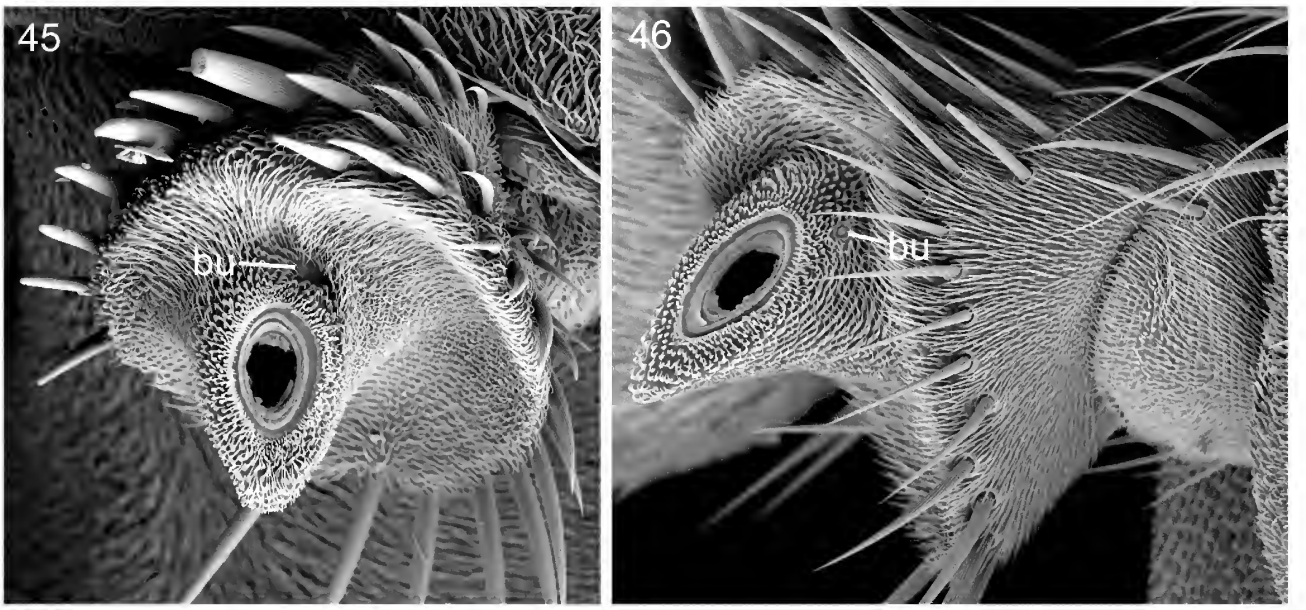

Figures 45, 46. Left antennal seg. 2. *(45) Maorimyia bipunctata* (Hutton) (fam. Helcomyzidae), distolateral view. *(46) Napaeosciomyza* sp. (fam. Helosciomyzidae), lateral view. *bu*, pedicellar button.

In *Australoconops* segment 2 (Fig. 43) is elongate, gradually expanding distally, with the distal articular surface oblique, concave ventrally and bearing the conus dorsally. The conus is elongate, irregularly subcylindrical, weakly sclerotized and apparently flexible. The distal foramen is exceptionally large, subcircular, without a marked annular ridge, and terminal on the conus. The button was not located, probably because of the irregular surface of the conus. Segment 3 (Fig. 44) is somewhat elongate, bulbous basally and tapered distally. There is a large basal hollow into which the conus is inserted. The apparent sacculus opens on to the lateral surface near the base of the segment. There is a relatively large opening facing basally on the basal swelling of segment 3, which leads into a cavity much larger than that of the sacculus. This cavity (Fig. 44, *pp*), which I term the postpedicellar pouch, in analogy with that of the orthogenyan genus *Hormopeza*, has a thick transparent wall with a pigmented lining. Its mouth, though microtrichose, lacks the scabrous surface of the sub-basal caecum of some families, and is unlikely to be homologous with that structure. The microstructure of the pouch is not visible in my preparations, and it is not evident whether its function is sensory or glandular. Under CLM the sacculus appears to be superimposed on the pouch (in lateral view), but it is not clear if there is any connection between their walls.

The postpedicellar pouch is present in both sexes of *Australoconops unicinctus*. It is also present in *Heteroconops* sp. and probably at least some other taxa of Conopinae. Its opening is usually concealed in whole specimens, as it is on the surface which faces into the concavity of the distal articular surface of segment 2, but it is readily visible in cleared antennae under CLM. The condition in *Physocephala texana* (Williston) appears to be more complex but has not been examined in detail. The conus of *Heteroconops* is similar to that of *Australoconops* but is more elongate. The remarkable resemblance in structure of segment 2 between certain taxa of Conopidae and Pyrgotidae is mentioned under the latter family. I have previously noted variation in the number of aristal segments in the Conopidae (D. McAlpine, 2002).

Various studies of the Conopidae have failed to demonstrate convincingly its nearest relatives among the schizophoran families. The peculiarities of the conus and postpedicellar pouch appear to be apomorphies restricted to the subfamily Conopinae, and are therefore not relevant to the broader problem of relationships.

During this rapid selective check of conopid morphology, I have noticed major differences in the subscutellum (*sensu* J. McAlpine, 1981) between taxa. In *Stylogaster* spp. the subscutellum is large, deep, and medially extended so as almost to divide the postscutellum; in other conopid taxa examined the subscutellum is quite narrowly transverse or vestigial above the large postscutellum. This variation may have taxonomic significance.

The Sciomyzoidea (including Lauxanioidea)

J. McAlpine (1989) gave detailed reasons for separating the superfamilies Sciomyzoidea and Lauxanioidea and, at first glance, particularly regarding his table 116.4, he seems to have made a strong case (comparable to his now refuted case for monophyly of the Acalyptratae). However, careful assessment of the 16 character differences given indicates that their reliability as indicators for a pair of sharply defined monophyletic sister groups is at best very weak. Some ambiguous characters seem to be interpreted in a particular way to support a desired hypothesis, when they could be as readily interpreted as supporting an alternative one. J. McAlpine's identification of character states "that are apomorphic with respect to ground plan of Acalyptratae" is invalid as there is no such monophyletic taxon. What is apparent to me is that his lauxanioid families Lauxaniidae s.l. and Chamaemyiidae form a more apomorphic group, which could be a clade, whereas the remaining sciomyzoid family collection is most probably paraphyletic. If J. McAlpine (1989) and Wiegmann *et al.* (2011) are correct in including *Cremifania* within the lauxanioid family Chamaemyiidae, then it is clear that the protandrial structure supposed by the former to indicate the apomorphic groundplan condition for

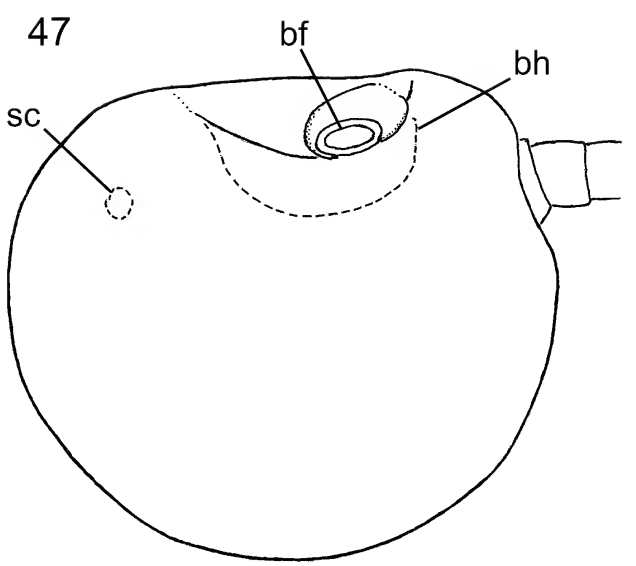

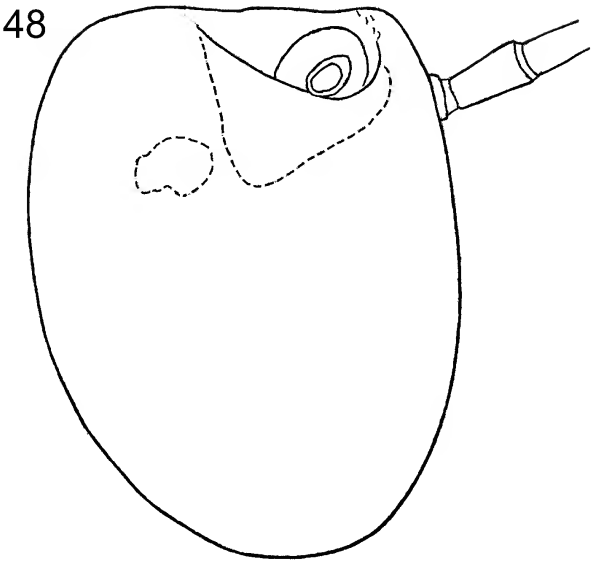

Figures 47–48. Left antennal seg. 3, medial view. *(47) Maorimyia bipunctata* (Hutton) (fam. Helcomyzidae). *(48) Napaeosciomyza* sp. (fam. Helosciomyzidae). *bf,* basal foramen; *bh*, basal hollow; *sc*, sacculus.

the Lauxanioidea (as distinct from the Sciomyzoidea) has no validity. Presentation of a more detailed analysis would be out of place here, but I retain the system used by Colless & McAlpine (1991) wherein the Lauxaniidae are placed in the Sciomyzoidea.

Those sciomyzoid taxa with antennal features more basic (and probably plesiomorphic) for the superfamily seem likely, from comparison with the outgroup Syrphidae, to retain the conditions most like the groundplan for the Schizophora. In *Maorimyia bipunctata* (Hutton) (family Helcomyzidae, Figs 45, 47) the rim is moderately developed for the Schizophora and does not form a pair of dorsal lobes. The conus is stout and prominent, located slightly medially of the centre of the distal articular surface, so that it encroaches slightly on the medial part of the rim-flange, with its distal surface and foramen very obliquely tilted dorsally and slightly laterally, with prominent ventral chin. The annular ridge is not prominent, and lacks any special development of microtrichia. The button is dorsolateral in position, more nearly dorsal than in related families (other than Coelopidae), and there is no dorsal longitudinal sulcus on the conus. Segment 3 is short, rounded, with moderately large basal hollow, the basal foramen on a marked, rounded gibbosity near the medial margin of the hollow. The sacculus is located ventrolaterally. *Napaeosciomyza* sp. (family Helosciomyzidae, Figs 46, 48) has the antenna structurally very similar to that of *Maorimyia*.

In typical Coelopidae (subfamily Coelopinae), e.g., *Gluma* (Fig. 49), *Coelopa*, and *Coelopella*, segment 2 resembles that of the Helcomyzidae in having the large conus situated almost centrally on the distal articular surface, almost symmetrical, and with distal foramen facing more dorsally than laterally. However, the coelopid conus, though slightly variable, is more elongate, and the button is situated dorsally at the base of the conus, where the latter merges with the distal articular surface, and is sunken into a shallow pedicellar sulcus, which extends distally on the dorsal surface of the conus for a variable length. Segment 3 of the coelopid antenna is short, rounded, and decumbent at rest, but is similar structurally to that of the Helcomyzidae, Helosciomyzidae, etc.

The position of the genus *Lopa* in the Coelopidae has been queried by Meier & Wiegmann (2002) from their molecular data. *Lopa* was originally placed in a separate subfamily, Lopinae, from other coelopids, the Coelopinae. The antenna of *Lopa convexa* McAlpine (Fig. 50) shares the peculiar apomorphic conditions of the Coelopidae, not known in other sciomyzoid families: conus large, centrally situated, with foramen dorsolateral; button dorsally situated at base of conus and at basal end of dorsal pedicellar sulcus. The last instar larva of *Lopa* also possesses the complete circle of hydrofuge hairs surrounding each posterior spiracle (D. McAlpine, 1991: 46), apparently absolutely diagnostic for the Coelopidae (larva of *Lopa* examined by both R. Meier and author). I consider that the sharing of these unique antennal and larval apomorphies between Lopinae and Coelopinae is strong evidence for their monophyly.

The sciomyzoid family Natalimyzidae (only genus *Natalimyza*, see Barraclough & McAlpine, 2006) is endemic to Africa, but a species has recently been recorded from Baltic amber (Eocene of Europe, Tschirnhaus & Hoffeins, 2009). I have examined antennal structure in *Natalimyza* "sp. B" (flagellar segments; Mount Elgon, Kenya) and *Natalimyza* "sp. A" (pedicel; Ukulinga Reserve, Natal). Segment 2 (Figs 51, 52) is of the basic sciomyzoid type with conus large, asymmetrical, prominent on median side, with foramen facing laterally and armature of annular ridge not particularly developed. Segment 3 (Fig. 53) is broad with broad, capacious basal hollow containing the basal foramen on its median side. The arista (Fig. 54) lacks segment 4, and segment 5 is short, rotund, and asymmetrical.

I have examined antennal structure in the following species of the family Lauxaniidae: *Minettia maculithorax* (Malloch), *Sapromyza sciomyzina* Schiner, *Rhagadolyra handlirschi* Hendel, *Trigonometopsis binotata* (Thomson), and *Homoneura* sp. (Figs 55–57).

The conus in these taxa is very asymmetrical, short, attached to the medial side of the distal articular surface and inclined so that it is little raised above that surface on

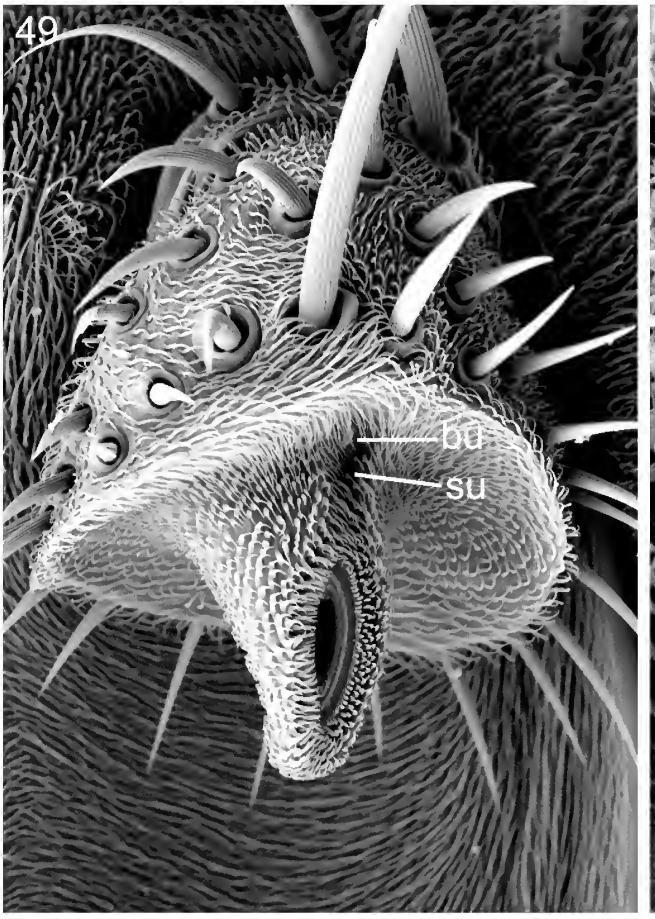

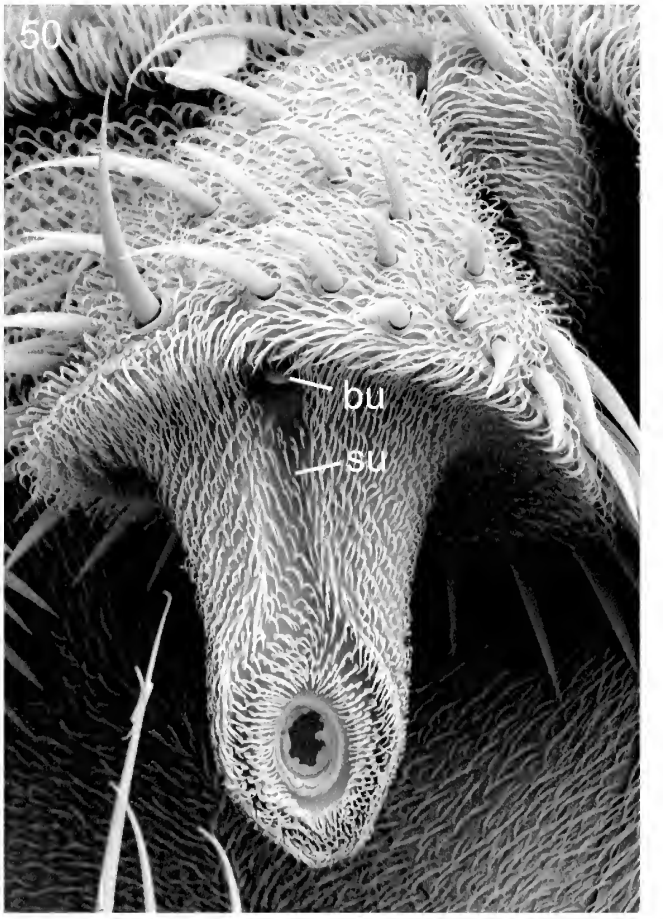

Figures 49, 50. Antennal seg. 2 of Coelopidae. *(49) Gluma keyzeri* McAlpine. *(50) Lopa convexa* McAlpine. *bu*, pedicellar button; *su*, pedicellar sulcus.

its lateral side. The distal foramen is so strongly inclined laterally as to be invisible when the segment is viewed distally. The microtrichose armature on the annular ridge is not differentiated from the general surface of the conus. The button is situated close to the upper lateral part of the annular ridge. Segment 3 differs from that of *Maorimyia*, *Napaeosciomyza*, and less markedly, from *Natalimyza* in that the basal outline is more oblique because of the prominent asymmetrical dorsobasal region bearing the foramen (Fig. 57).

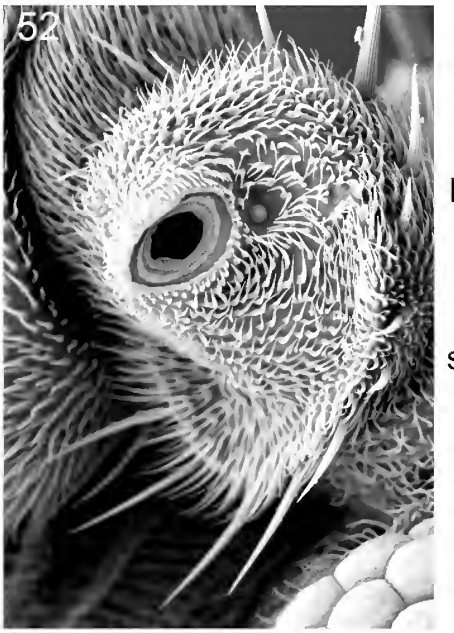

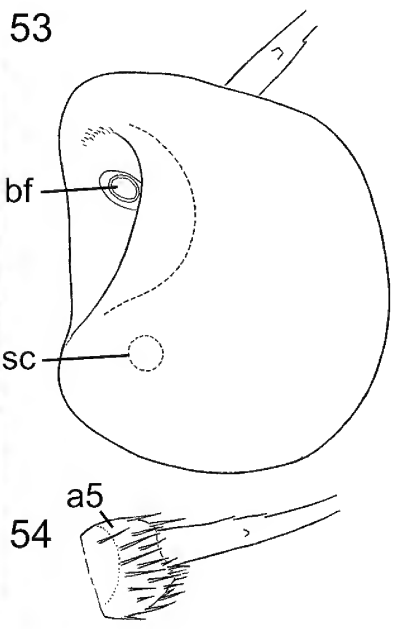

Figures 51–54. Antenna of *Natalimyza* sp. (Ukulinga Reserve Farm, Natal; fam. Natalimyzidae). *(51)* Pair of antennae, left seg. 3 removed. *(52)* Left seg. 2, lateral view. *(53)* Left seg. 3, medial view. *(54)* Basal part of left arista. *a5*, seg. 5; *bf*, basal foramen; *sc*, sacculus.

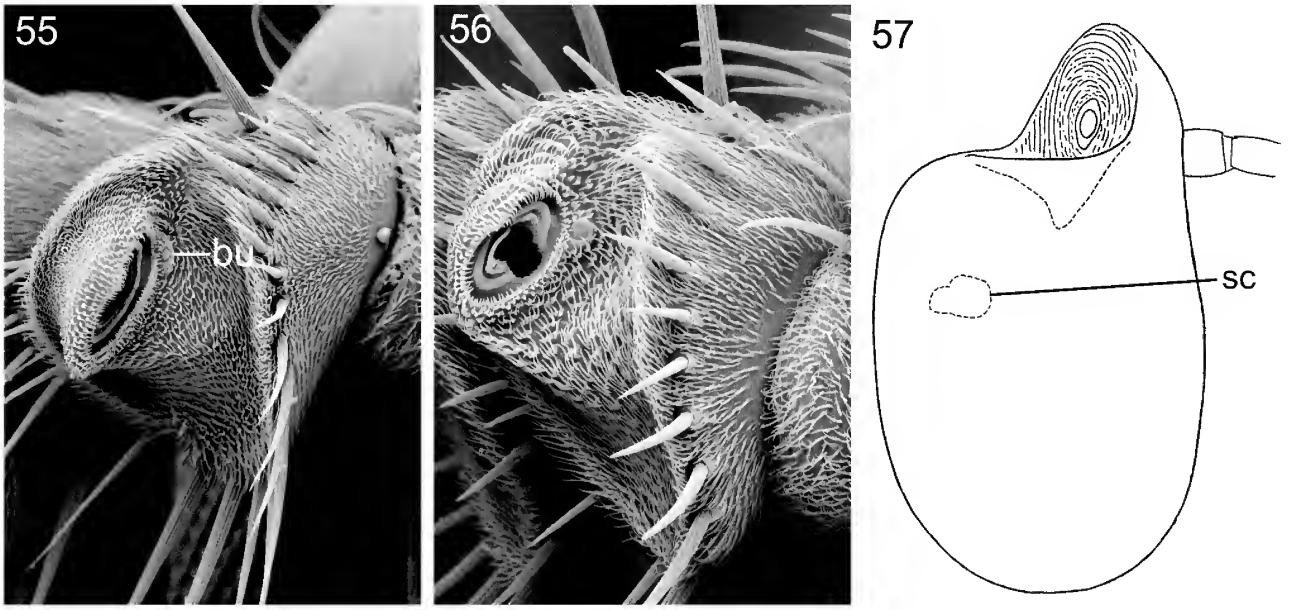

Figures 55–57. Antennae of Lauxaniidae. *(55) Sapromyza sciomyzina* Schiner, left seg. 2, lateral view. *(56) Trigonometopsis binotata* (Thomson), left seg. 2, lateral view. *(57) Homoneura* sp., left seg. 3, medial view. *bu*, pedicellar button; *sc*, sacculus.

The question arises as to whether antennal structure supports the segregation of Lauxaniidae and Chamaemyiidae together as a separate superfamily from the Sciomyzoidea. The above description suggests some differences between the Lauxaniidae and basal members of the Sciomyzoidea, but the sciomyzid genus *Pherbellia* has a conus somewhat approaching that of typical lauxaniids in shape. In the chamaemyiid genus *Pseudoleucopis* segment 2 and the conus are much more like those of *Maorimyia* than any of the lauxaniids examined, and segment 3 is almost transverse in basal outline. Thus, my very limited antennal studies for these families do not at present provide support for a superfamily Lauxanioidea *sensu* J. McAlpine.

The Milichiidae

Examples used for this study include *Stomosis* sp., *Milichiella* sp., and, in less detail, *Desmometopa* sp. In some species separation of segments 2 and 3 without damage to the conus is difficult.

In *Stomosis* (Figs 58–60) antennal structure retains many of the basal schizophoran features seen in various taxa of Sciomyzoidea and Canacidae s.l. The rim of segment 2 is prominently developed, without differentiated lobes, but is rather broadly interrupted dorsally. The distal articular surface is concave all around the conus, but has no differentiated cup or cavity. The conus is

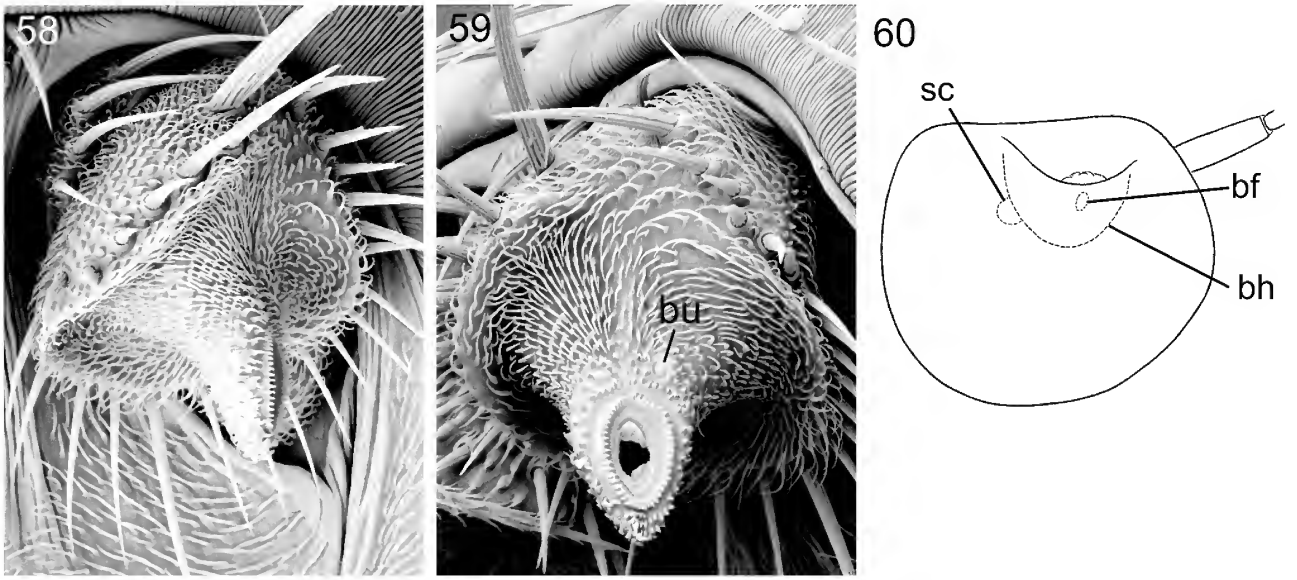

Figures 58–60. *Stomosis* sp. (fam. Milichiidae). *(58)* Left seg. 2, distodorsal view. (59) Left seg. 2 distolateral view. *(60)* Left seg. 3, medial view. *bf*, basal foramen; *bh*, basal hollow; *bu*, pedicellar button; *sc*, sacculus.

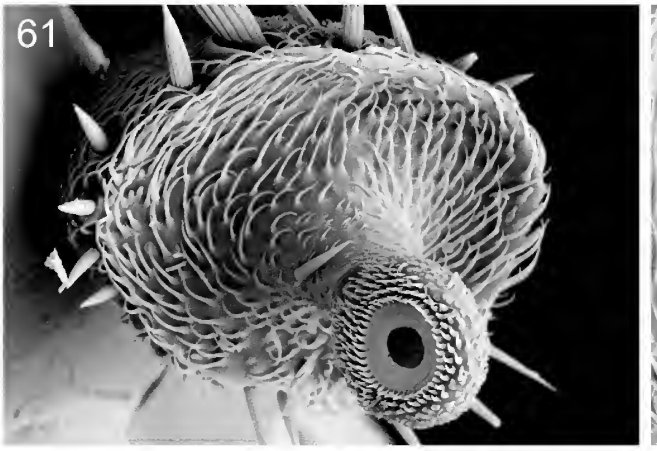

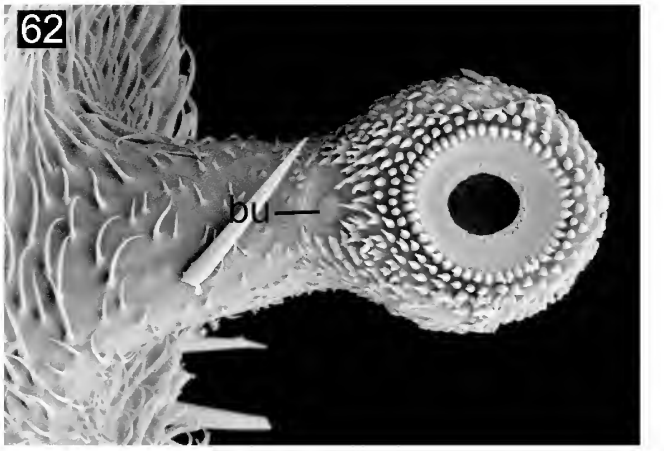

Figures 61, 62. *Milichiella* sp. (fam. Milichiidae). *(61)* Right seg. 2, distal view. *(62)* right conus, lateral view. *bu*, pedicellar button.

located near the centre of the distal articular surface and is large and prominent, with oval, dorsolateral annular ridge and foramen, and ventral chin; the button is situated dorsolaterally to the annular ridge. Segment 3 is short and compact with moderately deep basal hollow into which the conus is inserted and no basal stem; the basal foramen is contained within the hollow; the pore of the sacculus is situated on the lateral surface a little before mid-length of the segment.

Milichiella (Figs 61, 62) and *Desmometopa* differ mainly in having the rim uninterrupted dorsally and the conus more elongate and apically thickened, as in the Phoridae and Heteromyzidae-Sphaerocerinae; the annular ridge and associated foramen are subcircular, laterodistally located, and there is no chin.

The Milichiidae are often considered to be the possible sister group to the Chloropidae (e.g., Griffiths, 1972; Brake, 2000), but the few examples examined of the former show the distal articular surface of segment 2 to have no trace of cavity or cup and the conus to be rigidly sclerotized basally.

The Chloropidae

Study of the disarticulated pedicel of the following examples was carried out with SEM: *Apotropina ornatipennis* (Malloch) (subfamily Siphonellopsinae); *Chloropella bipartita* Malloch, *Lipara lucens* Meigen, *Pachylophus rufescens* (de Meijere), *Pemphigonotus mirabilis* Lamb (subfamily Chloropinae); *Batrachomyia atricornis* Malloch, *Cadrema* sp., *Merodonta* sp., *Rhodesiella magna* (Becker), *Tricimba carinifacies* Malloch, gen. and sp. undetermined, near *Elachiptera* and *Monochaetoscinella* (subfamily Oscinellinae); see Figs 63–67. In addition, the pedicel of several other taxa of Chloropidae has been examined on dry specimens with high magnification of a SLM, after removal of the postpedicel.

The distal articular surface of segment 2 is concave within the bounds of the well-developed, uninterrupted rim, but centrally a pedicellar cup is encircled by a sharply elevated ridge or collar. The conus is based within the cup which it almost fills, leaving a narrow encircling furrow. The conus is prominent and produced as a chin below the dorsolaterally facing foramen, and is armed with many denticles or spinules and sometimes with transverse ridges basal to the denticulate zone. The button is dorsolaterally located on the conus just clear of the collar. In *Apotropina* (subfamily Siphonellopsinae) and *Chloropella* (subfamily Chloropinae) the collar is not very prominent and the general covering of simple, separate microtrichia on the collar extends near the edge of the furrow. In *Rhodesiella*, *Cadrema*, and *Tricimba* (subfamily Oscinellinae) the collar is markedly higher and more prominent with smooth surface.

The condition in *Apotropina* and *Chloropella*, where the collar is relatively little raised and largely clothed with microtrichia, like those on the adjacent articular surface, somewhat resembles that of the possible outgroup Canacidae s.l. (*sensu* D. McAlpine, 2007a) and is probably plesiomorphic within the Chloropidae. The relatively high, glabrous collar, seen in *Rhodesiella*, *Cadrema*, and *Tricimba*, is perhaps an apomorphic state, but is not present in *Lipara* and *Batrachomyia*, also of the subfamily Oscinellinae.

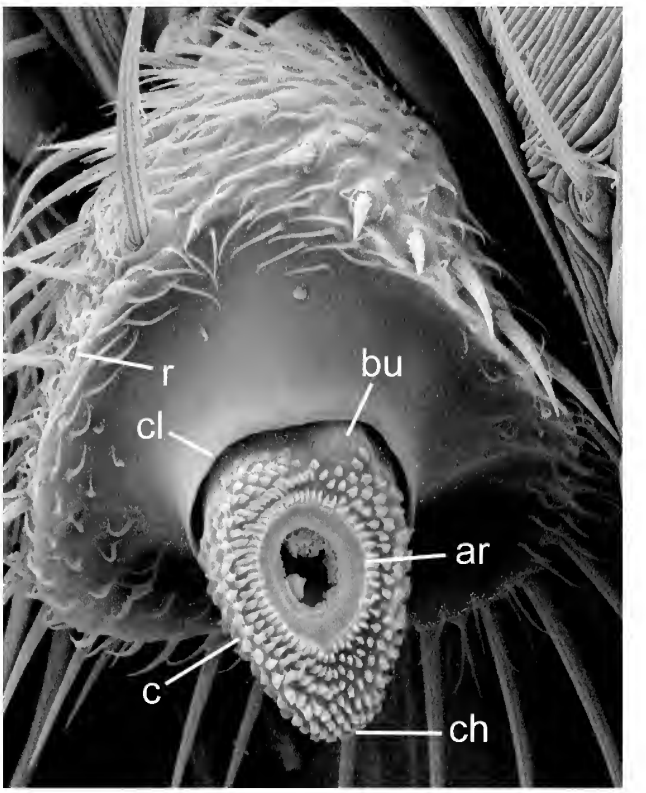

Figure 63. *Rhodesiella magna* (Becker) (fam. Chloropidae), left antennal seg. 2, seg. 3 removed. *ar*, annular ridge; *bu*, pedicellar button; *c*, conus; *ch*, chin; *cl*, collar; *r*, rim.

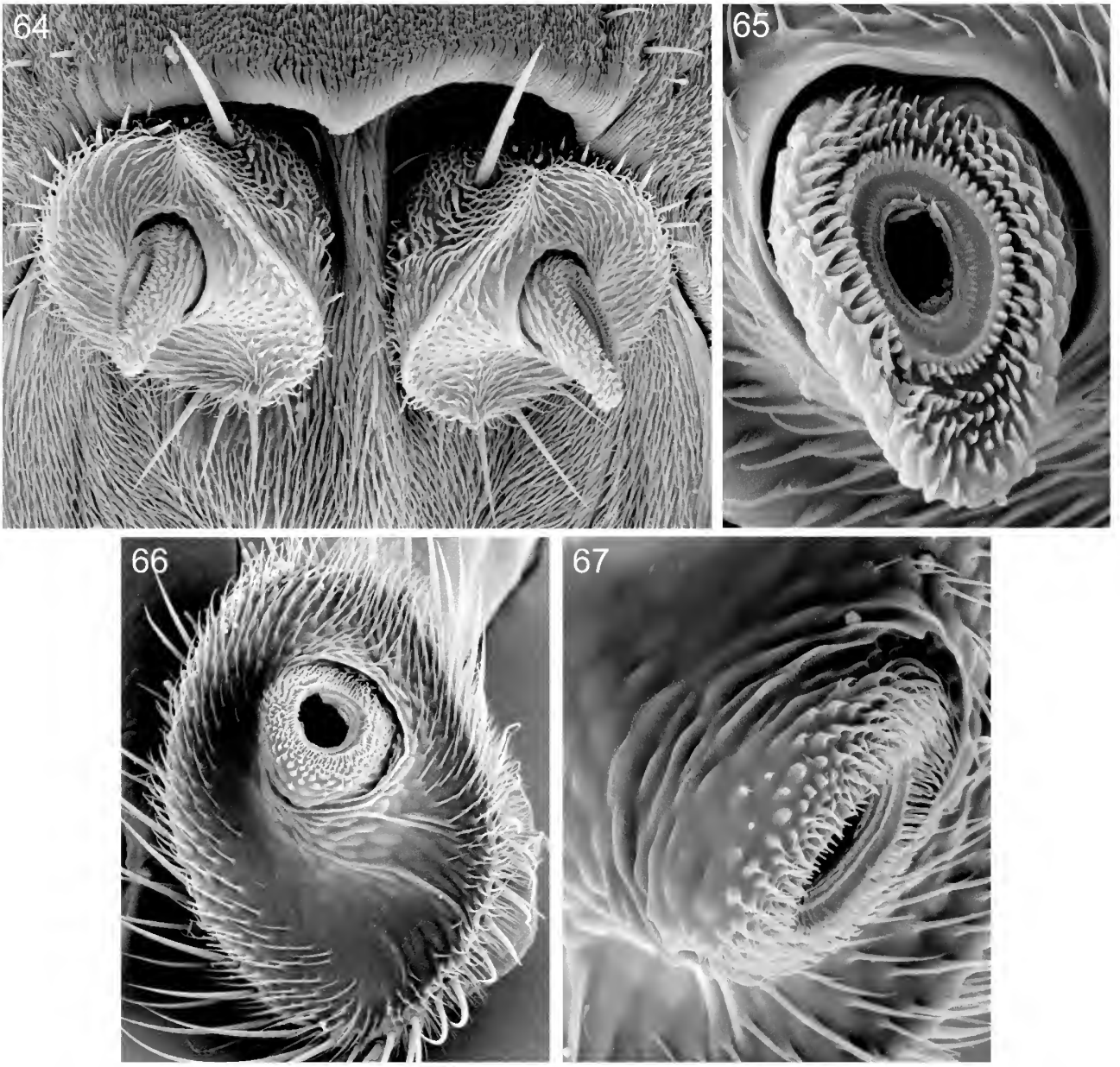

Figures 64–67. Antennae of Chloropidae. *(64) Apotropina ornatipennis* (Malloch), antennae in situ, disarticulated. *(65) Chloropella bipartita* Malloch, left conus. *(66) Batrachomyia atricornis* Malloch, distal articular surface of left seg. 2 with conus. *(67) B. atricornis*, laterally flexed conus of left antenna, part of collar and furrow thus obliterated.

I have seen evidence suggesting that the lining of the furrow is flexible, and that the collar system effectively provides another joint to the antenna. The illustrated pedicel of *Batrachomyia* (Figs 66, 67), shows how the cuticular fold forming the collar on the medial side of the conus can be stretched when the conus is flexed laterally, and the furrow is no longer apparent.

In view of the fact that the chloropid genera studied represent a wide range of relationships within the family, including examples of all three recognized subfamilies, it is probable that they are adequate to show both the groundplan conditions of the conus for the Chloropidae and the generally diagnostic features. I therefore suggest that the presence of a collar enclosing a narrow encircling furrow around the base of the conus is an autapomorphy for the family, and is a condition unknown in presumably closely related families (e.g., Milichiidae, Canacidae), but a similar condition occurs in some Pyrgotidae and some other Tephritoidea through convergence (see below).

The Cryptochetidae

This Old World family includes the polytypic genus *Cryptochetum*, also doubtfully the Australian *Librella* and the fossil *Phanerochaetum*. I have examined the antenna of all these genera, but the material has been inadequate for a detailed study.

Antennal structure in *Cryptochetum* is distinct from that of any other acalyptrate taxon (Figs 68–70). Segment 2 is completely encircled by the prominent, sharp-edged rim without an incision, notch or marked sinuosity. The distal articular surface is slightly concave, with large, elongate,

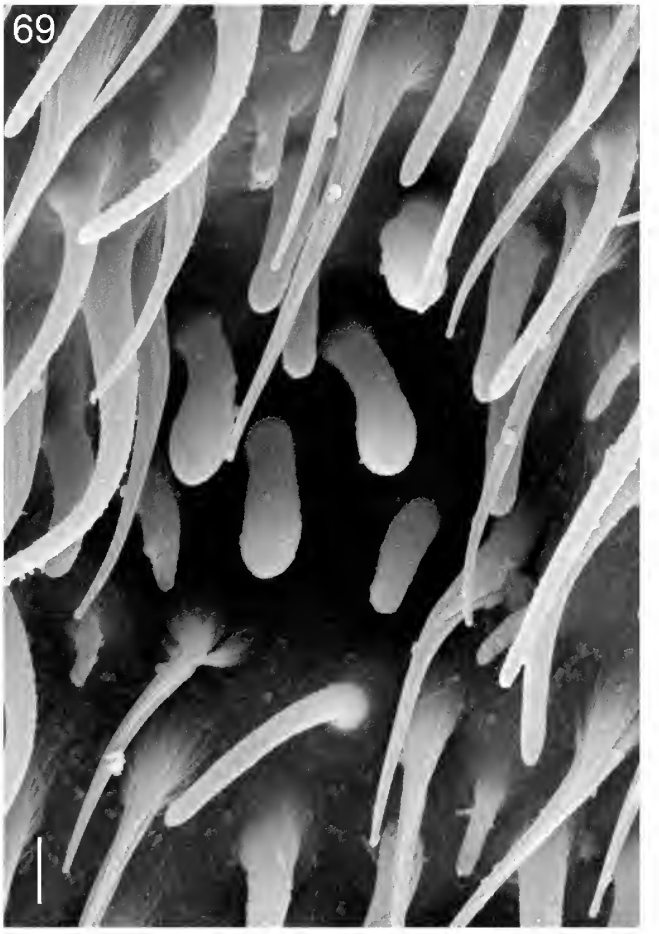

Figures 68–69. Antenna of *Cryptochetum* sp. (fam. Cryptochetidae). *(68)* Left seg. 2, dorsolateral view, conus broken. *(69)* Sensilla in sensory pit of seg. 3; scale = 2 μm.

erect, central conus. Because the conus is fragile and deeply embedded in segment 3, I am unable at present to describe it in detail, and the precise positions of the button and distal foramen have not been observed. Segment 3 is large, elongate, bilaterally compressed, with minute, unsegmented, subterminal arista or none and with the sacculus opening by a small pore on the ventrolateral surface before mid-length; the lateral and medial surfaces each support a number (9 to 12 or more) of shallow pits. These sensory pits each contain several club-like sensilla with thick, rounded apices (Fig. 69), probably to be classed as basiconic sensilla. Though such pits are of uncommon occurrence in acalyptrate schizophorans, similar ones are present on segment 3 of *Maorimyia bipunctata* (family Helcomyzidae), but they are differently distributed.

In *Cryptochetum* the elongate, centrally based conus, deeply inserted into the basal hollow of segment 3, resembles that of some conopids, some diopsids, and some milichiids (but probably not the more plesiomorphic taxa among the latter). Also, in the lower cyclorrhaphous family Phoridae the conus is deeply embedded in the centre of segment 3. The only claim of *Cryptochetum* to relationship to any of these families is to the Milichiidae, particularly in view of the interpretation of the venation of the anal region of *Cryptochetum* given by J. McAlpine (1989: 1476–1477). However, my thorough and prolonged investigation of the venation leaves no doubt that J. McAlpine was mistaken (see D. McAlpine, 2002), and that the venation of *Cryptochetum* (like that of *Librella*) approximates to that of the Ephydroidea (including Curtonotidae and Drosophilidae), not to that of the Milichiidae and Canacidae. Undoubtedly this development of the conus has evolved in a number of separate eremoneuran lineages, and is not always a reliable indicator of relationships.

The antennal structure of *Librella* is very different from that of *Cryptochetum*. Segment 2 is of a much more primitive form (Fig. 71). The rim expands on each side forming a broad lateral and a medial lobe, but these lobes are not approximated dorsally to produce the cucullate or cup-like condition as in most Ephydroidea (including Drosophilidae), but diverge from their origins on each side of the dorsal notch. The conus is stout, deep, and asymmetrical, slightly displaced on to the medial lobe of the rim, with the foramen facing dorsolaterally. Segment 3 (Fig. 72) is deep and bilaterally compressed, with medium-sized basal hollow and the foramen on a broad prominence near the margin of the hollow. The arista is three-segmented and of normal length.

I have examined the holotype (in amber) of *Phanerochaetum tuxeni* Hennig (ZMUC), and the most significant addition I have to add to the original description (Hennig, 1965) regards the relation of the free anal vein (vein 6, CuA+A1, or cu1b+1a) to the cell cup (or anal cell). Interpretation is difficult because there is partial separation of the wing surface from the amber, but reflected light off the wing surface gives an apparently more accurate representation than in Hennig's fig. 263, and indicates

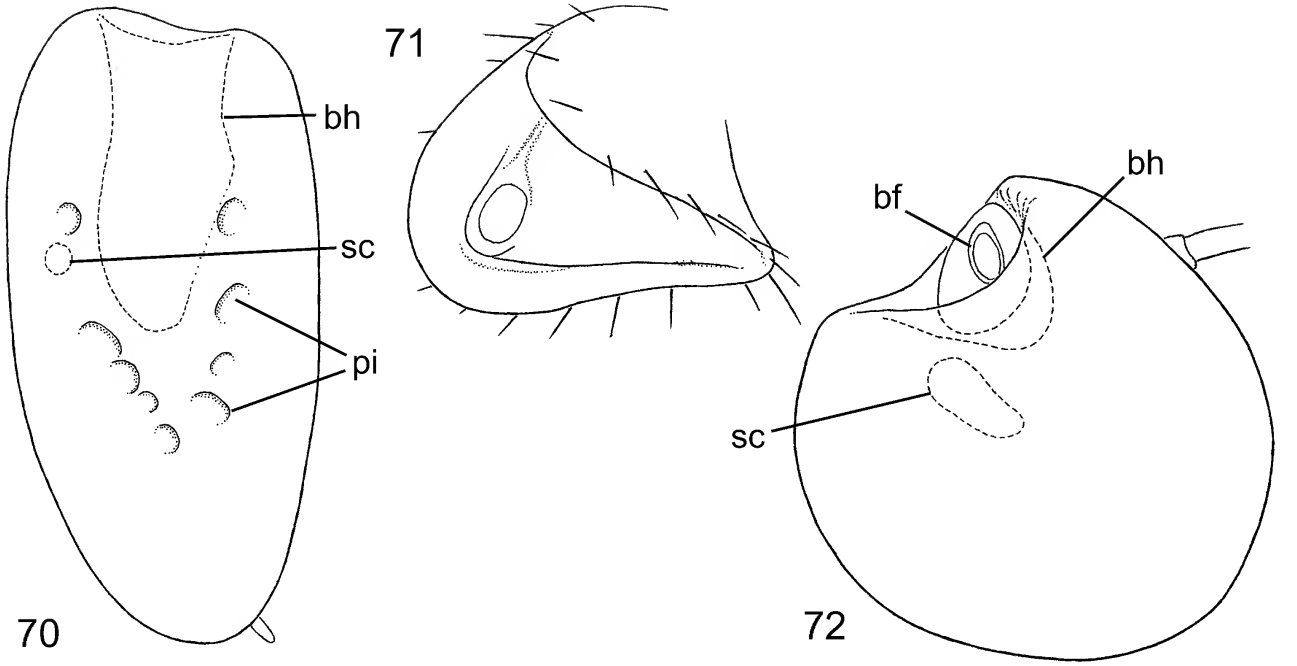

Figures 70–72. Antennae of Cryptochetidae. *(70) Cryptochetum* sp., seg. 3 of left antenna, medial view. *(71) Librella* sp., left seg. 2, lateral view. *(72)* The same, left seg. 3, medial view. *bf*, basal foramen; *bh*, basal hollow; *pi*, sensory pits; *sc*, sacculus.

that the anal cell is more like that of *Cryptochetum* and some ephydroid taxa, with anal crossvein strongly inclined distad and the vein delimiting the anal cell posteriorly little sclerotized. There is no trace of the basal crossvein, though Hennig (1969: fig. 43) found this to be distinct in a further specimen of *Phanerochaetum* (perhaps a second species).

The Ephydroidea

The following families of this superfamily are discussed below: Campichoetidae, Diastatidae, Curtonotidae, Drosophilidae, Ephydridae.

Some features and variation in the ephydroid antenna have been previously described, e.g., by Hennig (1971), and, in more detail, by Grimaldi (1990). Features common to all families include the great dorsal development of the pedicellar rim to form a pair of lobes separated by a narrow dorsal cleft (seam or slit), the adjacent margins of the two lobes usually appressed so that the cleft may not be obvious at low magnification, and the very asymmetrical conus. Typical caesti (separate from the annular ridge) are absent. The distal articular surface is particularly concave on its dorsolateral quarter (Fig. 73), or may abruptly give way to a deep cup containing the button and the sometimes much reduced conus

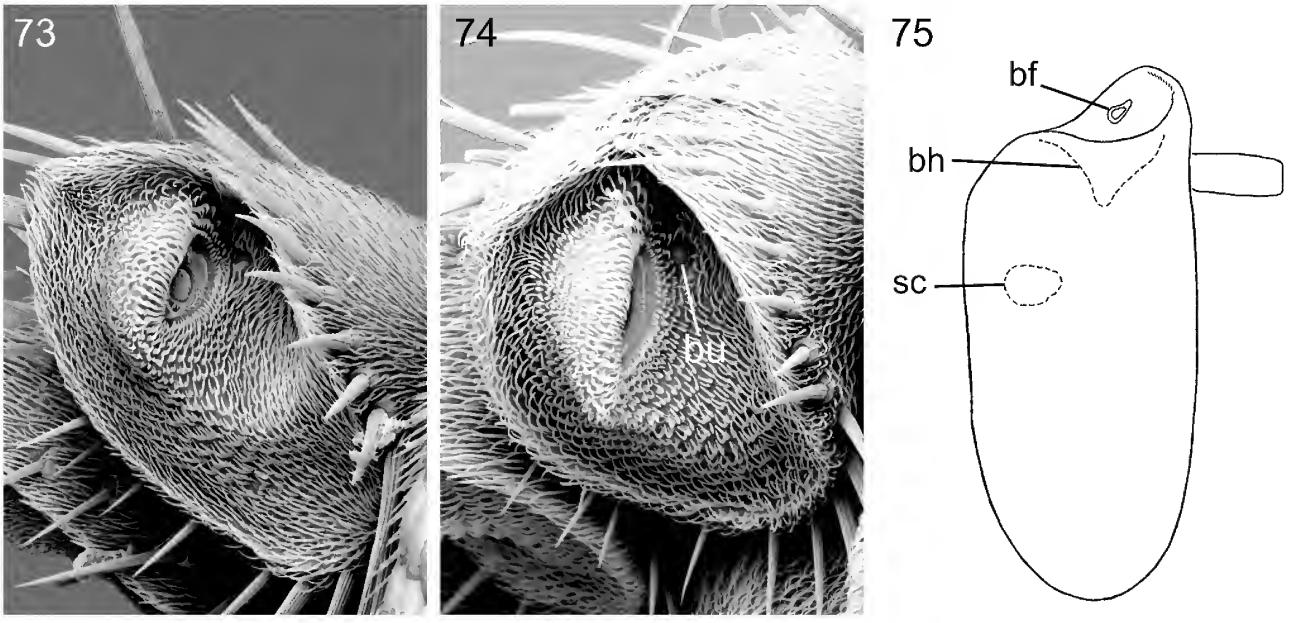

Figures 73–75. Antennae of Diastatidae and Campichoetidae. *(73)* Left antennal seg. 2 of *Diastata fuscula* (Fallén) (fam. Diastatidae), lateral view, seg. 3 removed. *(74) Campichoeta punctum* (Meigen) (fam. Campichoetidae), lateral view of seg. 2, seg. 3 removed. *(75)* The same, medial view of seg. 3. *bf*, basal foramen; *bh*, basal hollow; *bu*, pedicellar button; *sc*, sacculus.

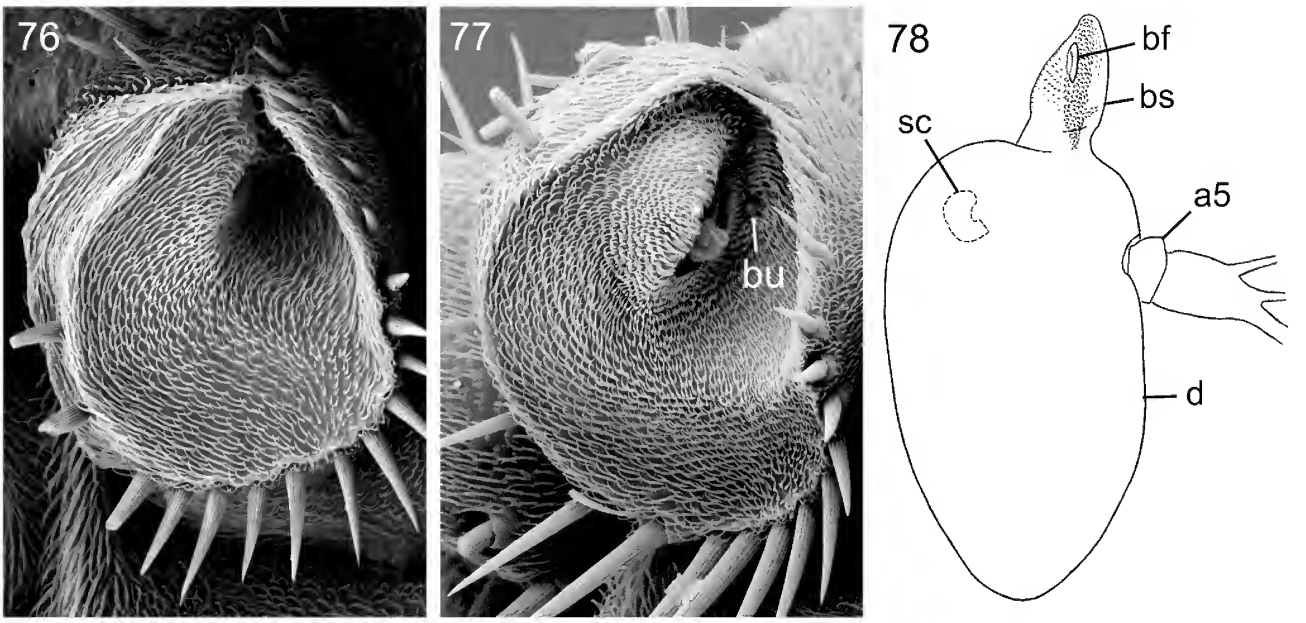

Figures 76–78. Antennae of Curtonotidae. *(76) Axinota pictiventris* Wulp, left seg. 2, seg. 3 removed, distolateral view. *(77) Cyrtona* sp., left seg. 2, similar view. *(78) A. pictiventris*, left seg. 3, medial view. *a5*, antennal seg. 5; *bf*, basal foramen of seg. 3; *bs*, basal stem; *bu*, pedicellar button; *d*, disc of seg. 3; *sc*, sacculus.

(Fig. 80). Several taxa show evidence of abrasive action using the dorsomedial surface of segment 2 (see p. 163).

Some of the apomorphies listed by J. McAlpine (1989: 1486) appear not to indicate accurately the groundplan condition for the superfamily, or are present in possible outgroups.

The Campichoetidae and Diastatidae

The antennae of *Campichoeta punctum* (Meigen) and *Diastata fuscula* (Fallén) have been studied.

In *Campichoeta* the distal articular surface of segment 2 (Fig. 74) is extensively concave, more deeply so on its lateral part, but there is no defined cup. The conus is located towards the medial side of this surface and is very asymmetrical. While the medial part of the conus is quite prominent, the part lateral to the foraminal ring is obsolete, so that the foramen and foraminal ring face laterally. The foraminal ring is crenulate laterally, but this condition is probably not homologous with the caestus of Neurochaetidae etc. The button is located on the articular surface a little laterally to the foraminal ring. Segment 3 (Fig. 75) has not a typical basal stem, but is more prominent dorsobasally than ventrobasally. The basal hollow is moderately large; the basal foramen is situated just beyond its medial margin and faces laterally. The sacculus is located slightly before mid length and has the usual lateral pore. The arista is three-segmented, with short annular segment 4 and long cylindrical segment 5.

The antenna of *Diastata* (Fig. 73) agrees in all essential details with that of *Campichoeta* as given above, the main differences being in proportions.

The Curtonotidae

The antennae of *Axinota pictiventris* Wulp (Figs 76, 78) and *Cyrtona* sp. (Karen, Kenya, Fig. 77) are here considered.

In *Axinota* segment 2 has the rim represented by a double ridge on its medial side. The distal articular surface is concave and more deeply recessed laterally to the conus. The conus is asymmetrical, broad and very short, with the foramen facing laterally. The foraminal ring is crenulate laterally as in *Campichoeta*, but is not entirely visible in the preparation. Segment 3 has a very marked differentiation into basal stem and distal disc. There is no basal hollow, and the caecum on the basal stem is minute. The basal stem bears the basal foramen on its ventromedial surface not far from its extremity. The arista lacks segment 4; segment 5 is very short and stout, and segment 6 is swollen basally.

The antenna of *Cyrtona* has a general resemblance to that of *Axinota*, with a few notable differences. Segment 2 lacks the additional ridge of the rim; the lateral part of the distal articular surface is less narrowly recessed so that the button is readily detected, just laterally to the foraminal ring; segment 3 has a less attenuated basal stem; segment 4 is distinctly sclerotized so that the arista is three-segmented.

The Drosophilidae

I have examined for this study the antenna of the following species: *Leucophenga scutellata* Malloch, *Scaptomyza australis* Malloch, *Drosophila (Drosophila) immigrans* Sturtevant, *Drosophila (Sophophora) melanogaster* Meigen, *Tambourella endiandrae* Wheeler. Grimaldi (1990) has given information and figures for some additional species. The true drosophilids (*sensu* Grimaldi, 1990) have many features in common with the Campichoetidae and Diastatidae, as discussed above, but are, to varying degrees, more apomorphic. All those studied by me have the conus short, asymmetrical, and undeveloped on the lateral side of the asymmetrically directed foramen.

In *Leucophenga* (Fig. 79) segment 2 has no well defined cup, but the distal articular surface deepens much dorsolaterally so that the button is almost concealed. Segment

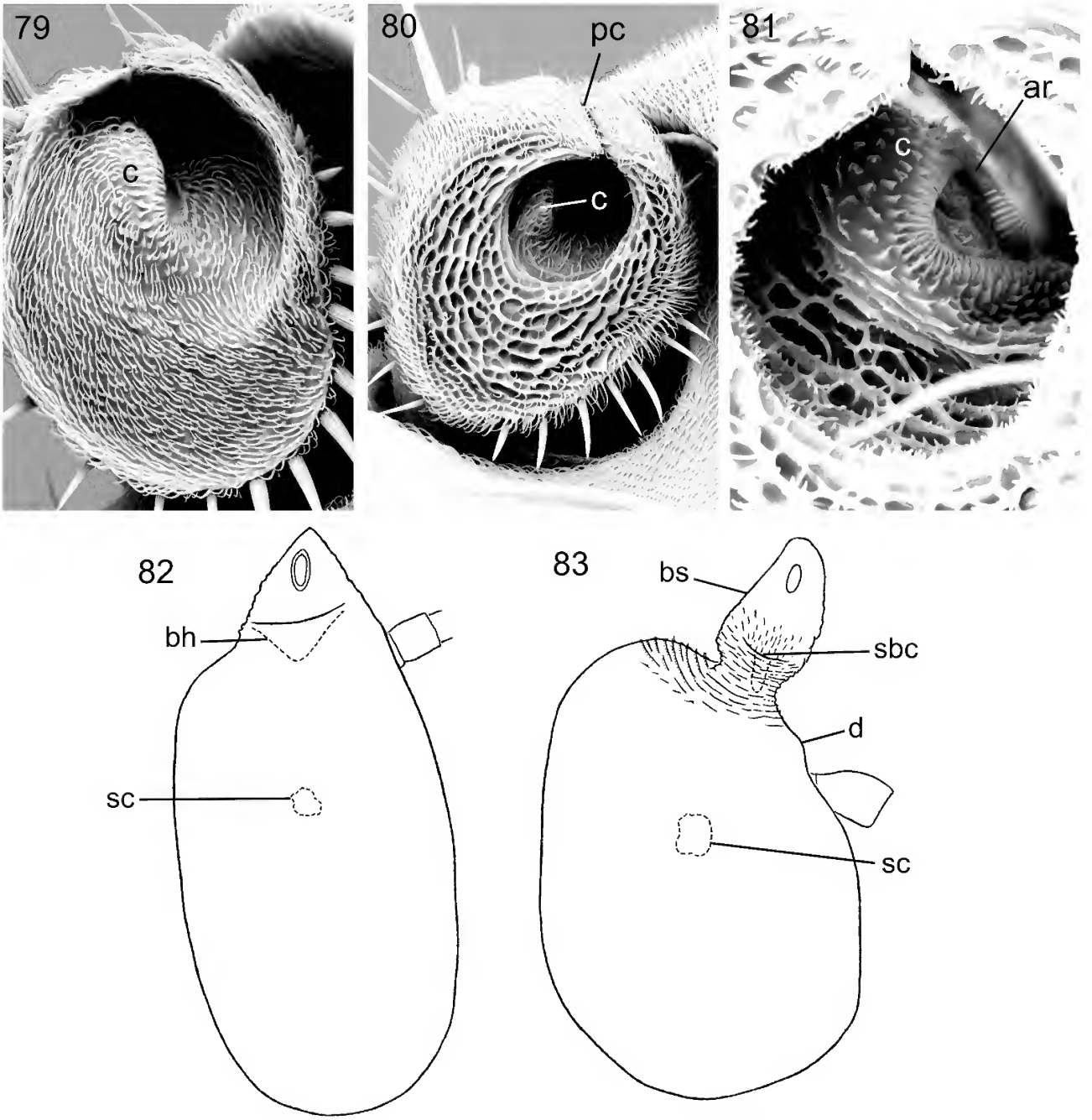

Figures 79–83. Antennae of Drosophilidae. *(79) Leucophenga scutellata* Malloch, distal articular surface of seg. 2. *(80) Drosophila immigrans* Sturtevant, the same. *(81) Tambourella endiandrae* Wheeler, contents of pedicellar cup. *(82) L. scutellata*, left seg. 3, medial view. *(83) T. endiandrae*, the same. *ar*, annular ridge of seg. 3; *bh*, basal hollow; *bs*, basal stem; *c*, conus; *d*, disc of seg. 3; *pc*, pedicellar cleft; *sbc*, sub-basal caecum; *sc*, sacculus.

3 (Fig. 82) has a basal stem, but this is broad where it joins the disc and less sharply defined than in the other genera. The moderately developed basal hollow opens on the broader part of the basal stem.

In *Drosophila* spp. and *Tambourella* the distal articular surface gives way much more abruptly to a deep, narrow cup into which the very short conus is sunken, but there is no raised collar (Figs 80, 81). Usually segment 3 has the basal stem well defined and more or less attenuated (Fig. 83). The basal hollow is generally present in some form, in contrast to the Curtonotidae, but may be contracted to a narrow caecum located on the basal stem. The arista is usually three-segmented.

The Ephydridae

For this study I examined the antennae of the following species: *Ochthera pilimana* Becker, *Scatella* sp., *Ephydrella marshalli* Bock, *Paralimna calva* Bock, *Hydrellia tritici* Coquillett, *Stratiothyrea cheesmanae* Cogan, *Risa longirostis* Becker, "ephydrid genus E", which includes several Australian species living in saline habitats. I previously examined the arista of numerous ephydrid taxa (D. McAlpine, 2002), and found it to be usually two-segmented through loss of segment 4, but in a few cases it is even further reduced. Wirth *et al.* (1987: particularly figs 41–44) show some of the variation in antennal form in the family.

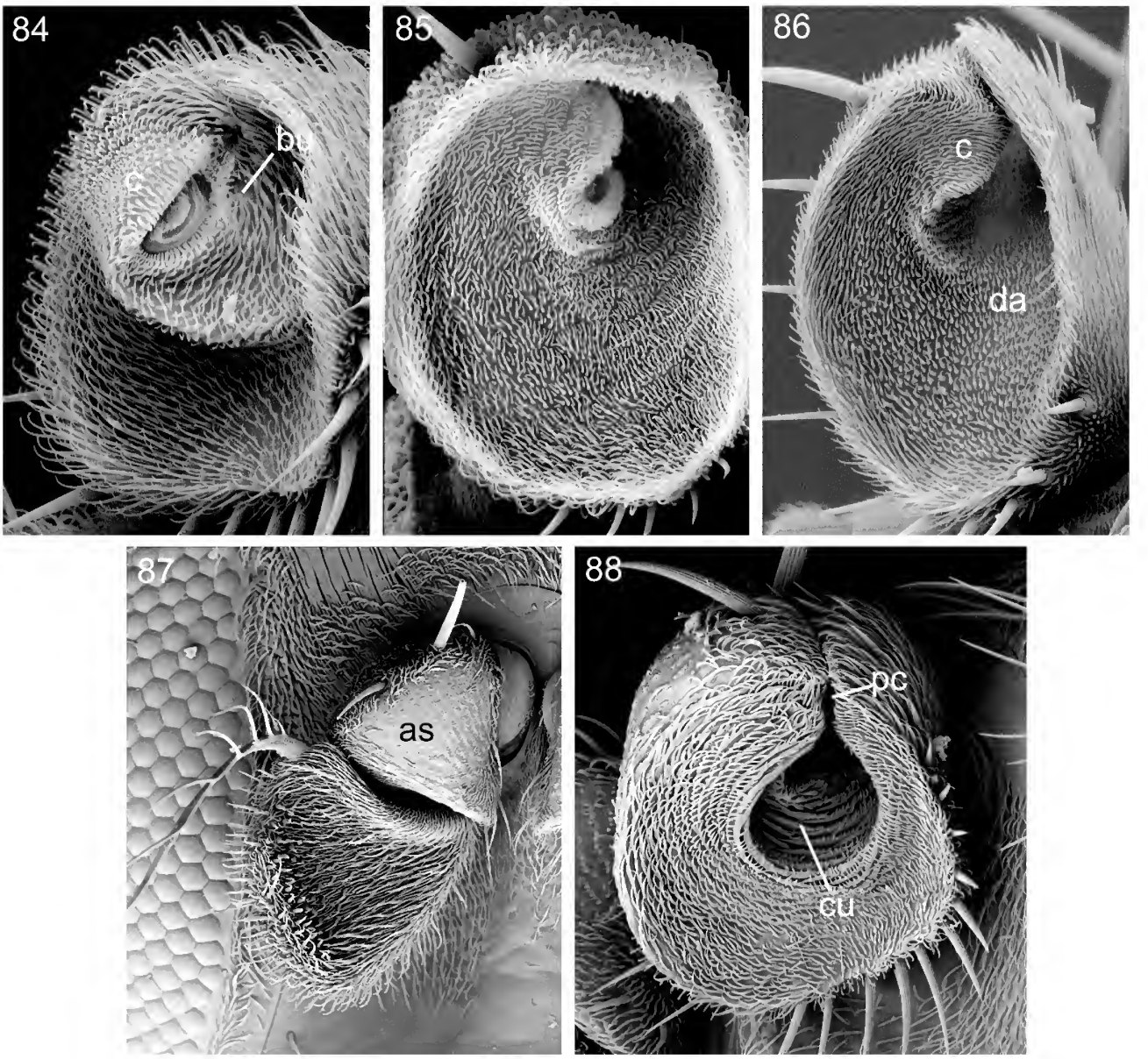

Figures 84–88. Antennae of Ephydridae. *(84) Ephydrella marshalli* Bock, left seg. 2, seg. 3 removed, distolateral view. *(85) Paralimna calva* Bock, the same view. *(86) Hydrellia tritici* Coquillett, the same view. *(87) Stratiothyrea cheesmanae* Cogan & Wirth, right antenna. *(88)* The same, left seg. 2, distal view, seg. 3 removed. *as*, abraded dorsomedial surface of seg. 2; *bu*, pedicellar button; *c*, conus; *cu*, pedicellar cup; *da*, distal articular surface; *pc*, pedicellar cleft.

Antennal structure in the family Ephydridae shows most of the range of variation occurring in the superfamily Ephydroidea (Figs 84–93). In *Scatella* and *Ephydrella* the conus arises from the medial side of the distal articular surface and is seen to project markedly beyond it in medial view; a ridge extends from the ventral base of the conus across the articular surface, defining a shallow cup-like depression which occupies the dorsolateral part of the surface. The annular ridge and foramen are asymmetrical and face laterally. Segment 3 has a shallow basal hollow, deepening to a central pit. The basal foramen is located in a concavity on a broadly rounded prominence on the margin of the hollow, which could be regarded as an incipient basal stem. The pore of the sacculus is located laterally, far from the ventral margin. In segment 2 of *Ochthera* the conus is somewhat similar but there is no transverse ridge extending from its base. Segment 3 has a distinct but short basal stem. *Hydrellia* and *Paralimna* have a more reduced conus, and, although the distal articular surface is markedly and narrowly deeper dorsolaterally, there is no defined cup. Segment 3 has a definite basal stem which is not strongly narrowed, though tapering to a point in *Paralimna*. In *Stratiothyrea* the distal articular surface of segment 2 is almost flat on much of its extent, with narrow dorsal cleft and very deep abrupt subcentral cup quite unlike any of the above examples. The conus is almost absent and the annular ridge is located only slightly asymmetrically on the floor of the cup. Segment 3 is markedly differentiated into the narrow, digitiform basal stem and broad disc; the rather narrow sub-basal caecum opens on to the medial surface of the stem a little distance from the disc; there is a slight indication of a separate basal hollow on the medial side of

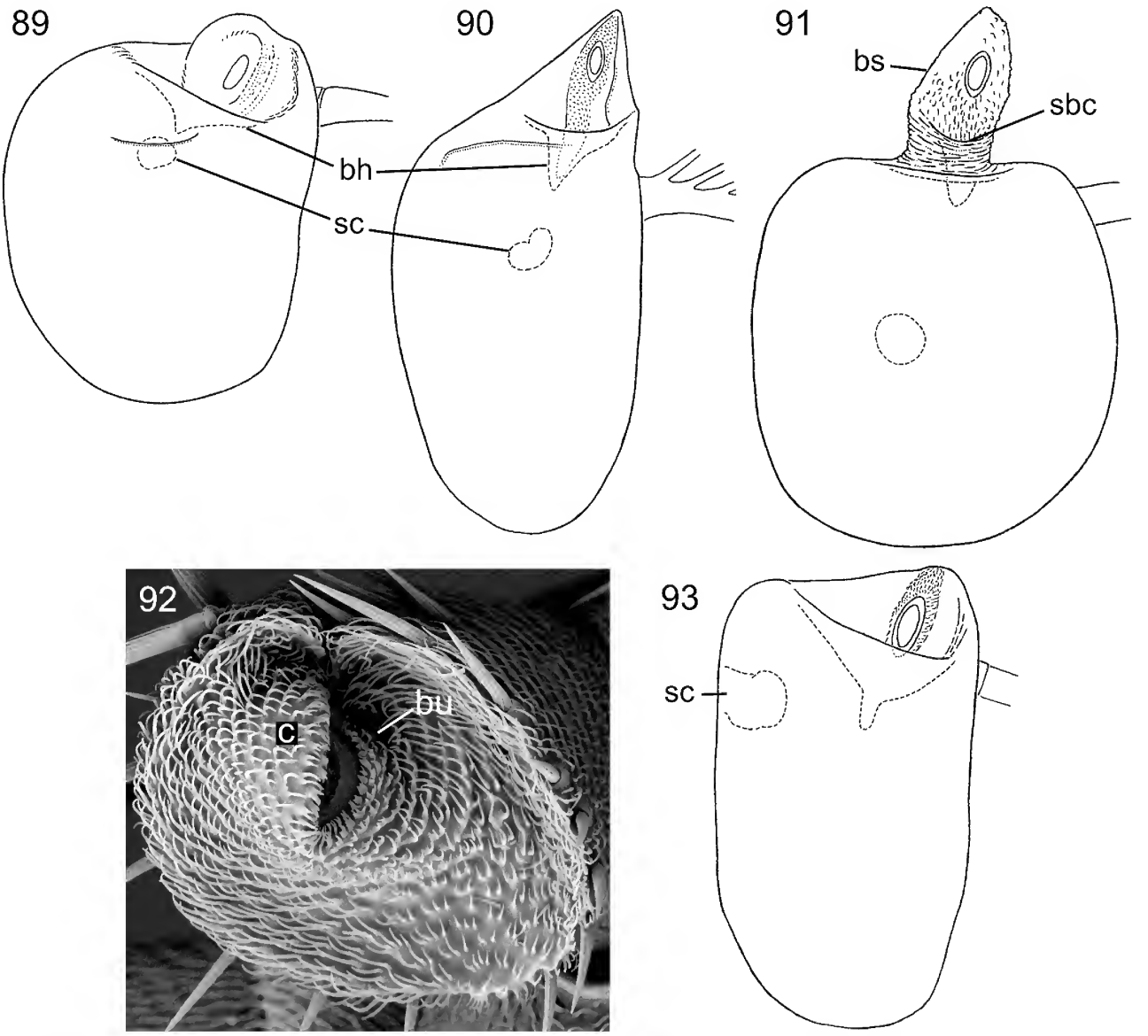

Figures 89–93. Antennae of Ephydridae. *(89) Scatella* sp., left seg. 3, medial view. *(90) Paralimna calva* Bock, the same. *(91) Stratiothyrea cheesmanae* Cogan & Wirth, the same. *(92)* Ephydrid genus E, Innaminka, S. Aust., left seg. 2, distal view, seg. 3 removed. *(93)* Ephydrid genus E, Lake Hindmarsh, Vic., left seg. 3, medial view. *bh*, basal hollow; *bs*, basal stem; *bu*, pedicellar button; *c*, conus; *sbc*, sub-basal caecum; *sc*, sacculus.

the broad basal surface of the disc. The antennal structure of *Stratiothyrea* is remarkable for its resemblance to that of such advanced drosophilids as *Tambourella*, evidently through detailed convergence. Like these two genera, *Camilla acutipennis* (Loew) (family Camillidae) also has an elongate basal stem (Hennig, 1971: fig. 8).

In "ephydrid genus E" segment 2 (Fig. 92) is more elongate than that of many ephydrids, with the lobe on the medial side of the dorsal seam more prominent than that on the lateral side; the distal articular surface is less deeply concave than that of most ephydrids and without any suggestion of a cup-like cavity; the conus is relatively narrow, but strongly projecting and arising close to the medial dorsal lobe; the foramen faces entirely laterally. Segment 3 (Fig. 93) has no basal stem; the basal foramen is on a slight scabrous prominence on the lateral margin of the basal hollow; the hollow is capacious, tilted medially, and its floor has a narrow caecum-like extension; the pore of the sacculus is in a ventral position, as in *Risa*, but in contrast to other examined ephydrids, which have it in a lateral position. The arista lacks segment 4; segment 6 is numerously and irregularly pubescent on c. the basal 0.4 of its length, but beyond this has only a dorsal series of c. 10 very short rays. The arista is thus fairly typical of the Ephydridae, while some other features, including the ventral position of the sacculus, the elongate prementum of the proboscis, the characteristic facial contour, the prominent vibrissa, the milky-white wing membrane, the rather long unpigmented but slightly sclerotized crease representing vein 6, and the almost complete suture separating abdominal tergites 1 and 2, suggest placement in the subfamily Risinae, which was formerly given separate family status.

The Mormotomyiidae

There has been difficulty in determining the relationships of this family within the Schizophora (see Kirk-Spriggs *et al.*, 2011, for most recent discussion). The only included species, the subapterous *Mormotomyia hirsuta* Austen, is only known from the type locality, Ukasi [Ukazzi] Hill, Eastern Province, Kenya, where all stages are associated with bat dung. Ashley Kirk-Spriggs has generously supplied adult males for antennal study (Figs 178–181, see p. 162). Hennig (1971) has described some features of the antenna.

Segment 2 is subconical in outward form; the cleft is long and deep, completely dividing the paired dorsal lobes of the rim, but their adjacent margins remain in contact (Fig. 178). The distal articular surface (Fig. 179) is deeply concave, extensively microtrichose, with some of the microtrichia grouped into combs, but without parallel or reticulate ridging. There is no well defined pedicellar cup, but the laterodorsal part of the surface has a deeper bowl-like concavity containing the conus, somewhat as in *Leucophenga*. The conus is asymmetrically developed, obsolete on the lateral side of the foramen, moderately prominent on the medial side, and well removed from the medial margin of the rim. The annular ridge is indistinct and the foramen is inclined laterally. The pedicellar button (Fig. 180) is located near the dorsolateral part of the annular ridge, but is weakly developed or almost indistinguishable externally.

Segment 3 (Fig. 181) has a broadly rounded, not well defined basal stem, with the basal foramen facing medially. The basal hollow is broad and of moderate depth. The sacculus is capacious, with relatively small pore near centre of lateral surface of disc. The three-segmented arista arises laterodorsally towards the base of the disc.

The deep pedicellar cleft of *Mormotomyia* is similar to that occurring in both the Ephydroidea and the Calyptratae. However, the asymmetrical conus, with laterally (not dorsally) inclined foramen, and the sclerotized prothoracic precoxal bridges are typical of the Ephydroidea, not of the Calyptratae. The general structure of the antenna is reminiscent of *Leucophenga*, a somewhat plesiomorphic example of the Drosophilidae, or could be classed between the more plesiomorphic and more apomorphic taxa of the Ephydridae (Figs 84–93). The three-segmented arista, the location of the preabdominal spiracles in the pleural membrane, and, in the male, the large tergite 6 and asymmetrical sternite 6 place *Mormotomyia* outside the limits of the Ephydridae, but general antennal structure supports its position in the Ephydroidea suggested by Kirk-Spriggs *et al.* (2011).

The Neurochaetidae and Periscelididae

These families share a distinctive antennal structure including possible synapomorphies, but only if the genera *Cyamops* and *Stenomicra* are omitted from consideration. The two last genera are so different that their antennae will be described separately (as subfamily Stenomicrinae). For comment on the recently published phylogenetic association of the Neurochaetidae with the Pallopteridae see p. 150.

Because of availability and ease of exposure of parts of segment 2, I describe the antenna of *Nothoasteia clausa* McAlpine first (Figs 94–96), and then draw comparisons with other taxa. Segment 2 is deflexed so that its broad distal articular surface faces downwards (Fig. 94). The rim forms a pair of dorsal lobes separated by a deep slit, or cleft, but their margins are not appressed as in the Ephydroidea. The medial lobe is larger than the lateral lobe, but the lobes are not as large and cucullate as in some related genera (e.g., *Neurochaeta*), so that most details of the articular surface are exposed by disarticulation (Fig. 95). The conus is absent. The distal articular surface is extensively microtrichose, with the ventral part extensively almost flat, the dorsal part with centrally placed shallow concavity almost filled by the nearly symmetrical, distally facing, complete annular ridge. The annular ridge is armed with two to three dense irregular encircling series of incurved spinescent microtrichia. A well-developed button is located just outside the annular ridge slightly dorsad of a mid-lateral position. There is a well-developed nodulose caestus on each side between the annular ridge and the foraminal ring. The latter is rather prominent and produced into a blunt cusp dorsally and ventrally. The short oval foramen faces distally and is approximately symmetrically placed, both within the annular ridge and on the segment as a whole.

Segment 3 of *Nothoasteia clausa* (Fig. 96) consists of a short, stout basal stem and rounded disc. The basal foramen is on the mid-ventral surface of the basal stem, in accordance with the symmetrically placed distal foramen of segment 2. The scabrous tongue is finely, irregularly ridged and runs from the basal extremity of the medial surface of the basal stem distad into the basal caecum of the disc. The ventrobasal surface of the disc has a shallow secondary cavity or postpedicellar pouch just beyond the opening of the basal cavity. Such secondary cavity has not been observed in other genera. The sacculus opens near the centre of the lateral surface of the disc.

The arista of *Nothoasteia clausa* lacks any trace of segment 4. Segments 5 and 6 are symmetrical, without trace of the oblique base of segment 6 seen in *Cyamops*, *Periscelis*, and some other genera. Segment 6 and the short segment 5 are both pubescent, the hairs beyond the basal enlargement of segment 6 tending to form slightly differentiated but not seriate rays which extend to the apex. In one specimen examined segments 5 and 6 appear to be fused, leaving no visible suture under high magnification of CLM, but in other specimens there is a visible suture but no annular membrane between these segments.

In the neurochaetid *Neurotexis primula* McAlpine the essential structure of segment 2 resembles that of *Nothoasteia* with some difference in proportions. The dorsal lobes are larger than in *Nothoasteia* but do not conceal much of the distal articular surface. The part of the dorsal articular surface immediately below the annular ridge is almost devoid of microtrichia but bears a reticulate pattern of fine, prominent ridges, which give way to an irregular covering of separate microtrichia towards the ventral margin. The button is larger than that of *Nothoasteia* but similarly located. The annular ridge is more vertically elongate than in *Nothoasteia* but has similar armature. The caesti are more vertically elongate and diffuse, with weak, almost horizontal nodulation.

I previously mentioned (D. McAlpine, 1993) the general features of segment 3 and the arista in *Neurotexis* spp., and illustrated the antenna of *Neurotexis freidbergi* McAlpine (D. McAlpine, 1993: fig. 8). This and *N. primula* have the basal stem longer than in *Nothoasteia* and the disc narrower and more ovate. In *Neurotexis freidbergi* the arista is three-

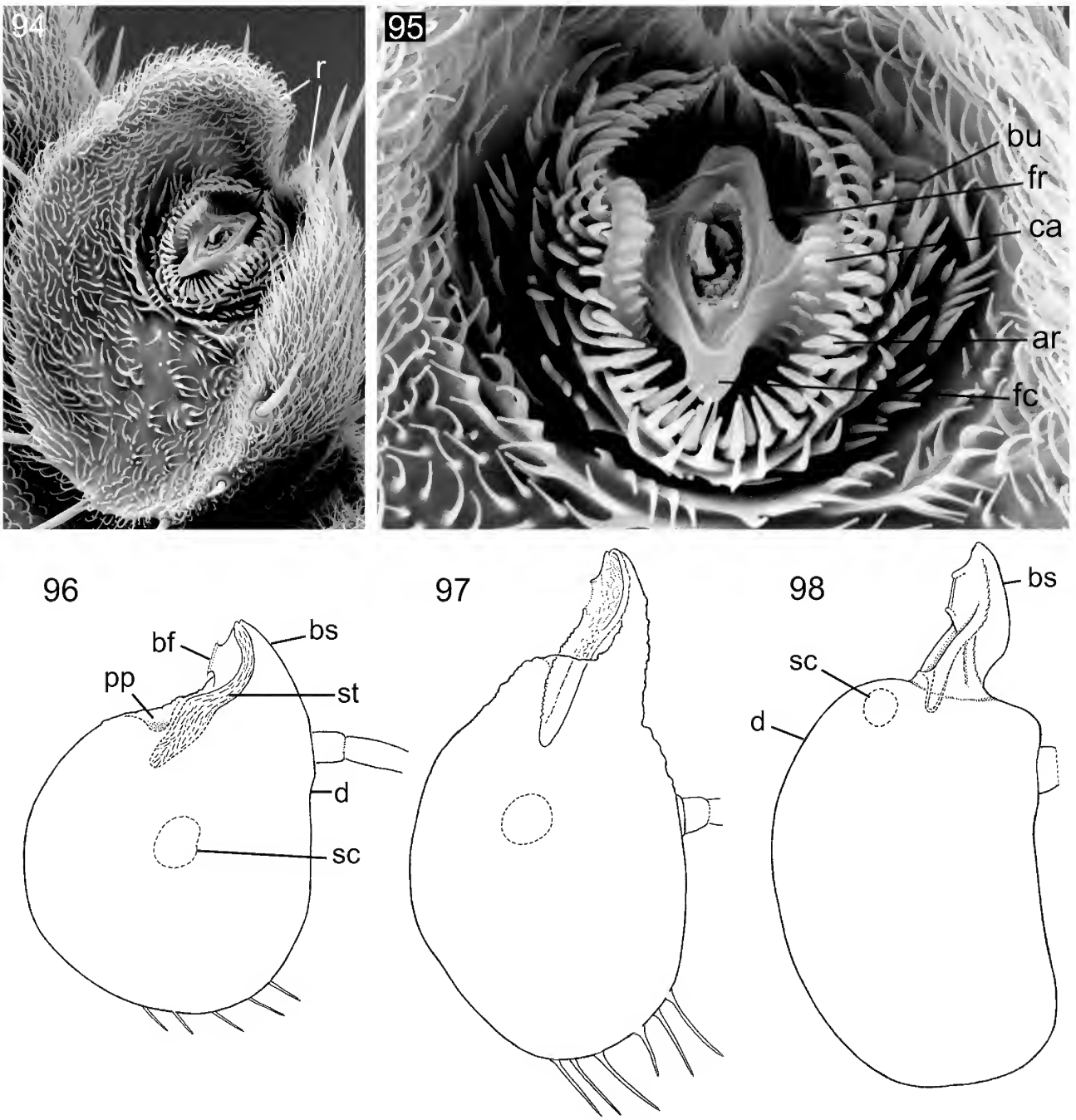

Figures 94–98. Antennae of Neurochaetidae and Periscelididae. *(94) Nothoasteia clausa* McAlpine, left seg. 2, distal view, seg. 3 removed. *(95)* The same, annular ridge of seg. 2 and associated structures. *(96)* The same, left seg. 3, medial view. *(97) Neurochaeta inversa* McAlpine, left seg. 3, medial view. *(98) Periscelis fasciata* Mathis, the same. *ar*, annular ridge; *bf*, basal foramen; *bs*, basal stem; *bu*, pedicellar button; *ca*, caestus; *d*, disc of seg. 3; *fc*, foraminal cusp; *fr*, foraminal ring; *pp*, postpedicellar pouch; *r*, dorsal lobes of rim; *sc*, sacculus; *st*, scabrous tongue.

segmented, with segments 4 and 5 small; in *N. primula* segment 5 is very short and distinct, but segment 4 is not clearly defined, perhaps fused with segment 3. Segment 6 has long dorsal and ventral rays and fewer short medial rays. It has not been possible to locate the sacculus in preparations because of the irregularly roughened cuticle of segment 3.

The antenna of *Neurochaeta inversa* McAlpine resembles that of *Neurotexis primula* in most features. The dorsal lobes of segment 2 are more deeply cucullate than in that species making examination of the dorsal part of the distal articular surface more difficult. The part of this surface ventral to the annular ridge is almost devoid of microtrichia, but has a reticulate pattern of ridges resembling *N. primula*. The incurved spinescent microtrichia on the annular ridge are particularly large and dense on the more ventral part of the ridge, but are less developed dorsally. The button could not be located, possibly because of difficulty in exposing the more dorsal part of the articular surface. The caesti are short, compact, and prominently raised, with relatively few nodules.

Segment 3 of *Neurochaeta inversa* (Fig. 97) resembles that of *Neurotexis primula* in most features, but the basal cavity, with its contained extension of the scabrous tongue, is

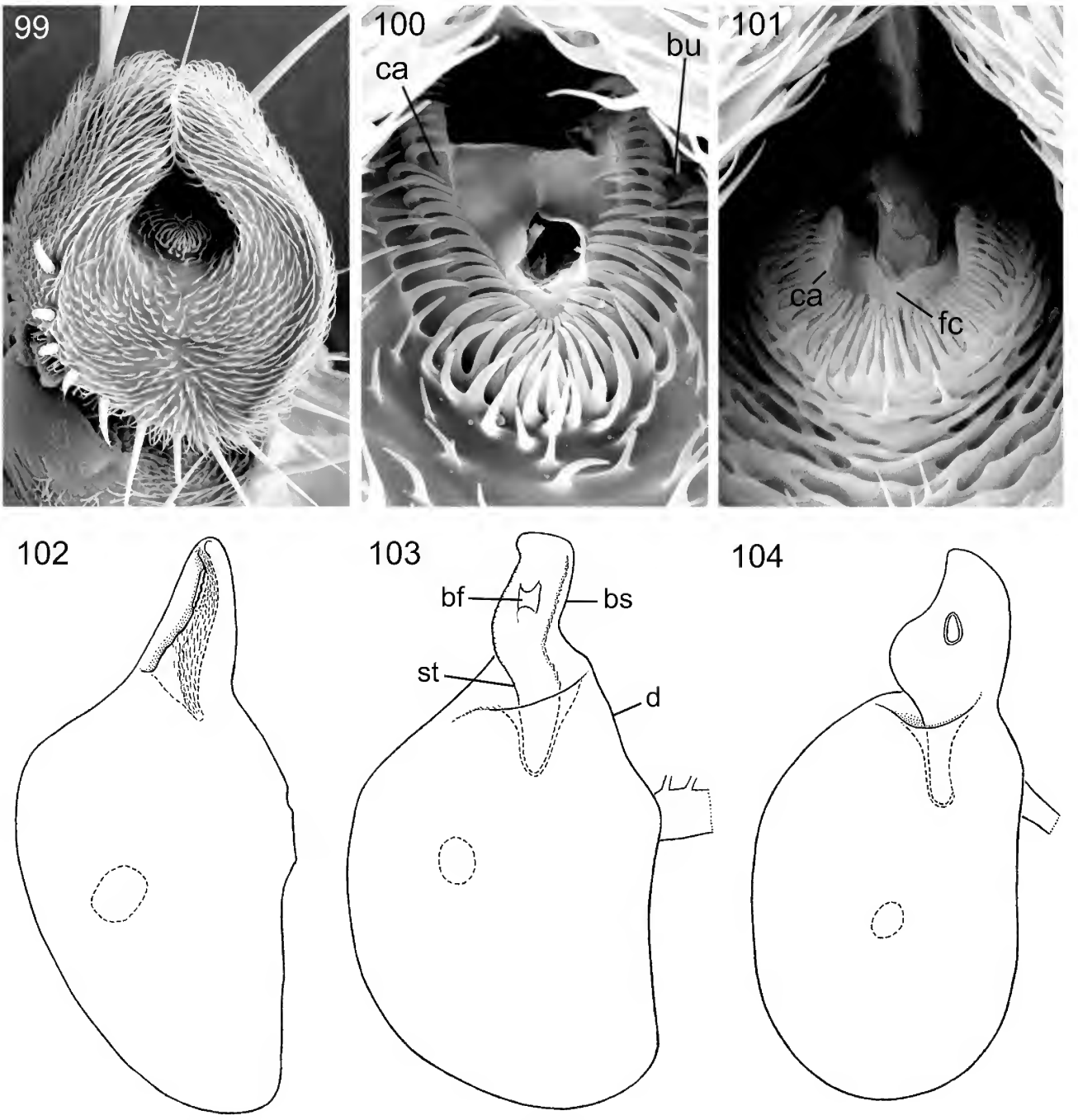

Figures 99–104. Antennae of Periscelididae. *(99) Periscelis fasciata* Mathis, right seg. 2, distal view, seg. 3 removed. *(100)* The same, annular ridge and associated parts. *(101) Planinasus* sp. (Brazil), annular ridge and associated parts of left antenna. *(102) Planinasus* sp. left seg. 3, medial view. *(103) Stenomicra* "sp. B" (Upper Allyn, N.S.W.), the same view. *(104) Cyamops* sp. (Tuglo, N.S.W.), the same. *bf*, basal foramen of seg. 3; *bs*, basal stem; *bu*, pedicellar button; *ca*, caestus; *d*, disc of seg. 3; *fc*, foraminal cusp; *st*, scabrous tongue.

deeply elongate, and none of the larger, fringing microtrichia is forked. There is a well-developed sacculus opening near the centre of the lateral surface of the disc.

The arista of *Neurochaeta inversa* resembles that of *Neurotexis* spp. in general features. Segments 4 and 5 are both very short, microtrichose, and approximately symmetrical.

I have examined segments 2 and 3 in *Periscelis fasciata* Mathis, and segment 3 and the aristal segments in *Periscelis annulata* (Fallén). Segment 2 of *P. fasciata* (Figs 99, 100) has much in common with that of the neurochaetids described above. The paired dorsal lobes are subequal, large and appressed, so that part of the distal articular surface is sunk in a cup, which is well differentiated from the rest of the distal articular surface. The part of the distal articular surface ventral to the annular ridge is clothed with many simple irregularly placed microtrichia and has no ridges. The structures on the distal articular surface are approximately symmetrical and symmetrically placed. The annular ridge resembles that of *Nothoasteia* and other neurochaetids, but its dorsal part is not visible in the preparation. The button is small and located near the outer lateral side of the ridge. The caesti are present, but elongate and not very prominent.

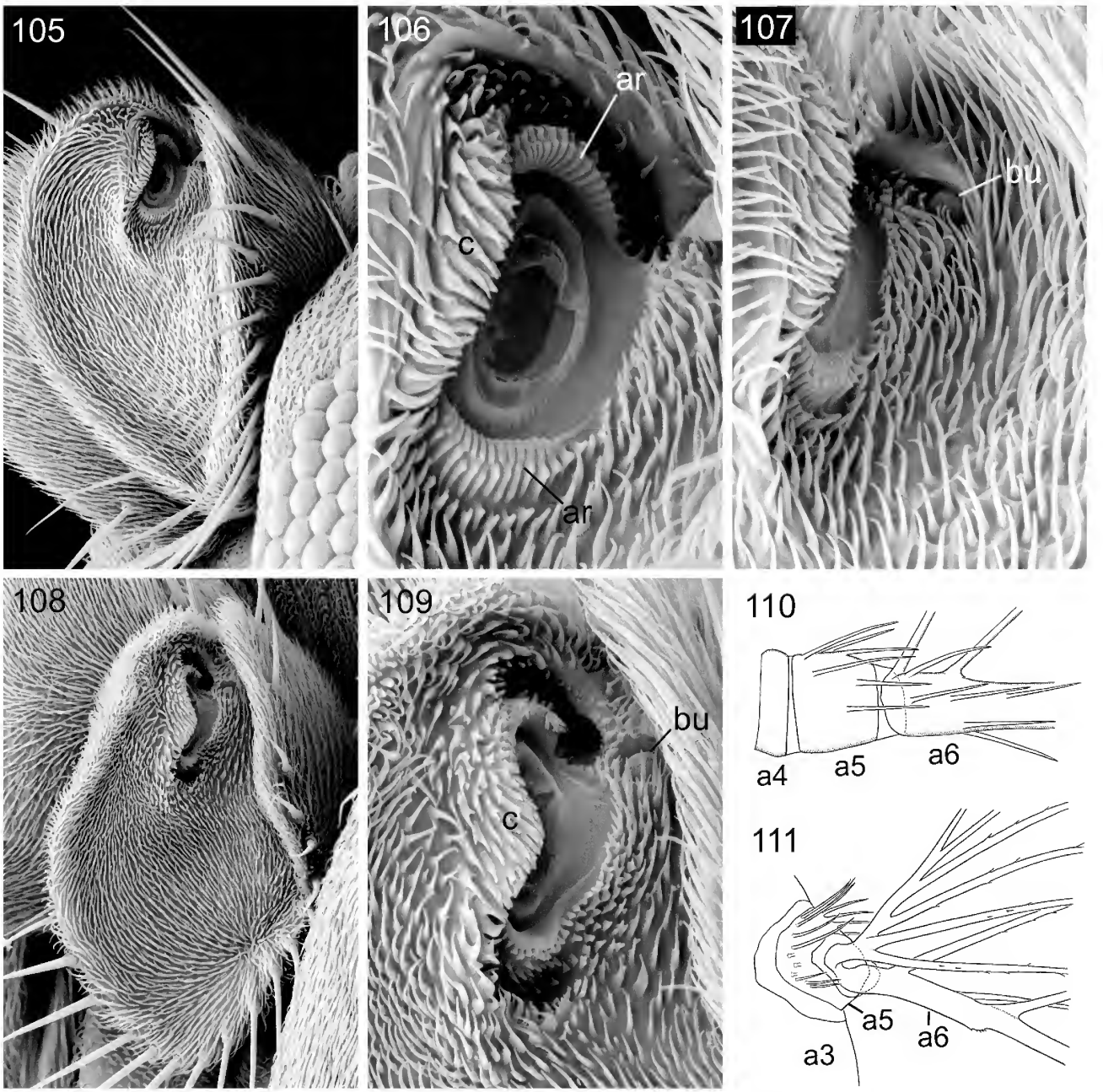

Figures 105–111. Antennae of Periscelididae. *(105) Stenomicra* "sp. NB" (Woitape, P.N.G.), left seg. 2, lateral view, seg. 3 removed. *(106)* The same, detail of annular ridge and adjacent parts. *(107)* The same, more distal view of same region. *(108) Cyamops* sp. (Tuglo, N.S.W.), left seg. 2, lateral view. *(109)* The same, detail of annular ridge and adjacent parts. *(110) Periscelis annulata* (Fallén), part of right arista. *(111) Planinasus* sp. (Brazil), part of right arista. *a3–a6*, antennal segments three to six; *ar*, annular ridge; *bu*, pedicellar button; *c*, vestige of conus.

In both *Periscelis fasciata* (Fig. 98) and *P. annulata* the basal stem of segment 3 is more abruptly narrowed and set off from the disc than in *Neurotexis* and *Neurochaeta*. The sacculus is located very near the ventral base of disc in both species (as it is also in *Scutops fascipennis* Coquillett), instead of the more central position on the lateral surface as in the other periscelidid taxa studied and in the neurochaetids.

As previously pointed out (D. McAlpine, 2002) the arista of the more typical Periscelidinae (e.g., *Periscelis* and *Scutops*) is three segmented with asymmetrical segment 5, and the base of segment 6 is obliquely fitted to the distolateral surface of segment 5 (Fig. 110). I have noted also that in a paratype of the periscelidid *Diopsosoma primum* Malloch (in BMNH) segment 6 is asymmetrical basally.

The genus *Planinasus* is placed in the Periscelididae in most recent literature, and sometimes in the subfamily Stenomicrinae (e.g., Grimaldi & Mathis, 1993). I find the antennal structure of *Planinasus* sp. (N. Friburgo, Brazil) to resemble more closely that of the subfamily Periscelidinae (Figs 101, 102). Segment 2 shows most of the features seen in the Periscelidinae and Neurochaetidae. These include the pair of large, cucullate dorsal lobes, the nearly symmetrical structure of the distal articulatory surface and annular ridge, the pair of prominent caesti, and the centrally located, distally

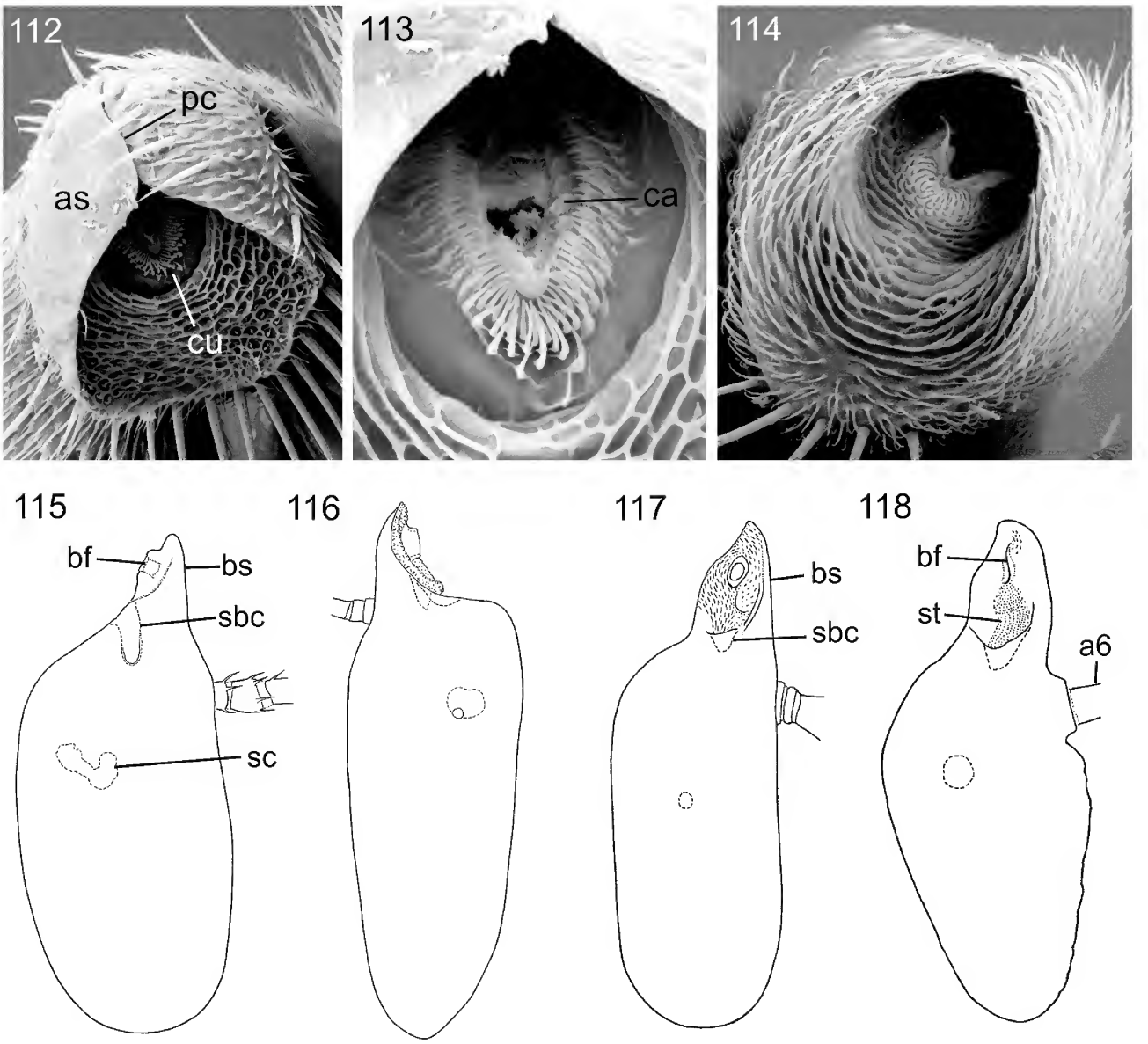

Figures 112–118. *(112) Chyliza* sp. (Imbia, P.N.G.; fam. Psilidae), left antennal seg. 2, distal view, seg. 3 removed. *(113)* The same, annular ridge and associated parts within pedicellar cup. *(114) Syringogaster* sp. (Costa Rica; fam. Syringogastridae), left antennal seg. 2, distal view. *(115) Chyliza* sp., left antennal seg. 3, medial view. *(116) Syringogaster* sp. left antennal seg. 3, lateral view. *(117) Nothybus decorus* de Meijere (fam. Nothybidae), left antennal seg. 3, medial view. *(118) Gobrya cyanea* (Enderlein) (fam. Gobryidae), the same. *a6*, antennal seg. 6; *as*, abraded surface; *bf*, basal foramen; *bs*, basal stem; *ca*, caestus; *cu*, pedicellar cup; *pc*, pedicellar cleft; *r*, dorsal lobes of rim; *sbc*, sub-basal caecum; *sc*, sacculus; *st*, scabrous tongue.

facing foramen. The part of the distal articulatory surface below the annular ridge has many, more or less transverse ridges supporting many microtrichia. The button is present just outside the lateral part of the annular ridge. The basal cavity of segment 3 opens obliquely along the basal stem (Fig. 102). It thus contains the elongate, somewhat obliquely facing basal foramen and the greater part of the scabrous tongue. The sacculus is located near mid-length of the disc.

The arista of *Planinasus* (Fig. 111) lacks segment 4. Segment 5 is dilated to cover much of the membranous socket of segment 3. It is asymmetrical and partly microtrichose. Segment 6, with its complex branching, is bifurcate from the base which is oblique—desclerotized on its medial side—to fit the oblique distal articular foramen of segment 5.

The most typical genera of the subfamily Stenomicrinae here considered are *Stenomicra* and *Cyamops* (Figs 103–109). In these segment 2 has the distal articular foramen and associated parts much more asymmetrical than in the Periscelidinae and Neurochaetidae, and more like that of the ephydrid genera *Hydrellia* and *Paralimna*. The reduced conus is present only on the medial side of the foramen as an irregularly rounded ridge, and the foramen faces laterally from inside this conus-remnant. The annular ridge with its dentate armature is variably developed, and is concealed by the conus-remnant from most angles. The button is located near the lateral margin of the foramen. Caesti are absent. Segment 3 has a very prominent basal stem (when disarticulated), with its basal foramen located

asymmetrically on its lateral surface (Figs 103, 104). Some *Stenomicra* spp. have the annular ridge and button more deeply recessed than in Figs 105–107 and difficult to examine.

These facts suggest that a rearrangement of genera within the currently recognized taxa Stenomicrinae (*sensu* Grimaldi & Mathis, 1993), Periscelidinae, and Neurochaetidae may be necessary. I do not formally make this reclassification because (1) I do not have access to a wide enough range of material, (2) the degree of symmetry in the articulation between segments 5 and 6 suggests a different segregation of taxa from that indicated by the structure of segment 2, (3) some other schizophoran families (e.g., Ephydridae) possess a comparable range of variation to that of Periscelididae s.l., (4) some of the distinctive features shared by Neurochaetidae and Periscelididae appear in other acalyptrate families (e.g., the Psilidae, see below), and (5) any major reclassification should take into consideration further evidence in addition to antennal morphology. Also, the Neurochaetidae should perhaps retain family status as a derivative or close relative of the Eocene genus *Anthoclusia*, possessing a more complete series of fronto-orbital bristles and a symmetrical antennal segment 5, in contrast to the genera recently placed in both the Periscelidinae and Stenomicrinae (see D. McAlpine, 1983).

The Psilidae and Syringogastridae

These families have been placed in the superfamily Diopsoidea by D. McAlpine (1997). Examples of Psilidae used for detailed antennal study include *Chyliza* sp. (from Imbia, Papua New Guinea, Figs 112, 113, 115) and *Psila fimetaria* (Linné) (from Switzerland). Specimens of *Syringogaster* spp. (from Costa Rica, Figs 114, 116, and Brazil) were used.

The Psilidae have often been characterized as having segment 2 with a dorsal cleft, slit, or seam, i.e. the rim is strongly produced to form a pair of broad, narrowly separated cucullate dorsal lobes, as in numerous other schizophoran families (see D. McAlpine, 1997). This structure produces a cap-like appearance with the hollowed distal articular surface facing distoventrally or ventrally. Much of the concave distal surface is covered with a reticulation of raised ridges and is microtrichose to a variable degree. The conus is virtually absent. The annular ridge forms an almost symmetrical convexity sunk within a deep median cavity of the upper part of the articular surface, sheltered or almost concealed by the lobes of the rim, and bearing numerous stout, incurved microtrichia. The button is located dorsolaterally, just outside this circlet of microtrichia in *Chyliza* sp. It could not be found in *Psila fimetaria*, apparently because of the extremely irregular and deeply recessed cuticular surface. The foraminal ring is vertically elongate, with a variably developed dorsal and ventral cusp. A caestus, consisting of a series of prominent, almost separate tubercles is present on each side of the foraminal ring.

These features coincide to a quite remarkable degree with those described for the Neurochaetidae and some taxa of Periscelididae. Though this may suggest at first glance a close relationship between these families, I can find no particular shared non-antennal characters to support such a relationship, and many of the antennal features also occur in other families.

In *Syringogaster* sp. (family Syringogastridae) both segments 2 and 3 are very similar to those of the Psilidae in essential structure. The distal articular surface of segment 2 (Fig. 114) is deeply concave because of the pair of large incompletely separated lobes formed from the rim; there is no elevated conus; the approximately symmetrical annular ridge is sunk into the cup; the foraminal ring has a dorsal and a ventral cusp; there appears to be a ridge close inside the annular ridge on each side representing a caestus (difficult to see because this region is deeply recessed). Segment 3 (Fig. 116) resembles that of the Psilidae particularly in the long basal stem bearing the ventrally directed symmetrical foramen on a ventral prominence.

The Syringogastridae have been regarded as the sister group of the Diopsidae s.l. (Griffiths, 1972; D. McAlpine, 1997), despite their greater resemblance to the Psilidae in antennal structure. The view of Feijen (1983) that the Syringogastridae form the sister group of the "Centrioncidae" (as distinct from the Diopsidae s.str.) was rejected by D. McAlpine (1997), and the present study seems to provide further evidence against Feijen's viewpoint. However, I am not at present inclined to abandon the theory of close relationship between Syringogastridae and Diopsidae s.l. solely on antennal characters. Of the six distinctive apomorphies shared by Syringogastridae and Diopsidae (D. McAlpine, 1997: table 1) none is present in the Psilidae. In addition, the small, transverse basal articular foramen of the syringogastrid fore coxa is like that of typical diopsids, in contrast to the longer, oblique foramen of the Gobryidae and Psilidae; and the complex, crazed cuticle of the central part of the face in Syringogastridae somewhat resembles that of various diopsid genera (see figs 20, 22, 24 in D. McAlpine, 1997), while the Psilidae have the face with continuous, unbroken sclerotization.

The Nothybidae and Gobryidae

These two families were referred to the superfamily Diopsoidea by D. McAlpine (1997), and each is only known from its type genus (respectively *Nothybus* and *Gobrya*). They show agreement in many aspects of antennal morphology (Figs 117–121).

The rim of segment 2 is developed into a pair of large hood-like lobes (approximately as in Ephydroidea and other groups), but the distal articular surface, though concave, has no defined cup containing the annular ridge and foramen; the conus is reduced to a low but distinct prominence on the medial side of the foramen, but is obsolete on the lateral side, and as a result the irregularly and asymmetrically developed annular ridge and the foramen face laterally; there are no caesti. Segment 3 (Figs 117, 118) has the strongly produced basal stem bilaterally compressed, and the basal foramen on its medial surface faces medially in *Nothybus*, ventromedially in *Gobrya*; the medial surface of the basal stem has a scabrous zone which extends into the small sub-basal caecum near where the basal stem adjoins the disc of the segment. Segments 4 and 5 of the arista are short but separately sclerotized in *Nothybus*, absent in *Gobrya*; in both groups the arista arises dorsally on segment 3, instead of in the usual dorsolateral position.

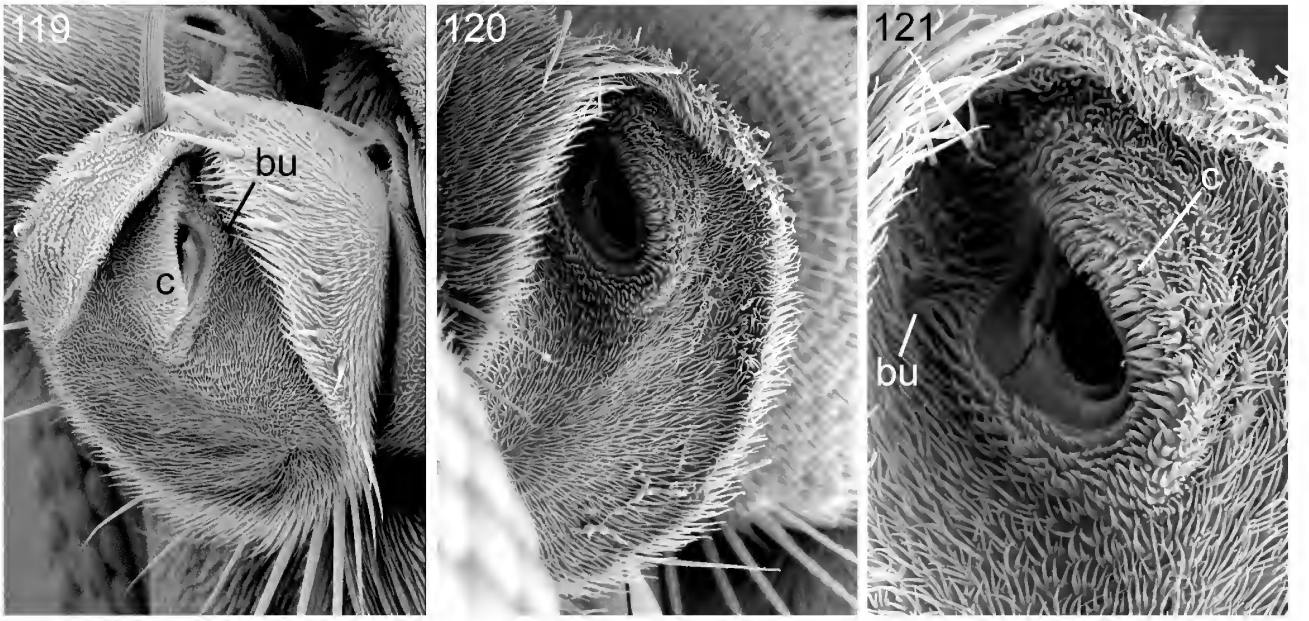

Figures 119–121. Antennae of Nothybidae and Gobryidae. *(119) Nothybus decorus* de Meijere, left seg. 2, distolateral view, seg. 3 removed. *(120) Gobrya cyanea* (Enderlein), right seg. 2, distolateral view, seg. 3 removed. *(121)* The same, detail of conus and adjacent parts. *bu*, pedicellar button; *c*, medial prominence of reduced conus.

The Diopsidae

The broad classification of the Diopsidae given by Hennig (1965: 62) is still preferred. This gives two subfamilies: Centrioncinae, including *Centrioncus* (synonym *Teloglabrus*, since added; D. McAlpine, 1997); and Diopsinae, including all other genera. I have examined details of antennal structure in *Centrioncus decoronotus* Feijen, *Sphyracephala (Hexechopsis) beccarii* (Rondani), and *Cyrtodiopsis* sp. (West Malaysia). Feijen (1983: figs 4–6) has illustrated the general features of some diopsid antennae.

The antennae of Diopsidae differ from those of the four diopsoid families treated above in the following conditions: segment 2, though having the rim well developed and encircling the distal articular surface, is not produced into a pair of dorsal lobes; the conus is relatively large, well removed from the medial margin of the distal articular surface, and the armature of the annular ridge is relatively slightly developed; caesti are absent; segment 3 has a large basal hollow, into which the conus is inserted, and has no basal stem—two features sharply distinguishing it from that of all other diopsoid families, including the Syringogastridae.

In *Centrioncus* (Fig. 122) the conus is deep, somewhat bilaterally compressed, and asymmetrical, with laterally facing preapical foramen; segment 3 (Fig. 124) has its basal foramen inside the basal hollow on its lateral wall; the arista is inserted slightly laterally to the dorsal margin of segment 3.

In *Sphyracephala* segment 2 (Fig. 123) is more nearly radially symmetrical (only slightly bilaterally compressed), with the conus erect, elongate, slightly clavate, arising from near the centre of the distal articular surface, and possessing a terminal foramen; the button is located preapically on the mediodorsal part of the conus (a most unusual location in the Cyclorrhapha); segment 3 (Fig. 125) has the basal hollow deep, almost symmetrical, with the basal foramen located on its floor; the arista is placed symmetrically on its dorsal margin. In *Cyrtodiopsis* the conus is even longer than in *Sphyracephala*, with the button on the dorsal surface at c. the distal quarter of its length. The form of segment 2 and its conus in these more advanced diopsids is remarkably convergent with that of the lower cyclorrhaphous family Lonchopteridae.

Other genera of Diopsinae (e.g., *Diopsis*) appear similar to the above examples in most details. The antenna of *Centrioncus* is more like that of various basal schizophoran types found in the Sciomyzoidea and Heteromyzoidea than is that of the Diopsinae, though it may partly retain the plesiomorphic structure from which that of the Diopsinae was derived.

The lower tephritoid families

In this informal category I include the families Lonchaeidae, Pallopteridae, Piophilidae, Richardiidae, and Ulidiidae (syn. Otitidae) as distinct from the higher tephritoid families Pyrgotidae, Platystomatidae, and Tephritidae. I have examined in at least moderate detail the antenna of one species of each family, viz. *Lonchaea* sp. (Lonchaeidae), *Palloptera muliebris* (Harris) (Pallopteridae), *Piophila vitrea* McAlpine (Piophilidae), *Richardia tephritina* Enderlein (Richardiidae), and *Herina macalpinei* Kameneva (Ulidiidae); see Figs 126–133.

Wiegmann *et al.* (2011) in their phylogenetic study of dipterous families remove the Pallopteridae far from the tephritoid families, with which they are usually associated, and place the family as the sister group of the Neurochaetidae. I find antennal segment 2 of *Palloptera* to be exceedingly similar structurally to that of the tephritoid genus *Richardia* Fig. 129) and without the distinctive characters of the Neurochaetidae. This fact, together with the distinctive tephritoid synapomorphies of the pallopterid female postabdomen, not approached

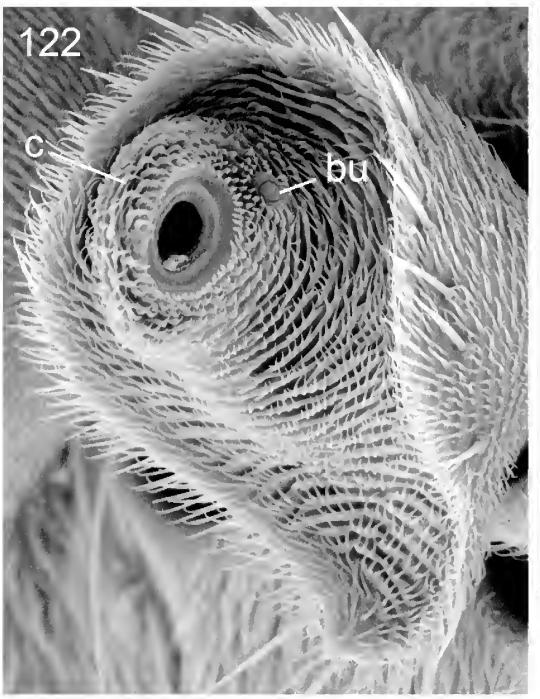

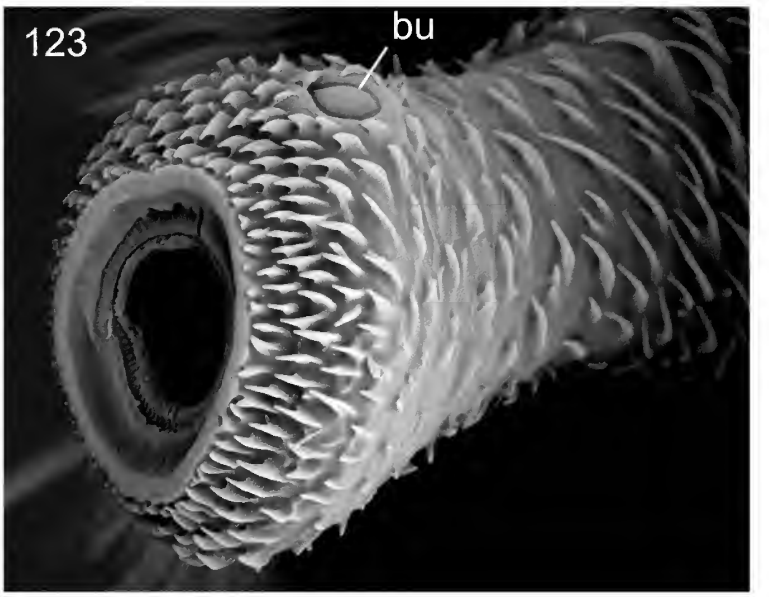

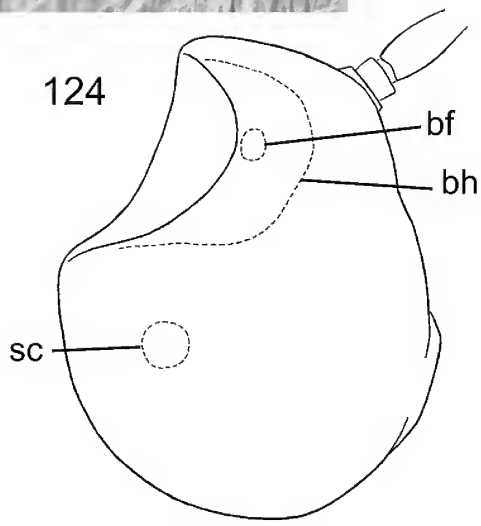

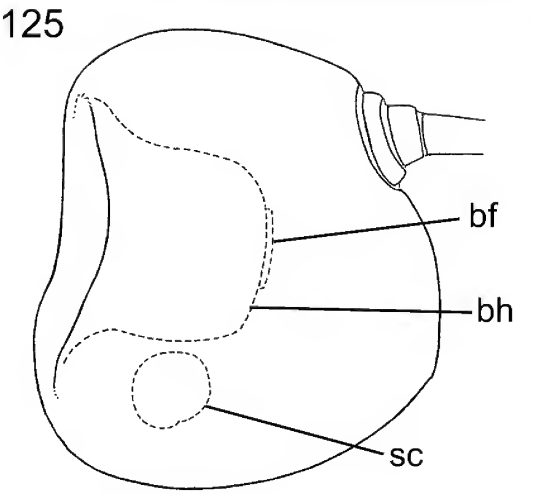

Figures 122–125. Antennae of Diopsidae. *(122) Centrioncus decoronotus* Feijen, left seg. 2, distolateral view, seg. 3 removed. *(123) Sphyracephala beccarii* (Rondani), conus of right seg. 2, distomedial view. *(124) C. decoronotus*, left seg. 3, medial view. *(125) S. beccarii*, the same. *bf*, basal foramen of seg. 3; *bh*, basal hollow; *bu*, pedicellar button; *c*, conus; *sc*, sacculus.

in the Neurochaetidae (see J. McAlpine, 1987: figs 5, 6; D. McAlpine, 1978: fig. 19), and the general lack of morphological and behavioural resemblances between the two families render the placement indicated by Wiegmann *et al.* very improbable. Also, the plesiomorphic Eocene neurochaetid genus *Anthoclusia* shows no significant points of resemblance to the Pallopteridae (Hennig, 1965, and author's unpublished study).

The lower tephritoid taxa show the general features of segments 2 and 3 somewhat as in the Sciomyzoidea, but with some modifications. The distal articular surface of segment 2 is generally somewhat concave and encircled or almost so by the prominent rim, but the latter is often interrupted by a slight mid-dorsal notch, not by a long cleft as in most platystomatids and calyptrates. The conus is broad, almost uniformly sclerotized, rather short, and, with a little variation, more nearly bilaterally symmetrical than in most sciomyzoid taxa; it is tilted so as to retain its ventral prominence, often with a slight chin, but dorsally it is often scarcely raised above the general level of the articular surface. The distal foramen is vertically more or less elongate and tilted dorsally but not or only slightly laterally (as in *Piophila*). The foraminal ring usually bears a dorsal and a ventral cusp (except in *Herina*). The button occupies a dorsolateral position rather near the annular ridge. No taxon in this group is known to possess an encircling furrow (round the base of the conus) or caesti between the foraminal ring and annular ridge.

Segment 3 has usually a capacious basal hollow, but in *Lonchaea* it is reduced and divided by a ridge (Fig. 132). The basal stem is generally absent or only slightly indicated. The basal foramen is on a very slightly developed prominence near the margin of the basal hollow and usually faces ventrally, almost symmetrically.

The examples studied all have a three-segmented arista.

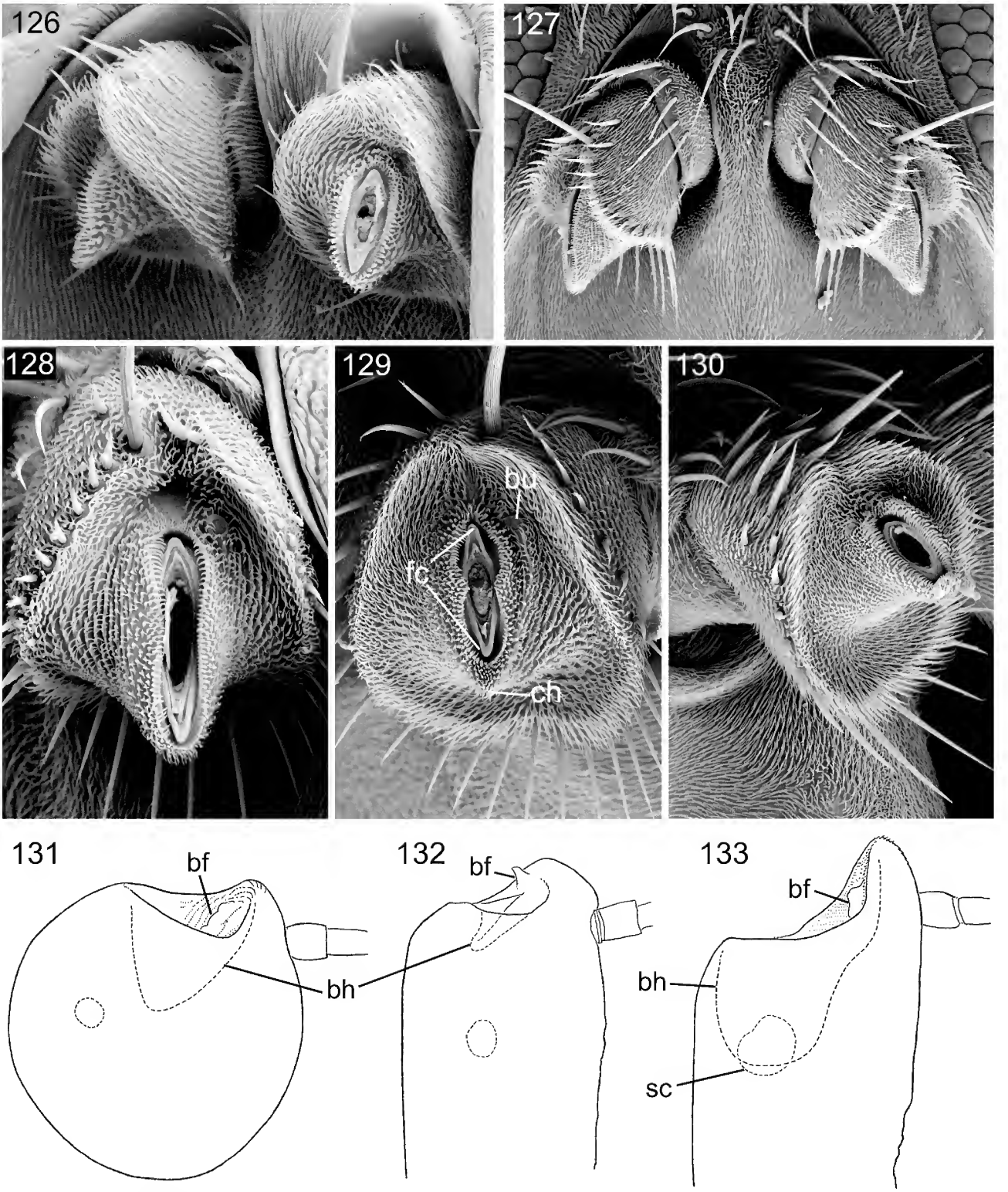

Figures 126–133. Antennae of lower tephritoids. *(126) Piophila vitrea* McAlpine (fam. Piophilidae), antennae, each with seg. 3 removed to expose conus. *(127) Lonchaea* sp. (Willoughby East, N.S.W.; fam. Lonchaeidae), the same. *(128) Lonchaea* sp., left antennal seg. 2, seg. 3 removed. *(129) Richardia tephritina* Enderlein (fam. Richardiidae), the same. *(130) Herina macalpinei* Kameneva (fam. Ulidiidae or Otitidae), right antennal seg. 2, seg. 3 removed. *(131) Piophila vitrea*, left antennal seg. 3, medial view. *(132) Lonchaea* sp., the same. *(133) Richardia tephritina*, the same. *bf*, basal foramen of seg. 3; *bh*, basal hollow of seg. 3; *bu*, pedicellar button; *ch*, chin; *fc*, foraminal cusps; *sc*, sacculus.

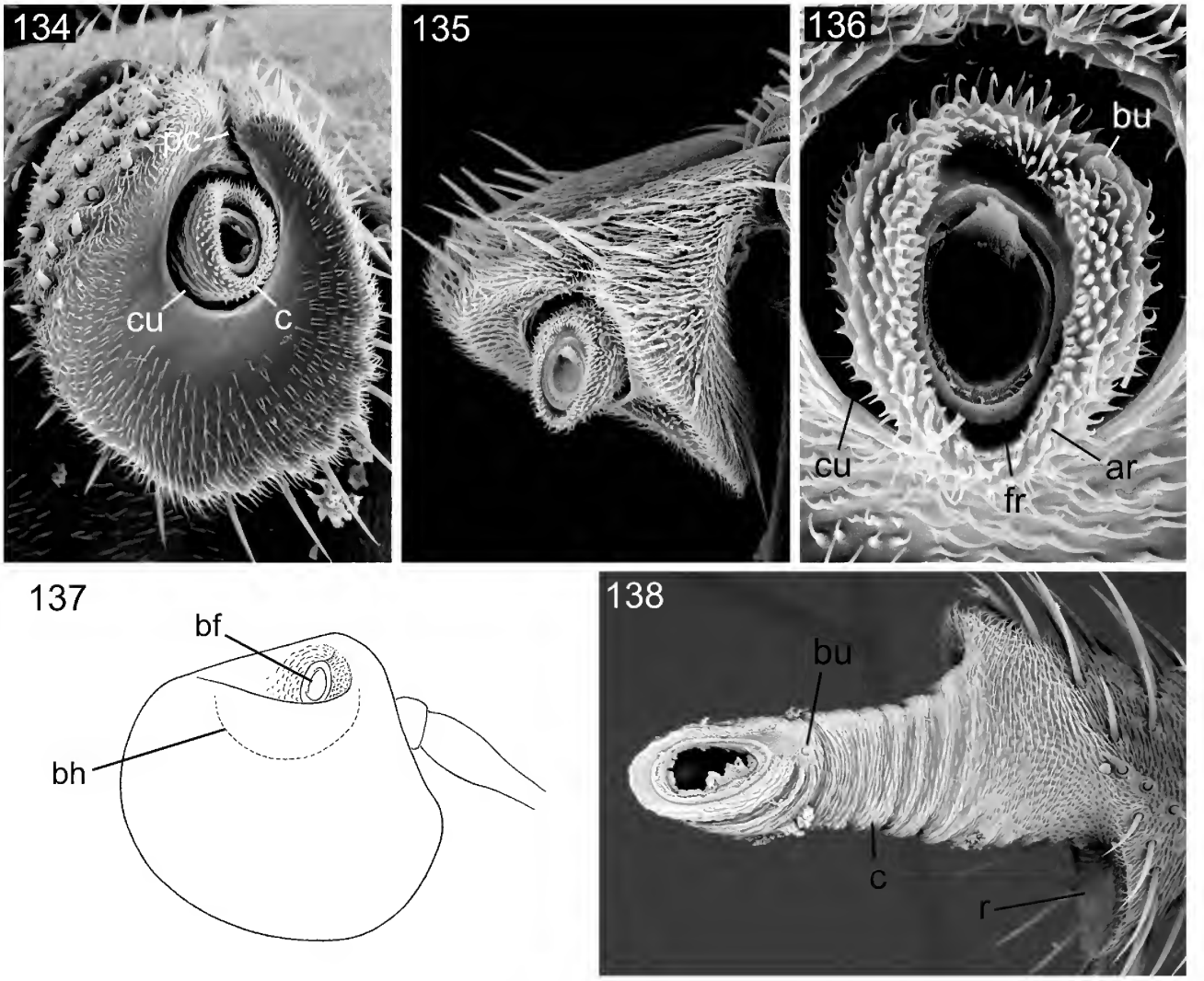

Figures 134–138. Antennae of Pyrgotidae. *(134) Cardiacera carnei* (Paramonov), left seg. 2, distal view, seg. 3 removed. *(135) Prodalmannia variabilis* Bezzi, left seg. 2, lateral view, seg. 3 removed. *(136) P. variabilis*, left conus and associated parts, distal view. *(137) P. variabilis*, left seg. 3, medial view. *(138) Adapsilia* sp. (Kuranda, Qld), male, part of left seg. 2, lateral view, seg. 3 removed to expose conus. *ar*, annular ridge; *bf*, basal foramen of seg. 3; *bh*, basal hollow; *bu*, pedicellar button; *c*, conus; *cu*, pedicellar cup; *fr*, foraminal ring of seg. 2; *pc*, pedicellar cleft; *r*, pedicellar rim.

The Pyrgotidae

I have examined antennal structure in the following species: *Cardiacera carnei* (Paramonov), *Maenomenus ensifer* Bezzi, *Prodalmannia variabilis* Bezzi, *Adapsilia* sp. (Kuranda, Queensland). The first three of these have fairly uniform antennal structure, but *Adapsilia* has some unusual features and will be described separately.

In the more typical genera segment 2 has a broad encircling rim, often interrupted by a dorsal notch or incipient cleft. The distal articular surface is more or less concave. The conus is moderately short, not markedly receding dorsally, arising from within a deep cup lined by largely membranous cuticle. This condition apparently confers considerable flexibility on the conus which therefore has the property of an additional articulated antennal segment (Figs 134–136). The foraminal ring is simple, rounded but not quite circular and only slightly tilted dorsally to dorsolaterally; caesti and cusps are absent. The button is located dorsolaterally near or on the annular ridge. This condition somewhat resembles that in the Chloropidae, but there is no chin and the collar is less developed; the chloropids studied have no cleft in the rim. Segment 3 (Fig. 137) is without a typical basal stem, though sometimes it may be more basally prominent dorsally than ventrally. The basal hollow is broad, but only of moderate depth. The basal foramen is located on the lateral wall of the hollow on a slight gibbosity, which is probably flexible. The sacculus of *Maenomenus* has a relatively large external pore. The external pore could not be detected in the other pyrgotid genera, but a sacculus is presumably present (certainly present in *Cardiacera*). The arista in these examples is three-segmented with strongly marked articulation between segments 5 and 6. Segment 4 is relatively large in *Cardiacera*, in some species almost as long as segment 5; in the other genera it is short but sclerotized.

In *Adapsilia* sp. (Fig. 138) the antenna is longer than in the above examples. The rim lacks the dorsal notch and the distal articular surface is only partly concave. There is no cup or encircling furrow. The conus is remarkably large, elongate, and apparently flexible over most of its length,

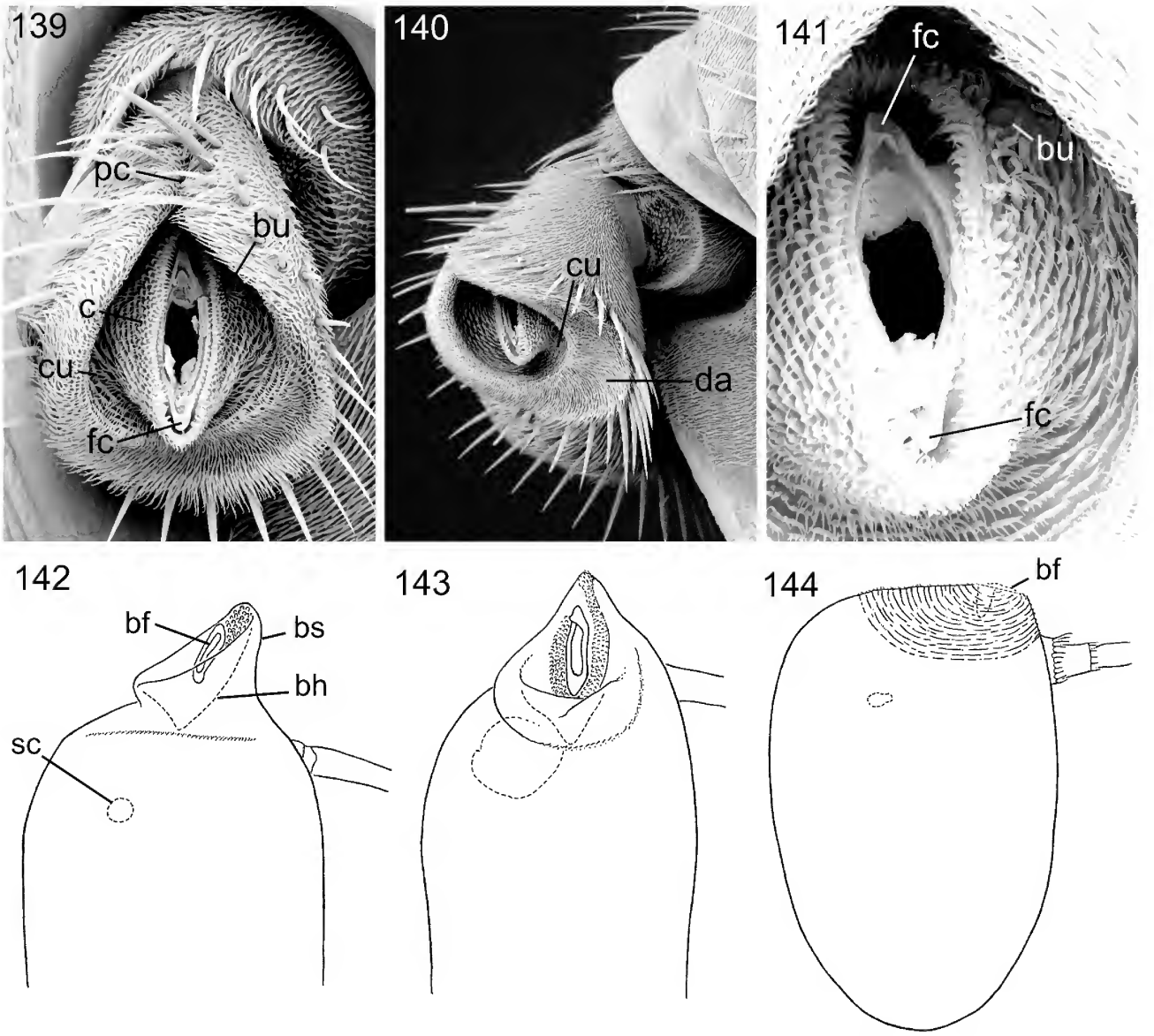

Figures 139–144. Antennae of Platystomatidae. *(139) Duomyia curta* McAlpine, left seg. 2, distodorsal view, seg. 3 removed. *(140) Lamprogaster stenoparia* Hendel, left seg. 2, lateral view, seg. 3 removed. *(141)* The same, parts contained in cup of seg. 2. *(142) Loxonevra* sp. (West Sumatra), part of left seg. 3, medial view. *(143) Euprosopia armipes* McAlpine, the same. *(144) Peltacanthina* sp. (Karen, Kenya), left seg. 3, medial view. *bf*, basal foramen of seg. 3; *bh*, basal hollow; *bs*, incipient basal stem; *bu*, pedicellar button; *c*, conus; *cu*, pedicellar cup; *da*, distal articular surface of seg. 2; *fc*, foraminal cusp; *pc*, pedicellar cleft; *sc*, sacculus.

but less so basally; its cuticle is thrown into many encircling folds and the surface has finer transverse ridging; the foramen is strongly tilted laterally. This structure is apparently derived from that of *Cardiacera* etc., but differs markedly in the great prolongation of the conus and extension of the flexibility of the cuticle over much of the length of the conus. Segment 3 has a deep, capacious basal hollow. Segment 4 is reduced to a minute vestige, so that the arista appears to be two-segmented. Korneyev (2004) drew attention to the numbers of aristal segments in the key to Palaearctic genera of Pyrgotidae.

The convergent resemblance in some characters between certain taxa of Conopidae and Pyrgotidae has been mentioned before (e.g., Hennig, 1952: 195). The structure of antennal segment 2 and the conus in *Adapsilia* provides an additional example (compare Figs 138 and 43). As these conditions differ from those in the groundplans of both families, the structural similarities are perhaps to be interpreted as due to similarities in habits of the adult flies.

In addition to the condition of antennal segment 4, possibly useful taxonomic characters in the Pyrgotidae include the structure and position of the prelabrum ("clypeus" in error) and various features of the proboscis.

The Platystomatidae and Tephritidae

Antennal structure in the Platystomatidae reflects some of the general diversity occurring in the family. I therefore divide the selection of taxa examined for antennal morphology into four categories for descriptive purposes. These categories (types A to D) are not necessarily sharply defined, nor do they consistently follow a natural classification.

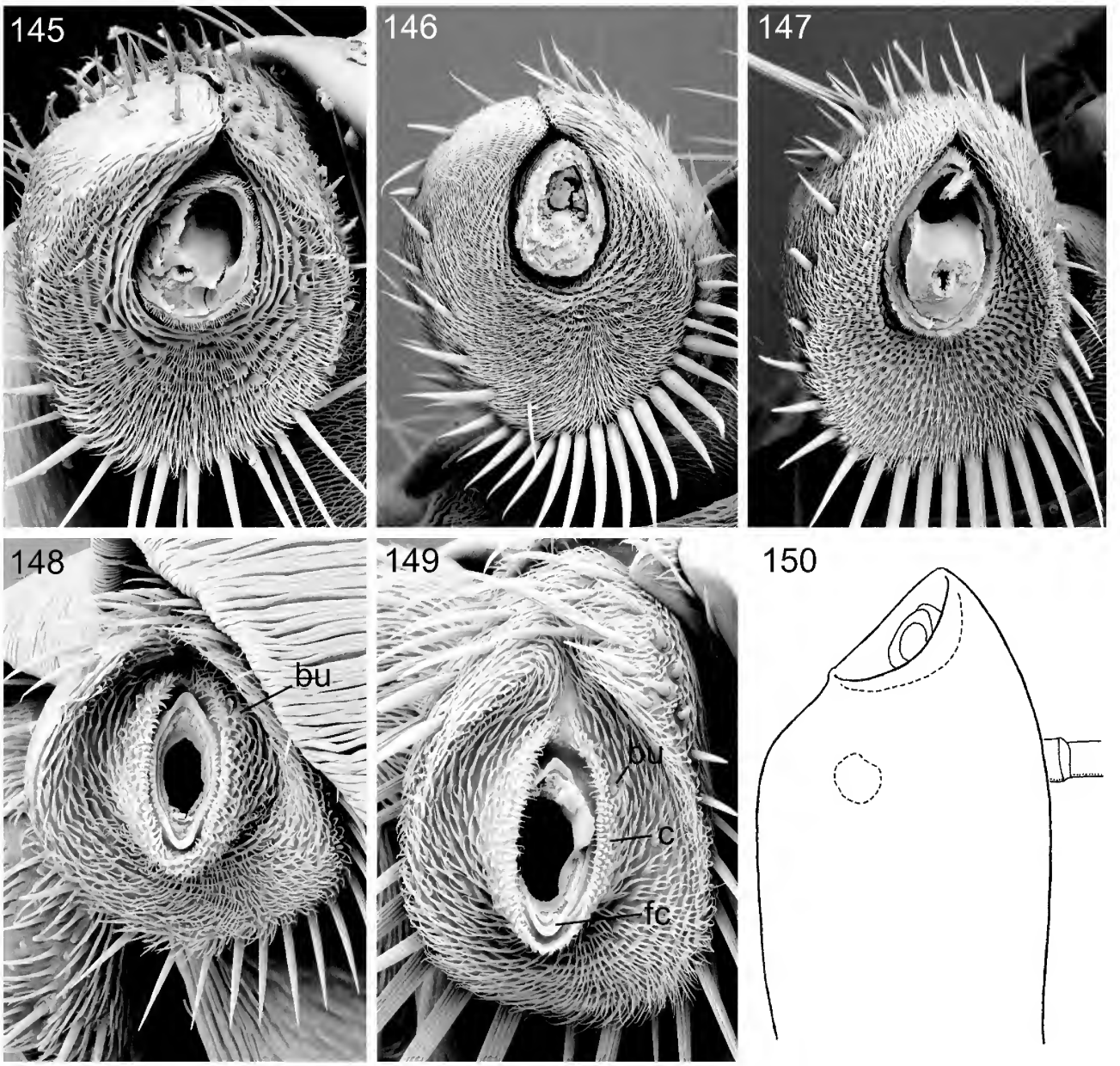

Figures 145–150. Antennae of Platystomatidae. *(145) Peltacanthina* sp. (Karen, Kenya), left seg. 2, distal view, seg. 3 removed. *(146) Cleitamia astrolabei* (Macquart), the same. *(147) Scholastes cinctus* (Guérin-Méneville), the same. *(148) Microepicausta* "sp. 1" (in AM), the same. *(149) Rhytidortalis averni* McAlpine, the same. *(150)* The same sp., part of left seg. 3, medial view. *bu*, pedicellar button; *c*, conus; *fc*, foraminal cusp.

Type A (Figs 139–143). Examples studied: *Achias kurandanus* Hennig, *Duomyia* spp., *Euprosopia vitrea* McAlpine, *E. armipes* McAlpine, *Lamprogaster stenoparia* Hendel, *Lenophila achilles* McAlpine & Kim, *Loxonevra* sp. (western Sumatra), *Plagiostenopterina* sp. (near *enderleini* Hendel), *Platystoma gemmationis* (Rondani). This is the most frequent type in the family, particularly in the subfamily Platystomatinae, and is perhaps the groundplan condition for the Platystomatidae, the other types being derived from it. It resembles the condition commonly found in the Tephritidae.

Segment 2 has a long dorsal cleft extending near its base (Figs 139, 152, pc). The distal articular surface immediately within the rim is flattened to slightly concave, but centrally it abruptly gives way to a capacious cup (Fig. 140). The collar separating the distal articular surface from the cup (as seen in the Chloropidae) is here at most slightly developed and dorsally interrupted. In some species of *Duomyia* it is almost obsolete, so that the surface of the cup is not so sharply differentiated from that of the surrounding articular surface. The short conus is often almost bilaterally symmetrical and almost symmetrically placed on the segment, but is tilted so that the annular ridge and distal foram face somewhat dorsally. Thus there is often a slight ventral chin and the dorsal extremity of the annular ridge is scarcely raised above the floor of the cup. Because of its small size, the conus does not nearly fill the cavity of the cup. The annular ridge and foraminal ring are vertically elongate, the latter usually with a dorsal and a ventral cusp. The button is located near the dorsolateral part of the annular ridge, virtually on the floor of the cup. Segment 3 is most often elongate, with both sacculus and arista located

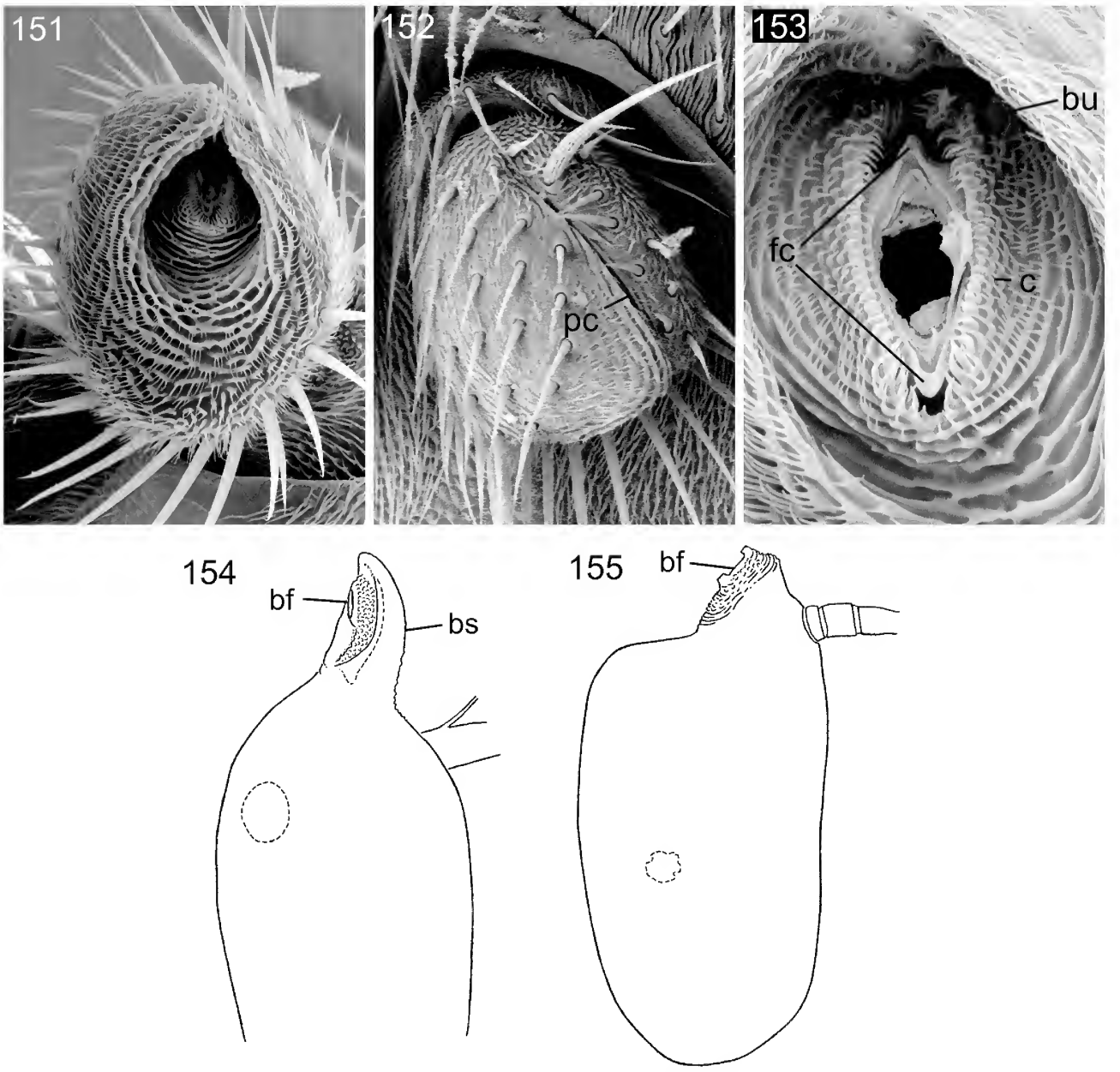

Figures 151–155. Antennae of Platystomatidae. *(151) Atopognathus complens* (Walker), left seg. 2, distal view, seg. 3 removed. *(152)* The same, dorsal view of left seg. 2. *(153) Mesanopin biplexum* Whittington, pedicellar cup and contents. *(154) A. complens*, part of left seg. 3, medial view. *(155) M. biplexum*, the same parts. *bf*, basal foramen of seg. 3; *bs*, basal stem of seg. 3; *bu*, pedicellar button; *c*, conus; *fc*, foraminal cusps; *pc*, pedicellar cleft.

not far from its base. The basal hollow is generally present but small and there may be slight development of the basal stem. The basal foramen is asymmetrically placed at or near the margin of the hollow. The arista is commonly three-segmented, but in numerous species of *Euprosopia* and some of other genera segments 5 and 6 are fused.

Type B (Figs 144–147). Examples studied: *Cleitamia astrolabei* (Macquart), *Peltacanthina* sp. (Karen, Kenya), *Scholastes cinctus* (Guérin-Méneville). The morphology of this group may not be well understood but a more detailed study should be completed by future students.

The most distinctive apparent feature is the deep, narrow cup of segment 2, which is almost plugged by the stout, apparently subcylindrical conus with distal foramen of greater area than usual. However, in all disarticulated specimens the conus has snapped or crumbled so that the features of its distal surface cannot be accurately ascertained. The tendency of the conus to break up may indicate that its distal part is flexible and incompletely sclerotized, as in the pyrgotid genus *Adapsilia*. Segment 3 appears not to have a typical hollow or sub-basal stem, but there is a narrow caecum next to the basal foramen, at least in *Peltacanthina* sp. (Fig. 144), and the cuticle of the convex basal zone of the segment is covered with a dense set of fine encircling ridges.

Mezona sp. (Sokoke Forest, Kenya, in AM) appears to have several sacculi on segment 3, but available material is too limited for detailed study. This genus is perhaps closely related to *Peltacanthina*.

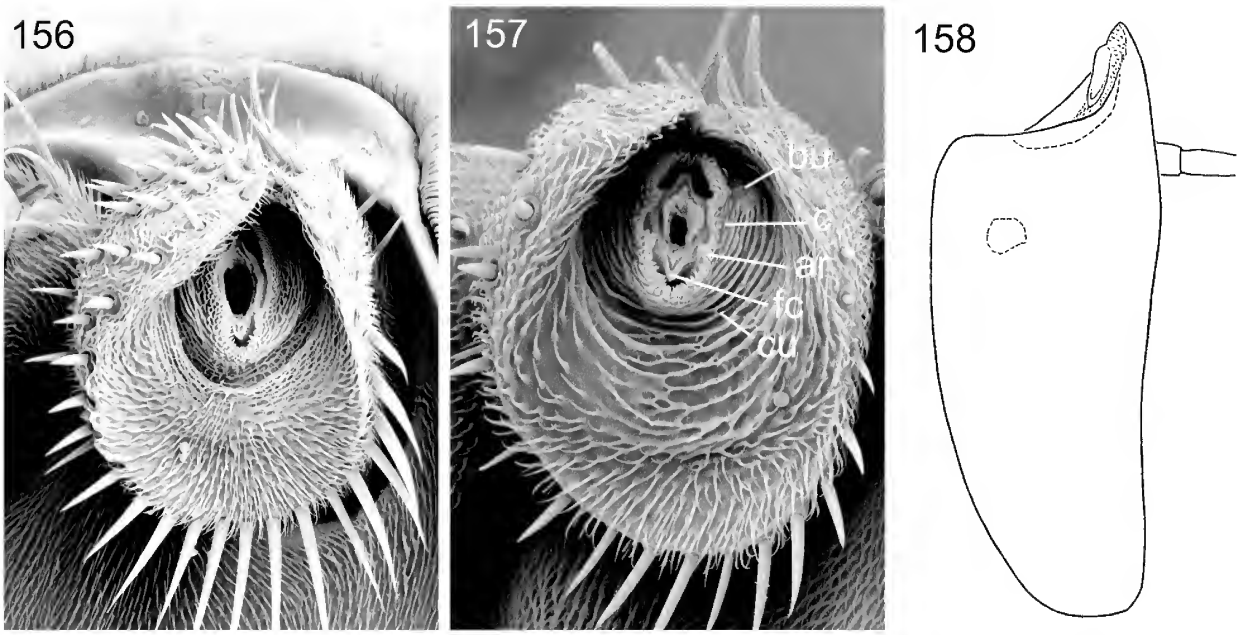

Figures 156–158. Antennae of Tephritidae. *(156) Euphranta marina* Permkam & Hancock, left seg. 2, distal view, seg. 3 removed. *(157) Spathulina acroleuca* (Schiner), the same parts. *(158) E. marina*, left seg. 3, medial view. *ar*, annular ridge; *bu*, pedicellar button; *c*, conus; *cu*, pedicellar cup; *fc*, foraminal cusp.

Type C (Figs 148–150). Examples studied: *Microepicausta* "sp. 1" (New South Wales, in AM), *Rhytidortalis averni* McAlpine.

These taxa resemble those listed under type A, but the cup is absent or incompletely differentiated from the surrounding articular surface of segment 2. The condition of the base of the conus is therefore not very different from that of such lower tephritoid families as Piophilidae and Ulidiidae, though the resemblance is probably secondary.

Type D (Figs 151–155). Examples studied: *Atopognathus complens* (Walker), *Mesanopin biplexum* Whittington, *Xiria* sp. (West Malaysia, in AM).

The cup is deep and capacious but not very sharply demarcated at its periphery. The conus is much reduced or shortened, but in *Mesanopin* it retains a degree of ventral prominence. In *Atopognathus* and *Xiria* the annular ridge is only slightly raised above the floor of the cup. In all three genera the basal hollow of segment 3 is absent and the basal stem is well developed, with the foramen near its extremity. *Mesanopin* is unusual in having the sacculus located beyond mid-length of segment 3. *Atopognathus* differs from the other two examples in having segments 5 and 6 fused (arista two-segmented as in some *Euprosopia* spp.).

Examples of the family Tephritidae examined for this study include the following: *Bactrocera tryoni* (Froggatt), *Euphranta marina* Permkam & Hancock, *Spathulina acroleuca* (Schiner) (see Figs 156–158). It is a family of great taxonomic diversity and these taxa are unlikely to show the full range of variation.

Segment 2 shows the main features described above for platystomatid type A. The conus is short in *Euphranta* and *Spathulina*, longer and more ventrally prominent in *Bactrocera*. Segment 3 has a small basal hollow, broader and shallower in *Euphranta* than in the other two genera. There is a short subacute basal stem, with the foramen on its ventral surface. The arista is three-segmented, with segment 4 very short.

The Calyptratae (Muscoidea s.l.)

Probably the most generally utilized recent superfamily and family classification for the calyptrates is still that of J. McAlpine (1989), though Hennig (1973) recognized a larger number of families. However, the phylogenetic study of Kutty *et al.* (2010) indicated that some major changes in superfamily and family classification are needed. Possibly the treatment of the calyptrates as a single superfamily (termed Muscoidea by Richards & Davies, 1977, Crosskey [ed.], 1980, and by Colless & D. McAlpine, 1991), is the best system, and is in accord with the analyses by Roback (1951), Griffiths (1972), Kutty *et al.* (2010), and Wiegmann *et al.* (2011), though Roback did not consider the pupiparous families.

The calyptrates show a general uniformity of antennal structure, particularly in details of segment 2, over the majority of included taxa. The main exceptions appear, from my limited selection of taxa, to be the highly derived Hippoboscidae and related so-called families (i.e. the Streblidae and Nycteribiidae, perhaps better not afforded separate family rank from the Hippoboscidae, if results of the phylogenetic study by Kutty *et al.*, 2010, gain general acceptance). These latter taxa (but not the related Glossinidae) have proved difficult for SEM work, but this need not affect the interpretation of morphology in the vast majority of calyptrate flies. Examples of Glossinidae, Hippoboscidae, and Nycteribiidae, previously studied by me, differ from other calyptrates and most other schizophorans (except for certain periscelidids) in having the rays (or primary branches) of the arista (segment 6) with secondary branching (see Fig. 167 and Theodor, 1967).

Calyptrate taxa which I have used for SEM study include: *Australofannia* sp. (family Fanniidae, Fig. 163), *Hydrotaea* sp. and *Musca vetustissima* Walker (family Muscidae, Figs 161, 162, 169), *Delia urbana* (Malloch) (family Anthomyiidae, Figs 159, 160), *Stomorhina discolor* (Fabricius) (family Rhiniidae, formerly in Calliphoridae, Fig.

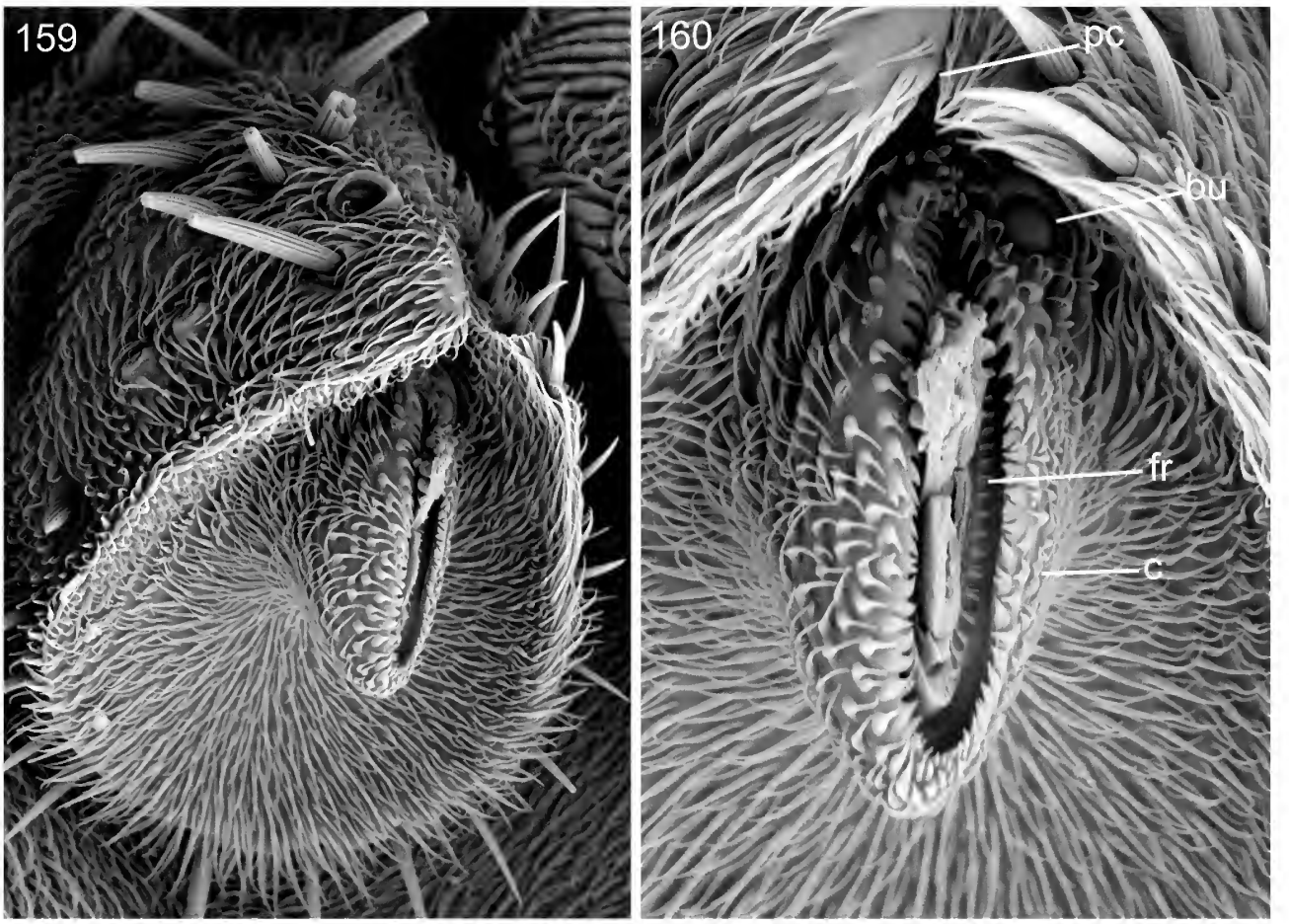

Figures 159, 160. Left antenna of *Delia urbana* (Malloch) (fam. Anthomyiidae), female. *(159)* Seg. 2, seg. 3 removed, distomedial view. *(160)* The same, upper part of distal articular surface. *bu*, pedicellar button; *c*, conus; *fr*, foraminal ring; *pc*, pedicellar cleft.

172), *Chrysomya* sp. and *Amenia chrysame* (Walker) (family Calliphoridae, Figs 164, 171), *Axinia lucaris* Colless (family Axiniidae or Rhinophoridae, Fig. 165), *Senostoma mcalpinei* Barraclough (family Tachinidae), "McAlpine's fly" (near family Anthomyiidae according to Ferrar, 1979; near family Mystacinobiidae according to Kutty *et al.*, 2010; Figs 170, 173), *Glossina* sp. (family Glossinidae, Figs 166–168). Several other taxa have been examined with CLM.

The following description applies, with little deviation, to segment 2 of the many typical examples studied (see Figs 159–166). The rim has a deep dorsal cleft, the margins of which remain in contact or almost so. The distal articular surface is broadly moderately concave, but recedes, often deeply and narrowly, on its central dorsal part between the dorsal extremity of the conus and the cleft. The conus is almost bilaterally symmetrical in shape and position on the mid-dorsal region of the articular surface, little raised from this surface at the dorsal end of the vertically elongate annular ridge, but always prominent at its ventral extremity (or chin) so that the annular ridge and distal foramen face dorsally rather than distally. The annular ridge generally does not have strongly differentiated armature, but is usually interrupted mid-dorsally below the cleft. The chin becomes particularly elongate and sharp apically in some examples of Calliphoridae and Tachinidae (though a broad representation of these families has not yet been examined), but is broadly rounded in *Stomorhina*. As in many other schizophorans with narrowly elongate distal foramen, the foraminal ring often has a distinct dorsal and ventral foraminal cusp (Fig. 164).

The conus of the examined calyptrate taxa does not arise from a cup or any recessed zone surrounding its base, described above in several acalyptrate groups. It is possible in such examples as *Australofannia* (Fig. 163) and *Musca* (Fig. 161), that the surrounding cuticular surface consisting of sclerotized ridges alternating with bands of thinner cuticle allows some side-to-side movement of the conus and of segment 3 which it supports. The conus of *Axinia* (Fig. 165) is much larger than in other calyptrate taxa studied, and, when exposed, projects beyond the distal articular surface for a distance greater than the length of the main body of segment 2.

The pedicellar button of calyptrates is generally located dorsolaterally to the annular ridge, often within the dorsal recess and near the pedicellar cleft. In *Musca* (Fig. 162) it is particularly deeply recessed and faces dorsally towards the cleft.

In the Calyptratae the number of sacculi in segment 3 is variable, but I have had time to examine very few taxa, especially as the usually darkly pigmented and rough cuticle makes study difficult with CLM.

Glossina has a sacculus on the more basal part of the lateral surface of segment 3 (Fig. 168, sc), and this appears to be the homologue of the one sacculus in most acalyptrate taxa; but there is also an apparent sacculus (presumably a secondary structure) on the medial surface of this segment a little further from the base (Fig. 167, *ss*).

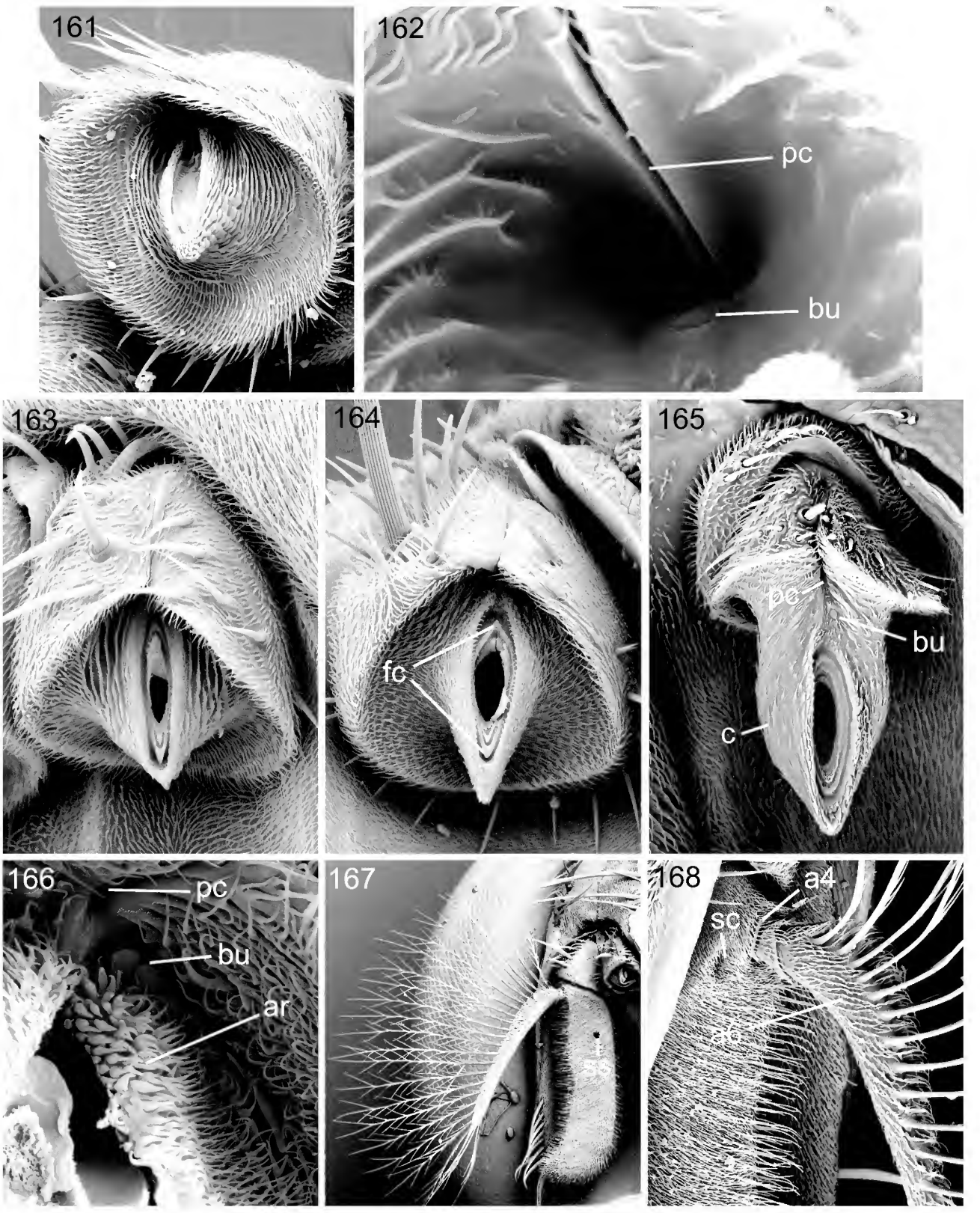

Figures 161–168. Antennae of Calyptratae. *(161) Musca vetustissima* Walker (fam. Muscidae), female, left seg. 2, distal view. *(162)* The same, dorsal recess of right seg. 2. *(163) Australofannia* sp. (fam. Fanniidae), female, left seg. 2, distodorsal view. *(164) Amenia chrysame* (Walker) (fam. Calliphoridae), female, left seg. 2, distodorsal view. *(165) Axinia lucaris* Colless (fam. Axiniidae or Rhinophoridae), male, left seg. 2, dorsal view. *(166) Glossina* sp. (fam. Glossinidae), male, part of recess of left seg. 2. *(167)* The same, right antenna, medial view. *(168)* The same, part of right antenna, lateral view, showing base of arista. *a4, a6*, antennal segments 4 and 6 (arista); *ar*, annular ridge; *bu*, pedicellar button; *c*, conus; *fc*, foraminal cusp; *pc*, pedicellar cleft; *sc*, opening of sacculus; *ss*, secondary sacculus.

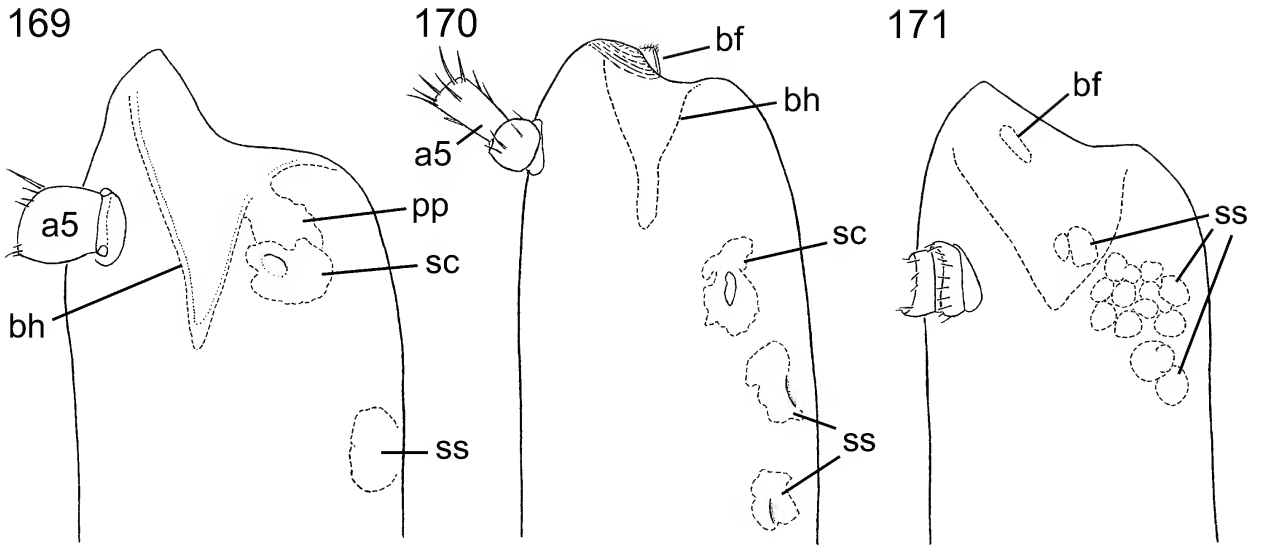

Figures 169–171. Basal part of left seg. 3, lateral view, of Calyptratae. *(169) Musca vetustissima* Walker (fam. Muscidae), male. *(170)* McAlpine's fly (fam. near Anthomyiidae or Mystacinobiidae), female. *(171) Amenia chrysame* (Walker) (fam. Calliphoridae), female. *a5*, antennal segment 5; *bf*, basal foramen, not visible in Fig. 169; *bh*, basal hollow; *pp*, postpedicellar pouch; *sc*, sacculus; *ss*, secondary sacculi.

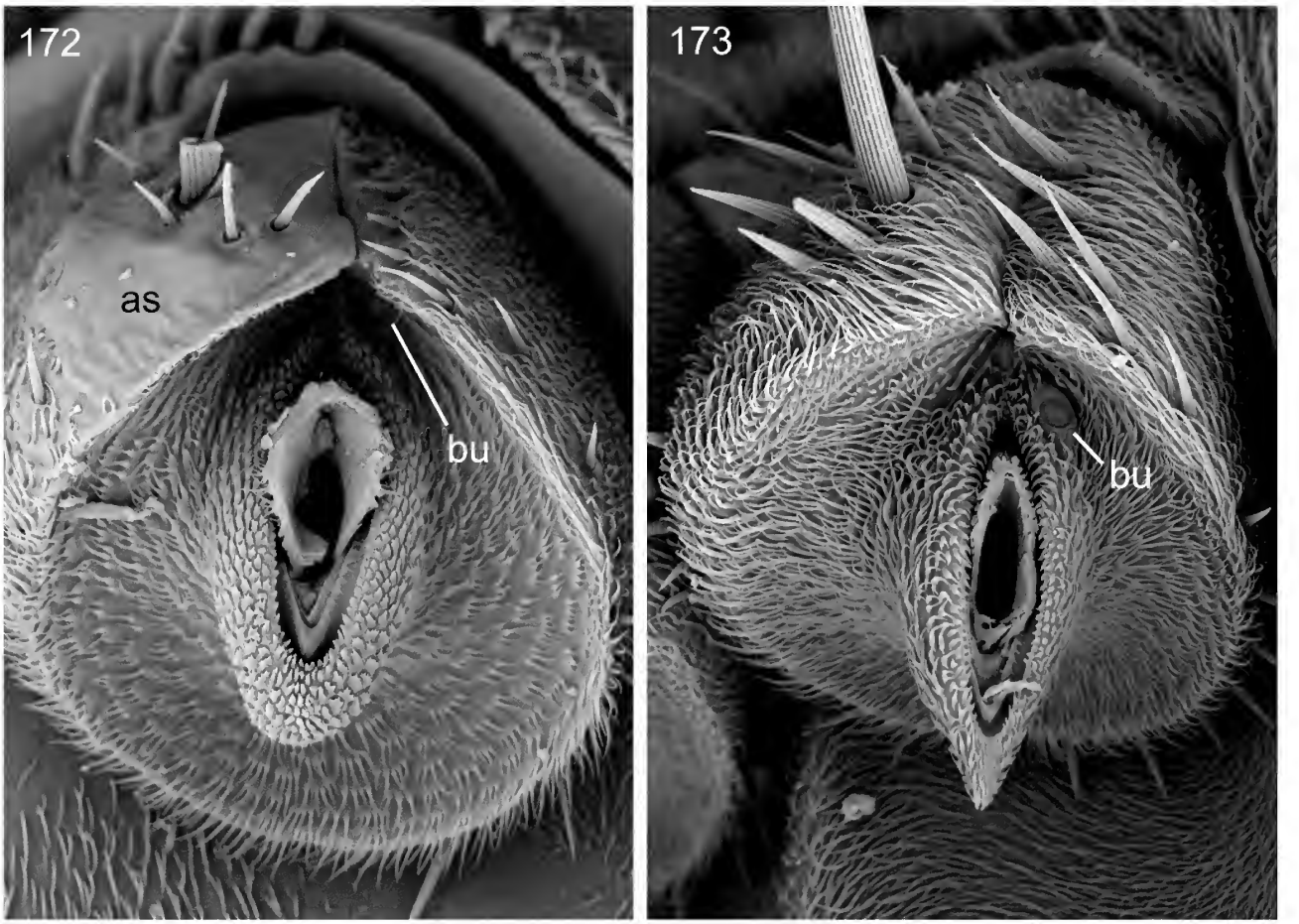

Figures 172–173. Antennal segment 2 of Calyptratae, distodorsal view. *(172) Stomorhina discolor* (Fabricius) (fam. Rhiniidae), male. *(173)* McAlpine's fly (? fam.), female. *as*, abraded surface; *bu*, pedicellar button.

As *Glossina* represents the morphologically most basal clade of the Pupipara—the sister group to the rest of the Calyptratae—it may be that it resembles the basal condition for the Calyptratae in these features (despite its apomorphic life history and aristal structure). In a sense, it typifies the common calyptrate condition of possession of a primary sacculus, with one or more secondary sacculi.

In *Fannia canicularis* (Linné) segment 3 has one major sacculus near the middle of the lateral surface, but there are also numerous smaller pit-like structures, some of

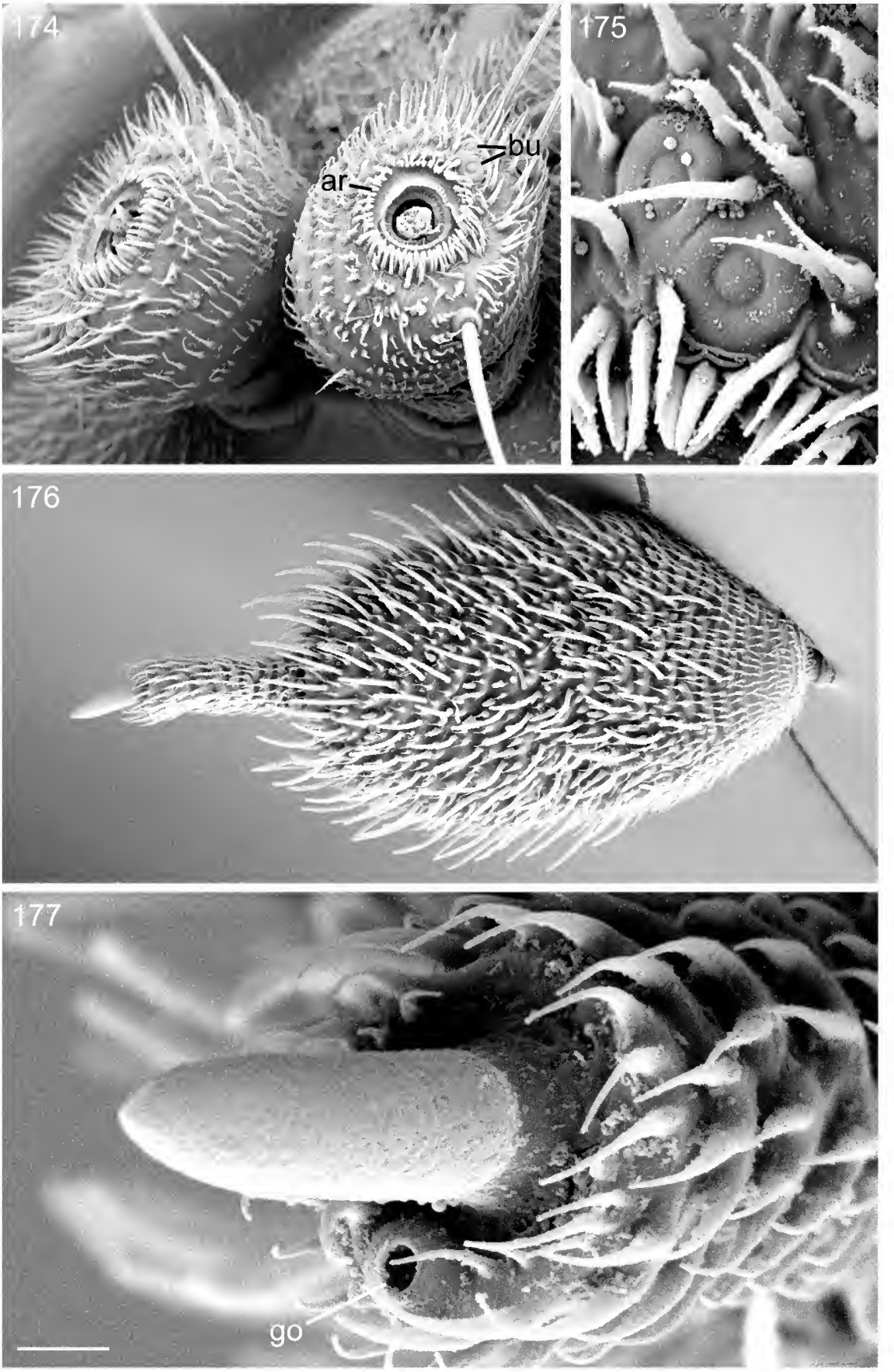

Figures 174–177. Antenna of *Apystomyia elinguis* Melander (fam. Apystomyiidae), male. *(174)* Both antennae, segs 3 removed. *(175)* Buttons of left seg. 2. *(176)* Right flagellum, medial view. *(177)* Distal part of right stylus, distomedial view; scale = 4 μm. *ar*, annular ridge; *bu*, pedicellar buttons; *go*, stylar goblet.

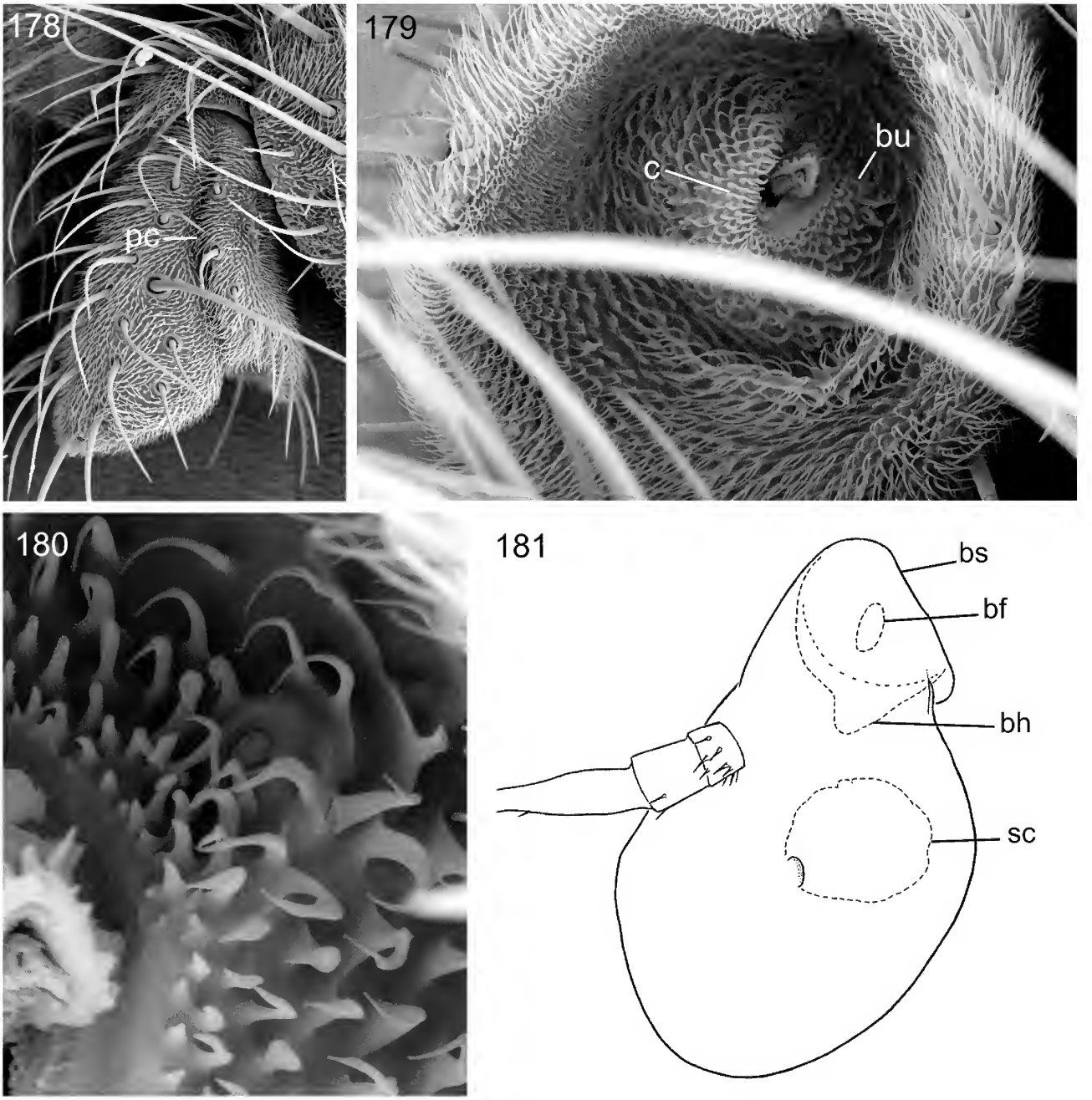

Figures 178–181. Antenna of *Mormotomyia hirsuta* Austen (fam. Mormotomyiidae), male. *(178)* Segs 1 and 2, dorsolateral view. *(179)* Distal articular surface of seg. 2, seg. 3 removed. *(180)* Part of distal articular surface, showing button. *(181)* Left seg. 3, lateral view. *bf*, basal foramen; *bh*, basal hollow; *bs*, basal stem; *bu*, pedicellar button; *c*, conus; *pc*, pedicellar cleft; *sc*, sacculus.

which contain several sensilla. In *Scathophaga* sp. (family Anthomyiidae or Scathophagidae) segment 3 has a sacculus on the lateral surface and another on the medial surface near the base. This condition resembles that of *Glossina*. In *Musca vetustissima* (Fig. 169) segment 3 carries a normal sacculus on the lateral surface rather close to the base and a secondary sacculus-like ventral organ more removed from the base, which may be divided in two in some individuals. There is also a postpedicellar pouch opening into the ventral side of the basal hollow, not seen by me in other calyptrate taxa. This is reminiscent of the pouch in *Australoconops* (family Conopidae), but in the latter the pouch opens to the exterior ventrally to the hollow (Fig. 44), not into the hollow. The phylogenetic distance between *Musca* and *Australoconops* renders it improbable that this pouch is homologous in the two taxa. In McAlpine's fly (Fig. 170), segment 3 resembles that of *Musca*. A large sacculus is located at c. the basal quarter of its length on the lateral surface and there are c. three ventral secondary sacculi near mid-length and beyond. In the calliphorid *Amenia* (Fig. 171), segment 3 has c. 14 sacculus-like organs of various sizes on the lateral surface ventrad of the aristal socket. I cannot identify any one of these as the primary sacculus seen in other families. Some of these contain rounded internal bodies (as seen with CLM), but the internal structure needs interpretation by ultramicroscopic technique. Also in *Chrysomya* and some other calliphorid

taxa there are numerous sacculus-like structures. By contrast *Stomorhina*, now placed in the separate family Rhiniidae, clearly has only one sacculus. Among the tachinids, *Chetogaster* and *Senostoma* have one large sacculus only. In the "axiniids" (family Axiniidae or Rhinophoridae; see Colless, 1994) there is commonly one sacculus ("sensory pore"), but it is multiple or absent in various taxa.

As the Calyptratae form an apparent clade derived from among the acalyptrate groupings, it may be profitable to ascertain which acalyptrate groups conform most closely to basal calyptrates in antennal morphology.

The features of the distal surface of segment 2 in typical calyptrates (e.g., *Delia*, Figs 159, 160; *Amenia*, Fig. 164) conform in some detail with those of such lower tephritoid families as Piophilidae (see Fig. 126), Lonchaeidae (Figs 127, 128), and Richardiidae (Fig. 129). Main common features include: segment 2 approaching bilateral symmetry, with conus centred on mid-line of distal articular surface, strongly tilted so that dorsal part of its distal surface is scarcely raised above level of distal articular surface, while the ventral part is produced as a prominent chin; foraminal ring and distal foramen narrowly elongate, former produced as an upper and a lower foraminal cusp; button located at lateral side of dorsal extremity of foraminal ring. These examples of Tephritoidea differ from my calyptrate examples in that the pedicellar cleft is absent or represented by a shallow notch in the rim. However, a more distinct cleft is present in numerous taxa of Tephritidae and Platystomatidae (classed as "higher tephritoids"), and in the latter family the cleft is often as long and distinct as in typical calyptrates (Fig. 152). This is of interest because numerous platystomatid taxa show the squama (lower calypter) larger than in any other acalyptrate family ("calyptrate" condition). In the past this character combination has occasionally caused species of the platystomatid genera *Achias* and *Euprosopia* to be classed erroneously as calyptrates.

Some comparative molecular studies (Vossbrinck & Friedman, 1989; Cameron *et al.*, 2007) have suggested an affinity of the Calyptratae to the Ephydroidea (Drosophiloidea). In antennal structure the most marked resemblance between these two groups is the well-developed pedicellar cleft. Otherwise the ephydroid pedicel is very unlike that encountered in the Calyptratae. In more plesiomorphic ephydroid forms (e.g., *Campichoeta*, Fig. 74; *Cyrtona*, Fig. 77; *Ephydrella*, Fig. 84) the conus is situated towards the medial part of the rim and is very bilaterally asymmetrical, so that the foramen faces laterally (without any dorsal inclination) and is not narrowly elongate, the chin and foraminal cusps are absent, and the button is less dorsally located. More apomorphic forms (e.g., *Drosophila* s.str., Fig. 80; *Tambourella*, Fig. 81; *Stratiothyrea*, Fig. 88) have the conus sunk into a deep pedicellar cup (scarcely resembling the dorsal recess of calyptrates) and remaining asymmetrical in form, a condition very unlike that of any calyptrates that I have observed.

For the above reasons it appears that antennal morphology is likely to support an origin of the Calyptratae nearer to the Tephritoidea than to the Ephydroidea, but certainly the problem of calyptrate origin must ultimately depend on a much broader analysis of evidence.

Greenberg's plaques and abrasive surfaces on segment 2

Greenberg (1970) and Greenberg & Ash (1972) described small button-like cuticular structures or "plaques" on the external surface of the dorsomedial lobe of the pedicellar rim of some taxa in several calyptrate families, including Calliphoridae, Sarcophagidae, Tachinidae, Muscidae, Fanniidae, and Scathophagidae. He also recorded their absence in examined material of *Stomoxys calcitrans* (Linné) (Muscidae), *Nemorilla maculosa* (Meigen) (Tachinidae), and *Drosophila melanogaster* Meigen (Drosophilidae). In their typical form in the Calliphoridae and Sarcophagidae each Greenberg's plaque bears a minute bulbous setula, which is liable to wear in older flies, and is overlapped by a group of fine microtrichia. I also noted these plaques in *Musca vetustissima* Walker and *Hydrotaea* sp. (Muscidae), but they are apparently absent in *Glossina* sp. (Glossinidae), *Australofannia* sp. (Fanniidae), *Axinia lucaris* Colless (Axiniidae or Rhinophoridae), and *Amenia chrysame* (Walker) (Calliphoridae, Ameniinae). Greenberg & Ash found the plaques apparently not to have an olfactory function, and they appear to be modified macrotrichia in which the membranous socket has become more conspicuous than the reduced setula.

I consider these modifications in the same broad category as the specialized abrasive dorsomedial surface of segment 2 observed in numerous taxa of acalyptrate schizophorans. Specially developed spination on this surface, often showing signs of abrasion under high magnification, occurs in *Myopa* sp. (family Conopidae), *Cardiacera carnei* (Paramonov) (family Pyrgotidae, see Fig. 134), in several tephritid genera (Figs 156, 157), in some *Rhytidortalis* spp. (family Platystomatidae, see D. McAlpine 2000), *Dayomyia molens* McAlpine (family Platystomatidae, see D. McAlpine, 2007b), and in *Tethinosoma fulvifrons* Malloch (family Canacidae, formerly in Tethinidae, see D. McAlpine 2007a). Also specimens of *Stratiothyrea* (family Ephydridae, Fig. 87), *Chyliza* (family Psilidae, Fig. 112), *Senostoma* (family Tachinidae), *Stomorhina* (family Rhiniidae, Fig. 172), and *Syringogaster* (family Syringogastridae, Fig. 114) show signs of abrasion on this surface, though without obvious morphological adaptation.

It is likely that a more thorough survey of schizophoran antennae would reveal evidence of such specialized usage in many additional taxa. The biological significance of the abrasive antennal surface remains unknown.

ACKNOWLEDGMENTS. I am greatly indebted to Suzanne M. Lindsay, under whose tireless application to electron microscopy so many unrecorded features of the dipterous antenna were discovered. David Britton, Shane McEvey, Daniel Bickel, Russell Cox, Jacqueline Recsei, and Helen Smith have helped in various ways, and the last processed the manuscript. The following have provided significant study material: A. Rung Baptista, D.A. Barraclough, D.R. Britton, D.H. Colless, G.W. Courtney, G. Daniels, G.B. Davies, A.H. Kirk-Spriggs, W.N. Mathis, B. Merz, B.R. Stuckenberg, S.L. Winterton, D.K. Yeates.

References

Amorim, D. de S., and D. K. Yeates. 2006. Pesky gnats: ridding dipteran classification of the Nematocera. *Studia dipterologica* 13: 3–9.

Arillo, A., and B. M. Mostovski. 1999. A new genus of Prioriphorinae (Diptera, Phoridae) from the Lower Cretaceous amber of Alava (Spain). *Studia dipterologica* 6: 251–255.

Barraclough, D. A., and D. K. McAlpine. 2006. Natalimyzidae, a new African family of acalyptrate flies (Diptera, Schizophora, Sciomyzoidea). *African Invertebrates* 47: 117–134.

Brake, I. 2000. Phylogenetic systematics of the Milichiidae (Diptera, Schizophora). *Entomologica scandinavica*. Supplement 57: 120 pp.

Brown, B. V. 2007. A further new genus of primitive phorid fly (Diptera: Phoridae) from Baltic amber and its phylogenetic implications. *Contributions in Science* 513: 14 pp.

Buck, M. 2006. A new family and genus of acalyptrate flies from the Neotropical region, with a phylogenetic analysis of Carnoidea family relationships (Diptera, Schizophora). *Systematic Entomology* 31: 377–404.

Cameron, S. L., C. L. Lambkin, S. C. Barker, and M. F. Whiting. 2007. A mitochondrial genome phylogeny of Diptera: whole genome sequence data accurately resolve relationships over broad timescales with high precision. *Systematic Entomology* 32: 40–59.

Chandler, P. J. 1994. The Oriental and Australasian species of Platypezidae (Diptera). *Invertebrate Taxonomy* 8: 351–434.

Chandler, P. J. 1998. Family Opetiidae. In *Contributions to a Manual of Palaearctic Diptera*, ed. L. Papp and B. Darvas, 3, 17–25. Budapest: Science Herald.

Chapman, R. F. 1971. *The Insects. Structure and Function* (edition 2): xii + 819 pp. New York: Elsevier.

Chapman, R. F. 1991. Chapter 2. General anatomy and function. *The Insects of Australia*, second edition, pp. 33–67. Carlton, Melbourne: Melbourne University Press.

Chen, L., and H. Y. Fadamiro. 2008. Antennal sensilla of the decapitating phorid fly, *Pseudacteon tricuspis* (Diptera: Phoridae). *Micron* (ScienceDirect) 39: 517–525.

Chvala, M. 1983. The Empidoidea (Diptera) of Fennoscandia and Denmark. II. General Part. The families Hybotidae, Atelestidae and Microphoridae. *Fauna entomologica scandinavica* 12: 5–279 + 2 unnumbered pages.

Clements, A. N. 1956. The antennal pulsating organs in mosquitoes and other Diptera. *Quarterly Journal of Microscopical Science* 97: 429–433.

Colless, D. H. 1994. A new family of muscoid Diptera from Australasia, with sixteen new species in four new genera (Diptera: Axiniidae). *Invertebrate Taxonomy* 8: 471–534.

Colless, D. H., and D. K. McAlpine. 1991. Chapter 39. Diptera (flies). *The Insects of Australia*, second edition, pp. 717–786. Carlton, Melbourne: Melbourne University Press.

Collins, K. P., and B. M. Wiegmann. 2002a. Phylogenetic relationships and placement of the Empidoidea (Diptera: Brachycera) based on 28S rDNA and EF-1α sequences. *Insect Systematics and Evolution* 33: 421–444.

Collins, K. P., and B. M. Wiegmann. 2002b. Phylogenetic relationships of the lower Cyclorrhapha (Diptera: Brachycera) based on 28S rDNA sequences. *Insect Systematics and Evolution* 33: 445–456.

Crampton, G. C. 1942. The external morphology of the Diptera. In *Guide to the Insects of Connecticut. State Geological and Natural History Survey Bulletin* 64: 10–165.

Crosskey, R. W., ed. 1980. Catalogue of the Diptera of the Afrotropical Region. 1437 pp. London: British Museum (Natural History).

Day, M. F. 1955. A new sense organ in the head of the mosquito and other nematocerous flies. *Australian Journal of Zoology* 3: 331–335.

Disney, R. H. L. 1988. The form of articulation between the pedicel and first flagellar segment of the antenna in flies (Diptera). *The Entomologist* 107: 93–103.

Disney, R. H. L. 1994. *Scuttle flies: the Phoridae*, 467 pp. London: Chapman and Hall.

Disney, R. H. L. 2001. Sciadoceridae (Diptera) reconsidered. *Fragmenta faunistica* 44: 309–317.

Disney, R. H. L. 2003. Tasmanian Phoridae (Diptera) and some additional Australasian species. *Journal of Natural History* 37: 505–639.

DuBose, W. P., and R. C. Axtell. 1968. Sensilla on the antennal flagella of *Hippelates* eye gnats. *Annals of the Entomological Society of America* 61: 1547–1561.

Eggers, F. 1923. Ergebnisse von Untersuchungen am Johnstonschen Organ der Insekten und ihre Bedentung der stiftführenden Sinnesorgane. *Zoologischer Anzeiger* 57: 224–240.

Faucheux, M. J. 2004a. Sensilla placodea on the antennae of Lepidoptera. *Annales de la Société Entomologique de France* 40: 105–107.

Faucheux, M. J. 2004b. Antennal sensilla of Trichoptera and Lepidoptera: phylogenetic considerations. *Bulletin de l'Institute Royal des Sciences Naturelles de Belgique*. Entomologie 74: 69–71.

Feijen, H. R. 1983. Systematics and phylogeny of Centrioncidae, a new Afromontane family of Diptera (Schizophora). *Zoologische Verhandelingen* (Leiden) 202: 137 pp.

Ferrar, P. 1979. The immature stages of dung-breeding muscoid flies in Australia, with notes on the species, and keys to the larvae and puparia. *Australian Journal of Zoology, Supplementary Series* 73: 106 pp.

Greenberg, B. 1970. Species distribution of new structures on fly antennae. *Nature* 28: 1338–1339.

Greenberg, B., and N. Ash. 1972. Setiferous plaques on antennal pedicels in muscoid Diptera: appearance in various species and tests of function. *Annals of the Entomological Society of America* 65: 1340–1346.

Griffiths, G. C. D. 1972. *The phylogenetic classification of the Diptera Cyclorrhapha with special reference to the structure of the male postabdomen*. 340 pp. The Hague: W. Junk.

Grimaldi, D. A. 1990. A phylogenetic revised classification of genera in the Drosophilidae (Diptera). *Bulletin of the American Museum of Natural History* 197: 139 pp.

Grimaldi, D. A., and J. Cumming. 1999. Brachyceran Diptera in Cretaceous amber and Mesozoic diversification of the Eremoneura. *Bulletin of the American Museum of Natural History* 239: 124 pp.

Grimaldi, D. A., J. M. Cumming, and A. Arillo. 2009. Chimeromyiidae, a new family of Eremoneuran Diptera from the Cretaceous. *Zootaxa* 2078: 33–54.

Grimaldi, D. A., and M. S. Engel. 2005. *Evolution of the Insects*: xv + 755 pp. Cambridge: Cambridge University Press.

Grimaldi, D. A., and W. N. Mathis. 1993. Fossil Periscelididae (Diptera). *Proceedings of the Entomological Society of Washington* 95: 383–403.

Hennig, W. 1952. *Die Larvenformen der Dipteren* 3: vii + 628 pp. Berlin: Akademie-Verlag.

Hennig, W. 1965. Die Acalyptratae des Baltischen Bernsteins und ihre Bedeutung für die Erforschung der phylogenetischen Entwicklung dieser Diptera–Gruppe. *Stuttgarter Beiträge zur Naturkunde* 145: 215 pp.

Hennig, W. 1969. Neue Übersicht über die aus dem Baltischen Bernstein bekannten Acalyptratae (Diptera: Cyclorrhapha). *Stuttgarter Beiträge zur Naturkunde* 209: 42 pp.

Hennig, W. 1971. Neue Untersuchungen über die Familien der Diptera Schizophora (Diptera: Cyclorrhapha). *Stuttgarter Beiträge zur Naturkunde* 226: 76 pp.

Hennig, W. 1973. Diptera (Zweiflügler). *Handbuch der Zoologie* 4(2) 2:337 + 4 unnumbered pp.

Hennig, W. 1976. Das Hypopygium von *Lonchoptera lutea* Panzer und die phylogenetischen Verwandtschaftsbeziehungen der Cyclorrhapha (Diptera). *Stuttgarter Beiträge zur Naturkunde* (A) 283: 63 pp.

Heymons, R. 1943. Biologische Beobachtungen an Sphaeroceriden (Borboriden). *Zeitschrift für Morphologie und Ökologie der Tiere* 40: 93–116.

Hicks, J. B.. 1857. On a new structure in the antenna of insects. *Transactions of the Linnean Society of London* 22(2): 147–154, pll. 29, 30.

Hu, F., G.-N. Zhang, F.-X. Jia, W. Dou, and J.-J. Wang. 2010. Morphological characterization and distribution of antennal sensilla in six fruit flies (Diptera: Tephritidae). *Annals of the Entomological Society of America* 103: 661–670.

Imms, A. D., O. W. Richards, and R. G. Davies. 1957. *A General Textbook of Entomology*, edition 9: x + 886 pp. London: Methuen & Co.

Kessel, E. L. 1960. The response of *Microsania* and *Hormopeza* to smoke (Diptera: Platypezidae and Empididae). *The Pan-Pacific Entomologist* 36: 67–68.

Kirk-Spriggs, A. H., M. Kotrba, and R. S. Copeland. 2011. Further details of the morphology of the enigmatic African fly *Mormotomyia hirsuta* Austen (Diptera: Mormotomyiidae). *African Invertebrates* 52: 145–165.

Korneyev, V. A. 2004. Genera of Palaearctic Pyrgotidae (Diptera, Acalyptrata), with nomenclatural notes and a key. *Vestnik zoologii* 38: 19–46.

Kutty, S. N., T. Pape, B. M. Wiegmann, and R. Meier. 2010. Molecular phylogeny of the Calyptratae (Diptera: Cyclorrhapha) with an emphasis on the superfamily Oestroidea and the position of Mystacinobiidae and McAlpine's fly. *Systematic Entomology* 35: 614–635.

Lowne, B. T.. 1895. *The anatomy, physiology, morphology, and development of the blow-fly* (*Calliphora erythrocephala*). Vol. II: i–viii, 351–778, pll. 22–52.

McAlpine, D. K. 1978. Description and biology of a new genus of flies representing a new family (Diptera, Schizophora, Neurochaetidae). *Annals of the Natal Museum* 23: 273–295.

McAlpine, D. K. 1983. A new subfamily of Aulacigastridae (Diptera: Schizophora), with a discussion of aulacigastrid classification. *Australian Journal of Zoology* 31: 55–78.

McAlpine, D. K. 1991. Review of the Australian kelp flies (Diptera: Coelopidae). *Systematic Entomology* 16: 29–84.

McAlpine, D. K. 1993. Review of the upside-down flies (Diptera: Neurochaetidae) of Madagascar and Africa, and the evolution of neurochaetid host plant associations. *Records of the Australian Museum* 45: 221–239.
doi:10.3853/j.0067-1975.45.1993.21

McAlpine, D. K. 1997. Gobryidae, a new family of acalyptrate flies (Diptera: Diopsoidea), with a discussion of relationships of the diopsoid families. *Records of the Australian Museum* 49: 167–194.
doi:10.3853/j.0067-1975.49.1997.1264

McAlpine, D. K. 2000. Australian signal flies of the genus *Rhytidortalis* (Diptera: Platystomatidae). *Proceedings of the Linnean Society of New South Wales* 121:147–174.

McAlpine, D. K. 2002. Some examples of reduced segmentation of the arista in Diptera-Cyclorrhapha, and some phylogenetic implications. *Studia dipterologica* 9: 3–17.

McAlpine, D. K. 2007a. The surge flies (Diptera, Canacidae, Zaleinae) of Australasia and notes on tethinid-canacid morphology and relationships. *Records of the Australian Museum* 59: 27–64.
doi:10.3853/j.0067-1975.59.2007.1468

McAlpine, D. K. 2007b. New taxa of signal flies (Diptera: Platystomatidae) of New Caledonia. *Records of the Australian Museum* 59: 65–77.
doi:10.3853/j.0067-1975.59.2007.1485

McAlpine, D. K. 2008. New extant species of ironic flies (Diptera: Ironomyiidae) with notes on ironomyiid morphology and relationships. *Proceedings of the Linnean Society of New South Wales* 129:17–38.

McAlpine, J. F., ed. 1981. *Manual of Nearctic Diptera*. Vol. 1. Hull, Quebec: Canadian Government Publishing Centre.

McAlpine, J. F. 1981. 2. Morphology and terminology — adults. In *Manual of Nearctic Diptera*, ed. J. F. McAlpine, 1: 9–63. Hull, Quebec: Canadian Government Publishing Centre.

McAlpine, J. F. 1987. 68. Pallopteridae. In *Manual of Nearctic Diptera*, ed. J. F. McAlpine, 2: 839–843. Hull, Quebec: Canadian Government Publishing Centre.

McAlpine, J. F. 1989. 116. Phylogeny and classification of the Muscomorpha. In *Manual of Nearctic Diptera*, ed. J. F. McAlpine, 3: 1397–1578. Hull, Quebec: Canadian Government Publishing Centre.

McIver, S. B. 1975. Structure of cuticular mechanoreceptors of arthropods. *Annual Review of Entomology* 20: 381–397.

Meier, R., and B. M. Wiegmann. 2002. A phylogenetic analysis of Coelopidae (Diptera) based on morphological and DNA sequence data. *Molecular Phylogenetics and Evolution* 25: 393–407.

Moulton, J. K., and B. M. Wiegmann. 2004. Evolution and phylogenetic utility of CAD (rudimentary) among Mesozoic-aged eremoneuran Diptera (Insecta). *Molecular Phylogenetics and Evolution* 31: 363–378.

Nagatomi, A., and N. Liu. 1994. Apystomyiidae, a new family of Asiloidea (Diptera). *Acta zoologica hungarica* 40: 203–218.

Oosterbroek, P., and G. W. Courtney. 1995. Phylogeny of the nematocerous families of Diptera. *Zoological Journal of the Linnean Society* 115: 267–311.

Peterson, B. V. 1987. Phoridae. In *Manual of Nearctic Diptera*, ed. J. F. McAlpine 2, 689–712. Hull, Quebec: Canadian Government Publishing Centre.

Pfeil, R. M., R. A. Walsh, and R. O. Mumma. 1994. Scanning electron microscopic examination of the putative olfactory structures possessed by the phorid fly, *Megaselia halterata* (Diptera, Phoridae). *Scanning Microscopy* 8: 687–694.

Richards, O. W., and R. G. Davies. 1977. *Imms' General Textbook of Entomology*. 2: Classification and Biology i–viii, 421–1354. London: Chapman & Hall.

Roback, S. S. 1951. A classification of the muscoid calyptrate Diptera. *Annals of the Entomological Society of America* 44: 327–361.

Ross, K. T. A., and M. Anderson. 1987. Morphology of the antennal sensilla of the cabbage root fly, *Delia radicum* L. (Diptera: Anthomyiidae). *International Journal of Insect Morphology and Embryology* 16: 331–342.

Ross, K. T. A., and M. Anderson. 1991. Ultrastructure of the funicular sensilla of the cabbage root fly, *Delia radicum* L. (Diptera: Anthomyiidae). *International Journal of Insect Morphology and Embryology* 20: 83–101.

Sabrosky, C. W. 1999. Family-group names in Diptera. *Myia* 10: 1–360.

Schlinger, E. I. 1981. Chapter 43, Acroceridae. In *Manual of Nearctic Diptera*, ed. J. F. McAlpine, 1: 575–584. Hull, Quebec: Canadian Government Publishing Centre.

Shanbhag, S. R., K. Singh, and R. N. Singh. 1995. Fine structure and primary sensory projections of sensilla located in the sacculus of the antenna of *Drosophila melanogaster*. *Cell Tissue Research* 282: 237–249.

Sinclair, B. J., and J. M. Cumming. 2006. The morphology, higher-level phylogeny and classification of the Empidoidea (Diptera). *Zootaxa* 1180: 172 pp.

Smith, K. M. 1919. Comparative study of certain sense-organs in the antennae and palpi of Diptera. *Proceedings of the Zoological Society of London* 1919: 31–69, pll. 1–4.

Snodgrass, R. E. 1935. *Principles of Insect Morphology*. ix + 667 pp. New York: McGraw-Hill.

Soenen, M. A. 1940. L'organe de Johnston des diptères brachycères. *Annales de la Société scientifique de Bruxelles* 40(2): 9–22, 1 pl.

Stocker, R. F. 2001. *Drosophila* as a focus in olfactory research; mapping of olfactory sensilla by fine structure, odor specificity, odorant receptor expression, and central connectivity. *Microscopy Research and Technique* 55: 284–296.

Stuckenberg, B. R. 1999. Antennal evolution in the Brachycera (Diptera), with a reassessment of terminology relating to the flagellum. *Studia dipterologica* 6, 33–48.

Sukontason, K., K. L. Sukontason, R. C. Vogtsberger, N. Boonchu, T. Chaiwong, S. Piangjai, and H. Disney. 2005. Ultrastructure of coeloconic sensilla on postpedicel and maxillary palp of *Megaselia scalaris* (Diptera: Phoridae). *Annals of the Entomological Society of America* 98: 113–118.

Theodor, O. 1967. An Illustrated Catalogue of the Rothschild Collection of Nycteribiidae (Diptera) in the British Museum (Natural History) viii + 506 pp, 5 pl. London: The British Museum (Natural History).

Trautwein, M. D., B. M. Wiegmann, and D. K. Yeates. 2010. A multigene phylogeny of the fly superfamily Asiloidea (Insecta): taxon sampling and additional genes reveal the sister-group to all higher flies (Cyclorrhapha). *Molecular Phylogenetics and Evolution* 56: 918–930.

Tschirnhaus, M. von, and C. Hoffeins. 2009. Fossil flies in Baltic amber—insights in the diversity of Tertiary Acalyptratae (Diptera, Schizophora), with new morphological characters and a key based on 1,000 collected inclusions. *Denisia* 26, neue Serie 86: 171–212.

Vockeroth, J. R., and F. C. Thompson. 1987. Chapter 52: Syrphidae. In *Manual of Nearctic Diptera*, ed. J. F. McAlpine, 2: 713–743. Hull, Quebec: Canadian Government Publishing Centre.

Vossbrinck, C. R., and S. Friedman. 1989. A 28s ribosomal RNA phylogeny of certain cyclorrhaphous Diptera based upon a hypervariable region. *Systematic Entomology* 14: 417–431.

Wada, S. 1991. Morphologische Indizien für das unmittelbare Schwestergruppeverhältnis der Schizophora mit den Syrphoidea ("Aschiza") in der phylogenetischen Systematik der Cyclorrhapha (Diptera: Brachycera). *Journal of Natural History* 25, 1531–1570.

Wellington, W. G. 1946. Some reactions of muscoid Diptera to changes in atmospheric pressure. *Canadian Journal of Research (D: Zoological Sciences)* 24: 105–117.

Wiegmann, B. M., *et al.* 2011. Episodic radiations in the fly tree of life. *PNAS* Early edition: 1–6.
doi:10.1073/pnas.1012675108

Wigglesworth, V. B. 1950. *The Principles of Insect Physiology* (edition 4): viii + 544 pp. London: Methuen & Co.

Wirth, W. W., W. N. Mathis, and J. R. Vockeroth. 1987. Chapter 98: Ephydridae. In *Manual of Nearctic Diptera*, ed. J. F. McAlpine, 2: 1027–1047. Hull, Quebec: Canadian Government Publishing Centre.

Zatwarnicki, T. 1996. A new reconstruction of the eremoneuran hypopygium and its implications for classification (Insecta: Diptera). *Genus* 7: 103–175.

Records of the Australian Museum (2011) Vol. 63: 167–202. ISSN 0067-1975
doi:10.3853/j.0067-1975.63.2011.1581

Descriptions of New Species of the Diverse and Endemic Land Snail *Amplirhagada* Iredale, 1933 from Rainforest Patches across the Kimberley, Western Australia (Pulmonata: Camaenidae)

FRANK KÖHLER

Department of Environment and Conservation of Western Australia, Science Division, Wildlife Place, Woodvale WA 6026, Australia and

Australian Museum, 6 College Street, Sydney NSW 2010, Australia
frank.koehler@austmus.gov.au

ABSTRACT. Fifteen species of the camaenid land snail *Amplirhagada*, which are endemic to the Kimberley region in Western Australia, are newly described in the present work based on material collected in 1987 during the Kimberley Rainforest Survey of the then Dept. Conservation and Land Management, Western Australia. These species were listed previously as new discoveries under preliminary species identifications but have never been validly described. All of them were collected in rainforest and vine thicket patches across the Kimberley, where they generally occur as narrow-range endemics. The species are most typically characterized by a peculiar penial anatomy while other morphological structures, such as the shell or radula, provide characters less or not suitable for unambiguous species identification. Three manuscript taxa listed as potentially new are here preliminarily subsumed under an already described taxon, *A. carinata* Solem, 1981. By contrast to all other species treated herein, *A. carinata* has a fairly large distribution around the Walcott Inlet in the Southwest Kimberley. This taxon also reveals a comparatively large amount of morphological variation not only with respect to the shell but also to its genital anatomy. This unusual morphological variation is discussed as being potentially indicative of on-going lineage differentiation and the presence of a species complex, which cannot be satisfactorily resolved at the present stage.

KÖHLER, FRANK. 2011. Descriptions of new species of the diverse and endemic land snail *Amplirhagada* Iredale, 1933 from rainforest patches across the Kimberley, Western Australia (Pulmonata: Camaenidae). *Records of the Australian Museum* 63(2): 167–202.

The Kimberley region in northwesternmost Western Australia has been found to harbour a hyper-diverse radiation of camaenid land snails, which matches in species richness some of the most diverse land snail faunas worldwide (Köhler, 2010a). Despite the valiant work of Alan Solem (1931–1990) over many years, a large proportion of this land snail fauna has remained undescribed. In contrast to many other groups of helicoid land snails worldwide, the Camaenidae in northwesternmost Australia (i.e., in the Kimberley and immediately adjacent regions of the Northern Territory) have micro-ranges and are usually restricted to small islands of rainforests and vine thickets, where they occur as local endemics.

Recently, molecular comparisons have revealed high levels of mitochondrial divergence between *Amplirhagada* species from several offshore islands along the Kimberley

coast. The amount of genetic differentiation of the island species had not been expected, for the islands have repeatedly been connected with the mainland during the past 500,000 years (Johnson, O'Brien & Fitzpatrick, 2010; Köhler, 2010b). Based on this observation, it has been concluded that the origin of species predates the formation of the islands and that the phylogeographic relationships among *Amplirhagada* species may reflect earlier events, likely connected to the fragmentation of rainforest habitats since about the late Miocene or early Pliocene (Köhler, 2010a).

In terms of species numbers, *Amplirhagada* Iredale, 1933 arguably is the most diverse camaenid genus in the Kimberley. Representatives of this group are found along the Kimberley coast within a distributional range from the Buccaneer Archipelago in the south to Kalumburu in the north as well as in inland areas of the Napier, Oscar, Harding, and King Leopold Ranges, the Drysdale River Reserve, Mt Elizabeth Station and the region south of Wyndham (Solem, 1981, 1988). Thirty species were described previously by nineteenth and twentieth century authors, such as Smith (1894), Iredale (1938, 1939) and Solem (1981, 1988), while an additional twenty-six species were recently described by Köhler (2010b) bringing the total number of currently recognized species to 56. However, this number does include only a few of the allegedly 23 new species briefly listed under preliminary taxon identifications in the inventory of the Kimberley rainforests (Solem, 1991), which have remained undescribed. These species were collected in rainforest and vine thicket patches across the Kimberley, where they were mostly found as micro-endemics (Fig. 1). The relevant material has since been kept in the Field Museum of Natural History, Chicago, where it has remained essentially untouched after Alan Solem passed away in 1990 (Cameron, Pokryszko & Wells, 2005).

To revise the status of these manuscript taxa and formally describe those that are considered to represent valid species is the foremost goal of the present publication as a contribution towards a more complete knowledge of the Camaenidae of the Western Australian Kimberley.

Material and methods

This study is primarily based on ethanol preserved specimens and supplementary dry shell material collected during the Kimberley Rainforest Survey (RFS) of the then Department of Environment and Land Management, Western Australia (now Department of Environment and Conservation, DEC) in 1987–1988. This material has been kept in the Field Museum of Natural History, Chicago (FMNH). The specimen series have now been split and shared with the Western Australian Museum, Perth (WAM) and the Australian Museum, Sydney (AM).

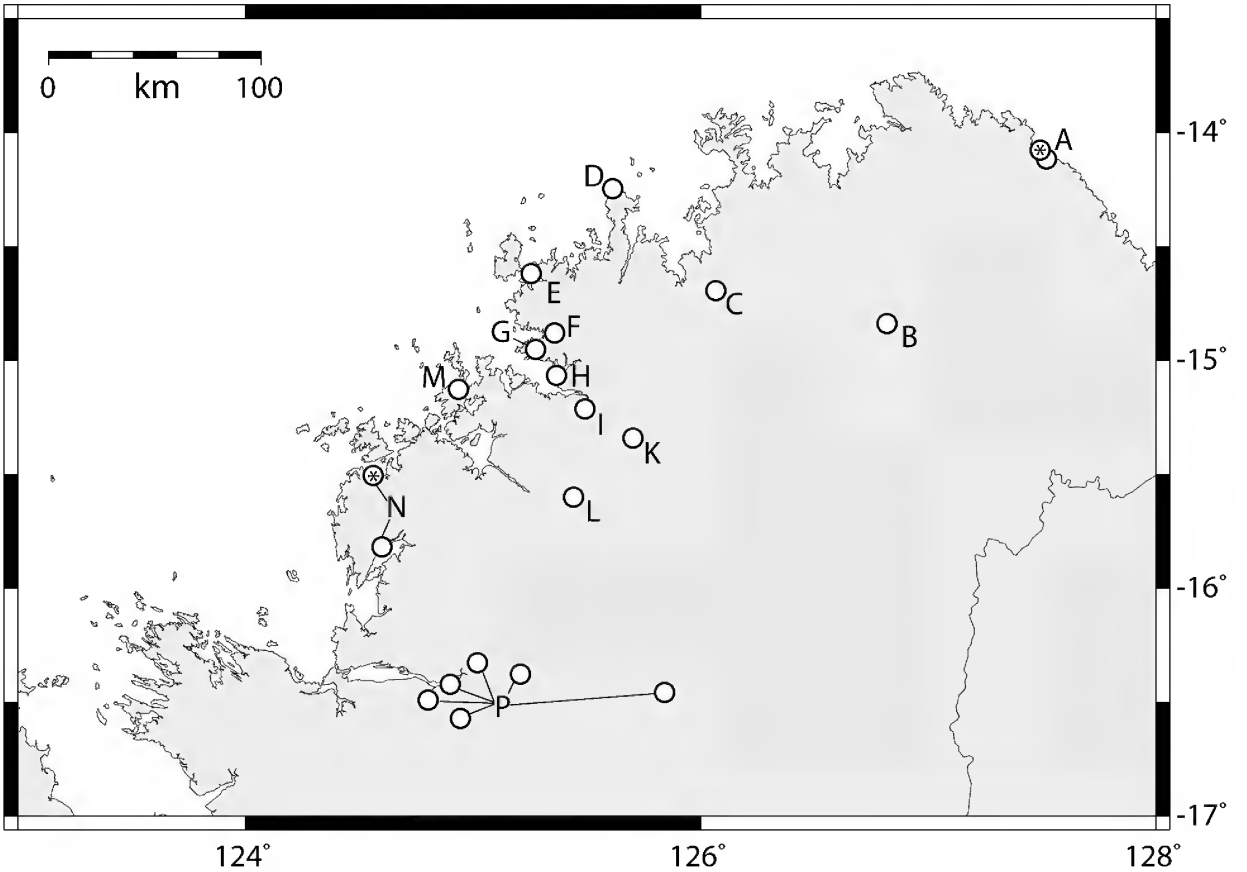

Figure 1. Distribution of *Amplirhagada* species described in the present work. *(A) A. atlantis* n.sp. *(B) A. carsoniana* n.sp. *(C) A. alicunda* n.sp. *(D) A. davidsoniana* n.sp. *(E) A. vialae* n.sp. and *A. discoidea* n.sp. *(F) A. forrestiana* n.sp. *(G) A. inusitata* n.sp. and *A. epiphallica* n.sp. *(H) A. lindsayae* n.sp. *(I) A. angustocauda* n.sp. *(K) A. moraniana* n.sp. *(L) A. gardneriana* n.sp. *(M) A. bendraytoni* n.sp. *(N) A. coffea* n.sp. *(P) A. carinata* Solem, 1981. When species occur at more than one locality, the type locality of newly described taxa is marked with an asterisk.

Morphological descriptions focus on characters of the shell, genital organs, and the radula. Morphometric shell parameters of adult shells (with calloused outer lip), such as height of shell (H), diameter of shell (D) and height of last whorl (LW) were measured with Vernier callipers precise to 0.1 mm. The numbers of whorls (N), including the protoconch, were counted as described in Barker (1999: Fig. 6). The parameter "angle of aperture" describes the angle formed between aperture and the horizontal in degrees when the shell is in an upright position. Anatomy of mantle and genital organs was studied using a binocular microscope with drawing mirror. The final inking of anatomical drawings was done by Martin Püschel (Sydney). Radulae and jaws were extracted manually, cleaned by soaking in 10% KOH solution for about six hours followed by rinsing in water and ethanol. They were mounted on carbon specimen tabs for electron scanning microscopy. Radular tooth formula gives the numbers of teeth as follows: C (central row of teeth) + number of lateral rows of teeth + number of transitional rows of teeth + number of marginal rows of teeth. Whenever the number of available specimens allowed, the anatomy was studied in two (in small series) to five specimens per sample in order to confirm that morphological features are consistently found among conspecific specimens.

Terminology for anatomical features is not always consistent and Alan Solem employed some terms that are otherwise not widely used. In order to gain clarity, terms used here are defined as follows. Anterior part of oviduct refers to the proximal portion of the oviduct from the atrium to the point where uterus and prostate fuse forming the spermoviduct. The anterior oviduct consists of vagina (most anterior portion between atrium and opening to bursa copulatrix) and free oviduct (between opening to bursa copulatrix and distal end of anterior part of oviduct). Spermoviduct consists of uterus and prostate fused to each other. Bursa copulatrix is the term used for the spermatolytic gland, which has erroneously been referred to as "spermatheca" by Alan Solem. The inner penial wall may support different structures, such as pustules (small, conical elevations) and pilasters (projecting longitudinal column). The main stimulatory pilaster is significantly larger than any other potentially present pilasters and frequently also differs in shape and structure.

Systematic descriptions

Gastropoda
Heterobranchia
Stylommatophora
Camaenidae Pilsbry, 1895

Amplirhagada Iredale, 1933

Amplirhagada Iredale, 1933: 52; Solem, 1981: 147–320; Solem, 1988: 28–32; Solem, 1991: 187–202; Solem & McKenzie, 1991: 247–263; McKenzie *et al.*, 1995: 251; Johnson, O'Brien & Fitzpatrick, 2010: 141–153; Köhler, 2010b: 217–284. Type species *Helix* (*Hadra*) *sykesi* Smith, 1894 by original designation.

Tenuigada Iredale, 1939: 68. Type species *Tenuigada percita* Iredale, 1939 by original designation.

Diagnosis

Rock or free sealer with medium sized (H = 8–23 mm, D = 15–30 mm, H/D = 0.5–1.1) shell, from thin and translucent to moderately thick, broadly conical to dome-shaped with moderately to strongly elevated spire. Umbilicus narrowly winding, entirely open to completely concealed by columellar reflection, frequently variable within species. Protoconch with weak to strongly developed radially elongated pustulations, transition to teleoconch inconspicuous. Teleoconch sculpture variable, ranging from presence of very weak axial growth lines only to presence of well-developed, regular radial lirae, which may be prominent on entire whorl surface or only on upper parts of whorls. Last whorl moderate to wide in cross-section, periphery well rounded to slightly angulated (often transitions are found within single populations). Shell colour variable, background often yellowish brown to horn, frequently banded, with brown sub-sutural and peripheral bands, or more rarely uniform with lighter base.

Mantle cavity extending between half and more than entire last whorl of shell; mantle roof with variably spotted or marbled, black pigmentation; kidney extending about half to two thirds of mantle cavity.

Genitalia typically camaenid with prostate and uterus being fused forming spermoviduct; development of gonads depending on seasonal activity and maturity. Penis with well-developed sheath, extending entire length, usually thin proximally, thick distally. Typically without well-developed epiphallus, rarely vas deferens reflecting as simple, elongated epiphallus. Penial retractor muscle attached at apex of penial complex, variable in length. Vas deferens entering penial sheath from halfway up to almost apically; entering penial chamber through variably developed verge. Inner penial wall supporting characteristic pustulation and basal pilasters (often species-specific); a main stimulatory pilaster may or may not be present, varying in development, shape and sculpture (often species-specific). Bursa copulatrix relatively simple, short, reaching or slightly extending base of spermoviduct; head usually well differentiated (inflated); inner wall of vagina and bursa copulatrix with longitudinal pilasters that vary in development and finer structure.

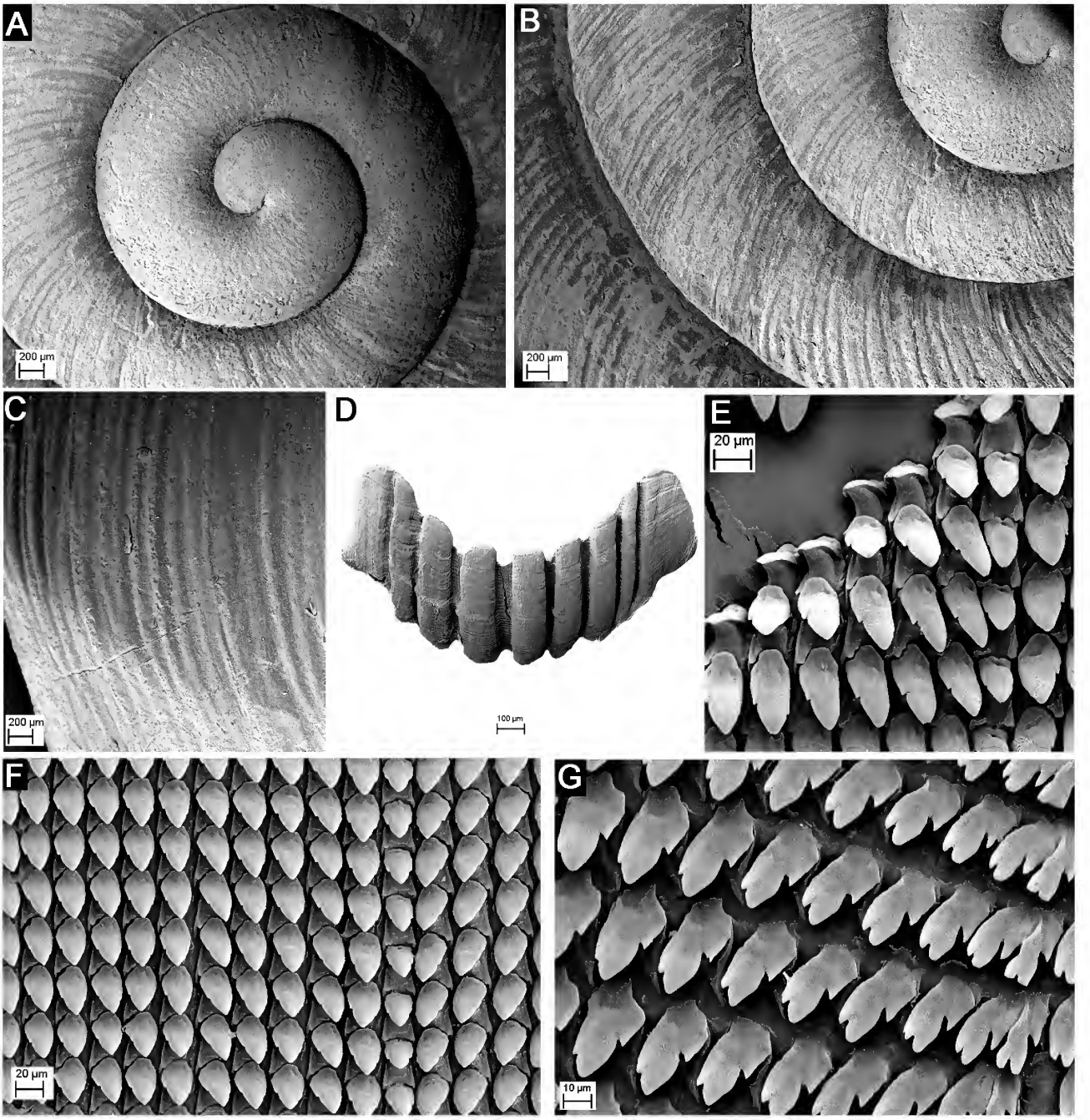

Figure 2. *Amplirhagada atlantis* n.sp. SEM of shell (AM C.472919), radula and jaw (AM C.472918). *(A)* Protoconch viewed from above. *(B)* Detail of first teleoconch whorls viewed from above. *(C)* Close-up showing sculpture on last whorl. *(D)* Jaw. *(E)* Close-up showing morphology of central and inner lateral teeth. *(F)* Central and lateral teeth viewed from above. *(G)* Inner and central marginal teeth viewed from above. Scale bars: *A–C*, 200 µm; *D*, 100 µm; *E–F*, 20 µm; *G*, 10 µm.

Albumen gland elongated. Talon embedded in albumen gland within proximal portion of albumen gland. Hermaphroditic duct tightly undulating. Radula rectangular in shape, usually between 3.5 and 5.5 mm long with 120–170 rows of teeth. Tooth formula variable, C + 12–20 + 3–4 + 15–22. Central teeth with pointed triangular mesocones, shorter than base of tooth; ectocones vestigial. Lateral teeth with bluntly pointed triangular mesocones, length equal to base of tooth; vestigial to small ectocones; endocones vestigial. Marginal teeth multicuspid, mesocones and endocones similar in length, ectocones smaller than endocones, occasionally subdivided. Species aestivating as rock or free sealers.

Amplirhagada atlantis n.sp.

Type locality. Western Australia, NW Kimberley, Joseph Bonaparte Gulf, 8.6 km SSE of Cape Bernier; 14°04'40"S 127°29'25"E (RFS-04-1; coll. V. Kessner, 04 Jun 1987) (Fig. 1).

Type material. Holotype WAM S34704 (preserved specimen) (Pl. 1.1; Table 1). Paratypes AM C.472918 (4 preserved specimens), WAM S34705 (8 preserved specimens), FMNH 220006 (12 preserved specimens), AM C.472919 (3 dried shells), WAM S34706 (10 dried shells), FMNH 220005 (13 dried shells).

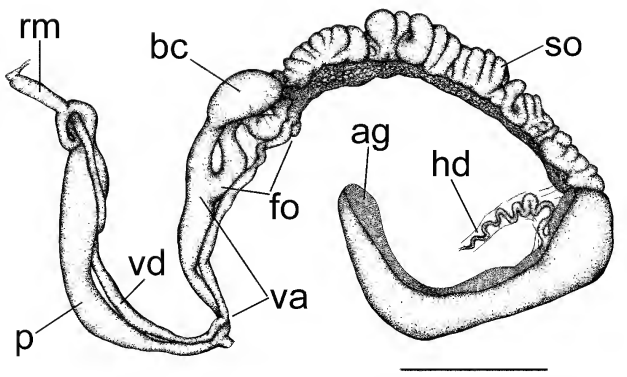

Figure 3. Genitalia of *Amplirhagada atlantis* n.sp. (AM C.472918). Abbreviations: *ag*, albumen gland; *bc*, bursa copulatrix; *fo*, free oviduct; *hd*, hermaphroditic duct; *p*, penis; *rm*, penial retractor muscle; *so,* sperm oviduct; *va*, vagina; *vd*, vas deferens. Scale bar = 5 mm.

Additional material (not dissected). WAM S34751 (5 preserved specimens), FMNH 220327 (10 preserved specimens), WAM S34752 (8 dried shells), FMNH 220328 (7 dried shells), all from 5.6 km W of Evelyn Island, mainland, behind beach and mangroves; 14°06'55"S 127°31'10"E (RFS 10-2; coll. V. Kessner, 10 Jun 1987).

Etymology. Specific name referring to the name of the seaplane "Atlantis 1925" of the two German aviators Hans Bertram and Adolph Klausmann, who in 1932 undertook a goodwill flight from Cologne, Germany, to Australia. On 14 May 1932 the aviators took off from Timor bound for Darwin but were stranded due to bad weather near Bertram Cove, where they survived for 40 days before being rescued. Being a noun the species epithet keeps its male suffix.

Description

Shell (Pl. 1.1, Fig. 2A–C). Broadly conical with moderately elevated spire. Rather thin but solid, translucent. Periphery well rounded to slightly angulate; upper and basal sectors rounded. Umbilicus 80–90% concealed by columellar reflection. Background colour horn to almost crème; no spiral bands visible; outer and inner lip colour whitish. Protoconch 2.6 mm in diameter, comprising about 1.5 whorls, with weak radially elongated pustulations. Teleoconch with faint, regular axial growth lines, evenly distributed across whorls of shell and across whorl diameter. Angle of aperture 45–60 degrees; outer lip thin, well rounded, well expanded, not or slightly reflected; basal node absent or weak. Parietal wall of inner lip inconspicuous. Average shell size 11.8±0.8 × 16.2±0.9 mm (Table 1).

Radular and jaw morphology (Fig. 2 D–G). Tooth formula C + 14 + 4 + ?; average number of rows of teeth 130 (n = 2). Jaw with nine plates.

Genital morphology (Figs 3–4). Penis straight, more or less of same length as anterior part of oviduct. Penial sheath delicate. Length of penial retractor muscle equivalent to about ¼ of length of penial complex. Penial verge extending about ¼ of length of penial chamber, slender with rounded tip. Almost entire inner penial wall covered by strongly developed pustules, which are arranged to form several corrugated longitudinal pilasters. Main stimulatory pilaster

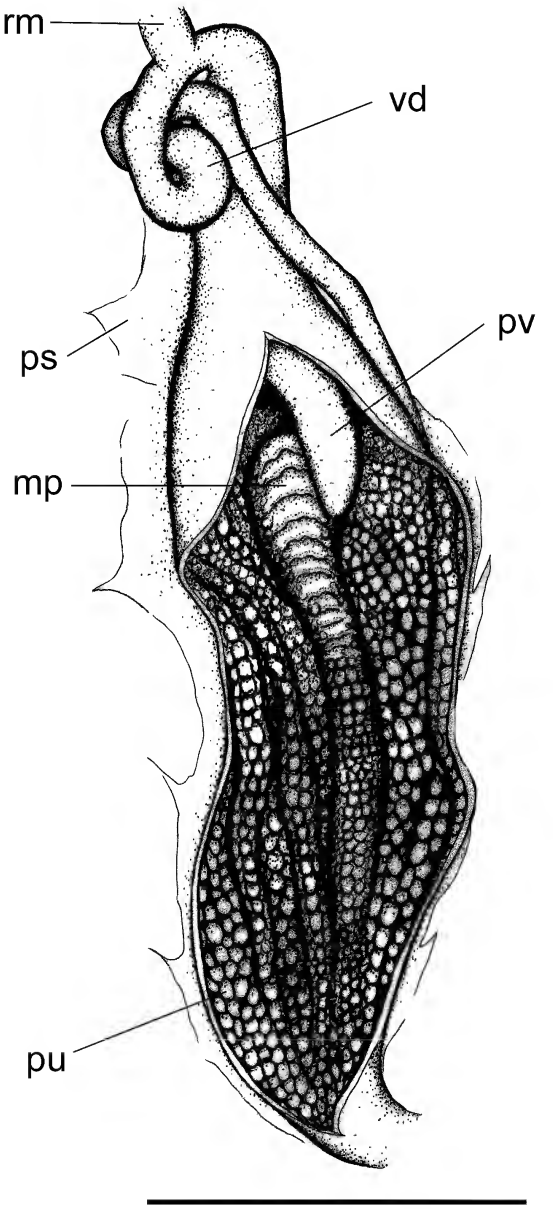

Figure 4. Penial anatomy of *Amplirhagada atlantis* n.sp. (AM C.472918). Abbreviations: *mp*, main pilaster; *ps*, penial sheath; *pu*, penis wall pustulation; *pv*, penial verge; *rm*, penial retractor muscle; *vd*, vas deferens. Scale bar = 3 mm.

well developed, elongate, comprising proximal third of inner penial wall; sculptured by smooth lateral ridges being formed by fused and flattened pustules. Vas deferens entering penial sheath near apex of penial complex. Vagina long, tubular, posteriorly slightly inflated; inner vaginal wall and inner wall of spermathecal duct support continuous, well-developed, smooth longitudinal pilasters. Bursa copulatrix short, reaching base of spermoviduct; head elongately inflated, connected with spermoviduct by connective tissue, wall of head delicate, smooth. Free oviduct rather straight comprising less than half of length of anterior part of oviduct. Spermoviduct longer than anterior part of oviduct.

Aestivation strategy. Free or rock sealer, in talus throughout vine thicket patches.

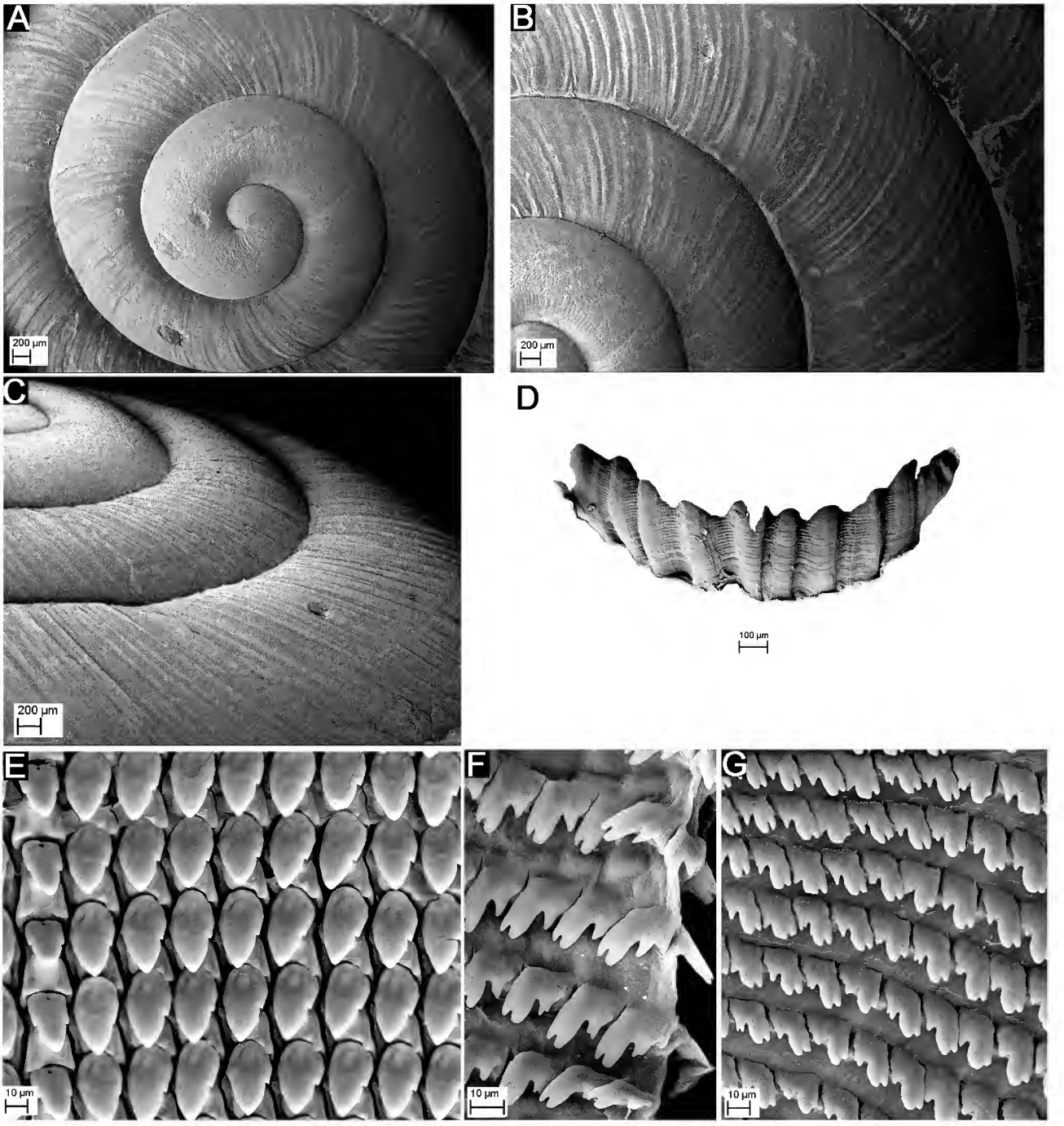

Figure 5. *Amplirhagada carsoniana* n.sp. SEM of shell (AM C.472920), radula and jaw (WAM S34708). *(A)* Protoconch viewed from above. *(B)* Detail of first teleoconch whorls viewed from above. *(C)* First teleoconch whorls viewed obliquely from above. *(D)* Jaw. *(E)* Central and lateral teeth viewed from above. *(F)* Close-up of marginal teeth. *(G)* Inner and central marginal teeth viewed from above. Scale bars: *A–C*, 200 µm; *D*, 100 µm; *E–G*, 10 µm.

Remarks. Anatomical description based on dissections of two type specimens. The non-type sample contains predominantly immature individuals not suitable for anatomical dissections. Listed by Solem (1991) as "*Amplirhagada* NSP17".

Amplirhagada carsoniana n.sp.

Type locality. Western Australia, NW Kimberley, Carson Escarpment, 2.5 km N of Face Point, base of escarpment; 14°50'20"S 126°49'10"E (RFS 10-4, coll. V. Kessner, 10 Jun 1987) (Fig. 1).

Type material. Holotype WAM S34707 (preserved specimen) (Pl. 1.2; Table 1). Paratypes WAM S34708 (preserved specimen), FMNH 220344 (preserved specimen), AM C.472920 (5 dried shells), WAM S34709 (12 dried shells), FMNH 220343 (17 dried shells).

Etymology. In reference to the Carson Escarpment, where this species was found.

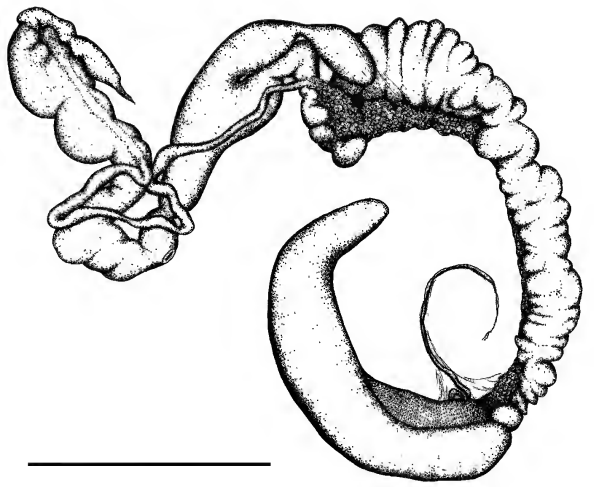

Figure 6. Genitalia of *Amplirhagada carsoniana* n.sp. (WAM S34708). For labelling of structures see Fig. 3. Scale bar = 5 mm.

Description

Shell (Pl. 1.2; Fig. 5 A–C). Broadly conical with low spire, almost discoid. Thin to delicate, translucent. Periphery rounded to slightly angulate; upper and basal sectors of whorls well rounded. Umbilicus 10–30% concealed by columellar reflection. Background colour brownish horn; peripheral band absent or well marked, thin, brown, visible on most whorls; sub-sutural diffuse, thin, visible on most whorls; outer and inner lip colour whitish. Protoconch 2.6 mm in diameter, comprising about one whorl, with weak radially elongated pustulations. Teleoconch with faint, regular axial growth lines, evenly distributed across shell surface. Angle of aperture about 45 degrees; outer lip thin, well rounded, expanded, weakly reflected; basal node absent. Parietal wall of inner lip absent or very inconspicuous. Average shell size 9.8±0.6 × 16.3±0.8 mm (Table 1).

Radular and jaw morphology (Fig. 5 D–G). Tooth formula C + 12–14 + 4 + 18–20; average number of rows of teeth 130 (n = 2). Jaw with ten plates.

Genital morphology (Figs 6–7). Penis coiled within thick penial sheath; penial complex about as long as anterior part of oviduct. Length of penial retractor muscle equivalent to about half of length of penial complex. Penial verge extending about 1/5 of length of penial chamber, slender with pointed tip. Inner penial wall entirely covered by dense pustulation; pustules forming indistinct, corrugated pilasters. Main stimulatory pilaster indistinct, formed by prolonged pustules, comprising proximal half of inner penial chamber. Vas deferens entering penial sheath within proximal third of penial complex. Vagina moderately long, distally inflated. Bursa copulatrix short, reaching base of spermoviduct. Free oviduct coiled, shorter than vagina. Spermoviduct longer than anterior part of oviduct.

Aestivation strategy. Free sealer.

Remarks. Description based on dissection of one specimen. Listed by Solem (1991) as "*Amplirhagada* NSP18" to be distinct from *A. drysdaleana* Solem, 1981. Both taxa are indeed very similar but *A. carsoniana* differs by coiled, shorter penis with shorter main pilaster, no extended basal pilasters of inner penial wall and shorter vagina. Vas deferens entering sheath half way up in *A. carsoniana* but within upper sector of penial sheath in *A. drysdaleana*. Being similar overall and occurring in close proximity to each other, both species are likely sister taxa.

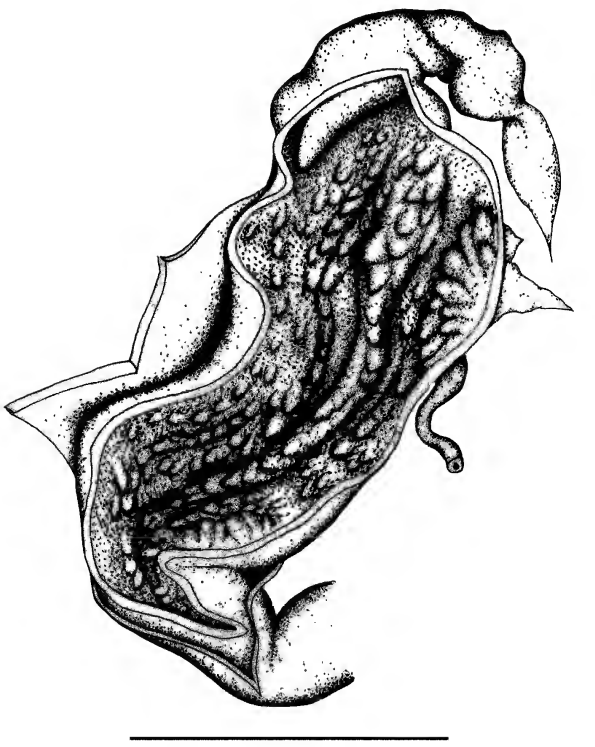

Figure 7. Penial anatomy of *Amplirhagada carsoniana* n.sp. (WAM S34708). For labelling of structures see Fig. 4. Scale bar = 3 mm.

Amplirhagada alicunda n.sp.

Type locality. Western Australia, NW Kimberley, 27 km SE Walsh Point, ca. 16 km SSW of Mt. Connor, 13 km from coast; 14°41'45"S 126°04'04"E (RFS 11-4, coll. V. Kessner, 11 Jun 1987) (Fig. 1).

Type material. Holotype WAM S34710 (preserved specimen) (Pl. 1.3; Table 1). Paratypes WAM S34711 (2 preserved specimens), FMNH 220384 (2 preserved specimens), AM C.472921 (10 dried shells), WAM S34712 (16 dried shells), FMNH 220385 (25 dried shells).

Etymology. Species epithet derived from "alicunde" (Latin = from somewhere, from any place), in reference to the remote type locality, far away from any named place.

Description

Shell (Pl. 1.3; Fig. 8 A–D). Broadly conical to semi-globose with elevated spire. Solid, not translucent. Periphery slightly compressed to slightly angulate; upper sector of whorl flattened, basal sectors rounded. Umbilicus 70–100% concealed by columellar reflection. Background colour crème to horn; peripheral band conspicuous, usually well developed, rather thin, clearly visible on most whorls;

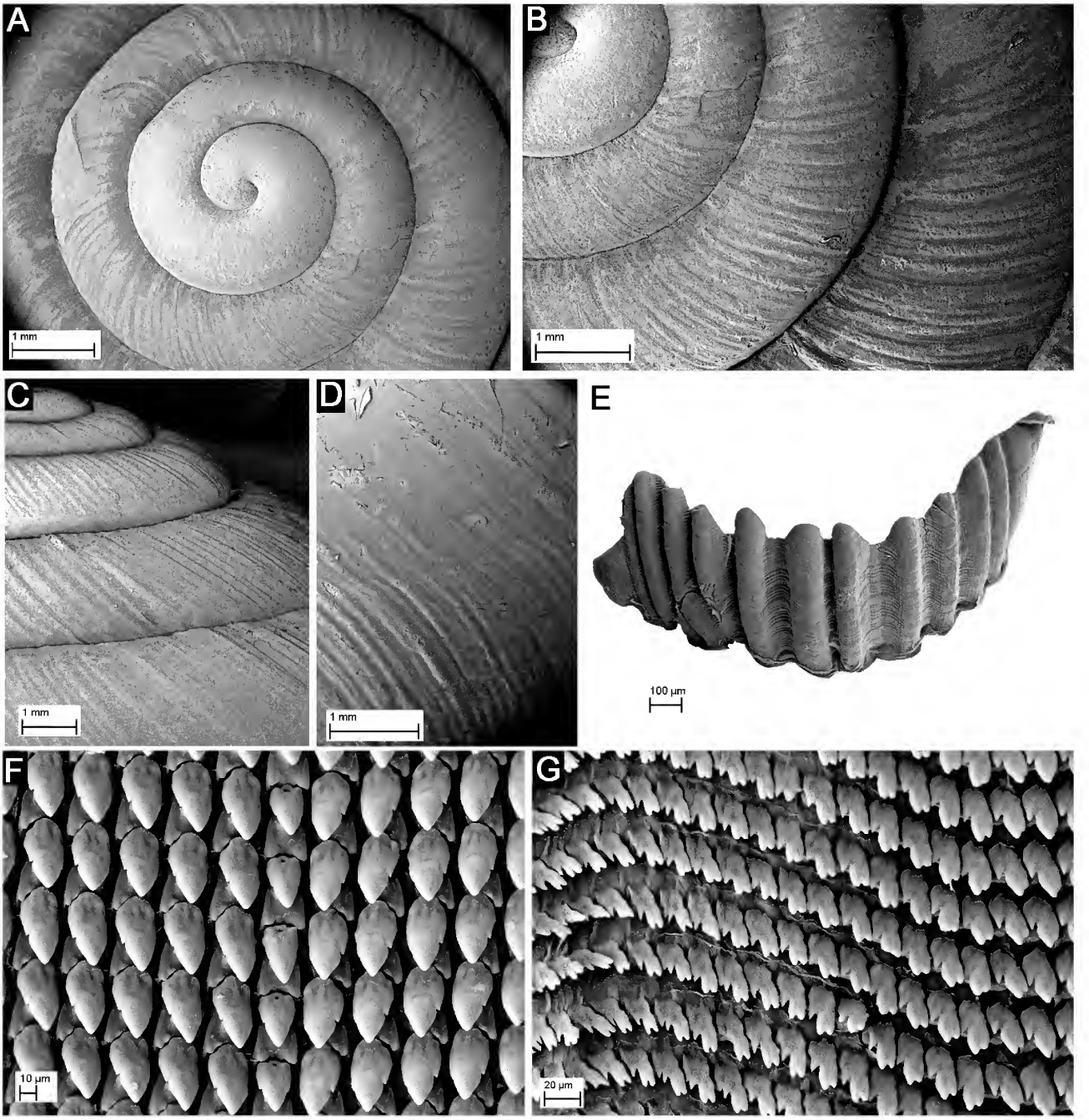

Figure 8. *Amplirhagada alicunda* n.sp. SEM of shell (AM C.472921), radula and jaw (WAM S34711). *(A)* Protoconch and first teleoconch whorls viewed from above. *(B)* Detail of first teleoconch whorls viewed from above. *(C)* First teleoconch whorls viewed obliquely from above. *(D)* Close-up showing sculpture on last whorl. *(E)* Jaw. *(F)* Central and inner lateral teeth viewed from above. *(G)* Marginal teeth viewed from above. Scale bars: *A–D*, 1 mm; *E*, 100 µm; *F*, 10 µm, *G*, 20 µm.

sub-sutural band broad, diffuse to well developed, brown, clearly visible on most whorls; outer and inner lip colour white, conspicuously contrasting shell colour. Protoconch 2.4 mm in diameter, comprising about one whorl, with very weak radially elongated pustulations. Teleoconch with faint, regular axial growth lines, evenly distributed across shell. Angle of aperture about 60 degrees; outer lip moderately thick, well rounded, slightly expanded, not reflected; basal node absent or weak. Parietal wall of inner lip very inconspicuous. Average shell size 16.0±1.4 × 20.2±0.7 mm (Table 1).

Radular and jaw morphology (Fig. 8 E–G). Tooth formula C + 16–18 + 4 + 18–20 (n = 1). Jaw with 12 plates.

Genital morphology (Figs 9–10). Penis straight, more or less of same length as anterior part of oviduct; distal part of penis proper narrow, proximal part inflated. Penial sheath delicate. Length of penial retractor muscle equivalent to about ¼ of length of penial complex. Penial verge extending about 1/10 of length of penial chamber, slender with pointed tip. Proximal part of inner penial wall entirely covered by extremely fine pustulation. Main stimulatory pilaster strongly enlarged, comprising proximal half of inner penial chamber,

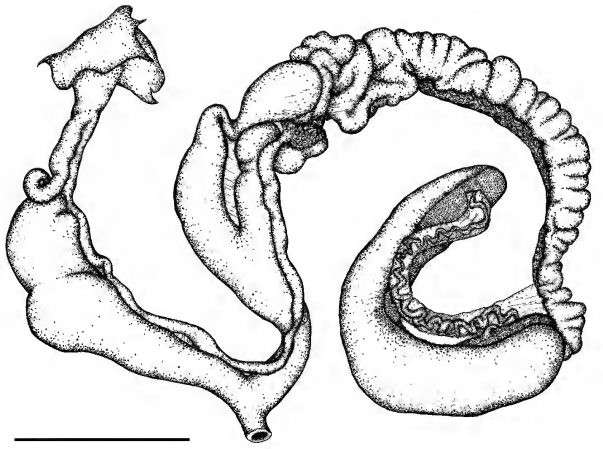

Figure 9. Genitalia of *Amplirhagada alicunda* n.sp. (WAM S34711). For labelling of structures see Fig. 3. Scale bar = 5 mm.

cone-shaped, sculptured by regularly spaced, lateral ridges that support dense rows of little hooks. Vas deferens entering penial sheath within proximal third of penial complex. Vagina moderately long, tubular; inner vaginal wall and inner wall of bursa copulatrix with continuous, well-developed, smooth longitudinal pilasters. Bursa copulatrix short, reaching base of spermoviduct. Free oviduct rather straight comprising less than half of length of anterior part of oviduct. Spermoviduct longer than anterior part of oviduct.

Aestivation strategy and ecology. Free sealer, inhabits locally restricted vine thicket.

Remarks. Anatomical description based on dissection of one specimen. Listed by Solem (1991) as "*Amplirhagada* NSP19". Shell similar to other relatively large, broadly conical species with spiral bands, such as *A. combeana* Iredale, 1938 and *A. mitchelliana* Solem, 1981 but anatomy of inner penial wall clearly different.

Amplirhagada moraniana n.sp.

Type locality. Western Australia, NW Kimberley, 25.6 km SSW of Mitchell River Homestead, N bank of Moran River, 15°20'30"S 125°42'05"E (RFS-18-2: coll. V. Kessner, 18 Jun 1987) (Fig. 1).

Type material. Holotype WAM S34713 (preserved specimen) (Pl. 1.4; Table 1). Paratypes WAM S34714 (2 preserved specimens), FMNH 220725 (3 preserved specimens), FMNH 220724 (20 dried shells), WAM S34715 (15 dried shells), AM C.472922 (6 dried shells).

Etymology. Named after the Moran River.

Description

Shell (Pl. 1.4; Fig. 11 A–E). Broadly conical with low to moderately elevated spire; thin, translucent. Periphery well rounded to slightly angulate; upper and basal sectors of whorls rounded. Umbilicus 70–90% concealed by columellar reflection. Background and ventral colour pale brownish horn; peripheral and sub-sutural bands usually absent or diffuse, visible on last whorl only; outer and inner lip whitish. Protoconch ~2.5 mm in diameter, comprising about 1.5

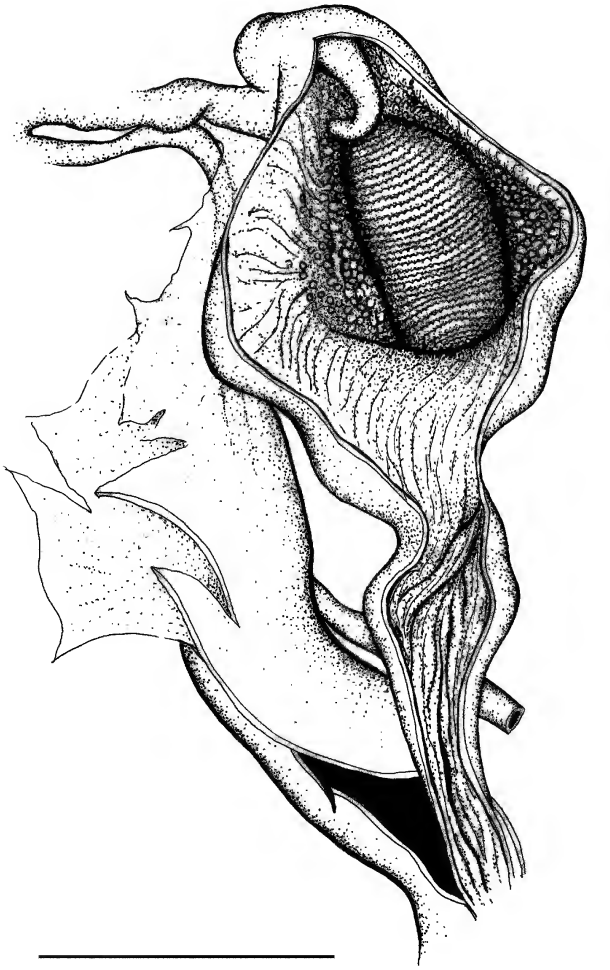

Figure 10. Penial anatomy of *Amplirhagada alicunda* n.sp. (WAM S34711). For labelling of structures see Fig. 4. Scale bar = 3 mm.

whorls, with radially elongated pustulations. Teleoconch with regular axial lirae, evenly distributed across shell surface. Angle of aperture about 45 degrees; outer lip thin, well rounded, slightly expanded, slightly reflected; basal node absent or weak. Parietal wall of inner lip inconspicuous. Average shell size 10.9±1.5 × 15.9±1.5 mm (Table 1).

Radular and jaw morphology (Fig. 1 F–J). Tooth formula C + 12–13 + 3–4 + 16–18, with 120 rows of teeth (n = 1). Jaw with nine plates.

Genital morphology (Figs 12–13). Penis straight, tubular, longer than anterior part of oviduct. Penial sheath very delicate. Length of penial retractor muscle very short, equivalent to about 1/10 of length of penial complex. Penial verge very long, extending about ¾ of length of penial chamber, slender with pointed tip. Inner penial wall almost entirely covered by reloped, rhomboid pustules that are arranged in honey-comb pattern. No main stimulatory pilaster differentiated; three to four longitudinal pilasters formed by fused, more elevated pustules are present, extending most of inner penial chamber, giving rise to corrugated longitudinal pilasters comprising distal end of inner penial wall. Vas deferens very thick, not undulating, entering penial sheath within proximal third of penial complex. Vagina long, tubular; inner vaginal wall and inner wall of bursa copulatrix with continuous, well-developed, smooth longitudinal pilasters. Bursa copulatrix slightly

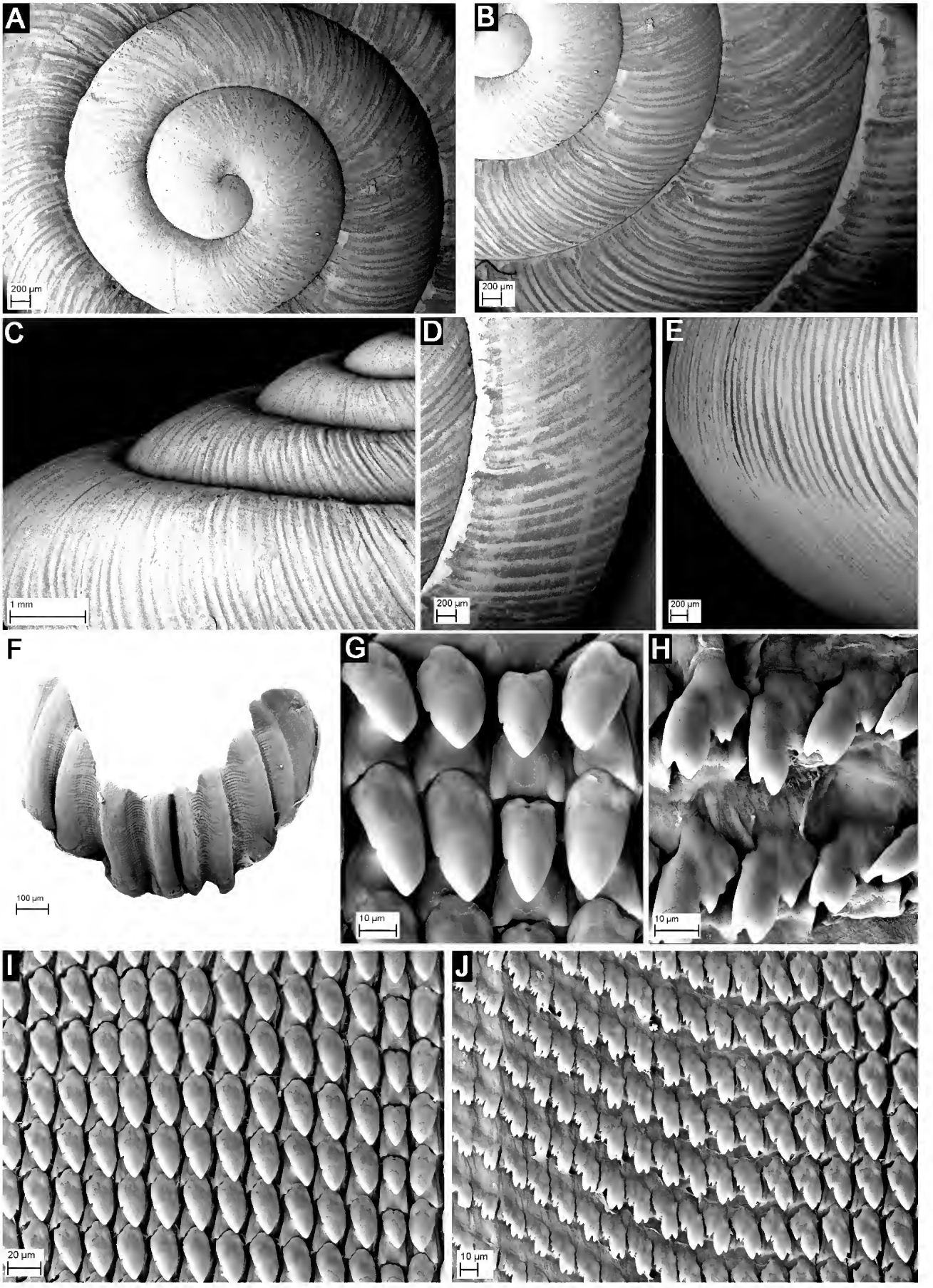
A
200 µm
B
200 µm
C
1 mm
D
200 µm
E
200 µm
F
100 µm
G
10 µm
H
10 µm
I
20 µm
J
10 µm

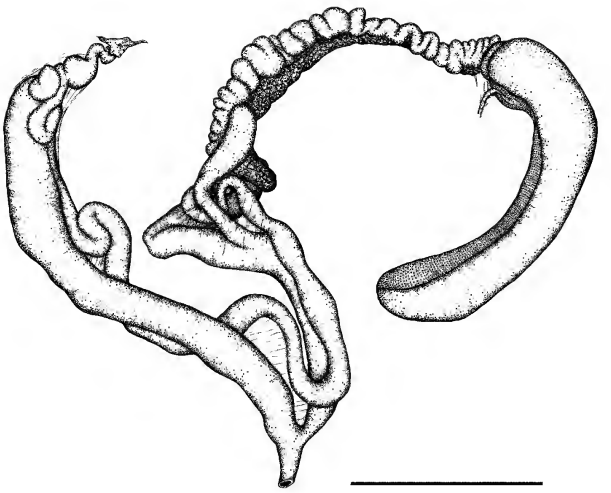

Figure 12. Genitalia of *Amplirhagada moraniana* n.sp. (WAM S34714). For labelling of structures see Fig. 3. Scale bar = 5 mm.

extending base of spermoviduct. Free oviduct comprising less than half of length of anterior part of oviduct. Spermoviduct about as long as anterior part of oviduct.

Aestivation strategy: Free sealer.

Remarks. Anatomical description based on dissection of one specimen. Listed by Solem (1991) as "*Amplirhagada* NSP20". One of the smallest species with respect to shell height and diameter; a similar shell with respect to size and shape is only found in *A. angustocauda* described further below. Elongated shape of penis and markedly elongated penial verge (almost as long as penial chamber), corrugated penial wall sculpture, and very thick vas deferens is combination of features typical only for this species.

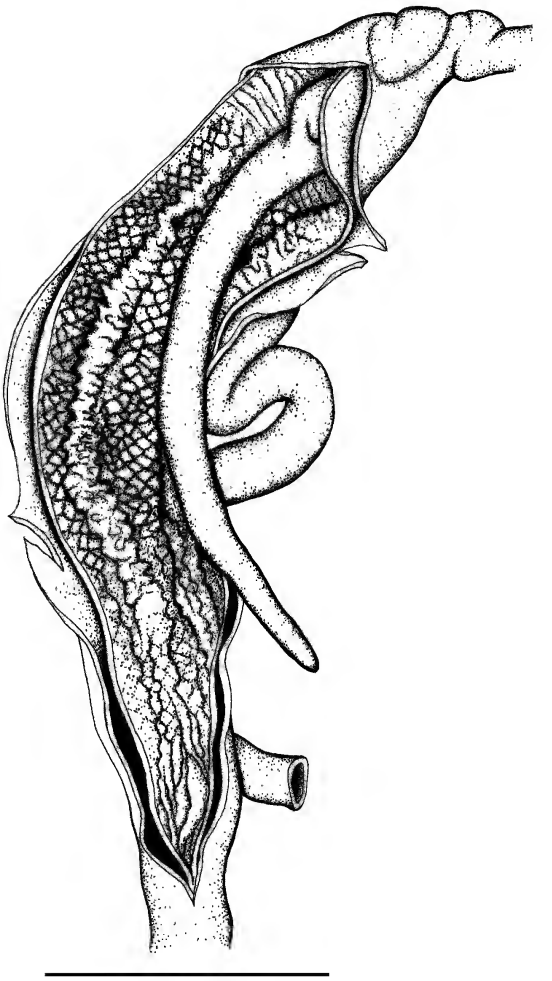

Figure 13. Penial anatomy of *Amplirhagada moraniana* n.sp. (WAM S34714). For labelling of structures see Fig. 4. Scale bar = 3 mm.

Amplirhagada davidsoniana n.sp.

Type locality. Western Australia, NW Kimberley, Admiralty Gulf, 2.6 km E Davidson Point, near Voltaire Passage; 14°14'55"S 125°36'50"E (RFS 09-2; coll. V. Kessner, 9 Jun 1987) (Fig. 1).

Type material. Holotype WAM S34716 (preserved specimen) (Pl. 1.5; Table 1). Paratypes AM C.472923 (14 preserved specimens), WAM S34717 (30 preserved specimens), FMNH 220282 (44 preserved specimens), paratypes AM C.472924 (15 shells), WAM S34718 (36 dried shells), FMNH 220283 (54 shells).

Etymology. In reference to Davidson Point.

Description

Shell (Pl. 1.5; Fig. 14 A–C). Broadly conical with moderately elevated spire. Thin to solid, translucent. Periphery evenly rounded to slightly angulate; upper and basal sectors of whorls well rounded. Umbilicus 50–80 percent concealed by columellar reflection. Background colour horn to yellowish brown; peripheral band absent to well developed, usually diffuse, rather thin, brown, visible on last whorls only; subsutural band absent or diffuse and very thin, brown, visible on last whorls only; ventral and outer lip colour horn; inner lip translucent, pale white. Protoconch c. 2.4 mm in diameter, comprising about one whorl, with well-developed, radially elongated pustulations. Teleoconch with fine, regular axial growth lines, rounded in cross-section; spaces equal to thickness of lines; sculpture evenly distributed across whorls of shell and across whorl diameter, height of lirae reduced

Figure 11 (facing page). *Amplirhagada moraniana* n.sp. SEM of shell (AM C.472922), radula and jaw (WAM S34714). *(A)* Protoconch and first teleoconch whorls viewed from above. *(B)* Detail of first teleoconch whorls viewed from above. *(C)* First teleoconch whorls viewed obliquely from above. *(D)* Close-up showing sculpture on last whorl, viewed from above. *(E)* Close-up showing sculpture on last whorl, lateral view. *(F)* Jaw. *(G)* Close-up showing detail of central and inner marginal teeth. *(H)* Close-up showing detail of central marginal teeth. *(I)* Central and inner lateral teeth viewed from above. *(J)* Marginal teeth viewed from above. Scale bars: *A–B, D–E*, 200 µm; *C*, 1 mm; *F*, 100 µm; *G–H, J*, 10 µm; *I*, 20 µm.

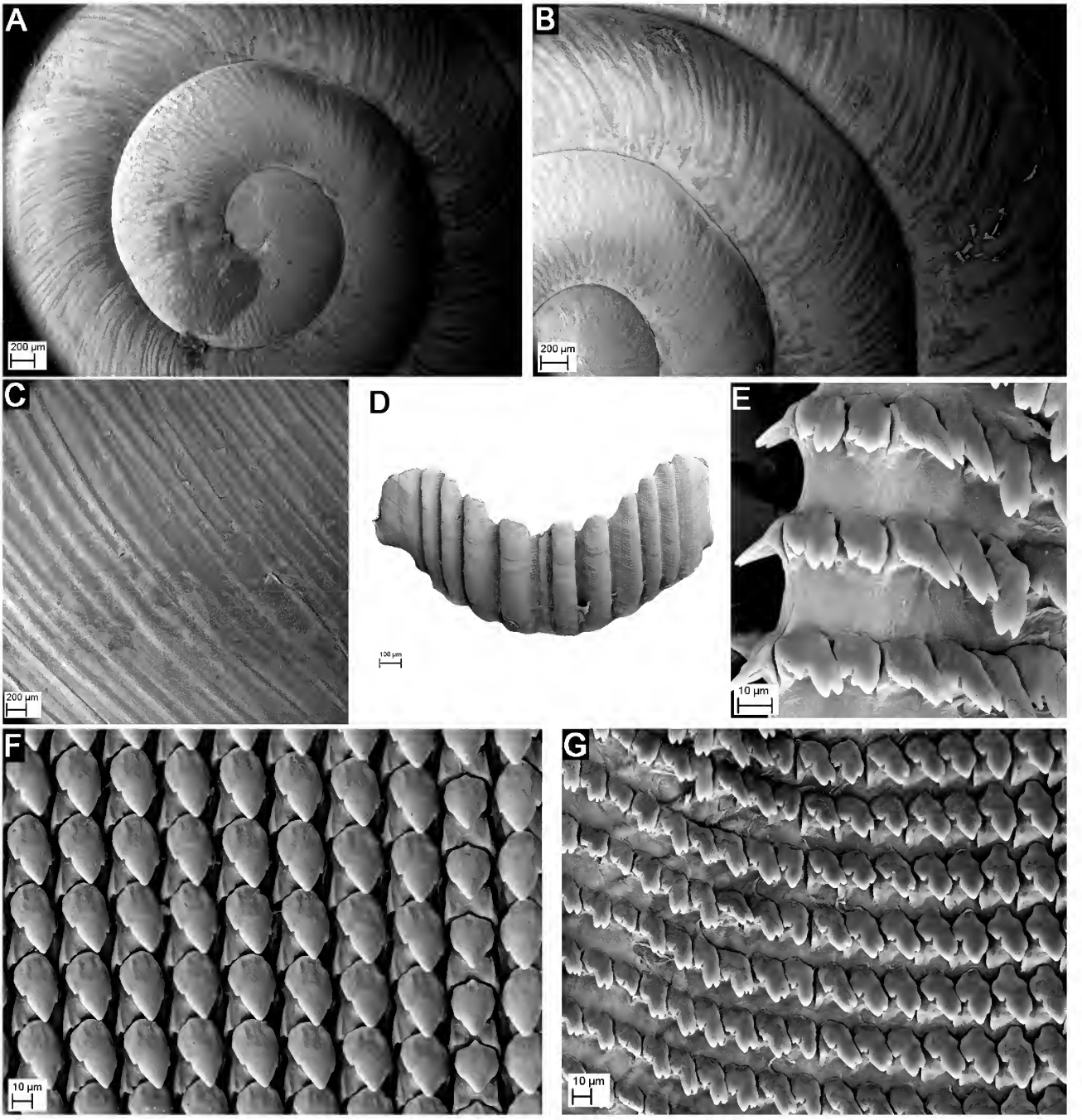

Figure 14. *Amplirhagada davidsoniana* n.sp. SEM of shell (AM C.472924), radula and jaw (AM C.472923). *(A)* Protoconch and first teleoconch whorls viewed from above. *(B)* Detail of first teleoconch whorls viewed from above. *(C)* Close-up showing sculpture on last whorl, viewed from above. *(D)* Jaw. *(E)* Close-up showing detail of central marginal teeth. *(F)* Central and inner lateral teeth viewed from above. *(G)* Marginal teeth viewed from above. Scale bars: *A–C*, 200 µm; *D*, 100 µm; *E–G*, 10 µm.

underneath suture. Angle of aperture less than 45 degrees; outer lip sharp to moderately thick, rounded, expanded, slightly reflected; basal node absent or very weak. Parietal wall of inner lip inconspicuous. Average shell size 13.1±0.8 × 18.3±0.9 mm (Table 1).

Radular and jaw morphology (Fig. 14 D–G). Tooth formula C + 12–14 + 4 + 24–28, with 150–160 rows of teeth (n = 2). Jaw with 11 plates.

Genital morphology (Figs 15–16). Penis straight, tubular, slightly longer than anterior part of oviduct. Penial sheath very delicate. Length of penial retractor muscle equivalent to length of penial complex. Penial verge elongately conical, with pointed tip, extending about 1/5 of length of penial chamber. Inner penial wall entirely covered by well-developed pustules arranged in longitudinal rows or pilasters. Main stimulatory pilaster relatively short, cone-shaped comprising proximal third of inner penial wall; with lateral corrugations. Vas deferens very thick, not undulating, entering penial sheath within proximal third of penial complex. Vagina long, tubular; inner vaginal wall with rows of laterally expanded pustules that are densely arranged in longitudinal rows. Rows of pustules giving rise

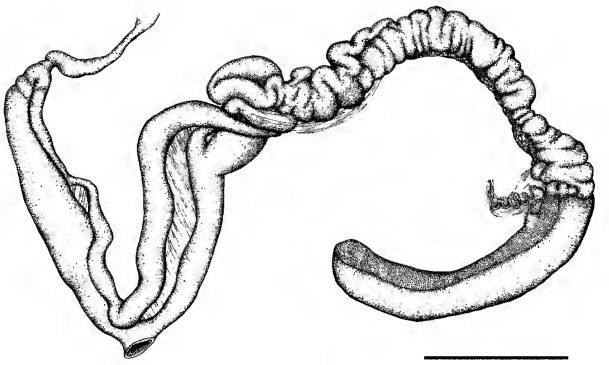

Figure 15. Genitalia of *Amplirhagada davidsoniana* n.sp. (AM C.472923). For labelling of structures see Fig. 3. Scale bar = 5 mm.

to corrugated pilasters at proximal end of vagina. Inner wall of bursa copulatrix with smooth longitudinal pilasters. Bursa copulatrix slightly extending base of spermoviduct. Free oviduct short, comprising less than half of length of anterior part of oviduct. Spermoviduct about longer than anterior part of oviduct.

Aestivation strategy: Rock sealer.

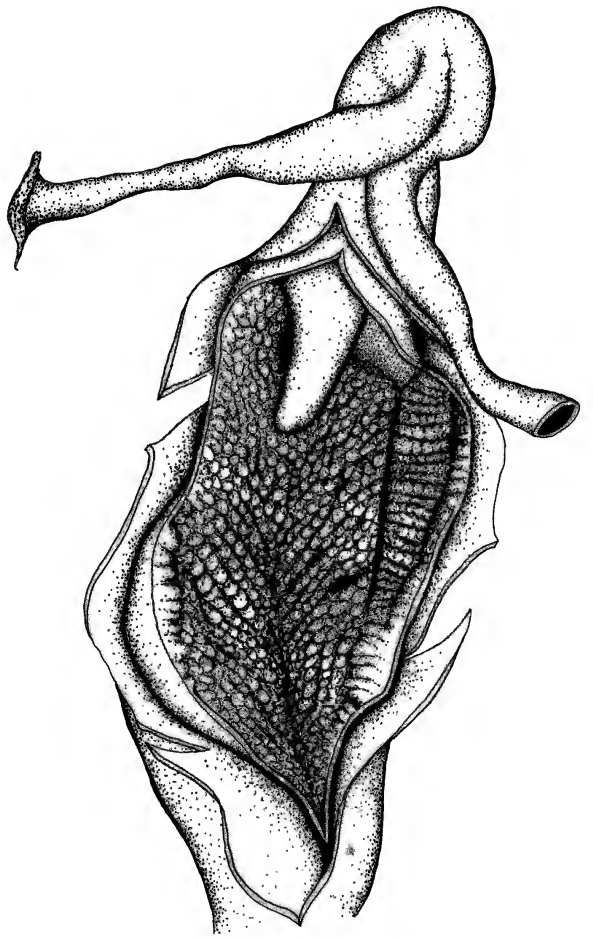

Figure 16. Penial anatomy of *Amplirhagada davidsoniana* n.sp. (AM C.472923). For labelling of structures see Fig. 4. Scale bar = 3 mm.

Remarks. Anatomical description based on dissections of three specimens. Listed by Solem (1991) as "*Amplirhagada* NSP21". Shell similar to *A. imitata* (Smith, 1894), *A. solemiana* Köhler, 2010 and *A. indistincta* Köhler, 2010, but differing by shell size, distinct corrugation of inner penial wall and much longer vagina.

Amplirhagada vialae n.sp.

Type locality. Western Australia, NW Kimberley, Bonaparte Archipelago, Montague Sound, Scott Strait, 8.3 km E of Savage Hill; 14°37'15"S 125°15'15"E (RFS-05–2; coll. V. Kessner, 05 Jun 1987) (Fig. 1).

Type material. Holotype WAM S34719 (preserved specimen) (Pl. 1.6; Table 1). Paratypes AM C.472925 (2 preserved specimens), WAM S34720 (5 preserved specimens), FMNH 220066 (9 preserved specimens), AM C.472926 (4 shells), WAM S34721 (10 dried shells), FMNH 220065 (12 shells).

Etymology. Named in honour of Marlene Vial in recognition for her help with SEM and other work.

Description

Shell (Pl. 1.6; Fig. 17 A–D). Semi-globose with highly elevated spire. Solid, not translucent. Periphery well rounded to slightly compressed, occasionally slightly angulate; upper sector of whorl flattened to slightly shouldered underneath suture, basal sectors rounded. Umbilicus completely concealed by columellar reflection. Background colour pale yellowish brown to horn; peripheral band conspicuous, well developed, moderately broad, clearly visible on last whorls; sub-sutural band broad, diffuse to well developed, brown, clearly visible on last whorls; both bands may blend into each other covering shell with a dark brown tone; outer and inner lip colour white, conspicuously contrasting shell colour. Protoconch 3.4 mm in diameter, comprising about 1.5 whorls, with weak radially elongated pustulations. Teleoconch with faint, regular axial growth lines, evenly distributed across shell. Angle of aperture about 30 degrees; outer lip moderately thick, well rounded, slightly expanded, not reflected; basal node absent or weak. Parietal wall of inner lip inconspicuous. Average shell size 17.1±1.8 × 19.8±1.0 mm (Table 1).

Radular and jaw morphology (Fig. 17 E–G). Tooth formula C + 14–16 + 4 + 20–22, with 160 rows of teeth (n = 1). Jaw with 10 plates.

Genital morphology (Figs 18–19). Penis curved, medially inflated, about as long as anterior part of oviduct. Penial sheath very delicate. Length of penial retractor muscle equivalent to about 1/3 of length of penial complex. Penial verge elongately conical, with pointed tip, short, extending about 1/10 of length of penial chamber. Inner penial wall entirely covered by well-developed, elongate pustules densely arranged in longitudinal rows. Main stimulatory pilaster huge, cone-shaped comprising 3/4 of length of inner penial wall; with regular lateral corrugations that support dense and regular rows of hooks. Vas deferens thick, not undulating, entering penial sheath close to penial apex. Vagina long, inflated; inner vaginal wall and wall of

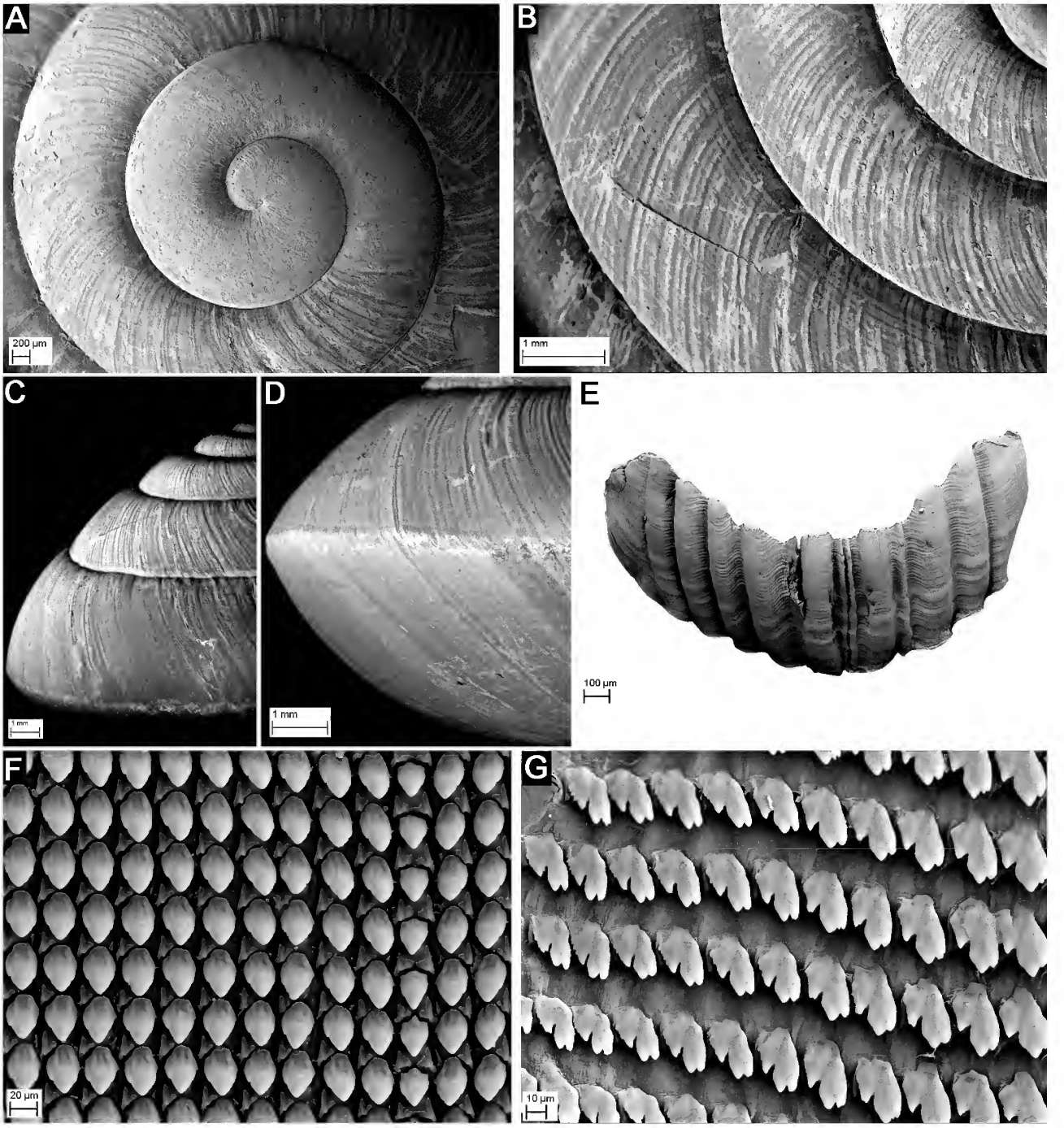

Figure 17. *Amplirhagada vialae* n.sp. SEM of shell (AM C.472926), radula and jaw (AM C.472925). *(A)* Protoconch and first teleoconch whorls viewed from above. *(B)* Detail of first teleoconch whorls viewed from above. *(C)* Lateral view of shell. *(D)* Lateral view of last whorl. *(E)* Jaw. *(F)* Central and inner lateral teeth viewed from above. *(G)* Marginal teeth viewed from above. Scale bars: *A*, 200 µm, *B–D*, 1 mm; *E*, 100 µm, *F*, 20 µm; *G*, 10 µm.

bursa copulatrix with smooth longitudinal pilasters. Bursa copulatrix reaching base of spermoviduct. Free oviduct rather long, tubular, comprising about half of length of anterior part of oviduct. Spermoviduct not much longer than anterior part of oviduct.

Aestivation strategy: Free sealer.

Remarks. Anatomical description based on dissections of two specimens. Listed by Solem (1991) as "*Amplirhagada* NSP22". The "bee-hive" shaped shell is similar to that of *A. decora* Köhler, 2010 (Bigge Island) and *A. boongareensis* Köhler, 2010 (Boongaree Island), but these species differ in shell colour. All three species are characterized by a huge,

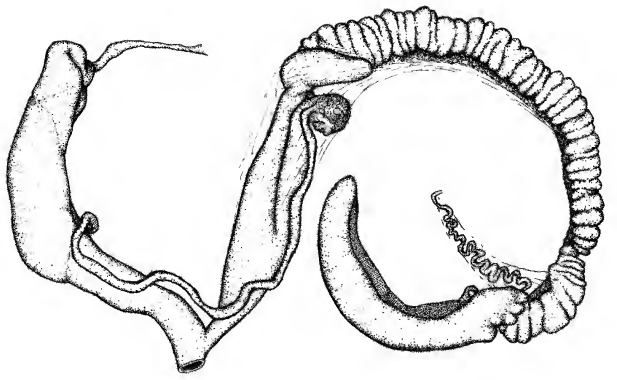

Figure 18. Genitalia of *Amplirhagada vialae* n.sp. (AM C.472925). For labelling of structures see Fig. 3. Scale bar = 10 mm.

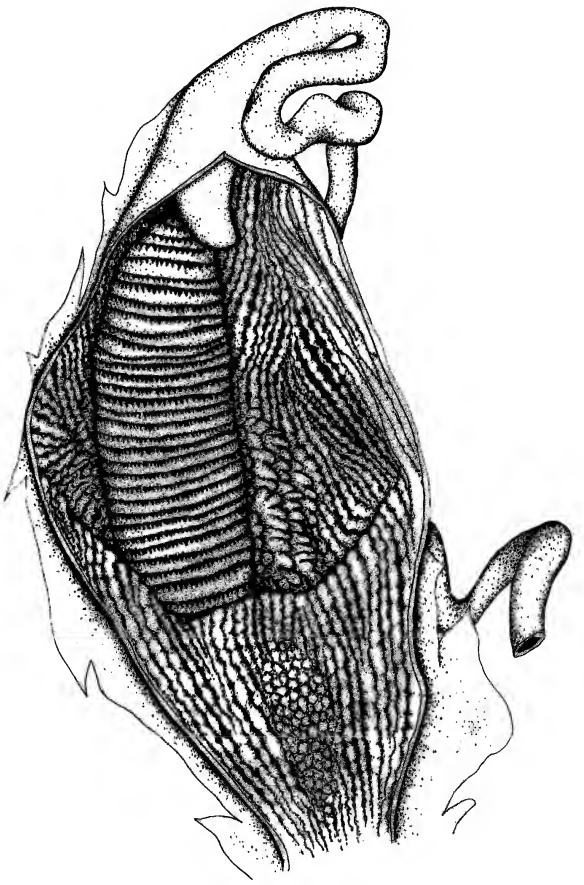

Figure 19. Penial anatomy of *Amplirhagada vialae* n.sp. (AM C.472925). For labelling of structures see Fig. 4. Scale bar = 3 mm.

cone-shaped main pilaster and by their inner penial wall being densely covered with large pustules. *Amplirhagada boongareensis* differs by possessing two additional pilasters and *A. decora* Köhler, 2010 has a shorter bursa copulatrix. The present species occurs in sympatry with *A. discoidea* n.sp. being described in the following.

Amplirhagada discoidea n.sp.

Type locality. Western Australia, NW Kimberley mainland, Scott Strait, 8.3 km E of Savage Hill on Bigge Island; 14°37'15"S 125°15'15"E (RFS 05-2; coll. V. Kessner, 5 Jun 1987) (Fig. 1).

Type material. Holotype WAM S34722 (preserved specimen) (Pl. 1.7; Table 1). Paratypes AM C.472927 (3 preserved specimens), WAM S34723 (5 preserved specimens), FMNH 220064 (8 preserved specimens), AM C.472928 (6 dried shells), WAM S34724 (12 dried shells), FMNH 220063 (20 dried shells).

Etymology. In reference to discoidal shape of shell.

Description

Shell (Pl. 1.7; Fig. 21A–D). Broadly conical with low spire, discoid. Rather thin but solid, slightly translucent. Periphery angulate; upper and basal sectors slightly flattened. Umbilicus 10–20% concealed by columellar reflection. Background colour light yellowish brown; peripheral band conspicuous, well developed, moderately broad, clearly visible on last whorl only; sub-sutural band broad, well developed, brown, visible on last whorl only; both bands may blend into each other covering shell with a dark brown tone; outer and inner lip colour white, conspicuously contrasting shell colour. Protoconch 3.1 mm in diameter, comprising about one whorl, with inconspicuous radially elongated pustulations. Teleoconch almost smooth, with very faint, regular axial growth lines. Angle of aperture about 45 degrees; outer lip thin, well rounded, slightly expanded, not or slightly reflected; basal node. Parietal wall of inner lip thin. Average shell size 12.4±0.7 × 20.9±0.9 mm (Table 1).

Radular and jaw morphology (Fig. 21 E–G). Tooth formula C + 13–15 + 4 + 16–22, with 120 rows of teeth (n = 2). Jaw with c. 10 plates.

Genital morphology (Figs 20, 22). Penis rather straight, tubular, about as long as anterior part of oviduct. Penial sheath very delicate, distally thicker. Length of penial retractor muscle equivalent to about 1/3 of length of penial complex. Penial verge elongately conical, with blunt tip, short, extending about ¼ of length of penial chamber. Inner penial wall entirely covered by densely arranged, very small pustules. Several more or less developed longitudinal

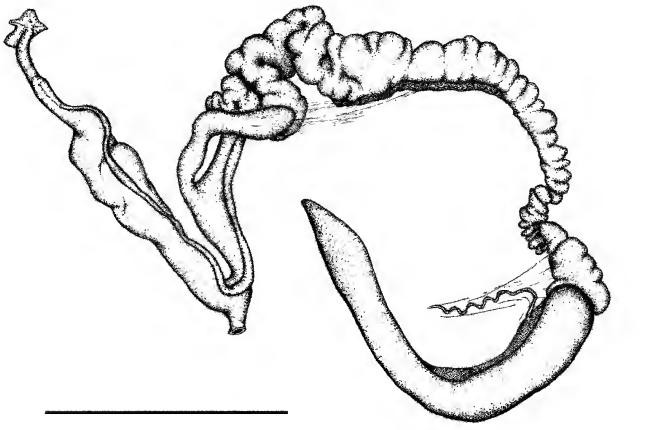

Figure 20. Genitalia of *Amplirhagada discoidea* n.sp. (AM C.472927). For labelling of structures see Fig. 3. Scale bar = 10 mm.

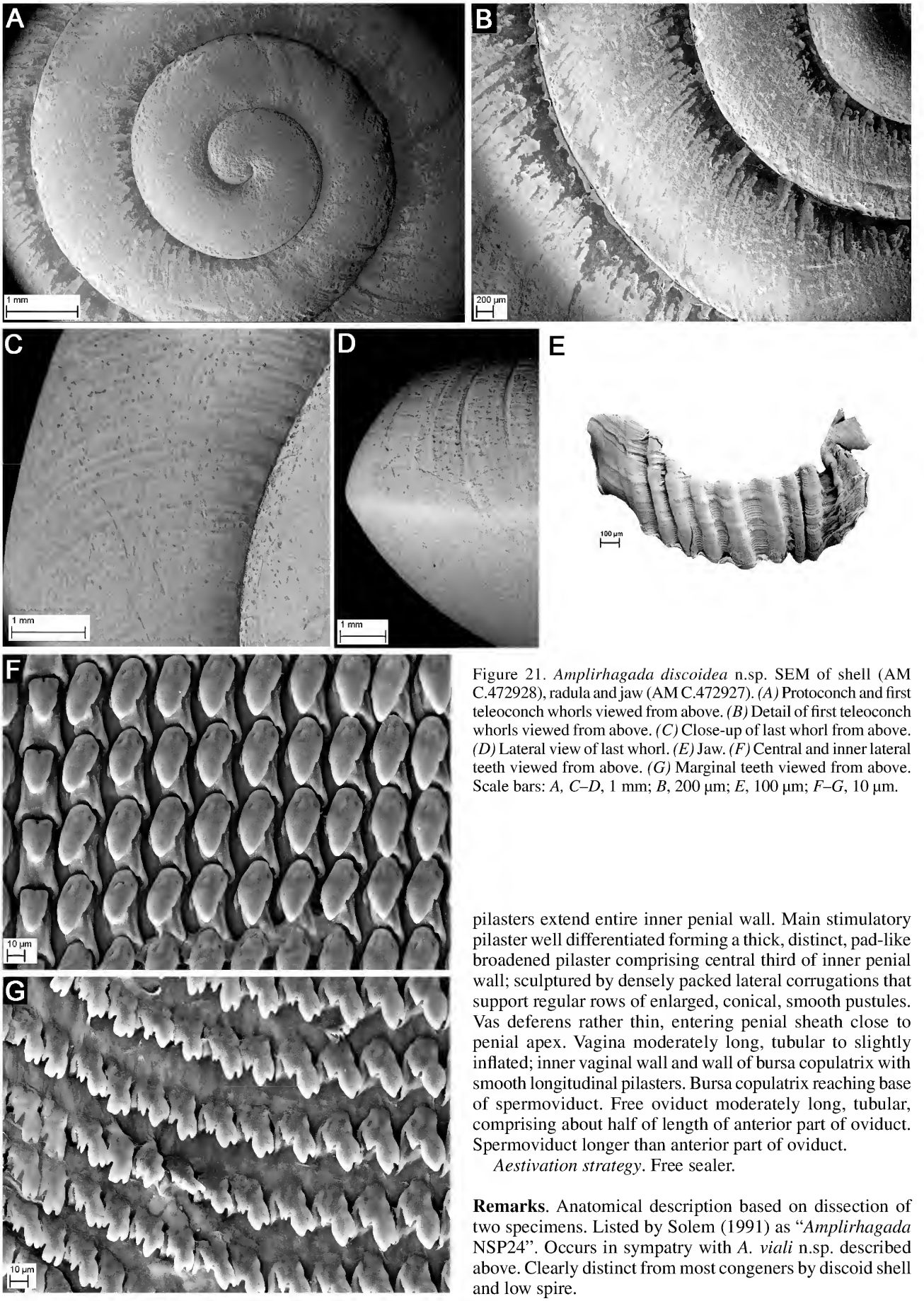

Figure 21. *Amplirhagada discoidea* n.sp. SEM of shell (AM C.472928), radula and jaw (AM C.472927). *(A)* Protoconch and first teleoconch whorls viewed from above. *(B)* Detail of first teleoconch whorls viewed from above. *(C)* Close-up of last whorl from above. *(D)* Lateral view of last whorl. *(E)* Jaw. *(F)* Central and inner lateral teeth viewed from above. *(G)* Marginal teeth viewed from above. Scale bars: *A, C–D*, 1 mm; *B*, 200 µm; *E*, 100 µm; *F–G*, 10 µm.

pilasters extend entire inner penial wall. Main stimulatory pilaster well differentiated forming a thick, distinct, pad-like broadened pilaster comprising central third of inner penial wall; sculptured by densely packed lateral corrugations that support regular rows of enlarged, conical, smooth pustules. Vas deferens rather thin, entering penial sheath close to penial apex. Vagina moderately long, tubular to slightly inflated; inner vaginal wall and wall of bursa copulatrix with smooth longitudinal pilasters. Bursa copulatrix reaching base of spermoviduct. Free oviduct moderately long, tubular, comprising about half of length of anterior part of oviduct. Spermoviduct longer than anterior part of oviduct.

Aestivation strategy. Free sealer.

Remarks. Anatomical description based on dissection of two specimens. Listed by Solem (1991) as "*Amplirhagada* NSP24". Occurs in sympatry with *A. viali* n.sp. described above. Clearly distinct from most congeners by discoid shell and low spire.

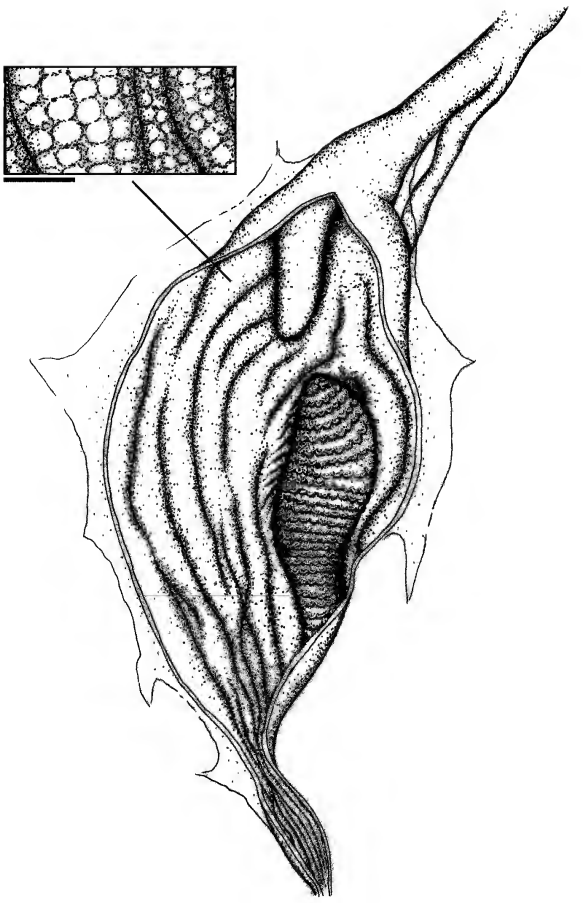

Figure 22. Penial anatomy of *Amplirhagada discoidea* n.sp. (AM C.472927). For labelling of structures see Fig. 4. Scale bar = 5 mm. Scale bar (inset) = 0.25 mm.

Amplirhagada forrestiana n.sp.

Type locality. Western Australia, NW Kimberley, York Sound, Prince Frederick Harbour, 9.7 km NW of Mt. Anderdon, 4 km from coast; 14°52'50"S 125°21'30"E (RFS-05-3; coll. V. Kessner, 05 Jun 1987) (Fig. 1).

Type material. Holotype WAM S34725 (preserved specimen) (Pl. 1.8; Table 1). Paratypes AM C.472930 (2 preserved specimens), WAM S34726 (5 preserved specimens), FMNH 220084 (8 preserved specimens), AM C.472931 (5 dried shells), WAM S34727 (9 dried shells), FMNH 220083 (12 dried shells).

Etymology. Named after Matthew Forrest, first Kimberley explorer, who in 1879 was instructed to map out the country between the De Grey River in Western Australia and the Victoria River in the Northern Territory.

Description

Shell (Pl. 1.8; Fig. 25 A–C). Broadly conical with low spire, almost discoid. Thin, translucent. Periphery sharply angulate; upper and lower sectors of whorls rounded. Umbilicus narrowly winding, 30–80% concealed by columellar reflection. Background colour pale brownish horn; peripheral band absent or diffuse, if present moderately broad, diffuse, brown, visible on last whorls only; sub-sutural band absent or diffuse, brown, visible on last whorls only; outer and inner lip colour whitish. Protoconch 4.7 mm in diameter, comprising about 1.5 whorls, with indistinct radially

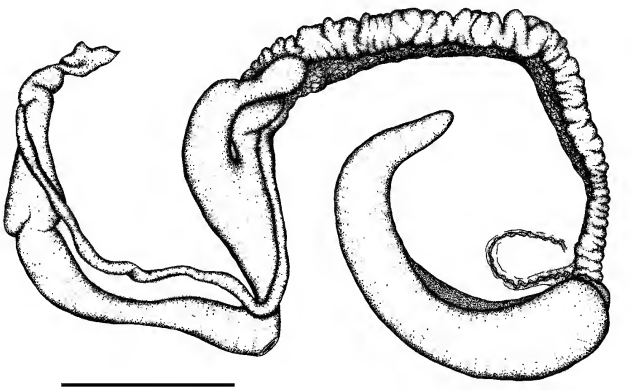

Figure 23. Genitalia of *Amplirhagada forrestiana* n.sp. (AM C.472930). For labelling of structures see Fig. 3. Scale bar = 5 mm.

elongated pustulations. Teleoconch with well-developed, regular lirae, evenly distributed across shell surface. Angle of aperture 45–60 degrees; outer lip thin, well rounded, slightly expanded, slightly reflected; basal node absent or weak. Parietal wall of inner lip inconspicuous. Average shell size 11.6±0.8 × 19.4±1.0 mm (Table 1).

Radular and jaw morphology (Fig. 25 D–G). Tooth formula C + 11 + 4 + 16; 150 rows of teeth (n = 1). Jaw with nine plates.

Genital morphology (Figs 23, 24). Penis rather straight, tubular, longer than anterior part of oviduct. Penial sheath delicate, proximally thicker. Penial retractor muscle stubby. Penial verge comparatively long, elongately conical, extending about ⅓

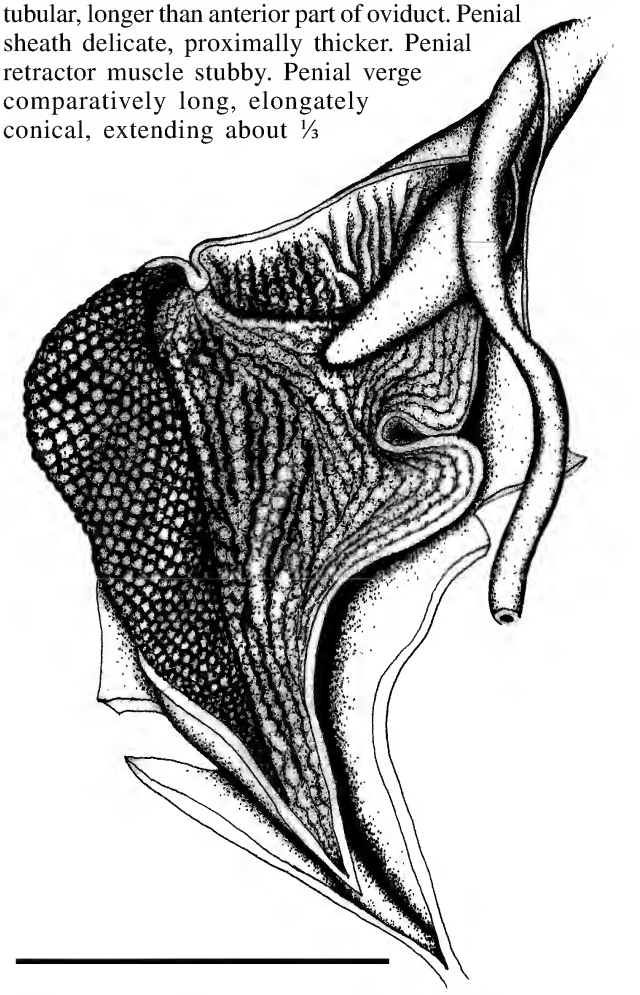

Figure 24. Penial anatomy of *Amplirhagada forrestiana* n.sp. (AM C.472930). For labelling of structures see Fig. 4. Scale bar = 3 mm.

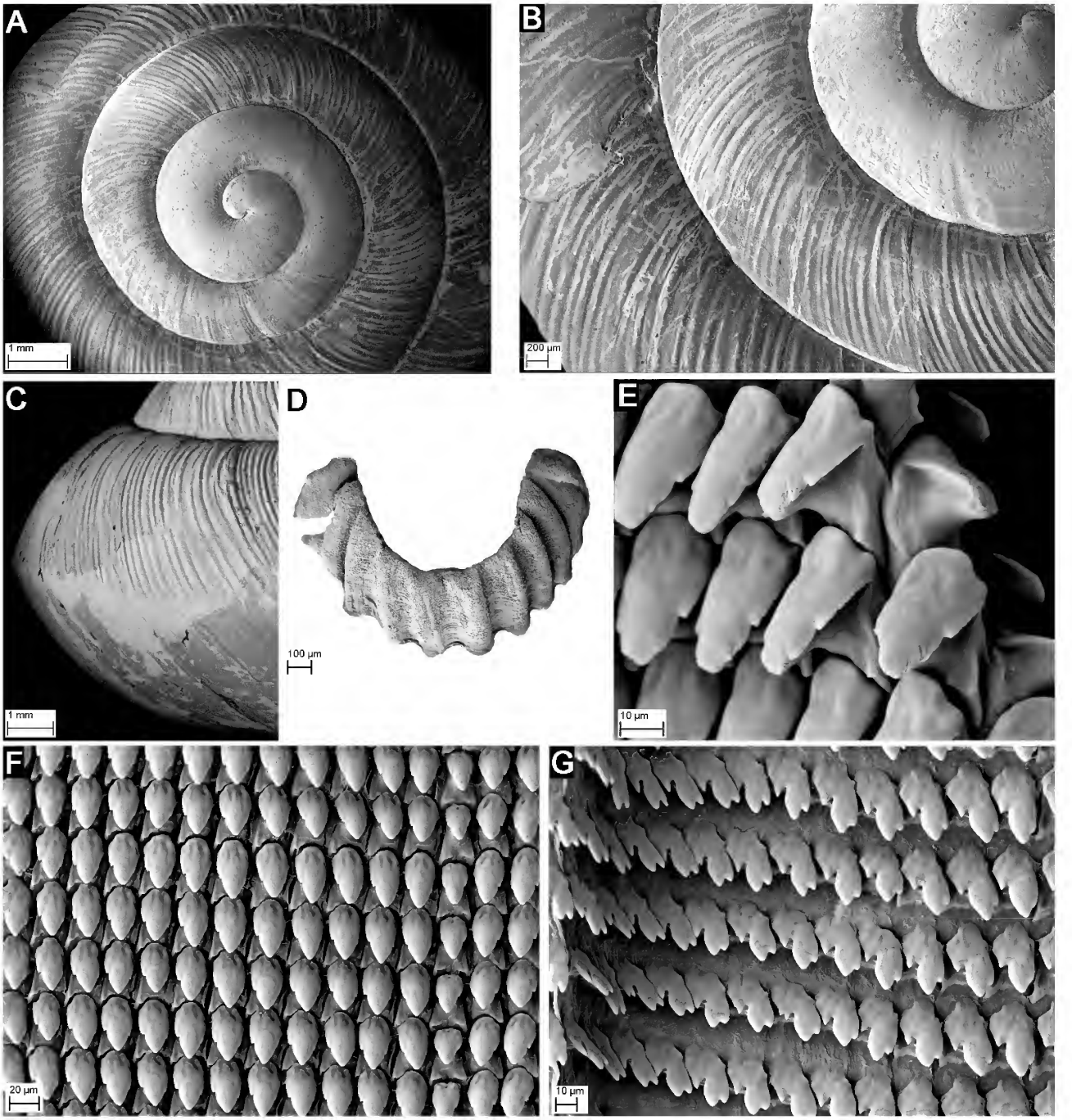

Figure 25. *Amplirhagada forrestiana* n.sp. SEM of shell (AM C.472931), radula and jaw (AM C.472930). *(A)* Protoconch and first teleoconch whorls viewed from above. *(B)* Detail of first teleoconch whorls viewed from above. *(C)* Lateral view of last whorl. *(D)* Jaw. *(E)* Close-up of inner lateral teeth. *(F)* Central and lateral teeth viewed from above. *(G)* Marginal teeth viewed from above. Scale bars: *A, C*, 1 mm; *B*, 200 µm; *D*, 100 µm; *E, G*, 10 µm; *F*, 20 µm.

of length of penial chamber. Inner penial wall entirely covered by densely in honey-comb pattern arranged, small and regular pustules. No main stimulatory pilaster. Vas deferens rather thin, entering penial sheath close to penial apex, long and winding. Vagina moderately long, distally inflated; inner vaginal wall and wall of bursa copulatrix with smooth longitudinal pilasters. Bursa copulatrix very wide, slightly extending base of spermoviduct. Free oviduct very long, tubular, coiling, comprising ¾ of length of anterior part of oviduct. Spermoviduct about as long as anterior part of oviduct.

Aestivation strategy. Free sealer.

Remarks. Listed by Solem (1991) as "*Amplirhagada* NSP25". A single specimen from Naturalist Island, assigned to the same manuscript name in the collection of the Field Museum (FMNH 220692) was not studied. Amongst medium-sized species, shell differs from other congeners by markedly wider diameter, resulting in a discoidal shape (shell proportions and size only similar in *A. discoidea*). *Amplirhagada discoidea* differs by having a more angulated shell periphery and a conspicuously different penial anatomy, with a large main pilaster (absent in *A. forrestiana*), rather smooth inner penial wall (markedly pustulose in *A. forrestiana*) and rather narrow bursa copulatrix (wide on *A. forrestiana*).

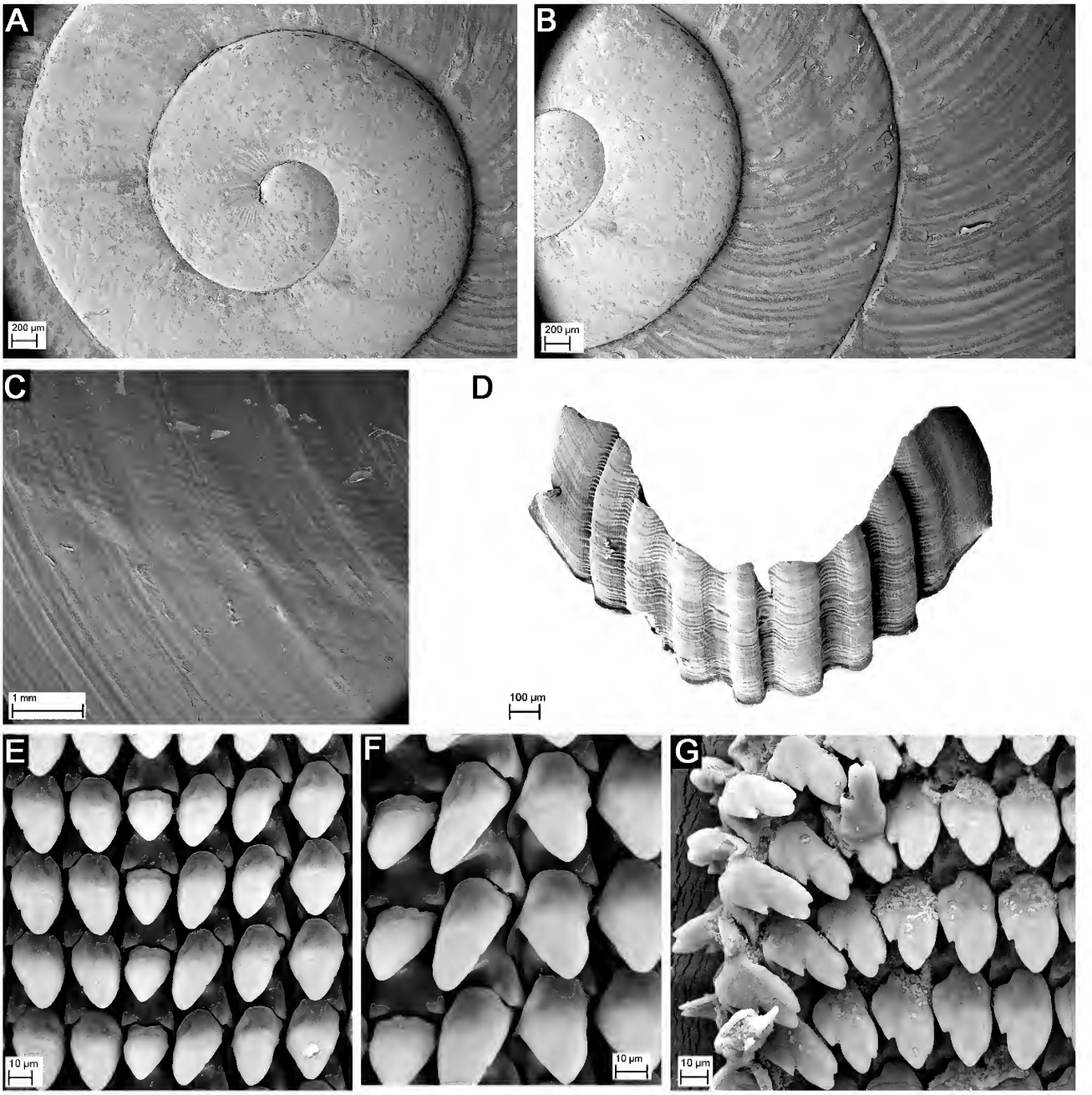

Figure 26. *Amplirhagada inusitata* n.sp. SEM of shell (AM C.472929), radula and jaw (WAM S34728). *(A)* Protoconch and first teleoconch whorls viewed from above. *(B)* Detail of first teleoconch whorls viewed from above. *(C)* Close-up of sculpture on last whorl, lateral view. *(D)* Jaw. *(E)* Central and inner lateral teeth. *(F)* Close-up of central and lateral teeth viewed from above. *(G)* Transition from outer lateral to inner marginal teeth viewed from above. Scale bars: *A–B*, 200 µm; *C*, 1 mm; *E–G*, 10 µm.

Amplirhagada inusitata n.sp.

Type locality. Western Australia, NW Kimberley, N side of Prince Frederick Harbour, near mouth, 16 km W of Mt. Anderdon, 0.3 km from coast; 14°57'10"S 125°16'30"E (RFS 14-1; coll. V. Kessner, 14 Jun 1987) (Fig. 1).

Type material. Holotype WAM S34728 (preserved specimen, dissected). Paratypes WAM S34729 (preserved specimen, juvenile), FMNH 220537 (preserved specimen), AM C.472929 (2 dried shells), WAM S34730 (3 dried shells) (Pl. 1.9), FMNH 220540 (6 dried shells).

Etymology. Species epithet derived from "inusitata" (Latin, unusual, uncommon, extraordinary; of female gender) in reference to its remarkably distinct penial morphology.

Description

Shell (Pl. 1.9; Fig. 26 A–C). Broadly conical with low spire. Thin, translucent. Periphery sharply angulate; upper sector of whorls flattened. Umbilicus 30–50% concealed by columellar reflection. Background colour pale yellowish brown; peripheral band diffuse to well developed, moderately broad, brown, visible on visible on last whorl only; sub-

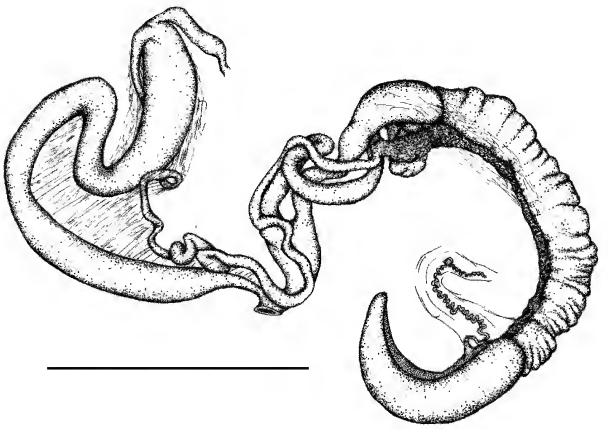

Figure 27. Genitalia of *Amplirhagada inusitata* n.sp. (WAM S34728). For labelling of structures see Fig. 3. Scale bar = 10 mm.

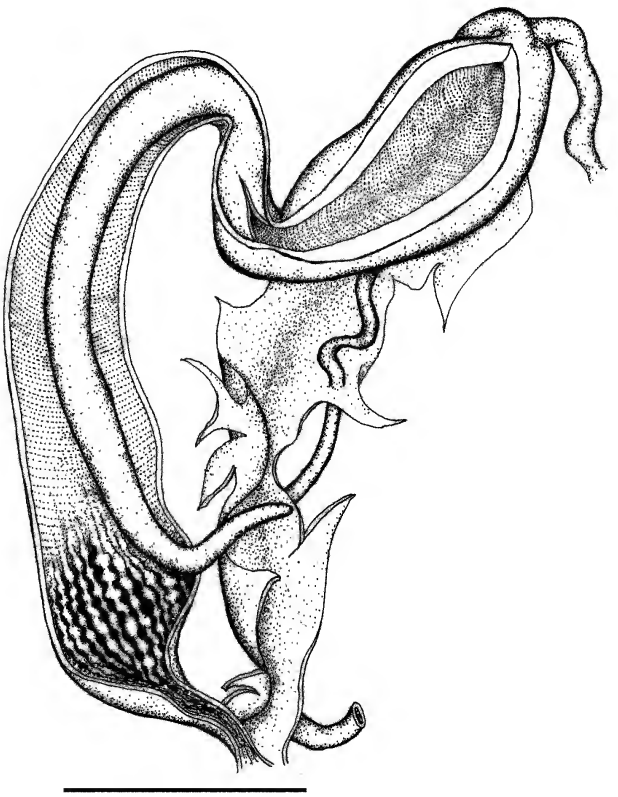

Figure 28. Penial anatomy of *Amplirhagada inusitata* n.sp. (WAM S34728). For labelling of structures see Fig. 4. Scale bar = 5 mm.

sutural band diffuse to well developed, brown, visible on last whorl only; outer and inner colour like shell. Protoconch 2.6 mm in diameter, comprising about one whorl, with very indistinct radially elongated pustulations. Teleoconch with faint axial growth lines, evenly distributed across shell surface. Angle of aperture 45–60 degrees; outer lip thin, well rounded, slightly expanded; basal node absent or weak. Parietal wall of inner lip inconspicuous. Average shell size 16.8±1.7 × 21.4±0.7 mm (Table 1).

Radular and jaw morphology (Fig. 26 D–G). Tooth formula C + 14–19 + 4 + ?; 125 rows of teeth (n = 1). Jaw with 10 plates.

Genital morphology (Figs 27–28). Penis long, curved to bending, tubular, clearly longer than anterior part of oviduct. Penial sheath very delicate. Penial retractor muscle very short. Penial verge extremely elongated, extending almost entire length of penis, with pointed tip, proximally the lumen of the penial verge forms an extended duct that is connected to vas deferens, possibly functioning as epiphallus. Penial chamber extending only distal half of entire length of penial complex, inner penial wall almost entirely smooth, in proximal third corrugated longitudinal pilasters are present consisting of fused pustules. No main stimulatory pilaster differentiated. Vas deferens rather thin, undulating, entering penial sheath close to penial apex. Vagina moderately long, tubular to slightly inflated; inner vaginal wall and wall of bursa copulatrix with smooth longitudinal pilasters. Bursa copulatrix reaching base of spermoviduct. Free oviduct long, bending, tubular, comprising more than half of length of anterior part of oviduct. Spermoviduct as long as anterior part of oviduct.

Aestivation strategy. Free sealer.

Remarks. Anatomical description based on dissection of the holotype. Listed by Solem (1991) as "*Amplirhagada* NSP26". Shell similar to other relatively large and broadly conical species with spiral bands, such as *A. combeana* Iredale, 1938 and *A. mitchelliana* Solem, 1981, differing from all other congeners by extremely long and tubular penial verge, narrowly elongated penis, smooth penial wall with only short corrugated pilasters at its base. Found in sympatry with *A. pusilla* Solem, 1981 and *A. epiphallica* n.sp. described below.

Amplirhagada coffea n.sp.

Type locality. Western Australia, NW Kimberley, George Water, 16 km SW of Mt. Grey, near Barlee Impediment; 15°49'10"S 124°36'00"E (RFS-23-3; coll. V. Kessner, 23 Jun 1987) (Fig. 1).

Type material. Holotype WAM S34731 (preserved specimen) (Pl. 1.10; Table 1). Paratypes AM C.472932 (3 preserved specimens, WAM S34732 (8 preserved specimens), FMNH 220945 (13 preserved specimens), AM C.472933 (6 dried shells), WAM S34733 (10 dried shells), FMNH 220948 (16 dried shells).

Etymology. Species epithet refers to the dark coffee-brown colour of the shell.

Description

Shell (Pl. 1.10; Fig. 29 A–C). Semi-globose, with rather high spire; solid. Periphery compressed to angulate; upper sector slightly shouldered, basal sector rounded. Umbilicus completely concealed by columellar reflection. Background colour crème to brown; sub-sutural and mid-whorl bands usually blend into each other covering entire shell surface in chestnut brown; ventral and outer lip colour light brownish horn; inner lip whitish. Shell surface glossy. Protoconch 3.3 mm in diameter, comprising about 1.2 whorls, with indistinct radially elongated pustulations. Teleoconch with well-developed, regular axial growth lines, evenly distributed

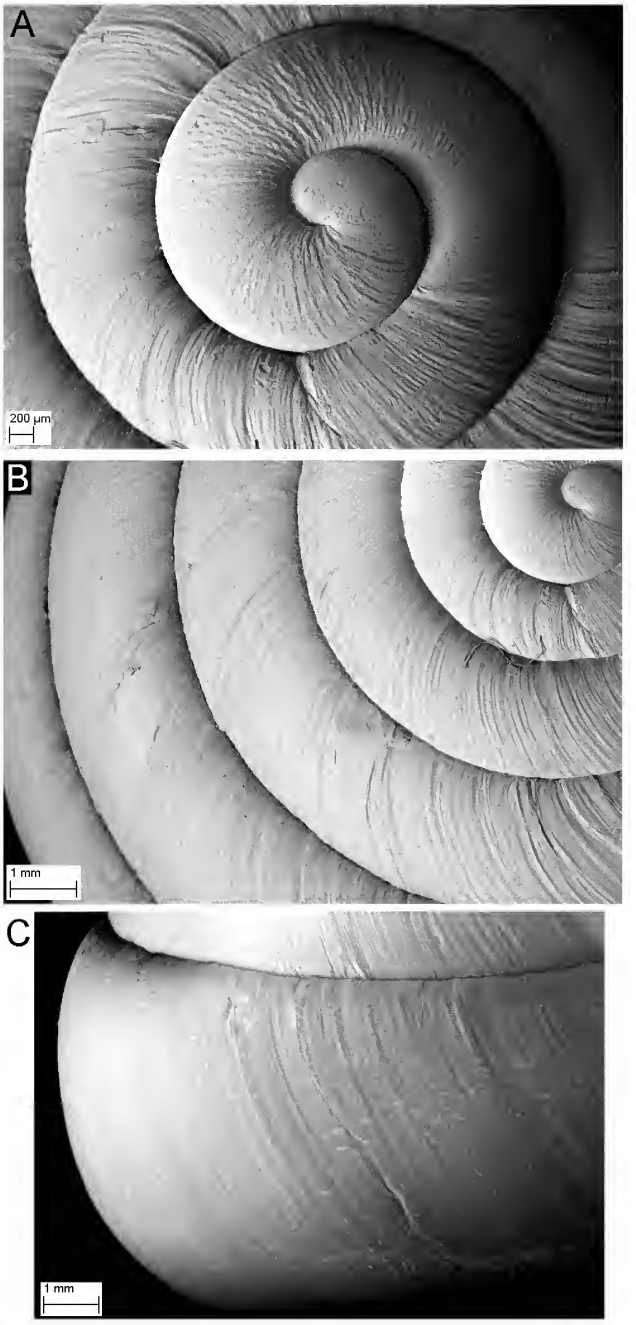

Figure 29. *Amplirhagada coffea* n.sp. SEM of shell (AM C.472933). *(A)* Protoconch and first teleoconch whorls viewed from above. *(B)* Detail of first teleoconch whorls viewed from above. *(C)* Close-up of sculpture on last whorl, lateral view. Scale bars: *A*, 200 µm; *B–C*, 1 mm.

across shell surface. Angle of aperture 30–45 degrees; outer lip rounded to slightly angulate, slightly expanded, well reflected, basal node of lip present, palatal node absent. Average shell size 17.9±1.6 × 21.4±1.1 mm (Table 1).

Genital morphology (Fig. 30). Penis straight, more or less of same length as anterior part of oviduct. Penial sheath proximally thick, distally delicate. Length of penial retractor muscle equivalent to about a third of length of penial complex. Penial verge slender, moderately long, extending about 1/6 of length of penial chamber. Distal part of inner penial wall entirely covered by regular pustulation; pustules relatively large, conical. Proximal part of inner penial wall

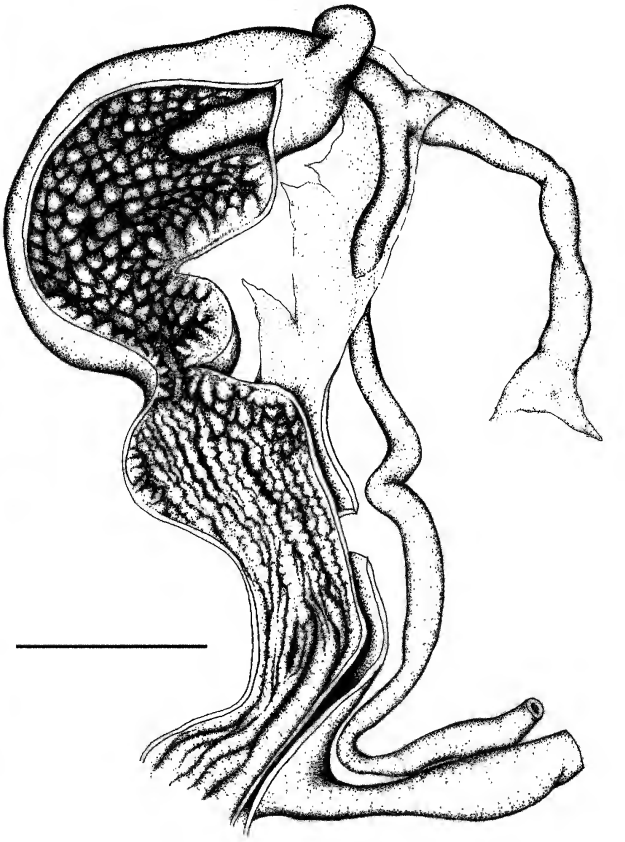

Figure 30. Penial anatomy of *Amplirhagada coffea* n.sp. (AM C.472932). For labelling of structures see Fig. 4. Scale bar = 3 mm.

covered by many irregular, corrugated pilasters formed from fused rows of pustules. No main stimulatory pilaster present. Vas deferens entering penial sheath within distal quarter of penial complex. Rest of genital system unknown.

Aestivation strategy. Rock sealer.

Remarks. Description based on dissection of one specimen. Listed by Solem (1991) as "*Amplirhagada* NSP27" together with dry shells found on Boongaree Island, which were tentatively considered conspecific as based on similar shell. The species from Boongaree was previously described as *A. boongareensis* Köhler, 2010. *Amplirhagada coffea* differs from the former by usually having a concealed umbilicus, different shell and inner lip colour, glossy surface, strongly reflected outer lip. Species with similar "bee-hive" shaped shells, such as *A. boongareensis*, *A. decora* Köhler, 2010 and *A. vialae* differ by having large cone-shaped main pilasters and distinct pustulation of inner penial wall. Material from a second sampling site at the mainland coast (RFS-26–3, Brecknock Harbour, opposite Camden Island) is tentatively being considered conspecific for its similar shell and penial anatomy.

Amplirhagada gardneriana n.sp.

Type locality. Western Australia, NW Kimberley, 15 km E of King Cascade, Princess May Ranges; 15°36'00"S 125°26'30"E (RFS 27-3; coll. V. Kessner, 27 Jun 1987) (Fig. 1).

Type material. Holotype WAM S34734 (preserved specimen) (Pl. 1.11; Table 1). Paratypes AM C.472934 (8 preserved specimens), WAM S34735 (13 preserved specimens), FMNH 221084 (22 preserved specimens), AM

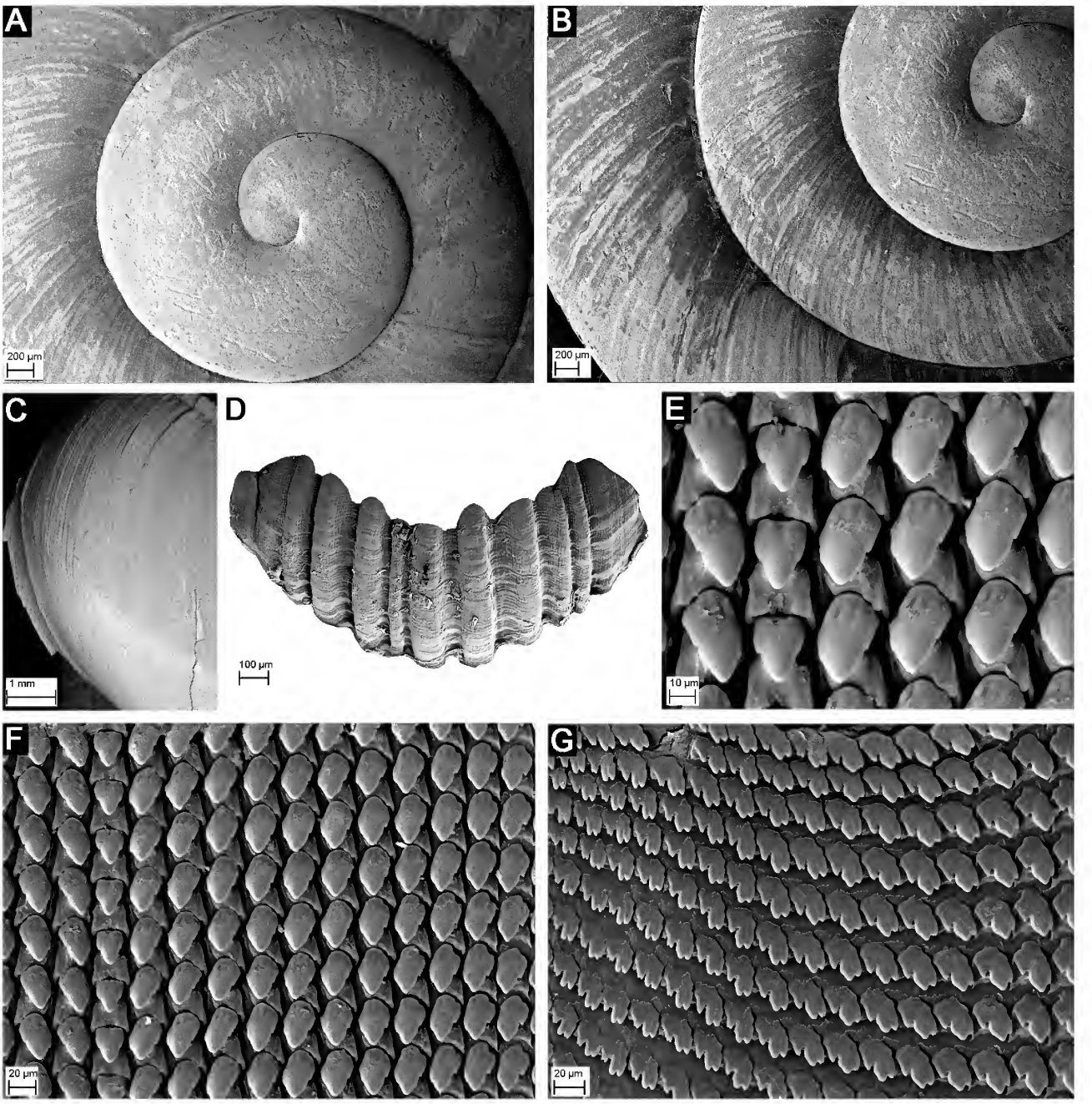

Figure 31. *Amplirhagada gardneriana* n.sp. SEM of shell (AM C.472935), radula and jaw (AM C.472934). *(A)* Protoconch and first teleoconch whorls viewed from above. *(B)* Detail of first teleoconch whorls viewed from above. *(C)* Close-up of sculpture on last whorl, lateral view. *(D)* Jaw. *(E)* Central and inner lateral teeth from above. *(F)* Marginal teeth viewed from above. Scale bars: *A–B*, 200 µm; *C*, 1 mm; *D*, 100 µm; *E*, 10 µm; *F–G*, 20 µm.

C.472935 (14 dried shells), WAM S34736 (25 dried shells), FMNH 221083 (34 dried shells).

Etymology. In reference to the Gardner Plateau, where this species occurs.

Description

Shell (Pl. 1.11; Fig. 31 A–C). Semi-globose with elevated spire. Solid, not translucent. Periphery well rounded to angulate; upper and basal sectors of whorls well rounded. Umbilicus narrowly winding, 50–80% concealed by columellar reflection. Background colour horn to pale brownish ochre; peripheral band rarely present, if present rather distinct, thin, brown, visible on last whorl only; sub-sutural band absent or diffuse, brown, thin; outer and inner lighter than shell. Protoconch 2.6 mm in diameter, comprising about one whorl, with very indistinct radially elongated pustulations. Teleoconch with faint, regular axial growth lines; evenly distributed across shell surface. Angle of aperture 45–60 degrees; outer lip thin, well rounded, expanded, not reflected; basal node absent or weak. Parietal wall of inner lip thin. Average shell size 14.2±1.2 × 18.0±0.7 mm (Table 1).

Radular and jaw morphology (Fig. 31 D–G). Tooth formula C + 11 + 4 + 16; 125 rows of teeth (n = 1). Jaw with 10 plates.

Genital morphology (Figs 32–33). Penis straight, tubular,

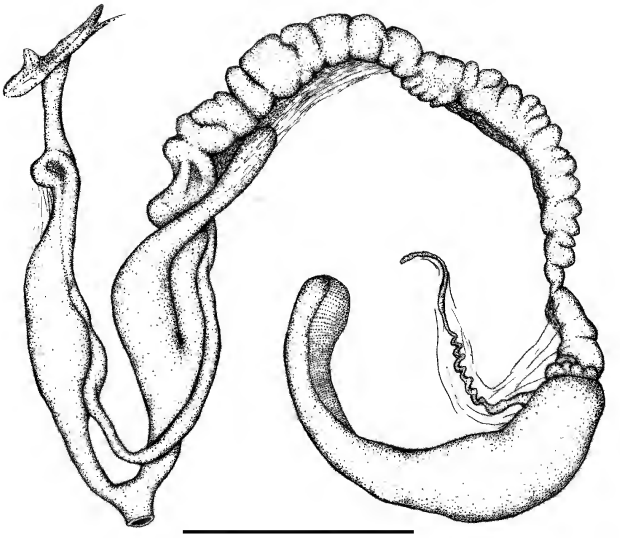

Figure 32. Genitalia of *Amplirhagada gardneriana* n.sp. (AM C.472934). For labelling of structures see Fig. 3. Scale bar = 5 mm.

thin, as long as anterior part of oviduct. Penial sheath distally thick, proximally delicate. Penial retractor about half as long as penis. Penial verge conical, with pointed tip, extending about ¼ of length of penial chamber. Inner penial wall entirely covered by very fine, dense pustulation. Main stimulatory pilaster weakly developed, extending distal half of inner penial wall, corrugated. Vas deferens rather thin, entering penial sheath in distal third of penial complex. Vagina moderately long, tubular to slightly inflated; inner vaginal wall and wall of bursa copulatrix with smooth longitudinal pilasters. Bursa copulatrix slightly extending base of spermoviduct. Free oviduct comprising about half of length of anterior part of oviduct. Spermoviduct longer than anterior part of oviduct.

Aestivation strategy. Free sealer.

Remarks. Anatomical description based on dissections of three specimens. Listed by Solem (1991) as "*Amplirhagada* NSP28". According to Solem (1991) the species differs from *A. pusilla* Solem, 1981 by its narrower umbilicus and more elevated spire and from *A. drysdaleana* Solem, 1981 by a shorter vagina. It also differs by a distinct pustulation of inner penial wall.

Amplirhagada lindsayae n.sp.

Type locality. Western Australia, NW Kimberley, Prince Frederick Harbour, 40.5 km NE of Mt. Trafalgar, S of Hunter River mouth; 15°03'55"S 125°21'55"E (RFS-14-2; coll. V. Kessner, 14 Jun 1987) (Fig. 1).

Type material. Holotype WAM S34737 (preserved specimen) (Pl. 1.12; Table 1). Paratypes AM C.472936 (4 preserved specimens), WAM S34738 (12 preserved specimens), FMNH 220561 (18 preserved specimens), AM C.472937 (3 dried shells), WAM S34739 (8 dried shells), FMNH 220560 (12 dried shells).

Additional, non-type material. WAM S34753 (6 dried shells), FMNH 219312 (7 dried shells), all from S side of Hunter River mouth, Prince Frederick Harbour; 15°02'58"S 125°23'53"E (KC–079; coll. V. Kessner, A. Longbottom, 22 Jul 1988).

Etymology. Named in honour of Sue Lindsay (Australian Museum) in recognition of her help with SEM work.

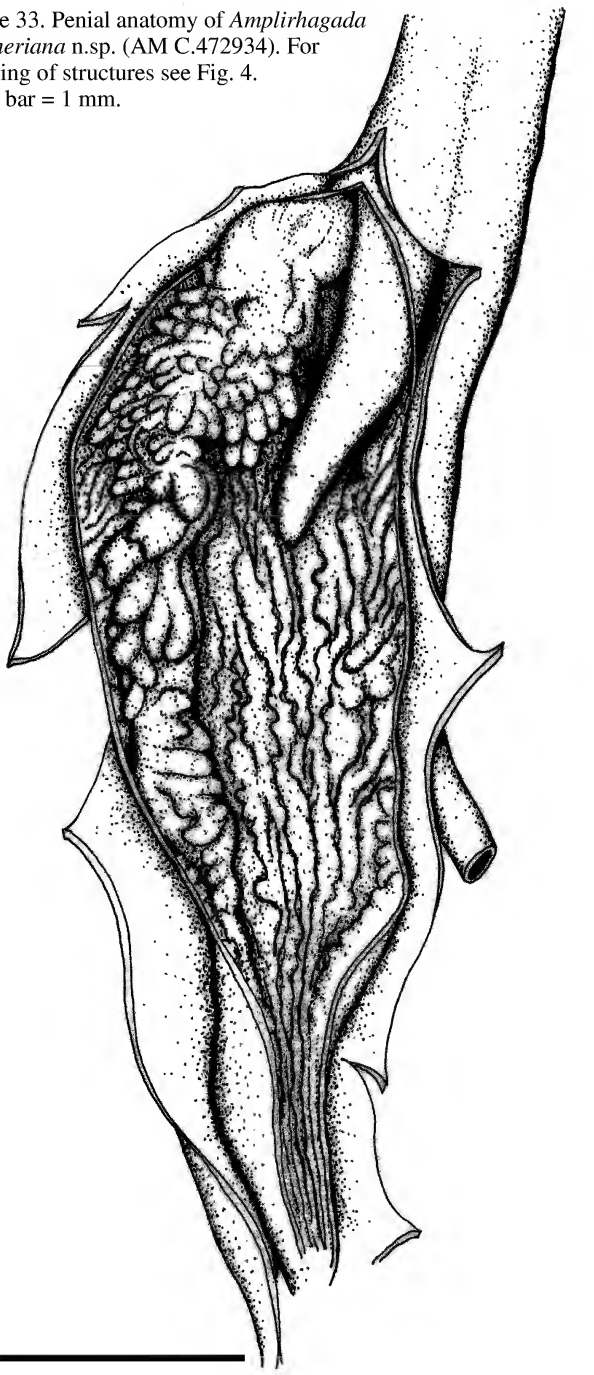

Figure 33. Penial anatomy of *Amplirhagada gardneriana* n.sp. (AM C.472934). For labelling of structures see Fig. 4. Scale bar = 1 mm.

Description

Shell (Pl. 1.12; Fig. 34 A–C). Semi-globose with elevated spire. Solid, not translucent. Periphery angulate to keeled; upper and basal sectors of whorls well rounded. Umbilicus almost entirely concealed by columellar reflection, forming a chink. Background colour pale greenish-ochre; peripheral band mostly visible, usually diffuse, blending into brownish tone that may cover upper part of whorls, thin to moderately broad, brown, visible on last whorls only; sub-sutural band absent or very inconspicuous and diffuse, brown, visible on last whorl only; ventral colour pale horn, outer lip like shell, inner lip pale white. Protoconch 2.8 mm in diameter, comprising about one whorl, with very indistinct radially elongated pustulations. Teleoconch with faint, regular axial

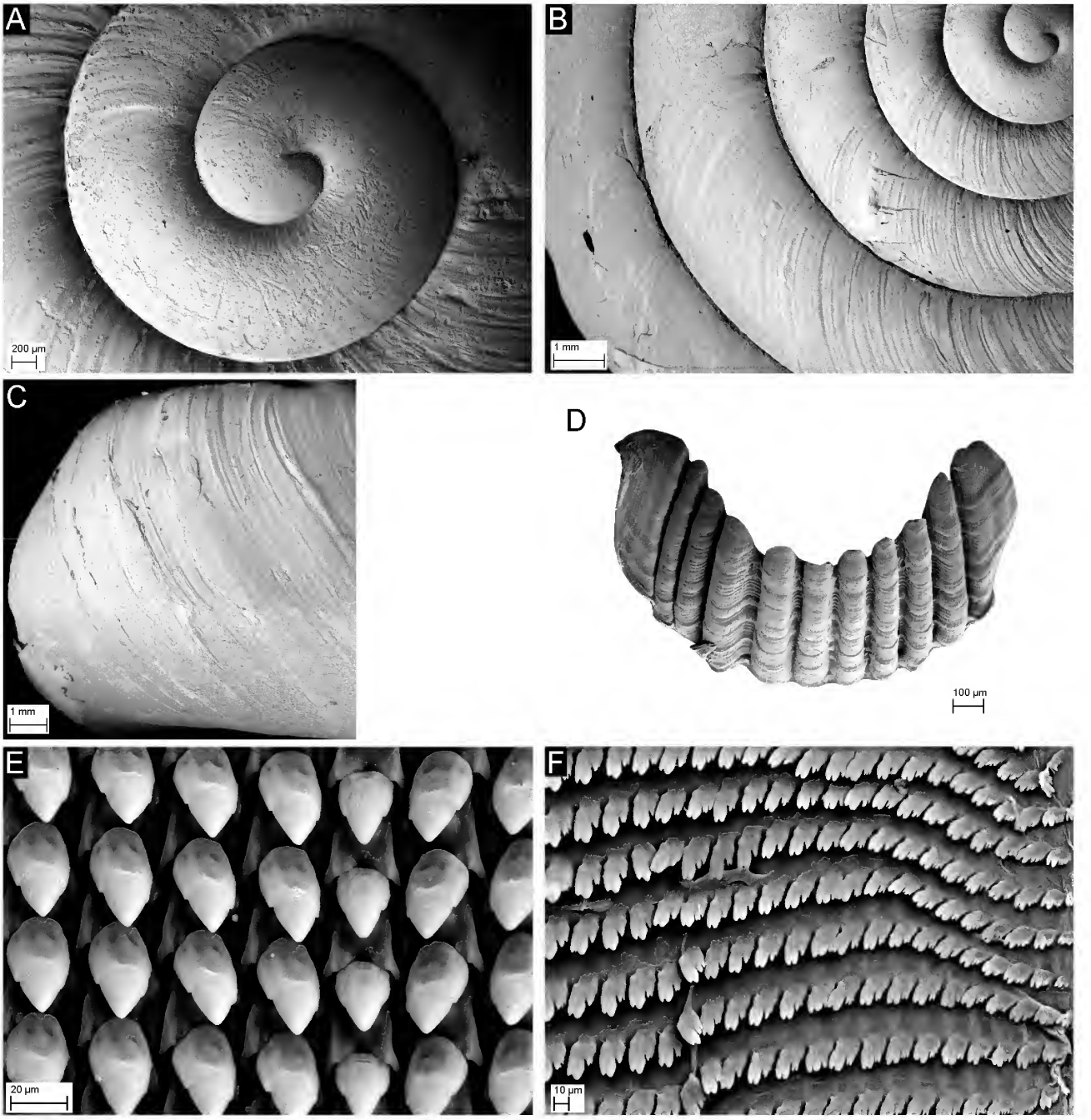

Figure 34. *Amplirhagada lindsayae* n.sp. SEM of shell (AM C.472937), radula and jaw (AM C.472936). *(A)* Protoconch and first teleoconch whorls viewed from above. *(B)* Detail of first teleoconch whorls viewed from above. *(C)* Close-up of sculpture on last whorl, lateral view. *(D)* Jaw. *(E)* Central and inner lateral teeth, detail from above. *(F)* Marginal teeth viewed from above. Scale bars: *A*, 200 µm; *B–C*, 1 mm; *D*, 100 µm; *E*, 20 µm; *F*, 10 µm.

growth lines; evenly distributed across shell surface. Angle of aperture about 45 degrees; outer lip sharp to moderately thick, well rounded, slightly expanded, not or slightly reflected; basal node absent or very weak. Parietal wall of inner lip thin. Average shell size 18.3±1.3 × 22.4±0.8 mm (Table 1).

Radular and jaw morphology (Fig. 34 D–F). Tooth formula C + 12–14 + 4 + 24–26, with 130 rows of teeth 130 (n = 1). Jaw with 11 plates.

Genital morphology (Figs 35–36). Penis straight, tubular, as long as anterior part of oviduct. Penial sheath distally thick, proximally thin. Penial retractor about as long as penis. Penial verge rather small, elongate with pointed tip. Inner penial wall entirely covered by relatively large pustules that are arranged in longitudinal rows. Main stimulatory pilaster formed by row of enlarged (broadened, more elongate), triangular pustules, each supporting a single hook. A weak gutter forms along inner penial wall. Vas deferens moderately thick, entering penial sheath close to penial apex, forming an extended loop. Vagina long, tubular, moderately inflated; inner vaginal wall and wall of bursa copulatrix with smooth longitudinal pilasters. Bursa copulatrix comparatively long, clearly extending base of spermoviduct. Free oviduct comprising about half of length of anterior part of oviduct. Spermoviduct longer than anterior part of oviduct.

Aestivation strategy. Free sealer.

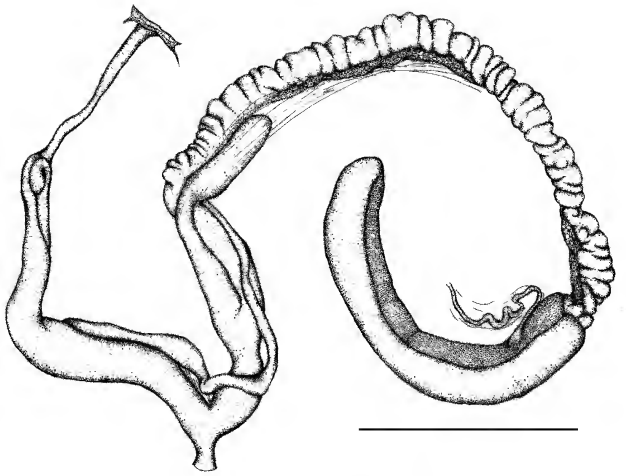

Figure 35. Genitalia of *Amplirhagada lindsayae* n.sp. (AM C.472936). For labelling of structures see Fig. 3. Scale bar = 10 mm.

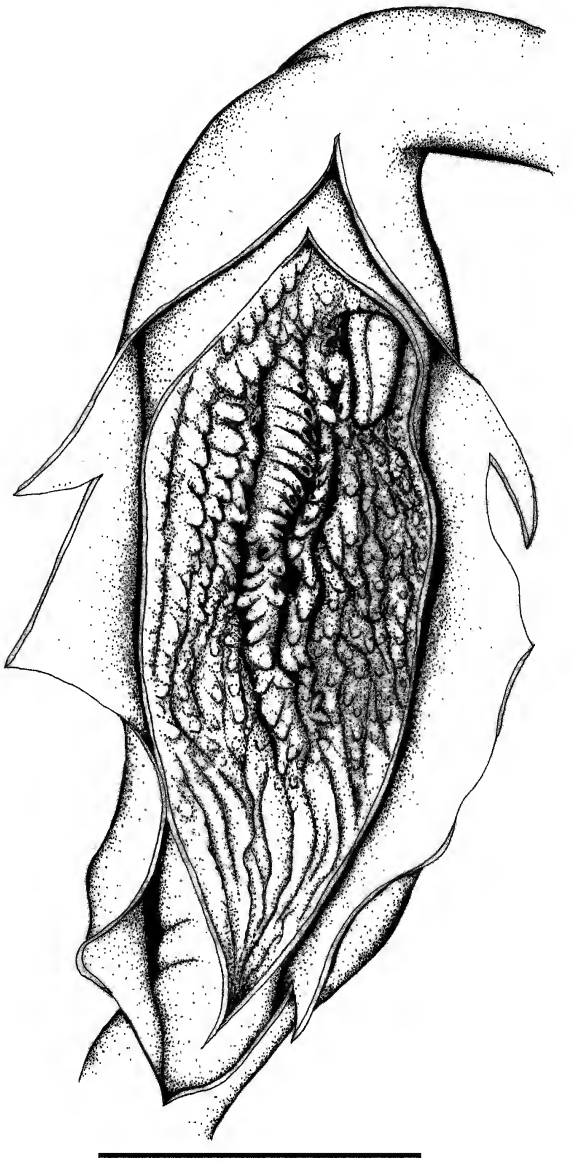

Figure 36. Penial anatomy of *Amplirhagada lindsayae* n.sp. (AM C.472936). For labelling of structures see Fig. 4. Scale bar = 3 mm.

Remarks. Anatomical description based on dissections of three specimens. Listed by Solem (1991) as "*Amplirhagada* NSP29". The "bee-hive" shaped shell is similar to that of other species, such as *A. boongareensis* Köhler, 2010, *A. decora* Köhler, 2010 and *A. vialae*, all of which differ from present species by possessing a huge cone-shaped main pilaster.

Amplirhagada bendraytoni n.sp.

Type locality. Western Australia, NW Kimberley, York Sound, 4 km SE of Cape Brewster, S of Coronation Island, between beach and base of escarpment; 15°07'40"S 124°56'15"E (RFS 12-3; coll. V. Kessner, 12 Jun 1987) (Fig. 1).

Type material. Holotype WAM S34740 (preserved specimen) (Pl. 1.13; Table 1). Paratypes WAM S34741 (2 preserved specimens), FMNH 220448 (3 preserved specimens), WAM S34742 (3 dried shells), FMNH 2200447 (5 dried shells).

Etymology. Named in honour of my friend and neighbour Ben Drayton from Sydney.

Description

Shell (Pl. 1.13; Fig. 37 A–B). Broadly conical to semi-globose with moderately elevated spire. Solid, not translucent. Periphery angulate; upper and basal sectors rounded. Umbilicus 50–80% concealed by columellar reflection. Background colour horn with a yellowish brown tone; spiral bands absent; outer and inner lip colour lighter than shell. Protoconch not differentiable on SEM micrograph. Teleoconch with very faint axial growth lines; evenly distributed across shell surface. Angle of aperture c. 45 degrees; outer lip moderately thick, well rounded, slightly expanded, not reflected; basal node absent. Parietal wall of inner lip absent. Average shell size 15.2±1.5 × 21.3±1.3 mm (Table 1).

Radular and jaw morphology (Fig. 37 C–G). Radular Tooth formula C + 13–18 + 4 + 18–22, with 130–140 rows of teeth (n = 2). Jaw with nine plates.

Genital morphology (Figs 38–39). Penis straight, tubular, thin, as long as anterior part of oviduct. Penial sheath thick. Penial retractor half as long as penis. Penial verge tiny, with pointed tip. Inner penial wall entirely smooth, with several rather indistinct longitudinal pilasters. Main stimulatory pilaster short, at proximal half of inner penial wall, corrugated by lateral lamellae, each lamella supporting usually three little hooks that are arranged into longitudinal rows that run along the central portion of the pilaster. Vas deferens thin, entering penial sheath close to penial apex, forming an extended loop. Vagina very short, proximally inflated; inner vaginal wall and wall of bursa copulatrix with smooth longitudinal pilasters. Bursa copulatrix slightly extending base of spermoviduct. Free oviduct comprising more than half of length of anterior part of oviduct. Spermoviduct longer than anterior part of oviduct.

Aestivation strategy. Free sealer.

Remarks. Anatomical description based on dissections of two specimens. Listed by Solem (1991) as "*Amplirhagada* NSP31". The combination of an almost entirely smooth inner penial wall with a sort main pilaster, a tiny verge and a thick penial sheath are peculiar to only this species.

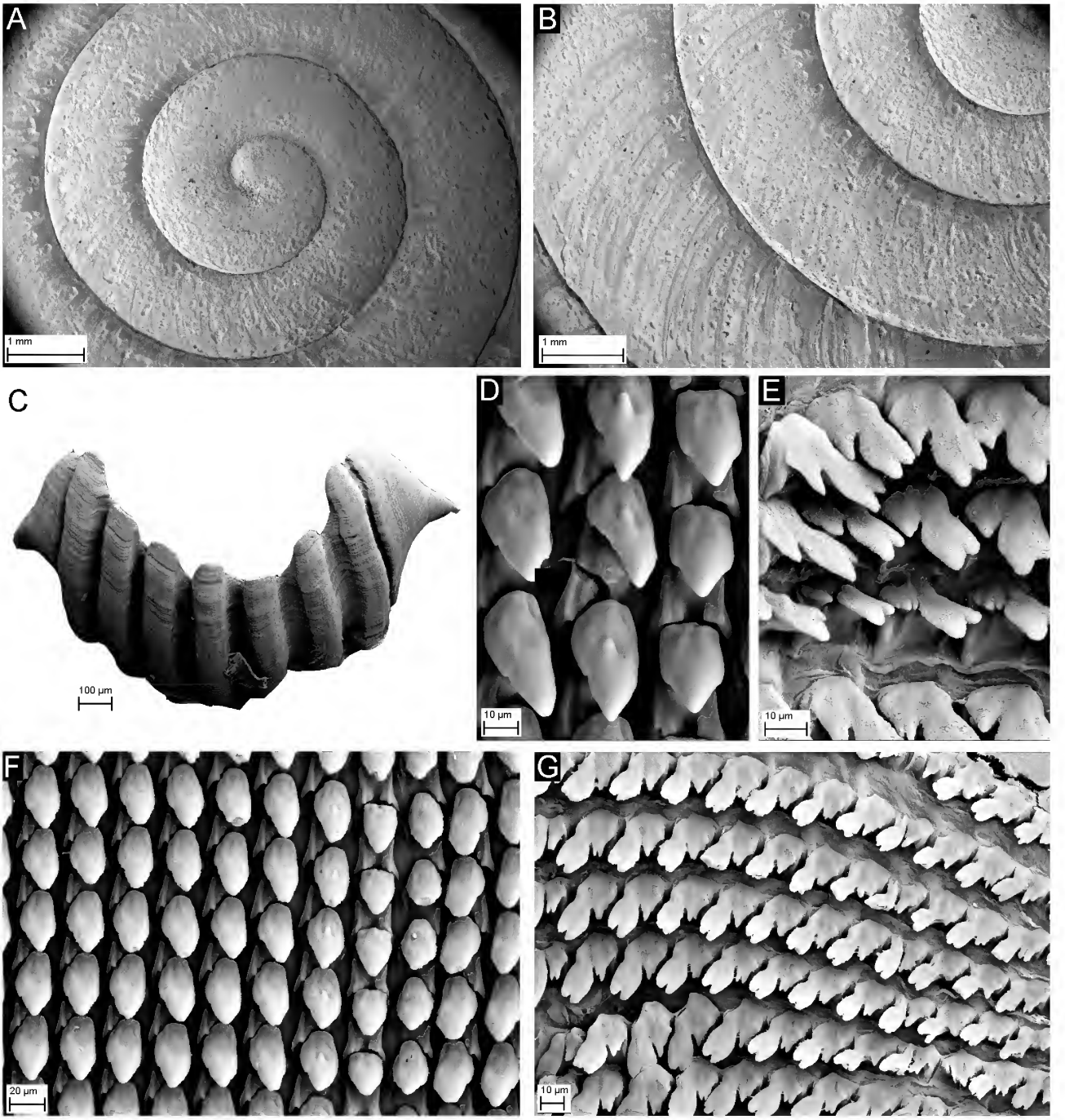

Figure 37. *Amplirhagada bendraytoni* n.sp. SEM of shell, radula and jaw (WAM S34741). *(A)* Protoconch and first teleoconch whorls viewed from above. *(B)* Detail of first teleoconch whorls viewed from above. *(C)* Jaw. *(D)* Close-up of central and inner lateral teeth. *(E)* Close-up of Marginal teeth. *(F)* Central and inner lateral teeth viewed from above. *(G)* Marginal teeth viewed from above. Scale bars: *A–B*, 1 mm; *C*, 100 µm; *D–E, G*, 10 µm; *F*, 20 µm.

Amplirhagada angustocauda n.sp.

Type locality. Western Australia, NW Kimberley, SE of Prince Frederick Harbour, 10.5 km E of Mt. Brookes, 6.5 km from coast; west bank tributary Roe River; 15°12'45"S 125°29'30"E (RFS 16-1; coll. V. Kessner, 16 Jun 1987) (Fig. 1).

Type material. Holotype WAM S34743 (preserved specimen, dissected). Paratypes FMNH 220650 (preserved specimen) (Pl. 1.14), WAM S34744 (2 dried shells), FMNH 220654 (dried shell).

Etymology. The species epithet is derived from "angustus" (Latin = narrow) and "cauda" (Latin = penis), in reference to the narrow and elongate epiphallus being a characteristic of this species.

Description

Shell (Pl. 1.14; Fig. 40 A–C). Broadly conical with moderately elevated spire. Thin, translucent. Periphery sharply angulate; upper and basal sectors rounded. Umbilicus 30% concealed by columellar reflection. Background colour yellowish brown; spiral bands absent; outer and inner lip

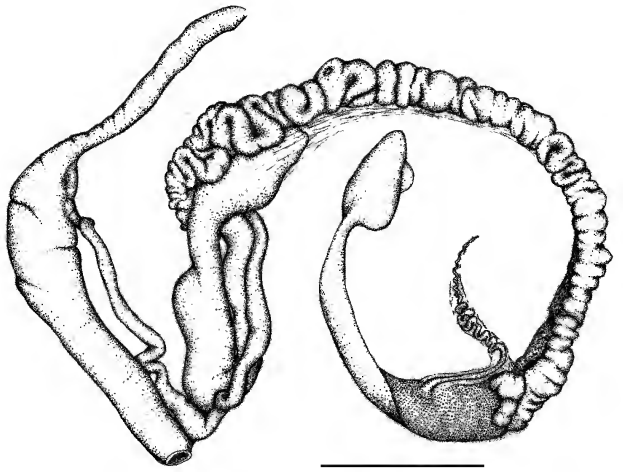

Figure 38. Genitalia of *Amplirhagada bendraytoni* n.sp. (WAM S34741). For labelling of structures see Fig. 3. Scale bar = 5 mm.

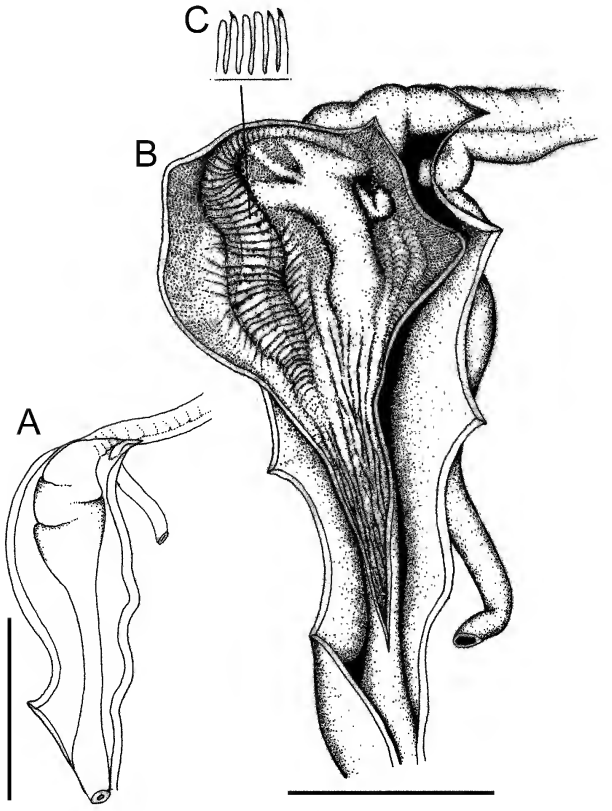

Figure 39. Penial anatomy of *Amplirhagada bendraytoni* n.sp. (WAM S34741). For labelling of structures see Fig. 4. *(A)* Schematic view of the penis with the penial sheath being removed. Scale bar = 5 mm. *(B)* Interior anatomy of the penial wall. Scale bar = 5 mm. *(C)* Schematic cross-section of the main pilaster (not to scale).

colour whitish. Protoconch 3.4 mm in diameter, comprising about 1.5 whorls, essentially smooth. Teleoconch with well-developed, irregular axial growth lines; evenly distributed across shell surface. Angle of aperture c. 60°; outer lip sharp, well rounded, slightly expanded; basal node absent. Parietal wall of inner lip absent. Average shell size 11.7±1.2 × 15.7±0.7 mm (Table 1).

Radular and jaw morphology (Fig. 40 D–F). Tooth formula C + 10–13 + 4 + 16, with 120 rows of teeth 130 (n = 1). Jaw with 11 plates.

Genital morphology (Figs 41–42). Penis straight, with a short, tubular, very thin penis proper; lumen of penial chamber short extending only about 1/3 to 1/4 of length of penial complex. Inner penial wall with few smooth longitudinal pilasters; no main stimulatory pilaster differentiated. Penial sheath distally thick, proximally thin. Penial retractor muscle stubby, no longer than 1/5 of penial complex. Vas deferens moderately thick, entering penial sheath at about half of length of penial complex, forming an extended loop, reflecting as an elongate, thin, tubular epiphallus, which gives rise to the short penis. Inner wall of epiphallus smooth, ciliated. Penial verge tiny, slender, with pointed tip. Vagina moderately long, proximally slightly inflated; inner vaginal wall and wall of bursa copulatrix with smooth longitudinal pilasters. Bursa copulatrix slightly extending base of spermoviduct. Free oviduct comprising about half of length of anterior part of oviduct. Spermoviduct longer than anterior part of oviduct.

Aestivation strategy. Unknown.

Remarks. Description is based on dissection of the holotype. The species was listed by Solem (1991) as "*Amplirhagada* NSP33". Shell smaller than in most other congeners. Various features of the penial anatomy are very characteristic: vas deferens reflecting as a narrow, elongated epiphallus, the penial chamber is very short supporting longitudinal pilasters but no pustules. Species differs by its markedly different penial anatomy from *A. wilsoni* Solem, 1981, which also occurs at the banks of the Roe River not too far from the type locality of this species. For comparison with *A. moraniana* having also a similar shell see remarks under this species.

Amplirhagada epiphallica n.sp.

Type locality. Western Australia, NW Kimberley, N side of Prince Frederick Harbour, near mouth, 16 km W of Mt. Anderdon, 0.3 km from coast; 14°57'10"S 125°16'30"E (RFS 14-1; coll. V. Kessner, 14 Jun 1987) (Fig. 1).

Type material. Holotype WAM S34745 (preserved specimen) (Pl. 1.15; Table 1). Paratypes WAM S34746 (3 preserved specimens), FMNH 200539 (4 preserved specimens), WAM S34747 (2 dried shells), FMNH 220541 (2 dried shells).

Etymology. The species epithet refers to the presence of an epiphallus, which is a very distinctive feature among species of *Amplirhagada*.

Description

Shell (Pl. 1.15; Fig. 43 A–C). Broadly conical with low spire, almost discoid. Thin to delicate, translucent. Periphery rounded to angulate; upper and basal sectors of whorls well rounded. Umbilicus 10–50% concealed by columellar reflection. Background colour pale yellowish brown; peripheral band well marked, moderately thick, brown, visible on most whorls; sub-sutural well marked to diffuse, moderately thick, visible on most whorls; outer and inner lip colour whitish. Protoconch 2.5 mm in diameter, comprising about 1.2 whorls, essentially smooth. Teleoconch with regular axial growth lines; evenly distributed across shell surface. Angle of aperture about 45 degrees; outer lip thin, well rounded, expanded, not reflected; basal node absent or weakly developed. Parietal wall of inner lip inconspicuous. Average shell size 13.7±0.8 × 20.1±0.7 mm (Table 1).

Radular and jaw morphology (Fig. 43 D–F). Tooth formula C + 13–14 + 4 + 18–20, with 150 rows of teeth 130 (n = 1). Jaw with 11 plates.

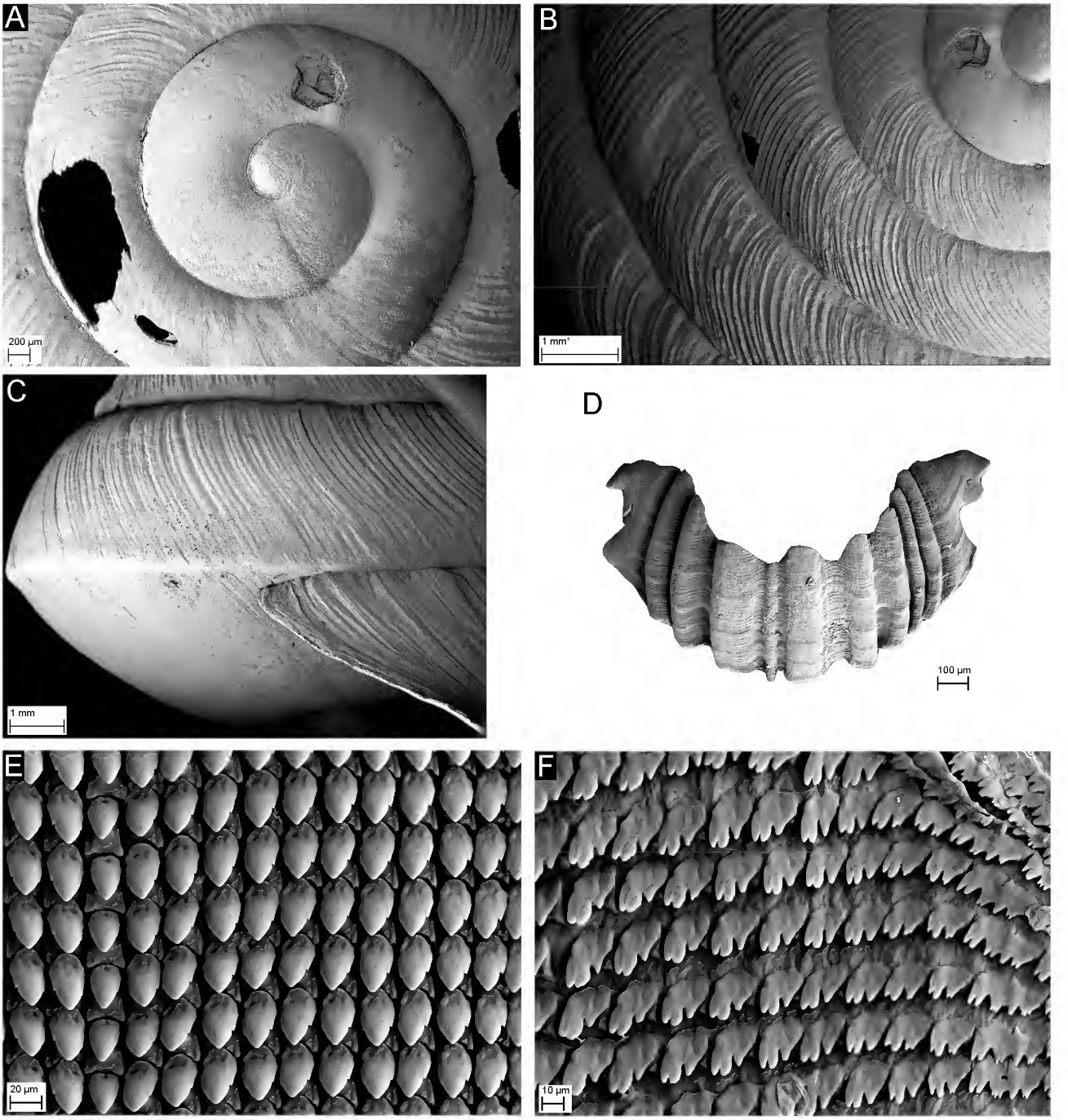

Figure 40. *Amplirhagada angustocauda* n.sp. SEM of shell, radula and jaw (WAM S34743). *(A)* Protoconch and first teleoconch whorls viewed from above. *(B)* Detail of first teleoconch whorls viewed from above. *(C)* Close-up of sculpture on last whorl, lateral view. *(D)* Jaw. *(E)* Central and inner lateral teeth viewed from above. *(F)* Marginal teeth viewed from above. Scale bars: *A*, 200 µm; *B–C,* 1 mm *D*, 100 µm; *E*, 20 µm; *F,* 10 µm.

Genital morphology (Figs 44–45). Penis complex elongated, tubular, coiled; actual penis extending proximal two thirds of penial complex. Inner penial wall completely lined with regular, fine pustulation arranged in corrugated pilasters; no main stimulatory pilaster differentiated. Penial sheath thick. Penial retractor muscle stubby, no longer than 1/10 of penial complex. Vas deferens moderately thick, entering penial sheath at apical end of penial complex, forming an extended loop, reflecting as an elongate, thin, tubular epiphallus, which gives rise to the short penis. Inner wall of epiphallus smooth, ciliated. Penial verge tiny, slender, forming a loop with pointed tip. Vas deferens elongated, winding before entering the uterus. Vagina long, tubular; inner vaginal wall and wall of bursa copulatrix with smooth longitudinal pilasters. Bursa copulatrix slightly extending base of spermoviduct, with bulbous head. Free oviduct elongated, coiled before entering the uterus, comprising more than half of length of anterior part of oviduct. Spermoviduct no longer than anterior part of oviduct. Albumen gland as long as spermoviduct.

Aestivation strategy. Free sealer.

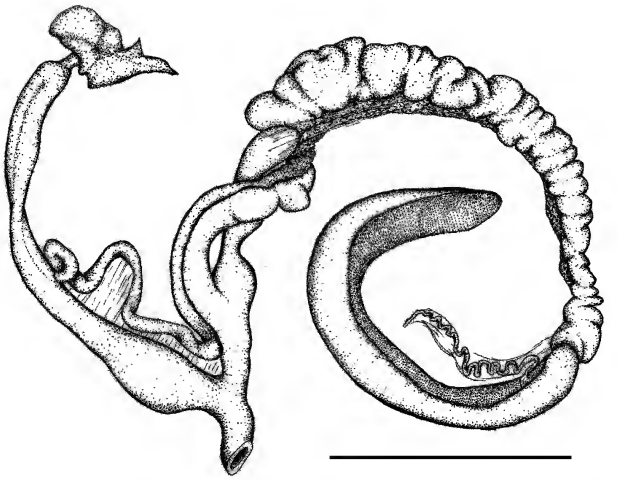

Figure 41. Genitalia of *Amplirhagada angustocauda* n.sp. (WAM S34743). For labelling of structures see Fig. 3. Scale bar = 5 mm.

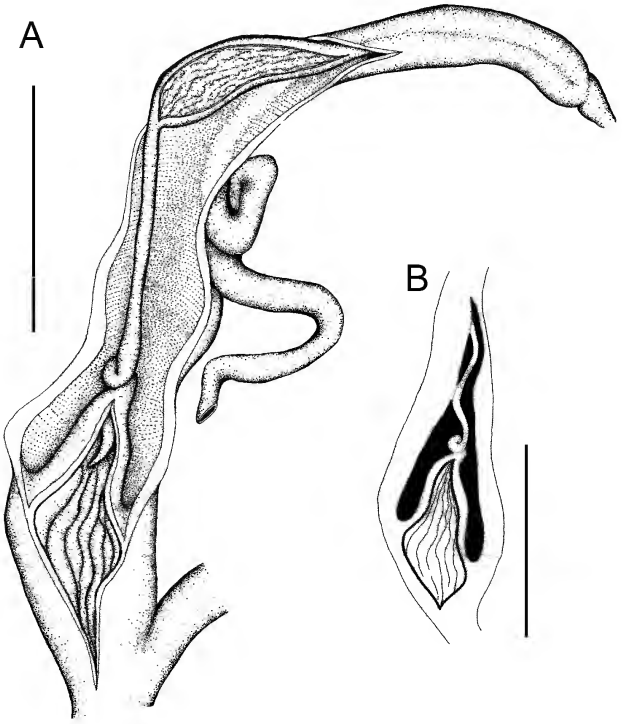

Figure 42. Penial anatomy of *Amplirhagada angustocauda* n.sp. (WAM S34743). For labelling of structures see Fig. 4. *(A)* Interior anatomy of the penial wall. *(B)* Schematic view of the penis with the penial sheath being removed. Scale bars = 3 mm.

Remarks. Anatomical description based on dissection of the holotype. Listed by Solem (1991) as "*Amplirhagada* NSP35" and found in sympatry with *A. inusitata* n.sp. and *A. pusilla* Solem, 1981. The flat shell is similar to that of *A. discoidea*. However, the genital anatomy of this species is very unusual for *Amplirhagada* showing a combination of exclusive features, such as a very long and winding vas deferens, a long tubular vagina, very long tubular penis and vas deferens reflecting as an epiphallus within the strongly developed penial sheath, and a short, thin and coiled penial verge.

Amplirhagada carinata Solem, 1981

Amplirhagada carinata Solem, 1981: 205–208, pl. 13e, figs. 37g, 43a–b, 45a–b

Type locality. Western Australia, SW Kimberley, 5 km N of Mt Hart Station, immediately W of Mt Matthew, Upper Barker Drainage, King Leopold Ranges.

Material examined (Fig. 1). WAM S34759 (8 preserved specimens), FMNH 220843 (7 preserved specimens), WAM S34760 (13 dried shells), FMNH 220842 (13 dried shells), all from 3.6 km SSE of Mt. Talbot, 3.2 km from coast, near Walcott Inlet; 16°29'25"S 124°48'05"E, RFS-21-3; coll. V. Kessner, 21 Jun 1987 ("NSP36"). WAM S34761 (8 preserved specimens), FMNH 221066 (8 preserved specimens), AM C.472938 (6 dried shells), WAM S34762 (13 dried shells), FMNH 221065 (19 dried shells), all from 34 km S of Mt. Kitchener, 9 km from coast, S of Calder River; 16°19'40"S 125°01'10"E; RFS-27-1, coll. V. Kessner, 27 Jun 1987 ("NSP36"). WAM S34763 (5 preserved specimens), FMNH 221096 (5 preserved specimens), AM C.472939 (5 dried shells), WAM S34764 (15 dried shells), FMNH 221095 (20 dried shells), all from NW hump of The Dromedaries, E of Isdell River; 16°34'20"S 124°56'40"E; RFS-28-1, coll. V. Kessner, 28 Jun 1987 ("NSP38"). WAM S34765 (4 preserved specimens), FMNH 220782 (4 preserved specimens), WAM S34766 (9 dried shells), FMNH 220781 (10 dried shells), all from Walcott Inlet, 6 km E of Mt. Talbot, 2 km from coast; 16°27'30"S 125°50'30"E; RFS 19-2, coll. V. Kessner, 19 Jun 1987 ("NSP42"). FMNH 220755 (2 preserved specimens), WAM S34767 (11 dried shells), FMNH 220755 (11 dried shells), all from Walcott inlet, 14.5 km E of Mt. Talbot; 16°25'20"S 124°54'00"E; RFS 18-4, leg. V. Kessner, 18 Jun 1987 ("NSP42"). AM C.472940 (6 preserved specimens), WAM S34768 (10 preserved specimens), FMNH 220987 (15 preserved specimens), WAM S34769 (17 dried shells), FMNH 220986 (16 dried shells), all from 25.3 km WSW of Mt. Blithe, on Charney River; 16°22'35"S 125°12'35"E; RFS 25-2, coll. V. Kessner, 25 Jun 1987 ("NSP42").

Diagnosis

Shell (Pl. 1.16; Fig. 46 A–C) broadly conical to discoid with low spire, slightly to sharply angulated periphery, well rounded upper and basal sectors of whorls. Umbilicus 10–80% concealed by columellar reflection. Background colour pale yellowish brown; peripheral band usually diffuse, thin, brown, visible on most whorls; sub-sutural band diffuse, brown, thin; outer and inner lip colour like shell. Protoconch c. 1.5 mm in diameter, with about 1.5 whorls, with very indistinct radially elongated pustulations. Teleoconch with faint, regular axial growth lines; evenly distributed across shell surface. Angle of aperture 45–60 degrees; outer lip thin to moderately thick, well rounded, slightly to well expanded, not reflected; basal node absent or weak. Parietal wall of inner lip inconspicuous. Average shell size 10.7±16.9 × 1.4±1.1 mm (Table 1).

Radular tooth formula C + 12–14 + 4 + 16–20, with on average 130 of rows of teeth (n = 4), jaw with 10 plates (Fig. 46 D–E).

Penis heavily coiled within penial sheath, thick, longer than anterior part of oviduct, with thick penial sheath. Penial verge moderate in size, comprising c. 1/10 of length of penial chamber, conical, with rounded tip. Inner penial wall penial wall with dense, fine pustulation, main stimulatory pilaster weakly to well developed, extending about half of length of penial chamber, consisting of enlarged and partly fused pustules forming hooked corrugations or an elongated, conical pilaster; a gutter forming along inner penial wall. Vas deferens moderately thick, winding, entering

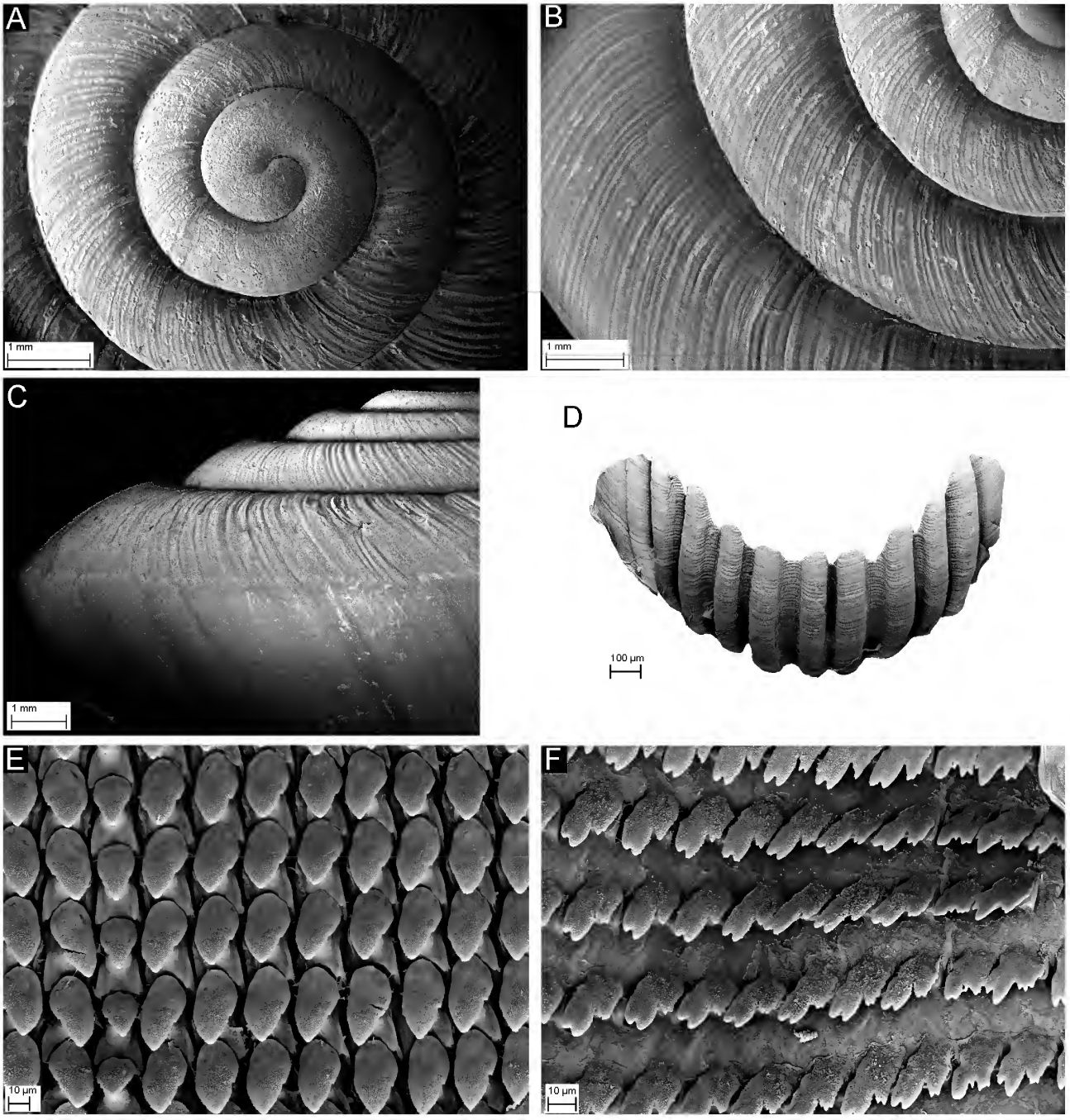

Figure 43. *Amplirhagada epiphallica* n.sp. SEM of shell, radula and jaw (WAM S34746). *(A)* Protoconch and first teleoconch whorls viewed from above. *(B)* Detail of first teleoconch whorls viewed from above. *(C)* Close-up of sculpture on last whorl, lateral view. *(D)* Jaw. *(E)* Central and inner lateral teeth viewed from above. *(F)* Marginal teeth viewed from above. Scale bars: *A–C*, 1 mm; *D*, 100 µm; *E–F*, 10 µm.

penial sheath close to penial apex. Vagina moderately long, distally inflated, inner wall with rows of densely arranged triangular pustules. Bursa copulatrix clearly extending base of spermoviduct (Figs 47–48). Aestivation strategy unknown.

Remarks. Description based on dissections of four specimens. Material of three distinct manuscript species differentiated by Solem (1991), *Amplirhagada* NSP36, NSP38, and NSP 42, are subsumed under *A. carinata* Solem, 1981. Solem (1991) indicated serious problems with the correct delimitation of *A. carinata* and was puzzled by its unusually large distributional range. However, there are other congeners, such as *A. burnerensis* (Smith, 1894), *A. pusilla* Solem, 1981 and *A. osmondi* Solem, 1988, that occupy similarly large ranges in the interior of the SW and E Kimberley.

The various populations currently included within *A. carinata* indeed reveal considerable levels of anatomical differentiation. While inner penial wall always supports dense and conspicuous pustulation, a main stimulatory pilaster may or may not be developed. However, anatomical variation in shell and penial anatomy is large also within populations and I am not able to unequivocally delimit taxa by using these features. As outlined by Cameron (1992) for similar patterns of shell differentiation found in a number of camaenid species in the Oscar and Napier Ranges of the

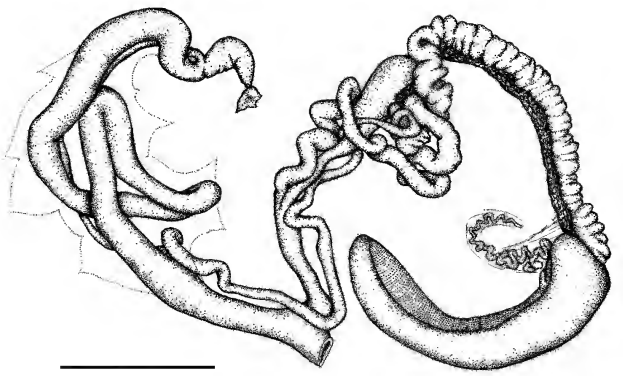

Figure 44. Genitalia of *Amplirhagada epiphallica* n.sp. (WAM S34746). For labelling of structures see Fig. 3. Scale bar = 5 mm.

Figure 45. Penial anatomy of *Amplirhagada epiphallica* n.sp. (WAM S34746). For labelling of structures see Fig. 4. *(A)* Interior anatomy of the penial wall. *(B)* Schematic view of the penis with the penial sheath being removed. Scale bars = 5 mm.

interior SW Kimberley, this might indicate the presence of unresolved species complexes that are currently undergoing the process of lineage differentiation (i.e., speciation). A careful analysis of the spatial patterns of anatomical and genetic differentiation is needed to resolve these problems and suggest a proper taxonomic solution for these species complexes.

Discussion

Significance of morphological characters for the delimitation of taxa

The genital anatomy, with special emphasis on penial anatomy, has been recognized as the most significant source of systematic information on all systematic levels within the Camaenidae (e.g., Solem, 1981). This observation was recently confirmed also for *Amplirhagada* by Köhler (2010b), who showed that the vast majority of species was characterized by distinct features, notably of inner penial wall and development of the main stimulatory pilaster. Species-taxa delineated by use of such features were consistently differentiated by large genetic distances in the mitochondrial marker *cytochrome c oxidase subunit 1* (COI).

Naturally, the development and relative size of some genital structures depends on the maturity of the animal and on its actual reproductive state. Among fully mature specimens (with adult shell features and fully developed albumen gland), a simple pattern of seasonal variation is found with the genitalia being inactive and reduced in size during the early to middle dry season between May and August (Solem & Christensen, 1984). As figures and descriptions of genital features herein are exclusively based on the examination of adult specimens collected during the dry season (June 1987), all reproductive organs should be in a comparable stage of seasonal development.

Species described herein (and earlier; Köhler, 2010b) reveal an amazing variety especially with respect to their penial anatomy. Most species are readily recognisable by a peculiarly developed inner penial wall (*A. alicunda*, *A. discoidea*, *A. bendraytoni*), the presence of an unusually long penial verge (*A. moraniana*, *A. inusitata*), a massively enlarged main pilaster (*A. alicunda*, *A. vialae*), absence of a main pilaster (*A. coffea*), peculiar shape of the main pilaster (*A. gardneriana*), an extremely elongated penis (*A. inusitata*), or even the presence of an epiphallus (*A. angustocauda*, *A. epiphallica*), and often a combination of several such characteristics.

The presence of an epiphallus in *A. angustocauda* and *A. epiphallica* is particularly remarkable because the lack of an epiphallus was thought to be a characteristic shared by all species of this genus. The species *A. epiphallica* is characterizedby additional features, such as a very long and coiled penis plus a long and winding vas deferens and free oviduct, which sets it apart from all other congeners. These features indicate that this is a species that likely occupies a distinct position in the phylogenetic tree of *Amplirhagada*. Still, it is retained within *Amplirhagada* for the time being because of its typical shell, the presence of a penial sheath and a penial verge being similar to the typical shape. The elongated, tubular penis, the presence of an epiphallus and the long and winding vas deferens and free oviduct can be seen as derivations from the typical anatomy. It is considered more likely that these structures are plesiomorphic and were lost or reduced in all other congeners than assuming that they have developed in *A. epiphallica* independently from similar character states in other camaenid genera. This assumption implies that *A. epiphallica* may be the most primitive species within *Amplirhagada*. This remains to be tested by a phylogenetic analysis.

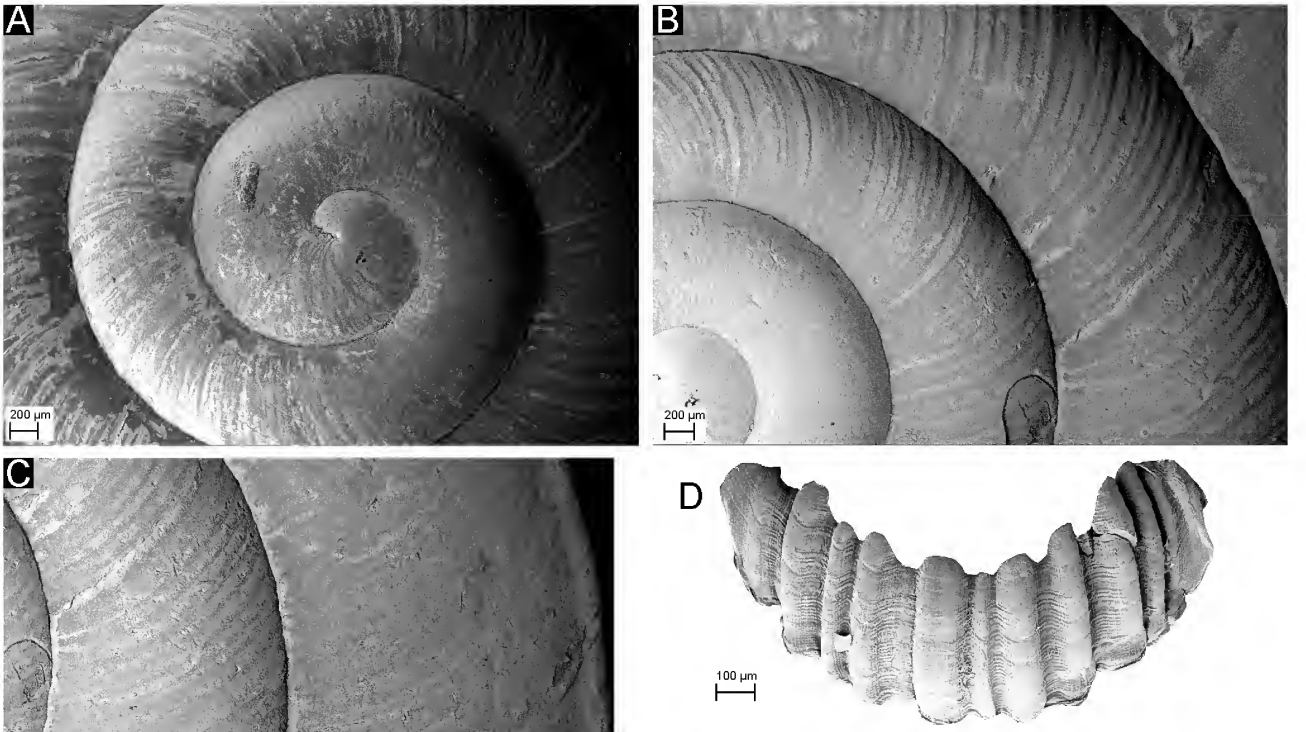

Figure 46. *Amplirhagada carinata* Solem, 1981 SEM of shell, radula and jaw (WAM S34759). *(A)* Protoconch and first teleoconch whorls viewed from above. *(B)* Detail of first teleoconch whorls viewed from above. *(C)* Close-up of sculpture on last whorl, lateral view. *(D)* Jaw. *(E)* Central and inner lateral teeth viewed from above. *(F)* Marginal teeth viewed from above. Scale bars: *A–C*, 200 µm; *D*, 100 µm; *E–F*, 10 µm.

The marked interspecific differentiation in the reproductive anatomy and the observation that differences are greater when species occur in sympatry led Solem (1981) to argue that the structure of penial and vaginal walls may have a significant function in mate recognition. Recent findings of reproductive character displacement in genital morphology of Asian camaenids (*Satsuma*) seem to provide evidence in support of this idea (Kameda, Kawakita & Kato, 2009). In accordance with this postulate, the species with the most highly derived penial anatomy described here (*A. vialae*, *A. discoidea*, *A.*

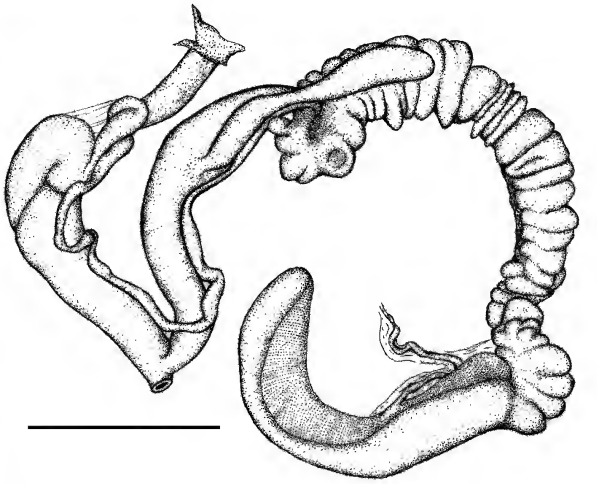

Figure 47. Genitalia of *Amplirhagada carinata* Solem, 1981 (WAM S34759). For labelling of structures see Fig. 3. Scale bar = 5 mm.

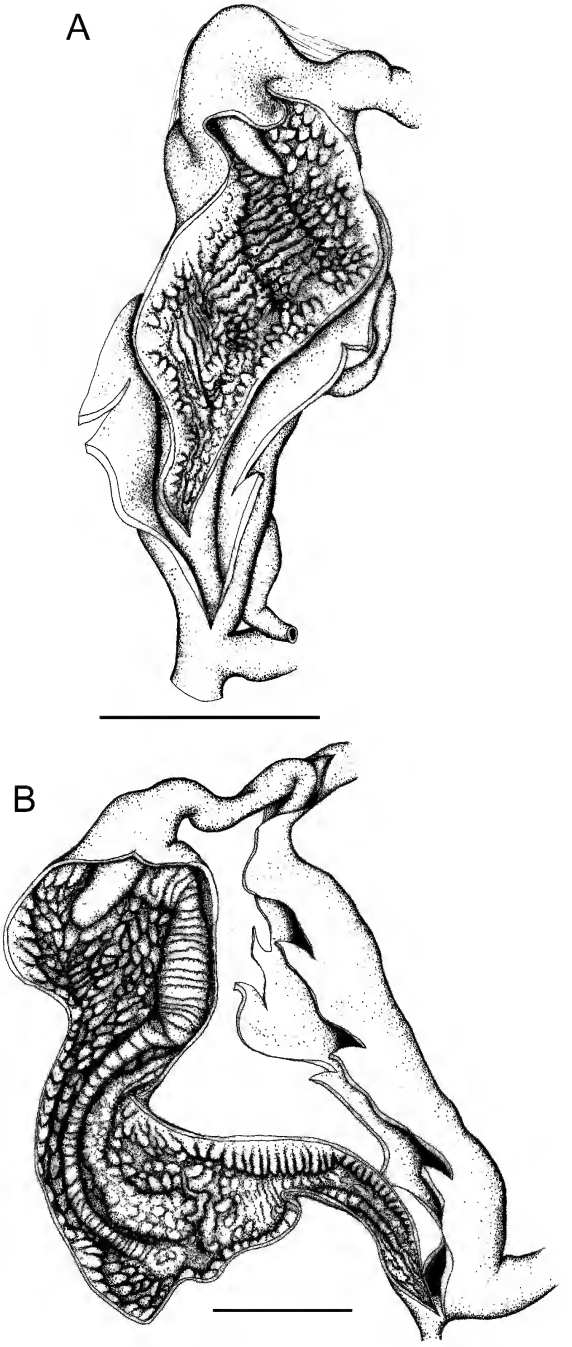

Figure 48. Penial anatomy of *Amplirhagada carinata* Solem, 1981. *(A)* Interior anatomy of the penial wall (WAM S34759). *(B)* Interior anatomy of the penial wall (WAM S34763). For labelling of structures see Fig. 4. Scale bars = 3 mm.

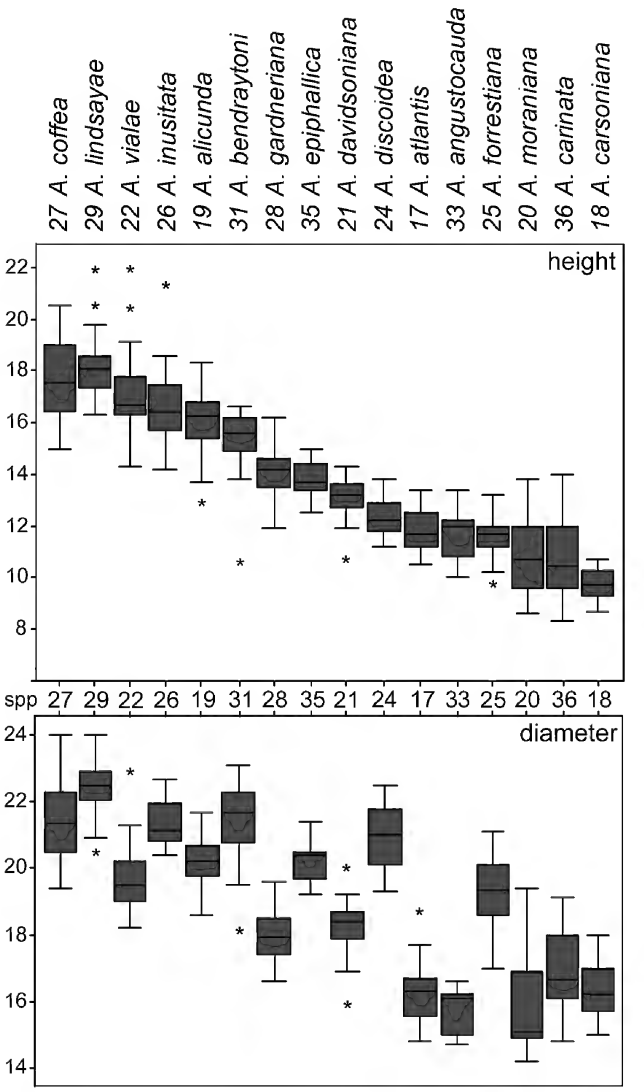

Figure 49. Shell size ranges of *Amplirhagada* species described herein. Box plot diagrams showing the median (line in box), the 25% (box) and 75% percentile (lines outside box) and extremes (asterisks) of shell height (above) and shell width (below) of species sorted by their height. Species numbers refer to the manuscript names of the described species as used by Solem (1991): 27, *A. coffea*. 29, *A. lindsayae*. 22, *A. vialae*. 26, *A. inusitata*. 19, *A. alicunda*. 31, *A. bendraytoni*. 28, *A. gardneriana*. 35, *A. epiphallica*. 21, *A. davidsoniana*. 24, *A. discoidea*. 17, *A. atlantis*. 33, *A. angustocauda*. 25, *A. forrestiana*. 20, *A. moraniana*. 36, *A. carinata*. 18, *A. carsoniana*.

inusitata, *A. epiphallica*, *A. angustocauda*) consistently occur in sympatry with at least a second congener. However, the picture is not as simple as there are also species that possess unusual features but are not known to co-occur with a second species, such as *A. moraniana* and *A. alicunda*. In addition, another species not treated herein (*Amplirhagada* NSP37, as preliminarily identified by Alan Solem) and *A. carinata* have overlapping ranges and a similar penial anatomy. However, these two species were never found in sympatry. *Amplirhagada* "NSP37" was ignored in this paper because of its currently unresolved relationships with another undescribed species from islands in the Collier Bay, and will be dealt with in future publications.

Contrasting with the systematic significance of the reproductive anatomy, Solem (1981) found that shell features often are of limited value for the recognition of species. In the first place, species recognition by shell features is complicated though by the usually large amount of variation in shell shape and colouration. In general, species that occur under allopatric conditions may exhibit quite similar shells while conversely species found in sympatry usually have distinct shell shapes or sizes, which was discussed as being indicative of ecological niche partitioning (Solem, 1981; Cameron, 1992). Although shell characters are of limited utility for inferring relationships, they are still useful for the recognition of most species. Among species of *Amplirhagada*

there are two conspicuously different shell types. Many species have moderately flat and broadly conical shells (the "standard shape") but some others have dome-shaped (or beehive-shaped) shells. Köhler (2010b) has shown that a least some of these species form a separate clade (*A. uwinensis* Köhler, 2010; *A. sphaeroidea* Köhler, 2010; *A. regia* Köhler, 2010; *A. camdenensis* Köhler, 2010) nested among other congeners. Species described here also differ in their shells with respect to shape, colour, and size (Table 1). With regard to adult shell height (H), they occupy ranges between about 10 and 22 mm (Fig. 49) with almost no overlap between the smaller (e.g., *A. moraniana*, *A. wilsoni, A. atlantis*) and the larger species (e.g., *A. coffea*, *A. lindsayae*). Even species of similar height may partly differ significantly in diameter (D), and thus also in their H/D ratio. This holds true, for example, for the species pairs *A. coffea–A. lindsayae*, *A. vialae–A. inusitata* or *A. discoidea*–all other species of similar height.

Besides shells and genitalia, radulae and jaws were considered rather useless for the differentiation of taxa at species level by Solem (1981), which is confirmed by the results of the present study. The radula was found to be highly conserved and therefore uninformative at the species and genus level.

Corresponding observations with regard to the significance of morphological characters in general were made in other Australian (Clark, 2009; Willan *et al.*, 2009; Köhler, 2010b, c, 2011), Asian (Chiba, 1999; Kameda, Kawakita & Kato, 2007; Chiba & Davison, 2008) and New Guinean Camaenidae (Jordaens *et al.*, 2009), respectively.

Patterns of distribution and lineage differentiation

The majority of *Amplirhagada* species are found exclusively in rainforest or vine thicket patches at more sheltered localities, which seems to indicate a strong correlation with this kind of habitat. Similar observations were made in most other camaenids in the Kimberley (Solem, 1991). As a result, species ranges are often very small; i.e., an average of 20 km in diameter (Solem & McKenzie, 1991). In accordance with this general statement, all but three species described herein were found only at one (or two very close) localities. Only *A. coffea* and *A. carinata* Solem, 1981 were found at localities that imply a larger distributional range. Other *Amplirhagada* species with larger distributions are *A. pusilla* Solem, 1981, *A. burnerensis* (Smith, 1894), *A. osmondi* Solem, 1988, *A. napierana* Solem, 1981 and *A. percita* (Iredale, 1939) (Cameron, 1992; Solem, 1981). All these species are found in the semi-arid interior of southern and southeastern Kimberley, where they predominantly occur on limestone outcrops in more open woodland. These more inhospitable habitats differ considerably from the rainforest-type habitats of species that live in the rainfall-rich coastal regions of the NW Kimberley. Rainforest habitats may accommodate up to four sympatric *Amplirhagada* species plus a range of additional camaenids from other genera. In sympatry these species seem to occupy distinct ecological niches—a conclusion essentially based on differences in shell shapes and sizes (Solem, 1991).

Table 1. Shell measurements of the type series. Given are maximum–minimum (mean±standard deviation) of N measured adult shells. Abbreviations used: HT = holotype.

species	n	height (H)	diameter (D)	height of first whorl	number of whorls	H/D ratio
A. atlantis	19	10.5–13.4 (11.8±0.8)	14.8–18.7 (16.2±0.9)	6.6–8.4 (7.2±0.4)	4.0–5.0 (4.6±0.3)	0.65–0.81 (0.73±0.04)
	HT	12.8	18.7	8.4	5.0	0.68
A. carsoniana	20	8.7–10.7 (9.8±0.6)	15.0–18.0 (16.3±0.8)	5.3–6.9 (6.3±0.4)	4.5–5.0 (4.8±0.2)	0.53–0.69 (0.60±0.04)
	HT	8.8	16.1	6.5	5.0	0.55
A. alicunda	22	12.9–18.3 (16.0±1.4)	18.6–21.7 (20.2±0.7)	7.9–10.1 (9.0±0.5)	4.7–5.7 (5.2±0.2)	0.66–0.88 (0.79±0.05)
	HT	14.8	19.7	9.2	5.0	0.75
A. moraniana	21	8.6–13.8 (10.9±1.5)	14.2–19.4 (15.9±1.5)	5.8–8.3 (6.3±0.7)	3.5–5.5 (4.8±0.4)	0.59–0.77 (0.68±0.04)
	HT	9.5	15.1	6.7	5.0	0.63
A. davidsoniana	21	10.7–14.3 (13.1±0.8)	15.9–20.0 (18.3±0.9)	6.5–8.6 (7.6±0.5)	5.0–5.9 (5.4±0.3)	0.64–0.77 (0.72±0.03)
	HT	14.0	20.0	8.6	5.9	0.70
A. vialae	21	17.9–21.9 (17.1±1.8)	18.2–22.9 (19.8±1.0)	7.9 -11.1 (9.1±0.7)	5.2–6.7 (5.8±0.4)	0.76–0.98 (0.86±0.06)
	HT	16.7	20.2	9.1	5.4	0.83
A. discoidea	21	11.2–13.8 (12.4±0.7)	19.3–22.5 (20.9±0.9)	6.9–8.2 (7.6±0.4)	5.1–5.9 (5.5±0.2)	0.55–0.64 (0.59±0.03)
	HT	13.3	22.5	8.2	5.2	0.59
A. forrestiana	22	9.8–13.2 (11.6±0.8)	17.0–21.1 (19.4±1.0)	6.3–8.2 (7.2±0.5)	5.0–6.1 (5.3±0.3)	0.55–0.64 (0.60±0.02)
	HT	12.0	20.3	7.1	6.1	0.59
A. inusitata	13	14.2–21.3 (16.8±1.7)	20.4–22.7 (21.4±0.7)	8.3–9.7 (8.9±0.4)	5.4–6.3 (5.7±0.3)	0.69–0.95 (0.79±0.07)
A. coffea	28	15.0–20.5 (17.9 1.6)	19.4–24.0 (21.4±1.1)	8.1–10.5 (9.3±0.6)	5.1–6.3 (5.8±0.3)	0.68–0.92 (0.84±0.05)
	HT	20.0	22.4	10.0	6.0	0.89
A. gardneriana	22	11.9–16.2 (14.2±1.2)	16.6–19.6 (18.0±0.7)	6.8–8.4 (7.6±0.4)	4.8–5.6 (5.4±0.2)	0.68–0.88 (0.79±0.05)
	HT	15.8	19.5	8.4	5.5	0.81
A. lindsayae	23	16.3–21.9 (18.3±1.3)	20.5–24.0 (22.4±0.8)	8.4–10.0 (9.2±0.4)	5.1–5.7 (5.4±0.2)	0.72–0.96 (0.81±0.05)
	HT	18.0	22.0	9.1	5.3	0.82
A. bendraytoni	13	10.6–16.6 (15.2±1.5)	18.1–23.1 (21.3±1.3)	8.2–12.0 (9.2±0.9)	5.0–6.0 (5.7±0.3)	0.59–0.78 (0.71±0.05)
	HT	15.4	21.7	9.0	6.0	0.71
A. angustocauda	5	10.0–13.4 (11.7±1.2)	14.7–16.6 (15.7±0.7)	6.2–7.1 (6.6±0.3)	5.0–5.6 (5.3±0.2)	0.67–0.81 (0.74±0.04)
A. epiphallica	9	12.5–15.0 (13.7±0.8)	19.2–21.4 (20.1±0.7)	7.6–8.1 (7.9±0.2)	5.6–6.0 (5.8±0.1)	0.63–0.75 (0.68±0.04)
	HT	13.7	21.4	7.6	6.0	0.64
A. carinata	63	8.3–14.0 (10.7±1.4)	14.8–19.1 (16.9±1.1)	5.6–8.6 (6.7±0.6)	4.5–6.1 (5.2±0.4)	0.51–0.76 (0.63±0.08)

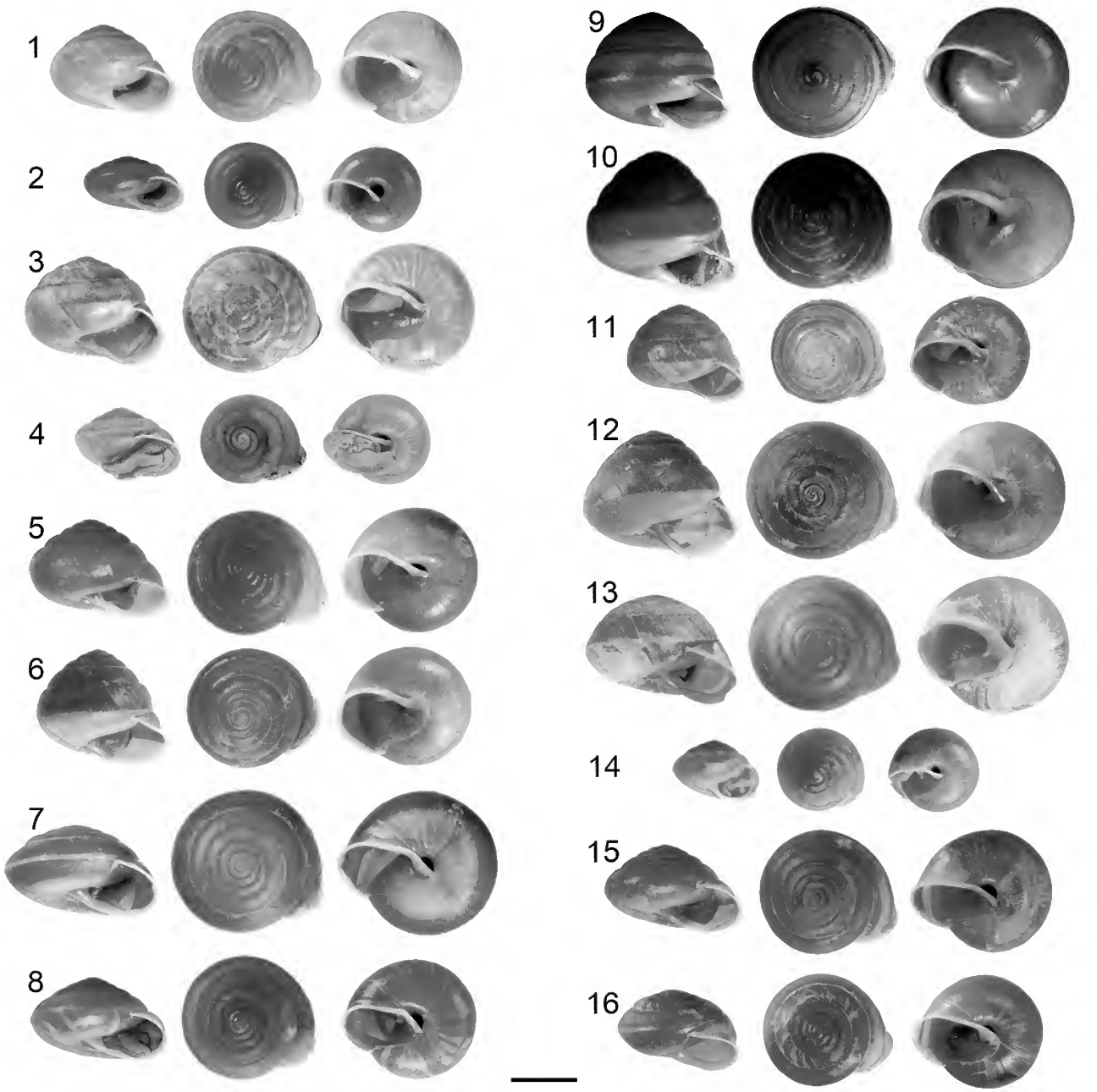

Plate 1. Shells of *Amplirhagada* species (from left to right viewed from side, above, and below). 1. Holotype of *A. atlantis* n.sp. WAM S34704. 2. Holotype of *A. carsoniana* n.sp. WAM S34707. 3. Holotype of *A. alicunda* n sp. WAM S34710. 4. Holotype of *A. moraniana* n.sp. WAM S34713. 5. Holotype of *A. davidsoniana* n.sp. WAM S34716. 6. Holotype of *A. vialae* n.sp. WAM S34719. 7. Holotype of *A. discoidea* n.sp. WAM S34722. 8. Holotype of *A. forrestiana* WAM S34725. 9. Paratype of *A. inusitata* n.sp. AM C.472929. 10. Holotype of *A. coffea* n.sp. WAM S34731. 11. Holotype of *A. gardneriana* n.sp. WAM S34734. 12. Holotype of *A. lindsayae* n.sp. WAM S34737. 13. Holotype of *A. bendraytoni* n.sp. WAM S34740. 14. Paratype of *A. angustocauda* n.sp. FMNH 220650. 15. Holotype of *A. epiphallica* n.sp. WAM S34745. 16. Shell of *A. carinata* Solem, 1981 WAM S34759. Scale bar = 10 mm. Notice that soft bodies protrude from some shells.

By contrast, the open woodland/rock habitats in the drier interior support only one *Amplirhagada* species each. In these regions, *Amplirhagada* species with similar ecological adaptations replace each other on local scales, which was attributed to the lack of available ecological niches (Cameron, 1992). On the other hand, it has been shown that areas of exposed, layered rock can act as litho-refugia for the persistence of rainforest lineages in areas where rainforest is currently, or was historically, marginal or absent (Couper & Hoskin, 2008). Rocks provide similar microclimatic conditions to rainforest, in being cool, moist, largely sheltered from fire and are stable and relatively buffered from short- and long-term climatic changes.

The species that are able to live in rocky landscapes outside of closed-canopy rainforests have generally larger distributions simply because the rocky ranges are spatially not as restricted as rainforest patches. These wider distributions in rather inhospitable landscapes provide

opportunities for differentiation along spatial gradients in concert with medium to long-termed climatic fluctuations, which may in the end lead to allopatric speciation (Cameron, 1992). Such processes are apparently responsible for the huge variation within *A. carinata* and other camaenid species from the drier interior of the Kimberley. Being apparently a more widespread phenomenon, they deserve the attention of future, more detailed studies.

ACKNOWLEDGMENTS. This work has been conducted as part of the Kimberley Island Survey of the Western Australian Department of Environment and Conservation (DEC), a project jointly funded by the Commonwealth of Australia and the Western Australian Government. I owe a debt of gratitude to Sue Lindsay, Martin Püschel and Marlene Vial for their help with SEM work, anatomical drawings and photography as well as to Lesley Gibson (Perth) for supporting my work over the last years. In addition, I wish to thank Jochen Gerber (FMNH), Shirley Slack-Smith and Corey Whisson (WAM) as well as Alison Miller and Janet Waterhouse (AM) for efficiently processing loans of samples.

References

Barker, G. M. 1999. *Naturalised terrestrial Stylommatophora (Mollusca: Gastropoda)*. Ed. Vol. 38, *Fauna of New Zealand*. Canterbury, New Zealand: Lincoln.

Cameron, R. A. D. 1992. Land snail faunas of the Napier and Oscar Ranges, Western Australia; diversity, distribution and speciation. *Biological Journal of the Linnean Society* 45: 271–286. doi:10.1111/j.1095-8312.1992.tb00644.x

Cameron, R. A. D., B. M. Pokryszko, and F.E. Wells. 2005. Alan Solem's work on the diversity of Australasian land snails: an unfinished project of global significance. *Records of the Western Australian Museum, Supplement* 68: 1–10.

Chiba, S. 1999. Character displacement, frequency-dependent selection, and divergence of shell colour in land snails *Mandarina* (Pulmonata). *Biological Journal of the Linnean Society* 66: 465–479.

Chiba, S., and A. Davison. 2008. Anatomical and molecular studies reveal several cryptic species of the endemic genus *Mandarina* (Pulmonata: Helicoidea) in the Ogasawara Islands. *Journal of Molluscan Studies* 74: 373–382. doi:10.1093/mollus/eyn029

Clark, S. A. 2009. A review of the land snail genus *Meridolum* (Gastropoda: Camaenidae) from central New South Wales, Australia. *Molluscan Research* 29: 61–120.

Couper, P. J., and C. J. Hoskin. 2008. Litho-refugia: the importance of rock landscapes for the long-term persistence of Australian rainforest fauna. *Australian Zoologist* 34: 554–560.

Iredale, T. 1933. Systematic notes on Australian land shells. *Records of the Australian Museum* 19(1): 37–59. doi:10.3853/j.0067-1975.19.1933.690

Iredale, T. 1938. A basic list of the land Mollusca of Australia - Part III. *Australian Zoologist* 9: 83–124.

Iredale, T. 1939. A review of the land Mollusca of Western Australia. *Journal of the Royal Society of Western Australia* 25: 1–88.

Johnson M. S., E. K. O'Brien and J. J. Fitzpatrick. 2010. Deep, hierarchical divergence of mitochondrial DNA in *Amplirhagada* land snails (Gastropoda: Camaenidae) from the Bonaparte Archipelago, Western Australia. *Biological Journal of the Linnean Society* 100: 141–153. doi:10.1111/j.1095-8312.2010.01407.x

Jordaens, K., L. Bruyndoncx, J. Van Goethem, and T. Backeljau. 2009. Morphological and anatomical differentiation of three land snails of the genus *Rhynchotrochus* (Gastropoda: Pulmonata: Camaenidae). *Journal of Molluscan Studies* 75: 1–8. doi:10.1093/mollus/eyn035

Kameda, Y. C., A. Kawakita, and M. Kato. 2007. Cryptic genetic divergence and associated morphological differentiation in the arboreal land snail *Satsuma* (*Luchuhadra*) *largillierti* (Camaenidae) endemic to the Ryukyu Archipelago, Japan. *Molecular Phylogenetics and Evolution* 45: 519–533. doi:10.1016/j.ympev.2007.03.021

Kameda, Y. C., A. Kawakita, and M. Kato. 2009. Reproductive character displacement in genital morphology in *Satsuma* land snails. *American Naturalist* 173: 689–697.

Köhler, F. 2010a. Uncovering local endemism in the Kimberley, Western Australia: Description of new species of the genus *Amplirhagada* Iredale, 1933 (Pulmonata, Camaenidae). *Records of the Australian Museum* 62(2): 217–284. doi:10.3853/j.0067-1975.62.2010.1554

Köhler, F. 2010b. Camaenid land snails in north-western Australia: A model case for the study of speciation and radiation. In *17th World Congress of Malacology*, edited by Panha, S., C. Sutcharit, and P. Tongkerd. Phuket: Chulalongkorn University, Bangkok.

Köhler, F. 2010c. Three new species and two new genera of land snails from the Bonaparte Archipelago in the Kimberley, Western Australia (Pulmonata, Camaenidae). *Molluscan Research* 30: 1–16.

Köhler, F. 2011. *Australocosmica*, a new genus of land snails from the Kimberley, Western Australia (Eupulmonata, Camaenidae). *Malacologia* 53: 199–216. doi:10.4002/040.053.0201

McKenzie, N. L., L. Fontanini, N. V. Lindus, and M. R. Williams. 1995. Biological inventory of Koolan Island, Western Australia, 2. Zoological notes. *Records of the Western Australian Museum* 17: 249–266.

Smith, E. A. 1894. On the land-shells of Western Australia. *Proceedings of the Malacological Society of London* 1: 84–99.

Solem, A. 1981. Camaenid land snails from Western and central Australia (Mollusca: Pulmonata: Camaenidae). II. Taxa from the Kimberley, *Amplirhagada* Iredale 1933. *Records of the Western Australian Museum* Suppl. 11: 147–320.

Solem, A. 1988. New camaenid land snails from the northeast Kimberley, Western Australia. *Journal of the Malacological Society of Australia* 9: 27–58.

Solem, A. 1991. Land snails of Kimberley rainforest patches and biogeography of all Kimberley landsnails. In *Kimberley rainforests of Australia*, ed. McKenzie, N.L., R.B. Johnston, and P.G. Kendrick. pp. 145–246. Canberra: Surrey Beatty & Sons and Department of Conservation and Land Management Western Australia.

Solem, A., and C. Christensen. 1984. Camaenid land snail reproductive cycle and growth patterns in semiarid area of north-western Australia. *Australian Journal of Zoology* 32: 471–491. doi:10.1071/ZO9840471

Solem, A., and N. L. McKenzie. 1991. The composition of land snail assemblages in Kimberley rainforests. In *Kimberley Rainforests of Australia*, ed. McKenzie, N.L., R.B. Johnston, and P.G. Kendrick. pp. 247–263. Canberra: Surrey Beatty & Sons and Department of Conservation and Land Management Western Australia.

Willan, R. C., F. Köhler, V. Kessner, and M. F. Braby. 2009. Description of four new species of limestone-associated *Torresitrachia* land snails (Mollusca: Pulmonata: Camaenidae) from the Katherine District of the Northern Territory, with comments on their conservation. *The Beagle. Records of the Museums and Art Galleries of the Northern Territory* 25: 85–98.

Records of the Australian Museum (2011) Vol. 63: 203–266. ISSN 0067-1975
doi:10.3853/j.0067-1975.63.2011.1586

Middle to Late Ordovician (Darriwilian-Sandbian) Conodonts from the Dawangou Section, Kalpin Area of the Tarim Basin, Northwestern China

YONG YI ZHEN[1]*, ZHIHAO WANG[2], YUANDONG ZHANG[2], STIG M. BERGSTRÖM[3], IAN G. PERCIVAL[4] AND JUNFENG CHENG[2]

[1] Australian Museum, 6 College Street, Sydney NSW 2010, Australia
yongyi.zhen@austmus.gov.au

[2] LPS, Nanjing Institute of Geology and Palaeontology,
Chinese Academy of Sciences, Nanjing 210008, China
zhwang@nigpas.ac.cn · ydzhang@nigpas.ac.cn · cjfcjf1983@163.com

[3] School of Earth Sciences, Division of Earth History,
The Ohio State University, Columbus, Ohio 43210, United States of America
stig@geology.ohio-state.edu

[4] Geological Survey of New South Wales, W B Clarke Geoscience Centre,
947–953 Londonderry Road, Londonderry NSW 2753, Australia
ian.percival@industry.nsw.gov.au

ABSTRACT. Forty-four conodont species are documented from the Dawangou section in the Tarim Basin, which spans the Darriwilian to Sandbian interval and is the global auxiliary stratotype for the base of the Upper Ordovician. Five conodont zones are recognized in this section, including the *Yangtzeplacognathus crassus*, *Histiodella holodentata* and *H. kristinae* zones in the upper part of the Dawangou Formation, the *Pygodus anserinus* Zone from the upper part of the Saergan Formation to the lower part of the Kanling Formation, and the *Baltoniodus alobatus* Zone in the upper part of the Kanling Formation. Presence of the *P. serra* Zone is based on occurrences of this species on shale bedding planes in the lower and middle Saergan Formation, but could not be confirmed in acid-leached samples studied from this interval. The Middle/Upper Ordovician boundary occurs within graptolitic black shale of the upper Saergan Formation. Although the boundary interval was intensively sampled, conodonts were very rare, probably due to stagnant or stratified basinal environments. This documentation of the conodont faunas and biostratigraphy of the Dawangou section is considered preliminary and more detailed conodont studies are required, but the remoteness of the site hinders the further extensive sample collection needed for this purpose.

ZHEN, Y. Y., Z. H. WANG, Y. D. ZHANG, S. M. BERGSTRÖM, I. G. PERCIVAL, AND J. F. CHEN. 2011. Middle to Late Ordovician (Darriwilian-Sandbian) conodonts from the Dawangou section, Kalpin area of the Tarim Basin, northwestern China. *Records of the Australian Museum* 63(3):203–266.

KEYWORDS: Conodonts, Ordovician, Darriwilian, Sandbian, biostratigraphy, Tarim, China

* author for correspondence

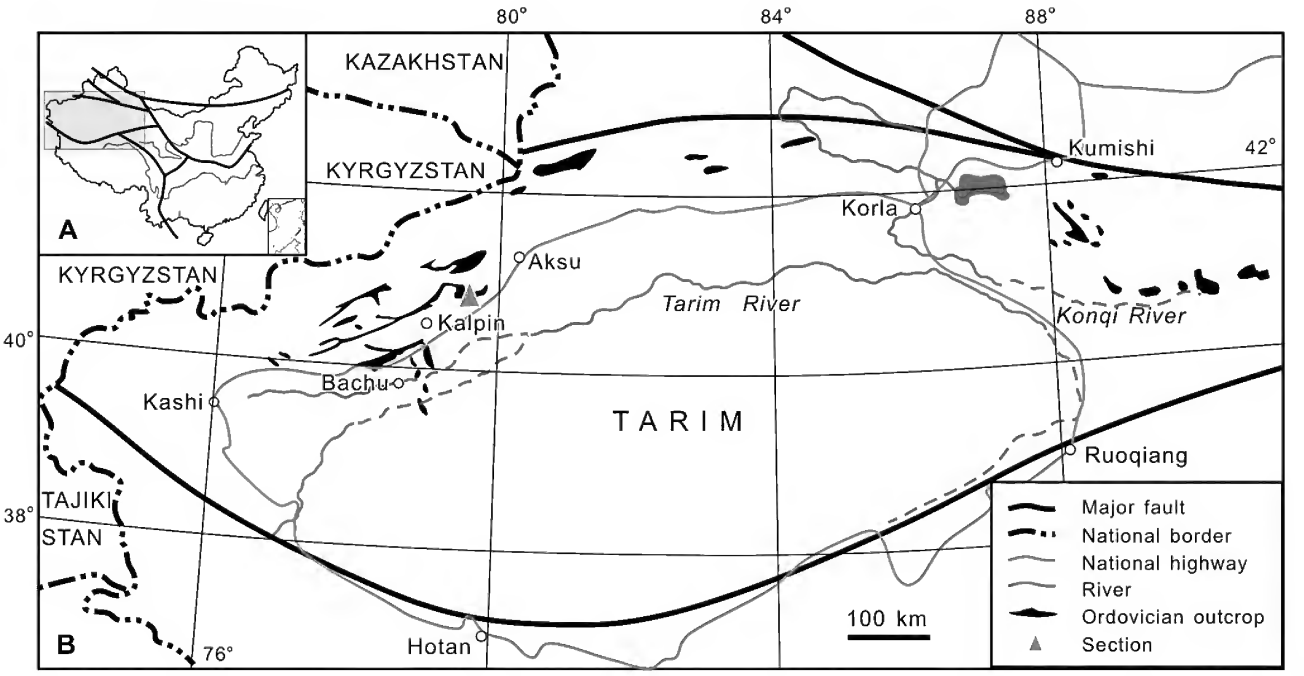

Figure 1. Locality map. ***A***, map of China showing the location of the Tarim Basin in northwestern China; ***B***, Map showing the outline of the Tarim Basin, outcrops of the Ordovician strata, and the location of the Dawangou section (red triangle), Kalpin, Xinjiang Autonomous Region, China.

Ordovician conodonts from the Dawangou section of the Tarim Basin were first reported by Zhou *et al.* (in Zhou & Chen, 1990, 1992, p. 66–79) who listed occurrences from the Dawangou Formation (Upper Qiulitag Group) to the Qilang Formation. They recognized eight conodont zones from the Dawangou Formation to the Kanling Formation (Zhou & Chen, 1992, fig. 3.2). Ordovician conodonts from this section were also reported briefly in several other publications (Gao, 1991; Bergström & Wang, 1998; Wang & Zhou, 1998; Bergström *et al.*, 1999; 2000; Wang, 2001), but no detailed systematic treatment of the conodont faunas from the Dawangou section has previously been published.

In the late 1990's, the Dawangou section was considered, along with the Fågelsång Section of southern Sweden and the Calera Section of USA, as potential GSSP candidates for the base of the Upper Ordovician (Bergström *et al.*, 1999). Through a world-wide assessment process organized by the Ordovician Subcommission of the International Commission on Stratigraphy, the Fågelsång Section was chosen as the global boundary stratotype (defined by the FAD of graptolite *Nemagraptus gracilis*), and the Dawangou section of the Tarim Basin was selected as an auxiliary stratotype (Bergström *et al.*, 2000). To fulfill its role as a standard reference assisting precise regional and international correlation of the Middle/Upper Ordovician boundary, detailed documentation of the conodont faunas from this level in the upper part of the Saergan Formation and lower part of the Kanling Formation is of great importance. This contribution, mainly based on collections made in 1987 by the Nanjing Institute of Geology and Palaeontology, supplemented by additional material collected on a field trip during 2008, addresses this imperative.

Regional geological and stratigraphic setting

Located in the central and southern part of the Xinjiang Autonomous Region of far northwestern China, the Tarim Basin (Fig. 1) is the largest inland sedimentary basin of China, covering an area of about 570,000 km^2 with the Tianshan Mountains bordering to the north and northwest, the Kunlun Mountains to the southwest and the Altun Mountains to the southeast. Much of the interior of the basin is covered by China's largest desert, the Taklamakan Desert. The Kunlun Mountains extending over 2,000 km represent a complex geological entity evolved through sedimentation, volcanism, deformations, subduction–accretions, collisions between Gondwana (or peri-Gondwanan terranes) and several Kunlun Terranes primarily during various orogenic episodes throughout the Palaeozoic and the Early Mesozoic, and the closure of the eastern parts of the Palaeo-Tethys Ocean (Yao & Hsü, 1994; Pan *et al.*, 1996). They are widely regarded as the "back bone" of today's China by joining the Pamir Mountains to the west and the Qilian Mountains to the east along the north edge of the Tibetan Plateau, with the Qinling Mountains further to the east. The Tianshan Mountains form an intracontinental mountain range stretching some 2,800 km eastward from Tashkent in Uzbekistan, that initially formed in the Late Palaeozoic following the collision and coalescence of the Tarim Plate and the Siberia-Kazakhstan plates (Windley *et al.*, 1990; Zhou & Chen, 1992). This region was reactivated in the Cenozoic during the Himalayan Orogeny (Molnar & Tapponnier, 1975), and remains active as a modern example of large-scale continental deformation resulting from the India-Eurasia convergence (Wang *et al.*, 2001).

The Tarim Basin is the remnant of an independent palaeo-plate with a long and complicated geological history, characterized by collisions, accretions and amalgamations, compressions, and intracontinental mountain building on its edges, which were mainly associated with the Indian Plate moving northward against Eurasia since the Mesozoic (Zhou & Chen, 1992; Zhou & Lin, 1995). It consists of basement comprising Proterozoic and Archaean metamorphic complexes, overlain by a very thick succession (locally exceeding 31 km) of shelf-marine-dominated Upper Proterozoic (Sinian) to Palaeozoic sediments, and predominantly non-marine deposits of the latest Palaeozoic (Late Permian) to Cenozoic (Wang *et al.*, 1992, table 2).

Owing to the development of a huge overburden of the Taklamakan Desert that came into existence in the late Miocene, in association with the formation and depression of the basin, and the accumulation of thick successions of foreland deposits fringing the uplifted mountain ranges, Palaeozoic and older rocks are mainly exposed along the basin margins. Outcrops of Late Proterozoic (Sinian) and Early Palaeozoic strata are largely restricted to two areas on the western and northeastern margins of the Tarim Basin, whereas the Late Palaeozoic rocks are more widely distributed (Zhou & Chen, 1992).

During the Ordovician, the Tarim Basin, as a peri-Gondwanan palaeo-plate, was situated at low to middle latitudes of the Southern Hemisphere (Zhao *et al.*, 1996; Huang *et al.*, 2000; Li & Powell, 2001), and received carbonate-dominated marine shelf deposits with a total thickness up to 6000 m (He *et al.*, 2007) that are now only exposed in western Tarim (Kalpin-Bachu areas) and in northeastern Tarim (Queerqueke-Uligezhitag areas; see Fig. 1). However, subsurface data revealed by petroleum boreholes and seismic stratigraphy indicate that Ordovician rocks are much more widely distributed underneath the extensive Cenozoic desert cover (Zhou & Chen, 1992; Zhao *et al.*, 2000).

Analysis of the Ordovician lithofacies and biofacies (Zhou & Chen, 1992; He *et al.*, 2007; Wang *et al.*, 2007) indicated the existence of an intracratonic basin in the northeast part of Tarim Basin that extended further westward, crossing the entire northern Tarim plate on an east-west trend. It is characterized by turbidite successions with radiolarian siliciclastics (bathyal to abyssal), graptolitic black shale (shallow and stagnant basin), and rhythmically alternating sandstones, siltstones, shales and minor calcarenites (shallow trough; more than 2500 m in thickness in the Queerqueke area) (Zhong & Hao, 1990; Wang *et al.*, 2008). The basinal facies is flanked on its southern side by a narrow and continuous zone of slope facies (Nileid trilobite biofacies). As the transitional zone between the basin (or trough) and the platform, the slope facies is mainly composed of argillaceous-laminated or nodular calcilutite, calcarenite and calcirudite intercalated with shale. The Mid-Tianshan Islands of Ordovician time, situated along the northern margin of the Tarim plate, and the uplifts on the southeastern margin of the basin, were subjected to erosion, and might be the major source regions of the terrigenous material, while the carbonate platform (occupying a vast area in the central-western part of the Tarim plate) received shallow marine carbonate deposits during the Ordovician. Spatial and temporal distribution patterns reflecting the expansion and contraction of these two contrasting sedimentary systems (or megafacies) throughout the Ordovician, namely the deeper siliciclastic basin or trough regime and the shallow carbonate platform regime, were largely controlled by sea level changes and regional transgressive and regressive events.

Ordovician rocks are well exposed along the Dawangou, a narrow but deep erosional stream-cut gorge on the western slope of the Tianshan Mountains, about 15 km northwest of the Yingan Village in Kalpin County, northwestern Tarim Basin (Fig. 1). Zhou & Chen (1992, p. 66–79, fig. 3–2) provided a detailed stratigraphic log of the section and faunal lists. Part of the material in the current study (39 samples with prefix Nj, see Fig. 2, Table 1) formed the basis of the conodont data presented by Zhou & Chen (1992). The Ordovician System at the Dawangou gorge conformably overlies the Late Cambrian Awatag Group and is itself disconformably overlain by the Early Silurian Kalpintag Formation. The Ordovician section consists of 26 Beds that are grouped into six lithostratigraphic units with a total thickness of 748.44 m. The area was located in a transitional facies zone, with the lower part of the succession (Early Ordovician Qiulitag Group) deposited in a shallow water carbonate platform setting, the Saergan Formation (late Darriwilian to early Sandbian age) and the Yingan Formation (Katian) accumulated in a basinal setting, whereas the Middle Ordovician Dawangou Formation and the Late Ordovician Kanling and Qilang formations were primarily deposited in a slope setting.

The stratotype of the Dawangou Formation proposed by Zhou *et al.* (1991; also see Zhao & Zhang, 1991, p. 66) is exposed on the north side of Yingan Mountain located to the northwest of the Yingan village (not far from the Dawangou section). It consists of 15.1 m of greyish medium- to thinly-bedded nodular biocalcilutites, with glauconitic algal-bound biocalcilutites in the middle part and irregular cherty bands in the basal part. In the Dawangou section, the Dawangou Formation is equivalent to Bed 10 of Zhou & Chen (1990, 1992; see Wang & Zhou, 1998, text-fig. 1; Zhou *et al.*, 1998, text-fig. 2), and consists of 22 m of greyish medium- to thinly-bedded nodular biocalcilutites and biocalcarenites with glauconite and cherty masses and bands. It forms a lithologically distinctive unit that can be easily differentiated from the underlying mainly thick-bedded algal-laminated limestones of the upper part of the Upper Qiulitag Group, and from black shales of the overlying Saergan Formation. The Dawangou Formation, which is extensively exposed along the northwestern margin of the Tarim Basin, was deposited in a generally calm, upper slope environment with a depositional depth generally not much greater than 70 m (Zhou *et al.*, 1998). A significant transgressive event occurred in the region during the late Middle Ordovician (Darriwilian) and earliest Late Ordovician, indicated by a conformable transition from the open, shallow water carbonate platform setting of the Upper Qiulitag Group, through the slope setting of the Dawangou Formation, to the basinal setting of the Saergan Formation.

The name Saergan Formation is derived from the Saergan Series that was initially proposed for all the Ordovician rocks above the Qiulitag Group. It was restricted to only about 14 m of black calcareous graptolitic shale with limestone lenses distributed in the Kalpin area (Chen *et al.*, 1995). As one of the most important Ordovician source rocks for petroleum in the Tarim Basin, this condensed black shale unit with abundant pyrite and organic material (Cai *et al.*, 2009) was likely deposited in an euxinic bottom

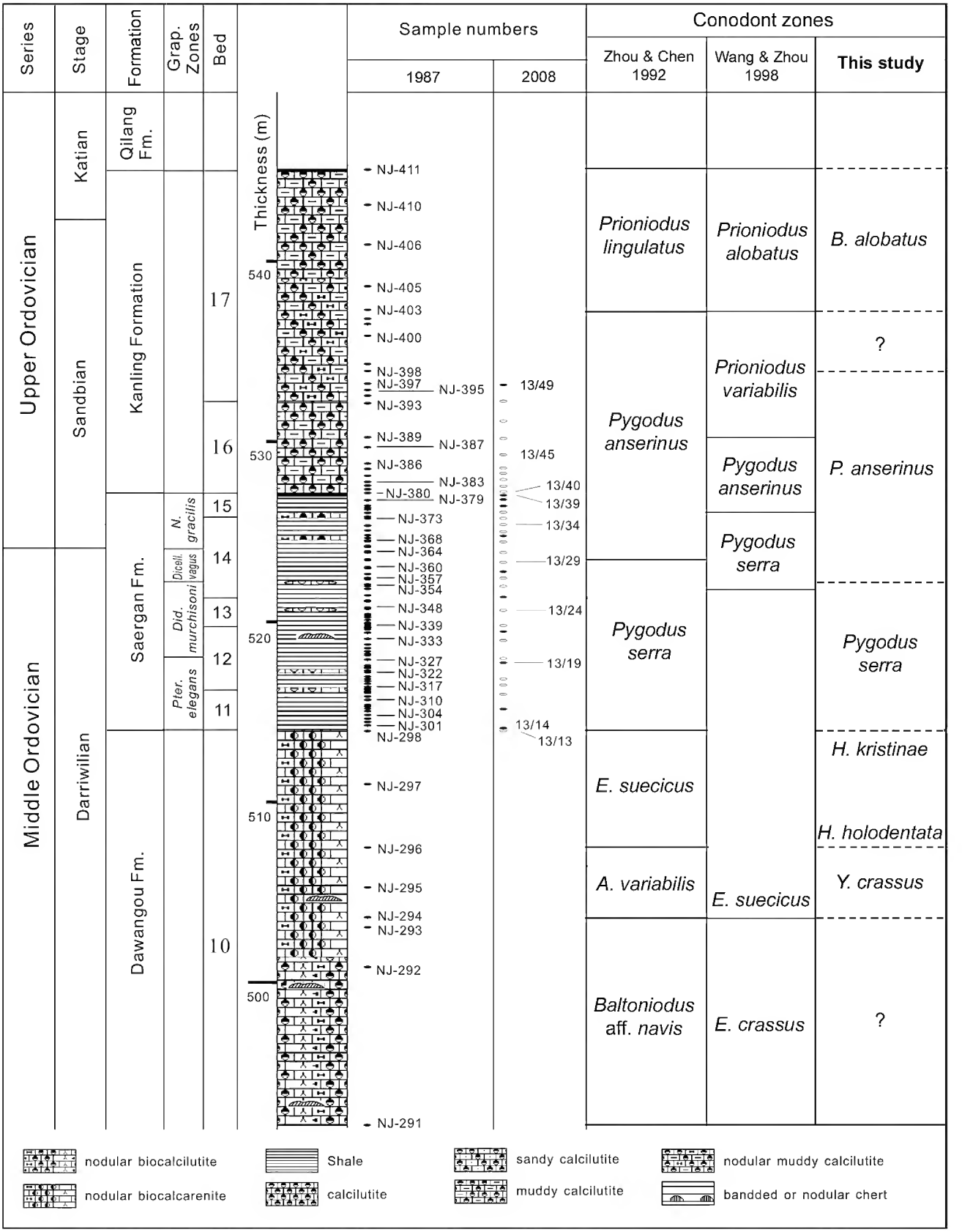

Figure 2. Stratigraphy and conodont sampling positions of the Dawangou section (Dawangou, Saergan and Kanling formations), Kalpin, Xinjiang Autonomous Region, China.

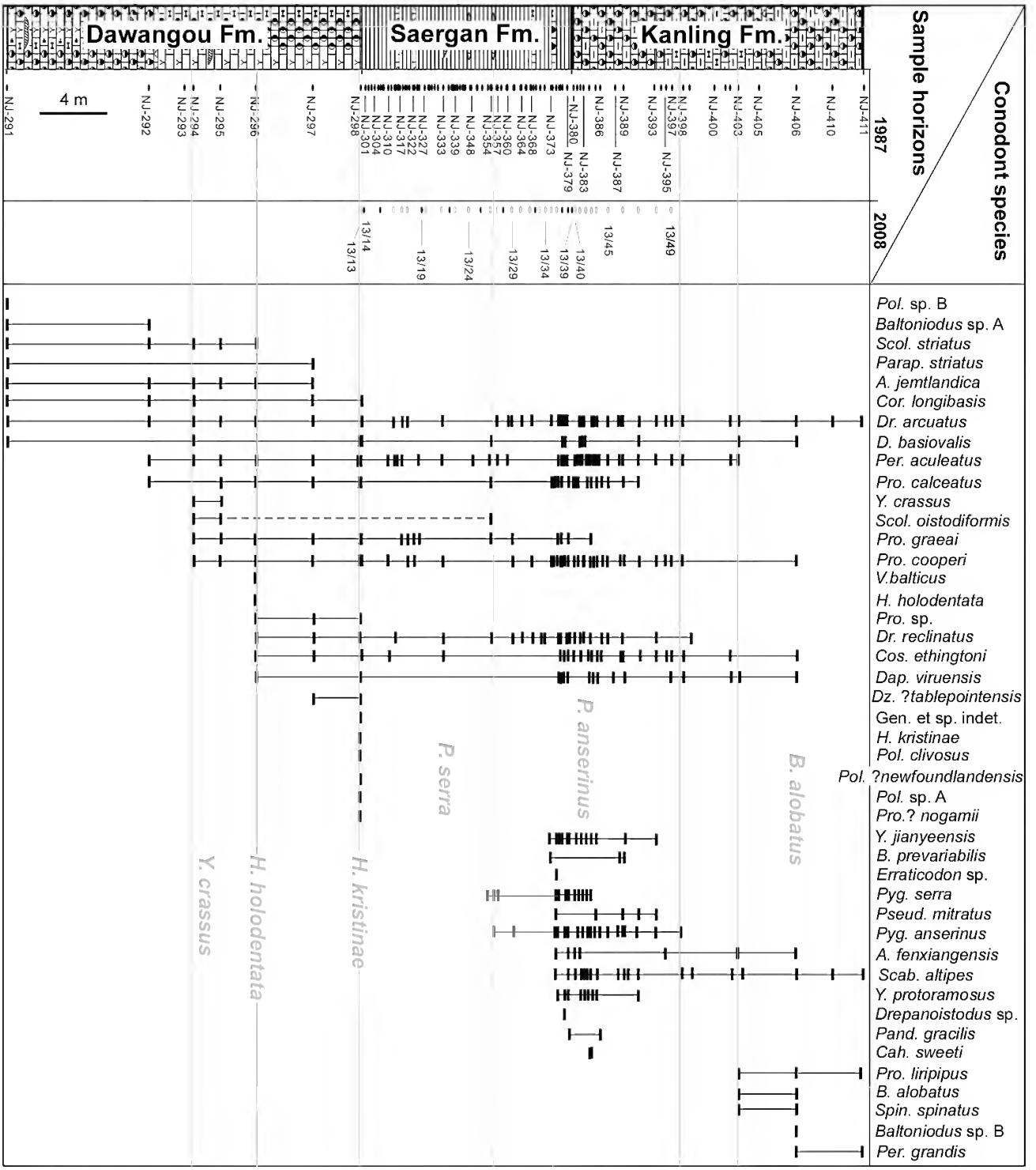

Figure 3. Conodont occurrences recorded in this study from the Dawangou section (Dawangou, Saergan and Kanling formations), Kalpin, Xinjiang Autonomous Region, China.

water environment of restricted circulation and stagnant or stratified conditions. The overlying Kanling Formation (Sandbian), consisting of 17–36 m of purplish red and greyish green to grey thin-to medium-bedded calcilutites, is widely exposed in the Kalpin area, with its stratotype located at Kanling, near Yingan Village, where it is also 18 m in thickness as in the Dawangou section (Fig. 2).

Systematic studies of the other fossil groups from the Dawangou section include the trilobites from the Dawangou Formation (Zhou *et al.*, 1998), chitinozoans from the Saergan Formation (Hennissen *et al.*, 2010), and acritarchs (Li *et al.*, 2006). A detailed monographic documentation of the trilobite faunas from this section is currently in preparation (Z. Y. Zhou pers. comm.).

Conodont biostratigraphy and regional correlation

Zhou & Chen (1990, 1992) recognized six informal conodont zones from the Dawangou Formation to Kanling Formation of the Dawangou section at Kalpin in the Tarim Basin (Fig. 2; also see Zhou & Chen, 1992, p. 80, fig. 3–2), which were further revised by Wang & Zhou (1998, fig. 1). Bergström *et al.* (1999) recognized two conodont zones (the *P. serra* and *P. anserinus* zones) in the Saergan Formation. In this study the conodont biostratigraphic framework proposed by previous authors was re-assessed, based on material collected from two field trips (Tables 1–2). Five conodont zones can now be recognized, although due to data limitation, their upper and lower boundaries are yet to be precisely defined (Fig. 2). As an auxiliary stratotype for the base of the Upper Ordovician, more detailed conodont studies are required, but the remoteness of the site hinders collection of the numerous samples needed for this purpose.

***Baltoniodus alobatus* Zone**: In the upper part of the Kanling Formation (from samples Nj 403 to Nj 411), Zhou & Chen (1992) recognized the *Prioniodus lingulatus* Zone with some 11 conodont species (authors' original identifications) recovered from this interval including *Dapsilodus mutatus, Prioniodus lingulatus, Protopanderodus liripipus, P. rectus, Periodon grandis, Scabbardella altipes, Spinodus spinatus*, *Drepanodus* sp., *Eoplacognathus* sp., *Panderodus* sp., and *Prioniodus* sp. Wang & Zhou (1998, text-fig. 1) referred to this interval as the *Prioniodus alobatus* zone and recorded the occurrence of 22 conodont species (authors' original identifications) from the Dawangou section, including *Ansella nevadensis*, *Cornuodus longibasis*, *Dapsilodus mutatus, Drepanoistodus venustus, D.* sp., *Eoplacognathus jianyeensis*, *E.* sp. B, gen. et sp. indet., *Paltodus? jemtlandicus*, *Periodon grandis, Protopanderodus cooperi, P. liripipus, P. rectus*, *P. robustus*, *P. varicostatus*, *Prioniodus alobatus*, *P. variabilis*, *P.* sp., *Scabbardella altipes, Spinodus spinatus*, and *Walliserodus ethingtoni*. Our re-examination of conodont specimens recovered from five samples through this interval has confirmed the occurrence of the following 13 species (Fig. 3): *Ansella fenxiangensis, Baltoniodus alobatus, B.* sp. B, *Costiconus ethingtoni, Dapsilodus viruensis, Drepanodus arcuatus, Drepanoistodus basiovalis, Periodon aculeatus, P. grandis, Protopanderodus cooperi, P. liripipus, Scabbardella altipes,* and *Spinodus spinatus*.

Prioniodus lingulatus An, 1987 is considered herein as a junior synonym of *Baltoniodus alobatus* (Bergström, 1971) (see further discussion under Systematic Palaeontology section). This morphologically distinctive species with a wide platform-like posterior process has been widely reported in Europe (Bergström, 1971; Dzik, 1994), North America (Kennedy *et al.*, 1979; Nowlan, 1981; Leslie, 2000), Precordilleran Argentina (Ortega *et al.*, 2008), Tarim (Zhong, 1990; Wang & Zhou, 1998; Zhao *et al.*, 2000; Xiong *et al.*, 2006; this study), South China (An, 1981; Zeng *et al.*, 1983; An, 1987; Chen *et al.*, 2011) and southeast Asia (Agematsu *et al.*, 2006, 2008a). Based on a collection of more than 100,000 identified conodont specimens from some 40 stratigraphic sections of the Swedish Middle-Upper Ordovician, Bergström (1971) established the conodont biostratigraphic zonal succession (including five zones and ten subzones) for Baltoscandia, and recognized *B. alobatus* as the index species for the upper Subzone of the *Amorphognathus tvaerensis* Zone of the Upper Ordovician. The *B. alobatus* Subzone, with its base marked by the first appearance (FAD) of *B. alobatus* and with top defined by the first appearance (FAD) of *Amorphognathus superbus* (Rhodes), was originally correlated with the upper part of the British graptolite *Diplograptus multidens* zone (Bergström, 1971, p. 101), equivalent to the *C. bicornis* Zone of late Sandbian age (Webby *et al.*, 2004; Bergström *et al.*, 2009). The upper boundary of the *B. alobatus* Subzone (*A. tvaerensis* Zone) is generally correlated with the basal part of the *Belodina confluens* Zone of the North American Midcontinent succession (Webby *et al.*, 2004; Bergström *et al.*, 2010, fig. 3).

The *B. alobatus* Subzone spanned the interval when enormous explosive volcanic eruptions took place in the Iapetus Ocean with volcanic ash layers (K-bentonites) widespread over much of eastern and central North America (Millbrig) and in Baltoscandia (Kinnekulle), representing the largest volcanic ash falls in the Earth's Phanerozoic history (Bergström *et al.*, 2004). In Baltoscandia, the Kinnekulle K-bentonite Bed forms a prominent stratigraphical marker defining the base of the Keila Stage (Hints & Nõlvak, 1999). Biostratigraphic studies suggest a correlation of the North American Millbrig K-bentonite with the upper part of the *Phragmodus undatus* conodont Zone (upper *C. bicornis* graptolite Zone). The Baltoscandian Kinnekulle K-bentonite Bed is in the upper part of the *D. foliaceus* (formerly *multidens*) graptolite Zone (Huff *et al.*, 1992; Bergström *et al.*, 2004), which was correlated with the *B. alobatus* conodont Subzone (Webby *et al.*, 2004).

In the Tarim Basin, *B. alobatus* was reported from the Queerqueke Formation of the northeastern part of the Tarim Basin (Zhong, 1990), the Qiaerbake Formation in Bachu (Xiong *et al.*, 2006), the Tumuxiuk Formation in subsurface core (Zhao *et al.*, 2000), and from the upper part of the Kanling Formation near Kalpin (Zhou & Chen, 1992; Wang & Zhou, 1998; Zhao *et al.*, 2000; this study). In South China, An (1987) proposed the *P. lingulatus* Zone based on the conodont assemblage from the upper part of the Datianba Formation of Guizhou and Jiangsu, with the holotype of *P. lingulatus* recovered from the top Datianba Formation in the Ganxi Section of Yanhe County, Guizhou (An, 1987, p. 35, pl. 25, fig. 17) in association with *Belodella* sp., *Drepanoistodus* sp., *Panderodus gracilis, Prioniodus* sp. and *Scabbardella similaris* (An's original identifications). In the lower part of the Datianba Formation the *Eoplacognathus jianyeensis* Zone includes the nominate species associated with *Complexodus pugionifer*, *Panderodus gracilis, Periodon aculeatus*, *Prioniodus alobatus*, *P. variabilis*, *P.* sp., and *Protopanderodus* sp. An (1987, table 3) correlated the *P. lingulatus* Zone with the *B. alobatus* Subzone of the North American Midcontinent succession. As *B. lingulatus* is now considered a junior synonym of *B. alobatus* (see discussion under Systematic Palaeontology Section), the *B. alobatus* Subzone should then be correlated with the entire 3.4 m thick Datianba Formation in the Ganxi section in Guizhou. However, in the Dawangou section of the Tarim Basin, *Y. jianyeensis* occurs in a stratigraphically slightly lower interval (in the top part of the Saergan Formation and the lower part of the Kanling Formation) in association with *P. anserinus* and others, an assemblage similar to that documented from the top part of the Datianba Formation in Hunan, South China (Zhang, 1998c).

Protopanderodus liripipus is a widely distributed species with a relatively long stratigraphic range from the upper *A. tvaerensis* Zone to *A. ordovicicus* Zone (Sweet, 1988), reported from North America (Kennedy *et al.*, 1979; McCracken, 1989; Leslie, 2000; Pyle & Barnes, 2001), Europe (Bergström, 1990, 2007; Dzik, 1994), Australia (Burrett *et al.*, 1983; Trotter & Webby, 1994; Zhen *et al.*, 1999), North China (Wang & Lou, 1984; An & Zheng, 1990), Tarim Basin (Gao, 1991; Zhao *et al.*, 2000; Wang, 2001; Wang & Qi, 2001), South China (An *et al.*, 1981; An *et al.*, 1985; An, 1987; Ding *et al.* in Wang, 1993) and southeast Asia (Agematsu *et al.*, 2007, 2008a). *Periodon grandis* also had a wide distribution globally, with first appearance in the *undatus* Zone and disappearing in the upper part of the *A. superbus* Zone (Webers, 1966), a level slightly younger than the *velicuspis* Zone in the North American Midcontinent succession.

***Pygodus anserinus* Zone**: This zone is represented by the whole range of *P. anserinus* from the upper part of the Saergan Formation with the lowest level represented by the specimens from acid residue (from sample 96B50-6) to the lower part of the Kanling Formation (sample Nj 398). It is associated with two other biostratigraphically important species, *Y. jianyeensis* (from sample Nj 374 to Nj 389) and *P. serra* (from sample Nj 375 to AFT-X-K14/43; specimens observed on shale bedding surface at the levels equivalent to samples Nj359, Nj356, and Nj353, see Bergström *et al.*, 1999; see also Tables 1–2).

Zhou & Chen (1992, p. 74) and Bergström *et al.* (1999) reported the lowest occurrence of *P. anserinus* on the bedding surface of shale at the same stratigraphic level as sample Nj 362, and suggested this represented the lower boundary of this zone (see Figs 2, 3). However, as this bedding plane specimen of *P. anserinus* has been lost, Wang & Zhou (1998) considered sample Nj 375 as the base of the *P. anserinus* Zone. As the most diverse assemblage in the Dawangou section, this sample yields 21 species including *Ansella fenxiangensis, Baltoniodus prevariabilis, Cahabagnathus sweeti, Costiconus ethingtoni, Dapsilodus viruensis, Drepanodus arcuatus, D. reclinatus, D.* sp., *Drepanoistodus basiovalis, Erraticodon* sp., *Panderodus gracilis, Periodon aculeatus, Protopanderodus calceatus, P. cooperi, P. graeai, Pseudooneotodus mitratus, Pygodus anserinus, P. serra, Scabbardella altipes, Yangtzeplacognathus jianyeensis* and *Y. protoramosus*. *Cahabagnathus sweeti* and *Baltoniodus prevariabilis* are two other distinctive species of the *P. anserinus* Zone in Sweden (Bergström, 1971). Sample 96B50-6 was collected by Bergström in 1996 from a limestone lens exposed 4.6 m below the top of the Saergan Formation (about the same stratigraphical level as sample Nj355, see Figs 2–3). *Pygodus serra* and an early form of *P. anserinus* (with only a couple of nodes in a weakly developed fourth row directly comparable with Lindström's holotype from Sweden) were recovered from this sample. Such early forms of *P. anserinus* are found right at the base of the *P. anserinus* Zone in Sweden. Therefore, it would be appropriate to move the base of the *P. anserinus* Zone to the level 4.6 m below the top of the Saergan Formation.

Yangtzeplacognathus jianyeensis is a highly distinctive platform species with a stratigraphic range confined to the *P. anserinus* Zone, and has not been reported outside of China (see Systematic Palaeontology Section) where its species definition and stratigraphic range have been subject to debate among Chinese authors. An *et al.* (1981) established the *P. miaopoensis* (= *Y. jianyeensis*) Zone in the lower part of the Miaopo Formation in Hubei. Chen & Zhang (1984b) proposed the *P. anserinus–Y. jianyeensis* Zone for the conodont assemblage recovered from the middle part of the Datianba Formation in Jiangsu Province, and considered it equivalent to the *P. anserinus* Zone in Sweden. This view was accepted by Zhang (1998c) in defining the base of the *P. anserinus–Y. jianyeensis* Zone by the first appearance of both *P. anserinus* and *Y. jianyeensis*. However, An *et al.* (1985, p. 31) defined the *Y. jianyeensis* Zone for the conodont assemblage of the Miaopo Formation in Hubei, South China and correlated it with the upper part of the *P. serra* Zone to lower part of the *A. tvaerensis* Zone of the Swedish succession. Later, An (1987, tables 2–3) revised the *Y. jianyeensis* Zone with its base marked by the disappearance of *P. anserinus* and the top by the first appearance of his *P. lingulatus*, and correlated the *Y. jianyeensis* Zone with the lower and middle parts of the *A. tvaerensis* Zone of the Swedish succession (= *variabilis* + *gerdae* subzones). Co-occurrence of *Y. jianyeensis* and *P. anserinus* in the upper part of the Saergan Formation and the lower part of the Kaling Formation supports the definition given by Zhang (1998c).

Pygodus anserinus is a morphologically distinctive species with a stratigraphic range spanning the *P. anserinus* Zone and the lower *A. tvaerensis* Zone (Sweet, 1988, p. 192). In Swedish sections, the *P. anserinus* Zone has a thickness of 10 to 15 metres with the base defined by the first appearance of *P. anserinus*, and the top by the first appearance of *A. tvaerensis*, and was correlated with the upper part of the *H. teretiusculus* and the lower part of the *N. gracilis* graptolite zones (Bergström, 1971, pp. 97–98; Bergström *et al.*, 2000, fig. 6). Bergström (1971, p. 98) subdivided the *P. anserinus* Zone into two informal subzones, subsequently naming these as the *A. inaequalis* Subzone and *A. kielcensis* Subzone (Bergström, 1983, fig. 1). The primary marker to define the Middle/Upper Ordovician Boundary is the first appearance datum (FAD) of the graptolite *N. gracilis*, which is within the conodont *P. anserinus* Zone. Efforts to subdivide the *P. anserinus* Zone in the Dawangou section have been largely hindered by the fact that the boundary level is condensed (similar to the GSSP stratotype section at Fågelsång in southern Sweden), and the graptolitic shale contains only several intercalated (temporally discontinuous) carbonate bands or nodules, from which only a low diversity conodont fauna dominated by long ranging species can be extracted. It is anticipated that detailed sampling in the Dawangou Formation of the Yangjikan Section (also in Kalpin) will have high potential for resolving this biostratigraphic problem, because in this section, the Middle/Upper Ordovician boundary level lies within the carbonates of the Dawangou Formation, which are age equivalent to the black shale of the Saergan Formation in the Dawangou section.

Wang & Zhou (1998, fig. 1) established the *B. variabilis* Zone in the middle part of the Kanling Formation based on the occurrence of *Baltoniodus variabilis* (Bergström, 1962) in the middle and upper part of the Kanling Formation, but both figured specimens (Wang & Zhou, 1998, pl. 1, figs 4, 6) were from sample Nj 406 and cannot be confidently assigned to *B. variabilis*. Moreover, no specimens are currently recognized from sample Nj 389 as belonging to *B. variabilis*, although Wang & Zhou (1998, fig. 1) reported its occurrence in this sample. Therefore, more detailed collecting is required

to confirm the occurrence of the *B. variabilis* Zone in this section (Fig. 2).

***Pygodus serra* Zone:** Zhou & Chen (1992, fig. 3–2) considered the lower and middle part of the Saergan Formation (beneath Nj 362, where the occurrence of *P. anserinus* was reported on a bedding surface) as belonging to the *P. serra* zone. Bergström *et al.* (1999, p. 71) also indicated the occurrence of *P. serra* at the level of 8.87 m above the base of the Saergan Formation, based on samples collected in 1996 (that unfortunately were not able to be relocated for the current study). Our extensive sampling of every calcareous bed in this interval has produced a low diversity assemblage including *Costiconus ethingtoni, Dapsilodus viruensis, Drepanodus arcuatus, D. reclinatus, Drepanoistodus basiovalis, Periodon aculeatus, Protopanderodus calceatus, P. cooperi, P. graeai,* and *Scolopodus? oistodiformis*, which are all long ranging species of little use in defining this zone (Tables 1–2, Figs 2–3). However, occurrence of *Histiodella kristinae* at the top of the Dawangou Formation suggests that this interval (middle and lower part of the Saergan Formation) may correlate with the *P. serra* Zone and possibly part of the *E. suecicus* Zone. Occurrence of *Pygodus anitae* on shale bedding surfaces in the lower Saergan Formation (Goldman & Leslie, personal comm. to Bergström) also supports this correlation.

The graptolite zonation for the lower and middle part of the Saergan Formation has been recently redefined to include three zones in ascending order, the *Pterograptus elegans*, the *Didymograptus murchisoni*, and the *Dicellograptus vagus* zones (Chen *et al.*, 2008; Chen *et al.*, in press; Fig. 2). The *Dicellograptus vagus* Zone, with its base placed at the FAD (first appearance datum) of the eponymous species, replaces the poorly-defined *Hustedograptus teretiusculus* Zone, which was conventionally recognized by the disappearance of *Didymograptus murchisoni* together with the common occurrence of *H. teretiusculus*. However, the FAD of *Dicellograptus vagus* is slightly higher than the LAD (last appearance datum) of *Didymograptus murchisoni* in the Dawangou section, leaving a short interval below the boundary lacking stratigraphically diagnostic species.

***Histiodella kristinae* zone:** This level is represented by a diverse assemblage recovered from the top of the Dawangou Formation, and includes 18 species, *Cornuodus longibasis, Costiconus ethingtoni, Dapsilodus viruensis, Drepanodus arcuatus, D. reclinatus, Drepanoistodus basiovalis, Dzikodus tablepointensis,* gen. et sp. indet., *Histiodella kristinae, Periodon aculeatus, Polonodus clivosus, P. newfoundlandensis, P.* sp. A, *Protopanderodus calceatus, P. cooperi, P. graeai, P.* sp. and *P.? nogamii* (Fig. 3). *H. kristinae* Stouge, 1984 is the most distinctive species of this assemblage, along with several pectiniform species including *Dzikodus tablepointensis, Polonodus clivosus, P. newfoundlandensis,* and *P.* sp. A. Based on the inferred phylogeny of *Histiodella* species recovered from the Table Head Formation of western Newfoundland, Stouge (1984, table 3) proposed two conodont zones, namely the *H. tableheadensis* (= *H. holodentata*) Zone in the lower Table Head Formation and the *H. kristinae* Zone in the upper Table Head Formation, correlating the latter with the *E. suecicus* Zone of the Baltoscandian succession. *Histiodella kristinae* is widely distributed in North America (Barnes & Poplawski, 1973; Landing, 1976; Stouge, 1984; Nowlan & Thurlow, 1984), Europe (Dzik, 1994; Rasmussen, 2001; Löfgren, 2004), Argentine Precordillera (Heredia *et al.*, 2005; Heredia, pers. com., 2010), South China (Ni, 1981; Ding *et al.* in Wang, 1993; Zhang, 1998c), North China (Wang & Lou, 1984; An & Zheng, 1990), and the Tarim Basin (Wang & Zhou, 1998; Zhao *et al.*, 2000; Du *et al.*, 2005; this study). Based on a large collection of *Histiodella* species from the Yangjikan section and other localities of the Tarim Basin, Du *et al.* (2005) recognized four conodont zones in ascending order: *H. sinuosa* Zone, *H. holodentata* Zone, *H. kristinae* Zone, and *H. bellburnensis* Zone, and correlated the *H. kristinae* Zone with the uppermost *A. variabilis* Zone and the lower part of the *E. suecicus* Zone. However, Bergström *et al.* (2009) suggested that the top of the *H. kristinae* Zone could approximate the base of the *P. serra* Zone, indicating a correlation of the *H. kristinae* Zone with the *E. suecicus* Zone of the Baltoscandian succession.

***Histiodella holodentata* zone**: This assemblage recovered from sample Nj 296 is characterized by the occurrence of *H. holodentata* Ethington & Clark, 1982 along with 15 other species including *Ansella jemtlandica, Cornuodus longibasis, Costiconus ethingtoni, Dapsilodus viruensis, Drepanodus arcuatus, D. reclinatus, Drepanoistodus basiovalis, Parapanderodus striatus, Periodon aculeatus, Protopanderodus calceatus, P. cooperi, P. graeai, P.* sp., *Scolopodus striatus*, and *Venoistodus balticus* (Fig. 3). *Histiodella holodentata* is a widely distributed and biostratigraphically useful species reported from North America (Ethington & Clark, 1982; Nowlan & Thurlow, 1984; Stouge, 1984; Johnston & Barnes, 2000; Bauer, 2010), Kazakhstan (Zhylkaidarov, 1998), Argentine Precordillera (Albanesi & Ortega, 2003; Heredia, pers. com., 2010), Australia and New Zealand (Zhen *et al.*, 2004a, 2009b; Percival & Zhen, 2007), North Europe (Rasmussen, 2001), South China (An *et al.*, 1985; An, 1987; Zhang, 1998c), North China (An *et al.*, 1983; An & Zheng, 1990), Tarim Basin (Gao, 1991; Wang & Zhou, 1998; Zhao *et al.*, 2000; Du *et al.*, 2005), and southeast Asia (Agematsu *et al.*, 2006, 2008b).

Ethington & Clark (1982) proposed two informal conodont zones with *H. sinuosa* and *H. holodentata* as the index species based on their occurrences in the Ibex area of Utah, which were later recognized as the two formal conodont zones within the Whiterockian of the North American Midcontinent succession (Sweet, 1988, chart 1, p. 190). However, correlations of the *H. holodentata* Zone, with its base defined by the first appearance of *H. holodentata*, with the Baltoscandian succession were debated among conodont biostratigraphers. For instance, Stouge (1984, table 3) correlated this zone with the upper part of the *Lenodus variabilis* Zone, whereas Harris *et al.* (1995) suggested a correlation with the upper *L. variabilis* Zone to the lower *E. suecicus* Zone. Rasmussen (2001) correlated the base of the *H. holodentata* Zone with the basal *L. variabilis* Zone, and Webby *et al.* (in Webby *et al.*, 2004, fig. 2.2) considered the *H. holodentata* Zone as the time equivalence of the *L. variabilis* Zone. Based on study of the Tarim material, Du *et al.* (2005, table 11) preferred a correlation with the middle part of the *L. variabilis* Zone.

Bergström (1971) subdivided the *Pygodus serra* conodont Zone into five subzones with *E. suecicus* as

the zonal index species for the lowermost subzone, and defined its base by the first appearance (FAD) of *P. serra* and the top by the disappearance of *E. suecicus* and the appearance of *Y. foliaceus*. Lindström (1971) established the *Amorphognathus variabilis* Zone for the conodont fauna from the Kundan Stage. Subsequent studies of conodonts from the middle Darriwilian of Baltoscandia and South China have supported recognition of these as two formal conodont zones. Furthermore, significant taxonomic revisions of both *E. suecicus* and *L. variabilis* have resulted in the recognition of two more conodont zones (the *E. pseudoplanus* Zone and the *Y. crassus* Zone) between the revised *E. suecicus* and *L. variabilis* zones (Viira, 1974; An *et al.*, 1985; Zhang, 1998c, 1998d; Löfgren & Zhang, 2003; Löfgren, 2003, 2004). The *E. suecicus* Zone was then subdivided into the *Pygodus anitae* Subzone and *P. lunnensis* Subzone and correlated to the Aserian Stage, and the *L. variabilis* Zone was restricted to an interval more or less corresponding to the middle-upper part of the Hunderum Substage of the Kundan (Zhang, 1998a; Löfgren & Zhang, 2003).

Löfgren, (2004, fig. 1) correlated both the *H. kristinae* Zone and *H. holodentata* Zone of the North American Midcontinent succession to the *E. pseudoplanus* Zone of the Baltoscandian succession. Considering that in the Dawangou section, *H. holodentata* occurs above the range of *Y. crassus*, it is best to correlate the occurrence of *H. holodentata* in the Dawangou Formation to only part of the *E. pseudoplanus* Zone. However, due to environmental changes resulting from a significant transgressive event in the late Darriwilian, occurrences of these zonal index species as recorded in the Dawangou section (Figs 2–3) clearly do not represent their full stratigraphic ranges, and their boundaries are still poorly defined (Fig. 2).

***Yangtzeplacognathus crassus* Zone:** *Y. crassus* was recovered from two samples (Nj294 and Nj 295) in the middle part of the Dawangou Formation associated with 10 other species including *Ansella jemtlandica, Cornuodus longibasis, Drepanodus arcuatus, Drepanoistodus basiovalis, Periodon aculeatus, Protopanderodus calceatus, P. cooperi, P. graeai, Scolopodus? oistodiformis*, and *S. striatus* (Table 1, Fig. 3). The distinctive pectiniform species, *Y. crassus*, has a wide distribution in the lower Darriwilian in South China (An, 1981, 1987; An *et al.*, 1985; Ni & Li, 1987; Chen & Zhang, 1989; Wang, 1993; Zhang, 1997, 1998c; Wang & Bergström, 1999a, 1999b), Tarim (Wang *et al.*, 1996; Bergström & Wang, 1998; Wang & Zhou, 1998), Baltoscandia (Viira, 1974; Stouge & Bagnoli, 1990; Wang, 1997; Viira *et al.*, 2001; Löfgren, 2003; Löfgren & Zhang, 2003) and Poland (Podhalańska, 1979; Dzik, 1994). Prior to its formal recognition by Chen & Zhang (in Wang, 1993, pl. 37, figs 12–17) based on type material recovered from the Guniutan Formation near Tangshan of Nanjing, it was reported from the Guniutan Formation in Jiangsu (An, 1981, 1987), Hubei (Ni & Li, 1987; An *et al.*, 1985), and Anhui (Chen & Zhang, 1989), and also from basal Hulo Formation of the Huangnitang Section of Changshan, west Zhejiang (Wang & Bergström, 1995; Zhang *et al.*, 2007) and the Dawangou Formation of the Dawangou section near Kalpin, Tarim Basin (Wang *et al.*, 1996), but assigned to different species names (see synonymy lists of Zhang, 1997 and Löfgren & Zhang, 2003). Detailed taxonomic studies of this species (Zhang, 1997, 1998c; Löfgren & Zhang, 2003) have made it one of the best documented conodont species in the lower Darriwilian, and biostratigraphically useful for regional correlations (Bergström & Wang, 1998).

The *Y. crassus* Zone was defined as a range zone marked by the occurrence of *Y. crassus* (Zhang, 1998c, table 2) in the Guniutan Formation of Hubei (Fenxiang Section—the type section of the Guniutan Formation) and Hunan (Cili and Maocaopu sections) provinces, South China, and correlated with the lower part of the Valaste Substage of the Baltic successions (Löfgren, 2003). Bergström & Wang (1998, fig. 1) suggested a correlation with the middle part of the *A. ellesae* graptolite Zone (Pacific Province) or *D. artus* graptolite Zone (Atlantic Province). Wang & Bergström (1995) and Zhang *et al.* (2007) reported the occurrence of *Y. crassus* in the lower part of the Hulo Formation at the Huangnitang Section, Changshan, west Zhejiang, and equated the *Y. crassus* Zone with the mid-upper part of the *A. ellesae* graptolite Zone. In the Maocaopu Section of Hunan Province, *H. holodentata* first appears in the upper part of the *Y. crassus* Zone (Zhang, 1998c, fig. 22), suggesting that the lowest part of the *H. holodentata* Zone overlaps with the uppermost part of the *Y. crassus* Zone (if the latter is retained as a range zone).

Material and methods

This study is based on a large collection of nearly twenty thousand identifiable, well-preserved (CAI 2-3) conodont specimens recovered from 63 samples collected during two separate field trips, in 1987 and in 2008 (Tables 1–2). Thirty-nine conodont samples collected in 1987 were processed with acetic acid (10%) and picked by one of the authors (ZHW) at the Nanjing Institute of Geology and Palaeontology, Chinese Academy of Sciences. He subsequently briefly reported identifications of the fauna in several publications, particularly important amongst which is a detailed listing of conodont species identified from each sample in a biostratigraphic description of the Dawangou section (in Zhou & Chen, 1992, pp. 71–78). Three of the authors (YYZ, YDZ, and JFC) participated in the 2008 field work, during which 24 conodont samples (about 5kg each) were collected from the top of the Dawangou Formation to the lower part of the Kanling Formation with particular focus on the carbonate or calcareous lenses within the black shale of the Saergan Formation. These 24 samples were each split into two halves, one of which was processed at the Nanjing Institute of Geology and Palaeontology and picked to completion by lab contractors. The other half of each of the 24 samples was acid leached (10% acetic acid) and the residues were separated and concentrated by using sodium polytungstate at the Londonderry laboratory of the Geological Survey of New South Wales; these residues were sorted and picked by the senior author at the Australian Museum. Interestingly, those samples processed in Australia had a much higher yield in comparison with the other halves processed in Nanjing, where they were not subjected to heavy-liquid separation techniques. One of the most productive samples from the top of the Dawangou Formation yielded nearly ten thousand specimens (Table 2).

All photographic illustrations shown in Figs 4 to 32 are SEM photomicrographs captured digitally (numbers with the prefix IY are the file names of the digital images).

Table 1. Distribution of conodont species recovered from 39 samples collected from the Dawangou, Saergan and Kanling formations of the Dawangou section, near Kalpin, Tarim Basin in 1987 field work.

	Nj 411	Nj 410	Nj 406	Nj 403	Nj 402	Nj 399	Nj 398	Nj 395	Nj 389	Nj 388	Nj 386	Nj 385	Nj 384	Nj 383	Nj 382	Nj 379	Nj 378	Nj 377	Nj 376	Nj 375	Nj 368	Nj 364	Nj 362	Nj 360	Nj 357	Nj 354	Nj 348	Nj 325	Nj 323	Nj 316	Nj 314	Nj 310	Nj 298	Nj 297	Nj 296	Nj 295	Nj 294	Nj 292	Nj 291	total
Ansella jemtlandica																																		3	4	36	65	3	3	114
Ansella fenxiangensis			2	6				2								2				3																				15
Baltoniodus alobatus			21	15																																				36
Baltoniodus prevariabilis									1	3																														4
Baltoniodus sp. A																																						2	1	3
Baltoniodus sp. B			2																																				2
Cahabagnathus sweeti													1																											1
Cornuodus longibasis																																		6			1	1	1	9
Costiconus ethingtoni			27		1		1	4	6	6	1	5			7	16	27	9	12												1	4	15	4					146
Dapsilodus viruensis			3				1	5	4	3	1	6	5			20	8	1	4	4														1						66
Drepanodus arcuatus	9	1	68	5	3		3	6	8	8		21		4	9	51	32	4	15	42	2	2		4	2								23	91	12	21	8	5	6	465
Drepanodus reclinatus						7							9			3	4		3	4		2				2				2		4	8	1					49
Drepanoistodus basiovalis	11			3												20	14									1						4				1		3	57
Drepanoistodus sp.																	1																						1
Dzikodus ?tablepointensis																																	29						29
Histiodella holodentata																																			3				3
Panderodus gracilis											1					3																							4
Parapanderodus striatus																																		5				2	7
Periodon aculeatus				2	8		3		15	19	2	21	6	12	18	49	189	13	43	13				1	2		6	5		2	10	3	62	1437	4	153	1255	1		3354
Periodon grandis	7		101																																				108
Polonodus sp. B																																						2	2
Protopanderodus calceatus															1	3			3	3													1	6	5	1		4		27
Protopanderodus cooperi			6				3	4	7	16	2	13	11	2	5	64	98	12	35	6	2		1						1		1	31	18	3	18	19			378
Protopanderodus graeai													4			10	3	3	7	4			3			2?		2	4			25	79	27	22	80			273
Protopanderodus liripipus	7		13	6																																			26
Protopanderodus sp.																																		3	1					4
Pseudooneotodus mitratus																				1																				1
Pygodus anserinus							5		1	93	29	43	177	75	57	59	5		11	2																				557
Pygodus serra															2?	57	4		12	255																				328
P. serra+anserinus (Pb and S)																357	215	128	145																					845
Scabbardella altipes	20	1	15	21	10	23	5		17	7	3		29			1																								152
Scolopodus striatus																																			2?	10	18	6	3	37
Scolopodus? oistodiform																																				1	4			5
Spinodus spinatus			6	1																																				7
Venoistodus balticus																																			2					2
Yangtzeplacognathus crassus																																				14	49			63
Yangtzeplacognathus jianyeensis									1							11	5?		1	9																				22
Yangtzeplacognathus protoramosus																6	3			1																				10
Total	43	2	275	59	22	30	21	21	60	155	39	109	242	93	97	732	603	170	291	347	4	4	4	5	4	3	6	7	5	2	12	5	154	1700	67	276	1500	22	21	7212

Table 2. Distribution of conodont species recovered from 24 samples collected from the Dawangou, Saergan and Kanling formations of the Dawangou section, near Kalpin, Tarim Basin in 2008 field work.

total	AFT-X-K13/49	AFT-X-K13/48	AFT-X-K13/47	AFT-X-K13/46	AFT-X-K13/45	AFT-X-K13/44	AFT-X-K13/43	AFT-X-K13/42	AFT-X-K13/41	AFT-X-K13/40	AFT-X-K13/36	AFT-X-K13/35	AFT-X-K13/34	AFT-X-K13/33	AFT-X-K13/31	AFT-X-K13/30	AFT-X-K13/29	AFT-X-K13/27	AFT-X-K13/26	AFT-X-K13/21	AFT-X-K13/18	AFT-X-K13/17	AFT-X-K13/16	AFT-X-K13/13	total
Ansella fenxiangensis									5	10															15
Baltoniodus prevariabilis												5													5
Cahabagnathus sweeti							7																		7
Cornuodus longibasis																								6	6
Costiconus ethingtoni	10	6	18	8		28	35	8	8	2										1				204	328
Dapsilodus viruensis	1			2																				5	8
Drepanodus arcuatus	2	6	13	53	6	25	81	12	16	48	12					2		4		4	1	1	4	103	393
Drepanodus reclinatus		1		6	2	3		6	5	3			1	2	4		2		2	4				26	67
Drepanoistodus basiovalis			5				17	13	12															6	53
Dzikodus ?tablepointensis																								2	2
Erraticodon sp.											5														5
Gen. et sp. indet.																								1	1
Histiodella kristinae																								30	30
Periodon aculeatus		38	50	91	3	142	78	75	85	2								2	9	63		3	11	6400	7052
Polonodus clivosus																								2	2
Polonodus newfoundlandensis																								36	36
Polonodus sp. A																								1	1
Protopanderodus calceatus			3	19	4	1	9	1	8	16	10	1							1					147	220
Protopanderodus cooperi	3	5	30	83	8	145	135	30	62	23	3	1								10	1			159	698
Protopanderodus graeai																					1	1		974	976
Protopanderodus? *nogamii*																								37	37
Protopanderodus sp.																								1	1
Pseudooneotodus mitratus		3	1	2		2																			8
Pygodus anserinus		47	125	640	9	293	107	9	24	5															1259
Pygodus serra							212	45	117	137															511
P. serra + *P. anserinus* (Pb+S)							327	87	162	97															673
Scabbardella altipes			13	2		48		8	5	2	2														80
Scolopodus? oistodiform																			1						1
Yangtzeplacognathus jianyeensis		6				97	24	6	6	14		1													154
Yangtzeplacognathus protoramosus			3			2	4	4	1																14
Total	16	112	261	906	32	786	1036	304	516	359	32	8	1	2	4	2	2	6	13	82	3	5	15	8140	12643

Figured specimens bearing the prefix NIGP are deposited in the collections of the Nanjing Institute of Geology and Palaeontology, Chinese Academy of Sciences in Nanjing, China. Fourteen topotype specimens of *Protopanderodus varicostatus* and *P. cooperi* from the Pratt Ferry Formation of Alabama are illustrated in Fig. 20 and Fig. 22 for comparison, and these (bearing the prefix OSU 53802 to OSU 53815 inclusive) are housed at the Orton Geological Museum, Ohio State University, Columbus, Ohio, USA.

Synonymy lists of the species documented in this contribution have emphasis on the Chinese literature in order to provide complete data for the distribution of the species in China. Fifteen species, including *Ansella fenxiangensis* (An, Du, Cao, Chen & Lee, 1981), *Baltoniodus* sp. A, *Baltoniodus* sp. B, *Cornuodus longibasis* (Lindström, 1955a), *Drepanoistodus* sp., *Erraticodon* sp., *Panderodus gracilis* (Branson & Mehl, 1933), *Periodon grandis* (Ethington, 1959), *Polonodus* sp. A, *Polonodus* sp. B, *Protopanderodus*? *nogamii* (Lee, 1975), *Protopanderodus* sp., *Spinodus spinatus* (Hadding, 1913), *Venoistodus balticus* Löfgren, 2006, and gen. et sp. indet. (a single quadriramate ramiform element), are documented by illustration only, as they are either represented by insufficient material to warrant an appropriate taxonomic treatment, or have lesser biostratigraphic significance. Conventional conodont terminology and notation as defined in the Treatise Part W (Clark *et al.* 1981) is employed in this contribution, except for the M elements (makellate), whose orientation, morphology and terminology was introduced by Nicoll (1990, 1992).

Systematic Palaeontology

Class Conodonta Pander, 1856

Ansella Fåhraeus & Hunter, 1985

Type species. *Belodella jemtlandica* Löfgren, 1978.

Ansella jemtlandica (Löfgren, 1978)

Fig. 4A–O

Roundya n. nov. Sweet & Bergström, 1962: 1244–1245, text-fig. 5.

Belodella jemtlandica Löfgren, 1978: 46, pl. 15, figs 1–8, fig. 24A–D; An *et al.*, 1983: 77, pl. 25, figs 8–12; Zhao *et al.*, 1984: 210, pl. 90, figs 1, 4, 11, 14; An & Zheng, 1990: pl. 10, figs 4–7.

Belodella? *jemtlandica* (Löfgren).–Ding *et al.* in Wang, 1993: 165, pl. 30, figs 9, 11, 14, 19.

Ansella jemtlandica (Löfgren).–Fåhraeus & Hunter, 1985: 1173, pl. 1, figs 1–5, 9, pl. 2, fig. 12, Fig. 1 (*cum syn.*); Ding, 1987: pl. 5, figs 11–12; Ni & Li, 1987: 396, pl. 60, figs 21–22, 24–25; An & Zheng, 1990: pl. 10, figs 4–7; Gao, 1991: 128, pl. 11, figs 3–6; Pohler, 1994: pl. 1, figs 15–16; Lehnert, 1995: 70, pl. 9, figs 1, 2, 5; pl. 10, fig. 8, pl. 12, fig. 1, pl. 13, fig. 1; Albanesi in Albanesi *et al.*, 1998:160–161, pl. 1, figs 18–23, text-fig. 27; Zhang, 1998c: 50, pl. 1, figs 5–9; Zhao *et al.*, 2000: 188, pl. 35, figs 13, 14; Rasmussen, 2001: 51, pl. 1, figs 4–9; Wang & Qi, 2001: pl. 1, figs 10, 12; Pyle & Barnes, 2002: 57, pl. 19, figs 1, 2; Pyle & Barnes, 2003: fig. 11.1–11.4; Zhen & Percival, 2004a: 84–86, fig. 5A–Q (*cum syn.*); Zhen & Percival, 2004b: fig. 4A–G; Zhen *et al.*, 2009b: 32, fig. 2A–I; Bauer, 2010: pl. 1, figs 1–2, 4–5.

Material. 114 specimens from six samples of the Dawangou Formation (see Table 1).

Remarks. Several species of *Ansella* introduced in the Chinese literature, including *A. fenxiangensis* (An, Du, Gao, Chen & Li, 1981) = *Belodella guniutanensis* Ni *in* Ni & Li, 1987, *A. longicuspica* Zhang, 1998c, *A. rigida* (An *in* An *et al.*, 1983) and *A. baotaensis* Ni *in* Ni & Li, 1987, show close morphological similarities to *A. jemtlandica*. They were differentiated from the latter mainly based on the depth of the basal cavities in the P elements (An *et al.*, 1983, p. 78; Zhang, 1998c, text-fig. 25). Zhang (1998c) suggested a possible evolutionary lineage from oldest *A. longicuspica* with a shallower basal cavity (about half of the P element length) to intermediate *A. jemtlandica* (basal cavity about three-fourths of the P element length), and then to the most derived *Ansella fenxiangensis* (see Fig. 5A–C) with a deep basal cavity (four-fifths to five-sixths of total P element length). Although in theory, recognition of these species with their shorter stratigraphical ranges might be more useful than a broad concept of the long ranging *A. jemtlandica*, in practice it may be difficult to correctly assign the material to a species based solely on the depth of the basal cavity in the P elements.

Baltoniodus Lindström, 1971

Type species. *Prioniodus navis* Lindström, 1955a.

Baltoniodus alobatus (Bergström, 1971)

Figs 5L, Q, 8M–N

Prioniodus alobatus Bergström, 1971: 145, pl. 2, figs 4–5; Zeng *et al.*, 1983: pl. 12, fig. 33; An, 1987: 169–170, pl. 25, figs 7–9 (*cum syn.*); Zhong, 1990: 150, pl. 17, figs 1–2; Wang & Zhou, 1998: pl. 1, figs 11–13.

Prioniodus lingulatus An, 1987: 170–171, pl. 25, figs 10–17 (*cum syn.*).

Baltoniodus alobatus (Bergström).–Dzik, 1994: 83, fig. 14d; Leslie, 2000: 1127, fig. 7.2–7.13 (*cum syn.*); Zhao *et al.*, 2000: 189, pl. 34, figs 11–13, pl. 39, figs 16–20, 23 (*cum syn.*); Xiong *et al.*, 2006: 368, pl. 1, figs 2–3; Agematsu *et al.*, 2008a: 967, fig. 11.1–11.21; Ortega *et al.*, 2008: fig. 6.1.

Prioniodus cf. *P. alobatus* Bergström.–An, 1981: pl. 4, fig. 9a–b.

Baltoniodus sp. cf. *B. variabilis* (Bergström).–Agematsu *et al.*, 2007: 33–35, fig. 10.1–10.17.

Material. Thirty-six specimens from two samples of the Kanling Formation (see Table 1).

Remarks. Bergström (1971, pl. 2, figs 4–5) described and illustrated only the amorphognathiform element of *Prioniodus alobatus* represented by the holotype, indicating that the other five or six types of elements comprising the apparatus were closely similar to those of *B. variabilis* (Bergström, 1962). According to the original description, the most distinctive feature of its amorphognathiform (Pa herein) element was "a wide, but low, platform-like posterior process" (Bergström, 1971, p. 145). More recently, Leslie (2000) fully described and illustrated this species as consisting of a seximembrate apparatus including geniculate M, alate ramiform Sa, bipennate Sc, quadriramate Sd, pastinate Pa and Pb elements.

Figure 4. *Ansella jemtlandica* (Löfgren, 1978). A, B, M element; ***A***, NIGP 152839, anterior view (IY147-004); ***B***, NIGP 152840, posterior view (IY147-005). C–F, Sa element; ***C–D***, NIGP 152841, C, lateral view (IY146-040), D, anterior view (IY146-039); ***E–F***, NIGP 152842, E, basal view (IY147-006), F, lateral view (IY147-008). ***G–H***, Sb element, NIGP 152843, G, antero-basal view (IY147-010), H, inner lateral view (IY147-011). I–K, Sc element; ***I***, NIGP 152844, outer lateral view (IY147-012); ***J***, NIGP 152845, inner lateral view (IY147-013); ***K***, NIGP 152846, outer lateral view (IY146-043). L–M, Pa element; ***L***, NIGP 152847, outer lateral view (IY147-003); ***M***, NIGP 152848, inner lateral view (IY148-001). N–O, Pb element; ***N***, NIGP 152849, inner lateral view (IY147-002); ***O***, NIGP 152850, outer lateral view (IY147-001). All from sample Nj294; scale bars 100 μm.

The illustrated Pa element (Fig. 8N) from the upper part of the Kanling Formation is a broken specimen with only the posterior process preserved. Similar specimens with a wide platform and a centrally positioned row of denticles were also reported as *B. alobatus* from subsurface core samples of the Yingmai-10 well (Zhao *et al.*, 2000, pl. 39, fig. 18), from the Tumuxieke Formation of Bachu (Wang & Zhou, 1998, pl. 1, fig. 11), from the Qiaerbake Formation in Bachu (Xiong *et al.*, 2006, pl. 1, figs 2–3), and from the same sample (Nj406) of the Kanling Formation of the Dawangou section (Wang & Zhou, 1998, pl. 1, fig. 13). The illustrated Pb element (Fig. 5Q) is identical with the specimen previously illustrated as *B. alobatus* by Wang & Zhou (1998, pl. 1, fig. 12) from a slightly higher level (sample Nj406) in the Kanling Formation of the same section, and also corresponds exactly to the ambalodiform (Pb herein) element of *Prioniodus lingulatus* (An, 1987, pl. 25, fig. 12) from the Datianba Formation of Ganxi, Guizhou Province.

The illustrated Pa element (Fig. 8N) is also identical with the holotype of *B. lingulatus* An, 1987, which was defined as consisting of a seximembrate apparatus including amorphognathiform, ambalodiform, cordylodiform,

tetraprioniodiform, trichonodelliform and oistodiform elements. An (1987) suggested that *B. lingulatus* was closely similar to *B. alobatus*, but the posterior process in the amorphognathiform element of the latter had a more convex upper surface, which was undulose in lateral view. One illustrated specimen of the Pa element of *P. lingulatus* (An, 1987, pl. 25, fig. 15) from the Datianba Formation of Jiangsu is identical with the specimen illustrated by Leslie (2000, fig. 7.3) as the Pa element of *B. alobatus* in having a distinctive inner-lateral lobate expansion on the posterior process. Leslie (2000, p. 1127) indicated that this feature was seen in many of the specimens referred to as the Pa element of *B. alobatus*. Based on his description, one of the most distinctive features of *B. alobatus* is that its S elements have small closely spaced denticles intercalated with several much larger denticles, particularly on the posterior process of the Sc element (Fig. 5L; see also Leslie, 2000, fig. 7.9). This feature is also developed in the type specimens of *Prioniodus lingulatus* An, 1987 (pl. 25, fig. 13), indicating that the latter, if not conspecific with *B. alobatus*, is certainly closely related to it. However, some specimens from a stratigraphically slightly lower level (Nj388, Fig. 5H–I) that are assigned to *B. prevariabilis* also show a similar denticle pattern on the posterior process.

Specimens representing the Pa element of *B. alobatus* recorded from the Tarim Basin (Fig. 8N; also see Wang & Zhou, 1998; Xiong *et al.*, 2006) are more comparable with the holotype of *P. lingulatus* in having a wider posterior platform than the holotype of *B. alobatus*. Considering that the width and the shape of the posterior platform varies significantly amongst the type material of *B. lingulatus*, that species is regarded herein as a junior synonym of *B. alobatus* as indicated by Zhao *et al.* (2000, p. 189). The Sc element of *B. alobatus* (Fig. 5L) differs from the corresponding element of the stratigraphically slightly older species *B. prevariabilis* (Fig. 5O–P) in having smaller denticles intercalated with a number of larger denticles on the posterior process, and the same feature is also observed in the Sd element (Fig. 8M). The specimens of *B. alobatus* assigned by Agematsu *et al.* (2007, fig. 10) to *B.* sp. cf. *B. variabilis* are similar to the Tarim form. Their M element has an unusually long inner lateral process compared to the Swedish specimens (although those are usually broken).

The Pa element representing *Baltoniodus* sp. B (Fig. 8I–L) that co-occurs with *B. alobatus* in sample Nj406 has a platform-like anterior process (rather than posterior process), which is narrower with the row of denticles near the outer lateral margin (Fig. 8J–K). Furthermore, the anterior process is straight, extending downward in lateral view (Fig. 8I) in comparison to the posterior process of *B. alobatus*. It shows some resemblance to *B. variabilis*, but the Pa element of the latter has a "triangular lateral expansion of the inner side of the posterior process" (Bergström, 1971, p. 148, pl.2, fig. 2).

Baltoniodus prevariabilis (Fåhraeus, 1966)

Fig. 5H–K, M–P, ?R

Prioniodus prevariabilis Fåhraeus, 1966: 29, pl. 4, fig. 5a–b; Bergström, 1971: 146, pl. 2, fig. 1.

Prioniodus (Baltoniodus) prevariabilis prevariabilis Fåhraeus.–Löfgren, 1978: 87, pl. 12, figs 37–43 (*cum syn.*).

Baltoniodus prevariabilis Fåhraeus.–Lindström, 1971: 56 *partim*; An & Ding, 1982: pl. 5, figs 1–3, 7; An *et al.*, 1985: pl. 7, figs 15, 18–19, pl. 16, figs 1–13; An, 1987: 127–128, pl. 20, figs 21–25, pl. 21, figs 1–7; Chen & Zhang, 1989: pl. 1, figs 10–14; Gao, 1991: 127, pl. 9, figs 1–3, 6; Ding *et al.* in Wang, 1993: 163, pl. 26, figs 1–17; Dzik, 1994: 82, pl. 18, figs 17–22, text-fig. 14b; Bednarczyk, 1998: pl. 1, figs 9–10, 12–13; Zhang, 1998c: 54, pl. 3, figs 1–8; Zhao, *et al.*, 2000: 189, pl. 34, fig. 15, pl. 39, figs 1–6; Viira, 2011: fig. 6D–F, H, K, M–N, Q–S.

Material. Nine specimens from three samples (see Tables 1–2).

Remarks. *Prioniodus prevariabilis* was erected as a form species with the only figured specimen (holotype) exhibiting straight, denticulated posterior and outer lateral processes and a denticulated, inner laterally deflected anterior process (Fåhraeus, 1966, pl. 4, fig. 5a–b). It represents the ambalodiform element in the multielement species apparatus that was first proposed by Löfgren (1978) to include the oistodiform (M), trichonodelliform (Sa herein), belodiform (Sb herein), tetraprioniodiform (Sd herein), amorphognathiform (Pa herein) and ambalodiform (Pb herein) elements. The cordylodiform (Sc herein) was also included in the species apparatus to form a septimembrate apparatus (An & Ding, 1982; An *et al.*, 1985; Zhang, 1998c). Specimens referable to *B. prevariabilis* are rare in the Dawangou samples, and only Sa, Sc, Pa and Pb elements of this species are recovered from the Kanling Formation and the upper part of the Saergan Formation. The Sa element is alate with a long denticulate posterior process and a denticulate, downward-extending lateral process on each side (Fig. 5H–I); the Sc element is bipennate with a long denticulate posterior process and a long, adenticulate anticusp-like anterior process (Fig. 5O–P); the Pa element has low and long denticulate posterior and anterior processes (Fig. 5J–K), and the Pb element displays a long denticulate, inner laterally curved, and strongly downward-extending anterior process (Fig. 5M–N). These specimens are comparable with those documented from Jämtland of northern Sweden (Löfgren, 1978) and from the Guniutan Formation of South China (Zhang, 1998c).

Several specimens recovered from the upper part of the Dawangou Formation are assigned to *Baltoniodus* sp. A (Fig. 5D–G). It is characterized by the Pa element (Fig. 5G) having the straight anterior and outer lateral processes adjoining at approximately right angles, and a Pb element (Fig. 5E) with an inner laterally deflected anterior process and a posteriorly curved outer lateral process, which are remarkably different from that of *B. prevariabilis*. The denticulate lateral processes of this species are also higher and more laterally extended (Fig. 5D) compared with *B. prevariabilis*.

Cahabagnathus Bergström, 1983

Petalognathus Drygant, 1974b (a junior homonym of *Petalognathus* Duméril & Bibron, 1854, a reptile, see Clark *et al.*, 1981, p. W129).

Type species. *Polyplacognathus sweeti* Bergström, 1971.

Figure 5. A–C, *Ansella fenxiangensis* (An, Du, Cao, Chen & Lee, 1981). ***A***, M element, NIGP 152851, Nj403, posterior view (IY161-019); ***B***, Sb element, NIGP 152852, Nj403, outer lateral view (IY161-020); ***C***, P element, NIGP 152853, Nj403, outer lateral view (IY161-018). D–G, *Baltoniodus* sp. A. ***D***, Sa element, NIGP 152854, Nj292, posterior view (IY158-019); ***E–F***, Pb element, NIGP 152855, Nj292, E, upper view (IY158-016), F, inner lateral view (IY158-015); ***G***, Pa element, NIGP 152856, Nj294, upper view (IY158-030). H–K, M–P, *Baltoniodus prevariabilis* (Fåhraeus, 1966). ***H–I***, Sa element, NIGP 152857, Nj388, H, lateral view (IY162-002), I, upper view (IY162-001); ***J–K***, Pa element, NIGP 152858, Nj388, J, inner lateral view (IY162-003), K, outer lateral view (IY162-006); ***M***, Pb element, NIGP 152860, Nj403, outer lateral view (IY161-016); ***N***, Pb element, NIGP 152861, AFT-X-K13/35, outer lateral view (IY163-022); ***O***, Sc element, NIGP 152862, AFT-X-K13/35, outer lateral view (IY163-20); ***P***, Sc element, NIGP 152863, AFT-X-K13/35, inner lateral view (IY163-021). L, Q, *Baltoniodus alobatus* (Bergström, 1971). ***L***, Sc element, NIGP 152859, Nj403, outer lateral view (IY161-017); ***Q***, Pb element, NIGP 152864, Nj403, outer lateral view (IY161-015). ***R***, *Baltoniodus prevariabilis*? (Fåhraeus, 1966). M element, NIGP 152865, AFT-X-K13/35, anterior view (IY163-029). Scale bars 100 μm.

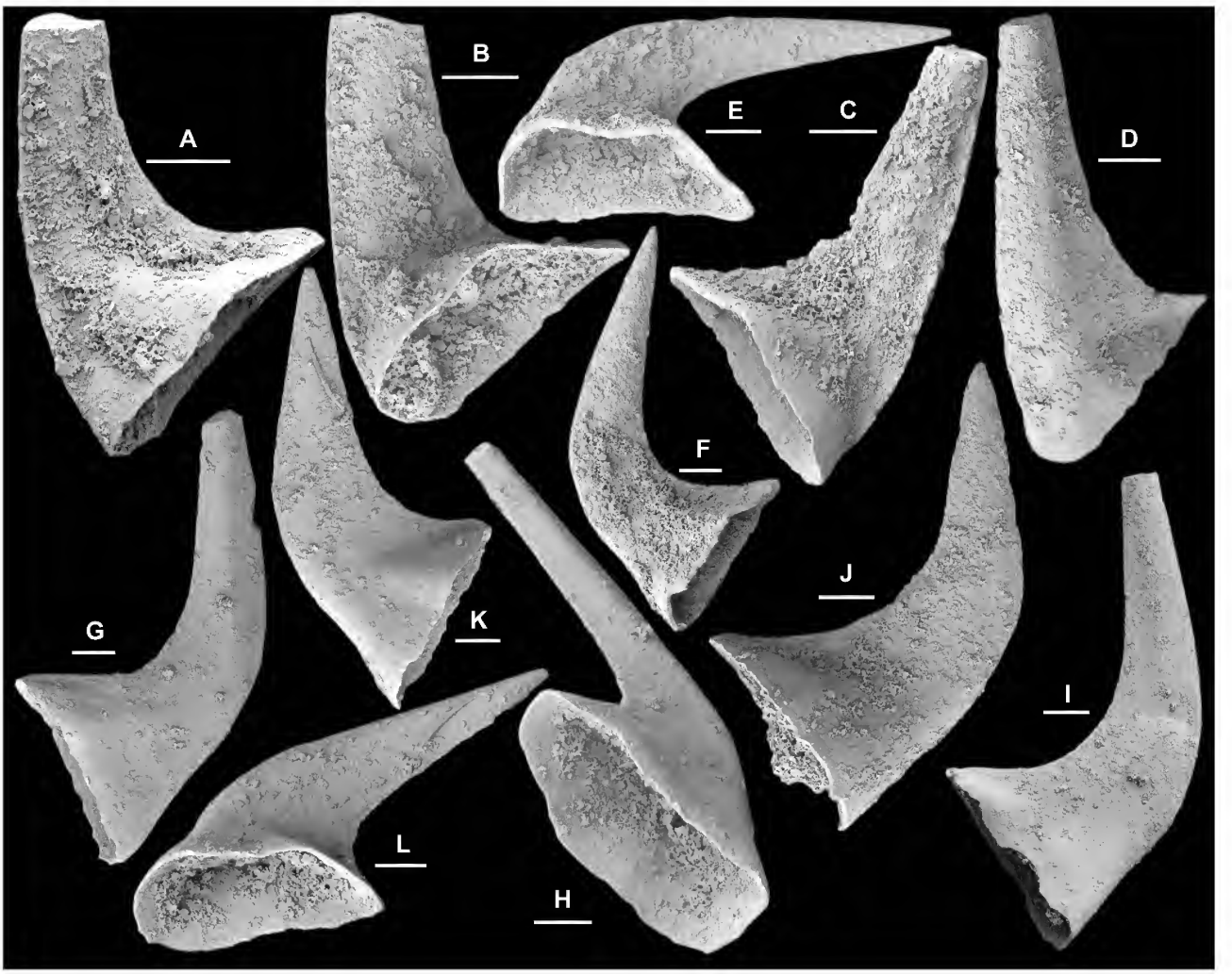

Figure 6. *Costiconus ethingtoni* (Fåhraeus, 1966). A–D, M element; ***A–B***, NIGP 152866, A, posterior view (IY166-016), B, basal-posterior view (IY166-017); ***C***, NIGP 152867, posterior view (IY166-008); ***D***, NIGP 152868, anterior view (IY166-015). E–I, Pb element; ***E–F***, NIGP 152869, E, basal view (IY166-002), F, inner lateral view (IY166-001); ***G–H***, NIGP 152870, G, outer lateral view (IY166-013), H, basal view (IY166-014); ***I***, NIGP 152871, outer lateral view (IY166-009). J–L, Pa element; ***J***, NIGP 152872, inner lateral view (IY166-010); ***K–L***, NIGP 152873, K, inner lateral view (IY166-004), L, inner-basal view (IY166-003). All from sample AFT-X-K13/13, scale bars 100 μm.

Remarks. Eight species belonging to *Cahabagnathus* are known in the literature, ranging in age from the early *P. serra* Zone to early *A. tvaerensis* Zone. Seven of these (the exception being *C. sweeti*) are recorded only from Laurentia, primarily in warm, shallow water facies (Leslie & Lehnert, 2005, Table 1). Leslie & Lehnert (2005) indicated that episodes of wider dispersals of this genus, dominated by endemic species and centered in Laurentia, were associated with major sea level transgressions. *Cahabagnathus sweeti* represents the acme of the cahabagnathid development at or near the Middle/Late Ordovician transition, when it became more cosmopolitan and also invaded deeper and cooler water environments.

Cahabagnathus sweeti (Bergström, 1971)

Fig. 8A–H

Polyplacognathus sweeti Bergström, 1971: 143–144, pl. 1, figs 1–2, text-fig. 14C–D; Harris *et al*., 1979: pl. 2, figs 12–13; Wang & Lou, 1984: 257, pl. 11, fig. 20, pl. 12, figs 5–6.

Petalognathus bergstroemi Drygant, 1974b: 54, pl. 1, figs 1–2.

Cahabagnathus sweeti (Bergström).–Bergström, 1983: 51, fig. 6I–J; Bauer, 1990: pl. 1, figs 16–17; Bergström, 1990: pl. 1, fig. 18; Gao, 1991: 128, pl. 8, figs 4–6; Bauer, 1994: pl. 4, figs 1–3; Wang *et al*., 1996: pl. 1, figs 24, 27, pl. 4, fig. 11; Zhang, 1998b: fig. 9G–H; Wang & Zhou, 1998: pl. 1, fig. 1; Lehnert *et al*., 1999: pl. 3, fig. 11; Zhao *et al*., 2000: 192, pl. 29, figs 7–10; Leslie & Lehnert, 2005: figs 1–2; Bergström, 2007: fig. 3C.

Material. Eight specimens from two samples of the lower Kanling Formation (see Tables 1–2).

Description. This species is rare in the Dawangou samples, being represented by only a few specimens. It has a bimembrate apparatus consisting of paired (sinistral and dextral) stelliplanate Pa and pastiniplanate Pb elements. Both elements bear an indistinct cusp and four processes (anterior, posterior, antero-lateral and postero-lateral) with a central row of nodes on each one. The sinistral and dextral elements

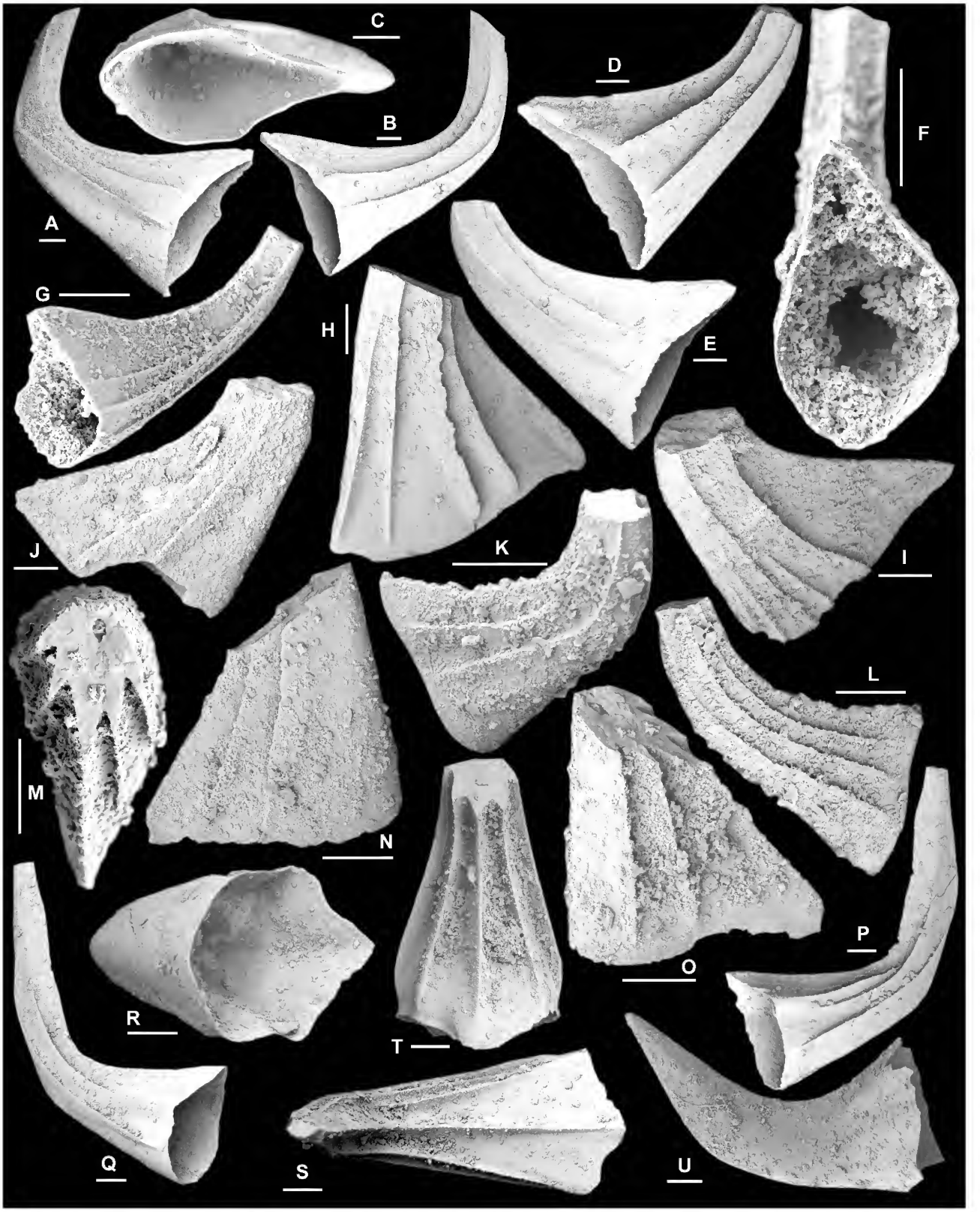

Figure 7. *Costiconus ethingtoni* (Fåhraeus, 1966). A–E, Sa element; ***A–C***, NIGP 152874, Nj379, A–B, lateral views (IY154-010, IY154-011), C, basal view (IY154-009); ***D–E***, NIGP 152875, 14/45, lateral views (IY155-032, IY155-033). ***F–G***, Sb element, NIGP 152876, 13/40, F, basal view (IY155-022), G, inner lateral view (IY155-021). H–L, Sc element; ***H***, NIGP 152877, Nj388, inner lateral view (IY162-010); ***I–J***, NIGP 152878, Nj378, I, inner lateral view (IY160-016), J, outer lateral view (IY160-015); ***K–L***, NIGP 152879, Nj297, K, outer lateral view (IY159-008), L, inner lateral view (IY159-009). M–T, Sd element; ***M–O***, NIGP 152880, Nj298, M, upper view (IY151-001), N, outer lateral view (IY151-002), O, inner lateral view (IY151-003); ***P–S***, NIGP 152881, Nj379, P–Q, lateral views (IY154-016, IY154-014), R, basal view (IY154-015), S, posterior view (IY154-017); ***T***, NIGP 152882, 13/45, posterior view (IY155-034). ***U***, Pa element, NIGP 152883, Nj388, inner lateral view (IY162-013). Scale bars 100 μm.

Figure 8. A–H, *Cahabagnathus sweeti* (Bergström, 1971). ***A–B***, sinistral Pa (stelliplanate) element, NIGP 152884, Nj384, A, upper view (IY154-019), B, upper-lateral view (IY154-020); ***C***, dextral Pb (pastiniplanate) element, NIGP 152885, AFT-X-K13/43, upper view (IY164-019); ***D***, sinistral Pb (pastiniplanate) element, NIGP 152886, AFT-X-K13/43, upper view (IY164-020); ***E***, sinistral Pb (pastiniplanate) element, NIGP 152887, AFT-X-K13/43, upper view (IY164-021); ***F***, dextral Pa (stelliplanate) element, NIGP 152888, AFT-X-K13/43, upper view (IY164-022); ***G–H***, dextral Pa (stelliplanate) element, NIGP 152889, AFT-X-K13/43, G, upper view (IY164-024), H, lateral view (IY164-026). I–L, *Baltoniodus* sp. B. ***I–J***, ***L***, Pa element, NIGP 152890, Nj406, I, outer lateral view (IY155-011), J, upper view (IY155-012), L, upper view, close up showing fine striation on the upper surface (IY155-013); ***K***, Pa element, NIGP 152891, Nj406, antero-outer lateral view (IY161-012). M–N, *Baltoniodus alobatus* (Bergström, 1971). ***M***, Sd element, NIGP 152892, Nj406, postero-lateral view (IY161-010); ***N***, Pa element, NIGP 152893, Nj406, upper view (IY161-009). O–P, *Cornuodus longibasis* (Lindström, 1955). ***O***, Sb element, NIGP 152894, AFT-X-K13/13, outer lateral view (IY167-001); ***P***, Sa element, NIGP 152895, Nj291, lateral view (IY158-004). Scale bars 100 µm, unless otherwise indicated.

form mirror-images of each other (Fig. 8C–D). Pa element has a short, blade-like anterior process nearly linear with the longer posterior process; antero-lateral process narrower and longer, being nearly perpendicular to the anterior and posterior processes; postero-lateral process shorter with a wider platform, forming an obtuse angle (about 110°) with the anterior process (Fig. 8A–B). A couple of specimens from the same sample have a rather prominent cusp, and their postero-lateral process has a narrower platform and forms a narrower angle (about 60°) with the anterior process (Fig. 8F–G), hence they are only questionably included in this species. Pb element with a short anterior process and a long posterior process represented by a row of nodes arranged more or less in straight line across the centre of the platform; posterior process with a wide and rounded platform in upper view; antero-lateral process long and tapering distally with the mid-row of nodes approximately perpendicular to the row of nodes on the anterior or posterior process; postero-lateral process shorter, with central row of nodes forming an angle of about 130° with the row of the nodes on the posterior process; nodes also developed along the platform margins of posterior and postero-lateral processes (Fig. 8C–E).

Remarks. Bergström (1983) suggested that five distinctive species of *Cahabagnathus* occurring in successive stratigraphic order in North America formed an evolutionary lineage from the oldest *C.* sp. A (=*C. directus* Bauer, 1987) of mid-late Darriwilian age (early *P. serra* Zone) to the youngest *C. carnesi* in the early Sandbian (early *A. tvaerensis* Zone). He proposed the generic name *Cahabagnathus* for this group and indicated that its direct ancestor might be a species of *Eoplacognathus*, such as *E. foliaceus* and *E. reclinatus*. Bergström (1983, p. 41) and Zhang (1998b, p. 14–15) also discussed in detail the evolutionary trends and character transformations through several recognized stages of the *Cahabagnathus* lineage. Within the eight known species of *Cahabagnathus*, Leslie & Lehnert (2005) recognized two lineages that shared an unknown common ancestor, and suggested that their dispersals and speciation were largely influenced by the transgressive and regressive events of sea level changes.

Cahabagnathus sweeti differs from *C. carnesi* Bergström, 1983 in having the short anterior process in the Pb element more or less extending straight, rather than bending towards the antero-lateral process as in the Pb element of *C. carnesi*. In China, *C. sweeti* has only been recorded from the Kanling Formation (Gao, 1991; Wang *et al.*, 1996; Wang & Zhou, 1998) and subsurface age equivalents (Zhao *et al.*, 2000) of the Tarim Basin, and from the Sandaogou Formation of Longxian County, Shaanxi Province in North China (Wang & Lou, 1984; Wang *et al.*, 1996).

Costiconus Rasmussen, 2001

Type species. *Panderodus ethingtoni* Fåhraeus, 1966.

Costiconus ethingtoni (Fåhraeus, 1966)

Figs 6–7

Panderodus ethingtoni Fåhraeus, 1966: 26, pl. 3, fig. 5a–b.

Walliserodus ethingtoni (Fåhraeus).–Bergström *et al.*, 1974: pl. 1, fig. 12; An & Ding, 1982: pl. 2, figs 7–8; An *et al.*, 1983: 162, pl. 26, figs 16–18; An & Xu, 1984: pl. 2, fig. 6; Wang & Lou, 1984: 288, pl. 3, figs 1–5; An *et al.*, 1985: pl. 10, figs 19–22; Ding, 1987: pl. 5, fig. 24; Chen & Zhang, 1989: pl. 5, fig. 24; Pohler & Orchard, 1990: pl. 2, fig. 19; Ding *et al.* in Wang, 1993: 213, *partim* only pl. 18, figs 4–6, 9, 11; Chen & Bergström, 1995: pl. 8, figs 13–14; Wang *et al.*, 1996: pl. 1, fig. 15; Albanesi in Albanesi *et al.*, 1998: 114, pl. 14, figs 20–25, text-fig. 8; Zhang, 1998c: 95–96, pl. 18, figs 10–15; Wang & Bergström, 1999a: 344, pl. 3, figs 6–7; Lehnert *et al.*, 1999: pl. 2, fig. 6; Wang & Qi, 2001: pl. 2, fig. 27; Wang, 2001: pl. 1, figs 25–26; Pyle & Barnes, 2002: pl. 22, figs 19–22.

Costiconus ethingtoni (Fåhraeus).–Rasmussen, 2001, 62–64, pl. 3, figs 16–18 (*cum syn.*); Zhen *et al.*, 2009a: 139–140, fig. 3A–W; Zhen *et al.*, 2009b: 31–33, fig. 4H–W (*cum syn.*); Viira, 2011: fig. 7O, Q.

Material. 443 specimens from 27 samples (see Tables 1–2).

Remarks. Specimens of this species recovered from the Dawangou section are identical with those recently described from the Yenwashan Formation of the JCY area of South China (Zhen *et al.*, 2009a) and from the Thompson Creek area in New Zealand (Zhen *et al.* 2009b). Based on a large collection from Dawangou, *C. ethingtoni* is interpreted as a septimembrate apparatus including a non-geniculate short-based M element (Fig. 6A–D), multicostate long-based S (Sa, Sb, Sc and Sd) elements (Fig. 7A–T) that show a wide variation in respect to the number of costae, and non-costate Pa (Figs 6J–L, 7U) and Pb (Fig. 6E–I) elements. The four types of the S elements were described in detail by Zhen *et al.* (2009a). The M element defined herein was previously referred to as a P element (see Zhang, 1998c, pl. 18, fig. 10; Zhen *et al.*, 2009a, fig. 3R–W; Zhen *et al.*, 2009b, fig. 4T-W) from which it can be distinguished by having a shorter and more posteriorly flared base. The P elements defined herein were previously referred to as representing the M element (e.g., Zhang, 1998c, pl. 18, fig. 11), and show a rather wide variation from long-based (Fig. 7U) to relatively short-based (Fig. 6G).

Dapsilodus Cooper, 1976

Type species. *Distacodus obliquicostatus* Branson & Mehl, 1933.

Dapsilodus viruensis (Fåhraeus, 1966)

Fig. 9A, ?B–C

Acodus viruensis Fåhraeus, 1966: 12, pl. 2, fig. 2a–b, text-fig. 2A.

Acontiodus sulcatus Fåhraeus, 1966: 17, pl. 2, fig. 6a–b, text-fig. 2F.

Acodus? mutatus (Branson & Mehl).–Löfgren, 1978: 44, pl. 2, figs 9–21 (*cum syn.*); Zeng *et al.*, 1983: pl. 12, figs 39–40.

Dapsilodus mutatus (Branson & Mehl).–An, 1987: 142, *partim* only pl. 4, figs 14, 17–18, 22–23, 27; An & Zheng, 1990: 164, pl. 4, figs ?1, 2–5; Stouge & Bagnoli, 1990: 14, pl. 9, figs 19, 26–27; Gao, 1991: 130, pl. 12, figs 10, 17; Ding *et al.* in Wang, 1993: pl. 15, figs ?22, 23–24, 26; Armstrong, 1997: 786, pl. 5–8, ?3–4; Ferretti & Serpagli, 1999: 230, pl. 3, figs 20–23; Wang, 2001: 351, pl. 2, figs 8–9 (*cum syn.*).

Dapsilodus striatus Chen & Zhang, 1984b: 126, 134, pl.1, figs 17–20; Duan, 1990: pl. 3, fig. 1.

Dapsilodus viruensis (Fåhraeus).–Zhang, 1998b: 58–59, pl. 4, figs 1–6 (*cum syn.*); Rasmussen, 2001: 67–68, pl.

4, figs 15–17 (*cum syn.*); Zhen *et al.*, 2009a: 142, fig. 4A–O (*cum syn.*).

Material. 74 specimens from 17 samples (see Tables 1–2).

Remarks. Löfgren (1978), An (1987) and Stouge & Bagnoli (1990) regarded *Acodus viruensis* Fåhraeus, 1966 as a junior synonym of *Belodus* (?) *mutatus* Branson & Mehl, 1933, whereas others, including Zhang (1998b), Ferretti & Serpagli (1999) and Rasmussen (2001), considered them as separate species. The taxonomic position of *Belodus* (?) *mutatus* has been discussed for many decades, and it remains as a poorly known species until its species apparatus and constituent elements are revised according to the multielement species concept. In particular, Rasmussen (2001, p. 68) pointed out that the original description of *Belodus* (?) *mutatus* by Branson & Mehl (1933, p. 126) indicated the presence of "one or two minute denticles" on "the posterior end" in some of the specimens from the basal Maquoketa Shale of Missouri. However, this taxonomically important character has not been observed in the type specimens (holotype and other topotype material) and from any of the Swedish and Chinese material previously assigned to *D. mutatus*, and more likely the Chinese specimens belong to *D. viruensis* (see Zhang, 1998b).

Drepanodus Pander, 1856

Type species. *Drepanodus arcuatus* Pander, 1856.

Drepanodus arcuatus Pander, 1856

Fig. 10A–N

Drepanodus arcuatus Pander, 1856: 20, pl. 1, figs 2, 4–5, 17, 30, ?31; An, 1981: pl. 3, fig. 22; An *et al.*, 1985: pl. 4, figs 6–11, pl. 12, 10–13, 15; An, 1987: 143–144, pl. 8, figs 7–9, 11–12, 15–18, 24; Ni & Li, 1987: 403, pl. 59, figs 6–7; Bergström, 1988: pl. 1, figs 4–5; Duan, 1990: pl. 2, figs 25–26; Ding *et al.* in Wang, 1993: 171, pl. 10, figs 1–4, 8–11, 17, ?20; Chen & Bergström, 1995: pl. 8, figs 10, 16; Zhang, 1998c: 59–60, pl. 4, figs 7–11, 15–16 (*cum syn.*); Wang & Bergström, 1999a: 334, pl. 2, figs 4–5; Wang, 2001: 352, pl. 1, figs 2, 6; Löfgren & Tolmacheva, 2003b: 211–215, figs 2, 3A–C, E–H, 5K–V, 6M–U, 7H–N, 8A–G (*cum syn.*); Zhen *et al.*, 2004a: 52–53, pl. 3, figs 1–12; Agematsu *et al.*, 2007: 31, fig. 13.9; Ortega *et al.*, 2008: fig. 6.27–6.28; Zhen *et al.*, 2009b: fig. 5A–N (*cum syn.*); Zhen & Nicoll, 2009: 11, fig. 5A–F; Viira, 2011: figs 14A, ?B, C–G, ?H, I, K, S, 15A–E, ?F–G.

Material. 858 specimens from 44 samples (see Tables 1–2).

Remarks. Both species of *Drepanodus*, *D. arcuatus* and *D. reclinatus* are rather common in collections from the Dawangou section, and can be easily recognized by their generally large size in the fauna. They are morphologically similar except that costae are generally absent in all the constituent elements of *D. arcuatus*. Armstrong (2000) included in *D. arcuatus* various forms of costate elements, which were reassigned to *D. reclinatus* by Löfgren & Tolmacheva (2003), who revised both species as having a septimembrate apparatus. Specimens from Dawangou (Fig. 10A–N) are identical with those illustrated by Löfgren & Tolmacheva (2003) from Sweden, except that the Sd element is not distinguished. As indicated by Löfgren & Tolmacheva (2003, p. 215), the Sd element represents the end member of a symmetry transition series and the general morphology is rather similar to the Sb element but with a more compressed base. It is likely that the Sb element documented herein (Fig. 10E–G) incorporates the Sd element as defined by Löfgren & Tolmacheva (2003).

Drepanodus reclinatus (Lindström, 1955a)

Fig. 11A–P

Acontiodus reclinatus Lindström, 1955a: 548, text-fig. 3C, pl. 2, figs 5–6.

Drepanodus reclinatus (Lindström).–Zhang, 1998c: 60–61, pl. 4, figs 12–14, 17–20 (*cum syn.*); Löfgren & Tolmacheva, 2003: 216–217, figs 5A–J, 7A–G (*cum syn.*); Ortega *et al.*, 2007: fig. 6M; Ortega *et al.*, 2008: fig.6.17–6.18.

Drepanodus arcuatus Pander.–Armstrong, 2000: 49, pl. 3, figs 1–18.

Drepanodus sp. A.–Zhen & Percival, 2004b: 159–160, *partim*, only fig. 3D, F–I; non fig. 3E = *Protopanderodus*.

Protopanderodus robustus (Hadding).–An *et al.*, 1983: 132, pl. 15, fig. 21; An & Zheng, 1990: pl. 6, figs 15–17; Chen & Bergström, 1995: *partim* only pl. 8, figs 3–4; Wang & Bergström, 1998: 342, *partim* only pl. 2, figs 7, 9.

Cornuodus longibasis (Lindström, 1955).–Wang & Qi, 2001: pl. 1, fig. 11.

Paroistodus sp. An & Zheng, 1990: pl. 6, fig. 11.

Material. 116 specimens from 26 samples (see Tables 1–2).

Remarks. All seven elements (except for the Sd) recovered from Dawangou (Fig. 11A–P) are identical with those illustrated by Löfgren & Tolmacheva (2003). Elements of *D. reclinatus* can be distinguished from *D. arcuatus* and other species of *Drepanodus* by being laterally costate.

Some specimens ascribed to *Drepanodus* sp. A from the Weemalla Formation (Darriwilian) of central New South Wales should be re-assigned to *D. reclinatus* representing the M (Zhen & Percival, 2004b, fig. 3D) and Pa (Zhen & Percival, 2004b, fig. 3F–I) elements. One figured specimen of *D.* sp. A (Zhen & Percival, 2004b, fig. 3E) represents an asymmetrical bicostate element of a *Protopanderodus* species, comparable to those described by Zhen & Percival (2004b, p. 172, fig. 11G–O) as *Protopanderodus robustus* (Hadding, 1913). However, *P. robustus* remains a poorly-known species, and may be more closely related to multicostate species rather than bicostate *Protopanderodus* species (see discussion under remarks of *P. cooperi*). Specimens previously assigned to *P. robustus* by various authors may belong to *D. reclinatus* (see synonymy list; also Löfgren & Tolmacheva, 2003).

Drepanoistodus Lindström, 1971

Type species. *Oistodus forceps* Lindström, 1955a.

Drepanoistodus basiovalis (Sergeeva, 1963)

Fig. 12A–Q

Oistodus basiovalis Sergeeva, 1963: 96, pl. 7, figs 6, 7, text-fig. 3.

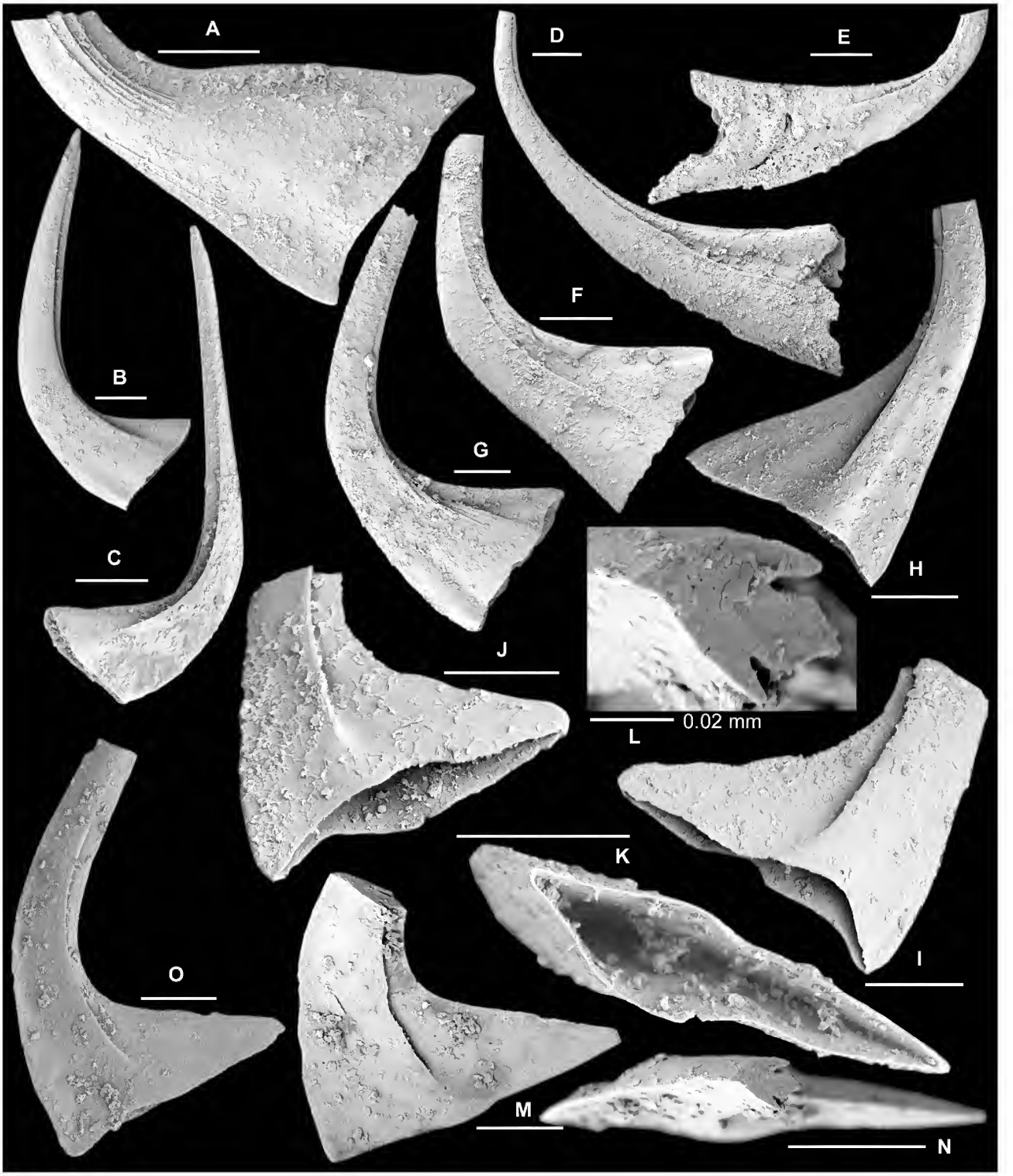

Figure 9. A–C, *Dapsilodus viruensis* (Fåhraeus, 1966). ***A***, Sc element, NIGP 152896, Nj375, outer lateral view (IY159-024). B–C, Sa element; ***B***, NIGP 152897, Nj375, lateral view (IY159-025), tentatively assigned to this species; ***C***, NIGP 152898, Nj375, lateral view (IY159-026). D–O, *Scabbardella altipes* (Henningsmoen, 1948). D–E, long-based acodiform element; ***D***, NIGP 152899, Nj378, outer lateral view (IY153-016); ***E***, NIGP 152900, Nj403, outer lateral view (IY161-021). F–G, medium-based acodiform element; ***F***, NIGP 152901, Nj297, outer lateral view (IY159-012); ***G***, NIGP 152902, AFT-X-K13/13, outer lateral view (IY167-002). H–O, asymmetrical distacodiform element; ***H***, NIGP 152903, Nj376, outer lateral view (IY159-029); ***I–K***, NIGP 152904, Nj378, I, outer lateral view (IY160-017), J, inner lateral view (IY160-017), K, basal view (IY160-020); ***L–N***, NIGP 152905, Nj379, L, upper view, close up of cross section of the cusp (IY160-035), M, inner lateral view (IY160-036), N, upper view (IY160-034); ***O***, NIGP 152906, Nj379, outer lateral view (IY160-033). Scale bars 100 μm, unless otherwise indicated.

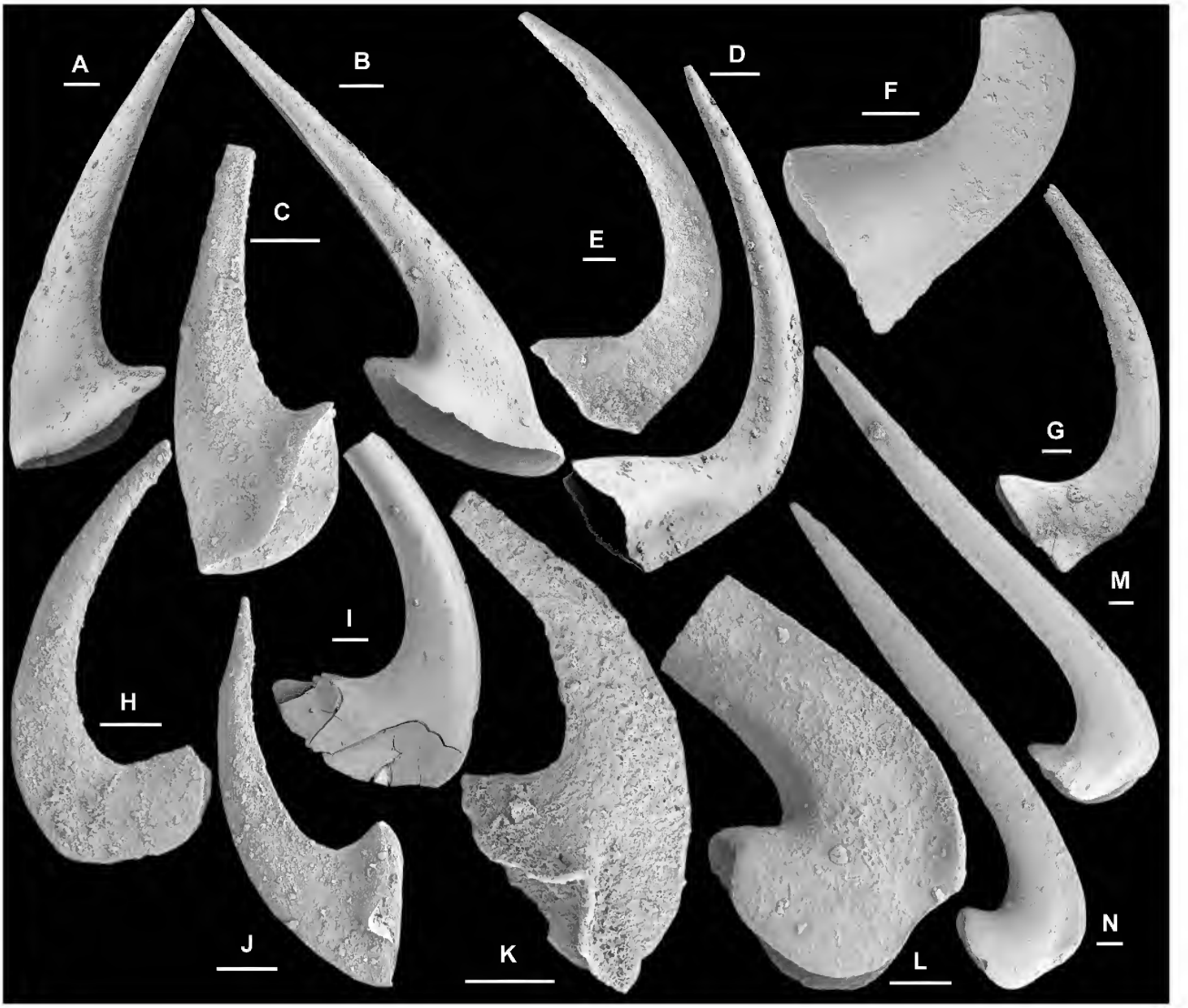

Figure 10. *Drepanodus arcuatus* Pander, 1856. A–C, M element; ***A***, NIGP 152907, AFT-X-K13/13, posterior view (IY166-021); ***B***, NIGP 152908, AFT-X-K13/13, anterior view (IY166-019); ***C***, NIGP 152909, Nj297, posterior view (IY150-034). ***D***, Sa element, NIGP 152910, Nj375, lateral view (IY162-024). E–G, Sb element; ***E***, NIGP 152911, Nj297, inner view (IY150-036); ***F***, NIGP 152912, Nj294, outer lateral view (IY147-035); ***G***, NIGP 152913, Nj297, inner lateral view (IY150-035). H–I, Sc element; ***H***, NIGP 152914, Nj297, inner lateral view (IY150-031); ***I***, NIGP 152915, Nj406, outer lateral view (IY161-004). J–K, Pa element; ***J***, NIGP 152916, Nj297, outer lateral view (IY150-033); ***K***, NIGP 152917, Nj294, outer lateral view (IY147-036). L–N, Pb element; ***L***, NIGP 152918, Nj295, inner lateral view (IY149-010); ***M***, NIGP 152919, AFT-X-K13/13, outer lateral view (IY166-023); ***N***, NIGP 152920, AFT-X-K13/13, inner lateral view (IY166-018). Scale bars 100 µm.

Drepanoistodus basiovalis (Sergeeva).–Lindström, 1971: 43, figs 6, 8; Löfgren, 1978: 55, pl. 1, figs 11–17, text-fig. 26B, C (*cum syn.*); An *et al.*, 1985: pl. 13, figs 17–20; An, 1987: 145–146, pl. 9, figs 30–31; An & Zheng, 1990: 164, pl. 8, fig. 9; Ding *et al.* in Wang, 1993: 173, *partim* only pl. 12, figs 1–2, 4; Albanesi in Albanesi *et al.*, 1998: 135, pl. 3, figs 15–18; Johnston & Barnes, 2000: 18, pl. 11, figs 10, 11, 15, 16 (*cum syn.*); ?Zhen *et al.*, 2003b: 191, fig. 14A–K; Zhen *et al.*, 2007: pl. 1, figs 27–37.

Drepanoistodus suberectus (Branson & Mehl).–Cooper, 1981: 164, pl. 26, figs 1, 2, 6.

Material. 110 specimens from 12 samples (Tables 1–2).

Remarks. *Drepanoistodus* is one of the most common genera widely distributed in the Ordovician with nearly 30 species names proposed in the literature. Due to their simple, coniform elements, the majority of these species remain inadequately documented. Recent studies of the group suggest that its species had a seximembrate or septimembrate apparatus (Zhen *et al.*, 2007). *Drepanoistodus basiovalis* was originally erected as a form species based on a geniculate coniform element from the Lower Ordovician of the St Petersburg region, Russia (Sergeeva, 1963, pl. 7, figs 6–7, text-fig. 3). Our current understanding of *D. basiovalis* is largely based on the revision of the species by Löfgren (1978) on material from the Middle Ordovician of Jämtland, northern Sweden (also see Zhen *et al.*, 2007, pl. 1, figs 27–37). Löfgren (1978) suggested a trimembrate apparatus including homocurvatiform (= P element herein), oistodiform (= M element) and suberectiform (= Sa element). We interpret the homocurvatiform element as P elements having an extended, inwardly flexed antero-basal corner (Löfgren, 1978, pl. 1, fig. 13 and probably also fig. 12), with the S elements forming a

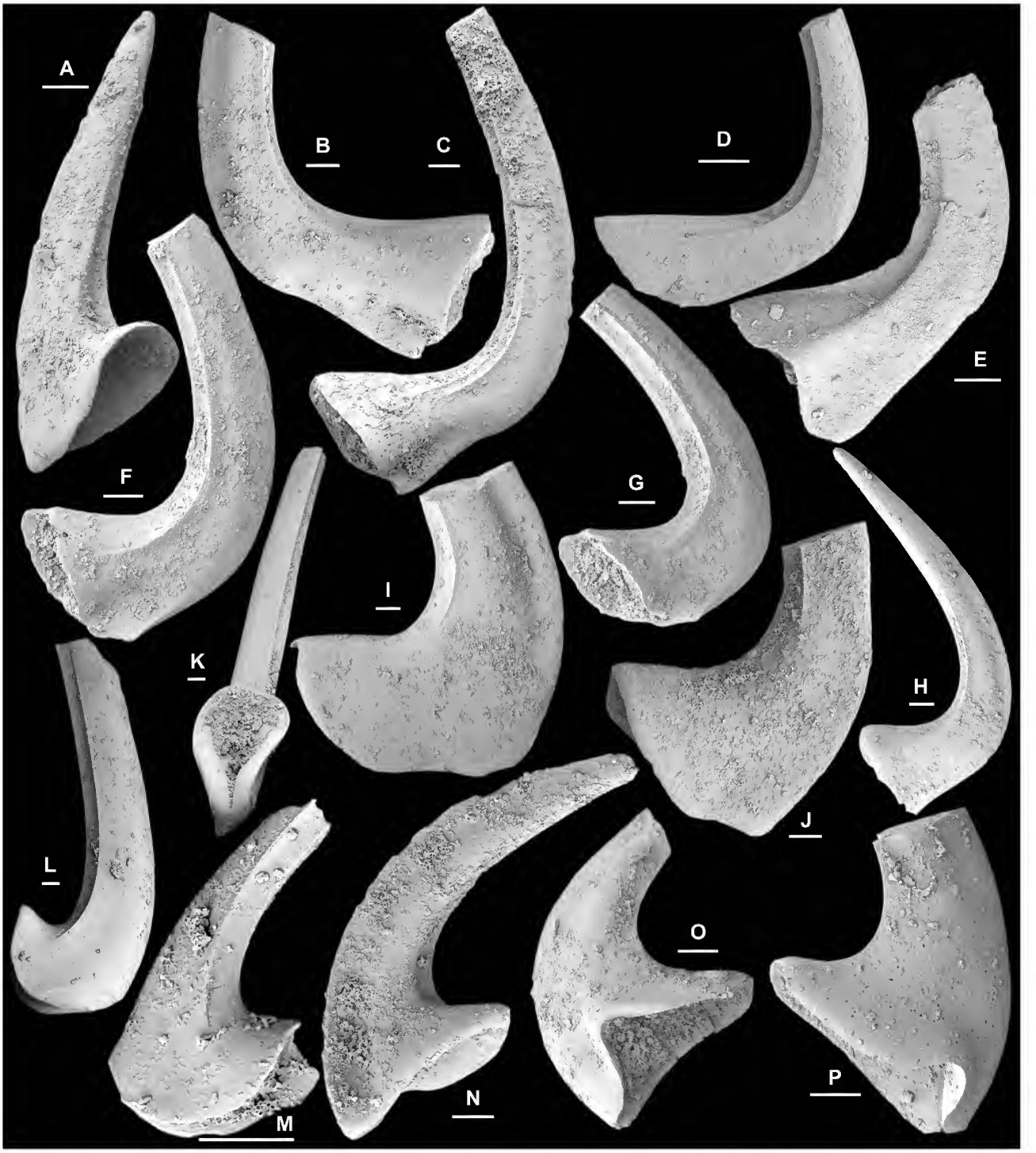

Figure 11. *Drepanodus reclinatus* (Lindström, 1955). ***A***, M element, NIGP 152921, AFT-X-K13/13, posterior view (IY166-005). B–E, Sa element; ***B***, NIGP 152922, AFT-X-K13/13, lateral view (IY166-031); ***C***, NIGP 152923, AFT-X-K13/13, lateral view (IY166-032); ***D***, NIGP 152924, Nj375, lateral view (IY162-025); ***E***, NIGP 152925, Nj295, lateral view (IY149-011). F–H, Sb element; ***F–G***, NIGP 152926, AFT-X-K13/13, F, inner lateral view (IY166-030), G, basal-inner lateral view (IY166-029); ***H***, NIGP 152927, AFT-X-K13/13, outer lateral view (IY166-033). I–J, Sc element; ***I***, NIGP 152928, AFT-X-K13/13, inner lateral view (IY166-026); ***J***, NIGP 152929, AFT-X-K13/13, inner lateral view (IY166-024). K–M, Pb element; ***K–L***, NIGP 152930, Nj375, K basal view (IY152-016), L, antero-inner lateral view (IY152-015); ***M***, NIGP 152931, AFT-X-K13/13, inner lateral view (IY169-010). N–P, Pa element; ***N***, NIGP 152932, AFT-X-K13/13, inner lateral view (IY166-034); ***O***, NIGP 152933, AFT-X-K13/13, outer lateral view (IY166-028); ***P***, NIGP 152934, AFT-X-K13/13, outer lateral view (IY166-036). Scale bars 100 μm.

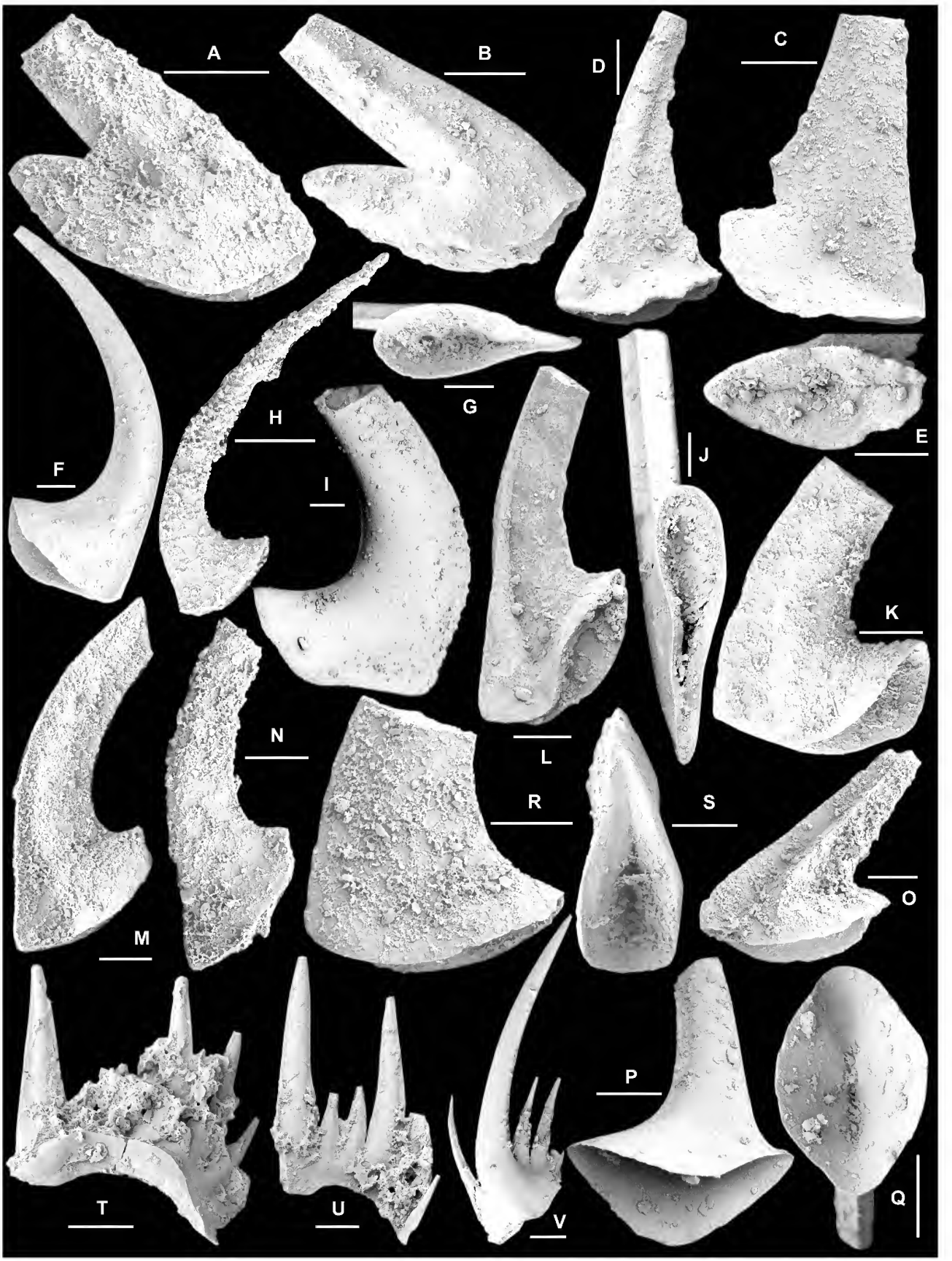

Figure 12. A–Q, *Drepanoistodus basiovalis* (Sergeeva, 1963). A–B, M element; ***A***, NIGP 152935, Nj378, anterior view (IY160-004), ***B***, NIGP 152936, Nj378, posterior view (IY160-005). C–E, Sa element; ***C***, NIGP 152937, Nj379, lateral view (IY160-039); ***D–E***, NIGP 152938, Nj291, D, lateral view (IY158-008), E, basal view (IY158-011). F–H, Sb element; ***F–G***, NIGP 152939, Nj379, F, inner lateral view (IY160-040), G, basal view (IY160-041); ***H***, NIGP 152940, Nj378, outer lateral view (IY160-011)… (continued on facing page)

symmetry transition series (Löfgren, 1978, pl. 1, figs 11, 14). Löfgren also included an element with a prominent costa on the outer lateral face (Löfgren, 1978, pl. 1, fig. 12), which may represent the additional P element. Based on study of the Swedish material, Zhen (in Zhen *et al.* 2007) suggested a septimembrate apparatus for this species, with the Sa element showing a symmetrical outline of the base, which is widest in the middle and tapers anteriorly and posteriorly (Zhen *et al.*, 2007, pl. 1, fig. 30).

Lindström (*in* Ziegler, 1974, p. 73) suggested that *D. basiovalis* could be differentiated from the stratigraphically older *D. forceps* in having a rounded outline of the base in the M element, and a more flattened cross-section in the S elements. Zhen *et al.* (2007, pl. 1, fig. 7) noted that the Sa element of *D. forceps* has a oval-shaped outline of the base that is widest anteriorly and only tapers posteriorly.

Drepanoistodus sp. (Fig. 12R–S) shows some resemblance to *Drepanoistodus* sp. cf. *D. nowlani* Ji & Barnes, 1994, a stratigraphically older species described from the Honghuayuan Formation (Early Ordovician) of South China (Zhen *et al.*, 2007, pl. 2, figs 4–5) in having the base widest posteriorly, but the Dawangou species has a shorter, laterally less flared base.

The M element of *D. basiovalis* from the Dawangou section typically shows a broad carina or a weakly developed costa on the posterior face (Fig. 12B), but some specimens from sample Nj298 at the top of the Dawangou Formation exhibit a sharp costa on the posterior face (Fig. 12O), and are identical with the M element of *D. basiovalis* recently illustrated from the lower Darriwilian (lowermost *Lenodus antivariabilis* Subzone) of Sweden (Zhen *et al.*, 2007, pl. 1, fig. 27). The posterior face of the M element of *Drepanoistodus stougei* Rasmussen, 1991 also has a prominent costa (see Rasmussen, 2001, pl. 6, figs 10, 13), but the holotype of *D. stougei* exhibits a narrower angle between the cusp and the outer-lateral proto-process and a more rounded outline of the basal margin (Rasmussen, 1991, fig. 6J). The M element of *Drepanoistodus costatus* (Abaimova, 1971) also bears a sharp costa on the posterior face, but has a less extended base and is associated with costate S elements (Zhen *et al.*, 2003b, fig. 15).

Dzikodus Zhang, 1998

Type species. *Polonodus tablepointensis* Stouge, 1984.

Remarks. Definition of *Dzikodus* and its morphological and phylogenetic relationship with *Polonodus* were reviewed recently by Zhen & Percival (2004b). Zhang's (1998c) original concept is followed herein to define *Dzikodus* as consisting of a septimembrate apparatus including makellate M, ramiform S, stelliscaphate paired Pa, and stelliscaphate but unpaired Pb elements.

Dzikodus ?tablepointensis (Stouge, 1984)

Fig. 13A–K

Polonodus tablepointensis Stouge, 1984: 72, pl. 12, fig. 13, pl. 13, figs 1–5 (*cum syn.*).
Dzikodus tablepointensis (Stouge).–Zhang, 1998c: 65–69, pl. 7, figs 1–12, pl. 8, figs 1–6 (*cum syn.*).

Material. 31 specimens from two samples at the top of the Dawangou Formation (Tables 1–2).

Remarks. This species is rarely represented in the Dawangou samples with stelliscaphate Pb (Fig. 13A–B), alate Sa (Fig. 13C–G), tertiopedate Sb (Fig. 13H–I), and quadriramate Sd (Fig. 13J–K) elements recovered. The Pb element has four processes, an inconspicuous cusp and a wide open basal cavity, and is comparable with those illustrated from the Guniutan Formation of South China (Zhang, 1998c, pl. 7, figs 7–9). However, as the two illustrated specimens assigned to the Pb element are incomplete with one lateral process broken off, they are only tentatively referred to *D. tablepointensis*.

Histiodella Harris, 1962

Type species. *Bryantodina sinuosa* Graves & Ellison, 1941.

Histiodella holodentata Ethington & Clark, 1982

Fig. 14A–B

Histiodella holodentata Ethington & Clark, 1982: 47–48, pl. 4, figs 1, 3, 4, 16 (*cum syn.*); Nowlan & Thurlow, 1984: pl. 1, figs 1, 3, 5; Wang & Zhou, 1998: pl. 4, fig. 12; Zhang, 1998c: 72, pl. 9, figs 14–15; Zhao *et al.*, 2000: 205, pl. 27, figs 12–14; Johnston & Barnes, 2000: pl. 15, fig. 7; Du *et al.*, 2005: 365, pl. 1, figs 22–26, 28 (*cum syn.*); Agematsu *et al.*, 2006: fig. 7.18; Chen *et al.*, 2006: fig. 10W; Percival & Zhen, 2007: 391, pl. 1, figs 22–23; Agematsu *et al.*, 2008b: 189, fig. 7.7; Zhen *et al.*, 2009b: 38–39, fig. 2O; Bauer, 2010: pl. 2, fig. 9.
Histiodella tableheadensis Stouge, 1984: 87–88, pl. 18, figs 8, 12–14, text-fig. 17; Zhang, 1998c: 72, pl. 9, figs 14, 15 (*cum syn.*); Albanesi & Ortega, 2003: pl. 1, fig. 4.
Histiodella intertexta An.–An *et al.*, 1985: pl. 14, figs 15, 16; An, 1987: 154, pl. 18, figs 15, 16, pl. 30, fig. 10; Gao, 1991: 131–132, pl. 9, fig. 5.
Histiodella infrequensa An in An *et al.*, 1983: 105–106, pl. 25, figs 1–2, text-fig. 14–12; An & Zheng, 1990: 166–167, *partim* only pl. 7, fig. 4, non fig. 1 (probably a broken Pa element of Rhipidognathidae).
Histiodella kristinae Stouge.–Zhen *et al.*, 2004a: 97–98, fig. 14A–L.

Material. Three specimens (Pa only) from one sample in the upper Dawangou Formation (see Table 1).

(Figure 12 caption, continued from facing page)... I–K, Sc element; ***I–J***, NIGP 152941, Nj375, I, iner lateral view (IY152-017), J, basal view (IY152-018); ***K***, NIGP 152942, Nj378, inner lateral view (IY160-009). L–N, P element; ***L***, NIGP 152943, Nj291, inner lateral view (IY158-010); ***M***, NIGP 152944, Nj378, inner lateral view (IY160-007); ***N***, NIGP 152945, Nj378, outer lateral view (IY160-006). ***O***, M element, NIGP 152946, Nj298, posterior view showing a sharp costa on the posterior face (IY159-020); ***P–Q***, Sa element, NIGP 152947, AFT-X-K13/43, P, lateral view (IY172-009), Q, basal view (IY172-010). ***R–S***, *Drepanoistodus* sp. Sa element, NIGP 152948, Nj378, R, lateral view (IY160-003), S, basal view (IY160-001). T-V, *Erraticodon* sp. ***T***, Pa element, NIGP 152949, AFT-X-K13/36, posterior view (IY172-005); ***U***, Pa element, NIGP 152950, AFT-X-K13/36, anterior view (IY172-004); ***V***, Sc element, NIGP 152951, AFT-X-K13/36, outer lateral view (IY172-001). Scale bars 100 μm.

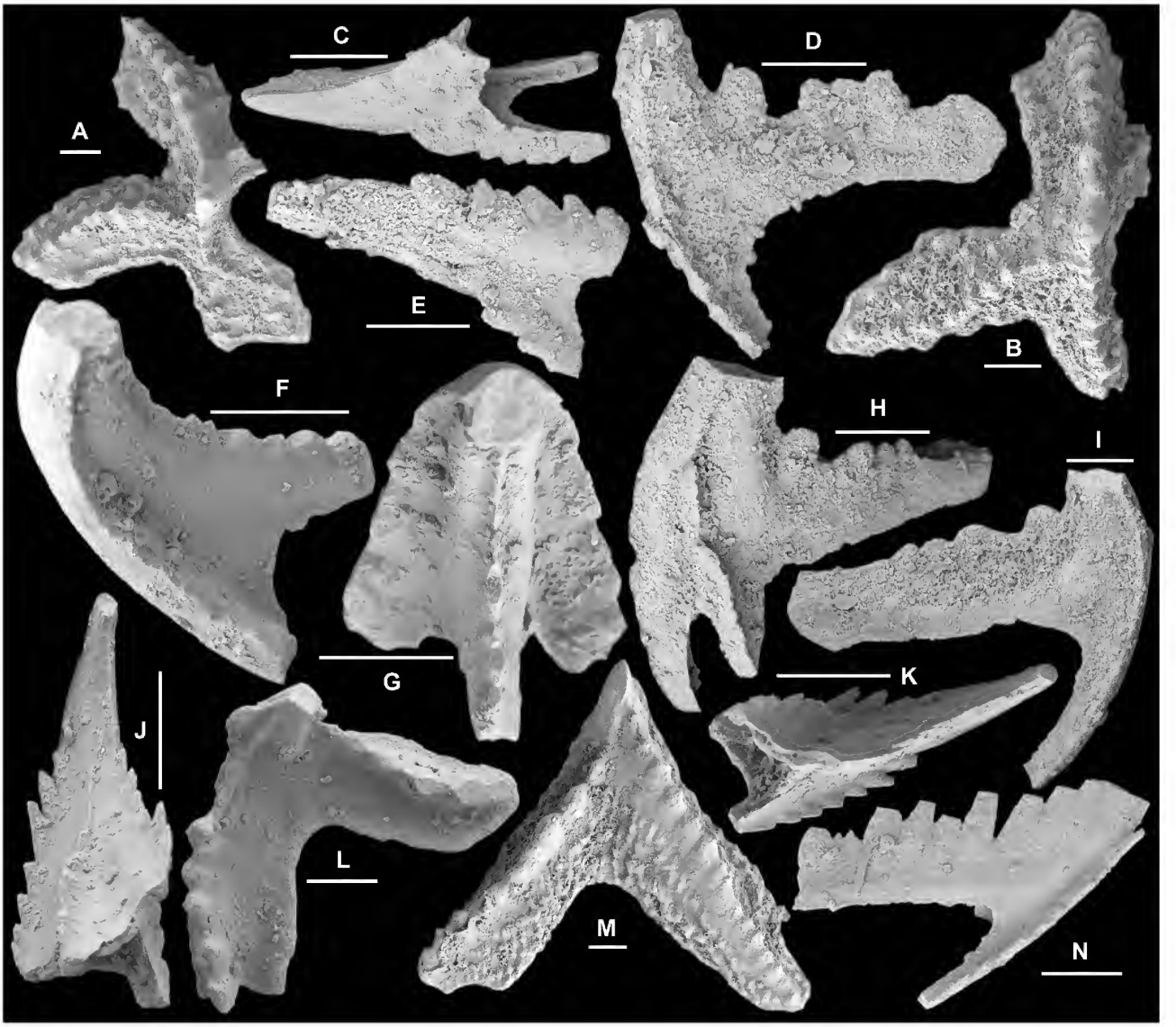

Figure 13. A–K, *Dzikodus ?tablepointensis* (Stouge, 1984). A–B, Pb element; ***A***, NIGP 152952, Nj297, upper view (IY150-001); ***B***, NIGP 152953, Nj297, upper view (IY150-002). C–G, Sa element; ***C***, NIGP 152954, Nj297, posterior view (IY150-003); ***D–E***, NIGP 152955, Nj297, D, lateral view (IY150-008), E, anterior view (IY150-010); ***F–G***, NIGP 152956, Nj297, F, lateral view (IY159-006), G, posterior view (IY159-007). ***H–I***, Sb element, NIGP 152957, Nj297, H, outer lateral view (IY150-006), I, inner lateral view (IY150-007). ***J–K***, Sd element, NIGP 152958, Nj297, J, postero-outer lateral view (IY159-005), K, posterior view (IY159-004). L–N, *Polonodus* sp. B. ***L***, P element, NIGP 152959, Nj291, upper view (IY158-002); M, P element, NIGP 152960, Nj291, upper view (IY158-001); ***N***, Sc element, NIGP 152961, Nj291, inner lateral view (IY158-003). Scale bars 100 μm.

Remarks. This species is rare in the Dawangou material and is represented only by the Pa element, which is identical with the holotype of *H. tableheadensis* from the Table Head Formation of western Newfoundland (see Stouge, 1984, pl. 18, fig. 14), and the holotype of *H. holodentata* from the Pogonip Group of the Ibex area of Utah (Ethington & Clark, 1982). Four species of *Histiodella*, including *H. sinuosa* (Graves & Ellison, 1941), *H. holodentata, H. kristinae*, and *H. bellburnensis* Stouge, 1984, were recovered from the Yangjikan Section of Kalpin County, located some 50 km SW of the Dawangou section (Du *et al.*, 2005). These authors recognized four biozones defined by the first appearance of (in ascending order): *H. sinuosa* Zone, *H. holodentata* Zone, *H. kristinae* Zone, and *H. bellburnensis* Zone. The phylogenetic relationship of these species is therefore similar to that reported in Middle Ordovician successions of North America, such as from the Table Head Formation of Newfoundland. Stouge (1984, p. 18, text-fig. 17) demonstrated that the *Histiodella* lineage occurring in the Table Head Formation evolved from older species with a larger cusp and a distally declining upper margin of the anterior process, to younger species with an inconspicuous cusp and a distally raised anterior process. This same evolutionary trend among the *Histiodella* species was also documented by Du *et al.* (2005).

Histiodella infrequensa was erected by An (in An *et al.*, 1983) based on Pa elements recovered from the Beianzhuang Formation of Tangshan, Hebei Province. The holotype (An *et al.*, 1983, pl. 25, fig. 1) shows a large cusp (over three times as wide as the adjacent denticles), whereas the paratype

figured (An *et al.*, 1983, pl. 25, fig. 2) exhibits a slightly smaller cusp (about twice as wide as adjacent denticles). An's original definition suggests that *H. infrequensa* is characterized by having an outline more or less quadrilateral with the L/H ratio about 3:2 in lateral view. However, both specimens illustrated by An (in An *et al.*, 1983) had the distal part of the cusp broken. Du *et al.* (2005) reassigned to *H. holodentata* the paratype of *H. infrequensa* originally illustrated by An (An *et al.*, 1983, pl. 25, fig. 2). An (in An *et al.*, 1983) compared his *H. infrequensa* to *H. sinuosa* (Graves & Ellison, 1941) rather than to *H. holodentata*, implying that when he proposed *H. infrequensa*, An (in An *et al.*, 1983) was unaware of the existence of *H. holodentata*. In fact the holotype of *H. infrequensa* is closely comparable with the holotype of *H. holodentata* (Ethington & Clark, 1982, pl. 4, fig. 3) except that the former shows a larger cusp. Therefore, *H. infrequensa* is regarded herein as a junior synonym of *H. holodentata*, with holotype of *H. infrequensa* representing an early form of this species.

Histiodella kristinae Stouge, 1984

Fig. 14C–F

Histiodella kristinae Stouge, 1984: 87, pl. 18, figs 1–7, 9–11, fig. 17 (*cum syn.*); Dzik, 1994: 110, pl. 24, figs 28–30, text-fig. 30; Wang & Zhou, 1998: pl. 3, fig. 5; Zhang, 1998c: 72–73, pl. 9, figs 16–17 (*cum syn.*); Zhao *et al.*, 2000: 206, pl. 27, fig. 11; Rasmussen, 2001: 84, pl. 8, figs1–3, 5; Löfgren, 2004: fig. 7u; Du *et al.*, 2005: 365, pl. 1, figs 6–21; Chen *et al.*, 2006: fig. 10X–Y; Viira, 2011: fig. 9N–O.

Histiodella holodentata Ethington & Clark.–Nowlan & Thurlow, 1984: pl. 1, figs 1, 3, 5; Wang *et al.*, 1996: pl. 1, figs 12–13; Rasmussen, 2001: 82, *partim* only pl. 7, fig. 19; Löfgren, 2004: fig. 7t.

Histiodella intertexta An in An *et al.*, 1981: pl. 1, fig. 20 (*nomen nudum*); Ding *et al.* in Wang, 1993: 181, pl. 29, fig. 11.

Histiodella serrata Harris.–Landing, 1976: 633–634, pl. 1, fig. 20; Wang & Lou, 1984: 262–263, pl. 10, fig. 1, pl. 11, figs 6–7.

Histiodella sp. nov. 1 Ni, 1981: pl. 1, fig. 26.

Material. 30 specimens from one sample at the top of the Dawangou Formation (Table 2).

Remarks. *Histiodella* species are morphologically distinctive, and several including *H. kristinae*, *H. holodentata* and others have been widely used as index fossils in the Middle Ordovician of the North American Mid-Continent, Argentine Precordillera, South China, Tarim and Australasia. However, definitions of *H. kristinae* and morphologically closely related forms, like *H. holodentata*, have been interpreted rather differently by various authors. In an earlier study of this species from central New South Wales, Zhen & Percival (2004a) attempted to use the H:L ratio to distinguish *H. kristinae* (H:L ratio = 0.50–0.58) from *H. holodentata* (H:L ratio varying from 0.64 to 0.70). Subsequently more material has been made available for examination and comparison, particularly abundant specimens of both species from the Tarim Basin, which has shown that the H:L ratio is rather variable in these two species of *Histiodella*. *H. kristinae* has more recently been interpreted as having a smaller cusp with its tip lower than those of the highest denticles on the anterior process (Zhen *et al.*, 2009b, p. 38). Following this definition of *H. kristinae* (more or less as originally given by Stouge, 1984), material from allochthonous limestones in the Oakdale Formation has been re-assigned to *H. holodentata* (Percival & Zhen, 2007; Zhen *et al.*, 2009b). Other specimens previously referred to as *H. holodentata* should now also be re-assigned to *H. kristinae*, such as those illustrated by Rasmussen (2001) and Löfgren (2004). The specimen illustrated by Rasmussen (2001, pl. 7, fig. 19, from sample 69668) as *H. holodentata* seems morphologically identical with the specimen assigned to *H. kristinae* (Rasmussen, 2001, pl. 8, fig. 1). This re-assignment is consistent with the information shown in figure 26 of Rasmussen (2001), where *H. kristinae* was recorded as occurring in sample 69668 with *H. holodentata* occurring in the samples immediately below, but not in sample 69668. Löfgren (2004) illustrated both *H. holodentata* (Löfgren, 2004, fig. 7t from sample H6) and *H. kristinae* (Löfgren, 2004, fig. 7u from sample H4) in the Kårgärde section in Sweden, but these two illustrated specimens are nearly identical and can be confidently assigned to *H. kristinae*.

Histiodella intertexta was introduced by An (*in* An *et al.*, 1981) as a *nomen nudum* (Zhang, 1998c, p. 73), and the only figured specimen (designated as the holotype: An *et al.*, 1981, pl. 1, fig. 20) is rectangular in outline and identical with the type material of *H. kristinae*. However, Zhang (1998c) correctly pointed out that two specimens subsequently identified and illustrated as *H. intertexta* by An *et al.* (1985, pl. 14, figs 15–16) and An (1987, pl. 18, figs 15–16, pl. 30, fig. 10) should be reassigned to *H. holodentata*. They show a much larger cusp which, although distally broken, would extend higher than any of the denticles on the anterior process.

The holotype of *H. sinuosa* (Graves & Ellison, 1941, pl. 2, fig. 13) from the Fort Peña Formation of Texas is a broken Pa element with a large, upward-pointing cusp. Based on the studies of Bradshaw (1969) and Ethington & Clark (1982), the Pa element of *H. sinuosa* (with *H. serrata* Harris, 1962 as a junior synonym) differs from both *H. holodentata* and *H. kristinae* in having a triangular outline in lateral view with the upper margins of the longer anterior and shorter posterior processes gradually declining distally (see Bradshaw, 1969, pl. 137, fig. 24; Sweet *et al.*, 1971, pl. 1, fig. 39). Bauer (2010) treated *H. sinuosa* and *H. serrata* as separate species, indicating that small denticles were well-developed in the posterior process of the Pa element in *H. serrata* (pl. 2, fig. 16–17), but they were generally absent in the Pa element of *H. sinuosa* (pl. 2, fig. 19). Although the apparatus configuration of these two species and their ontogeny was well documented by McHargue (1982), specific identifications for some of the specimens previously assigned to either *H. serrata* or *H. sinuosa* by various other authors need to be reassessed (see synonymy list).

Parapanderodus Stouge, 1984

Type species. *Parapanderodus arcuatus* Stouge, 1984 = *Parapanderodus striatus* (Graves & Ellison, 1941) emended by Smith (1991).

Remarks. *Parapanderodus* was erected by Stouge (1984) to accommodate several coniform species characterized by a posterior groove, an unexpanded base, and fine striation

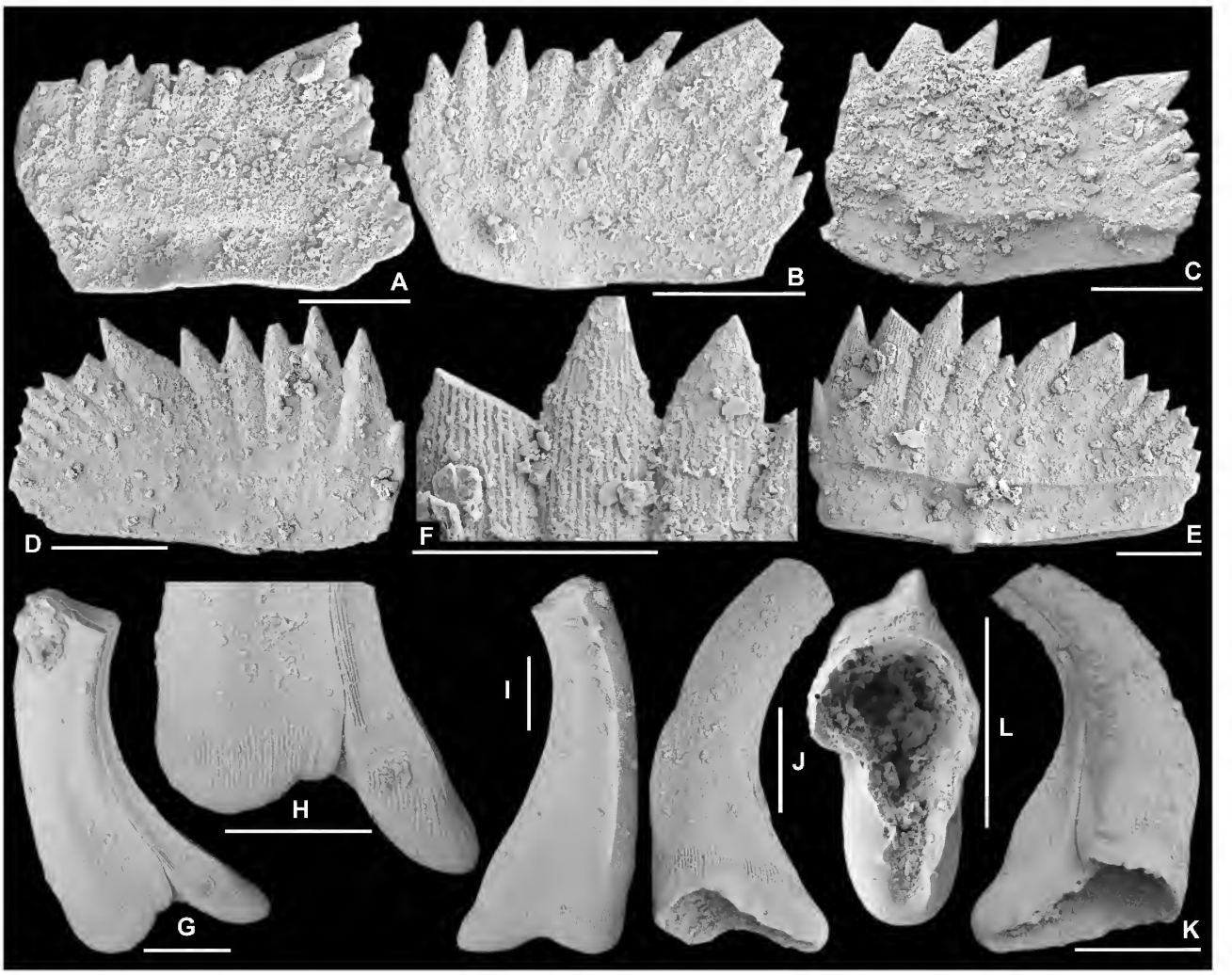

Figure 14. A–B, *Histiodella holodentata* Ethington & Clark, 1982. Pa element, ***A***, NIGP 152962, Nj296, outer lateral view (IY149-023); ***B***, NIGP 152963, Nj296, inner lateral view (IY149-024). C–F, *Histiodella kristinae* Stouge, 1984. Pa element; ***C***, NIGP 152964, AFT-X-K13/13, outer lateral view (IY163-001); ***D***, NIGP 152965, AFT-X-K13/13, inner lateral view (IY163-005); ***E–F***, NIGP 152966, AFT-X-K13/13, E, outer lateral view (IY163-003), F, outer lateral view, close up showing fine surface striation (IY163-004). G–L, *Panderodus gracilis* (Branson & Mehl, 1933). ***G–I***, tortiform element, NIGP 152967, Nj379, G, outer lateral view (IY160-024), H, outer lateral view showing furrow and fine striation on the base (IY160-025), I, inner lateral view (IY160-026). ***J–L***, falciform element, NIGP 152968, Nj379, J, inner lateral view (IY160-027), K, outer lateral view (IY160-028), L, basal view (IY160-029). Scale bars 100 μm.

on the surface. The type species *P. arcuatus* was interpreted as having two element types, but the other four species documented from the Table Head Formation of western Newfoundland—*P.* cf. *consimilis* (Moskalenko, 1973), *P. elegans* Stouge, 1984, *P. striatus* (Graves & Ellison, 1941), and *P.*? aff. *triangularis* (Ethington & Clark, 1964)—were described as form species. Stouge & Bagnoli (1988) revised the genus and considered the two species referred to *Semiacontiodus* by Stouge (1984), *S. asymmetricus* (Barnes & Poplawski, 1973) and *S. preasymmetricus* Stouge, 1984, to form part of the *P. arcuatus* species apparatus, thereby regarding *P. arcuatus* as a junior synonym of *P. asymmetricus* (Barnes & Poplawski, 1973). Subsequently however, Stouge & Bagnoli (1990, p. 21) and Bagnoli & Stouge (1997, p. 151) treated *P. arcuatus* Stouge, 1984 as a valid species.

Based on study of a large collection from Greenland including fused clusters with the occurrence of all the *Parapanderodus* species described by Stouge (1984), Smith (1991) considered all five *Parapanderodus* species, as well as *Semiacontiodus asymmetricus* (Barnes & Poplawski, 1973) and *S. preasymmetricus* Stouge, 1984, described by Stouge (1984) from the Table Head Formation, to represent a single species. Consequently Smith (1991) regarded the originally-designated type species (*P. arcuatus*) and subsequently-redesignated type species (*P. asymmetricus*) as junior synonyms of *P. striatus*, although he acknowledged that the Middle to early Late Ordovician (Whiterockian) representatives described by Barnes & Poplawski (1973) and Stouge (1984) tended to be albid. However, Ji & Barnes (1994) restricted *P. striatus* to the Early Ordovician hyaline elements. As *Parapanderodus* is only represented by a few specimens in the Dawangou material, it is impossible to re-assess the uncertainties and debates arising from the earlier work regarding to the species concept of *P. striatus*, *P. arcuatus* and *P. asymmetricus* and their taxonomic relationships. Therefore Smith's (1991) definition of *P. striatus* is followed herein until a more comprehensive revision of these related species is undertaken.

Smith (1991) erected *Toxotodus* as a coniform genus characterized by having antero-posteriorly compressed symmetrical and asymmetrical elements with a striate cusp and a very shallow or reduced basal cavity. However, the type species of *Toxotodus*, *Scolopodus carlae* Repetski, 1982 was regarded as a species of *Parapanderodus* by Stouge & Bagnoli (1988) and Ji & Barnes (1994). Considering that the species of *Toxotodus* show some rather distinctive characters that readily distinguish them from the type species of *Parapanderodus*, *Toxotodus* is considered herein as a valid genus. Consequently, several species that were assigned to *Parapanderodus* previously by various authors are here regarded as species of *Toxotodus*, such as *Parapanderodus carlae* (Repetski, 1982), and *P. retractus* Ji & Barnes, 1994, from the upper part of the St. George Group of western Newfoundland.

Parapanderodus and *Toxotodus* were sister taxa as evidenced by sharing of several distinctive characters, such as a striate cusp, a conspicuous posterior groove and a shallow basal cavity. It is likely that they are also closely related to Early Ordovician species of *Decoriconus* that, as revised by Löfgren (1998), consist of a seximembrate apparatus.

Parapanderodus striatus (Graves & Ellison, 1941) emended Smith (1991)

Fig. 15A–D

Drepanodus striatus Graves & Ellison, 1941: 11, pl. 1, figs 3, 12.

Scolopodus gracilis Ethington & Clark, 1964: 699, pl. 115, figs 2–4, 8–9; An, 1981: pl. 3, fig. 6; An *et al.*, 1985: pl. 6, fig. 6; Pohler, 1994: pl. 4, fig. 11.

Glyptoconus gracilis (Ethington & Clark).–Zhao *et al.*, 2000: 204, pl. 7, figs 4–7.

Scolopodus triangularis Ethington & Clark, 1964: 700, pl. 115, figs 6, 11, 13, 17, text-fig. 21.

Protopanderodus asymmetricus Barnes & Poplawski, 1973: 781–782, pl. 1, figs 12, 12a, 14, 16, text-fig. 2A.

Parapanderodus arcuatus Stouge, 1984: 65–66, pl. 9, figs 10–15; Pohler, 1994: pl. 4, fig. 10.

Parapanderodus elegans Stouge, 1984: 66–67, pl. 9, figs 20–27.

Parapanderodus striatus (Graves & Ellison).–Stouge, 1984: 67, pl. 10, figs 1–3; Smith, 1991: 49–52, figs 28a–f, 29a–d, 30 (*cum syn.*); Ji & Barnes, 1994: 49–50, pl. 21, figs 1–10, text-fig. 31A.

Material. Seven specimens from two samples of the Dawangou Formation (see Table 1).

Remarks. Smith (1991) defined *P. striatus* as consisting of a trimembrate apparatus represented by four form species including the s (= form species *Scolopodus gracilis* with a narrow posterior groove and *S. triangularis* with a v-shaped posterior groove), t (= form species *Protopanderodus asymmetricus*), and u (= form species *Scolopodus paracornuformis* Ethington & Clark, 1982) elements. Based on the material from the Lower Catoche Formation of the St. George Group of western Newfoundland, Ji & Barnes (1994) suggested a quadrimembrate apparatus for *P. striatus* (Graves & Ellison, 1941) including a suberect symmetrical element (referred to as the *c* element), subrounded symmetrical element (*a* element), slightly asymmetrical element (*b* element), and laterally compressed element (*e* element), which formed a symmetry transition series.

This species is rarely represented in the Dawangou Formation, and only the slightly asymmetrical element was recovered (Fig. 15A–D). These specimens are identical with those assigned by Zhao *et al.* (2000, pl. 7, figs 4–7) to *Glyptoconus gracilis* (Ethington & Clark, 1964) from the upper part of the Dawangou Formation in the Yangjikan Section of the Tarim Basin. They exhibit a prominent nonstriated rim on the base next to the basal margin, which is the characteristic feature of the form species *P. elegans* Stouge (1984, pl. 9, figs 20–27). Although most of the illustrated type specimens of this form species show a longer base than the Dawangou specimens, Stouge (1984, p. 67) indicated that the length of the base in this form species could be variable.

Periodon Hadding, 1913

Type species. *Periodon aculeatus* Hadding, 1913.

Periodon aculeatus Hadding, 1913

Fig. 16A–P

Periodon aculeatus Hadding, 1913: 33, pl. 1, fig. 14; Lindström, 1955b: 110, pl. 22, figs 10, 11, 14–16, 35; Bergström *et al.*, 1974: pl. 1, figs 4–6; Landing, 1976: 636, pl. 3, figs 3–6, 14; Löfgren, 1978: 74, pl. 10, fig. 1; pl. 11, figs 12–26, text-fig. 29 (*cum syn.*); An & Ding, 1982: pl. 4, figs 22–24; An *et al.*, 1983: 120–121, pl. 28, figs 7–9; Zeng *et al.*, 1983: pl. 12, figs 9–17; An & Xu, 1984: pl. 3, figs 1–6; Chen & Zhang, 1984b: 128, pl. 2, figs 1–7; Zhao *et al.*, 1984: 228–229, pl. 92, figs 3, 11, 17; An *et al.*, 1985: pl. 13, figs 1–14; An, 1987: 167, pl. 24, figs 7–17; Chen & Zhang, 1989: pl. 3, figs 21–26; Bergström, 1990: *partim* only pl. 1, fig. 15–16, non pl. 2, fig. 15 = *P. grandis*; Duan, 1990: pl. 3, figs 11, 17–20; Pohler & Orchard, 1990: pl. 3, fig. 3; Zhong, 1990: *partim* only pl. 19, figs 3–4, 7–8, 12, 16; Gao, 1991: 134, pl. 7, figs 10, 14–16; Zhang & Chen, 1992: pl. 1, figs 7–12; Ding *et al.* in Wang, 1993: 189–190, pl. 28, figs 1–15; Pohler, 1994: pl. 4, figs 25–27, 30–32; Chen & Bergström, 1995: pl. 6, figs 12, 15–16; Armstrong, 1997: 774–775, pl. 2, figs 13–21, text-fig. 3; Wang & Zhou, 1998: pl. 4, figs 2–4; Zhang, 1998b: 80, 81, pl. 14, figs 1–8 (*cum syn.*); Lehnert *et al.*, 1999: pl. 3, fig. 10; Ottone *et al.*, 1999: 240, text-fig. 3.8–3.11; Wang & Bergström, 1999a: 340–341, pl. 2, figs 18–19, pl. 3, fig. 11; Wang & Bergström, 1999b: pl. 2, fig. 20; Armstrong, 2000: 52, 56, pl. 6, figs 14–18, pl. 7, figs 1–6; Johnston & Barnes, 2000: 32–35, pl. 13, figs 12–13, 17–18, 20–31, pl. 14, figs 1–7, text-figs 4–5; Rasmussen, 2001: 110, pl. 13, figs 8–11 (*cum syn.*); Wang, 2001: 354, pl. 1, figs 10–11, 13, 16–22; Wang & Qi, 2001: pl. 2, figs 8–11; Norford *et al.*, 2002: pl. 2, figs 9–19; Pyle & Barnes, 2002: 107, pl. 21, figs 7–9; Pyle & Barnes, 2003: fig. 15.6–15.8; Xiong *et al.*, 2006: pl. 2, fig. 10; Bergström, 2007: 81, fig. 3K–M; Percival & Zhen, 2007: pl. 1, figs 10, 12; Ortega *et al.*, 2008: fig. 6.13; Viira, 2008: fig. 6S; Zhen *et al.*, 2009a: 145–148, figs 6A–R, 8N, 10L (*cum syn.*).

Material. Over 10406 specimens (see Tables 1–2).

Remarks. *Periodon aculeatus* is a widely distributed species and its apparatus configuration is well established. It is the dominant species in many of the samples from the Dawangou section (Tables 1, 2), and the material is morphologically identical with specimens recently documented from the basal Yenwashan Formation of western Zhejiang (Zhen *et al.*, 2009a).

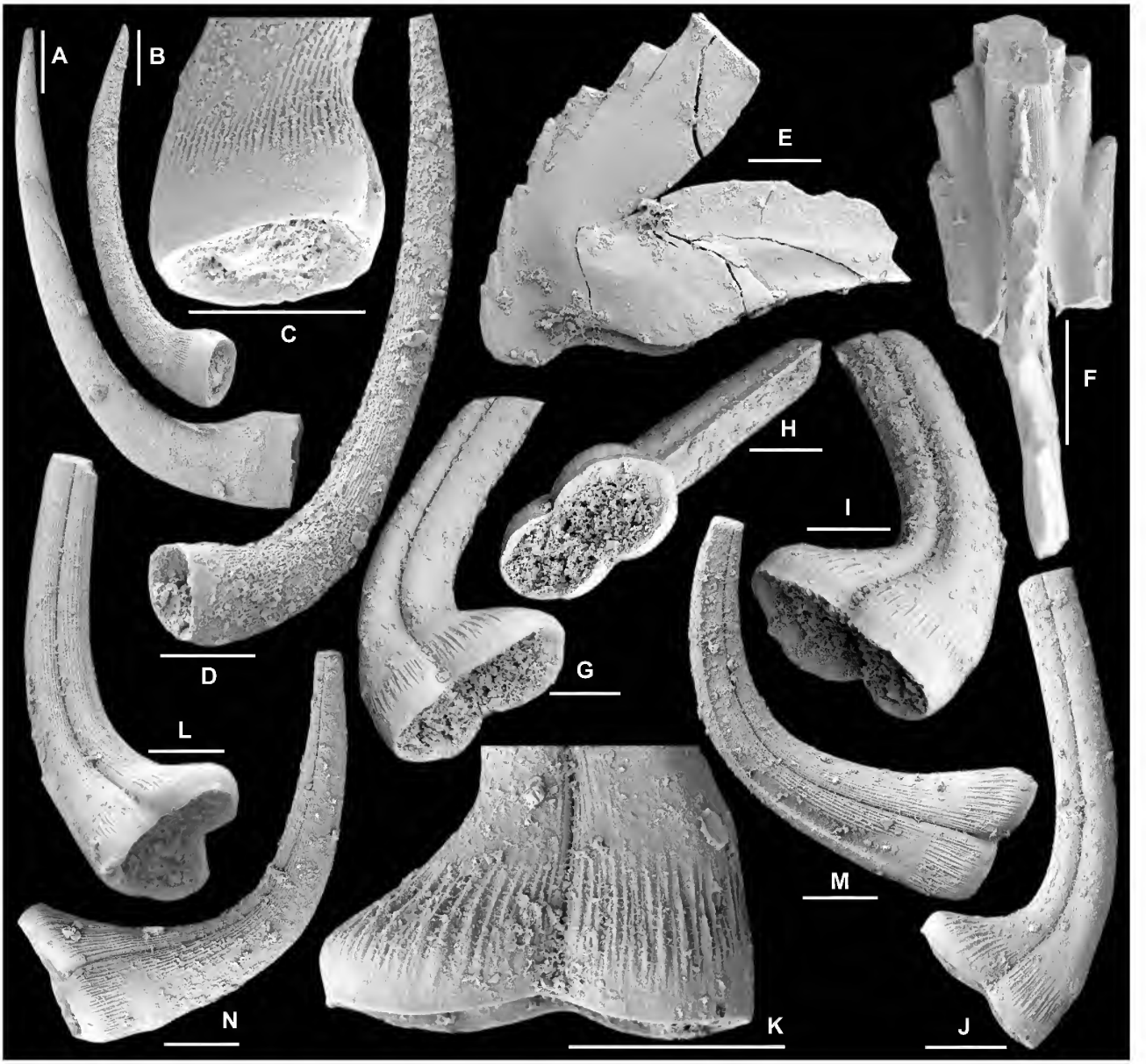

Figure 15. A–D, *Parapanderodus striatus* (Graves & Ellison, 1941). Slightly asymmetrical element; ***A***, NIGP 152969, Nj291, lateral view (IY158-013); ***B–C***, NIGP 152970, Nj297, B, lateral view (IY159-001), C, lateral view, close up showing fine surface striation (IY159-002); ***D***, NIGP 152971, Nj297, lateral view (IY159-003). E–F, *Periodon grandis* (Ethington, 1959). ***E***, M element, NIGP 152972, Nj406, anterior view (IY161-006); ***F***, Sa element, NIGP 152973, Nj406, posterior view (IY161-008). G–N, *Protopanderodus*? *nogamii* (Lee, 1975). G–K, Pa element; ***G–I***, NIGP 152974, AFT-X-K13/13, G, I, lateral views (IY167-009, IY167-011), H, basal view (IY167-010); ***J–K***, NIGP 152975, AFT-X-K13/13, J, lateral view (IY167-014), K, lateral view, close up showing striation, basal wrinkles and longitudinal furrow (IY167-015). ***L***, Sa element, NIGP 152976, AFT-X-K13/13, basal-lateral view (IY167-016). M–N, Sb element; ***M***, NIGP 152977, AFT-X-K13/13, inner lateral view (IY167-019); ***N***, NIGP 152978, AFT-X-K13/13, outer lateral view (IY167-021). Scale bars 100 μm.

The specimens illustrated as *P. aculeatus* from the Kuruktag area of the Tarim Basin by Zhong (1990) included both species, *P. aculeatus* and *P. grandis* (Zhong, 1990, pl. 19, fig. 6). The M element of *P. grandis* typically bears 5–7 denticles on the inner lateral process (Fig. 15E; Wang & Zhou, 1998, pl. 3, fig. 14), whereas only 2–4 denticles characterize the M element of *P. aculeatus* (Fig. 16A–B; also see Zhang & Chen, 1992).

Polonodus Dzik, 1976

Type species. *Ambalodus clivosus* Viira, 1974.

Remarks. Based on the pectiniform elements of the monotypic species, *Ambalodus clivosus* Viira, 1974, Dzik (1976, p. 423) provided a brief diagnosis for *Polonodus* as "conical conodonts with four lobes covered with concentric and radial rows of tubercles" having a "very large basal cavity", and illustrated three specimens showing a wide range of morphology including four-lobed (Dzik, 1976, fig. 29c), three-lobed (Dzik, 1976, pl. 43, fig. 1a–b), and an incomplete specimen with a well-developed anterior

platform (Dzik, 1976, fig. 29d). By applying a form species approach, Löfgren (1978) suggested that the Polish specimens illustrated by Dzik (1976) were not conspecific with the holotype of *P. clivosus*, and in fact they represented two species that were doubtfully included in *Polonodus* as *P.*? sp. A (= Dzik, 1976, pl. 43, fig. 1a–b) and *P.*? sp. B (= Dzik, 1976, fig. 29c–d). Stouge (1984) revised the type species, *P. clivosus*, and also named two new species (*Polonodus tablepointensis* and *P.*? *newfoundlandensis*) from the Table Head Formation of western Newfoundland. In the synonymy list of bimembrate *P. tablepointensis* he included specimens illustrated by Dzik (1976, fig. 28c–d) as *P. clivosus* and those ascribed to *P.*? sp. A and *P.*? sp. B by Löfgren (1978). Stouge (1984) then divided three species occurring in the Table Head Formation into two groups. His first group included *P. clivosus* and *P. newfoundlandensis*, with *P. tablepointensis* comprising the second group. Zhang (1998c) erected *Dzikodus* with *P. tablepointensis* as the type species, and also included M and S elements in the species apparatus of the latter.

Stouge (1984) only doubtfully considered his first group (*P. clivosus* and *P. newfoundlandensis*) as *Polonodus*, preferring to accept a generic definition based on Dzik's (1976) material from Polish erratic boulders rather than the type material of *Ambalodus clivosus* Viira, 1974. However, Löfgren (1990) argued that *P. clivosus* (Viira) might be more closely related to *P. tablepointensis* rather than *P. newfoundlandensis* as Stouge (1984) suggested.

Stouge (1984) recognized two paired pectiniform elements (polyplacognathiform and ambalodiform) in *Polonodus*. Löfgren (1990) recognized geniculate M and ramiform S (including trichnodelliform = Sa, gothodiform = Sb, and tetraprioniodiform = Sd) elements in the species apparatus of *Polonodus*. It is likely that the species apparatus might also include a modified bipennate ramiform element similar to that illustrated by Löfgren (1990, fig. 1e) to take the Sc position.

Polonodus clivosus (Viira, 1974)

Fig. 17L–M

Ambalodus n.sp. Viira, 1967: 323, fig. 3.24a–b.
Polyplacognathus n.sp. A Fåhraeus, 1970: fig. 3F–G.
Ambalodus n.sp. A Fåhraeus, 1970: fig. 3J–K.
Ambalodus clivosus Viira, 1974: 51–52, 134, pl. 8, fig. 1, text-figs 37–38.
Ambalodus? n.sp. Viira, 1974: 52, pl. 8, figs 2–3, text-fig. 39.
Polonodus clivosus (Viira).–Löfgren, 1978: 76, *partim* only pl. 16, figs 12–13; Stouge, 1984: 73, pl. 13, figs 6–13; Ding *et al.* in Wang, 1993: 191, pl. 32, figs 16, ?17.
Polonodus sp. H Ding *et al.* in Wang, 1993: *partim* only pl. 37 fig. 5.

Material. Two specimens from one sample at top of the Dawangou Formation (see Table 2).

Remarks. *Polonodus clivosus* was erected as a form species recovered from subsurface core material of Darriwilian age in the east Baltic (Viira, 1974, pl. 8, fig. 1, text-figs 37–38), and is interpreted herein as representing paired sinistral and dextral Pa (polyplacognathiform) elements. These have a node-like cusp with a row of node-like denticles extending the whole length of the longer anterior process and the short posterior process, and are also present on the inner lateral and secondary inner lateral processes. The anterior and posterior platforms of the holotype (Viira, 1974, pl. 8, fig. 1) form a gently curved outline in upper view without the outer lateral process. Specimens with four processes from the same core sample as the holotype of *P. clivosus* were referred to as *Ambalodus*? sp. n. by Viira (1974, pl. 8, figs 2–3, text-fig. 39), and are considered herein as representing the paired sinistral and dextral Pb (ambalodiform) elements of *P. clivosus*. Although Löfgren (1978) recognized that the Polish specimens from the erratic boulders accommodated in *P. clivosus* by Dzik (1976) belonged to separate species (see discussion above), her definition of *P. clivosus* also doubtfully included Newfoundland material (Table Head Formation) ascribed to *Polyplacognathus* n.sp. A and *Ambalodus* n.sp. A by Fåhraeus (1970). However, the Swedish specimens she illustrated (Löfgren, 1978, pl. 16, figs 12–13) bear a long outer lateral process, implying that the holotype of *P. clivosus* might have the outer lateral process broken off. This view was then accepted by Stouge (1984), who was the first to revise this species as consisting of a bimembrate species apparatus, but his definition of this species was largely based on the material from Newfoundland. *P. clivosus* differs from the corresponding elements of *P. newfoundlandensis* in lacking a prominent notch between the anterior process and the secondary inner lateral process of the Pa element (Stouge, 1984, pl. 13, fig. 13), and in having larger denticles on the anterior process of the Pb element (Stouge, 1984, pl. 13, fig. 11). The definition of *P. clivosus* given by both Löfgren (1978) and Stouge (1984) was also endorsed by Viira (per. comm., 2010), who confirmed that the original holotype of *P. clivosus* (Viira, 1974, specimen Cn 245, text-fig. 37, pl. 8, fig. 1) "has a broken outer lateral process which is seen clearly on the basal view".

One specimen (Fig. 17L–M) recovered from the same sample AFT-X-K13/13 in association with *P. newfoundlandensis* also had the outer lateral process broken off, and is identical with the holotype of *P. clivosus* (Viira, 1974, text-fig. 37, pl. 8, fig. 1). It differs from *P. newfoundlandensis* in lacking a prominent notch between the anterior process and the secondary inner lateral process, and in having a more prominent and laterally more compressed cusp and denticles on the anterior and posterior processes.

Polonodus newfoundlandensis Stouge, 1984

Fig. 17A–K

Polonodus newfoundlandensis Stouge, 1984: 73–74, pl. 13, figs 14–16, text-fig. 28.
Polonodus cf. *newfoundlandensis* Stouge.–Zhao *et al.*, 2000: 215, pl. 30, figs 16–17.
Polonodus kunshanensis Ding in Wang, 1993: 191, *partim*, only pl. 33, fig. 17, non figs 15, 18 = ?*Dzikodus tablepointensis*.
?*Polonodus* sp. Gao, 1991: *partim* only pl. 9, figs 8–9, ?13.

Material. 36 specimens from one sample at the top of the Dawangou Formation (Table 2).

Remarks. Stouge (1984) erected *P. newfoundlandensis* as consisting of a bimembrate apparatus including paired (in mirror image) Pa (polyplacognathiform) and paired Pb (ambalodiform) elements, and suggested that it differed from the type species, *P. clivosus* in having smaller denticles on the anterior process of the Pb element and in having a

Figure 16. *Periodon aculeatus* Hadding 1913. A–B, M element; ***A***, NIGP 152979, posterior view (IY145-001); ***B***, NIGP 152980, anterior view (IY145-002). C–E, Sa element; ***C–D***, NIGP 152981, C, anterior view (IY145-003), D, lateral view (IY145-004); ***E***, NIGP 152982, lateral view (IY145-006). F–I, Sb element; ***F–G***, NIGP 152983, F, inner lateral view (IY145-010), G, outer lateral view (IY145-013); ***H–I***, NIGP 152984, H, upper view (IY145-018), I, inner lateral view (IY145-020). J–K, Sc element; ***J***, NIGP 152985, outer lateral view (IY145-016); ***K***, NIGP 152986, inner lateral view (IY145-017). L–N, Pa element; ***L***, NIGP 152987, inner lateral view (IY145-023); ***M***, NIGP 152988, outer lateral view (IY145-024); ***N***, NIGP 152989, basal view (IY145-025N). O–P, Pb element; ***O***, NIGP 152990, outer lateral view (IY145-027); ***P***, NIGP 152991, inner lateral view (IY145-026). All from sample Nj294; scale bars 100 µm.

deeper inner notch on the anterior process. The holotype is a sinistral Pa element from the lower part of the Table Head Formation (A3, *H. holodentata* Zone) of western Newfoundland (Stouge, 1984).

Only pectiniform P elements have been recovered in our material from the Dawangou Formation. The Pa element (Fig. 17A–D) shows some features intermediate between *P. newfoundlandensis* and *P. clivosus* (Viira, 1974). It is comparable with the holotype of *P. newfoundlandensis* in having a prominent notch on the inner side of the anterior process. However, the denticle row on the anterior process of the Pa element from Dawangou is more strongly curved inner laterally than that of the holotype, a feature that is more comparable with the specimen that Stouge (1984, pl. 13, fig. 13) referred to as *P. clivosus*. The Pb element of the Dawangou material (Fig. 17E–K) is comparable with the type material in having small denticles on a narrower platform of the anterior process, but the angle between the denticle rows on the outer lateral process and the anterior process is more acute (around 50°) and the denticle row on the inner lateral process forms an acute angle with that on the posterior process (Fig. 17F) rather than a right angle as

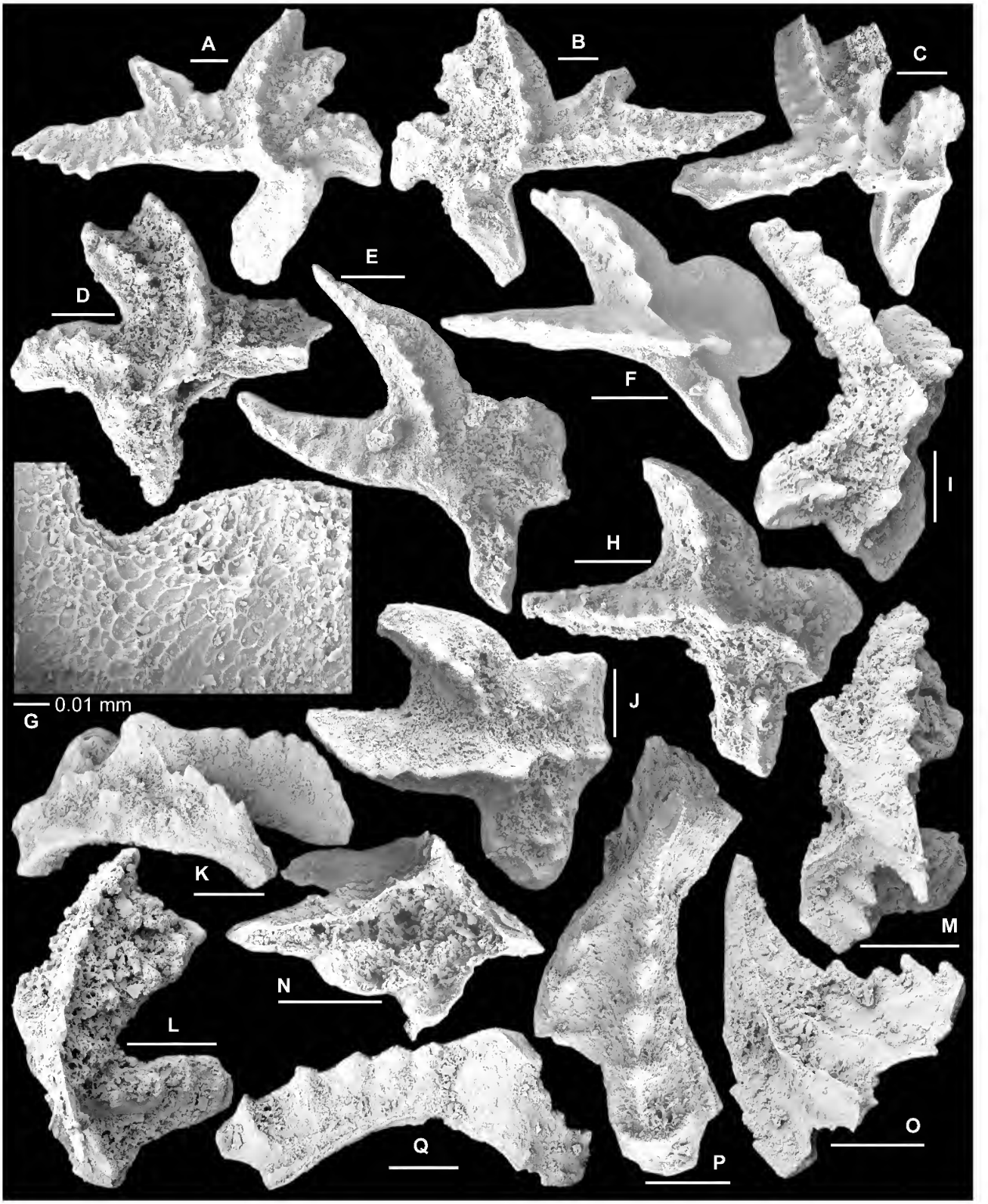

Figure 17. A–K, *Polonodus newfoundlandensis* Stouge, 1984. A–D, Pa (polyplacognathiform) element; ***A***, NIGP 152992, AFT-X-K13/13, sinistral, upper view (IY165-026); ***B***, NIGP 152993, AFT-X-K13/13, dextral, upper view (IY165-027); ***C***, NIGP 152994, AFT-X-K13/13, sinistral, upper view (IY165-031); ***D***, NIGP 152995, AFT-X-K13/13, dextral, upper view (IY165-025). E–K, dextral Pb (ambalodiform) element; ***E***, NIGP 152996, AFT-X-K13/13, upper view (IY165-032); ***F–G***, NIGP 152997, AFT-X-K13/13, F, upper view (IY165-029), G, upper view, close up showing reticulate surface structure (IY165-030); ***H–I***, NIGP 152998, AFT-X-K13/13, H, upper view (IY165-020), I, lateral view (IY165-022); ***J–K***, NIGP 152999, AFT-X-K13/13, J, upper view (IY165-021), K, lateral view (IY165-023). ***L–M***, *Polonodus clivosus* (Viira, 1974). Pa (polyplacognathiform) element, NIGP 153000, AFT-X-K13/13, L, upper view (IY163-018), M, outer lateral view (IY163-017). ***N–O***, Gen. et sp. indet. Sd element, NIGP 153001, AFT-X-K13/13, N, basal view (IY163-014), O, inner lateral view (IY163-014). ***P–Q***, *Polonodus* sp. A. ?Pb element, NIGP 153002, AFT-X-K13/13, P, upper view (IY163-008), Q, inner lateral view (IY163-009). Scale bars 100 μm, unless otherwise indicated.

in the type material (Stouge, 1984, pl. 13, fig. 15). In some of the Dawangou specimens, a weak secondary row with several low nodes may also be developed on the posterior lobe (Fig. 17J).

No ramiform S and geniculate M elements have been recognized for *P. newfoundlandensis* in the literature. However, one specimen of a quadriramate element from the same sample (AFT-X-K13/13) is nearly symmetrical, with denticulate anterior and posterior processes, and an adenticulate, blade-like costa on each lateral side. This specimen, assigned herein as gen. et sp. indet. (Fig. 17N–O), possibly represents the Sd element of *P. newfoundlandensis*.

An incomplete pectiniform specimen recovered from the same sample (AFT-X-K13/13) has a robust, laterally compressed cusp, a long anterior process with a row of node-like denticles, a short (possibly broken) posterior process, and an outer lateral process with a denticle row forming an angle of about 30° with that on the anterior process (Fig. 17P–Q). Likely a Pb element, it is morphologically different from the Pb element of *P. newfoundlandensis* associated in this sample from the top of the Dawangou Formation, and is therefore referred to herein as *Polonodus* sp. A.

The three illustrated specimens of *Polonodus kunshanensis* Ding in Wang, 1993 represent poorly preserved Pa (polyplacognathiform) elements recovered from the Guniutan Formation of Kunshan, Jiangsu Province. Zhang (1998c) considered this species to be a junior synonym of *Dzikodus tablepointensis* (Stouge, 1984). However, the holotype (Wang, 1993, pl. 33, fig. 18) is badly preserved with distal parts of the processes broken off, making its identification at the species level almost impossible. The illustrated paratype (Wang, 1993, pl. 33, fig. 15) seems comparable with the dextral Pa element of *D. tablepointensis* illustrated by Zhang (1998c, pl. 7, fig. 6) from the Guniutan Formation of Hunan Province, South China, but the other figured specimen (Wang, 1993, pl. 33, fig. 17) with the posterior process broken off can be well compared with both the material from the Dawangou Formation and the holotype of *P. newfoundlandensis* from the Table Head Formation of western Newfoundland (Stouge, 1984, pl. 13, fig. 16), in having a prominent notch between the anterior process and the secondary inner lateral process, and in having the inner lateral process posteriorly curved.

Tarim specimens illustrated as *P.* cf. *newfoundlandensis* by Zhao *et al.* (2000, pl. 30, figs 16–17) exhibit a more prominent cusp in comparison with the Dawangou material and the types from western Newfoundland.

Protopanderodus Lindström, 1971

Type species. *Acontiodus rectus* Lindström, 1955a.

Remarks. McCracken (1989) and Mellgren & Eriksson (2006) presented a comprehensive study of this genus, particularly reconstruction of the species apparatuses, and the latter revision was based on a large, well-preserved, collection of several species of *Protopanderodus* from the Swedish Middle Ordovician. Three species, *P. cooperi*, *P. graeai* and *P. calceatus*, dominate many of the Dawangou samples. Our study of the Tarim material supports, in general, the apparatus reconstruction and notation system proposed by Mellgren & Eriksson (2006), namely, the antero-posteriorly compressed M elements with a non-costate anterior face and costate or carinate posterior face, the short-based and costate P elements, and generally long-based and costate S elements that form a symmetry transition series. However, as Zhen *et al.* (2009a) suggested, material that Mellgren & Eriksson (2006) described as *Protopanderodus robustus* (Hadding, 1913) should in fact be referred to *P. cooperi*. Our current study also indicates that *Protopanderodus parvibasis* Löfgren, 1978 may be a junior synonym of *P. graeai* (see further discussion under remarks of the relevant species).

Protopanderodus calceatus Bagnoli & Stouge, 1997

Fig. 18A–Y

?Acontiodus robustus (Hadding).–Sweet & Bergström, 1962: 1222, pl. 169, fig. 11, text-fig. 11.

Protopanderodus robustus (Hadding).–Gao, 1991: 135, pl. 12, fig. 7 = Pb element.

Protopanderodus sp. cf. *varicostatus* (Sweet & Bergström).–Löfgren, 1978: 91, pl. 3, figs 26–31; McCracken, 1989: 22, 23, pl. 3, figs 1–8, fig. 3F; Stouge & Bagnoli, 1990: 23, pl. 8, figs 9–12; Rasmussen, 1991: 283, fig. 8D–E; Löfgren, 1994: fig. 7:3; Lehnert, 1995: 118, pl. 13, fig. 17, pl. 17, figs 5–6, 8–9; Norford *et al.*, 2002: pl. 3, figs 2–3; Zhen *et al.*, 2009b: 47–48, fig. 10A–O.

Protopanderodus calceatus Bagnoli & Stouge, 1997: 154–156, pl. 8, figs 13–19 (*cum syn.*); Zhang, 1998c: 82, 83, pl. 15, figs 6–13 (*cum syn.*); Wang & Bergström, 1999a: 341, pl. 1, figs 12–13; Wang & Bergström, 1999b: pl. 2, figs 3, 5; Rasmussen, 2001: 122, 124, pl. 15, figs 20–21; Mellgren & Eriksson, 2006: 108–110, figs 14, 15 (*cum syn.*).

Protopanderodus graeai (Hamar).–Ding *et al.* in Wang, 1993: *partim* only pl. 16, figs 10–11.

Protopanderodus varicostatus (Sweet & Bergström).–Wang & Lou, 1984: 278, pl. 5, figs 2–3, 7, 9–11; An *et al.*, 1985: pl. 6, fig. 5, pl. 12, figs 1–4; An, 1987: 173–174, pl. 11, figs 2–3; Duan, 1990: pl. 3, figs 27–29; Gao, 1991: 135–136, pl. 12, figs 9, 15; Ding *et al.* in Wang, 1993: 196, *partim* only pl. 16, figs 1, 5–6; Wang *et al.*, 1996: pl. 1, fig. 17; Wang, 2001: 356, pl. 1, figs 5, 7, 24, 28; Wang & Qi, 2001: pl. 1, fig. 6; Zhen *et al.*, 2004b: 157, fig. 8N–X.

Material. 247 specimens from 20 samples (see Tables 1–2).

Remarks. Bagnoli & Stouge (1997) originally defined *Protopanderodus calceatus* as consisting of a trimembrate apparatus including scandodiform, bicostate symmetrical and multicostate asymmetrical elements. Zhang (1998c) assigned the scandodiform element to the M position and differentiated the P, Sa, Sb and Sc elements. She (1998c, p. 83) suggested that *P. calceatus* could be distinguished from *P. varicostatus* by having only a weakly developed indentation of the basal margin. Mellgren & Eriksson (2006) suggested a septimembrate apparatus for *P. calceatus* including scandodiform M (differentiated as M1 and M2), bicostate (one costa each side) Sa, multicostate Sb, Sc and Sd, and short-based P (differentiated as Pa, Pb1 and Pb2) elements. Swedish material documented by Mellgren & Eriksson (2006) showed the occurrence of a bifurcated "twin" costa in the Sa, Sb, Sd and Pa elements of *P. calceatus*, but this feature is not recognized in the Dawangou material.

Specimens referred to *P. calceatus* from Dawangou are comparable with those from Sweden (Löfgren, 1978;

Bagnoli & Stouge, 1997; Mellgren & Eriksson, 2006), South China (Zhang, 1998c) and New Zealand (Zhen *et al.*, 2009b). *P. calceatus* is interpreted as consisting of a septimembrate apparatus with Sa (Fig. 18G–J) and Sb (Fig. 18K–L) elements represented by bicostate (one lateral costa on each side) symmetrical and slightly asymmetrical forms respectively (Fig. 18G–J, K–L), with Sc (Fig. 18M–P), Pa (Fig. 18T-V) and Pb (Fig. 18X–Y) elements represented by multicostate strongly asymmetrical forms (one costa on the outer lateral face and two costae separated by a groove on the inner lateral face), and with the Sd element represented by the multicostate weakly asymmetrical form (two costae separated by a groove on each lateral face, Fig. 18Q–S). The Pa element with a rounded antero-basal corner and the Pb element with a more or less quadrate outline in lateral view differ from the S elements in having a shorter base. The M elements have a gently curved basal margin and a prominent shallow groove on the posterior face located more towards the inner-lateral margin (Fig. 18A–F), and can be further differentiated into M1 without additional costa (Fig. 18 A–E) and M2 with a broad mid costa (or several costae) on the posterior face (Fig. 18F). These two morphotypes of the M element were also represented in the type material of early Darriwilian age from Sweden with the holotype comparable with the M2 morphotype (Bagnoli & Stouge, 1997; pl. 8, fig. 18), and also are present in the Guniutan Formation of South China (Zhang, 1998c, pl. 15, fig. 12 =M1, fig. 13 =M2).

Before *P. calceatus* was formally established, Stouge & Bagnoli (1990) and other authors followed Löfgren (1978) who referred to specimens informally as *Protopanderodus* cf. *varicostatus* (see synonym list). This assignment conveyed the fact that these species were closely similar to each other. In fact, Löfgren (1978) did a detailed study on this form and noted the highly variable nature of *P.* cf. *varicostatus*. She suggested that the elements were very similar to those of *P. varicostatus*, except that the symmetrical elements were not represented in her material from Jämtland of northern Sweden. This is also true in the specimens from the Dawangou section in that the element with two costae on each side is weakly asymmetrical and is assigned herein to the Sd position (Fig. 18Q–S).

Protopanderodus calceatus resembles *P. varicostatus* in having two costae separated by a groove on one or both sides of some constituent elements. The symmetrical element (=Sa herein) represented by a paratype (Bagnoli & Stouge, 1997; pl. 8, fig. 15) is clearly a bicostate element with a postero-laterally located costa on each lateral face. The symmetrical element (=Sa herein) of *P. varicostatus* as represented by the holotype (Sweet & Bergström, 1962; pl. 168, fig. 8) is apparently multicostate with two costae separated by a groove on each lateral face. Re-examination of topotype material of *P. varicostatus* from the Pratt Ferry Formation of Alabama has convinced us that this and *P. calceatus* represent separate species. *P. varicostatus* has multicostate S and P elements characterized by having a strongly curved basal margin with a distinctive indentation near the antero-basal corner and often with an anticusp-like extension similar to that of *P. cooperi*. Differing from those of *P. varicostatus*, the Sa and Sb elements of *P. calceatus* have the costa bordering the posterior side of the groove varying from weakly developed (Mellgren & Eriksson, 2006; fig. 14C, N) to nearly absent (Fig. 18I), and the costa bordering the anterior side of the groove being more posteriorly directed. These bicostate forms were often assigned to *P. robustus* by some authors (see synonymy list). Moreover, the basal margin of the M element of *P. calceatus* is generally less strongly curved (Fig. 18A–F), and the P elements of *P. calceatus* are strongly asymmetrical with two costae separated by a groove only on the inner lateral face (Fig. 18V, X), and the outer lateral face is ornamented with a postero-lateral costa (Fig. 18T, U, Y).

Protopanderodus cooperi (Sweet & Bergström, 1962)

Figs 19A–R, 20A–E

Acontiodus cooperi Sweet & Bergström, 1962: 1221–1222, pl. 168, figs 2, 3, text-fig. 1G; Burrett *et al.*, 1983: 180, fig. 9E; Wang & Lou, 1984: 249, pl. 5, figs 12–13, 16, 18, pl. 11, fig. 1; Bergström, 1990: pl. 2, fig. 9.

Scandodus sp. Sweet & Bergström, 1962: 1246, pl. 168, figs 13, 16.

Protopanderodus cooperi (Sweet & Bergström).–Chen & Zhang, 1989: pl. 4, figs 23–25; An & Zheng, 1990: *partim* only pl. 6, fig. 13, not fig. 14 = *P. varicostatus*; Gao, 1991: 135, pl. 12, fig. 6; Ding *et al.*, in Wang, 1993: 194–195, pl. 16, figs 7–9; Wang *et al.*, 1996: pl. 1, figs 22–23; Zhang, 1998c: 81, 82, pl. 14, figs 13–17 (*cum syn.*); Wang, 2001: 354–355, pl. 1, fig. 14; Wang & Qi, 2001: pl. 8, fig. 8; Pyle & Barnes, 2003: fig. 15.33; Zhen & Percival, 2004b: 170, fig. 11C–F; Zhen *et al.*, 2004b: 155, fig. 8A–E; Zhen *et al.*, 2009a: 148–150, fig. 7A–S (*cum syn.*); Zhen *et al.*, 2009b: 47, fig. 10S.

Protopanderodus gradates Serpagli.–Ortega *et al.*, 2008: fig. 6.32.

Protopanderodus rectus (Lindström).–Zhao *et al.*, 2000: 217–218, pl. 21, figs 1–17; Wang, 2001: 355–356, pl. 1, fig. 23.

Protopanderodus robustus (Hadding).–Löfgren, 1978: 94–95, *partim*, only pl. 3, figs 32–33; Pohler & Orchard, 1990: pl. 1, fig. 17; Rasmussen, 2001: 125, pl. 16, figs 5–8; Mellgren & Eriksson, 2006: 106–108, figs 9H–N, 13A–K.

Protopanderodus parvibasis Löfgren.–Mellgren & Eriksson, 2006: 104–105, *partim* only fig. 11A, H.

Material. 1076 specimens from 39 samples (see Tables 1–2).

Remarks. *Acontiodus cooperi* was erected as a form species based on the symmetrical acontiodiform element. The holotype (Sweet & Bergström, 1962, pl. 168, figs 2–3) has a suberect cusp with a postero-lateral costa on each side, a moderately extended base with a sinuous basal margin, and a prominent anticusp-like antero-basal extension. Specimens originally assigned to *Scandodus* sp. by Sweet & Bergström (1962, p. 1246, pl. 168, figs 13, 16) are likely to represent the M position of *P. cooperi*, which was recently revised as a multielement taxon consisting of a septimembrate apparatus including scandodiform M element, bicostate short-based P element, and bicostate longer-based S elements forming a symmetry transition series (Mellgren & Eriksson, 2006; Zhen *et al.*, 2009a). However, the development of the anticusp-like extension varies amongst the constituent elements of *P. cooperi* from the same fauna and also amongst various faunas reported. For instance, this feature is strongly developed in the holotype and in some specimens reported from the Yenwashan Formation of South China (Zhen *et al.*, 2009a, fig. 7M) and from the Tarim Basin (Zhao *et al.*, 2000, pl. 21, figs 2, 6), but is less strongly developed in the material from the Dawangou section (Fig. 19). Generally it is more strongly developed in the S elements (Fig. 19D, H, K), and

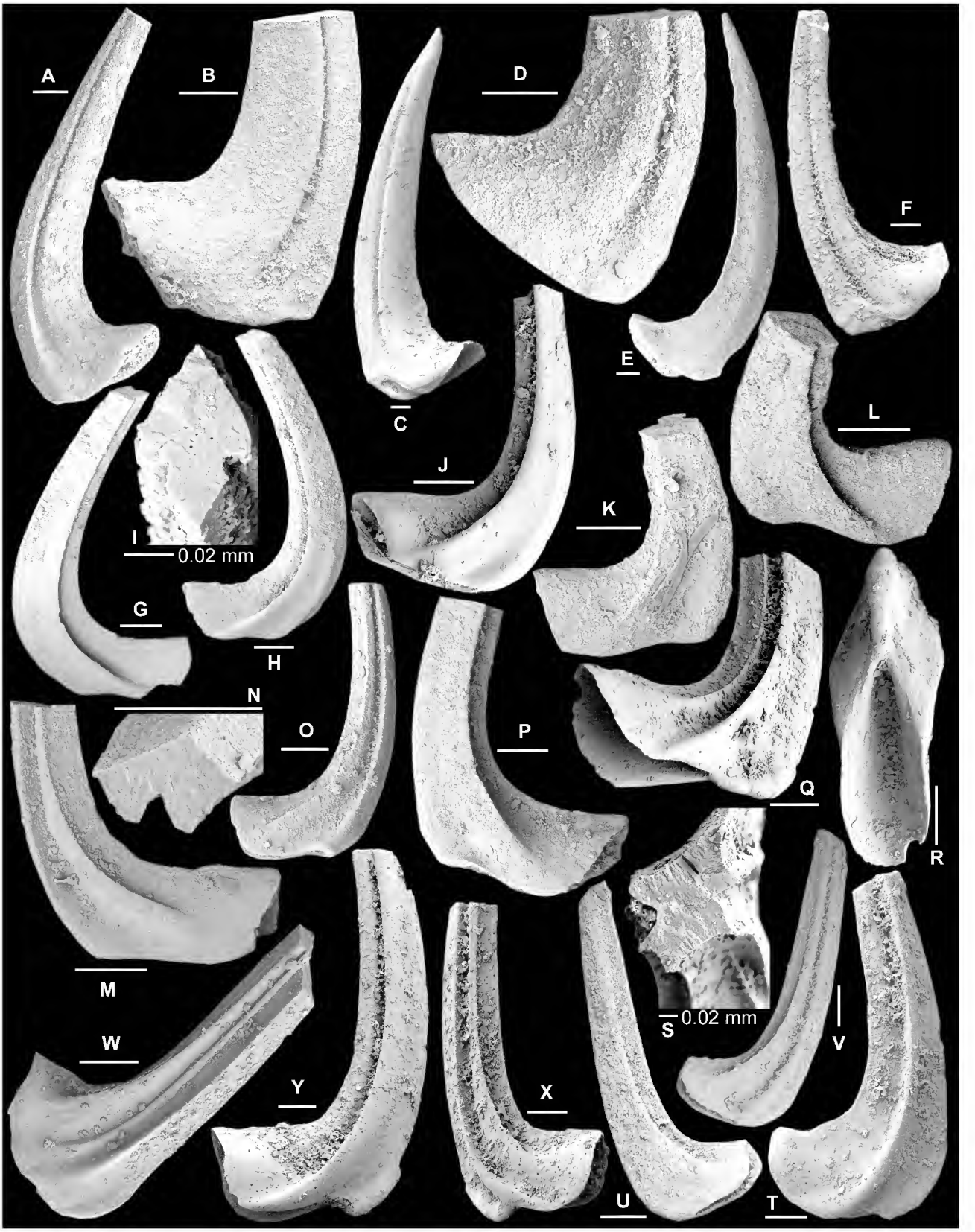

Figure 18. *Protopanderodus calceatus* Bagnoli & Stouge, 1997. A–E, M1 element; ***A***, NIGP 153003, Nj297, posterior view (IY150-016); ***B***, NIGP 153004, Nj295, posterior view (IY149-012); ***C***, NIGP 153005, AFT-X-K13/13, posterior view (IY168-007); ***D***, NIGP 153006, Nj296, posterior view (IY149-029); ***E***, NIGP 153007, AFT-X-K13/13, anterior view (IY168-008). ***F***, M2 element, NIGP 153008, AFT-X-K13/13, posterior view (IY168-006). G–J, Sa element; ***G–I***, NIGP 153009, Nj297, G, H, lateral views (IY162-022, IY162-018), I, upper view showing cross section of cusp (IY162-021); ***J***, NIGP 153010, AFT-X-K13/13, lateral view (IY168-013). ***K–L***, Sb element, NIGP 153011, Nj294, K, inner lateral view (IY147-020), L, outer lateral view (IY147-021). M–P, Sc element; ***M–N***, NIGP 153012, Nj294, M, inner lateral view (IY147-022), N, upper view showing cross section of cusp (IY147-023)… (caption continued on facing page)

less so in the P (Fig. 19N, R) and M (Fig. 19A–B) elements. Two topotypes of *P. cooperi* from the Pratt Ferry Formation of Alabama are illustrated herein (Fig. 20A–E) for detailed comparison. They represent the M (Fig. 20A–C) and weakly asymmetrical Sb (Fig. 20D–E) elements, and are identical with specimens from the Dawangou section (Fig. 19), and material from the Yenwashan Formation of South China (Zhen *et al.*, 2009a, fig. 7). The types and topotypes of *P. cooperi* mostly have a basal funnel attached (see Sweet & Bergström, 1962; pl. 168, figs 2, 3), and the base often shows a recessive basal margin (Fig. 20B), which is also preserved in some specimens from the Dawangou section (Fig. 19F–I).

Protopanderodus cooperi is widely distributed in North America (Sweet & Bergström, 1962), Australia (Burrett *et al.*, 1983; Zhen *et al.*, 2004), New Zealand (Zhen *et al.*, 2009b), South China (Chen & Zhang, 1989; Wang *et al.*, 1996; Zhang, 1998c; Zhen *et al.*, 2009a), North China (Wang & Lou, 1984), Tarim (Zhao *et al.*, 2000; Wang & Qi, 2001; this study), and Europe (Löfgren, 1978; Rasmussen, 2001; Mellgren & Eriksson, 2006). Although *P. cooperi* is readily distinguished from other species of *Protopanderodus* by having an anticusp-like extension at the antero-basal corner and an undulating basal margin of the bicostate P and S elements, it was considered by various authors as a junior synonym of a number of *Protopanderodus* species that are less well documented. Zhao *et al.* (2000) regarded P. *cooperi* as a junior synonym of *P. rectus* Lindström, 1955a. The type material of the latter from the Lower Ordovician (Floian) of Sweden shows a curved basal margin with development of a weak extension at the antero-basal corner (Lindström, 1955a, pl. 2, figs 7–11). This character was also well-documented by material included in *P. rectus* from Sweden, such as Löfgren (1978, pl. 3, figs 1–2), Rasmussen (2001, pl. 16, figs 1–4), and Mellgren & Eriksson (2006, fig. 8E, H, fig. 9D–G). As evidenced by this and other shared characters of these two species, it is likely that *P. cooperi* evolved from its direct ancestor (and also stratigraphically older species) *P. rectus* (Rasmussen, 2001, p. 125). Stouge (1984, p. 52) considered *Acontiodus cooperi* Sweet & Bergström, 1962 as the senior synonym of *Scolopodus varicostatus* Sweet & Bergström, 1962, representing the symmetrical acontiodiform element of a single species apparatus, and suggested that *A. cooperi* could only be differentiated from the latter by "having one pair of lateral costae". However, Landing (1976) regarded *P. varicostatus* as a junior synonym of *P. cooperi*. The specimens that he illustrated as *P. cooperi* should be excluded from this species. In fact one of the specimens is multicostate (Landing, 1976, pl. 4, fig. 6) and the other is likely a drepanodiform element (Landing, 1976, pl. 4, fig. 7).

Löfgren (1978, p. 94–95) indicated that many of her specimens assigned to *P. robustus* (Hadding, 1913) developed "an antero-basal 'hook' as in the acondiodiform elements described as *Acontiodus cooperi* by Sweet & Bergström (1962)". One of her illustrated specimens (Löfgren, 1978, pl. 3, fig. 33) is comparable with the holotype of *P. cooperi* (Sweet & Bergström, 1962, pl. 168, figs 2–3). Rasmussen (2001) and Mellgren & Eriksson (2006) followed the concept of *P. robustus* given by Löfgren (1978), and the Swedish material that they described and illustrated as *P. robustus* are identical both with the types of *P. cooperi* and with material from the Dawangou section (this study, Fig. 19) and from South China (Zhang, 1998c; Zhen *et al.*, 2009a).

The holotype of *P. robustus* was re-illustrated and described in detail by Lindström (1955b, pl. 22, fig. 1). It is a symmetrical element with a suberect cusp and a short, non-expanded base, and has a sharp anterior and posterior margins and more than one lateral costa (one major postero-lateral costa and two shorter minor costae) on each side. Bergström (2007, p. 81) also indicated that the holotype of *P. robustus* "possesses several small but distinct lateral costae". It is certain that *P. robustus* is a species of *Protopanderodus* (Bergström, 2007) rather than a species of *Drepanodus* (Dzik, 1994; Armstrong, 2000), but it seems more closely related to multicostate species like *Protopanderodus calceatus* rather than to bicostate *P. cooperi*. However, as Hadding's (1913) type material is preserved in shale, and the published illustrations are drawings only, *P. robustus* remains as a poorly known species until detailed taxonomic revision of the type material can be undertaken.

Protopanderodus graeai (Hamar, 1966)

Fig. 21A–V

Acontiodus rectus Lindström.–Hamar, 1964: 258, pl. 1, figs 10, 12, 13, 17, text-fig. 4a–b.
Acodus graeai Hamar, 1966: 47, pl. 3, figs 11–14, text-fig. 3.5.
Protopanderodus graeai (Hamar).–Löfgren, 1978: 93–94, pl. 3, figs 19–25, text-fig. 31K–M (*cum syn.*); Mellgren & Eriksson, 2006: 105–106, figs 9V–BB, 12 (*cum syn.*).
Protopanderodus parvibasis Löfgren, 1978: 93, pl. 3, figs 11–18, text-fig. 31D–F (*cum syn.*); Mellgren & Eriksson, 2006: 104–105, figs 9O–U, 11 (*cum syn.*).
Protopanderodus robustus (Hadding).–Wang, 2001: 356, pl. 1, figs 3–4.

Material. 1249 specimens from 18 samples (see Tables 1–2).

Diagnosis. A species of *Protopanderodus* with a septimembrate apparatus; all the elements having an erect or suberect cusp and a short, non-expanded base, except for the Sb element bearing a longer base; M element with acostate anterior and posterior faces; S and P elements bearing a sharp posterior margin and a postero-lateral costa on each side, except for the strongly asymmetrical Sc element only having a sharp postero-lateral costa on the inner lateral side; basal margin straight or gently arched except for the Pb element.

Description. M element scandodiform, antero-posteriorly strongly compressed; cusp suberect in posterior or anterior view and curved posteriorly, with sharp inner and outer lateral margins; anterior face smooth and gently convex; posterior face less convex, varying from smooth to bearing a broad carina; basal margin straight (Fig. 21A–C).

(Figure 18 caption, continued from facing page)... ***O***, NIGP 153013, Nj296, inner lateral view (IY149-025); ***P***, NIGP 153014, Nj296, outer lateral view (IY149-026). Q–S, Sd element; ***Q–R***, NIGP 153015, AFT-X-K13/13, Q, lateral view (IY168-016), R, basal view (IY168-017); ***S***, NIGP 153016, Nj378, upper view showing cross section of cusp (IY160-012). T–V, W, Pa element; ***T***, NIGP 153017, AFT-X-K13/13, outer lateral view (IY168-012); ***U–V***, NIGP 153018, Nj295, U, outer lateral view (IY149-022); V, inner lateral view (IY149-021); ***W***, NIGP 153019, Nj384, outer lateral view (IY162-014), tentatively assigned to this species. X–Y, Pb element; ***X***, NIGP 153020, AFT-X-K13/13, inner lateral view (IY168-009); ***Y***, NIGP 153021, AFT-X-K13/13, outer lateral view (IY168-010). Scale bars 100 μm, unless otherwise indicated.

Figure 19. *Protopanderodus cooperi* (Sweet & Bergström, 1962). A–B, M element; ***A***, NIGP 153022, Nj376, posterior view (IY159-030); ***B***, NIGP 153023, Nj376, posterior view (IY159-033). C–G, Sa element; ***C–D***, NIGP 153024, Nj297, C, basal view (IY147-014), D, lateral view (IY147-015); ***E–G***, NIGP 153025, AFT-X-K13/13, E, basal view (IY168-020), F–G, lateral views (IY168-021, IY168-022). H–I, Sb element; ***H***, NIGP 153026, AFT-X-K13/13, outer lateral view (IY168-032); ***I***, NIGP 153027, AFT-X-K13/13, inner lateral view (IY168-029). J–M, Sc element; ***J***, NIGP 153028, AFT-X-K13/13, outer lateral view (IY168-034); ***K–M***, NIGP 153029, Nj294, K, inner lateral view (IY147-017), L, outer lateral view (IY147-019), M, upper view, close up showing cross section of the cusp (IY147-018). ***N–O***, Pa element, NIGP 153030, AFT-X-K13/13, N, inner lateral view (IY169-023), O, basal view (IY169-024). P–R, Pb element; ***P***, NIGP 153031, AFT-X-K13/13, antero-outer lateral view (IY168-018); ***Q***, NIGP 153032, AFT-X-K13/13, inner lateral view (IY168-030); ***R***, NIGP 153033, AFT-X-K13/13, inner lateral view (IY169-029). Scale bars 100 µm.

Figure 20. A–E, *Protopanderodus cooperi* (Sweet & Bergström, 1962), from the Pratt Ferry Formation of Alabama. ***A–C***, M element, OSU 52802, from the topotype locality, A–B, posterior views (IY170-024, IY170-025), C, anterior view (IY171-011). ***D–E***, Sb element, OSU 52803, from the topotype locality, D, outer lateral view (IY171-012), E, inner lateral view (IY170-023). F–L, *Protopanderodus varicostatus* (Sweet & Bergström, 1962); from the Pratt Ferry Formation of Alabama. ***F–H***, M2 element, OSU 52804, topotype, sample 64B2-12 from the top bed of the formation, F–G, posterior views (IY170-002, Iy170-001), F, anterior view (IY171-015); ***I–J***, M2 element, OSU 52805 from the topotype locality, I, posterior view (IY170-007), J, anterior view (IY171-018). K–L, M1 element, OSU 52806, topotype, sample 64B2-12 from the top bed of the formation, K, posterior view (170-026), L, anterior view (IY171-013). Scale bars 100 μm.

Sa element symmetrical; cusp suberect with a sharp posterior margin and a posterolateral costa on each side (Fig. 21D–G). Sb element like Sa, but asymmetrical, and often with a longer base, and with costa on the outer lateral face more strongly developed and located more towards posterior margin (Fig. 21H–J). Sc element strongly asymmetrical with a convex, smooth outer lateral face and a less convex inner lateral face; cusp suberect with a sharp posterior margin and a sharp posterolateral costa on the inner lateral face (Fig. 21K–P). Sd element nearly symmetrical, with a sharp posterior margin and a sharp posterolateral costa on each side; similar to Pa element, but less asymmetrical (Fig. 21Q–R).

Pa element asymmetrical, with a convex outer lateral face and a less convex (or even concave) inner lateral face to form sharp anterior and posterior margins, and with a gently arched basal margin; cusp suberect with a strongly developed sharp postero-lateral costa on the outer lateral face and a only weakly developed costa on the inner lateral face, costa on the outer lateral face more towards posterior margin (Fig. 21S–T). Pb element slightly asymmetrical; cusp erect with a sharp posterior margin and a sharp postero-lateral costa on each side; basal margin strongly curved with anterior portion and the posterior portion nearly normal to each other, forming a rectangular outline of the base (Fig. 21U–V).

Remarks. In their recent revision of this species, Mellgren & Eriksson (2006) referred the strongly asymmetrical element (herein designated as Sc) to the M position, and split the Sb element defined herein into Sb1, Sb2, and Sc elements. They also assigned the M element (as defined herein) to the M element of *P. cooperi* (referring to it as *P. robustus*; see Mellgren & Eriksson, 2006, fig. 13E), and to the M element of *P. parvibasis*.

The Sc element of *P. graeai* is morphologically more closely related to the other S and the P elements of this species (by its size and location of the postero-lateral process on the

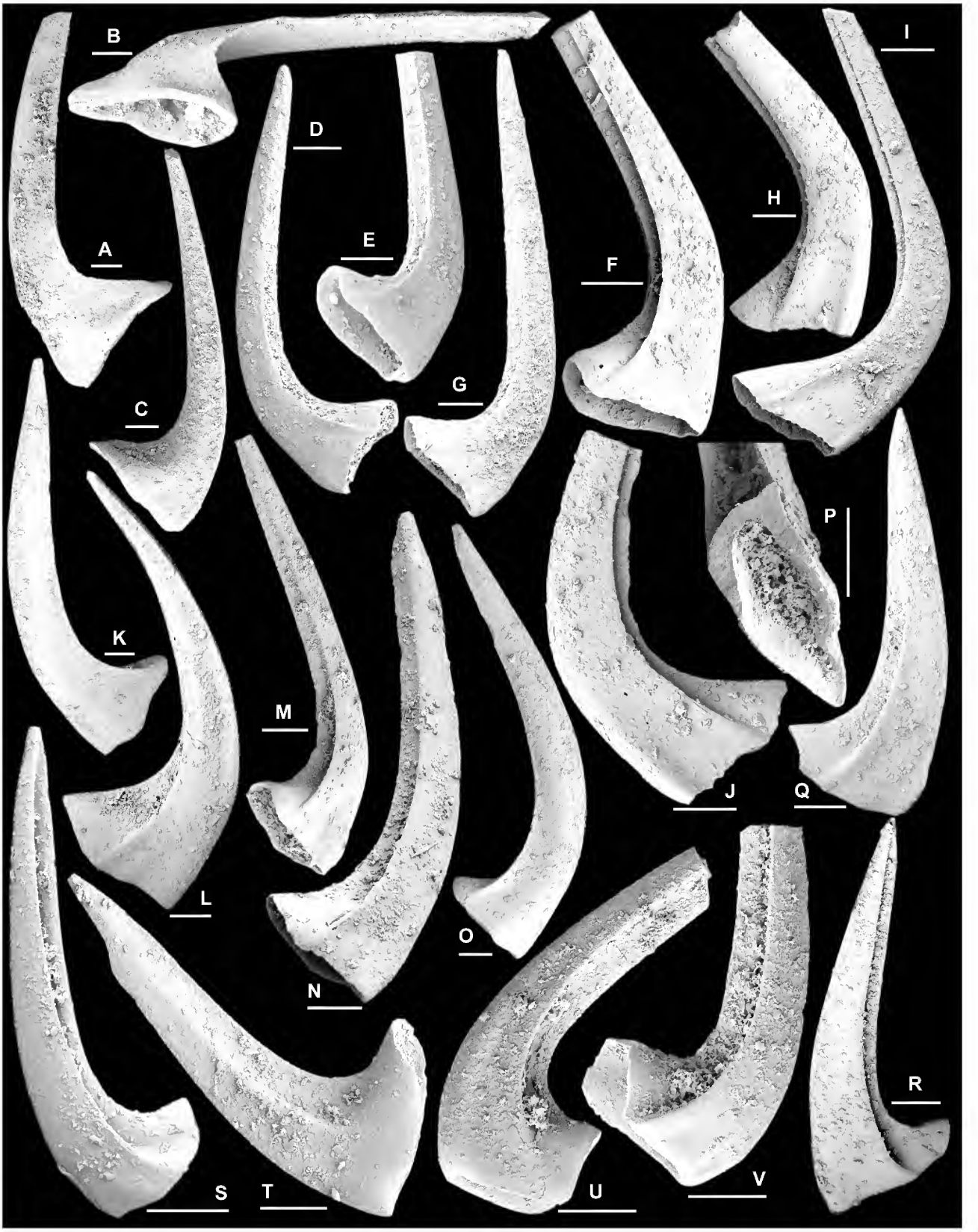

Figure 21. *Protopanderodus graeai* (Hamar, 1966). A–C, M element; ***A–B***, NIGP 153034, A, anterior view (IY167-045), B, basal-posterior view (IY167-044); ***C***, NIGP 153035, posterior view (IY169-006). D–G, Sa element; ***D***, NIGP 153036, lateral view (IY168-001); ***E–F***, NIGP 153037, E, basal-lateral view (IY168-003), F, lateral view (IY168-002); ***G***, NIGP 153038, lateral view (IY167-030). H–J, Sb element; ***H***, NIGP 153039, outer lateral view (IY167-036); ***I***, NIGP 153040, outer lateral view (IY167-029); ***J***, NIGP 153041, inner lateral view (IY167-037). K–P, Sc element; ***K–L***, NIGP 153042, K, outer lateral view (IY167-038), L, inner lateral view (IY167-039); ***M***, NIGP 153043, inner lateral view (IY167-032); ***N***, NIGP 153044, inner lateral view (IY167-033); ***O***, NIGP 153045, outer lateral view (IY167-035); ***P***, NIGP 153046, basal view (IY169-002). ***Q–R***, Sd element, NIGP 153047… (continued on facing page)

inner surface), and is also rather different from the M elements recognized in other species of *Protopanderodus,* which are generally larger than the P and S elements and strongly compressed antero-laterally. The M element of *P. graeai* defined herein is comparable with the M element of *P. cooperi*, but the latter characteristically has a sinuous basal margin and a prominent anticusp-like basal extension (Fig. 19; also see Zhang, 1998c, pl. 14, figs 13–17; Mellgren & Eriksson, 2006, fig. 13A–D, F–K). *P. graeai* differs from *P. cooperi* in having a straight basal margin and in lacking the anticusp-like antero-basal corner; it is distinguished from the bicostate elements of *P. calceatus* in having a less expanded base.

The long-based element assigned to the Sb1 and Sb2 position by Mellgren & Eriksson (2006) is only rarely represented in our collection from the Dawangou section (Fig. 21I).

Löfgren (1978) originally defined *P. parvibasis* as having a trimembrate apparatus including symmetrical and asymmetrical bicostate elements, and an acostate scandodiform element. The holotype of this species is a scandodiform element (Löfgren, 1978, pl. 3, fig. 18) bearing a suberect cusp with a faintly developed groove near the inner lateral margin on the posterior face and a short base with straight basal margin. It is morphologically closely related to M elements of the associated species *P. cooperi* and *P. calceatus*. Löfgren (1978, p. 93) suggested that the asymmetrical bicostate element of *P. parvibasis* was difficult to distinguish from the corresponding elements of other *Protopanderodus* species, and could only be differentiated by its shallower basal cavity, and differed from the corresponding element of *P. graeai* by having "the apex of the basal cavity placed more centrally". These minor differences between *P. graeai* and *P. parvibasis* may be recognizable in the well-preserved Swedish material, but are of little use when dealing with less well preserved specimens with a higher CAI.

Detailed comparison between *P. parvibasis* and *P. graeai* using the recently revised and illustrated Swedish material (Mellgren & Eriksson, 2006) and our collections indicates that most likely these represent only one species. Elements referable to both species are well represented among our material from Tarim, but we had extreme difficulty in distinguishing one from the other. Close examination of the *P. parvibasis* specimens illustrated by Mellgren & Eriksson (2006, fig. 11A, 11H) suggests that their Sb1 and Sb2 elements should be reassigned to *P. cooperi*, and all the other figured specimens except the M element (Mellgren & Eriksson, 2006, fig. 11D, 11I) are identical with those illustrated by them as *P. graeai*. However, if we consider the M element of *P. graeai* defined by Mellgren & Eriksson (2006) to represent the Sc position of this species, and the M element of *P. parvibasis* as defined by Mellgren & Eriksson (2006) to represent the M position in the *P. graeai* apparatus, and further combining the Sb1, Sb2 and Sc elements of Mellgren & Eriksson (2006) as the Sb element of *P. graeai*, then *P. parvibasis* becomes a junior synonym of *P. graeai*. These two species also have similar stratigraphical ranges (Mellgren & Eriksson, 2006, fig. 10).

Protopanderodus liripipus Kennedy, Barnes & Uyeno, 1979

Fig. 23C–E

Protopanderodus liripipus Kennedy, Barnes & Uyeno, 1979: 546–550, pl. 1, figs 9–19; An, 1981: pl. 3, fig. 29; An *et al.*, 1981: pl. 1, figs 16–17; An & Ding, 1982: pl. 2, figs 4, 13; Zeng *et al.*, 1983: pl. 12, fig. 34; An & Xu, 1984: pl. 1, fig. 21; Chen & Zhang, 1984b: 129, pl. 2, figs 22–24; Wang & Lou, 1984: 278, pl. 8, figs 6–10; An *et al.*, 1985: pl. 12, figs 5–9; An, 1987: 173, pl. 11, figs 4, 11–14; Ding, 1987: pl. 5, fig. 28; Chen & Zhang, 1989: pl. 4, figs 26, ?27; McCracken, 1989: 18–20, pl. 3, figs 15–16, 18, 20–25, text-fig. 3G–J (*cum syn.*); An & Zheng, 1990: pl. 6, figs ?5, 9–10; Bergström, 1990: pl. 2, figs 7–8, pl. 4, figs 1–4; Duan, 1990: pl. 3, figs 2, 4; Gao, 1991: 135, pl. 12, fig. 8; Ding *et al.* in Wang, 1993: 195, pl. 38, fig. 17; Trotter & Webby, 1994: 485, pl. 4, figs 2–6; Zhen *et al.*, 1999: 92, fig. 9.10–9.13 (*cum syn.*); Leslie, 2000: 1125, fig. 6.19–6.24; Zhao *et al.*, 2000: 217, pl. 20, figs 1–2, 5, 7, 10–13; Pyle & Barnes, 2001: pl. 2, figs 6–7; Wang, 2001: pl. 1, fig. 12; Wang & Qi, 2001: pl. 1, figs 5, 22; Agematsu *et al.*, 2007: 29, fig. 13.4, 13.5, 13.8, 13.10 (*cum syn.*); Agematsu *et al.*, 2008a: 969, fig. 12.23–12.28.

Material. 12 specimens from two samples of the upper Kanling Formation (see Table 1).

Remarks. *P. liripipus* was originally interpreted as a quadrimembrate apparatus including the scandodiform element (= M element herein) and a transition series of protopanderodiform (symmetrical = Sa, slightly asymmetrical = Sb, and strongly asymmetrical = Sc) elements, with the holotype representing the Sa element (Kennedy *et al.*, 1979, pl. 1, fig. 14), from the Tetagouche Group (upper Sandbian) at Camel Back Mountain in New Brunswick, Canada. This species was defined as having an extended and distally tapering base with the scandodiform element bearing a narrow groove near the inner lateral margin on the posterior face, the symmetrical and slightly asymmetrical elements bearing two costae separated by a groove on each side, and the strongly asymmetrical element bearing two costae on one side and one costa on the other. Some specimens among the illustrated types which have a shorter and lower base (Kennedy *et al.*, 1979, pl. 1, figs 16–17) are defined herein as representing the P positions. Amongst the type material the short-based P elements showed symmetry variations. The short-based P elements have also been reported from Australia (Trotter & Webby, 1994, pl. 4, fig. 4), North China (An & Zheng, 1990, pl. 6, fig. 10) and from the Tarim Basin (Gao, 1991, pl. 12, fig. 8; Zhao *et al.*, 2000, pl. 20 figs 10, 13; this study, Fig. 23C–D). Therefore, *P. liripipus* is considered herein as consisting of a seximembrate or septimembrate apparatus. Zhen *et al.* (1999, fig. 9.10–9.11) illustrated a Sc element that was strongly asymmetrical with a smooth outer lateral face and a costa-bounded deep groove on the inner lateral face.

Wide variations of the S elements in respect of the number of costae and their positions on the lateral faces were observed by Kennedy *et al.* (1979) among the type material,

(Figure 21 continued from facing page)... Q, inner lateral view (IY167-040), R, outer lateral view (IY167-041). S–T, Pa element; ***S***, NIGP 153048, outer lateral view (IY167-023); ***T***, NIGP 153049, inner lateral view (IY167-024). U-V, Pb element; ***U***, NIGP 153050, inner lateral view (IY167-028); ***V***, NIGP 153051, outer lateral view (IY167-026). All from sample AFT-X-K13/13; scale bars 100 μm.

Figure 22. *Protopanderodus varicostatus* (Sweet & Bergström, 1962); from the Pratt Ferry Formation of Alabama. ***A–C***, Sa element, OSU 52807, from the topotype locality, A–B, lateral views (IYIY170-010, IY171-019), C, upper view showing cross section of cusp (IY170-012). ***D–E***, Sb element, OSU 52808, from the topotype locality, D, inner lateral view (IY171-021), E, outer lateral view (IY170-017). ***F–G***, Pa element, OSU 52809, topotype, sample 64B2-12 from the top bed of the formation, F, inner lateral view (IY170-029), G, outer lateral view (IY171-016). H–M, Sc element; ***H–I***, OSU 52810, from the topotype locality, H, outer lateral view (IY170-018), I, inner lateral view (IY171-022); ***J–K***, OSU 52811, from the topotype locality, J, inner lateral view (IY170-020), K, outer lateral view (IY171-023); ***L–M***, OSU 52812, from the topotype locality, L, inner lateral view (IY170-021)… (continued on facing page)

but none of the illustrated S elements in the type collection showed the development of an anticusp-like extension on the antero-basal corner, as do those specimens documented from Australia (Trotter & Webby, 1994, pl. 4, fig4 1, 5), Tarim (Gao, 1991, pl. 12, fig. 8), South China (e.g., Chen & Zhang, 1984b, pl. 2, fig. 22; An *et al.*, 1985, pl. 12, figs 5–7; Ding *et al.* in Wang, 1993, pl. 38, fig. 17), and Malaysia (Agematsu *et al.*, 2008a). Further study of these forms with a prominent anticusp-like extension may lead to the conclusion that they represent a separate species, which was more closely related to *P. cooperi-P. rectus*, while *P. liripipus* might be derived from the multi-costate *P. calceatus-P. varicostatus* group, which formed a separate lineage more closely related to *P. gradatus* Serpagli, 1974 (see McCracken, 1989, fig. 2).

Protopanderodus varicostatus (Sweet & Bergström, 1962)

Figs 20F–L, 22A–R

Scolopodus varicostatus Sweet & Bergström, 1962: 1247–1248, pl. 168, figs 4–9, text-fig. 1A, C, K.

Scandodus unistriatus Sweet & Bergström, 1962: 1245, pl. 168, fig. 12, text-fig. 1E.

Protopanderodus varicostatus (Sweet & Bergström).–Bergström *et al.*, 1974: pl. 1, figs 9–10; An *et al.*, 1983: 132, pl. 16, figs 9–12; Burrett *et al.*, 1983: 184, fig. 9C, D; Fåhraeus & Hunter, 1985: 183, text-fig. 2; Dzik, 1994: 74, pl. 14, figs 1–5, text-fig. 11b; Zhang, 1998b: 83, 84, pl. 15, figs 14–19 (*cum syn.*); Lehnert *et al.*, 1999: pl. 2, fig. 16, pl. 3, fig. 14; Zhen & Percival, 2004b: 172–175, fig. 12A–M (*cum syn.*); Xiong *et al.*, 2006: pl. 2, fig. 22; Ortega *et al.*, 2008: fig. 6.20–6.21; Zhen *et al.*, 2009a: 151, fig. 8B–I.

Protopanderodus sp. cf. *calceatus* Bagnoli & Stouge.–Zhen & Percival, 2004a: 102–104, partim only figs 17A–J, M–S, not K–L.

Protopanderodus gradates Serpagli.–Ding *et al.* in Wang, 1993: 196, *partim* only pl. 16, figs 14, 16.

Material. 18 topotype specimens recovered from two samples (sample at topotype locality and sample 64B2–12 at the top bed) of the Pratt Ferry Formation of Alabama (see Sweet & Bergström, 1962).

Diagnosis. A multicostate species of *Protopanderodus* consisting of a septimembrate apparatus including scandodiform M, longer-based S (Sa, Sb, Sc, and Sd) and short-based P (Pa and Pb) elements; all elements bearing a suberect and distally reclined cusp, and a slightly expanded base with a shallow basal cavity and a strongly curved basal margin, which shows a characteristic indentation near the antero-basal corner and often an anticusp extension at the antero-basal corner in the S and P elements.

Description. M element scandodiform, antero-posteriorly compressed, asymmetrical with a suberect to reclined cusp and a rather extended base with a strongly curved basal margin (Fig. 20F–L); cusp with a smooth and convex anterior face (Fig. 20H, J, L) and costate posterior face (Fig. 20F–G, I, K). Two morphological variants are recognized based on development of costae on the posterior face: M1 element bearing a shallow groove on the posterior face more towards inner-lateral margin (Fig. 20K) with least development of the costae; M2 element bearing one or more costae to the outer-lateral side of the groove on the posterior face (Fig. 20 F–G, I).

Sa element symmetrical and multicostate (Fig. 22 A–C) with a suberect cusp and a long, non-expanded base; cusp laterally compressed with costate anterior and posterior margins, and two sharp costae separated by a narrow groove on each lateral face; basal margin sharply curved with posterior portion nearly normal to the anterior portion, and with a well-developed indentation near the antero-basal corner (Fig. 22A–B).

Sb element like Sa but asymmetrical, with more convex outer lateral face (Fig. 22E) and with sharp anterior margin slightly curved inner laterally (Fig. 22D).

Sc element strongly asymmetrical and multicostate (Fig. 22H–M) with a suberect cusp and a long, non-expanded base; cusp laterally compressed with sharply costate anterior and posterior margins, a sharp costa on the inner lateral face (Fig. 22 I, J, L), and two costae separated by a groove on the more convex outer lateral face (Fig. 22H, K, M); anterior margin slightly curved inner laterally.

Sd element weakly asymmetrical and multicostate (Fig. 22N–O) with a suberect cusp and a long, posteriorly curved base; cusp laterally compressed with sharply costate anterior and posterior margins; each lateral face ornamented with a prominent groove with a strong, sharp costa forming its anterior border and two less well-developed costa forming its posterior border; outer lateral face slightly more convex; anterior margin thin and slightly inner laterally curved, and forming a long blade-like anticusp projecting downward.

Pa element weakly asymmetrical and multicostate (Fig. 22F–G) with a suberect cusp and a short base; cusp laterally compressed with thin and sharply costate anterior and posterior margins; each lateral face ornamented with a prominent groove bordered by a strong costa on each side; anterior margin slightly curved inner laterally and forming a rounded antero-basal corner; basal margin strongly curved posteriorly, with the indentation near the antero-basal corner only weakly developed or even absent.

Pb element like Pa, but with a more or less quadrate outline of the base in lateral view (Fig. 22P–R) with well-developed indentation of the basal margin near the antero-basal corner to form a small, but prominent anticusp; anterior margin straight or only slightly curved and more or less perpendicular to the anterior portion of the basal margin (Fig. 22P, R).

Remarks. Sweet & Bergström (1962) proposed the species as consisting of a trimembrate apparatus including the bilaterally symmetrical (= Sa herein) element represented by the holotype (Sweet & Bergström, 1962; pl. 168, fig. 8), the slightly asymmetrical element represented by two illustrated paratypes that are interpreted herein as the Pb element (Sweet & Bergström, 1962; pl. 168, fig. 6) and the Sb element

(Figure 22 continued from facing page)... M, outer lateral view (IY171-007). ***N–O***, Sd element, OSU 528013, from the topotype locality, N, inner lateral view (IY170-016), O, outer lateral view (IY171-020). P–R, Pb element; ***P–Q***, OSU 528014, topotype, sample 64B2-12 from top bed of the formation, P, outer lateral view (IY171-014), Q, inner lateral view (IY170-027); ***R***, OSU 528015, topotype, sample 64B2-12 from the top bed of the formation, outer lateral view (IY171-017). Scale bars 100 μm, unless otherwise indicated.

Figure 23. A–B, *Venoistodus balticus* Löfgren, 2006. M element; ***A***, NIGP 153052, Nj296, posterior view (IY158-034); ***B***, NIGP 153053, Nj296, posterior view (IY158-032). C–E, *Protopanderodus liripipus* Kennedy, Barnes & Uyeno, 1979. C–D, P element (low based); ***C***, NIGP 153054, Nj406, inner lateral view (IY161-013); ***D***, NIGP 153055, Nj406, outer lateral view (IY161-014). ***E***, Sa element, NIGP 153056, Nj406, lateral view (IY155-010). F–L, *Protopanderodus* sp. ***F–G***, Sa element, NIGP 153057, Nj297, lateral views (IY150-027, IY150-026). H–I, Sc element; ***H***, NIGP 153058, Nj297, inner lateral view (IY150-028); ***I***, NIGP 153059, Nj297, inner lateral view (IY150-029). ***J–L***, Sb element, NIGP 153060, Nj296, J, outer lateral view (IY149-032), K, inner lateral view (IY149-031), L, basal view (IY149-030). M–N, *Pseudooneotodus mitratus* (Moskalenko, 1973). Pa element; ***M***, NIGP 153061, Nj375, upper view (IY159-022); ***N***, NIGP 153062, AFT-X-K13/44, upper view (IY164-029). O–P, *Spinodus spinatus* (Hadding, 1913). Sc element; ***O***, NIGP 153063, Nj406, outer lateral view (IY161-001); ***P***, NIGP 153064, Nj406, inner lateral view (IY161-002). Scale bars 100 μm.

(Sweet & Bergström, 1962; pl. 168, fig. 7), and the markedly asymmetrical (= Sc herein) element. As indicated by their choice of species name, Sweet & Bergström (1962) noted a wide variation in respect of the number and disposition of the lateral costae.

Protopanderodus varicostatus, characterized by strongly multicostate elements, was widely distributed and many variants or closely related forms have been described as *P.* sp. cf. *varicostatus* or *P.* sp. cf. *calceatus* (e.g., Zhen & Percival, 2004a). However, in the most of the material we studied previously, multicostate species of *Protopanderodus* comprised only a minor component of the faunas, which hindered a better understanding of variations, thereby sometimes leading to inconsistencies in interpretation of the species apparatus. Therefore, a close comparison of *P. varicostatus* and *P. calceatus* is essential to resolve this taxonomic uncertainty. For this purpose, the topotype material of *P. varicostatus* was re-examined and documented herein (see discussion under *P. calceatus*). We now suspect that material described as *P.* cf. *varicostatus* from a limestone lens exposed on Kirkup Station of central New South Wales may represent a separate species (Zhen & Pickett, 2008). These resemble specimens described as *P.* cf. *calceatus* from allochthonous limestones in the Oakdale Formation of central New South Wales (Zhen & Percival, 2004a) in having a broad anterior margin of the Sa element. The Oakdale specimens with multicostate S and P elements showing an indentation on the base are comparable with *P. varicostatus*, but some of

the figured specimens have a relatively shorter base without indentation (Zhen & Percival, 2004a, fig. 17K–L), suggesting they may not belong to this species. The Kirkup species is similar to both *P. varicostatus* and *P. calceatus* in having multicostate elements in the apparatus, but these elements have a less extended base (Zhen & Pickett, 2008, fig. 10J) and its bicostate Sa element has a broad anterior face (Zhen & Pickett, 2008, fig. 10 A–E), whereas the bicostate Sa element of *P. calceatus* (Fig. 18G–J) and multicostate Sa element of *P. varicostatus* (Fig. 22A–C) have a sharp anterior margin.

Pseudooneotodus Drygant, 1974a

Type species. *Oneotodus*? *beckmanni* Bischoff & Sannemann, 1958.

Pseudooneotodus mitratus (Moskalenko, 1973)

Fig. 23M–N

Ambalodus mitratus mitratus Moskalenko, 1973: 86, pl. 17, figs 9–11.

Ambalodus mitratus nostras Moskalenko, 1973: 87, pl. 17, figs 12–14, ?15.

Pseudooneotodus mitratus (Moskalenko).–Orchard, 1980: 25, pl. 3, figs 35, 42; Nowlan & Barnes, 1981: 23, pl. 2, figs 17–19; Nowlan, 1983: 667, pl. 3, figs 17, 21; Chen & Zhang, 1989: pl. 4, fig. 29; Pohler & Orchard, 1990: pl. 6, fig. 12; Dzik, 1994: 55, pl. 11, fig. 7; Zhen & Webby, 1995: 285, pl. 4, figs 16–17 (*cum syn.*); Zhang, 1998c: 85, pl. 14, fig. 12; Zhen *et al.*, 1999: fig. 9.14–9.15; Leslie, 2000: 1139, fig. 5.37 (*cum syn.*); Sweet, 2000: fig. 9.7; Pyle & Barnes, 2001: 1396, 1398, pl. 2, fig. 13; Zhen *et al.*, 2003a: fig. 6Q; Zhen *et al.*, 2004b: fig. 9A; Zhen & Pickett, 2008: 79, fig. 9A–B (*cum syn.*).

Pseudooneotodus mitratus mitratus (Moskalenko).–Zhao *et al.*, 2000: 219, pl. 43, figs 19, 23.

Pseudooneotodus mitratus nostras (Moskalenko).–Zhao *et al.*, 2000: 219, pl. 43, figs 20–22, 24–25.

Material. Nine specimens from five samples (see Tables 1–2).

Remarks. This species, characterized by a trilobate basal outline, is a very minor component of the Dawangou fauna, comparable to its rarity in various faunas from New South Wales (Zhen & Webby, 1995; Zhen *et al.*, 1999; Zhen *et al.*, 2003a; Zhen *et al.*, 2004b; Zhen & Pickett, 2008). Nowlan & Barnes (1981) and Nowlan (1983) regarded the two subspecies originally erected by Moskalenko (1973), *A. mitratus mitratus* and *A. mitratus nostras*, as constituent elements of a single species apparatus, and recognized a symmetry transition series among its elements. Although *P. mitratus* was a widely distributed species, its relative rarity in many faunas has hindered a formal reconstruction of its species apparatus in the literature. From our experience, the two morphotypes represented by Moskalenko's (1973) two subspecies are often found co-occurring, but forms with nodes on the upper surface are much rarer and have not been recovered in the Dawangou samples.

The broad-conical morphotype of *Pseudooneotodus triangulus* Chen & Zhang, 1984b is similar to *P. mitratus* in having a triangular outline in upper view, but the former species has the three processes more extended with a tendency to form a secondary ridge splitting from the posterior process (Chen & Zhang, 1984b, pl. 2, figs 25–26).

Pygodus Lamont & Lindström, 1957

Type species. *Pygodus anserinus* Lamont & Lindström, 1957.

Remarks. Most Ordovician conodont workers accept that species of *Pygodus* consisted of a seximembrate or septimembrate apparatus including pygodiform Pa, pastinate Pb, ramiform S (alate Sa, tertiopedate Sb, bipennate Sc and quadriramate Sd), and possibly geniculate M elements (Zhang, 1998a; Rasmussen, 2001; Zhen *et al.*, 2009a, table 2). The M elements of the two *Pygodus* species (*P. anserinus* and *P. serra*) occurring in the Dawangou section have not been recovered, although the Pa, Pb and S elements of both species were represented by a large collection (Tables 1–2). Very rare reports of a geniculate M element occurring in association with other elements of *Pygodus* have cast doubts on the inclusion of the M element in the *Pygodus* species apparatus (Dzik, 1994; Zhen *et al.*, 2009a). Armstrong (1997, 2000) provided an alternative reconstruction for *P. anserinus* and *P. serra*, interpreting the *P. anserinus* species apparatus to include a pygodiform Pa with four rows of denticles and a pygodiform Pb element with three rows of denticles, the latter generally considered by other workers as representing the Pa element of P. *serra* (Zhang, 1998a).

Pygodus anserinus Lamont & Lindström, 1957

Fig. 24A–P

Pygodus anserinus Lamont & Lindström, 1957: 67, pl. 5, figs 12–13, Fig. 1a–c (non d); Bergström, 1971: 149, pl. 2, figs 20, 21; Bergström *et al.*, 1974: pl. 1, figs 16–17; Harris *et al.*, 1979: pl. 3, figs 16–17, pl. 4, fig. 17; An & Ding, 1982: pl. 5, figs 15, 17, 18; Chen *et al.*, 1983: pl. 1, figs 5, 6; Zeng *et al.*, 1983: pl. 12, figs 4, 22; Chen & Zhang, 1984b: 130, pl. 2, figs 18–21; Wang & Luo, 1984: 279, pl. 11, figs 10, 19, pl. 12, figs 14; An *et al.*, 1985: pl. 17, figs 7–9; An, 1987: 176–177, pl. 26, figs 9–12, 14; Ding, 1987: pl. 5, fig. 8; Ni & Li, 1987: 435, pl. 59, fig. 26; Chen & Zhang, 1989: 222–223, pl. 5, figs 3–5; An & Zheng, 1990: pl. 14, figs 1, 2, 5, 6; Pohler & Orchard, 1990: pl. 2, fig. 20; Zhong, 1990: 152, pl. 16, figs 17, 18, pl. 20, 13, 15; Bergström, 1990: pl. 1, figs 19–22; Gao, 1991: 136, pl. 10, figs 6–12; Ding *et al.*, in Wang, 1993: 198, pl. 35, figs 22, 23, 25; Dzik, 1994: 105, 106, pl. 17, figs 7, 8, text-figs 26, 27; Armstrong, 1997: 777–778, *partim* only pl. 4, figs 1–3, 5–7, non fig. 4 = *P. serra*; Bednarczyk, 1998: pl. 2, figs 4, 16; Wang & Zhou, 1998: pl. 2, figs 5–8, 13; Zhang, 1998a: pl. 3, figs 1–8, text-fig. 2E; Zhang, 1998b: 87–88, pl. 16, figs 1–5 (*cum syn.*); Lehnert *et al.*, 1999: pl. 3, fig. 6; Zhao *et al.*, 2000: 220, pl. 30, figs 1–4, 19–21; Rasmussen, 2001: 127–127, pl. 16, figs 13–17 (*cum syn.*); Wang, 2001: pl. 2, figs 5–6, 10, 13–15, 17–18, 20–26 (*cum syn.*); Wang & Qi, 2001: pl. 2, figs 19, 21, 25, 26; Pyle & Barnes, 2003: fig. 13.8–13.10; Xiong *et al.*, 2006: pl.1, figs 17, 19; Agematsu *et al.*, 2007: 25, fig. 9.1–9.4; Bergström, 2007: fig. 3A; Ortega *et al.*, 2008: fig. 6.11; Viira, 2008: fig. 6O; Zhen *et al.*, 2009a: 152–157, figs 8N, 9A–I, 10A–L (*cum syn.*); Bergström, 2007: fig. 3A–B.

Pygodus serrus-anserinus transition.–An & Zheng, 1990: pl. 14, figs 3, 4; Zhao *et al.*, 2000: 221, *partim*, only pl. 30, fig. 6; Xiong *et al.*, 2006: pl. 1, fig. 14.

Pygodus serrus (Hadding).–Zhong, 1990: 152, pl. 20, *partim* only, fig. 17.

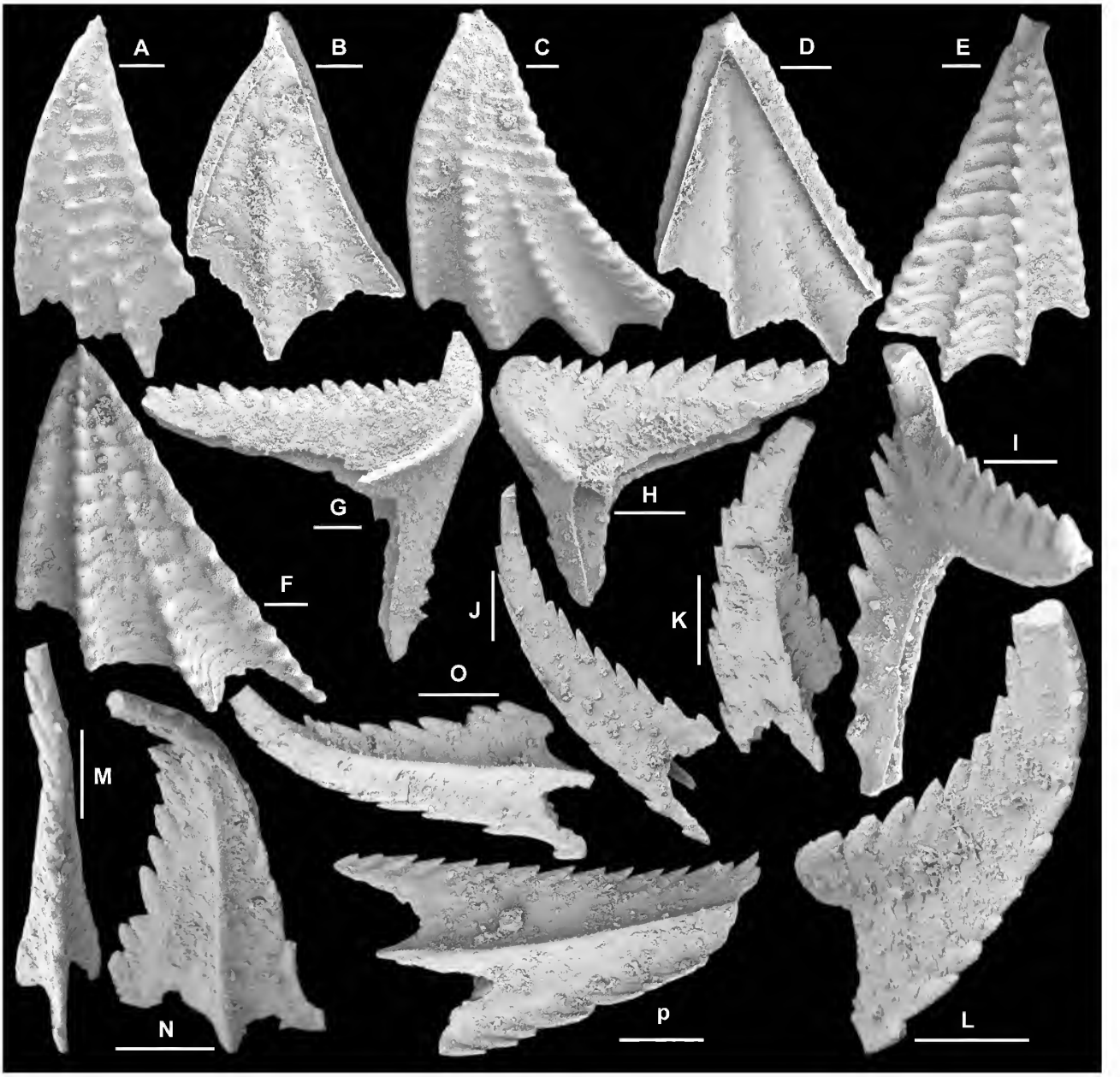

Figure 24. *Pygodus anserinus* Lamont & Lindström, 1957. A–F, Pa element; ***A***, NIGP 153065, Nj276, upper view (IY152-022); ***B***, NIGP 153066, Nj276, basal view (IY152-023); ***C***, NIGP 153067, Nj388, upper view (IY155-002); ***D***, NIGP 153068, Nj388, basal view (IY155-003); ***E***, NIGP 153069, Nj379, upper view (IY154-004); ***F***, NIGP 153070, Nj389, upper view (IY155-004). G–I, Pb element; ***G***, NIGP 153071, Nj378, outer lateral view (IY153-015); ***H***, NIGP 153072, Nj376, basal-outer lateral view (Iy153-001); ***I***, NIGP 153073, Nj376, inner lateral view (IY153-002). ***J***, Sa element, NIGP 153074, Nj376, lateral view (IY153-003). ***K–L***, Sb element, NIGP 153075, Nj377, K, outer lateral view (IY153-012), L, inner lateral view (IY153-013). M–P, Sd element; ***M–O***, NIGP 153076, Nj376, M, posterior view (IY153-006), N, inner lateral view (IY153-007), O, outer lateral view (IY153-008); ***P***, NIGP 153077, Nj379, outer lateral view (IY154-008). Scale bars 100 μm.

Material. 1816 specimens plus 1518 specimens of undifferentiated Pb and S elements of both *P. anserinus* and *P. serra* (see Tables 1–2).

Remarks. *P. anserinus* differs from the slightly older or contemporaneous *P. serra* in having four rows of denticles on the platform of the Pa element (Bergström, 2007; Zhen *et al*., 2009a). The fourth row of denticles inserted between the middle row and the inner row of the Pa element in *P. anserinus* is variably developed in transitional forms from *P. serra* to *P. anserinus*. The lowest occurrence of *Pygodus* in the Dawangou section was recorded in sample Nj375 near the top of the Saergan Formation, where the early form of *P. anserinus* (with the fourth row of denticles represented by a few weakly developed nodes near the distal margin of the platform) is associated with *P. serra*.

Morphologically, *P. anserinus* and *P. serra* can only be differentiated from each other by their Pa elements. When the two species are co-occurring as in the upper part of the Saergan Formation and in the lower part of the Kanling Formation, it is difficult or nearly impossible to tell the differences between Pb and S elements of these two species

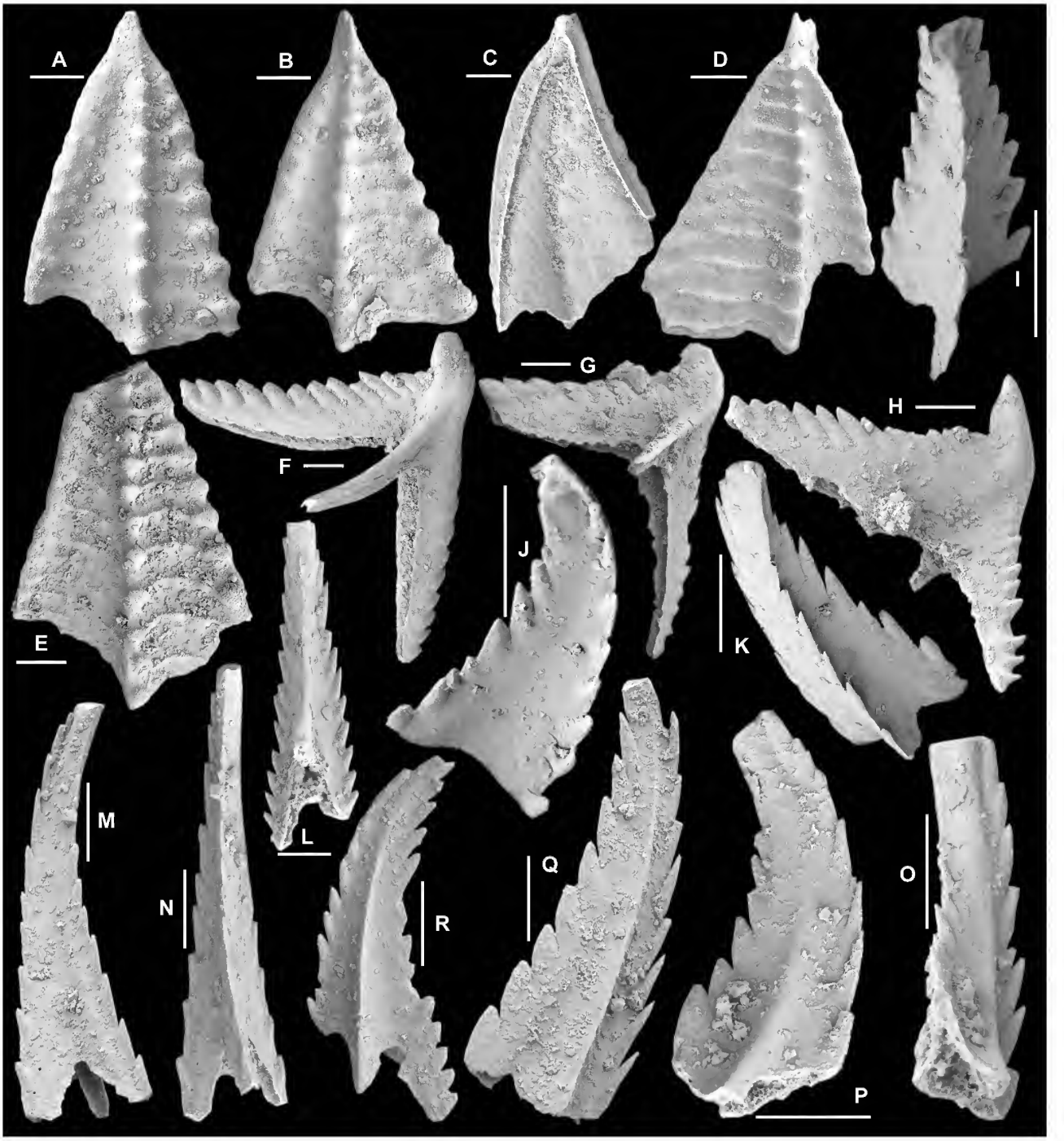

Figure 25. *Pygodus serra* (Hadding, 1913). A–E, Pa element; ***A***, NIGP 153078, 13/40, upper view (IY155-018); ***B***, NIGP 153079, Nj375, upper view (IY151-016); ***C***, NIGP 153080, Nj375, basal view (IY151-010); ***D***, NIGP 153081, Nj375, upper view (IY151-014); ***E***, NIGP 153082, 13/40, upper view (IY155-019). F–H, Pb element; ***F***, NIGP 153083, 13/40, outer lateral view (IY155-020); ***G***, NIGP 153084, Nj375, outer lateral view (IY151-017); ***H***, NIGP 153085, Nj375, inner lateral view (IY151-018). I–L, Sa element; ***I–K***, NIGP 153086, Nj375, I, posterior view (IY151-015), J, lateral view (IY151-020), K, antero-lateral view (IY151-22); ***L***, NIGP 153087, Nj375, posterior view (IY152-001). ***M–N***, Sb element, NIGP 153088, Nj375, M, lateral view (IY152-005), N, posterior view (IY152-006). ***O–P***, Sc element, NIGP 153089, Nj375, O, posterior view (IY152-009), P, inner lateral view (IY152-010). Q–R, Sd element; ***Q***, NIGP 153090, Nj375, outer lateral view (IY152-004); ***R***, NIGP 153091, Nj375, outer lateral view (IY152-011). Scale bars 100 μm.

(Tables 1–2). The ancestor-descendent relationship from *P. serra* to *P. anserinus* was well documented by their closely comparable morphological similarities and transformation of the Pa elements from a three-ridged platform of *P. serra* to a four-ridged platform of *P. anserinus* (Zhang, 1998a). Based on detailed studies of the distribution and palaeoecology of these two species in the Cobbs Arm Formation of north-central Newfoundland (Fåhraeus & Hunter, 1981), Fåhraeus (1982b, p. 5) favoured an allopatric speciation for *P. anserinus*, suggesting that *P. serra* was generally restricted to near shore setting, whereas *P. anserinus* "preferred the more open, probably deeper and cooler environment".

However, co-occurrence of these two species found in the lower part of the *P. anserinus* Zone in the Tarim Basin (this study) and other regions (Zhang, 1998a) points towards a sympatric speciation for *P. anserinus*, and co-occurrence of both *P. serra* and *P. anserinus* in the basinal shales does not support the ecological differentiation of these two species as suggested by Fåhraeus.

Pygodus serra (Hadding, 1913)

Fig. 25A–R

Arabellites serra Hadding, 1913, p. 13, pl. 1, figs 12, 13.
Pygodus aff. *anserinus* Lamont & Lindström.–Viira, 1967: fig. 4.6.
Haddingodus serra (Hadding).–Viira, 1967: fig. 4.7.
Pygodus serrus (Hadding).–Bergström, 1971: 149, pl. 2, figs 22, 23; Bergström *et al.*, 1974: pl. 1, fig. 18; Nicoll, 1980: fig. 3H–L; An, 1981: pl. 4, figs 1–3; Ni, 1981: pl. 1, figs 28–29; An & Ding, 1982: pl. 5, figs 4, 13, 14, 16, 19, 22; Chen *et al.*, 1983: pl. 1, figs 11, 12; Zeng *et al.*, 1983: pl. 12, figs 3, 5; Chen & Zhang, 1984b: 130–131, pl. 2, figs 16–17; Wang & Luo, 1984: 279, pl. 11, fig. 18; An *et al.*, 1985: pl. 17, figs 2–6; An, 1987: 177, pl. 24, fig. 25, pl. 26, figs 1–8, 13, 15, pl. 29, figs 2–3; Ding, 1987: pl. 5, figs 6–7; Chen & Zhang, 1989: 223, pl. 5, figs 1–2; An & Zheng, 1990: pl. 13, figs 11–14, 17–21; Zhong, 1990: 152, pl. 16, figs 10–11, 13–15, pl. 20, *partim* only, figs 14, 16, 18 (not fig. 17 = *P. anserinus*); Gao, 1991: 136, pl. 10, fig. 5; Ding *et al.*, in Wang, 1993: 198, pl. 30, figs 10, 13, 15–18, 20–22, 24, pl. 35, 24, 26; Wang *et al.*, 1996: pl. 1, fig. 14; Wang & Zhou, 1998: pl. 3, figs 1–2; Lehnert *et al.*, 1999: pl. 2, fig. 12; Zhao *et al.*, 2000: 220–221, *partim* only, pl. 30, figs 7–10, 18; Wang, 2001: 357, pl. 2, figs 4, 11, 16, 19; Wang & Qi, 2001: pl. 2, fig. 24; Xiong *et al.*, 2006: pl. 1, figs 15–16, 18.
Pygodus serra (Hadding).–Harris *et al.*, 1979: pl. 2, fig. 18; Zeng *et al.*, 1983: pl. 12, figs 3, 5; Ni & Li, 1987: 435, pl. 59, fig. 25; Bergström, 1990: pl. 1, figs 23–24; Pohler & Orchard, 1990: pl. 1, fig. 18; McCracken, 1991: p. 51, pl. 2, figs 4, 6 7, 9, 11, 12, 14–18, 20–23, 28–30; Dzik, 1994: 103–105, pl. 17, figs 9–12, text-fig. 26; Wang *et al.*, 1996: pl. 1, fig. 14; Wang & Zhou, 1998: pl. 3, figs 1–2; Zhang, 1998a: 96, pl. 2, figs 3–5, 8–14, text-figs 2C1, C3, 4B (doubtful pl. 2, figs 1, 2, 6, 7, text-fig. 2C2 = *P. xinjiangensis*) (*cum syn.*); Lehnert *et al.*, 1999: pl. 2, fig. 12; Ottone *et al.*, 1999: 242, pl. 6, figs 2–3; Percival *et al.*, 1999: fig. 8.18; Stouge & Bagnoli, 1999: 154, text-fig. 5; Pickett & Percival, 2001: fig. 4C; Wang, 2001: p. 357, pl. 2, figs 4, 11, 16, 19 (*cum syn.*); Wang & Qi, 2001: pl. 2, fig. 24; Norford *et al.*, 2002: pl. 3, figs 7–10; Bergström, 2007: fig. 4; Percival & Zhen, 2007: pl. 1, figs 1–3, 19.
Pygodus protoanserinus Zhang, 1998a: 96, text-fig. 2D, pl. 3, figs 9–18 (*cum syn.*); Zhang, 1998b: 86–87, pl. 16, figs 6–8 (*cum syn.*); Zhen *et al.*, 2004b: 158, fig. 9B–J (*cum syn.*); Percival & Zhen, 2007: pl. 1, figs 17–18.
Pygodus serrus-anserinus transition.–Zhao *et al.*, 2000: 221, *partim*, only pl. 30, fig. 5.
Pygodus anserinus Lamont & Lindström, 1957: 68, *partim*, only fig. 1d; Armstrong, 1997: 777–778, *partim* only pl. 4, fig. 4.
Pygodus cf. *anserinus* Lamont & Lindström.–Dong & Wang, 2006: pl. 7, fig. 17.
?Pygodus serra (Hadding).–Zhen *et al.*, 2004b: 158, fig. K–L = *Pygodus xinjiangensis*.
?Pygodus xinjiangensis Wang & Qi, 2001: 144, pl. 2, figs 18, 20.

Material. 839 specimens plus 1518 specimens of undifferentiated Pb and S elements of both *P. anserinus* and *P. serra* (see Tables 1–2).

Remarks. Zhang (1998a) proposed *Pygodus protoanserinus* to accommodate intermediate forms between *P. serra* and *P. anserinus*, and defined it as having three rows of denticles on the Pa element with the middle row situated more towards the outer lateral row rather than in a mid position or towards the inner row as in *P. serra*. However, based on examination of topotypes of *P. serra*, Bergström (2007) considered *P. protoanserinus* to be a junior synonym of *P. serra*, and indicated that Zhang's definition of *P. serra* also include forms ascribed to *Pygodus xinjiangensis* by Wang and Qi (2001). The latter has a Pa element bearing a narrower platform with outer and inner margins parallelling each other distally and with the middle row of the denticles located more closely to the inner lateral margin (Wang & Qi, 2001, pl. 2, fig. 18) rather than closer to the outer margin as in *P. serra*.

The abundant material of *Pygodus* species (both *P. serra* and *P. anserinus*) from the Dawangou section shows a distally expanding triangular outline of the platform, and the Pa element of *P. serra* exhibits the middle row of denticles varying from nearly centrally-positioned (Fig. 25E) to closer to the outer lateral margin (Fig. 25D). Zhang (1998a) also illustrated some specimens of *P. serra* bearing a narrow platform with parallel distal margins and a centrally positioned middle row of denticles from the Hällekis section of Sweden (Zhang, 1998a, text-fig. 2C2, pl. 2, fig. 7). Similar forms were also reported from the Guniutan Formation of South China (An, 1987, pl. 26, figs 1, 2, 5). These intermediate forms between typical *P. serra* and those referred to as *P. xinjiangensis* by Wang and Qi (2001) made it difficult to distinguish between these species on the characters originally employed. Moreover, forms referable to *P. xinjiangensis* occurred in association with *P. serra* (An, 1987; Zhang, 1998a, fig. 2). Therefore, we follow Bergström's (2007) opinion that *P. xinjiangensis* is a possible junior synonym of *P. serra* pending further study. Forms typical of *P. xinjiangensis* have not been recognized in the Dawangou material.

Scabbardella Orchard, 1980

Type species. *Drepanodus altipes* Henningsmoen, 1948.

Remarks. Orchard (1980) originally defined *Scabbardella* as a multielement genus consisting of three morphotypes (drepanodiform, acodiform and distacodiform), and suggested that it could be distinguished from *Dapsilodus* mainly by including the drepanodiform elements in the apparatus and in absence of striations on the lateral faces of elements, particularly near the anterior margin. The type species, *S. altipes* (Henningsmoen) was revised by Orchard (1980) as having a seximembrate apparatus, including two drepanodiform, two acodiform and two distacodiform elements differentiated mainly by the curvature of the cusp. Orchard (1980) regarded *Scabbardella similaris* (Rhodes, 1953) as a junior synonym of *S. altipes*. However, An (1987, p. 179–180) considered them as separate species (based on curvature of the cusp and length of the base), and re-assigned to *S. similaris* the material from England and Wales that Orchard (1980) referred to as *S. altipes*. Our interpretation concurs with that of Orchard (1980).

Figure 26. *Scolopodus striatus* Pander, 1856. ***A–B***, P element (acontiodiform), NIGP 153092, Nj294, A, anterior view (IY148-14), B, posterior view (IY148-015). ***C–D***, Sa element (subrounded), NIGP 153093, Nj294, C, posterior view (IY148-012), D, postero-lateral view (IY148-011). E–I, Sb element (short-based variant of compressed paltodiform); ***E–G***, NIGP 153094, Nj294, E, inner lateral view (IY148-007), F, posterior view (IY148-008), G, antero-outer lateral view (IY148-006); ***H–I***, NIGP 153095, Nj294, H, outer lateral view (IY148-029), I, upper view showing cross section of cusp (IY148-028). J–O, Sc element (medium-based variant of paltodiform); ***J***, NIGP 153096, Nj292, inner lateral view (IY158-025); ***K–L***, NIGP 153097, Nj292, K, inner lateral view (IY158-022), L, outer lateral view (IY158-020); ***M–O***, NIGP 153098, Nj294, M, basal view of basal cavity (IY148-017), N, outer lateral view (IY148-016), O, inner lateral view (IY148-018). ***P–Q***, Sd element (long-based variant of compressed paltodiform), NIGP 153099, Nj294, P, inner lateral view (IY148-009), Q, basal view of cusp (IY148-010). R–W, M element (short-based variant of paltodiform); ***R–S***, NIGP 153100, Nj294, R, inner lateral view (IY148-004), S, outer lateral view (IY148-005); ***T–U***, NIGP 153101, Nj292, T, inner lateral view (IY158-023), U, outer lateral view (IY158-024); ***V***, NIGP 153102, Nj295, inner lateral view (IY149-009); ***W***, NIGP 153103, Nj294, inner lateral view (IY158-031). Scale bars 100 μm.

Scabbardella altipes (Henningsmoen, 1948)

Fig. 9D–O

Drepanodus altipes Henningsmoen, 1948: 420, pl. 25, fig. 14; Wang & Lou, 1984: 257, pl. 2, figs 3–4, 15, 17.

Scabbardella altipes (Henningsmoen).–Orchard, 1980: 25–26, pl. 5, figs 2–5, 7–8, 12, 14, 18, 20, 23–24, 28, 30, 33, 35, text-fig. 4C (*cum syn.*); Nowlan, 1983: 668, pl. 1, figs 6–7, 11–14; Chen & Zhang, 1984b: 131, pl. 2, figs 29–30; Ni & Li, 1987: 437, pl. 55, figs 19–20, pl. 59, figs 21–22, 31–32; Chen & Zhang, 1989: pl. 5, figs 8–9; Gao, 1991: 137, pl. 12, fig. 18; Ding *et al.* in Wang, 1993:199, pl. 12, figs 26–27; Trotter & Webby, 1994: 487, pl. 3, figs 1–6, 8–11; Wang *et al.*, 1996: pl. 1, fig. 18; Wang & Zhou, 1998: pl. 2, fig. 3; Ferretti & Serpagli, 1999: pl. 2, figs 17–23; Leslie, 2000: 1125, fig. 3.36–3.37; Sweet, 2000: fig. 9.14–9.15; Zhao *et al.*, 2000: 221–222, pl. 23, figs 10–12; Rasmussen, 2001: 130, pl. 17, figs 4–5; Agematsu *et al.*, 2007: 29–30, fig. 11.4, 11.8–11.10, 11.12–11.17 (*cum syn.*); Agematsu *et al.*, 2008a: 969, fig. 10.25–10.34.

Dapsilodus similaris (Rhodes).–An, 1981: pl. 3, figs 4–5; An & Ding, 1982: pl. 1, figs 17–18; An *et al.*, 1983: 91, pl. 15, fig. 22; An & Xu, 1984: pl. 1, figs 8, 15; An *et al.*, 1985: pl. 11, figs 9–10, 13–14; Ding, 1987: pl. 5, fig. 23; Duan, 1990: pl. 3, figs 13–15.

Scabbardella similaris (Rhodes).–An, 1987: 179–180, pl. 5, figs 14–17, 19–24, 26–27; Ding *et al.* in Wang, 1993: 199, pl. 17, figs 22–28.

Material. 232 specimens from 17 samples (see Tables 1–2).

Remarks. The revised multielement concept given by Orchard (1980) is followed herein. Amongst the specimens of *S. altipes* illustrated by Orchard (1980) from the Upper Ordovician of England and Wales, seven morphotypes can be differentiated. They are short-based drepanodiform (Orchard, 1980, pl. 5, figs 23, 33), long-based drepanodiform (pl. 5, fig. 24), acodiform with short base and erect or reclined cusp (pl. 5, figs 18, 20), acodiform with medium base (Fig. 9F–G herein; Orchard, 1980, pl. 5, figs 14, 30), long-based acodiform (Fig. 9D–E; pl. 5, figs 3–4, 7–8, 12), long-based symmetrical distacodiform (pl. 5, figs 2, 35), and asymmetrical distacodiform (Fig. 9H–O; pl. 5, fig. 28).

Scolopodus Pander, 1856

Type species. *Scolopodus sublaevis* Pander, 1856.

Remarks. *Scolopodus* is well-defined and widely understood as a dominantly hyaline, robust, thick-walled coniform genus with a non-expanded base and sharp costae. However, as Pander's (1856) original material was lost, there has long been confusion and misinterpretations concerning various species erected by Pander (1856) and several subsequent authors (e.g., Lindström, 1955a). Pander (1856) recognized six form species of *Scolopodus*, including *S. sublaevis, S. striatus, S. costatus, S. semicostatus, S. aequilateralis*, and *S. quadratus*. Fåhraeus (1982a) considered that only two species were valid, namely the type species, *S. sublaevis* (= *S. aequilateralis*), and *S. quadratus* (= *S. costatus* and *S. striatus*); furthermore he regarded *S. rex* Lindström, 1955a as a junior synonym of *S. quadratus*. Based on material recovered from the Mining Institute in St. Petersburg that is believed to be part of Pander's type collection, and additional new material collected from one of Pander's original localities on the Popowka River of St. Petersburg, Tolmacheva (2006) provided a comprehensive revision of Pander's species of *Scolopodus*. She concluded that all Pander's form species belonged to a single species, except for the type species, *S. sublaevis*, which was not recognized in her material. Tolmacheva (2006) suggested that *S. striatus* was the valid name for this multielement species, with the widely-used *S. rex* forming a junior synonym. Her conclusion is supported by a large collection of *Scolopodus* collected by one (SB) of the authors from the type locality (Popowka River).

Scolopodus rex Lindström, 1955a was erected as a form species of a multicostate symmetrical element with rounded cross section (Lindström, 1955a, pl. 3, fig. 32), and *S. rex* var. *paltodiformis* Lindström, 1955a was proposed originally as a form species represented by a short-based, strongly compressed element with multicostate inner lateral face and only faintly costate outer lateral face (Lindström, 1955a, pl. 3, figs 33–34). Tolmacheva (2006, fig. 2) considered them to represent the Sa (subrounded) and M (scandodiform) positions respectively of her revised multielement species, *S. striatus*.

Our current understanding of *Scolopodus* is largely based on the now well-established multielement species *S. striatus*, as the type species originally designated by Pander remains as a poorly known species, whose validity may also be questionable (Tolmacheva, 2006). In the revision by Tolmacheva, *S. striatus* was defined as having five or more nongeniculate elements representing the M, S and P positions. However, some species of *Scolopodus*, such as *S.? oistodiformis* An & Ding, 1985 from China, and *S. subrex* Ji & Barnes, 1994 and *S. cornutiformis* (Branson and Mehl, 1933) from North America, have a distinctive geniculate M element in their species apparatus, rather a nongeniculate scandodiform M element as in *S. striatus*. *S.? oistodiformis* is widely reported in the Darriwilian of South China and Tarim. Its M element from the Dawangou Formation (Fig. 27A–C) is geniculate with a recurved, robust and antero-laterally strongly compressed cusp, which has a smooth, non-costate anterior face and a costate less convex posterior face. It remains uncertain whether this distinctive species group with a geniculate M element should be included in *Scolopodus*.

Scolopodus? oistodiformis An & Ding, 1985

Fig. 27A–I

Scolopodus rex oistodiform An & Ding, 1982: pl. 1, fig. 9 (*nomen nudum*); An & Ding, 1985: 8, pl. 1, figs 16–18; An *et al.*, 1985: pl. 8, fig. 5, pl. 10, figs 2–4; An, 1987: 187, pl. 7, figs 12, 24, 30; Gao, 1991: 140–141, pl. 6, fig. 20; Ding *et al.* in Wang, 1993: 205–206, pl. 14, figs 13–15; Zhao *et al.*, 2000: 224, pl. 14, figs 1, 9.

Scolopodus rex Lindström.–Zhang, 1998c: 90–91, pl. 17, figs 5–8.

Scolopodus longibasis Ni *in* Ni & Li, 1987: 439, pl. 57, figs 47–50.

Material. Six specimens from three samples (see Tables 1–2).

Remarks. *Scolopodus rex oistodiformis* was first introduced into the literature as a *nomen nudum* by illustration only (An & Ding, 1982). Subsequently, An & Ding (1985) formally defined this subspecies as consisting of a bimembrate apparatus including an asymmetrical geniculate element and a symmetrical, short-based multicostate scolopodiform element. They indicated that the geniculate element was

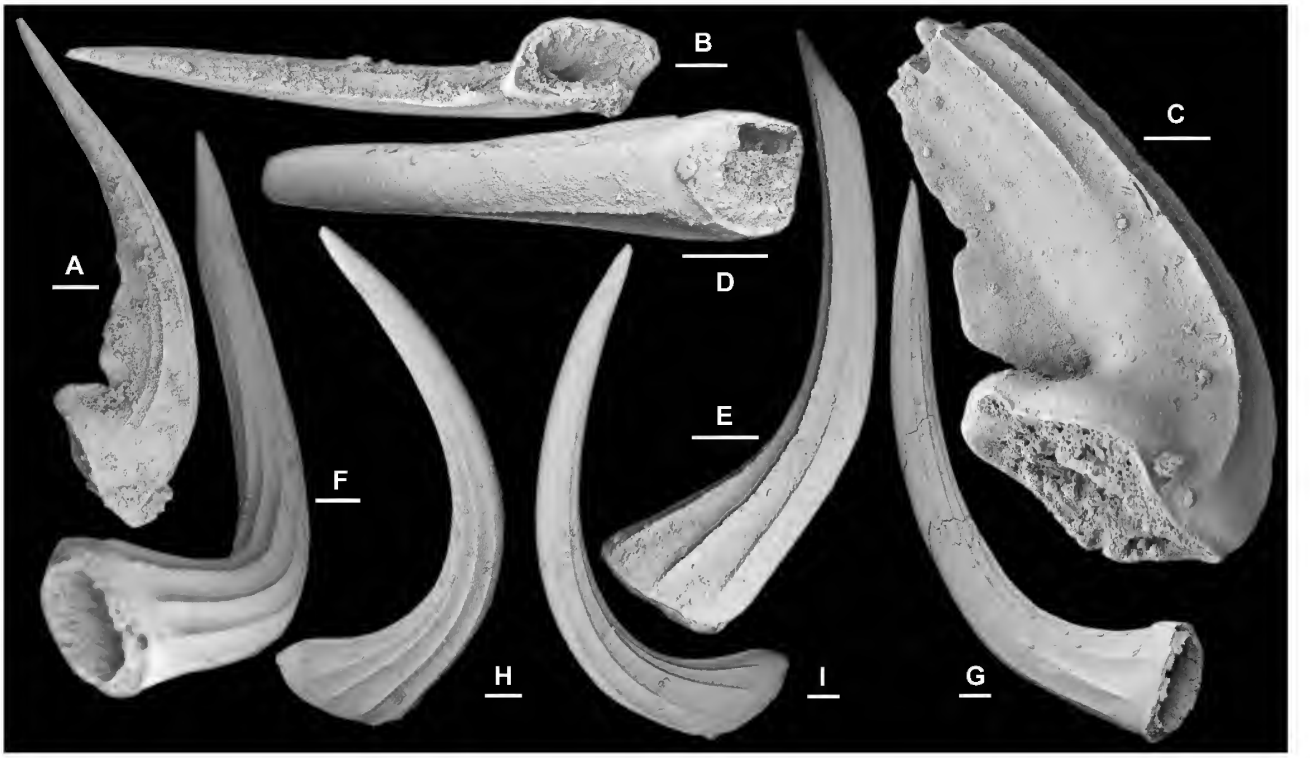

Figure 27. *Scolopodus*? *oistodiformis* An & Ding, 1985. A–C, M element; ***A–B***, NIGP 153104, Nj294, posterior view (IY148-020), B, basal view (IY148-019); ***C***, NIGP 153105, Nj295, posterior view (IY149-008). ***D–E***, Sa element, NIGP 153106, Nj294, D, anterior view (IY148-023), E, lateral view (IY148-031); ***F–G***, Sb element, NIGP 153107, Nj294, F, basal-inner lateral view (IY148-022), G, outer lateral view (IY148-021). ***H–I***, Sc element, NIGP 153108, Nj294, inner lateral view (IY148-030), I, outer lateral view (IY148-031). Scale bars 100 μm.

closely comparable with the form species *S. rex* var. *paltodiformis* Lindström, 1955a. Zhang (1998c) considered *S. rex oistodiformis* as a junior synonym of *S. rex* and included geniculate M, short-based scolopodiform P and long-based scolopodiform S elements with the S elements forming a symmetry transition series. In the recent revision of *S. striatus*, Tolmacheva (2006) regarded *S. rex* as a junior synonym of *S. striatus*, but rejected the specimens figured as *S. rex* by Zhang (1998c) from her revised multielement species, *S. striatus*. Therefore *S.*? *oistodiformis* is considered herein as representing a separate species as defined by Zhang (1998c). *S. longibasis* Ni in Ni & Li, 1987 is identical with the long-based S elements of this species from the Guniutan Formation of South China (Zhang, 1998c) and from the Dawangou Formation of the Tarim Basin (Fig. 27D–I). Therefore it is considered to be a junior synonym of *S.*? *oistodiformis*. In the Dawangou samples, *S.*? *oistodiformis* and *S. striatus* co-occur, and the short-based P and long-based S elements of *S.*? *oistodiformis* are difficult to differentiate from those of *S. striatus*. In particular, some of the long-based specimens referred to as the Sd element of *S. striatus* might likely belong to the S elements of *S.*? *oistodiformis*, which typically have a lesser number of costae, a longer base and a cusp varying from proclined to suberect (Fig. 27D–I).

Scolopodus? oistodiformis shows close resemblance to *S. subrex* Ji & Barnes, 1994, particularly the M elements which are nearly identical (see Ji & Barnes, 1994, pl. 19, figs 9–14), but *S. subrex* has S elements with a relatively shorter base (Ji & Barnes, 1994, pl. 19, figs 1–8), and the Pa element is rather distinctive with a very short base and a prominent notch on the basal margin (Ji & Barnes, 1994, pl. 19, fig. 15).

Scolopodus striatus Pander, 1856

Fig. 26A–W

?Scolopodus costatus Pander, 1856: 26, pl. 2, fig. 7a–d, pl. A, fig. 5e.

Scolopodus semicostatus Pander, 1856: 26, pl. 2, fig. 4a–b.

Scolopodus aequilateralis Pander, 1856: 26, pl. 2, fig. 5a–c, pl. A, fig. 5c.

Scolopodus quadratus Pander, 1856: 26, pl. 2, fig. 6a–d, pl. A, fig. 5d; Fåhraeus, 1982a: 21, pl. 2, figs 1–14, pl. 3, figs 1–8, 15 (*cum syn.*); Rasmussen, 2001: 131, pl. 17, fig. 12; Zhen *et al.*, 2003b: 212, fig. 27A–O (*cum syn.*); Zhen *et al.*, 2004a: 58–59, pl. 5, figs 15–21 (*cum syn.*).

Scolopodus striatus Pander, 1856: 26, pl. 2, figs 8a–d, pl. A, fig. 5f; Tolmacheva, 2006: 255–259, figs 5A–B, D, ?E, F, 6–8 (*cum syn.*); Viira, 2011: fig. 11E.

Scolopodus rex Lindström, 1955a: 595–596, pl. 3, fig. 32; van Wamel, 1974: 94, pl. 5, fig. 18; Landing, 1976: 640, pl. 4, fig. 14; Löfgren, 1978: 109–110, pl. 1, 38–39; An, 1981: pl. 3, fig. 10; An & Ding, 1982: pl. 1, fig. 22; Zeng *et al.*, 1983: pl. 12, fig. 35; An *et al.*, 1985: pl. 10, figs 8, 13; An, 1987: 187, pl. 7, figs 1–4, 6–8, pl. 9, fig. 6; Ding, 1987: pl. 5, fig. 20; Ni & Li, 1987: 440, pl. 57, figs 23, 32–34; Stouge & Bagnoli, 1990: 25, pl. 9, figs 1–6; Duan, 1990: pl. 2, fig. 6; Gao, 1991: 140, pl. 7, fig. 1; Ding *et al.* in Wang, 1993: 205, pl. 14, figs 21–26; Löfgren, 1994: fig. 7.1; Chen & Bergström, 1995: pl. 7, fig. 7; Wang *et al.*, 1996: pl. 2, figs 18–19; Wang & Bergström, 1999a: 342, pl. 2, fig. 14; Zhao *et al.*, 2000: 224, pl. 14, figs 2–8.

Scolopodus rex var. *paltodiformis* Lindström, 1955a: 596, pl. 3, figs 33–34.

Paltodus scolopodiformis Sergeeva, 1974: pl. 1, figs 10–11.

Scolopodus multicostatus Ni *in* Ni & Li, 1987: 439, pl. 58, fig. 6.
?Scolopodus praerex Ni *in* Ni & Li, 1987: 440, pl. 57, figs 51–54.

Material. 37 specimens from five samples of the Dawangou Formation (see Table 1).

Remarks. As revised by Tolmacheva (2006), *Scolopodus striatus* consists of a quinquimembrate apparatus including scandodiform M (Fig. 26R–W), acontiodiform P (Fig. 26A–B), subrounded Sa (Fig. 26C–D), and paltodiform and compressed paltodiform S (undifferentiated) elements. Tolmacheva (2006, fig. 2) further differentiated the compressed paltodiform element into short-based and long-based variants, and the paltodiform element into short-based and medium-based variants. Her short-based paltodiform element (Tolmacheva, 2006, fig. 7A) exhibits a multicostate inner lateral face and smooth outer lateral face; such features are identical with those exhibited by what she defined as the M element, although that is more strongly compressed with a shorter, but more expanded base. We regard the scandodiform element and short-based variant of the paltodiform element as representing the M element, whereas the medium-based variant of the paltodiform element is interpreted as occupying the Sc position (Fig. 26J–O). The long-based variant of the compressed paltodiform element is assigned to the Sd position (Fig. 26P–Q), and the short-based variant of the compressed paltodiform element is regarded as the Sb element (Fig. 26E–I).

The M element from the Dawangou section (Fig. 26R–W) is identical with the short-based variant of Tolmacheva's paltodiform element (2006, fig. 7A). Both have an antero-posteriorly compressed cusp and a short base. The convex anterior face is smooth (Fig. 26U) or only faintly costate basally (fig. 24S), and the posterior face is less convex but strongly costate (Fig. 26R, T, V–W). The typical scandodiform element defined by Tolmacheva (2006, fig. 6F–G, fig. 8D–F) has not been recognized in our Tarim material.

Yangtzeplacognathus Zhang, 1998b

Type species. *Polyplacognathus jianyeensis* An & Ding, 1982.

Remarks. Species of *Yangtzeplacognathus* were previously assigned to *Eoplacognathus*, which has a bimembrate apparatus including stelliplanate Pa and pastiniplanate Pb elements. Both elements of *Eoplacognathus* are paired, but not in mirror images. Zhang (1998b) proposed *Yangtzeplacognathus* to accommodate a group of species with unpaired, markedly dissimilar sinistral and dextral Pa (stelliplanate) and Pb (pastiniplanate) elements. She suggested that species of *Yangtzeplacognathus* formed a separate evolutionary lineage that originated in central China, and was the sister group sharing a common ancestor with the *Baltoplacognathus* lineage centred in the Baltoscandic area. Both lineages are postulated to have formed sister groups with the *Eoplacognathus-Polyplacognathus* lineage (Zhang, 1998b, fig. 11).

Löfgren & Zhang (2003) recognized geniculate M, and ramiform S elements (referred to as alate Sa, quadriramate Sb, bipennate ScA, and tertiopedate ScB) for *Yangtzeplacognathus crassus* (Chen & Zhang). However, considering analogies to the other related genera with ramiform-pectiniform apparatus structures, the quadriramate and tertiopedate elements defined by Löfgren & Zhang (2003) are better assigned to the Sd and Sb positions respectively.

The following four species have been included in *Yangtzeplacognathus*: (1) *Y. foliaceus* (Fåhraeus, 1966): holotype representing a sinistral Pb (pastiniplanate) element, recorded from the Vikarby Limestone of south-central Sweden; (2) *Y. protoramosus* (Chen, Chen & Zhang, 1983): recorded from lower part of the Miaopo and Datianba formations in South China (Zhang, 1998c), Tarim (this study), Baltoscandia (Bergström, 1971), and Poland (Dzik, 1978, 1994); 3) *Y. crassus* (Chen & Zhang in Wang, 1993), recorded from South China (Chen & Zhang in Wang, 1993; Zhang, 1997; Bergström & Wang, 1998; Wang & Bergström, 1999a; Zhang, 1998c), Tarim Basin (Wang & Zhou, 1998; this study), Baltoscandia (Stouge & Bagnoli, 1990; Löfgren, 2000; Löfgren & Zhang, 2003), and Poland (Dzik, 1994); and 4) *Y. jianyeensis* (An & Ding, 1982): reported from the Miaopo and Datianba formations in South China (An *et al.*, 1981, 1985; An & Ding, 1982; Chen *et al.*, 1983; Chen & Zhang, 1984a, 1984b; An, 1987; Zhang, 1998b, 1998c), basal Sandbian of Yunnan Province (Dong & Wang, 2006), and from the top Saergan Formation and lower part of the Kanling Formation (lower Sandbian) of the Tarim Basin (this study).

Yangtzeplacognathus crassus (Chen & Zhang in Wang, 1993)

Figs 28A–O, 29A–O

Ambalodus pseudoplanus Viira.–Ni & Li, 1987: pl. 55, fig. 16.
Eoplacognathus pseudoplanus (Viira).–Viira *et al.*, 2001: fig. 8a–l, 8q-t; Wang *et al.*, 1996: pl. 4, fig. 6.
Amorphognathus variabilis (Sergeeva).–Wang *et al.*, 1996: pl. 4, fig. 17.
Eoplacognathus crassus Chen & Zhang in Wang, 1993: 174, pl. 37, figs 12–17; Zhang, 1997: 61–65, figs 2A–B, 3A–L, 4A–L (*cum syn.*); Bergström & Wang, 1998: 91–93; Wang & Zhou, 1998: pl. 1, fig. 2, ?pl. 4, fig. 8; Wang & Bergström, 1999a: 335, pl. 3, fig. 16; Wang & Bergström, 1999b: pl. 2, fig. 14; non Xiong *et al.*, 2006: 368, pl. 1a–b = element of *Dzikodus*.
Yangtzeplacognathus crassus (Chen & Zhang).–Zhang, 1998c: 96–97, pl. 20, figs 5–8 (*cum syn.*); Löfgren, 2003: fig. 8A–D; Löfgren & Zhang, 2003: 731–735, figs 6, 12 (*cum syn.*); Viira, 2011: fig. 9B.

Material. 63 specimens from two samples of the Dawangou Formation (see Table 1).

Remarks. Specimens from the Dawangou Formation are identical with those previously documented from the Guniutan Formation in South China (Chen & Zhang in Wang, 1993; Zhang, 1998c) and from Sweden (Löfgren, 2003; Löfgren & Zhang, 2003). Chen & Zhang (in Wang, 1993) recognized two types of pectiniform (Pa = stelliplanate = polyplacognathiform, and Pb = pastiniplanate = ambalodiform) elements, each of which also has morphologically distinctive and consistent sinistral and dextral variants, based on study of the type material of this species from the Guniutan Formation in Tangshan, near Nanjing. Detailed study of the pectiniform elements of this species from China and Baltoscandia led Zhang (1997) to suggest that *Y. crassus* had a restricted age range that was important for international stratigraphic correlation.

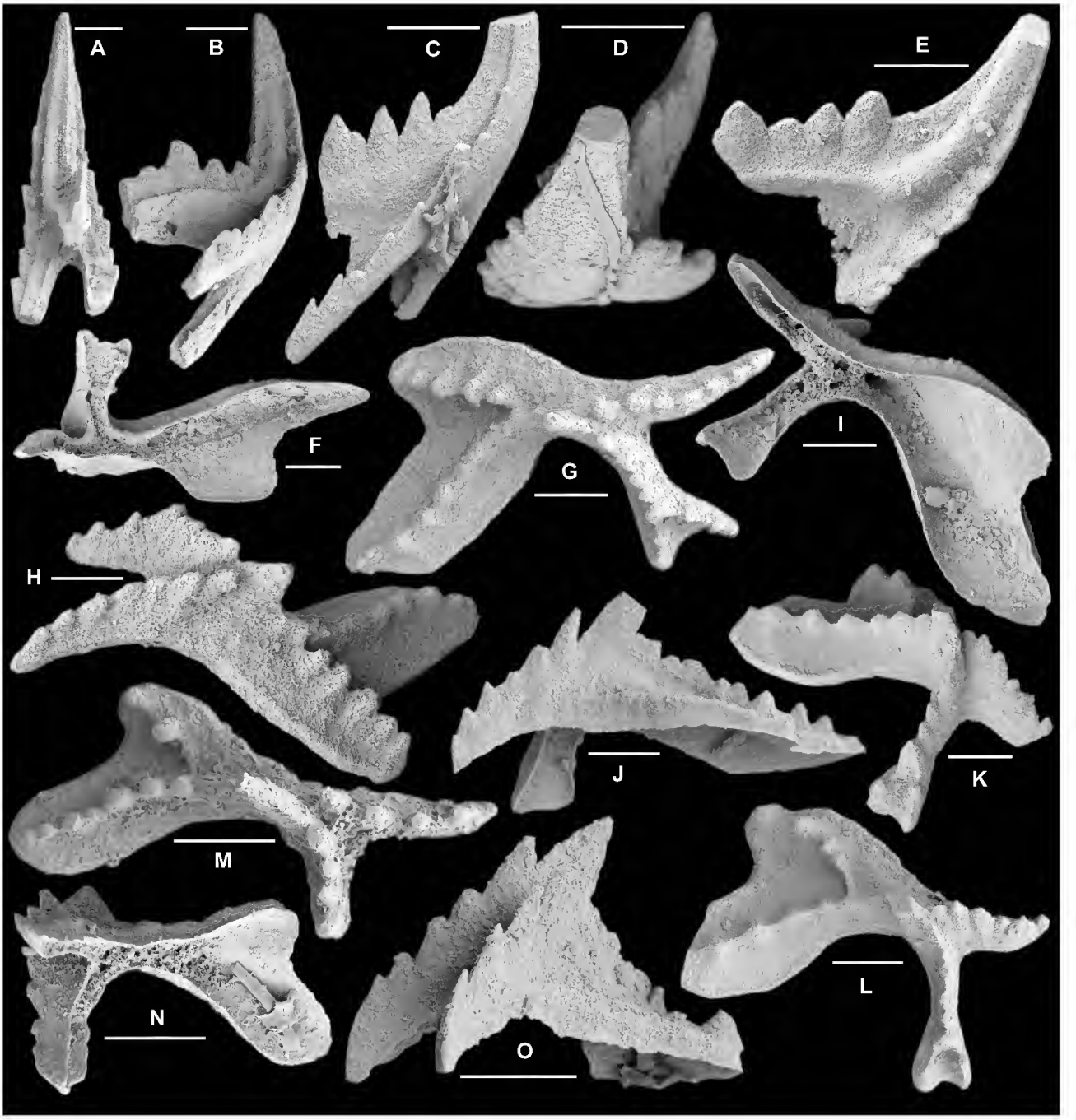

Figure 28. *Yangtzeplacognathus crassus* (Chen & Zhang, 1993). ***A–B***, Sa element, NIGP 153109, A, posterior view (IY146-036), B, lateral view (IY146-038); ***C***, Sa element, NIGP 153110, lateral view (IY146-033). ***D–E***, Sb element, NIGP 153111, D, antero-upper view (IY146-034), E, inner lateral view (IY146-035). ***F***, sinistral Pa element, NIGP 153112, basal view (IY146-003). G–O, dextral Pa element; ***G–H***, NIGP 153113, G, upper view (IY146-001), H, upper lateral view (IY146-002); ***I–J***, NIGP 153114, I, basal view (IY146-016), J, postero-lateral view (IY146-017); ***K–L***, NIGP 153115, K, antero-upper view (IY146-004), L, upper view (IY146-005); ***M***, NIGP 153116, upper view (IY146-020); ***N–O***, NIGP 153117, N, basal view (IY146-021), O, lateral view (IY146-022). All from sample Nj294; scale bars 100 μm.

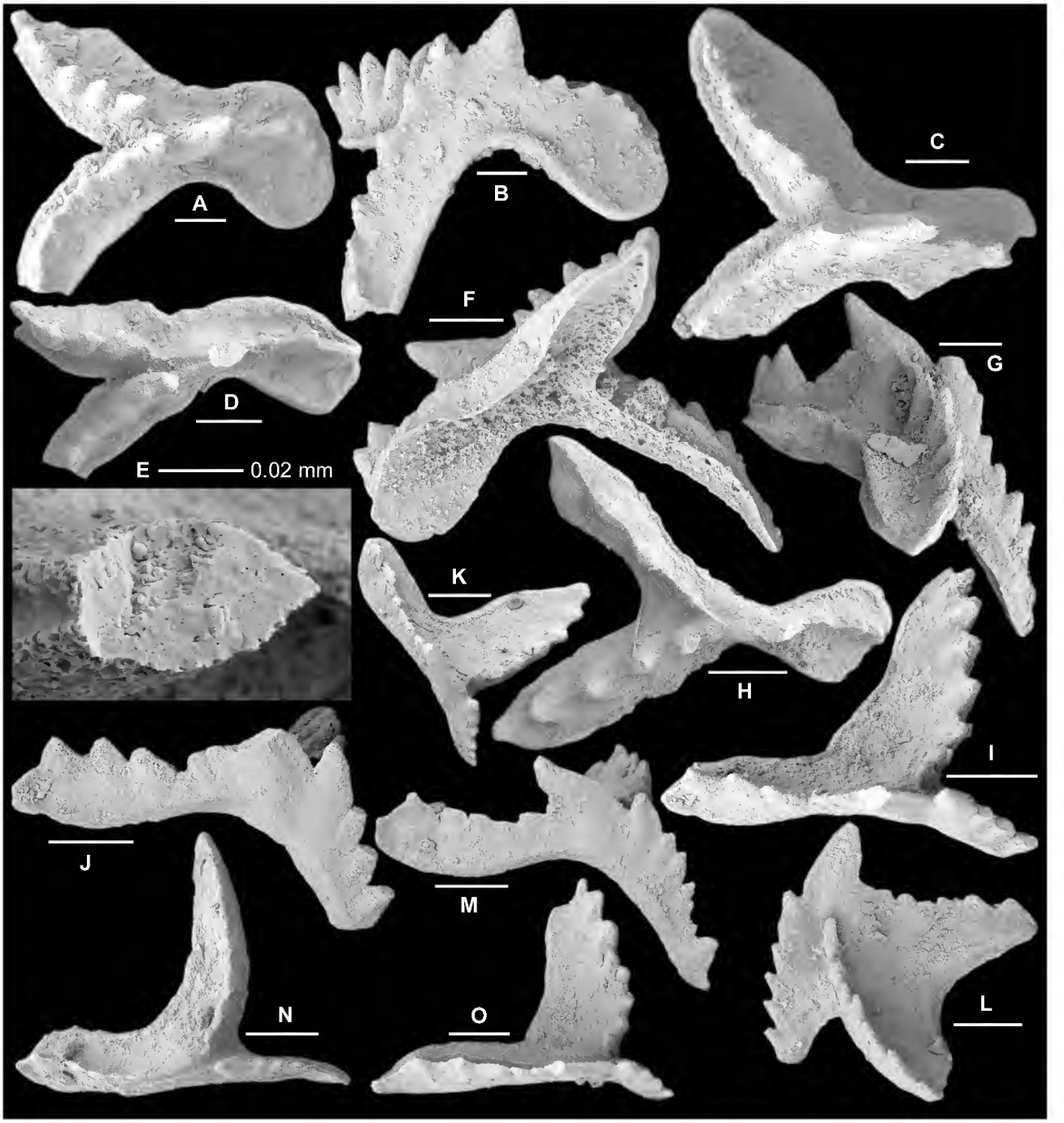

Figure 29. *Yangtzeplacognathus crassus* (Chen & Zhang, 1993). A–H, sinistral Pb element; ***A–B***, NIGP 153118, Nj295, A, upper view (IY149-001), B, lateral view (IY149-002); ***C***, NIGP 153119, Nj295, upper view (IY149-004); ***D–E***, NIGP 153120, Nj294, D, upper view (IY146-013), E, upper view, close up showing cross section of the cusp (IY146-015); ***F–G***, NIGP 153121, Nj294, F, basal view (IY146-010), G, lateral view (IY146-011); ***H***, NIGP 153122, Nj294, upper view (IY146-009). I–O, dextral Pb element; ***I–J***, NIGP 153123, Nj294, I, upper view (IY146-024), J, lateral view (IY146-023); ***K–L***, NIGP 153124, Nj294, K, upper view (IY146-032), L, lateral view (IY146-030); ***M–N***, NIGP 153125, Nj294, M, lateral view (IY146-029), N, upper view (IY146-031); ***O***, NIGP 153126, Nj294, upper view (IY146-025). Scale bars 100 μm, unless otherwise indicated.

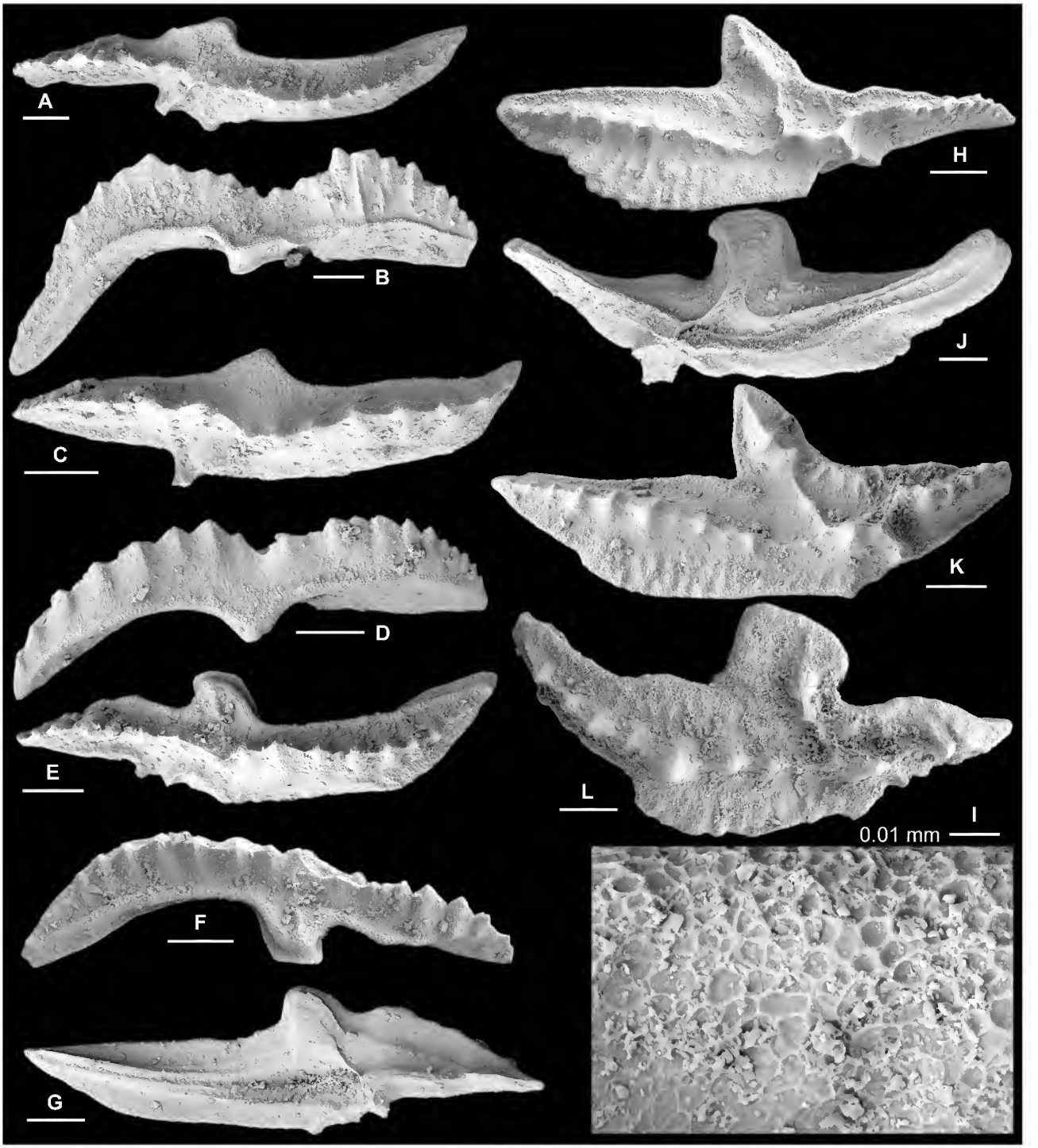

Figure 30. *Yangtzeplacognathus jianyeensis* (An & Ding, 1982). A–G, sinistral Pa element; ***A–B***, NIGP 153127, AFT-X-K13/44, A, upper view (IY165-011), B, lateral view (IY165-010); ***C–D***, NIGP 153128, AFT-X-K13/43, C, upper view (IY164-018), D, lateral view (IY164-016). ***E–F***, NIGP 153129, AFT-X-K13/41, E, upper view (IY164-008), F, upper-lateral view (IY164-007); ***G***, NIGP 153130, AFT-X-K13/44, basal view (IY165-012). H–L, dextral Pa element; ***H–I***, NIGP 153131, AFT-X-K13/44, H, upper view (IY165-003), I, upper view, close up showing fine reticular surface structure (IY166-005); ***J***, NIGP 153132, AFT-X-K13/44, basal view (IY165-006); ***K***, NIGP 153133, AFT-X-K13/43, upper view (IY164-014); ***L***, NIGP 153134, AFT-X-K13/40, upper view (IY164-001). Scale bars 100 μm, unless otherwise indicated.

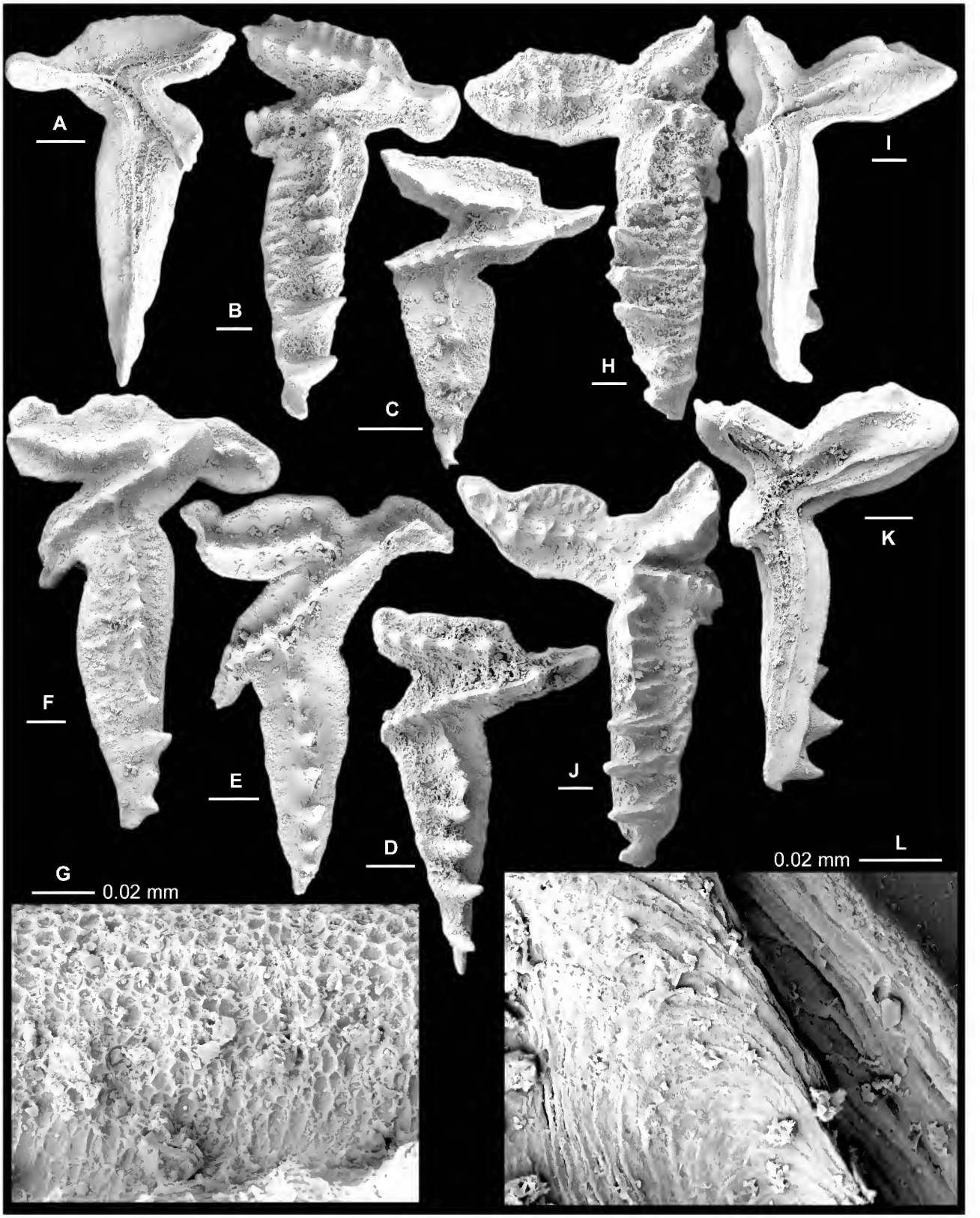

Figure 31. *Yangtzeplacognathus jianyeensis* (An & Ding, 1982). A–G, sinistral Pb element; ***A***, NIGP 153135, AFT-X-K13/44, basal view (IY165-008); ***B***, NIGP 153136, AFT-X-K13/44, upper view (IY165-001); ***C***, NIGP 153137, AFT-X-K13/44, juvenile, upper view (IY165-015); ***D***, NIGP 153138, AFT-X-K13/42, upper view (IY164-009); ***E***, NIGP 153139, AFT-X-K13/41, upper view (IY164-004); ***F–G***, NIGP 153140, AFT-X-K13/40, F, upper view (IY163-038), G, upper view, close up showing fine reticular surface structure (IY163-039). H–L, dextral Pb element; ***H***, NIGP 153141, AFT-X-K13/44, upper view (IY165-002); ***I***, NIGP 153142, AFT-X-K13/44, basal view (IY165-007); ***J***, NIGP 153143, AFT-X-K13/43, upper view (IY164-010); ***K–L***, NIGP 153144, AFT-X-K13/40, K, basal view (IY163-041), L, basal view, close up showing lamellar surface structure (IY163-042). Scale bars 100 μm, unless otherwise indicated.

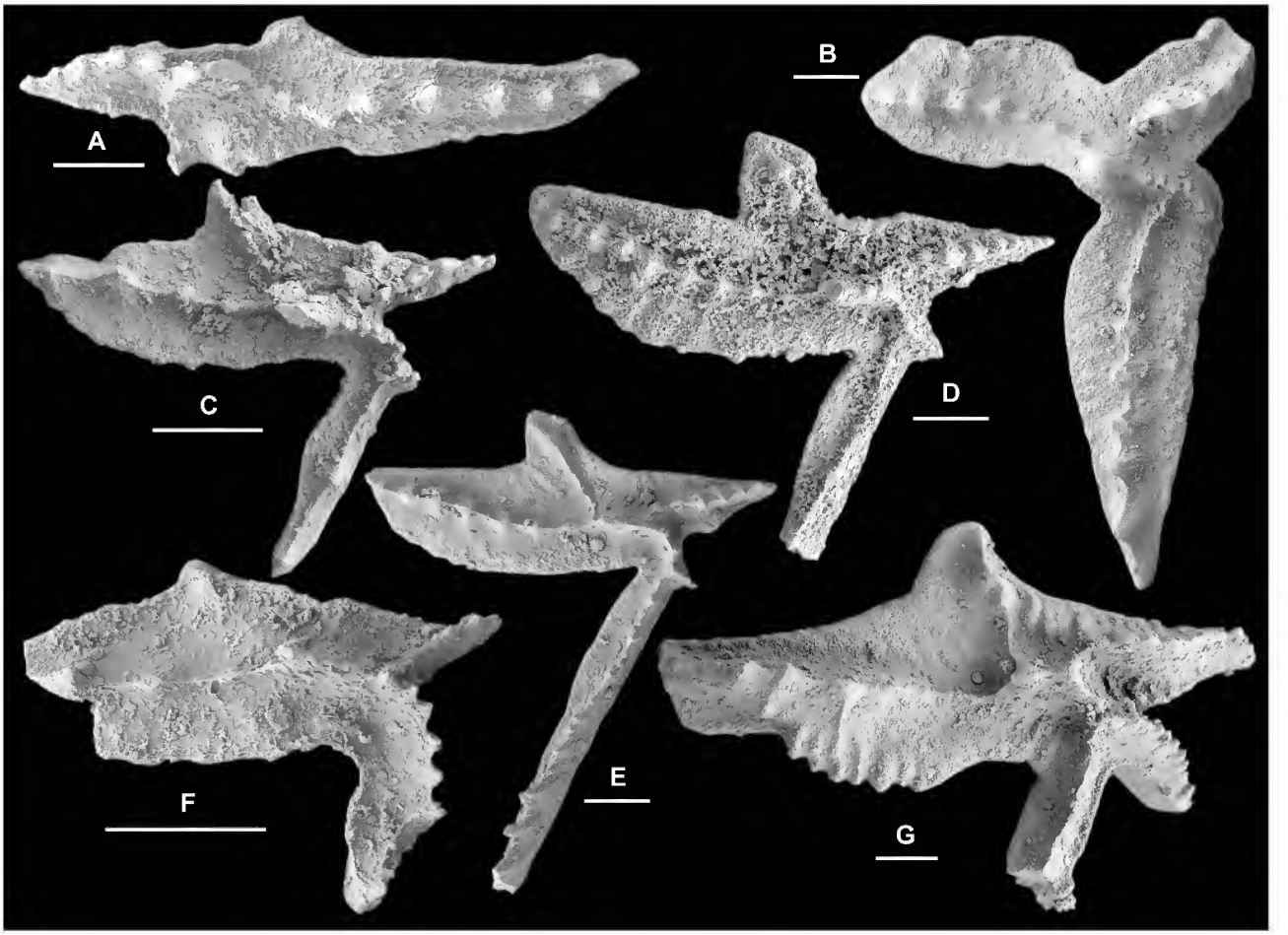

Figure 32. *Yangtzeplacognathus protoramosus* (Chen, Chen & Zhang, 1983). ***A***, sinistral Pa element, NIGP 153145, Nj378, upper view (IY153-018). ***B***, dextral Pb element, NIGP 153146, AFT-X-K13/40, upper view (IY163-040). C–G, dextral Pa element; ***C***, NIGP 153147, Nj378, upper view (IY153-017); ***D***, NIGP 153148, AFT-X-K13/44, upper view (IY165-014); ***E***, NIGP 153149, AFT-X-K13/43, upper view (IY164-023); ***F***, NIGP 153150, Nj378, upper view (IY153-021); ***G***, NIGP 153151, AFT-X-K13/44, upper view (IY165-013). Scale bars 100 μm.

Yangtzeplacognathus jianyeensis (An & Ding, 1982)

Figs 30A–L, 31A–L

Polyplacognathus miaopoensis An *et al.*, 1981: pl. 1, fig. 25 (*nomen nudum*); Zeng *et al.*, 1983: pl. 12, fig. 26; An *et al.*, 1985: 44–45, *partim* only pl. 18, figs 13–14, non figs 8, 15 = *Y. protoramosus*; Ni & Li, 1987: pl. 55, fig. 6, pl. 59, fig. 36.

Eoplacognathus cf. *reclinatus* (Fåhraeus).–Ni, 1981: pl. 1, fig. 32.

Polyplacognathus jianyeensis An & Ding, 1982: 9, pl. 3, figs 1–7; An & Xu, 1984: pl. 3, figs 18–19; An *et al.*, 1985: pl. 18, figs 16–18.

Eoplacognathus ramosus Chen *et al.*, 1983: 135, pl. 1, figs 1–4.

Eoplacognathus jianyeensis (An & Ding).–Chen & Zhang, 1984a: 329, pl. 1, figs 5–7, 12–14, 17–18, pl. 2, figs 3–4; Chen & Zhang, 1984b: 127, pl. 1, figs 30–33; An, 1987: 149, pl. 27, figs 1–7, 9–10; Chen & Zhang, 1989: 220, pl. 2, figs 26–29; Ding *et al. in* Wang, 1993: 175, pl. 31, figs 1–9; Wang & Zhou, 1998: *partim* only pl. 1, figs ?3, 10, non figs 5, 7–8 = *Y. protoramosus;* Dong & Wang, 2006: 149, pl. 7, figs 2, 5–6.

Eoplacognathus protoramosus Chen, Chen & Zhang.–Xiong *et al.*, 2006: pl. 1, fig. 13.

Yangtzeplacognathus jianyeensis (An & Ding).–Zhang, 1998b: 28, fig. 5M–S, fig. 6C, fig. 11C3, fig. 13; Zhang, 1998c: 99, pl. 19, figs 1–4 (*cum syn.*).

Material. 176 specimens from 12 samples (see Tables 1–2).

Remarks. Zhang (1998b) provided detailed description of this species as consisting of sinistral and dextral Pa (stelliplanate) and Pb (pastiniplanate) elements. It is characterized by the Pb element having four processes including a very short, narrow and downwardly-bent anterior process.

The nomenclatural history of this species is particularly confused. An & Ding (1982) erected *Polyplacognathus jianyeensis* as consisting of sinistral and dextral Pb (ambalodiform) and a Pa (polyplacognathiform) elements, with the type material recovered from the Datianba Formation of Tangshan, Jiangsu Province. *Polyplacognathus miaopoensis* was introduced into the literature without diagnosis or description as a *nomen nudum* by illustration of a designated holotype (sinistral Pb element) recovered from the Miaopo Formation of Xingtan, Hubei Province (An *et al.*, 1981, pl. 1, fig. 25). Later, An *et al.* (1985, p. 44) provided the diagnosis and description for *Eoplacognathus miaopoensis* based on the Pb element only, indicating that its Pa element was not recovered at the time, but in the illustration they also included a dextral Pa element (An *et al.*, 1985, pl. 18, fig. 8), which is actually referable to *Y. protoramosus* (see Zhang, 1998b, p. 25). Thus An *et al.* (1985) not only considered *E. miaopoensis* and

P. jianyeensis to represent separate species, but also to belong to different genera. Chen *et al.* (1983) proposed *Eoplacognathus ramosus* as consisting of sinistral and dextral Pa (polyplacognathiform) and Pb (ambalodiform) elements based on type material from the Datianba Formation of Tangshan, near Nanjing (same type locality as that of *Y. jianyeensis* and *Y. protoramosus*), and regarded *P. miaopoensis* as an invalid senior synonym (*nomen nudum*) of *E. ramosus*. An (1987) revised *Y. jianyeensis* as a species of *Eoplacognathus* by regarding both *P. miaopoensis* and *E. ramosus* as synonymous, but followed the original definition given by An & Ding (1982) without differentiation of the sinistral and dextral Pa elements in the species apparatus as Chen *et al.* (1983) had documented.

Based on a collection of over 200 specimens from central China, Zhang (1998b) revised *Y. crassus* as the type species of the new genus *Yangtzeplacognathus*, consisting of unpaired markedly dissimilar sinistral and dextral Pa (stelliplanate) and Pb (pastiniplanate) elements, and distinguished it from other species of *Yangtzeplacognathus* by having Pb elements with four processes.

Yangtzeplacognathus protoramosus (Chen, Chen & Zhang, 1983)

Fig. 32A–G

Eoplacognathus protoramosus Chen, Chen & Zhang, 1983: 135–136, pl. 1, figs 7–10; An, 1987: 149–150, pl. 27, figs 11–13, 17–18; Ding *et al.* in Wang, 1993: 175, *partim*, only pl. 32, figs 1–6 (*cum syn.*).

Yangtzeplacognathus protoramosus (Chen, Chen & Zhang).–Zhang, 1998c: 25–27, fig. 5E–L, fig. 6B, fig. 12 (*cum syn.*).

Eoplacognathus miaopoensis An *et al.*–An *et al.*, 1985: 44–45, *partim* only pl. 18, figs 8, 15.

Eoplacognathus jianyeensis (An & Ding).–Wang & Zhou, 1998: *partim* only pl. 1, figs 5, 7–8.

Eoplacognathus foliaceus (Fåhraeus).–Wang, 2001: 352, pl. 1, fig. 9.

Material. 24 specimens from eight samples (see Tables 1–2).

Remarks. Chen *et al.* (1983) erected *E. protoramosus* as consisting of sinistral and dextral Pa (polyplacognathiform) and Pb (ambalodiform) elements based on material from the Datianba Formation of Tangshan, near Nanjing, and regarded it as the most distinctive species defining their *E. protoramosus* Subzone in the upper part of the *P. serra* Zone. Zhang (1998c) indicated that this species had a stratigraphic range limited to the upper part of *P. serra* Zone in South China, but in the collections from the Dawangou section it has also been reported from the basal part of the Kanling Formation (Sandbian, *anserinus* Zone). The figured dextral Pb element (Fig. 32B) from the base of the Kanling Formation (sample AFT-X-K13/40) is identical with the specimen illustrated by Zhang (1998c, fig. 5J, fig. 12F) representing the late form of this species. In the Dawangou section *Y. protoramosus* is relatively uncommon, but extends well into the *anserinus* Zone. Zhao *et al.* (2006, p. 196) also recorded *Y. protoramosus* in the *anserinus* Zone at Lunnan in the Tarim Basin.

ACKNOWLEDGMENTS. YYZ's study was supported by the CAS/SAFEA International Partnership Program for Creative Research Teams. Part of the material studied in this contribution was collected by ZHW during 1987 with the support of a State Scientific Research Project on the correlation of the Phanerozoic strata in the Tarim Basin. Field work and collecting in the Tarim Basin during 2008 and processing of half of each sample was undertaken with the support of research grants to YDZ (2008ZX05008-001–001). Prof. Zhang Shiben from Petrol China is thanked for his guidance in the field work in 2008. Gary Dargan (formerly of Geological Survey of New South Wales, Londonderry) assisted with acid leaching and residue separation of the remaining half of each sample collected in 2008. Dr Viive Viira from Estonia is thanked for providing the senior author with her valuable monograph and for useful discussions on the type specimens of *Polonodus clivosus*. Scanning electron microscope photographs were prepared in the Electron Microscope Unit of the Australian Museum (Sydney). J. Repetski and R. L. Ethington are thanked for their careful and constructive reviews of the manuscript. IGP publishes with permission of the Executive Director, NSW Office of Resources and Energy.

References

Abaimova, G. P. 1971. New Early Ordovician conodonts from the southeastern part of the Siberian Platform. *Paleontological Journal* 1971(4): 486–493.

Agematsu, S., K. Sashida, S. Salyapongse, and A. Sardsud. 2006. Ordovician conodonts from the Thong Pha Phum area, western Thailand. *Journal of Asian Earth Sciences* 26:49–60. doi:10.1016/j.jseaes.2004.09.009

Agematsu, S., K. Sashida, S. Salyapongse, and A. Sardsud. 2007. Ordovician conodonts from the Satun area, southern peninsular Thailand. *Journal of Paleontology* 81(1):19–37. doi:10.1666/0022-3360(2007)81[19:OCFTSA]2.0.CO;2

Agematsu, S., K. Sashida, and A. B. Ibrahim. 2008a. Biostratigraphy and paleobiogeography of Middle and Late Ordovician conodonts from the Langkawi Islands, northwestern Peninsular Malaysia. *Journal of Paleontology* 82(5):957–973. doi:10.1666/07-058.1

Agematsu, S., K. Sashida, and A. Sardsud. 2008b. Reinterpretation of Early and Middle Ordovician conodonts from the Thong Pha Phum area, western Thailand, in the context of new material from western and northern Thailand. *Paleontological Research* 12(2):181–194. doi:10.2517/1342-8144(2008)12[181:ROEAMO]2.0.CO;2

Albanesi, G. L., and G. Ortega. 2003. Advances on conodont-graptolite biostratigraphy of the Ordovician System of Argentina. In *Aspects of the Ordovician System of Argentina, Serie Correlación Geológica,* ed. F. G. Aceñolaza, vol. 16, pp. 143–165. INSUGEO, Tucumán.

Albanesi, G. L., M. A. Hünicken, and C. R. Barnes. 1998. Bioestratigrafía, biofacies y taxonomia de conodontes de las secuencias ordovícicas del Cerro Porterillo, Precordillera central de San Juan, R. Argentina. *Actas de la Academia Nacional de Ciencias* 12:1–249.

An, T. X. 1981. Recent progress in Cambrian and Ordovician conodont biostratigraphy of China. *Geological Society of America Special Paper* 187:209–226.

An, T. X. 1987. *Early Palaeozoic Conodonts from South China.* Peking University Publishing House, Beijing, 238 pp. (in Chinese with English abstract).

An, T. X., and L. S. Ding. 1982. Preliminary studies and correlations on Ordovician conodonts from the Ningzhen Mountains, China. *Acta Petroleum Sinica* 3(4):1–11 (in Chinese).

An, T. X., and L. S. Ding. 1985. Ordovician conodont biostratigraphy in Hexian, Anhui Province. *Geological Review* 31:1–12 (in Chinese with English abstract).

An, T. X., and B. Z. Xu. 1984. Ordovician System and conodonts of Tungshan and Xianning, Hubei. *Acta Scientiarum Naturalium Universitatis Pekinensis* 1984(5):73–87 (in Chinese with English abstract).

An, T. X., and S. C. Zheng. 1990. *The Conodonts of the Marginal Areas around the Ordos Basin, North China*. Science Press, Beijing. 199 pp. (in Chinese with English abstract).

An, T. X., G. Q. Du, Q. Q. Gao, X. B. Chen, and W. T. Li. 1981. Ordovician conodont biostratigraphy of the Huanghuachang area of Yichang, Hubei. In *Selected Papers of the First Symposium of the Micropalaeontological Society of China*, Micropalaeontological Society of China, ed., Science Press, Beijing, 105–113 (in Chinese).

An, T. X., F. Zhang, W. D. Xiang, Y. Q. Zhang, W. H. Xu, H. J. Zhang, D. B. Jiang, C. S. Yang, L. D. Lin, Z. T. Cui, and X. C. Yang. 1983. *The Conodonts of North China and the Adjacent Regions*. Science Press, Beijing, 223 pp. (in Chinese with English abstract).

An, T. X., G. Q. Du, and Q. Q. Gao. 1985. *Ordovician conodonts from Hubei*. Geological Publishing House, Beijing, 64 pp. (in Chinese with English abstract).

Armstrong, H. A. 1997. Conodonts from the Ordovician Shinnel Formation, southern Uplands, Scotland. *Palaeontology* 40:763–797.

Armstrong, H. A. 2000. Conodont micropalaeontology of mid-Ordovician aged limestone clasts from Lower Old Red Sandstone conglomerates, Lanark and Strathmore basins, Midland Valley, Scotland. *Journal of Micropalaeontology* 19:45–59.
doi:10.1144/jm.19.1.45

Bagnoli, G., and S. Stouge. 1997. Lower Ordovician (Billingenian–Kunda) conodont zonation and provinces based on sections from Horns Udde, north Öland, Sweden. *Bollettino della Società Paleontologica Italiana* 35:109–163.

Barnes, C. R., and M. L. S. Poplawski. 1973. Lower and Middle Ordovician conodonts from the Mystic Formation, Québec, Canada. *Journal of Paleontology* 47:760–790.

Bauer, J. A. 1987. Conodonts and conodont biostratigraphy of the McLish and Tulip Creek formations (Middle Ordovician) of south-central Oklahoma. *Oklahoma Geological Survey, Bulletin* 141:1–55.

Bauer, J. A. 1990. Stratigraphy and conodont biostratigraphy of the upper Simpson Group, Arbuckle Mountains, Oklahoma. In *Early to Middle Paleozoic Conodont Biostratigraphy of the Arbuckle Mountains, Southern Oklahoma,* ed. S. M. Ritter. *Oklahoma Geological Survey Guidebook* 27:39–46.

Bauer, J. A. 1994. Conodonts from the Bromide Formation (Middle Ordovician), south-central Oklahoma. *Journal of Paleontology* 68:358–376.

Bauer, J. A. 2010. Conodonts and conodont biostratigraphy of the Joins and Oil Creek Formations, Arbuckle Mountains, South-central Oklahoma. *Oklahoma Geological Survey Bulletin* 150:1–44.

Bednarczyk, W. S. 1998. Ordovician conodont biostratigraphy of the Polish part of the Baltic syneclise. In *Proceedings of the Sixth European Conodont Symposium (ECOS VI)*, ed. H. Szaniawski. *Palaeontologia Polonica* 58:107–121.

Bergström, S. M. 1962. Conodonts from the Ludibundus Limestone (Middle Ordovician) of the Tvären area (S. E. Sweden): *Arkiv för Mineralogi och Geologi* 3(1):1–61.

Bergström, S. M. 1971. Conodont biostratigraphy of the Middle and Upper Ordovician of Europe and Eastern North America. *Geological Society of America Memoir* 127:83–157.

Bergström, S. M. 1983. Biogeography, evolutionary relationships, and biostratigraphic significance of Ordovician platform conodonts. *Fossils and Strata* 15:35–58.

Bergström, S. M. 1988. On Pander's Ordovician conodonts: distribution and of the *Prioniodus elegans* fauna in Baltoscandia. *Senckenbergiana lethaea* 69:217–251.

Bergström, S. M. 1990. Biostratigraphic and biogeographic significance of Middle and Upper Ordovician conodonts in the Girvan succession, south-west Scotland. *Courier Forschungsinstitut Senckenberg* 118:1–43.

Bergström, S. M. 2007. Middle and Upper Ordovician conodonts from the Fågelsång GSSP, Scania, southern Sweden. *GFF* 129:77–82.
doi:10.1080/11035890701292077

Bergström, S. M., and Z. H. Wang. 1998. Biostratigraphic significance of the Ordovician conodont *Eoplacognathus crassus* Chen & Zhang, 1993. *GFF* 120:91–93.
doi:10.1080/11035899801201091

Bergström, S. M., J. Riva, and M. Kay. 1974. Significance of conodonts, graptolites, and shelly faunas from the Ordovician of Western and North-central Newfoundland. *Canadian Journal of Earth Sciences* 11:1625–1660.
doi:10.1139/e74-163

Bergström, S. M., S. C. Finney, X. Chen, and Z. H. Wang. 1999. The Dawangou section, Tarim Basin (Xinjiang Autonomous Region), China: potential as global stratotype for the base of the *Nemagraptus gracilis* Biozone and the base of the global Upper Ordovician Series. *Acta universitatis Carolinae—Geologica* 43(1/2):69–71.

Bergström, S. M., S. C. Finney, X. Chen, C. Pålsson, Z. H. Wang, and Y. Grahn. 2000. A proposed global boundary stratotype for the base of the Upper Series of the Ordovician System: The Fågelsång section, Scania, southern Sweden. *Episodes* 23(3):102–109.

Bergström, S. M., W. D. Huff, M. R. Saltzman, D. R. Kolata, and S. A. Leslie. 2004. The greatest volcanic ash falls in the Phanerozoic: trans-Atlantic relations of the Ordovician Millbrig and Kinnekulle K-bentonites. *The Sedimentary Record* December: 4–8.

Bischoff, G., and D. Sannemann. 1958. Unterdevonische Conodonten aus dem Frankenwald. *Notizblatt Hessiches Landesamt Bodenforschung* 86:87–110.

Branson, E. B., and M. G. Mehl. 1933. Conodont studies. *University of Missouri Studies* 8:1–349.

Bradshaw, L. E. 1969. Conodonts from the Fort Peña Formation (Middle Ordovician), Marathon Basin, Texas. *Journal of Paleontology* 42:1137–1168.

Burrett, C., B. Stait, and J. Laurie. 1983. Trilobites and microfossils from the Middle Ordovician of Surprise Bay, southern Tasmania, Australia. *Association of Australasian Palaeontologists, Memoir* 1:177–193.

Cai, C. F., K. K. Li, M. Anlai, C. M. Zhang, Z. M. Xu, R. H. Worden, G. H. Wu, B. S. Zhang, and L. X. Chen. 2009. Distinguishing Cambrian from Upper Ordovician source rocks: evidence from sulfur isotopes and biomarkers in the Tarim Basin. *Organic Geochemistry* 40:755–768.
doi:10.1016/j.orggeochem.2009.04.008

Chen, M. J., and J. H. Zhang. 1984a. On two evolutionary continuums of conodonts in the Middle Ordovician. *Journal of Nanjing University (Natural Science)* 1984–2:327–334 (in Chinese with English abstract).

Chen, M. J., and J. H. Zhang. 1984b. Middle Ordovician conodonts from Tangshan, Nanjing. *Acta Micropalaeontologica Sinica* 1:120–137 (in Chinese with English abstract).

Chen, M. J., and J. H. Zhang. 1989. Ordovician conodonts from the Shitai region, Anhui. *Acta Micropalaeontologica Sinica* 6(3):213–228 (in Chinese with English abstract).

Chen, M. J., Y. T. Chen, and J. H. Zhang. 1983. Ordovician conodont sequence in Nanjing Hills. *Journal of Nanjing University, Natural Sciences* 1983(1):129–139 (in Chinese with English abstract).

Chen, X., and S. M. Bergström, eds. 1995. The base of the *austrodentatus* Zone as a level for global subdivision of the Ordovician System. *Palaeoworld* 5:1–117.

Chen, X., J. Y. Rong, X. F. Wang, Z. H. Wang, Y. D. Zhang, and R. B. Zhan. 1995. Correlation of the Ordovician rocks of China: charts and explanatory notes. *International Union of Geological Sciences, Publication* 31:1–104.

Chen, X., Y. D. Zhang, S. M. Bergström, and H. F. Xu. 2006. Upper Darriwilian graptolite and conodont zonation in the global stratotype section of the Darriwilian stage (Ordovician) at Huangnitang, Changshan, Zhejiang, China. *Palaeoworld* 15:150–170.
doi:10.1016/j.palwor.2006.07.001

Chen, X., S. M. Bergström, Y. D. Zhang, D. Goldman, and Q. Chen. 2011. Upper Ordovician (Sandbian–Katian) graptolite and conodont zonation in the Yangtze region, China. *Earth and Environmental Science Transactions of the Royal Society of Edinburgh* 101:1–24.

Chen, X., D. Goldman, S. A. Leslie, and N. A. Williams. 2008. Ordovician Dawangou section, Tarim Basin, western Xinjiang, China and its implication for biogeography. *Geological Society of America Abstracts with Programs* 40(5):85.

Chen, X., Y. D. Zhang, Y. Li, J. X. Fan, P. Tang, Q. Chen, and Y. Y. Zhang, (in press). A correlation of the Ordovician black organic rocks from the Tarim Basin and its peripheral regions. *Science China (Earth Sciences)*.

Clark, D. L., W. C. Sweet, S. M. Bergström, G. Klapper, R. L. Austin, F. H. T. Rhodes, K. J. Müller, W. Ziegler, M. Lindström, J. F. Miller, and A. G. Harris. 1981. Conodonta. In *Treatise on Invertebrate Paleontology, part W, Miscellanea, supplement 2*, ed. R. A. Robison. Geological Society of America, Boulder and University of Kansas, Lawrence, 202pp.

Cooper, B. J. 1976. Multielement conodonts from the St. Clair Limestone (Silurian) of southern Illinois. *Journal of Paleontology* 50(2):205–217.

Cooper, B. J. 1981. Early Ordovician conodonts from the Horn Valley Siltstone, central Australia. *Palaeontology* 24:147–183.

Ding, L. S. 1987. Preliminary probes into Ordovician conodont biostratigraphy from the Kunshan area, Jiangsu, China. In *Symposium on petroleum stratigraphy and palaeontology* (1987), 41–53, 375–380, Geological Publishing House, Beijing (in Chinese with English abstract).

Dong, D. Y., and W. Wang. 2006. *The Cambrian—Triassic Conodont Faunas in Yunnan, China—Correlative Biostratigraphy and the Study of Palaeobiogeographic Province of Conodont*. Yunnan Science and Technology Press, Kunming, 347 pp. (in Chinese with English summary).

Drygant, D. M. 1974a. Simple conodonts from the Silurian and lowermost Devonian. *Paleontologicheskiy Sbornik* 10:64–69.

Drygant, D. M. 1974b. New Middle Ordovician conodonts from North-western Volyn. *Paleontologicheskiy Sbornik* 11:54–58.

Du, P. D., Z. X. Zhao, Z. B. Huang, Z. J. Tan, C. Wang, Z. L. Yang, G. Z. Zhang, and J. N. Xiao. 2005. Discussion on four conodont species of *Histiodella* from Tarim Basin and their stratigraphic implication. *Acta Micropalaeontologica Sinica* 22(4):357–369.

Duan, J. Y. 1990. Ordovician conodonts from northern Jiangsu and indices of their colour alteration. *Acta Micropalaeontologica Sinica* 7(1):19–41 (in Chinese with English abstract).

Dzik, J. 1976. Remarks on the evolution of Ordovician conodonts. *Acta Palaeontologica Polonica* 21:395–455.

Dzik, J. 1978. Conodont biostratigraphy and paleogeographical relations of the Ordovician Mójcza Limestone (Holy Cross Mts., Poland). *Acta Palaeontologica Polonica* 23:51–72.

Dzik, J. 1994. Conodonts of the Mójcza Limestone. *Palaeontologia Polonica* 53:43–128.

Ethington, R. L., and D. L. Clark. 1964. Conodonts from the El Paso Formation (Ordovician) of Texas and Arizona. *Journal of Paleontology* 38:685–704.

Ethington, R. L., and D. L. Clark. 1982. Lower and Middle Ordovician conodonts from the Ibex area, western Millard County, Utah. *Brigham Young University, Geological Studies* 28(2):1–160.

Fåhraeus, L. E. 1966. Lower Viruan (Middle Ordovician) conodonts from the Gullhögen Quarry, Southern Central Sweden. *Sveriges Geologiska Undersökning* C 610:1–40.

Fåhraeus, L. E. 1970. Conodont-based correlations of Lower and Middle Ordovician strata in western Newfoundland. *Geological Society of America Bulletin* 81:2061–2076.
doi:10.1130/0016-7606(1970)81[2061:CCOLAM]2.0.CO;2

Fåhraeus, L. E. 1982a. Recognition and redescription of Pander's (1856) *Scolopodus* (form) species—constituents of multi-element taxa (Conodontophorida, Ordovician). *Geologica et Palaeontologica* 16:19–28.

Fåhraeus, L. E. 1982b. Allopatric speciation and lineage zonation exemplified by the *Pygodus serrus—P. anserinus* transition (Conodontophorida, Ordovician). *Newsletters on Stratigraphy* 11(1):1–7.

Fåhraeus, L. E., and D. R. Hunter. 1981. Paleoecology of selected conodontophorid species from the Cobbs Arm Formation (Middle Ordovician), New World Island, north-central Newfoundland. *Canadian Journal of Earth Sciences* 18:1653–1665.
doi:10.1139/e81-153

Fåhraeus, L. E., and D. R. Hunter. 1985. Simple-cone conodont taxa from the Cobbs Arm Limestone (Middle Ordovician), New World Island, Newfoundland. *Canadian Journal of Earth Sciences* 22:1171–1182.
doi:10.1139/e85-120

Ferretti, A., and E. Serpagli. 1999. Late Ordovician conodont faunas from southern Sardinia, Italy: bistratigraphic and paleogeographic implications. In *Studies on Conodonts—Proceedings of the Seventh European Conodont Symposium, Bologna-Modena, 1998*, ed. E. Serpagli. *Bollettino della Società Paleontologica Italiana* 37(2–3):215–236.

Gao, Q. Q. 1991. *Conodonts*. In *Sinian to Permian stratigraphy and Palaeontology of the Tarim Basin II, Keping-Bachu area*. Xinjiang Petroleum Administration Bureau and the Jianghan Petroleum Administration Bureau, ed, Petroleum Industry Press, Beijing, 125–149 (in Chinese with English abstract).

Graves, R. W., and S. Ellison. 1941. Ordovician conodonts of the Marathon Basin, Texas. *University of Missouri, School of Mines and Metallurgy, Bulletin of the Technical Series* 14:1–26.

Hadding, A. R. 1913. Undre dicellograptusskiffern i Skåne jämte några därmed ekvivalenta bildningar. *Lunds Universitets Årsskrift, Ny Följd, Afdelning 2*, 9(15):1–90.

Harris, A. G., S. M. Bergström, R. L. Ethington, and R. J. Ross Jr. 1979. Aspects of Middle and Upper Ordovician conodont biostratigraphy of carbonate facies in Nevada and southeast California and comparison with some Appalachian successions. *Brigham Young University Geology Studies* 26:7–43.

Harris, A. G., J. A. Dumoulin, J. E. Repetski, and C. Carter. 1995. Correlation of Ordovician rocks of Northern Alaska. In *Ordovician Odyssey: short Papers for the Seventh International Symposium on the Ordovician System,* ed. J. D. Cooper, M. L. Droser, and S. C. Finney. Fullerton, Calif., Pacific Section Society for Sedimentary Geology (SEPM), Book 77:21–26.

Harris, R. W. 1962. New conodonts from Joins (Ordovician) Formation of Oklahoma. *Oklahoma Geology Notes* 22:199–211.

Hamar, G. 1964. Conodonts from the lower Middle Ordovician of Ringerike. *Norsk Geologisk Tidsskrift* 44:243–292.

Hamar, G. 1966. Preliminary report on conodonts from the Oslo-Asker and Ringerike districts. *Norsk Geologisk Tidsskrift* 46:27–83.

He, D. F., X. Y. Zhou, C. J. Zhang, and X. F. Yang. 2007. Tectonic types and evolution of Ordovician proto-type basins in the Tarim region. *Chinese Science Bulletin* 52 (supp. 1):164–177.
doi:10.1007/s11434-007-6010-z

Henningsmoen, G. 1948. The Tretaspis Series of the Kullatorp core. In *Deep boring through Ordovician and Silurian strata at Kinnekulle, Vestergötland*, ed. B. Waern, P. Thorslund, and G. Henningsmoen. *Bulletin of the Geological Institution of the University of Uppsala* 32:374–432.

Heredia, S., S. Peralta, and M. Beresi. 2005. Darriwilian conodont biostratigraphy of the Las Chacritas Formation, Central Precordillera (San Juan Province, Argentina). *Geologica Acta* 3(4):385–394.

Hints, O., and J. Nõlvak. 1999. Proposal for the lower boundary-stratotype of the Keila Regional Stage (Upper Ordovician). *Proceedings of the Estonian Academy of Sciences, Geology* 48:158–169.

Huang, B. C., R. X. Zhu, Y. Otofuji, and Z. Y. Yang. 2000. The Early Paleozoic paleogeography of the North China block and the other major blocks of China. *Chinese Science Bulletin* 45(12):1057–1065.
doi:10.1007/BF02887174

Huff, W. D., S. M. Bergström, and D. R. Kolata. 1992. Gigantic Ordovician volcanic ash falls in North America and Europe: biological, tectonomagmatic, and event-stratigraphic significance. *Geology* 20:875–878.
doi:10.1130/0091-7613(1992)020<0875:GOVAFI>2.3.CO;2

Ji, Z. L., and C. R. Barnes. 1994. Lower Ordovician conodonts of the St. George Group, Port au Port Peninsula, western Newfoundland, Canada. *Palaeontographica Canadiana* 11:1–149.

Johnston, D. I., and C. R. Barnes. 2000. Early and Middle Ordovician (Arenig) conodonts from St. Pauls Inlet and Martin Point, Cow Head Group, western Newfoundland, Canada. 2. Systematic paleontology. *Geologica et Palaeontologica* 34:11–87.

Kennedy, D. J., C. R. Barnes, and T. T. Uyeno. 1979. A Middle Ordovician conodont faunule from the Tetagouche Group, Camel Back Mountain, New Brunswick. *Canadian Journal of Earth Sciences* 16:540–551.
doi:10.1139/e79-049

Lamont, A., and M. Lindström. 1957. Arenigian and Llandeilian cherts identified in the Southern Uplands of Scotland by means of conodonts, etc. *Transactions of the Edinburgh Geological Society* 17:60–70.

Landing, E. 1976. Early Ordovician (Arenigian) conodont and graptolite biostratigraphy of the Taconic allochthon, eastern New York. *Journal of Paleontology* 50:614–646.

Lee, H. Y. 1975. Conodonten aus dem unteren und mittleren Ordovizium von Nordkorea. *Palaeontographica Abteilung A* 150:161–186.

Lehnert, O. 1995. Ordovizische Conodonten aus der Präkordillere Westargentiniens: Ihre Bedeutung für Stratigraphie und Paläogeographie. *Erlanger Geologische Abhandlungen* 125:1–193.

Lehnert, O., S. M. Bergström, M. Keller, and O. Bordonaro. 1999. Ordovician (Darriwilian-Caradocian) conodonts from the San Rafael Region, west-central Argentina: biostratigraphic, paleoecologic, and paleogeographic implications. In *Studies on Conodonts—Proceedings of the Seventh European Conodont Symposium, Bologna-Modena, 1998,* ed. E. Serpagli, *Bollettino della Società Paleontologica Italiana* 37(2–3):199–214.

Leslie, S. A. 2000. Mohawkian (Upper Ordovician) conodonts of eastern North America and Baltoscandia. *Journal of Paleontology* 74(6):1122–1147.
doi:10.1666/0022-3360(2000)074<1122:MUOCOE>2.0.CO;2

Leslie, S. A., and O. Lehnert. 2005. Middle Ordovician (Chazyan) sea-level changes and the evolution of the Ordovician conodont genus *Cahabagnathus* Bergström, 1983. *Journal of Paleontology* 79(6):1131–1142.
doi:10.1666/0022-3360(2005)079[1131:MOCSCA]2.0.CO;2

Li, Z. X., and C. M. Powell. 2001. An outline of the palaeogeographic evolution of the Australasian region since the beginning of the Neoproterozoic. *Earth-Science Reviews* 53:237–277.
doi:10.1016/S0012-8252(00)00021-0

Lindström, M. 1955a. Conodonts from the lowermost Ordovician strata of south-central Sweden. *Geologiska Föreningens i Stockholm Förhandlingar* 76:517–604.

Lindström, M. 1955b. The conodonts described by A. R. Hadding, 1913. *Journal of Paleontology* 29(1):105–111.

Lindström, M. 1964. *Conodonts*. Amsterdam: Elsevier Publishing Company.

Lindström, M. 1971. Lower Ordovician conodonts of Europe. In *Symposium on Conodont Biostratigraphy,* ed. W. C. Sweet, and S. M. Bergström. *Geological Society of America, Memoir* 127:21–61.

Löfgren, A. 1978. Arenigian and Llanvirnian conodonts from Jämtland, northern Sweden. *Fossils and Strata* 13:1–129.

Löfgren, A. 1990. Non-platform elements of the Ordovician conodont genus *Polonodus*. *Paläontologische Zeitschrift* 64(3/4):245–259.

Löfgren, A. 1994. Arenig (Lower Ordovician) conodonts and biozonation in the eastern Siljan District, central Sweden. *Journal of Paleontology* 68:1350–1368.

Löfgren, A. 1998. Apparatus structure of the Ordovician conodont *Decoriconus peselephantis* (Lindström 1955). *Paläontologische Zeitschrift* 72(3/4):337–350.

Löfgren, A. 2000. Early to early Middle Ordovician conodont biostratigraphy of the Gillberga quarry, northern Öland, Sweden. *GFF* 122:321–338.
doi:10.1080/11035890001224321

Löfgren, A. 2003. Conodont faunas with *Lenodus variabilis* in the upper Arenigian to lower Llanvirnian of Sweden. *Acta Palaeontologica Polonica* 48:417–436.

Löfgren, A. 2004. The conodont fauna in the Middle Ordovician *Eoplacognathus pseudoplanus* Zone of Baltoscandia. *Geological Magazine* 141(4):505–524.
doi:10.1017/S0016756804009227

Löfgren, A. 2006. An *Oistodus venustus*-like conodont species from the Middle Ordovician of Baltoscandia. *Paläontologische Zeitschrift* 80(1):12–21.

Löfgren, A., and T. J. Tolmacheva. 2003. Taxonomy and distribution of the Ordovician conodont *Drepanodus arcuatus* Pander, 1856, and related species. *Paläontologische Zeitschrift,* 77(1):203–221.

Löfgren, A., and J. H. Zhang. 2003. Element association and morphology in some Middle Ordovician platform-equipped conodonts. *Journal of Paleontology* 77(4):721–737.
doi:10.1666/0022-3360(2003)077<0721:EAAMIS>2.0.CO;2

McCracken, A. D. 1989. *Protopanderodus* (Conodontata) from the Ordovician Road River Group, northern Yukon Territory, and the evolution of the genus. *Geological Survey of Canada Bulletin* 388:1–39.

McCracken, A. D. 1991. Middle Ordovician conodonts from the Cordilleran Road River Group, northern Yukon Territory, Canada. In *Ordovician to Triassic Conodont Paleontology of the Canadian Cordillera,* ed. M. J. Orchard, and A. D. McCracken. *Geological Survey of Canada, Bulletin* 417:41–63.

McHargue, T. R. 1982. Ontogeny, phylogeny, and apparatus reconstruction of the conodont genus *Histiodella*, Joins Fm., Arbuckle Mountains, Oklahoma. *Journal of Paleontology* 56:1410–1433.

Mellgren, J., and M. E. Eriksson. 2006. A model of reconstruction for the oral apparatus of the Ordovician conodont genus *Protopanderodus* Lindström, 1971. *Transactions of the Royal Society of Edinburgh: Earth Sciences* 97:97–112.
doi:10.1017/S0263593300001425

Molnar, P., and P. Tapponnier. 1975. Cenozoic tectonics of Asia: effects of a continental collision. *Science* 189:419–426.
doi:10.1126/science.189.4201.419

Moskalenko, T. A. 1973. Conodonts of the Middle and Upper Ordovician of the Siberian Platform. *Akademiy Nauk SSSR, Sibirskoe Otdelinie, Trudy Instituta Geologii i Geofiziki* 137:1–143.

Ni, S. Z. 1981. Discussion on some problems of Ordovician stratigraphy by means of conodonts in eastern part of Yangtze Gorges Region. In *Selected papers on the 1st Convention of Micropalaeontological Society of China*. Micropalaeontological Society of China, ed., Science Press, Beijing, 127–134 (in Chinese).

Ni, S. Z., and Z. H. Li. 1987. Conodonts. In *Biostratigraphy of the Yangtze Gorge area 2:Early Palaeozoic Era*, ed. X. F. Wang, S. Z. Ni, Q. L. Zeng, G. H. Xu, T. M. Zhou, Z. H. Li, L. W. Xiang, and C. G. Lai, Geological Publishing House, Beijing, p. 386–447, 549–555, 619–632 (in Chinese with English abstract).

Nicoll, R. S. 1980. Middle Ordovician conodonts from the Pittman Formation, Canberra, ACT. *BMR Journal of Australian Geology & Geophysics* 5:150–153.

Nicoll, R. S. 1990. The genus *Cordylodus* and a latest Cambrian-earliest Ordovician conodont biostratigraphy. *BMR Journal of Australian Geology & Geophysics* 11:529–558.

Nicoll, R. S. 1992. Analysis of conodont apparatus organisation and the genus *Jumudontus* (Conodonta), a coniform-pectiniform apparatus structure from the Early Ordovician. *BMR Journal of Australian Geology & Geophysics* 13:213–228.

Norford, B. S., D. E. Jackson, and G. S. Nowlan. 2002. Ordovician stratigraphy and faunas of the Glenogle Formation, southeastern British Columbia. *Geological Survey of Canada, Bulletin* 569:1–77.

Nowlan, G. S. 1981. Some Ordovician conodont faunules from the Miramichi Anticlinorium, New Brunswick. *Geological Survey of Canada, Bulletin* 345:1–35.

Nowlan, G. S. 1983. Biostratigraphic, paleogeographic, and tectonic implications of Late Ordovician conodonts from the Grog Brook Group, northwestern New Brunswick. *Canadian Journal of Earth Sciences* 20:651–671.
doi:10.1139/e83-060

Nowlan, G. S., and J. G. Thurlow. 1984. Middle Ordovician conodonts from the Buchans Group, central Newfoundland, and their significance for regional stratigraphy of the Central Volcanic Belt. *Canadian Journal of Earth Sciences* 21:284–296.
doi:10.1139/e84-031

Orchard, M. J. 1980. Upper Ordovician conodonts from England and Wales. *Geologica et Palaeontologica* 14:9–44.

Ortega, G., G. L. Albanesi, and S. E. Frigerio. 2007. Graptolite-conodont biostratigraphy and biofacies of the Middle Ordovician Cerro Viejo succession, San Juan Precordillera, Argentina. *Palaeogeography, Palaeoclimatology, Palaeoecology* 245:245–263.
doi:10.1016/j.palaeo.2006.02.023

Ortega, G., G. L. Albanesi, A. L. Banchig, and G. L. Peralta. 2008. High resolution conodont-graptolite biostratigraphy in the Middle-Upper Ordovician of the Sierra de La Invernada Formation (Central Precordillera, Argentina). *Geologica Acta* 6(2):161–180.

Ottone, E. G., G. L. Albanesi, G. Ortega, and G. D. Holfeltz. 1999. Palynomorphs, conodonts and associated graptolites from the Ordovician Los Azules Formation, Central Precordillera, Argentina. *Micropaleontology* 45(3):225–250.
doi:10.2307/1486135

Pan, Y. S., W. M. Zhou, R. H. Xu, D. A. Wang, Y. Q. Zhang, Y. W. Xie, T. E. Chen, and H. Luo. 1996. Geological characteristics and evolution of the Kunlun Montains region during the Early Paleozoic. *Science in China (Series D)* 39(4):337–347.

Pander, C. H. 1856. *Monographie der fossilen Fische des Silurischen Systems der Russisch-Baltischen Gouvernements*. 91 p., Akademie der Wissenschaften, St. Petersburg.

Percival, I. G., E. J. Morgan, and M. M. Scott. 1999. Ordovician stratigraphy of the northern Molong Volcanic Belt: new facts and figures. *Geological Survey of New South Wales, Quarterly Notes* 108:8–27.

Percival, I. G., and Y. Y. Zhen. 2007. Darriwilian conodonts of Eastern Australia: biostratigraphy and biogeographic distribution. In *Proceedings of the Tenth International Symposium on the Ordovician System, The Third International Symposium on the Silurian System, and IGCP 503 Annual Meeting, June, 2007, Nanjing*, ed. J. Li, J.-X. Fan and I. Percival. *Acta Palaeontologica Sinica* 46 (Supplement), pp. 387–392.

Pickett, J. W., and I. G. Percival. 2001. Ordovician faunas and biostratigraphy in the Gunningbland area, central New South Wales. *Alcheringa* 25:9–52.
doi:10.1080/03115510108619212

Podhalańska, T. 1979. Middle Ordovician biozones in the Łeba Elevation, NW Poland. *Bulletin de l'Académie Polonaise des Sciences. Série des Sciences de la Terre* 26(3–4):221–227.

Pohler, S. M. L. 1994. Conodont biofacies of Lower to lower Middle Ordovician megaconglomerates, Cow Head Group, Western Newfoundland. *Geological Survey of Canada, Bulletin* 459:1–71.

Pohler, S. M. L., and M. J. Orchard. 1990. Ordovician conodont biostratigraphy, western Canadian Cordillera. *Geological Survey of Canada Paper* 90–15:1–37.

Pyle, L. J., and C. R. Barnes. 2001. Conodonts from the Kechika Formation and Road River Group (Lower to Upper Ordovician) of the Cassiar Terrane, northern British Columbia. *Canadian Journal of Earth Sciences* 38:1378–1401.
doi:10.1139/e01-033

Pyle, L. J., and C. R. Barnes. 2002. *Taxonomy, evolution, and biostratigraphy of conodonts from the Kechika Formation, Skoki Formation, and Road River Group (Upper Cambrian to Lower Silurian), Northeastern British Columbia*. 227pp., NRC Research Press, Ottawa.

Pyle, L. J., and C. R. Barnes. 2003. Conodonts from a platform-to-basin transect, Lower Ordovician to Lower Silurian, northeastern British Columbia, Canada. *Journal of Paleontology* 77(1):146–171.
doi:10.1666/0022-3360(2003)077<0146:CFAPTB>2.0.CO;2

Rasmussen, J. A. 1991. Conodont stratigraphy of the Lower Ordovician Huk Formation at Slemmestad, southern Norway. *Norsk Geologisk Tidsskrift* 71:265–288.

Rasmussen, J. A. 2001. Conodont biostratigraphy and taxonomy of the Ordovician shelf margin deposits in the Scandinavian Caledonides. *Fossils and Strata* 48:1–180.

Rhodes, F. H. T. 1953. Some British Lower Palaeozoic conodont faunas. *Philosophical Transactions of the Royal Society of London, Series B, Biological Sciences* 237:261–334.
doi:10.1098/rstb.1953.0005

Sergeeva, S. P. 1963. Conodonts from the Lower Ordovician of the Leningrad region. *Paleontologicheskiy Zhurnal, Akademiya Nauk SSSR* 2:93–108.

Sergeeva, S. P. 1974. Some new conodonts from the Ordovician deposits of Leningrad region. *Paleontologičeskij sbornik* 2:79–84.

Serpagli, E. 1974. Lower Ordovician conodonts from Precordilleran Argentina (Province of San Juan). *Bollettino della Società Paleontologica Italiana* 13:17–98.

Simes, J. E. 1980. Age of the Arthur Marble: conodont evidence from Mount Owen, northwest Nelson. *New Zealand Journal of Geology and Geophysics* 23(4):529–532.

Smith, M. P. 1991. Early Ordovician conodonts of east and north Greenland. *Meddelelser om Grønland, Geoscience* 26:1–81.

Stouge, S. 1984. Conodonts of the Middle Ordovician Table Head Formation, western Newfoundland. *Fossils and Strata* 16:1–145.

Stouge, S., and G. Bagnoli. 1990. Lower Ordovician (Volkhovian-Kundan) conodonts from Hagudden, northern Öland, Sweden. *Palaeontographia Italica* 77:1–54.

Stouge, S., and G. Bagnoli. 1999. The suprageneric classification of some Ordovician prioniodontid conodonts. In *Studies on Conodonts—Proceedings of the Seventh European Conodont Symposium, Bologna-Modena, 1998*, ed. E. Serpagli. *Bollettino della Società Paleontologica Italiana* 37(2–3):145–158.

Sweet, W. C. 1988. *The Conodonta: Morphology, Taxonomy, Paleoecology, and Evolutionary History of a Long-Extinct Animal Phylum*. 212pp. Clarendon Press, Oxford.

Sweet, W. C. 2000. Conodonts and biostratigraphy of Upper Ordovician strata along a shelf to basin transect in central Nevada. *Journal of Paleontology* 74(6):1148–1160.
doi:10.1666/0022-3360(2000)074<1148:CABOUO>2.0.CO;2

Sweet, W. C., and S. M. Bergström. 1962. Conodonts from the Pratt Ferry Formation (Middle Ordovician) of Alabama. *Journal of Paleontology* 36:1214–1252.

Sweet, W. C., R. L. Ethington, and C. R. Barnes. 1971. North American Middle and Upper Ordovician conodont faunas. *Geological Society of America Memoir* 127:163–193.

Tolmacheva, T. J. 2006. Apparatus of the conodont *Scolopodus striatus* Pander, 1856 and a re-evaluation of Pander's species of *Scolopodus*. *Acta Palaeontologica Polonica* 51:247–260.

Trotter, J. A., and B. D. Webby. 1994. Upper Ordovician conodonts from the Malongulli Formation, Cliefden Caves area, central New South Wales. *AGSO Journal of Australian Geology & Geophysics* 15(4):475–499.

van Wamel, W. A. 1974. Conodont biostratigraphy of the Upper Cambrian and Lower Ordovician of north-western Öland, south-eastern Sweden. *Utrecht Micropalaeontological Bulletins* 10:1–125.

Viira, V. 1967. Ordovician conodont succession in the Ohesaare core. *Eesti NSV teaduste Akadeemia Toimetised, Keemia Geoloogia* 16(4):319–329.

Viira, V. 1974. *Konodonty ordovika Pribaltiki* (Ordovician conodonts of the east Baltic). 142 pp., Tallinn ("Valgus").

Viira, V. 2008. Conodont biostratigraphy in the Middle-Upper Ordovician boundary beds of Estonia. *Eastonian Journal of Earth Sciences* 57(1):23–38.
doi:10.3176/earth.2008.1.03

Viira, V. 2011. Lower and Middle Ordovician conodonts from the subsurface of SE Estonia and adjacent Russia. *Estonian Journal of Earth Sciences* 60(1):1–21.
doi:10.3176/earth.2011.1.01

Viira, V., A. Löfgren, S. Mägi, and J. Wickström. 2001. An Early to Middle Ordovician succession of conodont faunas at Mäekalda, northern Estonia. *Geological Magazine* 138(6):699–718.
doi:10.1017/S0016756801005945

Wang, C. Y., ed. 1993. *Conodonts of the Lower Yangtze Valley — an index to biostratigraphy and organic metamorphic maturity*. Science Press, Beijing, 326 pp. (in Chinese with English summary).

Wang, Q. M., T. Nishidai, and M. P. Coward. 1992. The Tarim basin, NW China: formation and aspects of petroleum geology. *Journal of Petroleum Geology* 15(1):5–34.
doi:10.1111/j.1747-5457.1992.tb00863.x

Wang, Q., P. Z. Zhang, J. T. Freymueller, R. Bilham, K. M. Larson, X. Lai, X. Z. You, Z. J. Niu, J. C. Wu, Y. X. Li, J. N. Liu, Z. Q. Yang, and Q. Z. Chen. 2001. Present-day crustal deformation in China constrained by global positioning system measurements. *Science* 294:574–577.
doi:10.1126/science.1063647

Wang, Y. J., J. F. Cheng, and Y. D. Zhang. 2008. New radiolarian genera and species of Heituao Formation (Ordovician) in the Kuruktag Region, Xinjiang. *Acta Palaeontologica Sinica* 47(4):393–404 (in Chinese with English Abstract).

Wang, Z. H. 2001. Ordovician conodonts from Kalpin of Xinjiang and Pingliang of Gansu across the base of Upper Ordovician Series. *Acta Micropalaeontologica Sinica* 18(4):349–363.

Wang, Z. H., and K. Q. Lou. 1984. Late Cambrian and Ordovician conodonts from the marginal areas of the Ordos Platform, China. *Bulletin of Nanjing Institute of Geology and Palaeontology, Academia Sinica* 8:237–304 (in Chinese with English abstract).

Wang, Z. H., and T. R. Zhou. 1998. Ordovician conodonts from western and northeastern Tarim and their significance. *Acta Palaeontologica Sinica* 37(2):173–193.

Wang, Z. H., and S. M. Bergström. 1999a. Conodonts across the base of the Darriwilian Stage in South China. *Acta Micropalaeontologica Sinica* 16(4):325–350 (in Chinese with English abstract).

Wang, Z. H., and S. M. Bergström. 1999b. Conodont-graptolite biostratigraphic relations across the base of the Darriwilian Stage (Middle Ordovician) in the Yangtze Platform and the JCY area in Zhejiang, China. In *Studies on Conodonts—Proceedings of the Seventh European Conodont Symposium, Bologna-Modena, 1998*, ed. E. Serpagli. *Bollettino della Società Paleontologica Italiana* 37(2–3):187–198.

Wang, Z. H., and Y. P. Qi. 2001. Ordovician conodonts from drillings in the Taklimakan desert, Xinjiang, NW China. *Acta Micropalaeontologica Sinica* 18(2):133–148.

Wang, Z. H., S. M. Bergström, and H. R. Lane. 1996. Conodont provinces and biostratigraphy in Ordovician of China. *Acta Palaeontologica Sinica* 35(1):26–59.

Wang, Z. H., Y. P. Qi, and S. M. Bergström. 2007. Ordovician conodonts of the Tarim region, Xinjiang, China: occurrence and use as palaeoenvironment indicators. *Journal of Asian Earth Sciences* 29:832–843.
doi:10.1016/j.jseaes.2006.05.007

Webby, B. D., F. Paris, M. L. Droser, and I. G. Percival, eds. 2004. *The great Ordovician biodiversification event*. Columbia University Press, New York, 484 pp.

Webers, G. F. 1966. The Middle and Upper Ordovician conodont faunas of Minnesota. *Minnesota Geological Survey Special Publication* 4:1–123.

Windley, B. F., M. B. Allen, C. Zhang, Z. Y. Zhao, and G. R. Wang. 1990. Paleozoic accretion and Cenozoic redeformation of the Chinese Tien Shan Range, central Asia. *Geology* 18:128–131.
doi:10.1130/0091-7613(1990)018<0128:PAACRO>2.3.CO;2

Xiong, J. F., T. Wu, and D. S. Ye. 2006. New advances on the study of Middle-Late Ordovician conodonts in Bachu, Xinjiang. *Acta Palaeontologica Sinica* 45(3):359–373 (in Chinese with English abstract).

Yao, Y. G., and K. J. Hsü. 1994. Origin of the Kunlun Mountains by arc-arc and arc-continent collisions. *The Island Arc* 3:75–89.
doi:10.1111/j.1440-1738.1994.tb00096.x

Zeng, Q. L., S. Z. Ni, G. H. Xu, T. M. Zhou, X. F. Wang, Z. H. Li, C. G. Lai, and L. W. Xiang. 1983. Subdivision and correlation on the Ordovician in the eastern Yangtze Gorges, China. *Bulletin of the Yichang Institute of Geology & Mineral Resources, Chinese Academy of Geological Sciences* 6:1–68.

Zhang, J. H. 1997. The Lower Ordovician conodont *Eoplacognathus crassus* Chen & Zhang, 1993. *GFF* 119:61–65.

Zhang, J. H. 1998a. The Ordovician conodont genus *Pygodus*. In *Proceedings of the sixth European conodont Symposium (ECOS VI)*, ed. H. Szaniawski. *Palaeontologia Polonica* 58:87–105.

Zhang, J. H. 1998b. Four evolutionary lineages of the Middle Ordovician conodont family Polyplacognathidae. *Meddelanden från Stockholms Universitets Institution för Geologi och Geokemi 298* (Paper 5):1–35.

Zhang, J. H. 1998c. Conodonts from the Guniutan Formation (Llanvirnian) in Hubei and Hunan Provinces, south-central China. *Stockholm Contributions in Geology* 46:1–161.

Zhang, J. H. 1998d. Review of the Ordovician conodont zonal index *Eoplacognathus suecicus* Bergström. *Meddelanden från Stockholms Universitets institution för geologi och geokemi* 298 (Paper 6):1–16.

Zhang, J. H., and Chen, M. J. 1992. Evolutionary trends and stratigraphic significance of *Periodon*. *Acta Micropalaeontologica Sinica* 9(4):391–396 (in Chinese with English abstract).

Zhang, Y. D., X. Chen, G. H. Yu, D. Goldman, and X. Liu. 2007. *Ordovician and Silurian rocks of northwest Zhejiang and northeast Jiangxi provinces, SE China*, 189 pp, University of Science and Technology of China Press, Hefei.

Zhao, S. Y., T. X. An, H. R. Qiu, S. L. Wan, and H. Ding. 1984. Conodonts. In *Palaeontological Atlas of North China, Volume III, Micropalaeontology*, ed. Tianjing Institute of Geology and Mineral Resources, 857 pp, Geological Publishing House, Beijing (in Chinese).

Zhao, X., R. S. Coe, S. A. Gilder, and G. M. Frost. 1996. Palaeomagnetic constraints on the palaeogeography of China: implications for Gondwanaland. *Australian Journal of Earth Sciences* 43:643–672.
doi:10.1080/08120099608728285

Zhao, Z. J., Z. X. Zhao, and Z. B. Huang. 2006. Ordovician conodont zones and sedimentary sequences of the Tarim Basin, Xinjiang, NW China. *Journal of Stratigraphy* 30(3):193–203 (in Chinese with English abstract).

Zhao, Z. X., and G. Z. Zhang. 1991. Subsurface Ordovician conodonts and stratigraphy of the Tarim Basin. Pp. 64–74 in *Papers on petroleum exploration in the Tarim Basin*. Science, Technology and Health Publishing House of Xinjiang, Ulumuqi (in Chinese with English abstract).

Zhao, Z. X., G. Z. Zhang, and J. N. Xiao. 2000. *Paleozoic stratigraphy and conodonts in Xinjiang*. 340 pp., Petroleum Industry Press, Beijing (in Chinese with English Abstract).

Zhen, Y. Y., and B. D. Webby. 1995. Upper Ordovician conodonts from the Cliefden Caves Limestone Group, central New South Wales, Australia. *Courier Forschungsinstitut Senckenberg* 182:265–305.

Zhen, Y. Y., and I. G. Percival. 2004a. Middle Ordovician (Darriwilian) conodonts from allochthonous limestones in the Oakdale Formation of central New South Wales, Australia. *Alcheringa* 28:77–111.
doi:10.1080/03115510408619276

Zhen, Y. Y., and I. G. Percival. 2004b. Middle Ordovician (Darriwilian) conodonts from the Weemalla Formation, south of Orange, New South Wales. *Memoirs of the Association of Australasian Palaeontologists* 30:153–178.

Zhen, Y. Y., and J. W. Pickett. 2008. Ordovician (Early Darriwilian) conodonts and sponges from west of Parkes, central New South Wales. *Proceedings of the Linnean Society of New South Wales* 129:57–82.

Zhen, Y. Y., and R. S. Nicoll. 2009. Biogeographic and biostratigraphic implications of the *Serratognathus bilobatus* fauna (Conodonta) from the Emanuel Formation (Early Ordovician) of the Canning Basin, Western Australia. *Records of the Australian Museum* 61(1):1–30.
doi:10.3853/j.0067-1975.61.2009.1520

Zhen, Y. Y., B. D. Webby, and C. R. Barnes. 1999. Upper Ordovician conodonts from the Bowan Park succession, central New South Wales, Australia. *Geobios* 32(1):73–104.
doi:10.1016/S0016-6995(99)80084-9

Zhen, Y. Y., I. G. Percival, and J. R. Farrell. 2003a. Late Ordovician allochthonous limestones in Late Silurian Barnby Hills Shale, central western New South Wales. *Proceedings of the Linnean Society of New South Wales* 124:29–51.

Zhen, Y. Y., I. G. Percival, and B. D. Webby. 2003b. Early Ordovician conodonts from far western New South Wales, Australia. *Records of the Australian Museum* 55(2):169–220.
doi:10.3853/j.0067-1975.55.2003.1383

Zhen, Y. Y., I. G. Percival, and B. D. Webby. 2004a. Early Ordovician (Bendigonian) conodonts from central New South Wales, Australia. *Courier Forschungsinstitut Senckenberg* 245:39–73.

Zhen, Y. Y., I. G. Percival, and B. D. Webby. 2004b. Conodont faunas from the Mid to Late Ordovician boundary interval of the Wahringa Limestone Member (Fairbridge Volcanics), central New South Wales. *Proceedings of the Linnean Society of New South Wales* 125:141–164.

Zhen, Y. Y., I. G. Percival, A. Löfgren, and J. B. Liu. 2007. Drepanoistodontid conodonts from the Early Ordovician Honghuayuan Formation of Guizhou, South China. *Acta Micropalaeontologica Sinica* 24(2):125–148.

Zhen, Y. Y., Y. D. Zhang, and I. G. Percival. 2009a. Early Sandbian (Late Ordovician) conodonts from the Yenwashan Formation, western Zhejiang, South China. *Alcheringa* 33:133–161.
doi:10.1080/03115510902844160

Zhen, Y. Y., I. G. Percival, R. A. Cooper, J. E. Simes, and A. J. Wright. 2009b. Darriwilian (Middle Ordovician) conodonts from Thompson Creek, Nelson Province, New Zealand. *Memoir of the Association of Australasian Palaeontologists* 37:25–53.

Zhong, D. 1990. Conodonts. 144–154, 243–247. In *Sinian to Permian Stratigraphy and Palaeontology of the Tarim Basin, Xinjiang Volume I—Kuruktag Area*, ed. South Xinjiang Petroleum Prospecting Corporation, Xinjiang Petroleum Administration Bureau, and the Institute of Petroleum and Geosciences, Dian-Qian-Gui Petroleum Prospecting Bureau. Nanjing University Press, Nanjing (in Chinese).

Zhong, D., and Y. X. Hao. 1990. Ordovician System. 40–104. In *Sinian to Permian stratigraphy and palaeontology of the Tarim Basin, Xinjiang Volume I—Kuruktag Area*, ed. South Xinjiang Petroleum Prospecting Corporation, Xinjiang Petroleum Administration Bureau, and the Institute of Petroleum and Geosciences, Dian-Qian-Gui Petroleum Prospecting Bureau. Nanjing University Press, Nanjing (in Chinese).

Zhou, D. K., T. R. Zhou, and P. Wang. 1991. Division of geological ages of Qiulitag Group in northeastern Tarim. In *Research of petroleum geology of northern Tarim Basin in China*, ed. R. X. Jia, pp. 37–43. China University of Geoscience Press, Wuhan (in Chinese with English abstract).

Zhou, Z. Y., and P. J. Chen, eds. 1990. *Biostratigraphy and Geological Evolution of Tarim*. 366 pp, Science Press, Beijing (in Chinese).

Zhou, Z. Y., and P. J. Chen, eds. 1992. *Biostratigraphy and Geological Evolution of Tarim*. 399 pp, Science Press, Beijing.

Zhou, Z. Y., and H. L. Lin. 1995. *Stratigraphy, Paleogeography and Plate-tectonics of Northwest China*. 299 pp, Nanjing University Press, Nanjing (in Chinese).

Zhylkaidarov, A. 1998. Conodonts from Ordovician ophiolites of central Kazakhstan. *Acta Palaeontologica Polonica* 43(1): 53–68.

Ziegler, W., ed. 1974. *Catalogue of Conodonts,* vol. 2. 403 pp. (Schweizerbart'sche Verlagsbuchhandlung, Stuttgart).

Addendum

While this paper was in review, it came to the attention of the authors that a paper by Stouge *et al.*, presented to the 11th International Symposium on the Ordovician System, gave a slightly different biostratigraphic zonation for the early to middle Darriwilian part of the Dawangou and Yangjikan sections. Without detail of the stratigraphic ranges of the critical species of conodonts, and systematic descriptions of the fauna, it is not possible at this point to discuss the relation between the biostratigraphic scheme outlined by Stouge *et al.* (2011), and our interpretation.

Stouge, S., P. D. Du, and Z. X. Zhao. 2011. Middle Ordovician (Darriwilian) global conodont zonation based the Dawangou and Saergan formations of the western Tarim region, Xinjiang Province, China. In *Ordovician of the World*, ed. J. C. Gutiérrez-Marco, I. Ràbano & D. García-Bellido. Spain. *Cuadermos del Museo Geominero, 14.* Instituto Geológico y Minero de España, Madrid, pp. 581–586.

Records of the Australian Museum (2011) Vol. 63: 267–272. ISSN 0067-1975
doi:10.3853/j.0067-1975.63.2011.1583

Sororsenexa—New Genus (Diptera: Empididae: Hemerodromiinae) from Australia

ADRIAN R. PLANT

Department of Biodiversity & Systematic Biology, National Museum of Wales,
Cathays Park, Cardiff, CF10 3NP, United Kingdom
adrian.plant@museumwales.ac.uk

ABSTRACT. *Sororsenexa,* new genus (Insecta: Diptera: Empididae: Hemerodromiinae), is described from Australia. The genus is monotypic with *Sororsenexa macalpinei* n.sp. its type species. Systematic relationships with other Hemerodromiinae are discussed and a key to Australian genera of the tribe Chelipodini presented.

PLANT, ADRIAN R. 2011. *Sororsenexa*—new genus (Diptera: Empididae: Hemerodromiinae) from Australia. *Records of the Australian Museum* 63(3): 267–272.

The Empididae subfamily Hemerodromiinae comprises small predatory flies with characteristically inflated raptorial forelegs. Most of the 17 extant genera and 453 species currently described have been assigned to two monophyletic tribes, Hemerodromiini and Chelipodini, although the systematic position of some genera remains uncertain (Plant, 2011). However, many taxa remain undescribed at both species and genus levels, particularly in moist tropical and southern temperate forests. In Australia a single species *Chelipoda biroi* (Bezzi, 1904) is known (Smith, 1989) but judging from museum collections, a rich fauna of Hemerodromiini and Chelipodini is present, especially in the eastern mountain ranges and in Tasmania.

Several undescribed Australian Hemerodromiinae were included in a recent phylogenetic appraisal of the subfamily (Plant, 2011). One of these (designated GENAU[C] in that study) was considered to belong in Chelipodini but showed rather weak support as the sister-group of the rest of the tribe. It exhibits several important apomorphies including having only a single row of short specialized setae beneath the front femur, an apicoventral spine on the front tibia, vein Sc fading not long after the branch point of Rs and especially the termination of the costa shortly beyond the apex of the wing and there can be little doubt that the taxon warrants generic status. The present work describes this taxon as a new genus comprising a single new species.

Materials and methods

Specimens used in this study were borrowed from or deposited in the Australian Museum, Sydney, Australia and National Museum of Wales, Cardiff, UK. The general morphological terms of McAlpine (1981) and antennal nomenclature of Stuckenberg (1999) were employed and interpretation of genitalic homology followed Cumming *et al.* (1995) and Sinclair (2000). Maceration of genitalia was performed in hot (90°C) lactic acid (85% v/v).

Taxonomy

Sororsenexa n.gen.

Figs 1–7.

Type species: *Sororsenexa macalpinei* n.sp., here designated.

Etymology. The generic name is a contraction of the Latin *soror* (sister) and *senex* (old person) in reference to the putative basal sister group relationship between *Sororsenexa* and the remaining Chelipodini. The genus is feminine.

Diagnosis. A characteristic genus of the Empididae subfamily Hemerodromiinae (Fig. 1) with raptorial forelegs widely separated from the midlegs. *Sororsenexa* can be distinguished from other Hemerodromiinae by the combination of characters *(a)* costa not circumambient, continued a short way only beyond apex of wing, *(b)* vein R_{4+5} forked, *(c)* front femur with a single ventral row of short specialized setae (denticles) and more or less lacking posteroventral or anteroventral rows of stronger "normal" setae on either side, *(d)* uniserial acrostichal setae well developed if small along entire length between anterior of scutum and front of prescutellar depression, *(e)* setulae present (if small) on laterotergite.

Description. (Description based on holotype and paratypes owing to shrinkage and distortion affecting all specimens). Head large, in dorsal view (Fig. 2) at least as wide as thorax and half its length; somewhat dorsoventrally compressed (at least in female, male specimens are distorted). Eyes with anterior ommatidia enlarged in both sexes; crena (eye notch) absent. Face short, hardly as long as three basal antennal segments, narrow, no wider than scape is long, narrower in male, parallel sided. Mouth cavity apparently deeply recessed, abruptly receding from frons ventrally (possibly a distortion artefact due to shrinkage on drying but present in all type specimens). Frons very broad triangular, margins almost linear; 2 pairs of weak marginal setae behind antenna and much stronger pair near margin just behind level of posterior ocellus. Ocellar tubercle hardly developed with one strong and one weak pair of setae. Vertex with 2 or more strong setae more or less contiguous with line of smaller stout postocular occiputal setae which become finer on lower occiput; some distinct setae on posterior occiput and behind mouth and some longer setae lateral to mouth opening. Antenna with scape almost bare; pedicel hardly longer than wide with subapical circlet of setae; postpedicel globose, covered with minute setulae and a few longer hairs subapically; stylus somewhat longer than basal antennal segments combined, tapering, micropilose, slightly swollen basal article and bristle-like apical mechanoreceptor present. Proboscis rather stout, apically pointed, as long as head is deep, directed vertically downwards. Palpus very small, almost globular, micropilose with 2–3 long fine setae.

Thorax short, hardly longer than deep, narrowed anteriorly in profile. Scutum rather strongly arched anteriorly in lateral view (Fig. 1), prescutellar area more or less flat; quadrate rectangular in dorsal view with pospronotal lobe well defined and slightly protuberant. Fused anepisternum + katepisternum rather narrowly triangular, in lateral view with longer anteroventral margin more or less linear. Scutellum with posterior margin rounded. Acrostichal setae small but distinct, uniserial extending posteriorly to anterior margin of prescutellar depression; 6–7 dorsocentral setae well developed, becoming longer posteriorly, anterior 1 or 2 setae displaced laterally such that line of dorsocentrals rather curving anteriorly; postpronotal setae long, incurved, strong, with much smaller seta below; 1 long strong seta extending laterally behind postpronotal lobe; 3–4 notopleural setae, lower pair very strong; 1 small supra-alar and stronger postalar setae; 1 strong outwardly directed seta on thoracic "collar". Laterotergite with 3–4 fine setulae.

Legs rather stout and conspicuously setose. Front coxa rather short and broad, only 4× as long as wide and 0.6–0.7× length of thorax, 1 row of long fine erect setae anteriorly (Fig. 3); mid and posterior coxae with similarly long setae anteroapically and on outer face. Front femur (Fig. 3) stout, evenly inflated 4–5× as long as wide, rather longer than front coxa; line of short stout denticle-like setae ventrally at the base of which are two larger but still stout setae (in females these basal setae often more or less of equal size while in males usually unequally developed); posteroventral row of fine distinct setae widely spaced from line of denticles; anteroventral row of small setulae very weakly developed and inconspicuous; dorsal ciliation of fine setae conspicuous; posterior face with distinct setae, anterior face almost bare. Posterior femur somewhat inflated but only about 0.5 as wide as front femur and slightly longer, distinctly hairy with dorsal and anteroventral series of setae about as long as depth of limb; mid femur more slender with less conspicuous but still strong setae throughout and rather stronger posteroventral series of setae.

Front tibia about 0.8× length of front femur, geniculate basally; small sharply pointed curving apical spine (Fig. 3) arising from slight ventral swelling juxtaposing with basal setae of femur when limb is reflexed; ventral row of numerous short rather spine-like adpressed setae. Mid and posterior tibiae about as long as their corresponding femora, conspicuously setose but setae not as long as depth of limb except dorsally on posterior tibia. All tarsi with segments 1–4 progressively shorter, second segment of front leg not shorter than third.

Abdomen with scattered fine hair like setae longest on posterior margins of sternites and tergites. Male terminalia (Figs 4–5) reflexed to more or less vertical position; hypandrium and epandrium separate; hypandrium large, rather oblong quadrate appearing somewhat keel-shaped in posterior (Fig. 5) or ventrolateral aspects, left and right lobes narrowly separated by weakly sclerotized area posteriorly (usually visible only after maceration) and bearing some long marginal setae; epandrium smaller than hypandrium, flattened ovate with numerous long setae from apex of which rather pointed leaf like subepandrial process emerges dorsally. Cercus projected vertically along anterodorsal margin of epandrium, narrow and rather strap-like in profile but viewed from in front (Fig. 6) inwardly curved with numerous small stout setae apically on inner face. Distal section of phallus strongly reflexed anteriorly when not withdrawn into sinusoidal phallic sheath; sheath strongly reflexed posteriorly on distal part.

Figure 1. *Sororsenexa macalpinei* n.sp., male habitus.

Female abdomen bluntly tapered apically, cercus about 2× as long as wide with long apical setae of equal length and a few shorter marginal setae.

Wing (Fig. 7) rather short and broad, 2.5× as long as widest, apically rounded, anterior and posterior margins almost subparallel, anal lobe very weakly developed. Vein C strong to wing tip, fading thereafter and completely absent along posterior margin. Vein Sc present, free, reaching almost to C but very weak beyond level of branching of Rs; crossvein h present. Rs short, originating at about 0.25 from base of wing, diverging narrowly from R_1. R_{2+3} long, ending in distal 0.3 of wing. R_{4+5} forked and diverging at angle of 60–65° with R_5 ending near wing tip. Median vein linear, fork M_{1+2} absent. CuA_1 linear, fading near wing margin. Cell br rather narrow, truncately pointed apically, longer than cells bm or cup. Cell cup closed, apically rectangular, A_1 strong continued for short distance beyond end of cup. Costal bristle strong.

***Sororsenexa macalpinei* n.sp.**

Figs 1–7

Type material. HOLOTYPE ♂, AUSTRALIA: Royal National Park near Sydney, NSW, 13 Aug. 1971, D.K. McAlpine (Australian Museum). Paratypes 7♂♂, 8♀♀, same data as holotype: 3♂♂, 3♀♀, Calga, Hawkesbury Distr., NSW, 29.9.1956, D.K. McAlpine (9♂♂, 10♀♀, Australian Museum; 1♂, 1♀, National Museum of Wales).

Description. Length 1.0–1.1 mm (♂), 1.1–1.3 mm (♀); wing 1.3–1.4 mm. Head black rather thickly and uniformly covered with silvery grey dust. Male antenna yellow, postpedicel not contrasting with basal segments, stylus black. Female antenna darker, postpedicel blackish contrasting with somewhat paler basal segments. Mouthparts yellowish with apex of proboscis black. Setae brownish in male, blackish

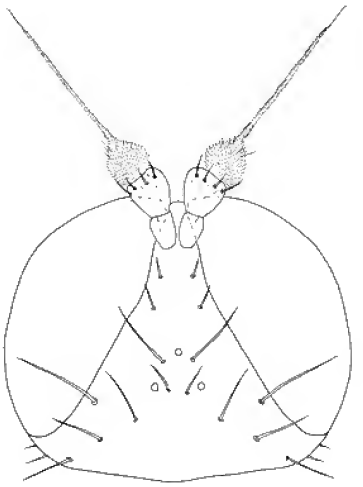

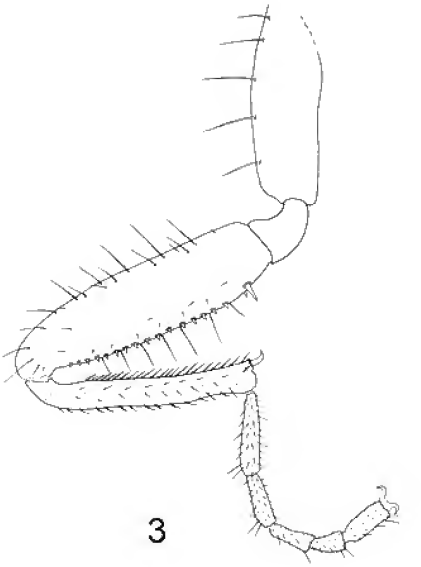

Figures 2–3. *Sororsenexa macalpinei* n.sp. (2) female head, dorsal; (3) male anterior leg, anterior aspect.

in female, rather paler on lower occiput near mouth cavity.

Thorax with ground colour of scutum and scutellum varying from dark yellow to almost black, generally paler in males but always heavily obscured by silvery grey dusting which in certain lights can appear blackish along median line or along line of dorsocentral setae on scutum; pleura somewhat paler and rather less strongly but uniformly dusted; all setae dark yellowish brown.

Legs yellow to yellowish brown, apical two segments of tarsi vaguely darker; all setae yellowish but front tibia with apical spine and front femur with ventral denticles and ventrobasal setae shining black.

Abdomen dark brown with similarly coloured or slightly paler setae; thinly but uniformly greyish dusted including hypandrium and epandrium. Subterminal segments progressively narrower than anterior segments in female, similarly sized in male.

Wings faintly tinged brownish yellow, veins yellow to yellowish brown, halter dirty yellow.

Etymology. The specific name honours David McAlpine who has collected all known specimens of *S. macalpinei*.

Comments. The precise collection localities we not recorded but the collector considers both known sites to have been a mixture of scattered eucalypts and sclerophyll heath. All specimens were taken in August or September which are cool months of the austral late winter and early spring.

Discussion

A recent cladistic analysis of Hemerodromiinae recovered *Sororsenexa* subtending a sister-group relationship between *Anaclastoctedon* Plant and the rest of the tribe Chelipodini (Plant, 2011). *Sororsenexa* exhibits several apomorphies important in the Chelipodini including the costa fading beyond the apex of the wing, front tibia with a strong apicoventral spine and only a single row of short denticles beneath the front femur without any closely adjacent anteroventral or posteroventral spine-like setae. In all other Hemerodromiinae the costa is circumambient and the ventral row of denticles is biserial, at least in part, on either side of which are obvious strong spine-like setae. Although a well-developed tibial spine is present in some Hemerodromiini genera, it is otherwise absent in Chelipodini. *Sororsenexa* is also the sole member of the Chelipodini in which the plesiomorphic conditions of forked of R_{4+5} and well-developed acrostichal setae are retained. The South American genus *Chelipodozus* Collin, formally included in Chelipodini but now considered *incertae sedis* in Hemerodromiinae (Plant, 2011) also has R_{4+5} forked. In *Chelipodozus* however cell dm is present and cup is apically rounded. The wings of all previously described Hemerodromiinae are long and narrow (usually at least 3× long as wide) and the relatively short and broad wings of *Sororsenexa* appear to be unique characters of the genus. The absence of a crena (eye notch) in *Sororsenexa* is a highly diagnostic character as it is present in almost all Empididae and is a conspicuous feature in all other described Hemerodromiinae.

Sororsenexa shares two important apomorphies with *Anaclastoctedon*; the loss of the fork in vein M_{1+2} and loss of crossvein dm-cu, although the latter in particular is subject to much homoplasy in Hemerodromiinae (Plant, 2011). Both these genera retain a plesiomorphic elongate second tarsal segment on the front leg, a condition otherwise characteristic of Hemerodromiini and the most basal Hemerodromiinae genera *Afrodromia* Smith and *Drymodromia* Becker. *Anaclastoctedon* however exhibits two highly distinctive and unique apomorphies; loss of the basal article of the antennal stylus and greatly enlarged, bilobed male cerci (Plant, 2010; 2011).

The single known species of *Sororsenexa* has only been collected from two localities in the Sydney Basin, New South Wales, Australia but further collecting will be required to establish if it is truly endemic to this area or merely overlooked, perhaps on account of its unusually small size or it emerging during the cooler winter months when collecting efforts are much less frequent.

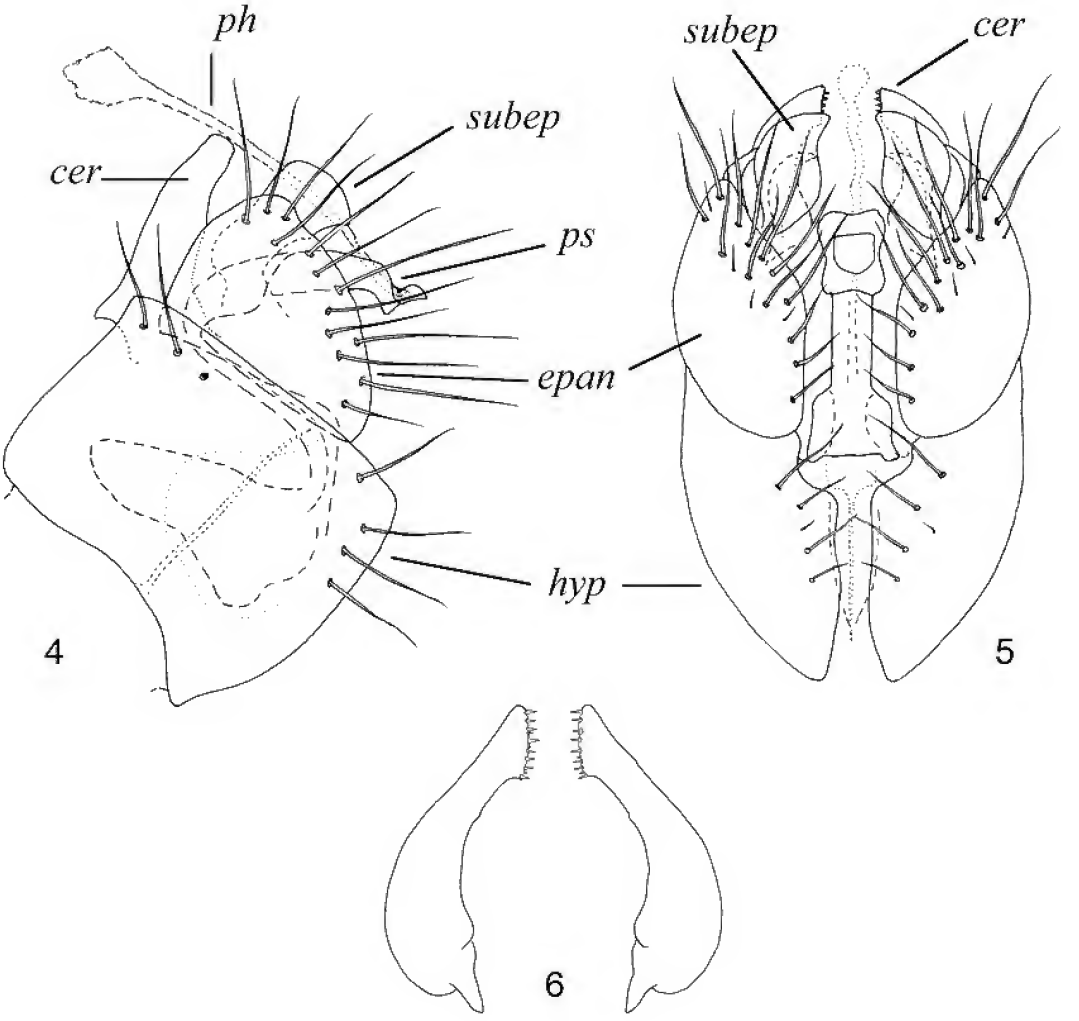

Figures 4–6. *Sororsenexa macalpinei* n.sp. male genitalia: (4) lateral view; (5) posterior view; (6) cerci in dorsal view. Abbreviations: cer, cercus; epan, epandrium; hyp, hypandrium; ph, phallus; ps, phallic sheath; subep, subepandrial process.

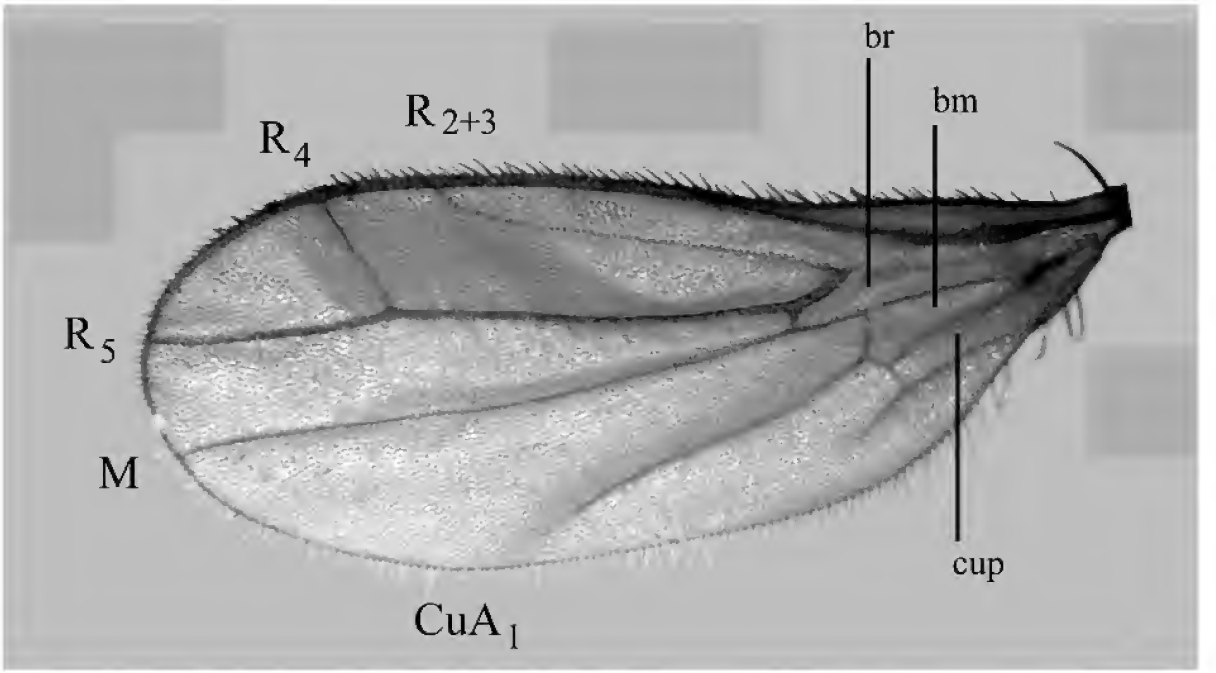

Figure 7. *Sororsenexa macalpinei* n.sp. male wing showing nomenclature of major veins and cells.

Key to Australian genera of Chelipodini

The following key is tentative as undescribed genera are almost certainly present in Australia and local forms of *Chelipoda* are subject to considerable but unstudied variation, especially in wing venation.

1 Vein C fading a short distance beyond apex of wing; R_{4+5} forked; eye notch (crena) absent ..... *Sororsenexa* n.gen.

—— Vein C circumambient, continued (if sometimes weakly) around posterior margin of wing; R_{4+5} linear; eye notch (crena) present and distinct 2

2 Crossvein dm-cu absent (cell dm absent); long veins R_{2+3}, R_{4+5}, M and CuA_1 unbranched; second tarsal segment of front leg longer than third segment; antenna lacking basal article to stylus; male cercus bilobed with upper lobe greatly enlarged and apically broadened ..... *Anaclastoctedon* Plant

—— Crossvein dm-cu usually present (cell dm closed); second tarsal segment of front leg shorter than or at most as long as third segment; antennal stylus with basal article; male cercus otherwise ..... *Chelipoda* Macquart

ACKNOWLEDGMENTS. I would like to thank David McAlpine and Dan Bickel for collecting the specimens on which this work was based and arranging loan of the material.

References

Cumming, J. M., B. J. Sinclair, and D. M. Wood. 1995. Homology and phylogenetic implications in male genitalia in Diptera—Eremoneura. *Entomologica scandinavica* 26: 121–151.

McAlpine, J. F. 1981. Morphology and terminology—Adults. In: *Manual of Nearctic Diptera*, cords. J. F. McAlpine, B. V. Peterson, G. E. Shewell, H. J. Teskey, J. R. Vockeroth, and D. M. Wood, volume 1, chapter 2, pp. 9–63. Agriculture Canada Monograph 27.

Plant, A. R. 2010. *Anaclastoctedon*, a new genus of Hemerodromiinae from Asia and Australia. *Raffles Bulletin of Zoology* 58: 15–25.

Plant, A. R. 2011. Hemerodromiinae (Diptera: Empididae): a tentative phylogeny and biogeographical discussion. *Systematic Entomology* 36: 83–103, published online 30 September 2010. doi:10.1111/j.1365-3113.2010.00547.x

Sinclair, B. J. 2000. 1.2. Morphology and terminology of Diptera male terminalia. In: *Contributions to a Manual of Palaearctic Diptera 1: General and Applied Dipterology,* ed. L. Papp, and B. Darvas, pp. 54–74.

Smith, K. G. V. 1989. 43. Family Empididae. In *Catalog of the Diptera of the Australasian and Oceanic Regions*, ed. N.L. Evenhuis, pp. 382–392. Honolulu: Bishop Museum Special Publication 86. Online version, updated 25 May 2007, consulted 22 October 2010 http://hbs.bishopmuseum.org/aocat/pdf/43empididae.pdf

Stuckenberg, B. R. 1999. Antennal evolution in the Brachycera (Diptera), with a reassessment of terminology relating to the flagellum. *Studia dipterologica* 6: 33–48.

Records of the Australian Museum (2011) Volume 63. ISSN 0067-1975

CONTENTS

Volume 63 • Numbers 1–3 • 2011

Main, B.Y., 1985b. Arachnida: Mygalomorphae. In *Zoological Catalogue of Australia*, ed. D.W. Walton, pp. 1–48. Canberra: Australian Government Publishing Service.

Main, B.Y., & R.M. Mascord, 1974. Description and natural history of a "tube building" species of *Dyarcyops* from New South Wales and Queensland (Mygalomorphae: Ctenizidae). *Journal of the Australian Entomological Society (NSW)* 1: 15–21.

Wishart, G., 1992. New species of the trapdoor spider genus *Misgolas* Karsch (Mygalomorphae: Idiopidae) with a review of the tube building species. *Records of the Australian Museum* 44(3): 263–278.
doi:10.3853/j.0067-1975.44.1992.35

Wishart, G., 1993. The biology of spiders and phenology of wandering males in a forest remnant (Araneae: Mygalomorphae). *Memoirs of the Queensland Museum* 33(2): 675–680.

Wishart, G., 2006. Trapdoor spiders of the genus *Misgolas* (Mygalomorphae: Idiopidae) in the Sydney Region, Australia, with notes on synonymies attributed to *M. rapax*. *Records of the Australian Museum* 58(1): 1–18.
doi:10.3853/j.0067-1975.58.2006.1446

Wishart, G., & D.M. Rowell, 1997. Phenotypic variation in sexual and somatic morphology in the trapdoor spider *Misgolas hubbardi* Wishart in relation to its genotypic variation (Mygalomorphae: Idiopidae). *Australian Journal of Entomology* 36: 213–219.
doi:10.1111/j.1440-6055.1997.tb01456.x

Wishart, G., & D.M. Rowell, 2008. Trapdoor spiders of the genus *Misgolas* (Mygalomorphae: Idopidae) from Eastern New South Wales, with notes on genetic variation. *Records of the Australian Museum* 60(1): 45–86.
doi:10.3853/j.0067-1975.60.2008.1495

Errata

* Through publisher-error this figure did not appear in the print version of Wishart's work published 29 June 2011 in volume 63, pages 33–51. The associated PDF doi:10.3853/j.0067-1975.63.2011.1553 was corrected to include the figure and uploaded 13 July 2011. Binders may replace volume 63, pages 51–52, with this leaf; page 52, the verso, has no text or figures. [Editor—21 October 2011]

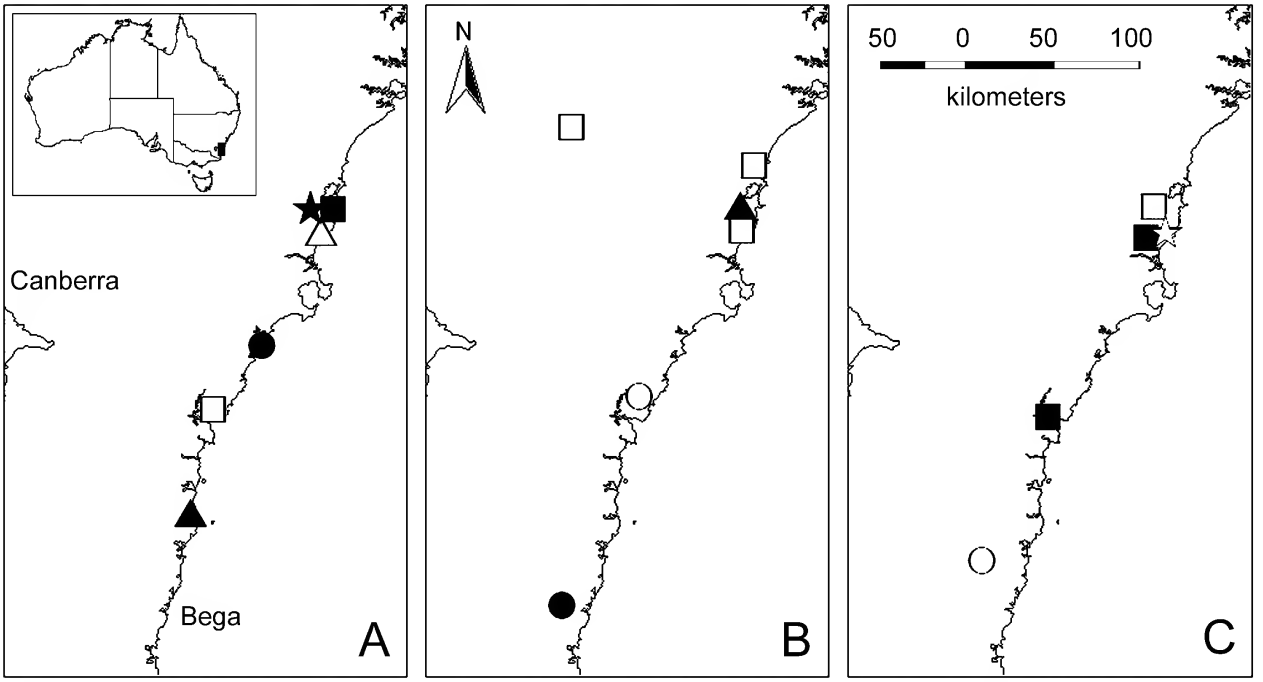

Fig. 14 A–C. Distribution of *Misgolas* species in the New South Wales Illawarra and South Coast (eastern Australia) based on material examined. (Inset [Fig. 14A] with catchment area). *(A)* ★ *M. gracilis*, ■ *M. rowelli*, △ *M. rapax*, ● *M. phippsi*, □ *M. kampenae*, ▲ *M. elegans*. *(B)* □ *M. dereki*, ▲ *M. robertsi*, ○ *M. horsemanae*, ● *M. shawi*. *(C)* □ *M. tannerae*, ■ *M. gwennethae*, ☆ *M. kirstiae*, ○ *M. paulaskewi*.

INSTRUCTIONS TO AUTHORS

Manuscripts must be submitted to The Editor. All manuscripts are refereed externally.

Only those manuscripts that meet the following requirements will be considered for publication.

Submit manuscripts and all images electronically; images should be high resolution TIFFs (see below). Attach one summary file or cover sheet giving: the title; the name, address and contact details of each author; the author responsible for checking proofs; a suggested running-head of less than 40 character-spaces; and the number of figures, tables and appendices. Manuscripts must be complete when submitted.

Tables and figures should be numbered and referred to in numerical order in the text. Electronic copy is stripped and reconstructed during production, so authors should avoid excessive layout or textual embellishments; a single font should be used throughout.

All copy is manipulated within a Windows (not Mac) environment using Microsoft and Adobe software. Maps should be submitted as high resolution TIFF.

Manuscripts should be prepared using recent issues as a guide. There should be a title (series titles should not be used), author(s) with their institutional addresses, an abstract (should be intelligible by itself, informative not indicative), introduction (should open with a few lines for general, non-specialist readers), materials and methods, results (usually subdivided with primary, secondary and rarely tertiary-level headings), discussion, acknowledgments and references. If appropriate, an appendix may be added after references.

In the titles of zoological works the higher classification of the group dealt with should be indicated. Except for common abbreviations, definitions should be given in the materials and methods section. Sentences should not begin with abbreviations or numerals; generic names should not be abbreviated if at the beginning of a sentence. Metric units must be used except when citing original specimen data. It is desirable to include geo-spatial coordinates; when reference is made to them, authors must ensure that their format precludes ambiguity, in particular, avoid formats that confuse arcminutes and arcseconds.

Label and specimen data should, as a minimum requirement, indicate where specimens are deposited, in addition to locality, date and collector. Original specimen data—especially that of type material—is preferred over interpreted data. If open to interpretation, cite original data between quotation marks or use "[sic]".

Rules of the International Code of Zoological Nomenclature must be followed; authors must put a very strong case if a Recommendation is not followed. When new taxa are proposed in works having multiple authors, the identity of the author(s) responsible for the new name(s) and for satisfying the criteria of availability, should be made clear in accordance with Recommendations in Chapter XI of the Code. A scientific name with more than two authors is unwieldy and should be avoided. Keys are desirable; they must be dichotomous and not serially indented. Synonymies should be of the short form: taxon author, year, pages and figures. A period and en-dash must separate taxon and author except in the case of reference to the original description. Proposed type material should be explicitly designated and, unless institutional procedure prohibits it, registered by number in an institutional collection.

Previously published illustrations will generally not be accepted. Extra costs resulting from colour production are charged to the author (AU$1000 for 1–8 pp, AU$2000 for 9–16 pp, etc.; these charges can be shared by authors of different papers that are printed consecutively). All images must (*a*) be rectangular or square and scalable to a width of 83 mm (one text column) or 172 mm (both text columns including gutter) and any depth up to 229 mm (the number of lines in a caption limits depth); (*b*) have lettering similar to 14 point, upper case, normal, Helvetica or Arial, in final print; (*c*) have no unnecessary white or black space; and (*d*) have vertical or horizontal scale bars, with the lengths given in the caption and with the thickness approximately equal to an upper case 14 point letter "I".

Digital images must be presented as TIFF, or as multilayered PSD files suitable for *Adobe Photoshop* version 5.0 or later. Halftone and colour images must be at a minimum resolution of 300 dpi at final size (at this resolution 2040 pixels = printed-page width) and all labelling must be sharp (with *anti-aliased* active). Black and white line images (bitmaps) must be at a minimum resolution of 1200 dpi at final size (at this resolution, 8160 pixels = page width = 172 mm).

When reference is made to figures in the present work use Fig. or Figs, when in another work use fig. or figs; the same case-rule applies to the words *tables* and *plates*. Figures and tables should be numbered and referred to in numerical order in the text.

Authors should refer to recent issues of the *Records of the Australian Museum* to determine the correct format for listing references and to *The Chicago Manual of Style* to resolve other matters of style. Insert URLs in the Reference section if they are known—use *digital object identifiers* (doi) if available (see www.doi.org and www.crossref.org).

Certain anthropological manuscripts (both text and images) may deal with culturally sensitive material. Responsibility rests with authors to ensure that approvals from the appropriate person or persons have been obtained prior to submission of the manuscript.

Stratigraphic practice should follow the *International Stratigraphic Guide* (second edition) and *Field Geologist's Guide to Lithostratigraphic Nomenclature in Australia*.

The Editor and Publisher reserve the right to modify manuscripts to improve communication between author and reader. Essential corrections only may be made to final proofs. No corrections can be accepted less than four weeks prior to publication without cost to the author(s). All proofs should be returned as soon as possible.

No reprints will be available.

All authors, or the Corresponding Author on their behalf, must sign a *Licence to Publish* when a manuscript is submitted, and certify that the research described has adhered to the Australian Museum's *Guidelines for Research Practice*—or those of their home institution providing they cover the same issues, especially with respect to authorship and acknowledgment. While under consideration, a manuscript may not be submitted elsewhere.

More information and examples are freely available at our website:

www.australianmuseum.net.au/Scientific-Publications

30 November 2011 Stock no. 011R63B

YOUR SUPPORT MAKES A DIFFERENCE

The Australian Museum strives to inspire the exploration of nature and cultures. We would like to acknowledge the benefactors and corporate partners who support us in achieving this vision.

These generous individuals contribute to scientific research, education programs, public programs and assist in the acquisition of items that enrich our collections. We would especially like to acknowledge those who generously leave a gift to the Australian Museum in their will—a lasting way to benefit generations to come.

If you would like to find out how your support can make a difference to the important work of the Australian Museum, please contact the Development Branch on +612 9320 6216 or development@austmus.gov.au. Donations to the Australian Museum and its Foundation are tax deductible.

NSW Government

PRINCIPAL PARTNERS

Australian Museum Members
BJ Ball Papers
City of Sydney
Geddes Group
IBM
JCDecaux
Lizard Island Reef Research Foundation
National Geographic Channel
Rio Tinto
Scitech
Sydney Grammar School
Sydney's Child
The Sydney Morning Herald

AUSTRALIAN MUSEUM FOUNDATION

President's Circle

Dr Zeny Edwards
Christopher Grubb
Ian and Stephanie Hardy
Mrs Judy Lee
Diccon Loxton
Helen Molesworth
Rob and Helen Rich
David and Daniela Shannon
The Sherman Foundation

Supporters

Antoinette Albert
James and Belinda Allen
Michelle Atkinson
Mr and Mrs KR Bell
Jane Beniac
Sir Ron Brierley
Alan Cameron
Elizabeth Cameron
Peter and Rose Cassidy
Ken Coles AM and Rowena Danziger AM
P Cornwell
Debra Cox
Patrick and Ailsa Crammond
John Dickinson
Suellen and Ron Enestrom
Estate of the late Clarence E Chadwick
Estate of the late Patricia M Porritt
Estate of the late Merrill Pye
Estate of the late Gwendoline A West
Leon Gorr
David Greatorex AO and Dee Greatorex
Owen Griffiths & Biodiversity Conservation Madagascar Assn
Ken Handley AO and Diana Handley
Ronnie Harding
Bill and Alison Hayward
Ann Hoban
John and Mary Holt
Dan Howard SC and Dr Rosemary Howard
Frank Howarth
Gilles Kryger
John Lamble Foundation
James E Layt AM
Margaret Mashford
Robert McDougall
Mabs Melville
Stephanie Miller and Martin Pool
Dame Elisabeth Murdoch AC DBE
John Neuhaus
Justice Henric Nicholas
The Noonan Family
David Norman
Alice Arnott Oppen OAM
Andrew Pardoe
John Pearson
Loris Peggie
Adrian and Dairneen Pilton
David Robb
Jane and Neville Rowden
Reid Family
Rosemary Swift
Senta Taft-Hendry
Vera Vargassoff
Tony White AM and Doffy White
Jennifer Wright

GIFTS TO COLLECTIONS

Steven and Janine Avery
Ursula Burgoyne
Louise and Sam Dawson
Rod and Robyn Dent in honour of Pat Dent and the Wanindilyaugwa tribe
John L Gordon
Mark Hanlon
Mrs J Holliday
The Late John Hume
John Rankin
Paul Scully-Power
Trevor Shearston

ISSN 0067-1975